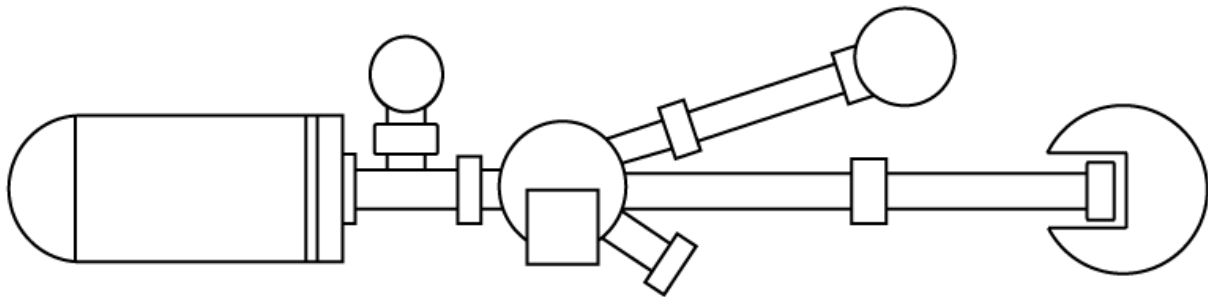


Welcome to the
**23rd International Conference
on the Application of Accelerators
in Research and Industry
(CAARI 2014)**



May 25-30, 2014

Grand Hyatt Hotel

San Antonio, Texas, USA

Contact Details

Holly Decker
Conference Coordinator
University of North Texas
1155 Union Circle, #311427
Denton, Texas
76203-5017 USA

Phone: +1-940-565-3256
Fax: +1-940-565-2227

E-mail:
holly.decker@unt.edu
Web: www.caari.com

CAARI 2014 COMMITTEES

Local Organizing Committee

Yongqiang Wang	Co-Chair	Los Alamos National Laboratory
Gary A. Glass	Co-Chair	University of North Texas
F. Del McDaniel	Co-Chair	University of North Texas
Barney L. Doyle	Co-Chair	Sandia National Laboratories
Jerome L. Duggan	Chair Emeritus	University of North Texas
Holly Decker	Conference Coordinator	University of North Texas
Carley Parriott	Conference Coordinator	Sandia National Laboratories
Barbara Diehl	Conference Assistant	Pacific Northwest National Laboratory
Jennifer Duckworth	Conference Assistant	University of North Texas
Zdenek Nejedly	Webmaster	AnzSolutions

Topic Editors

Arlyn Antolak	USA	Richard P. Levy	USA
John Baglin	USA	Daniel Marble	USA
Lucile Beck	France	Thomas Schenkel	USA
Mike Demkowicz	USA	David Schultz	USA
Alfredo Galindo-Uribarri	USA	Lin Shao	USA
Robert Garnett	USA	Valeriia Starovoitova	USA
Richard Greco	USA	S. (Theva) Thevuthasan	USA
Anna Hayes-Sterbenz	USA	Gyorgy Vizkelethy	USA
Peter Hosemann	USA	Yanwen Zhang	USA

Session Chairs

Elizabeth Auden	USA	Gregg McKinney	USA
John Baglin	USA	Vladimir Mozin	USA
Daniel Bardayan	USA	Xin Ou	Germany
Lucile Beck	France	Claire Pacheco	France
Mark Bradley	USA	Graham Peaslee	USA
Kevin Carnes	USA	Iva Bogdanovic Radovic	Croatia
Sergey Chemerisov	USA	Chintalapalle Ramana	USA
Marshall Cleland	USA	Jani Reijonen	USA
George Coutrakon	USA	Rex Richardson	USA
Aaron Couture	USA	Carl Rossi	USA
Miguel Crespillo	USA	Bibhu Rout	USA
Robert Cywinski	United Kingdom	Antonio Santos	Brazil
Arun Devaraj	USA	Reinhold Schuch	Sweden
Max Doebeli	Switzerland	Reinhard Schulte	USA
John Eley	USA	Lin Shao	USA
Alfredo Galindo-Uribarri	USA	Jefferson Shinpaugh	USA
Cameron Geddes	USA	Shuttha Shutthanandan	USA
Lyudmila Goncharova	Canada	David Silvermyr	USA
Tsahi Gozani	USA	Aliz Simon	Austria
Terry Grimm	USA	Ziga Smit	Slovenia
Bradley Hart	USA	Srinivasan Srivilliputhur	USA
Khalid Hattar	USA	Valeriia Starovoitova	USA
Anna Hayes	USA	Thomas Stoeckler	Germany
Jerry Hollister	USA	Daniel Stracener	USA
Peter Hosemann	USA	Jao Jung Su	USA
Daryush Ila	USA	Ming Tang	USA
Carole Johnstone	USA	Fredrik Tovesson	USA
Mike King	USA	Andrzej Turos	Poland
Tom Kirchner	USA	Duncan Weathers	USA
David Koltick	USA	Doug Wells	USA
Willy Langeveld	USA	Stephen Wender	USA
Rich Levy	USA	Dharshana Wijesundra	USA
Nan Li	USA	Isao Yamada	Poland
Bernhard Ludewigt	USA	Kaiyuan Yu	USA
Amanda Lupinacci	USA	Zihua Zhu	USA
Anita Mahajan	USA	Peter Zielinski	USA

Welcome to CAARI-2014

The organizers would like to welcome you to the 23rd International Conference on the Application of Accelerators in Research and Industry. This conference is being hosted by the University of North Texas (UNT) in Denton, TX, Sandia National Laboratories (SNL) in Albuquerque, NM, and Los Alamos National Laboratory (LANL) in Los Alamos, NM. CAARI 2014 is also being supported by several other U.S. National Laboratories, industries and agencies most identified with accelerator technology. The Conference Co-chairs and the Topic Editors worked with the Session Chairs to develop the sessions and speakers.

This is the 23rd International conference in the biennial series that began in 1968 as a *Conference on the Use of Small Accelerators for Teaching and Research* by Jerry Duggan, while he was a staff member at Oak Ridge Associated Universities. When Jerry moved to Denton, TX and joined the University of North Texas (UNT), he continued the Conference series in 1974, holding the meeting on the UNT campus. At this time, Jerry invited Lon Morgan to join him as a co-organizer. Lon Morgan brought in the industrial components of CAARI and it became known the International Conference on the Application of Accelerators in Research and Industry (CAARI). CAARI was held in Denton for 30 years. In 2004, Jerry Duggan asked Floyd "Del" McDaniel and Barney Doyle to be co-organizers of the CAARI Conference Series. In 2004, Barney and Del moved the conference to Fort Worth, Texas, where it was held biennially from 2004-2012. In 2012, Yongqiang Wang and Gary Glass were invited to become co-organizers of CAARI. For the 2014 Conference, we changed the conference dates to May 25-30 and moved the conference venue to the Grand Hyatt Hotel Riverwalk in San Antonio, Texas.

The CAARI Conference series is unique in that it brings together researchers from all over the world who use particle accelerators in their research and industrial applications. Each year the Topic Areas are reviewed and updated to reflect current research interests. The 2014 CAARI Conference is a collection of symposia for the following Topic Areas:

- Accelerator Technology & Facilities (ATF)
- Atomic and Molecular Physics (AMP)
- Homeland Security & Defense (HSD)
- Ion Beam Analysis (IBA)
- Ion Beam Modifications (IBM)
- Medical Applications (MA)
- Nuclear-Based Analysis (NBA)
- Nuclear Physics (NP)
- NanoScience & Technology (NST)
- Plenary Sessions (PS)
- Radiation Effects (RE)
- Teaching with Accelerators (TA)

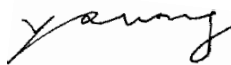
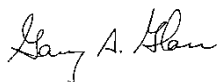
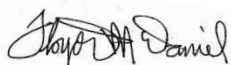
In addition to this brief Program Book with titles and presenting authors, the program with complete abstracts may be found at www.CAARI.com.

CAARI 2014 will be held at the beautiful Grand Hyatt Hotel located on the famous San Antonio Riverwalk. Please visit the following link, as this microsite will assist you in exploring great places to dine, shop, and visit while in San Antonio during the CAARI Conference. <http://visitsanantonio.com/2014caari>

We hope that you enjoy the conference and find it intellectually stimulating. In the schedule, we have provided several opportunities to renew friendships and talk science at this meeting: the Welcome Reception Sunday evening, the socials during each poster session Monday and Tuesday, the Conference outing on Wednesday afternoon, the Banquet on Thursday evening, and the Closing Ceremony on Friday at noon.

If there is anything we can do to make your conference experience and stay in San Antonio, Texas, more enjoyable, just ask Del, Gary, Yong, Barney, Holly, or Carley. We are very happy you have joined us in San Antonio and hope you have a memorable time!

Your Co-Chairmen, CAARI-2014



Financial Support

Financial support from sponsors, exhibitors, and advertisers is an essential element of a successful conference. This support enables us to provide support for conference events, students, and other attendees. We are very grateful to the sponsors, exhibitors, and advertisers listed below for their support of CAARI 2014.

Research and University Sponsors

Los Alamos National laboratory
Sandia National Laboratories
University of North Texas

Industrial Sponsors

High Voltage Engineering Europa B.V.
Impulse Technologies, Inc.
R&K Company Limited

Exhibitors

AccelSoft Inc.
Agilent Technologies
Behlke Power Electronics LLC
Buckley Systems Ltd
Daresbury Laboratory
Dean Technology
Engineering Stangenes Industries,
Inc.

Friatec NA
Impulse Technologies, Inc.
Kurt J. Lesker Company
National Electrostatics Corp
RadiaBeam Systems
TDK-Lambda
XIA LLC

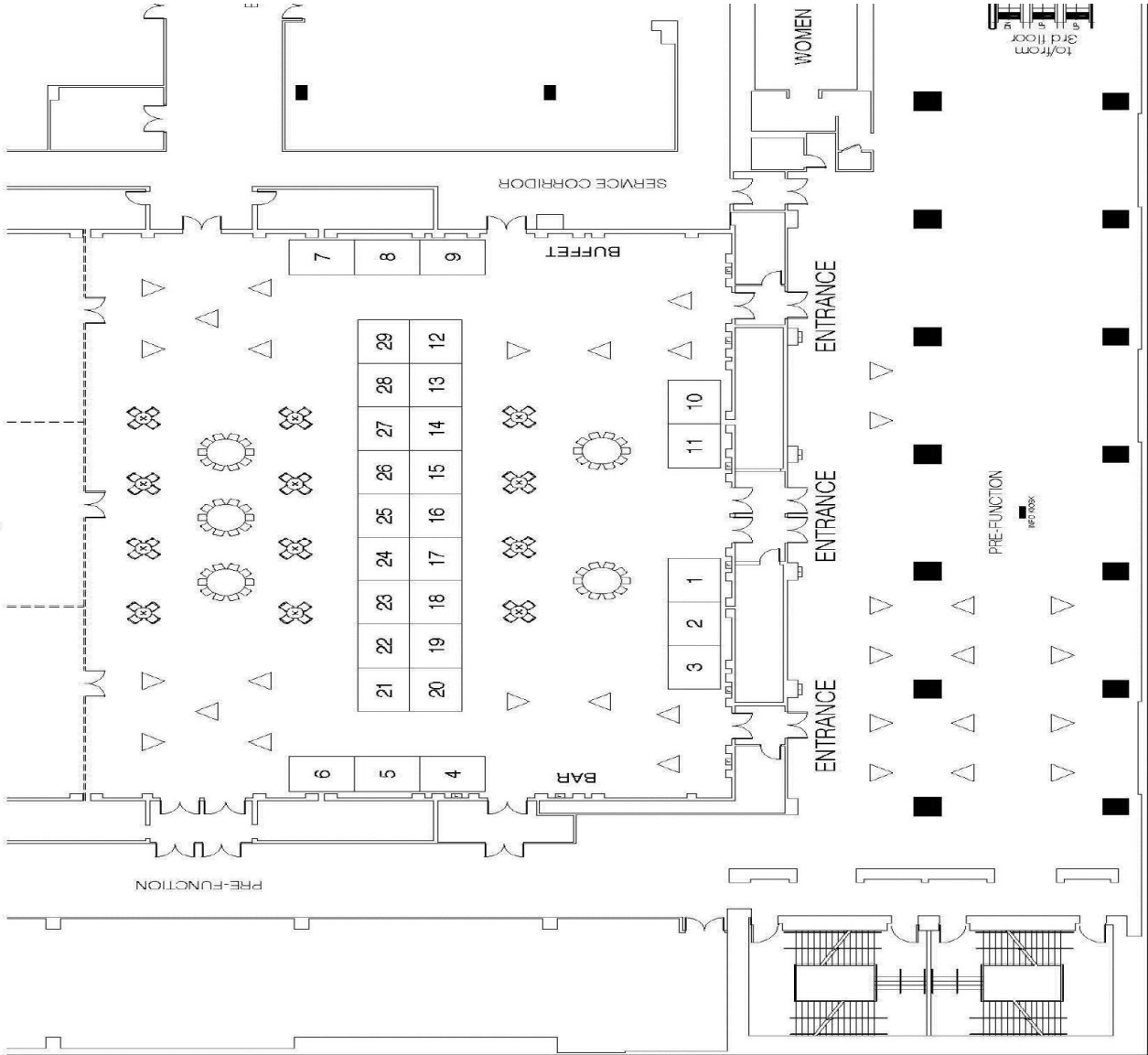
Advertisers

Amptek
American Elements

CAARI Conference Exhibitor Map

May 26-29, 2014

Grand Hyatt San Antonio / Lone Star Ballroom - Level 2
San Antonio, Texas



ADVERTISEMENTS

ACCELERATE ULTRA-HIGH VACUUM PERFORMANCE

Combine Agilent's leading UHV solutions to accelerate your results:

- Agilent Diode and StarCell Ion Pumps' UHV versatility
- Agilent 4UHV, the first true 4 channel ion pump controller
- Agilent TwisTorr FS turbo pumps' leading speed and compression
- Agilent Dry Scroll pumps' clean oil-free vacuum

Learn more: www.agilent.com/chem/vacuum

The Measure of Confidence



Scan the QR code
with your smartphone
for more information

© Agilent Technologies, Inc. 2014



Agilent Technologies

Now from AMPTEK

SDD, Si-PIN, AND CdTe DETECTORS FAST SDD™ DETECTORS WITH >1,000,000 CPS



FAST SDD™ WITH C2 WINDOW

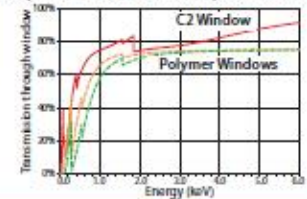
For SEM-EDS Applications

Features of the C2 Windows:

- High intrinsic efficiency
- Low energy response
- Measure elements down to Carbon
- Low cost



Comparison of C2 Window to Polymer Windows



GAMMA RAY DETECTION SYSTEM

Scintillation Detector (NaI) & Digital Pulse Processor



•Homeland Security •Nuclear Plant Monitor

Features of the GAMMA-RAD5:

- Ruggedized scintillator and PMT
- Gain stabilized in software
- Ethernet, RS232 & USB interfaces for robust communications
- USB powers entire system
- Flexible architecture for tailoring interface
- For OEMs and custom users

PMT DIGITAL TUBE BASE

Use with Your Scintillation Spectrometer



Includes

- Digital pulse processor with charge sensitive preamplifier, and MCA
- All power supplies (low voltage and high voltage)
- Interface hardware and PC software
- 14 pin photomultiplier tube base

Complete X-Ray Spectrometers • X-Ray and Gamma Ray Detectors • OEM X-Ray Components

• SEM Detectors • Digital Pulse Processors • XRF QA Software • X-Ray Sources

• Scintillation Detectors and Accessories • Digital Multichannel Analyzer

• Charge Sensitive Preamplifiers

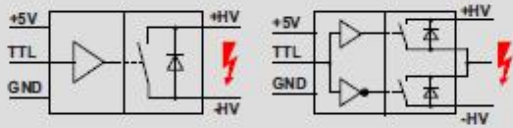
OEM's #1 Choice



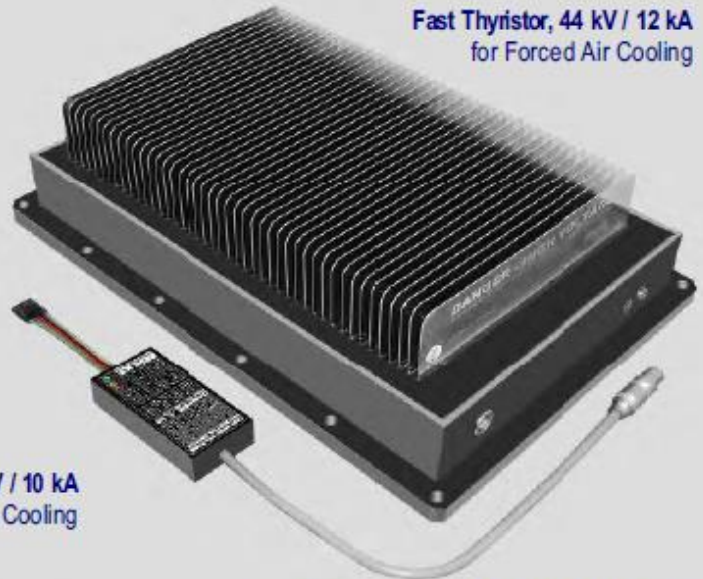
AMPTEK Inc. 14 DeAngelo Drive, Bedford, MA 01730-2204 USA
+1 781 275-2242 sales@amptek.com www.amptek.com



FAST HIGH VOLTAGE SOLID-STATE SWITCHES



- Operating voltages from 1 to 150 kV
- Peak currents from 15 A to 16 kA
- Short transition times and high di/dt
- AC, DC & push-pull switching modules
- MOSFET, IGBT and SCR technology
- Galvanic isolation for highside switching
- Various housing and cooling options
- Custom designed switches & pulsers



Fast Thyristor, 44 kV / 12 kA
for Forced Air Cooling



Fast Thyristor, 150 kV / 10 kA
for DLC Liquid Cooling



MOSFET AC Switch,
28 kVAC / 120 A
DLC Liquid
Cooling

NEW



Ultra compact MOSFET on-off switches for printed circuit boards. Voltages up to 18 kV at 79 x 38 x 17 mm and up to 36 kV at 140 x 38 x 20 mm (L x W x H). Pulse width from 50 ns to infinity.



Housing ▲

▼ Switch

DLC LIQUID COOLING

DLC - Direct Liquid Cooling.
The ultimate high performance
liquid cooling with fluorocarbon coolants.

www.behlke.com

Behlke Power Electronics LLC, 5 Alexander Rd, Billerica, MA 01821, USA

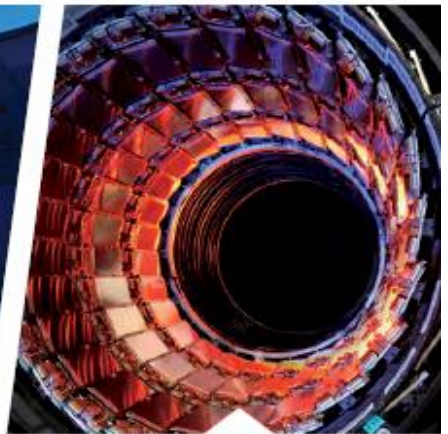


BEHLKE
HIGH-TECH IN HIGH VOLTAGE

BSL

Buckley Systems Ltd

WORLD LEADERS IN ELECTROMAGNETS AND PARTICLE ACCELERATOR SYSTEMS
DESIGN AND MANUFACTURING



< WE PARTNER WITH >

SEMICONDUCTOR
ION IMPLANT
INDUSTRIES

MEDICAL CANCER
THERAPY DESIGNERS
AND MANUFACTURERS

PARTICLE ACCELERATOR
LABORATORIES FOR
PHYSICS RESEARCH



Bill Buckley

Buckley Systems is pleased to announce that it has invested in D-Pace, a very exciting and promising Canadian Particle-Accelerator Design and Engineering company.

This investment will allow D-Pace to develop and commercialise various licensed product technologies. While it will be business as

usual for D-Pace and Buckley Systems, combining the pedigree of the two companies enhances the manufacturing and design synergies of both.

The aim is to deliver enhanced capabilities and address the emerging innovation opportunities of customers.

Head Office

PH + 64 9 573 2200
9 Bowden Road, Mt Wellington
Auckland 1060, New Zealand
info@buckleysystems.com

USA Office

PH + 1 978 948 3403
19 Turcotte Memorial Drive
Rowley, MA 01969, USA
office@buckleysystems.com

www.buckleysystems.com

HIGH VOLTAGE HIGH CURRENT

1 mA to
100 kA

- High Voltage Silicon Rectifiers
- High Voltage Diodes
- Voltage Multipliers
- Custom Assemblies
- Full Wave Bridges

e-mail: info@hvca.com

Semiconductors

*For Your High Current and/or
High Voltage Requirements*

- Silicon Rectifiers
 - Air-Cooled
 - Water Cooled
- Assemblies
 - Thyristor
 - Rectifier
 - SCR
 - Bridge Rectifier

e-mail: info@deantechnology.com



Products By:
DEAN
TECHNOLOGY



Our experienced
engineers will help you find
the perfect solution for
your high voltage or
high current application.

TO ORDER A FREE
CATALOG OR SAMPLES,
VISIT OUR WEBSITE.

www.hvca.com

www.cke.com

FRIALIT®- DEGUSSIT® Oxide Ceramics

Ceramics give particle accelerators a push

Whether kicker chamber, circular accelerator or particle source - ceramics and the joy of innovation lead to new horizons. Especially-designed alumina components with mature brazing technology solve problems for researchers and developers. Contact us for more information.



Single and multiple feedthroughs for ultra high-vacuum applications using FRIALIT-DEGUSSIT Oxide Ceramics ensure maximum electrical insulation with minimum outgassing and leakage rates.



FRIATEC insulation tubes provide maximum insulation and remain tight at extreme pressure and vacuum conditions and even resist temperatures exceeding 350°C.



Whether high current, high voltage or measurement signals, FRIATEC manufactures tailor-made and standard components to customer specifications.

FRIATEC N.A, LLC
11108 Challenger Ave, # 101
Odessa, Florida 33556
U.S.A.
Tel: 727-753-0880
info@friatecna.net
www.friatecna.net





HIGH VOLTAGE ENGINEERING EUROPA B.V.

The largest and most diverse manufacturer of particle accelerators

Products

HVE designs, manufactures, sells and markets ion beam technology based equipment for the scientific, educational and industrial research communities. The major product lines are:

Ion Accelerator Systems

- Air insulated accelerators up to 500 kV
- Singletron single ended accelerators up to 6.0 MV/TV
- Tandetron tandem accelerators up to 6.0 MV/TV

Research Ion Implanters

- Beam energies 10 - 60 MeV and higher
- Beam powers up to 25 kW

Systems for Ion Beam Analysis

- Rutherford Backscattering Spectroscopy (RBS)
- Particle Induced X-ray Emission (PIXE)
- Nuclear Reaction Analysis (NRA)
- Elastic Recoil Detection (ERD)
- Medium Energy Ionscattering Spectroscopy (MEIS)

Accelerator Mass Spectrometers

^3H , ^7Be , ^{10}Be , ^{14}C , ^{26}Al , ^{32}Si , ^{36}Cl , ^{41}Ca , ^{53}Mn , ^{79}Se , ^{129}I , ^{236}U etc.
analysis for use in

- Archeology
- Oceanography
- Geosciences
- Material sciences
- Biomedicine
- Etc.

Systems for Micro-beam applications

- Tandetron and Singletron based systems

Neutron Generator Systems

- DC and Pulsed Beam Systems

Electron Accelerator Systems

- Singletron electron accelerators up to 6.0 MV/TV

Components

Ion and electron accelerator tubes, ion and electron sources, beam handling & monitoring equipment, etc.



**MORE
ENERGY
FOR
RESEARCH**

High Voltage Engineering Europa B.V.

P.O. Box 99, 3800 AB Amersfoort, The Netherlands

Phone: +31-33-4619741. Fax +31-33-4615291

info@highvolteng.com • www.highvolteng.com

R.K R&K Company Limited

324MHz±5MHz
120kW Pulse

All Solid State Pulsed RF Power Amplifier
R&K-A324BW10-7181RP

R&K-A100BW2-7575RP
All Solid State Pulsed RF Power Amplifier

100MHz±1MHz
30kW Pulse

1.7MHz±0.1MHz
60kW CW

All Solid State RF High Power Amplifier
R&K-A1.7BW0.2-6878R

R&K-A1300BW10-6372R
All Solid State RF High Power Amplifier

1300MHz±5MHz
16kW CW

• All Solid State Power Amplifier of Excellent Linearity !

R&K RF Power Amplifiers are all solid state type designed for excellent linearity and low harmonic distortion Class-A, AB operation. Unlike vacuum tube amplifiers, it has long-term and continuous maintenance-free operation.

• Equipped with R&K unique technology Multi Monitoring System !

Each parameter, such as voltage, current, temperature, output power, reflection power, etc. at each internal active element or amplifier block are constantly monitored, and the monitor data can be saved in time sequence for over 10 years. The protection & alarm functions are activated as needed. This Multi Monitoring System makes it possible to diagnose, investigate, and analyze any failure.

• Power Combining by means of Broadband & High Power Radial Combiners !

The radial combiners used in some R&K Power Amplifiers give users technical advantage by its extremely low insertion loss at combining multiple power inputs and makes it possible to achieve high power very efficiently. With this technology, R&K offers low-cost and highly reliable power amplifiers compared with the conventional solid state power amplifiers. www.rk-microwave.com



Impulse Technologies, Inc. has partnered with R&K Company, Ltd. to promote and handle all inquiries within the United States. With over 20 years of experience, we have had the opportunity to reach and meet the needs of institutes worldwide.

For all inquiries within the US., please contact us at:

sales@impulse-tech.com TEL: +1 (631) 968-4116 FAX: +1 (631) 968-8339 www.impulse-tech.com

CUSTOM LINAC SYSTEMS

RadiaBeam Systems offers a full range of turnkey linac systems for a wide variety of commercial, industrial, and research applications. Unlike other manufacturers, we specialize in providing cost-optimized, customized systems to suit your exact needs.

All systems are designed, engineered, fabricated, and tested in our 16,000 ft² facility in Santa Monica, California, USA.

RADIOGRAPHY / CARGO INSPECTION

- Megavolt X-rays allow for the imaging of dense materials that are beyond the reach of isotope sources, without the security concerns and expense of radioisotopes
- Field deployable and compact portable systems available
- Multi-energy interlaced X-ray sources for cargo inspection systems with material discrimination



SELF-SHIELDED IRRADIATORS

- Ideal for space radiation effects testing, biological research, materials research, radiochemistry, and other applications
- Included shielding ensures safety for use in a laboratory or industrial environment

HIGH-POWER STERILIZATION & IRRADIATOR SYSTEMS

- E-beam and X-ray sterilization is a cost-effective and flexible way of sterilizing medical products and can greatly extend the shelf life and safety of food
- Full facilities with materials handling, beam delivery, controls, and shielding
- In-line irradiation systems can be integrated directly into a production line for optimal convenience and efficiency



OEM AND CUSTOM ACCELERATING GUIDES & SYSTEMS

- Standard and custom accelerating guides for industrial and research uses
- Fully custom systems for novel applications
- Any energy, frequency, or power available



www.radiabeamsystems.com | v: +1 310 822 5845 | f: +1310 582 1212 | info@radiabeam.com

#04.08.14



STANGENES INDUSTRIES, INC.

"The best in custom transformers."

For over 35 years, Stangenes Industries has been manufacturing critical components for government, industry, and research. As an OEM supplier to major medical and industrial equipment manufacturers, we have developed a reputation for quality and reliability at globally competitive prices. The foremost government and institutional particle accelerator facilities and research laboratories in the world rely on Stangenes Industries for innovation and excellence.

Pulse Transformers

Stangenes Industries has built its reputation on the design and manufacture of high power pulse transformers up to the extremes of 1.5 MV, 6 kA and 1kV, 600 kVA. We design and manufacture:

- Pulse Charging Transformers
- High Power Klystron Pulse Transformers
- Klystron/Gun Pulse Transformers
- Magnetron/Gun Pulse Transformer Assemblies
- Tanked Pulse Transformer Assemblies

High Voltage Pulse Modulators

Stangenes Industries designs and produces pulse modulators in standardized or custom configurations for military, medical, and industrial applications driving klystrons, magnetrons, lasers or accelerators. We offer both solid state and thyatron driven modulators ranging from a just a few kilovolts to over five hundred kilovolt pulses, pulse widths from 200 nanoseconds to 5 milliseconds and average power ratings of up to 150 kilowatts.

Configurations offered include:

- Classic PFN pulse transformer design with thyatron or solid state switching
- "Hard tube configuration" with pulse transformer using solid state switching
- Solid state fractional turn pulse transformer modulators
- Solid state Marx designs with or without a pulse transformer
- Dynamically adjustable repetition rate, pulse width and pulse amplitude
- Components or a complete "turnkey" systems

Power Supplies

Stangenes Industries has developed several advanced capacitor charging technologies. Our state-of-the-art power conversion units utilize IGBT switches operating at high frequency in a quasi-resonant design utilizing zero voltage switching topology. These units often contain no oil or other dielectric fluids, so these units are significantly lighter and more reliable than comparable units. The advanced Optimized Charging Cycle (OCC) that we have developed reduces the peak power consumption from the line. This feature enables charging of large capacitor banks without exceeding the allowed average power.

Stangenes has produced power supplies utilizing these technologies at many different power levels and output voltage configurations.

- Single kilowatt to tens of kilowatts
- Single digit kilovolts to tens of kilovolts
- High repetition modulators for magnetrons and klystron, as well as many industrial applications

We are constantly expanding our product line and many new configurations are in the pipeline today including designs for hundreds of kilovolts and hundreds of kilowatts.

Electromagnets

Stangenes Industries can design, fabricate, and test a wide variety of coils and electromagnets, from precision low current DC focusing magnets to pulsed coils operating at 300 kA generating fields as high as 40 Tesla.

- Dipole, quadrupole, sextupole, corrector, bending, and solenoid electromagnets
- Wire, hollow conductor, and foil conductors in both copper and aluminum
- Paper, film, fiberglass, b-stage, varnish, and vacuum epoxy casting insulation
- Air cooling and/or liquid cooling using water or oil running through hollow conductor, cooling loops, or cooling plates allowing current densities as high as 15 A/mm²
- 2d & 3d field modeling, thermal, mechanical stress, and fluid flow analysis capabilities
- Axial & transverse magnetic field, hi-pot, ring, turns-ratio, pressure and flow testing capabilities

SCR Controlled DC Power Supplies

Stangenes Industries produces SCR controlled DC power supplies in standardized configurations or to customer specifications. These supplies operate on conventional 50-400 Hz power sources and supply output voltages that range from a few kilovolts to over 100 kilovolts with power rating from ten kilowatts up to a few megawatts average. The DC power supplies can be supplied as components of a system or a complete "turnkey" system.

Transformers & Inductors

Stangenes Industries manufactures a broad range of transformers and inductors to our customer's specifications or design including but not limited to:

- Single and Three Phase Transformers to 1.1 MVA
- Isolation Transformers, air, epoxy, SF6 or oil insulated to 800 kV pulse
- Charging Inductors
- Constant Voltage Transformers
- Rectifier Transformers to 300 kVDC, 1.6 A
- Trigger Transformers
- Inverter Transformers
- Epoxy Cast Transformers

Current Transformers

For measurement of pulse and AC currents over a wide range of amplitudes, pulse lengths, and frequencies Stangenes Current Transformers have:

- Complete isolation from the circuit to be measured (no ground currents)
- Shielded construction
- Internal 50 ohm termination for coaxial cable matching
- High accuracy ($\pm 0.5\%$)
- A variety of hole sizes to fit most conductors and voltages

Stangenes Current Transformers are available in many sizes and configurations directly from stock. Custom sizes and configurations can be designed to meet nearly any requirement.

Capacitance Type Pulse Voltage Dividers

Our Voltage Dividers are used for measurements of pulse voltages up to 800 kilovolts. Units for still higher voltages are manufactured to the customer's requirements. The voltage division ratio is factory adjustable.

Stangenes Industries, Inc. 1052 East Meadow Circle, Palo Alto, CA 94303-4271

Phone: 650-493-0814 Fax: 650-855-9926 Email: info@stangenes.com

www.stangenes.com



TDK-Lambda

Turnkey HV Power Solutions

300kW DC power system in 5ft rack!

Features

Voltages to 50kV
Power - 30kW-1MW
Ripple < 0.1%
Low Stored Energy
Power Factor > 0.9
Efficiency > 88%
Water-cooled
Zero oil insulation
Remote/Local control
Scalable design

Applications

Microwave tubes
Accelerators
Amplifiers
Radar systems
Capacitor Charging



Call or email Andy Tydeman to discuss your application
Tel: +1-732-922-5408 or email: andy.tydeman@us.tdk-lambda.com



TDK-Lambda Americas Inc. - High Power Division
405 Essex Road, Neptune, NJ, 07753, USA
Tel: +1-732-922-5300 Fax: +1-732-922-1441

www.us.tdk-lambda.com/hp

Plug in. Turn on. Shine

Contact us for digital signal processors
for nuclear physics, nuclear medicine,
x-ray analysis and synchrotron research,
with optimized algorithms for:

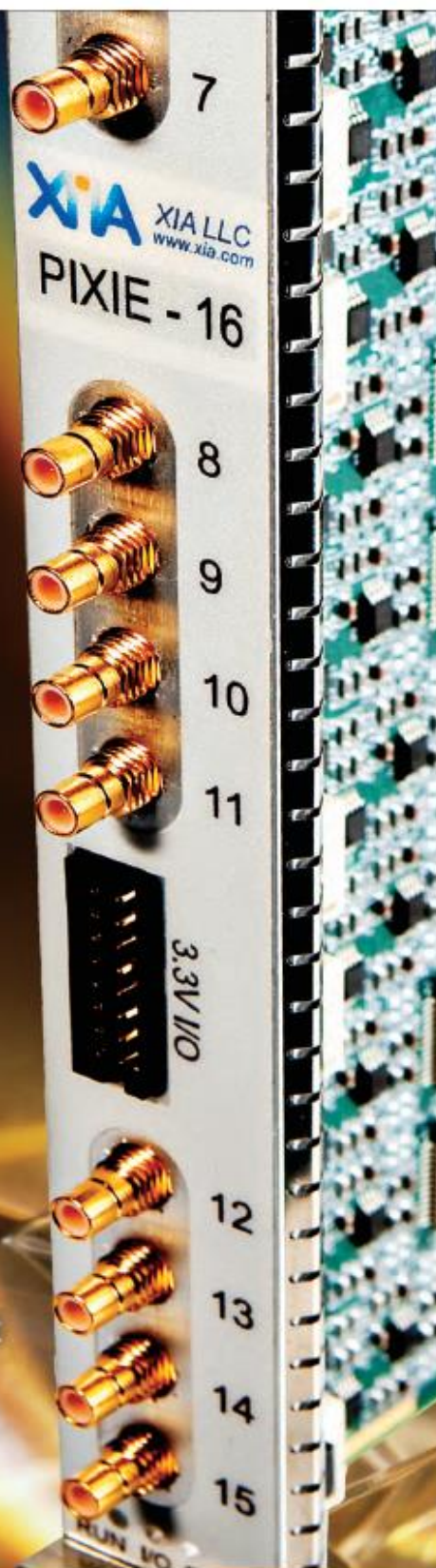
- Single & multi-channel input
- Timing coincidence
- Pulse shape analysis
- High counting rates.

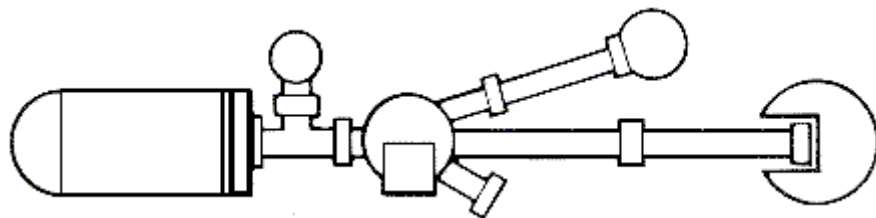


Instruments that Advance the Art

www.XIA.com

sales@XIA.com +1.510.401.5760





GENERAL INFORMATION

General Information

Oral Sessions

As with previous meetings in this conference series, there will be a mixture of plenary, invited talks, contributed talks, invited posters, and regular poster presentations. The Plenary sessions will begin each day on Monday, Tuesday, Thursday, and Friday with two presentations each day. Because of the Conference excursion Wednesday afternoon, there is no Plenary session on Wednesday. The oral presentations each day will be one 120 min. session in the mornings and two 90 min. sessions in the afternoons (except Wed. and Fri. afternoons). There will be a total of 83 oral sessions and 2 poster sessions.

Guidelines for Oral Presenters

- **Very important:** Each presentation **MUST** be in a PowerPoint or PDF file and read from a memory stick or CD. All presentations will be downloaded on the existing computer in the meeting room.
- All memory sticks or CDs **MUST** be given to the Session Chair or the Conference Assistant prior to the session, for downloading at least 15 minutes prior to the start of the session.
- At least 15-20% of your talk time should be reserved for questions and answers. If your talk is 30 minutes, reserve 5 minutes for Q & A; if it's a 20 minute talk, reserve 4 minutes and for a 15 minute talk, reserve 3 minutes.

Poster Sessions

All posters are to be put up on display boards no later than 1:00 PM on Monday. Poster sessions will be held in the early evenings of Monday and Tuesday and authors are welcome to present their posters both of these days. The Student Poster Competition will be held Tuesday evening from 6-7pm, please be available to present your poster at that time. Regular posters are required to be taken down by end of day Wednesday or they will have to be thrown away. Invited posters may be displayed throughout the entire week, in the hallway directly outside of Lone Star Ballroom and to be taken down by Friday. All Poster Sessions will be held in Lone Star Ballroom, alongside the Exhibitors. All posters in each session **MUST** be presented by an author in order to be published in the proceedings. Poster sessions will be held:

* Monday- 5:30 pm to 7:30 pm

* Tuesday- 5:00 pm to 7:00 pm

** Note that the invited posters will be kept up for the remainder of the week

Manuscripts

The Proceedings of CAARI-2014 will be published by Elsevier's Conference Journal Physics Procedia. Physics Procedia (<http://www.journals.elsevier.com/physics-procedia/>) is an e-only and open access journal focusing entirely on publishing conference proceedings in a dedicated online issue on ScienceDirect, which is then made freely available and searchable worldwide. In line with the improvements to the CAARI conference, each paper shall consist of a minimum of 3 pages and a maximum of 10 pages. Each submitted manuscript will now be reviewed by two referees. The Session Chairs, Topic Editors, and Conference Chairs will also be involved in the refereeing process to ensure that only high quality, original research work is included in the CAARI proceedings. Finally, the CAARI Chairs, in consultation with the topic editors, will recommend a small fraction of the reviewed manuscripts in 2014 to NIM-B editors for consideration as standalone publications in NIM-B. This recommendation will be in the form of a cover letter along with reviewers' comments to be sent to NIM-B by the CAARI Organizers. The selected authors will submit their revised manuscripts to NIM-B along with the response letter to CAARI reviewers' comments. The manuscript deadline is Monday, June 30.

Industrial Exhibit Show

The Industrial Exhibit show will run from 8 am to 6 pm Monday through Wednesday, in the Lone Star Ballroom. We have a variety of Exhibitors this year, so please stop by, see their products, and say “thank you” to the representatives for continuing to support the CAARI conference. Without our exhibitors, CAARI would not be able to support our students.

Hotel Internet Connections

The Grand Hyatt offers complementary wireless high-speed internet connection in the lobby area. The Hyatt has provided each sleeping room internet access for up to two devices. There will be limited Wi-Fi available in the meeting spaces located on floors two and three.

Continental Breakfast and Breaks

Each morning of the conference, continental breakfast will be served in the Lone Star Ballroom. Morning and afternoon breaks will be served each day as appropriate for the day’s events.

Lunch and Dinner

All lunches and dinners are on your own, except for the banquet on Thursday, which is included in your registration fee. We have information at the information booth regarding local restaurants and attractions.

Social Events

Welcome Reception

A Welcome Reception will be held Sunday, May 25th, from 6:00 pm to 8:00 pm in the Lone Star Ballroom.

Conference Assistant Briefing

The conference assistant briefing will be held on Sunday evening @ 8:00 pm next to the registration booth (directly following the welcome reception). Please make sure to attend this meeting in order to receive important instructions and assignments for the conference.

Companion Outing

All registered companions are invited to attend a customized guided tour of the Historic King William District. Those who wish to attend may meet in the hotel lobby on May 27 at 8:30 and will return at 10:30. This outing is included in your registration fee.

Conference Excursions

For those participants who opted to register for an excursion on Wednesday, please meet in the hotel lobby at the sign designating the name of your tour. The excursion tours will depart from the hotel lobby at 12:30 or 1:00 pm (please check at registration) and return at 5:00 pm.

Conference Student Appreciation Event

The student appreciation event for students 18 and over will be held on Wednesday, May 28 at 6:00 pm at Pat O'Brien's on the Famous San Antonio Riverwalk.

Topic Editors Dinner Meeting

Topic Editors will meet with the Conference Co-Chairs on Monday, May 26 at 7:30 in Bowie A located on the 2nd floor, to discuss refereeing and publication of manuscripts.

Topic Editors and Session Chairs Meeting

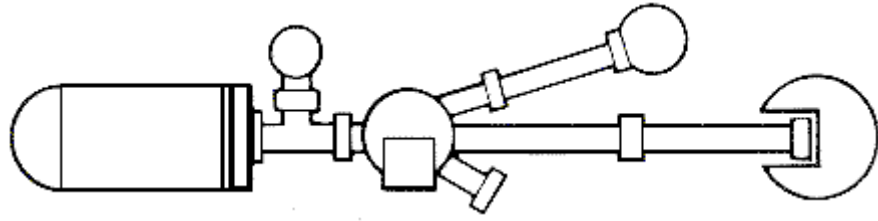
Topic Editors and Session Chairs will meet with the Conference Co-Chairs and their companions Tuesday, May 27 from 7:00 to 8:00 pm. This meeting is to review the conference setup, sessions, paper submissions and to discuss improvements to CAARI 2016. If you have any suggestions for the next CAARI Conference, please submit them to the information desk prior to this meeting.

Conference Banquet

The conference banquet will be held on Thursday, May 29th at 7:00 pm in the Texas Ballroom on the 4th floor. Entertainment will be provided.

Closing Ceremony

All participants and accompanying persons are cordially invited to attend the closing ceremony. It will be held on Friday, May 30, in the Bowie Prefunction area, located on the 2nd floor at 12:00 pm.



CONFERENCE PROGRAM SCHEDULE

Teaching with Accelerators Series: Vacuum Class

Introduction: Vacuum is a key enabling condition for many types of scientific inquiry and experimentation, and is a critical component to any accelerator systems. CAARI-2014 is pleased to offer a complimentary vacuum class to our attendees as a part of our efforts to enhance Teaching with Accelerators topic area. Topics will include an introduction to high vacuum and ultra-high vacuum, gas behavior at low pressure, the elements of system pressure and total gas load, materials selection, pumping technologies from primary vacuum to UHV, pressure measurement gauges, and system operation. The vacuum class is excerpted from Agilent's one-day UHV Seminar and is intended to provide an introduction to ultra-high vacuum systems and practice for scientists, engineers, technicians, and students. The class is divided into two 90 min. seminars, designated as TA03 and TA04 sessions under the topic area of Teaching with Accelerators in the conference program. Attendees will receive a copy of Agilent's seminar handbook, "High and Ultra-High Vacuum for Science Research", 2011, 133 pages.

Instructor: Walt van Hemert, Senior Trainer, Vacuum Products Division, Agilent Technologies

TA03: Vacuum seminar – Part I: Physics of Vacuum Tuesday, May 27, 3:30 – 5:00 pm Presido A

Introduction to high vacuum and ultra-high vacuum, gas behavior at low pressure, the elements of system pressure and total gas load, and materials selection for vacuum system.

TA04: Vacuum Seminar – Part II: Pumps and Gauges Wednesday, May 28, 8:00 – 9:30 am Presido A

Pumping technologies from primary vacuum to UHV, pressure measurement gauges, and integrated vacuum system operation.

Welcome to CAARI 2014

8:00 AM

Yongqiang Wang
Director
Ion Beam Materials Laboratory
Los Alamos National Laboratory

Gary A. Glass
Professor of Physics and Co-Director
Ion Beam Modification and Analysis Laboratory
University of North Texas

F. Del McDaniel
Professor of Physics and Co-Director
Ion Beam Modification and Analysis Laboratory
University of North Texas

Barney L. Doyle
Distinguished Member of the Technical Staff
Radiation Solid Interactions Department
Sandia National Laboratories

Guest Speakers

8:10 AM

David Schultz, Ph.D.
Professor of Physics
Associate Vice President for Research and Economic Development
University of North Texas

8:20 AM

John Sarrao
Associate Director for Theory, Simulation and Computation
Los Alamos National Laboratory

CAARI 2014 Program Schedule

May 25 - 30, 2014

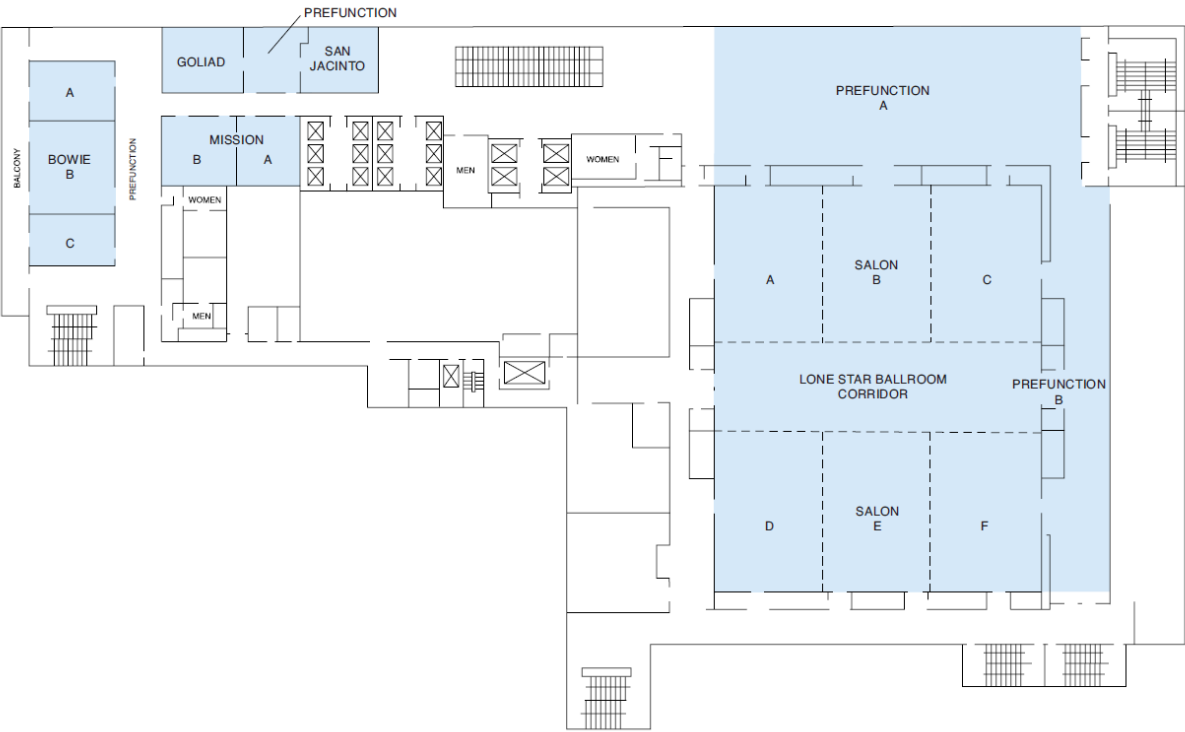
Sun. 12 - 5 PM Registration Open
6 - 8 PM Welcome Reception - Salon Rooms

		2nd Floor				3rd Floor				Legend	
		Lone Star Ballroom	Presidio A	Presidio B	Presidio C	Travis A/B	Travis C/D	Bonham B	Bonham C	Bonham D	
Monday, 5/26	8:00 AM	Opening Ceremony									AMP - Atomic & Molecular Physics
	8:30 AM	PS01									
	10:00 AM		ATF01	IBA06	RE05	HSD01	NP01	MA03	IBM01	NST03	ATF - Accelerator Technology & Facilities
	10:30 AM										
	12:30 PM		ATF02			HSD03	NP10	MA01	IBM04	NST05	HSD - Homeland Security & Defense
	2:00 PM										IBA - Ion Beam Analysis
Tuesday, 5/27	3:30 PM										IBM - Ion Beam Modifications
	4:00 PM			IBA08	RE02	HSD02	NP02	MA02		NST06	
	5:30 PM				Poster Social 1 - Salon Rooms (2nd Floor)						MA - Medical Applications
	8:00 AM	PS02									NBA - Nuclear Based Analysis
	9:30 AM		ATF05	IBA03	RE04		NP03	MA04	IBM02	NST01	NP - Nuclear Physics
	10:00 AM										NST - NanoScience & Technology
Wednesday, 5/28	12:00 PM		ATF03	IBA05	RE03	AMP01	NP04	MA06		NST07	PS - Plenary Sessions
	1:30 PM										RE - Radiation Effects
	3:00 PM		TA03	IBA09		AMP03	NP05	MA07		NST08	TA - Teaching with Accelerators
	3:30 PM				Poster Social 2 - Salon Rooms (2nd Floor)						
	5:00 PM										
	8:00 AM		TA04	IBA02	AMP02	HSD07	NP11	MA08			
Thursday, 5/29	9:30 AM		ATF04	IBA01	RE06	HSD04	NP07	NBA02	IBM05	NST09	
	9:45 AM										
	11:45 PM										
	1:00 PM				Excursions						
	8:00 AM	Lone Star Ballroom	Bowie A	Bowie B	Bowie C	Travis A/B	Travis C/D	Bonham B	Bonham C	Bonham D	
	9:30 AM	PS03									
Friday, 5/30	10:00 AM		ATF06	IBA07	RE08	HSD06	NP08	NBA03	IBM03	NST04	
	12:00 PM		ATF07		RE01		NP06	TA01	IBM07	NST02	
	1:30 PM										
	3:00 PM		ATF08	IBA04	RE07	AMP05		NBA04		TA02	
	3:30 PM										
	5:00 PM				Banquet - Texas Ballroom (4th Floor)						
Saturday, 5/31	7:00 PM										
	8:30 AM		PS04								
	9:30 AM										
	10:00 AM		AMP04	NP09	RE09			NBA01	IBM06		
	12:00 PM										
	1:00 PM				Closing Remarks - Held in Bowie Prefunction Area on 2nd Floor						

Floor Plan of Grand Hyatt Second Level

(Bowie, Mission, Goliad, San Jacinto, and Prefunction rooms, Lone Star Ballroom)

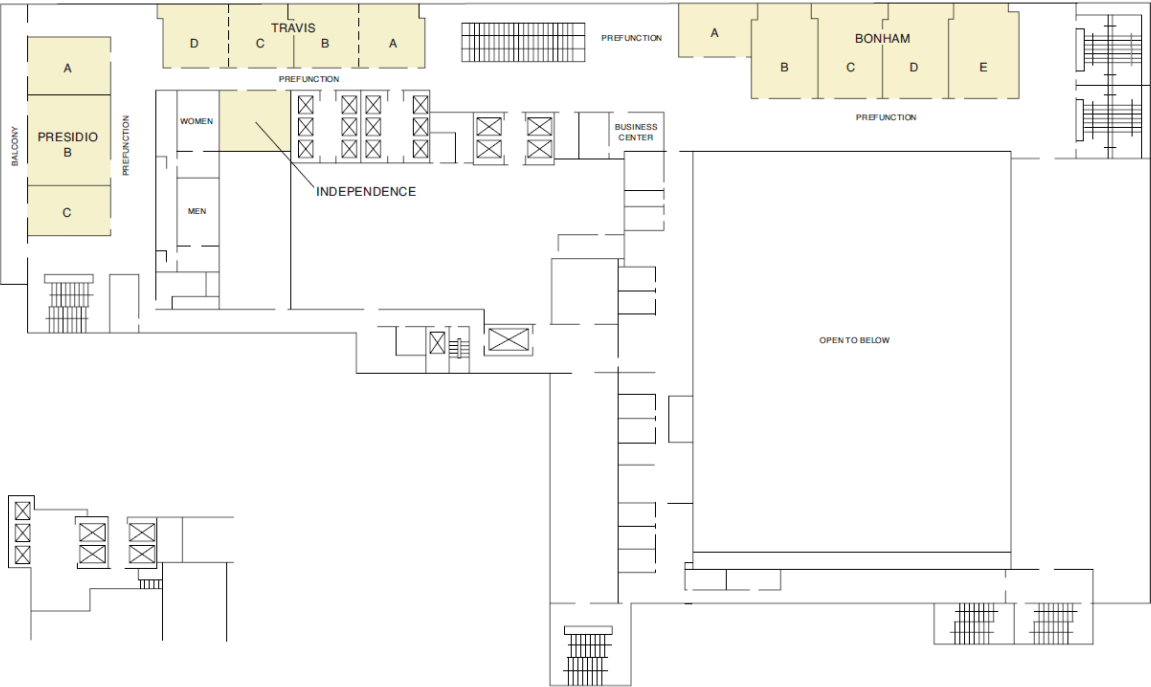
SECOND LEVEL



Floor Plan of Grand Hyatt Third Level

(Bonham, Presidio, Travis, and Independence rooms)

THIRD LEVEL



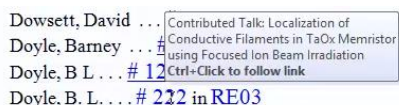
Using this Abstract Book

This Abstract Book contains the same front pages that are in the hardcopy Program plus new interactive:

1. the [session summary](#),
2. full text of accepted [abstracts](#), and
3. the [index of authors](#) and co-authors.

The Abstract Book can be downloaded from the conference website at <http://www.caari.com> and is available in several formats. All formats feature mutual hypertext links between the schedule, abstracts, and the author index.

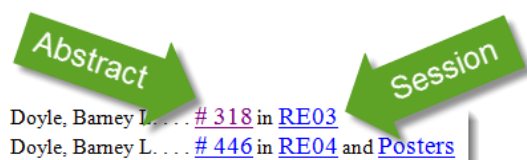
- Notebook, ultrabook, or desktop users: the Microsoft Word version offers popup hints. To see them hover the mouse over the hyperlink. Alternatively, a PDF version is also available.



- Users of small mobile devices (tablets or smartphones): While you can certainly use the Word and PDF versions above if your device supports them, we have re-flown the Abstract Book to about 4-inch width and 6-inch width so that if you are viewing the book on a small device you do not need to shift the screen horizontally (with some exceptions). Mobile version of the Adobe Reader can be downloaded, for example, from Google Play for Android, Windows Phone Store, etc.

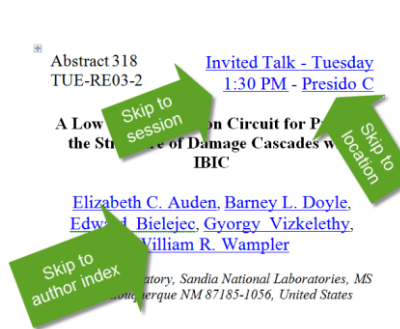
Based on the type of program you chose to read this book, you will be able to search for keywords in the abstracts that relate to your areas of interest or add your own notes or bookmarks.

This listing contains information about each presentation including all of the authors and their affiliations. If you wish to find out, for example, when Barney Doyle's talk is to be given, just look up his name in the [author index](#) at the end of this book:



Then click on the abstract number to read the full abstract or the session code to view other presentations in the same session.

When you are viewing the abstract click on the author's name to skip to the author index again or click on the session time and location to see all other presentations in this session.



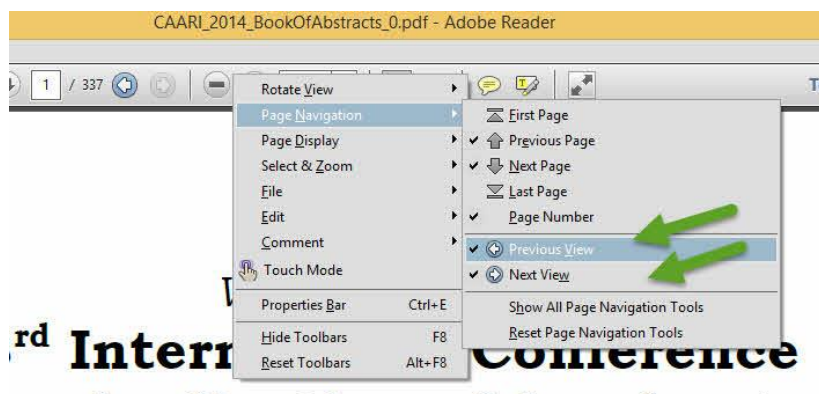
The abstract details include the abstract number: 318
The type of presentation: Invited Talk
The day and time Session RE03 starts: Tuesday 1:30 PM
The location: Presidio C

Going Back or Forward

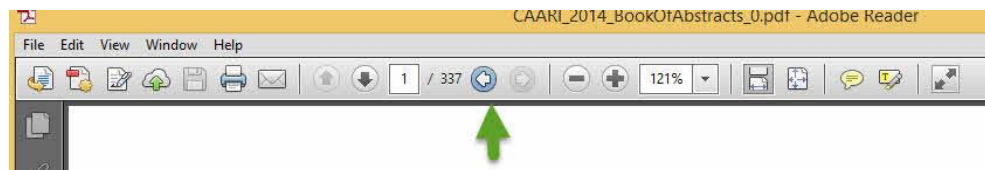
If you wish to skip back or forward you can use Alt + Left Arrow or Alt + Right Arrow in both MS Word and Adobe Reader. You can also add "back" and "forward" buttons to the tool bar in both MS Word and Adobe Reader: in Word right-click the toolbar, select Customize Quick Access Toolbar, select All commands, scroll down to the Back button, and click Add>>. Similar process for Adobe Reader is explained below.

Tip for Adobe Reader XI users

Adobe provides "back" and "forward" button capability within the PDF reader similar to that found in web browsers. If the "back" & "forward" buttons are not visible please right-click the toolbar and select "Page navigation" and then check the Previous view and Next view options.



The "back" and "forward" buttons will then appear on the tool bar.



Hypertext structure of this Abstract Book was facilitated by Meeting247 tools

Session Summary

PS01: Plenary Session - Monday

Monday at 8:30 AM in [Lone Star Ballroom](#)

[# 350](#) Thorium Based Energy Production Using Accelerators *by Robert Cywinski*

[# 314](#) LAST IMPROVEMENTS ON AGLAE FACILITY AND THEIR APPLICATION TO THE ANALYSIS OF CULTURAL HERITAGE ARTEFACTS *by Claire PACHECO*

ATF01: Accelerator Technology for Energy

Monday at 10:30 AM in [Presidio A](#)

[# 62](#) The MYRRHA ADS project in Belgium enters the Front End Engineering Phase *by Didier J De Bruyn*

[# 304](#) Fixed field ring methods for high power beams *by Francois G Meot*

[# 360](#) Experimental Subcritical Facility Driven by D-D/D-T Neutron Generator at BARC, India *by Amar Sinha*

[# 194](#) A Strong Focusing Cyclotron capable of producing 10 mA of proton beam up to 800 MeV and its applications. *by Nathaniel Pogue*

[# 23](#) A Fast Spectrum Neutron Source for Material Irradiation Using a Superconducting Electron Linac *by Valeriia N Starovoitova*

[# 460](#) Compact CW Racetrack FFAG for High-intensity Applications *by Carol Joanne Johnstone*

HSD01: Container Security - Part I

Monday at 10:30 AM in [Travis A/B](#)

[# 108](#) Domestic Nuclear Detection Office's Approach to Detect Concealed Threats *by Joel Rynes*

[# 486](#) Photofission based interrogation techniques for nuclear materials *by Tsahi Gozani*

[# 82](#) Non-intrusive Inspection Using CW Photon Beams *by Cody M. Wilson*

[# 166](#) Mixed source interrogation of steel shielded special nuclear material using an intense pulsed source *by Cassie E Hill*

[# 30](#) A light transportable neutron based inspection system for nuclear material and other contraband *by Michael J King*

IBA06: Chemical and Molecular Speciation and Imaging

Monday at 10:30 AM in [Presidio B](#)

[# 155](#) Elemental, Chemical & Molecular Speciation Using MeV Ion Beams: What, How and Why? *by Roger P Webb*

[# 436](#) Imaging and Analysis of Fixed Charge Density in the Brain using PIXE and Fe(III)-Ions as a Probe *by Tilo Reinert*

[# 256](#) SIMS Analysis of Biological Material in 1-, 2- and 3 Dimensions *by Alex Henderson*

[# 300](#) MeV-SIMS: A new chemical imaging technique for organic materials *by Jiro Matsuo*

[# 348](#) Pharmaceutical and biomedical application possibilities of ambient pressure MeV-SIMS *by Julien Demarche*

[# 106](#) Molecular imaging of organic samples using MeV SIMS setup at the heavy ion microprobe in Zagreb *by Ivancica Bogdanovic Radovic*

IBM01: Ion Implantation - New Directions

Monday at 10:30 AM in [Bonham C](#)

[# 255](#) In-situ characterization by RBS/C of damage evolution and thermal recovery on irradiated 3C-SiC *by Haizhou Xue*

[# 388](#) Synthesis of silver nanoparticles in MgO and YSZ using low energy ion implantation *by A. Dissanayake*

[# 425](#) Possible interface superconductivity with coherent quantum CDW transport and soliton condensation phase transition in heterogeneously doped ion implanted NbSe₃ single crystals *by kalyan sasmal*

[# 246](#) Electroluminescence of NV centers in diamond induced by ion-beam micro-fabricated graphitic electrodes *by Jacopo Forneris*

[# 219](#) High Energy (MeV) Ion Beam Implantation in INT-WS₂ *by Mihai Straticiuc*

[# 454](#) Low Energy Ar⁺ Ion Irradiation Induced Surface Modification in Cadmium Zinc Telluride (CdZnTe) *by Jitendra Kumar Tripathi*

[# 392](#) XPS Characterization of β -FeSi₂ formed in Si (100) by high fluence implantation of 50 keV Fe ion and post-thermal vacuum annealing *by Wickramaarachchige Jayampath Lakshantha*

MA03: Accelerator Production of Medically Relevant Isotopes

Monday at 10:30 AM in [Bonham B](#)

[# 305](#) Medical isotope production using high intensity accelerator neutrons *by Yasuki Nagai*

[# 153](#) Direct Production of ^{99m}Tc via ¹⁰⁰Mo(p,2n) on Small Medical Cyclotrons *by Peter A Zavodszky*

[# 282](#) Progress Related to Domestic Production of Mo-99: Accelerator Induced Fission in LEU Solution. *by Sergey Chemerisov*

[# 43](#) Design and Thermal-Hydraulic Performance of a Helium Cooled Target for the Production of Medical Isotope ^{99m}Tc *by Keith Woloshun*

[# 321](#) Converter and Target Optimization for the Photonuclear Production of Radioisotopes Using Electron Linear Accelerators *by Bindu KC*

[# 337](#) The Potential of a Compact Accelerator for Low Energy Production of Copper Isotopes *by Robert Cywinski*

NP01: New Facilities and Initiatives I

Monday at 10:30 AM in [Travis C/D](#)

[# 308](#) The IAEA new Accelerator Knowledge Portal *by Aliz Simon*

[# 239](#) Proposal for New World Laboratory: XFEL for protein spectroscopy, Higgs Factory for a million Higgs decays, 100 TeV Hadron Collider for supersymmetry *by Peter McIntyre*

[# 346](#) Experimental nuclear astrophysics research using stable beams at small scale accelerators *by Gabor gyula Kiss*

[# 402](#) The TIGRESS Integrated Plunger Device and In-Beam Gamma-Ray Spectroscopy at TRIUMF *by Philip J. Voss*

[# 141](#) ROSPHERE - a dedicated in-beam fast timing HPGe-LaBr₃(Ce) array *by Nicolae Marginean*

NST03: Graphene, Carbon Nanotubes and Composites

Monday at 10:30 AM in [Bonham D](#)

[# 383](#) Radiation effects on nano mechanics of low dimensional carbon systems *by Joseph Wallace*

[# 190](#) An ion-beam-based technique to characterize thermal property changes of irradiated carbon nanotubes *by Di Chen*

[# 197](#) Irradiation induced thermal property changes of carbon nanotubes *by Jing Wang*

[# 264](#) Laser induced periodic surface structures in nickel-fullerene hybrid composites *by Jiri Vacik*

RE05: Radiation Effects in Complex Structures and Materials

Monday at 10:30 AM in [Presidio C](#)

[# 443](#) Atomic Structure and Radiation Effects in Complex Oxides *by Kurt Edward Sickafus*

[# 122](#) Ion radiation damage in Sr₂Fe_{1.5}Mo_{0.5}O_{6-δ} Perovskite *by Ming Tang*

[# 406](#) Micro-bumps on the surface of borosilicate glasses induced by ion irradiation *by Tieshan wang*

[# 451](#) Ion beams studies of the radiation chemistry and radiation damage of materials important in nuclear power. *by Andrew D Smith*

[# 428](#) Defect Analysis of Heavy Ion-Irradiation of Polyethylene and Composites with Martian Regolith *by Naidu V. Seetala*

ATF02: Accelerators for Isotope Production

Monday at 2:00 PM in [Presidio A](#)

- [# 143](#) Accelerator-Driven Subcritical Assembly for the Production of Molybdenum-99 *by Evan Sengbusch*
[# 476](#) Development of a Visualization System for Charged Particles Shapes Superimposed on the Waveform of the Cyclotron Frequency *by Faisal M Alrumayan*
[# 24](#) Production of Medical and Industrial Isotopes Using a Superconducting Electron Linac *by Valeriia N Starovoitova*
[# 280](#) Accelerator Based Domestic Production of Mo-99: Photonuclear Approach *by Sergey Chemerisov*

HSD03: Long Standoff Detection

Monday at 2:00 PM in [Travis A/B](#)

- [# 329](#) An Overview of Active Interrogation *by James D Silk*
[# 146](#) APPLICATION OF INTENSE, SINGLE-PULSE BREMSSTRAHLUNG TO THE PROBLEM OF FINDING FISSILE MATERIAL* *by R. J. Commisso*
[# 243](#) Narrowband and tunable all-laser-driven inverse-Compton x-ray source *by Sudeep Banerjee*
[# 364](#) Advanced Low-Beta Cavity Development for Proton and Ion Accelerators *by Zachary A Conway*
[# 404](#) A Novel Compact Accelerator for Proton Interrogation *by Carol Johnstone*

IBM04: New Challenges in SIMS

Monday at 2:00 PM in [Bonham C](#)

- [# 98](#) Probing Environmental and Energy Liquid Surfaces and Interfaces Using Time-of-Flight Secondary Ion Mass Spectrometry *by Xiao-Ying Yu*
[# 88](#) Possibilities and Limitations of MeV-SIMS for Biological Applications *by Makiko FUJII*
[# 158](#) AP-MeV-SIMS at Surrey - a new ambient pressure SIMS system for molecular concentration mapping. *by Roger P Webb*
[# 165](#) Ambient Pressure MeV-SIMS analysis of contaminated PTFE aerosol filters. *by Julien Demarche*
[# 162](#) Modeling the Transport of Secondary Ion Fragments Into a Mass Spectrometer Through Ambient Pressure Using COMSOL Multiphysics Simulation Software. *by John-William Warmenhoven*

MA01: Particle Beam Radiobiology

Monday at 2:00 PM in [Bonham B](#)

- [# 467](#) Current advances in the biological optimization of proton treatment plans *by Alejandro Carabe*
[# 461](#) High-throughput Mapping of Proton Biologic Effect *by Lawrence Bronk*
[# 492](#) Radiobiological Modeling of High-Throughput Proton Irradiation Cell Survival Experiments *by Christopher Peeler*
[# 456](#) Predicted Risks of Second Cancers after Carbon-Ion Therapy versus Proton Therapy *by John G Eley*
[# 484](#) Tumor-targeting gold nanoparticles as engineered radiosensitizers for proton therapy: In Vivo Study at the SOBP and Beam Entrance *by Tatiana Wolfe*

NP10: New Facilities and Initiatives II

Monday at 2:00 PM in [Travis C/D](#)

- [# 353](#) Multi-Reflection Time-of-Flight Mass Spectrograph for Precision Mass Measurements of Short-Lived Nuclei and More *by Peter Schury*
[# 401](#) Search for ^{283,284,285}Fl decay chains* *by N. T. Brewer*
[# 339](#) New opportunities in decay spectroscopy with the GRIFFIN and DESCANT arrays *by Vinzenz Bildstein*
[# 187](#) Development of Fast, Segmented Trigger Detector for Decay Studies *by M. F. Alshudifat*
[# 385](#) Alpha- and proton-decay studies in the vicinity of 100Sn. *by Karolina Kolos*

NST05: Bio-Materials and Bio-Medical Applications - Part I

Monday at 2:00 PM in [Bonham D](#)

- [# 91](#) Cell Adhesion and Growth on Modified Surfaces by Plasma and Ion Implantation *by Maria Cecilia Salvadori*

[# 229](#) APPLICATIONS OF ELECTRON-BEAM IRRADIATION FOR THE PREPARATION OF NOVEL BIOMATERIALS - A REVIEW *by Esperidiana A. B. Moura*

[# 288](#) Ion Beam Analysis of Materials Used in Hermetic Single-Device Human Implants integrating Bio-sensors with Medical Electronics *by Mark W. Mangus, Jr.*

HSD02: Container Security - Part II

Monday at 4:00 PM in [Travis A/B](#)

[# 447](#) High Duty Factor Compact Linear Accelerator Systems *by Sami G Tantawi*

[# 147](#) ARCIS: Adaptive Rail Cargo Inspection System *by Anatoli Arodzero*

[# 148](#) Intra-Pulse Multi-Energy Method for Material Discrimination in X-ray Cargo and Container Inspection *by Aleksandr Saverskiy*

[# 85](#) Air Cargo Mobile Scanner Based on Associated Particle Imaging *by Vladimir G Solovyev*

[# 212](#) New Accelerator Design for Homeland Security X-Ray Applications *by Willem GJ Langeveld*

IBA08: IBA for Cultural Heritage Applications & Environment

Monday at 4:00 PM in [Presidio B](#)

[# 237](#) Accelerator based techniques at CEDAD for cultural heritage studies *by Lucio Calcagnile*

[# 234](#) High-throughput PIXE analysis of aerosol samples *by Giulia Calzolari*

[# 103](#) Characterization of pottery production of Tyre historical site using PIXE technique and cluster analysis *by Mohamad Roumie*

MA02: Evolving Accelerator Concepts for Medical Applications

Monday at 4:00 PM in [Bonham B](#)

[# 334](#) An Overview of Proton Accelerators for Cancer Therapy *by George Coutrakon*

[# 405](#) Overview of Carbon-ion Accelerators for a US-based National Center for Particle Beam Radiation Therapy Research *by Carol Johnstone*

[# 301](#) Multiple-room, continuous beam delivery hadrontherapy installation *by Francois G Meot*

[# 25](#) A High Intensity 10 MeV X-ray Generator to Eliminate High Activity Sources Used for Sterilization *by Terry L Grimm*

NP02: Nuclear Fission

Monday at 4:00 PM in [Travis C/D](#)

[# 170](#) The LANSCE Nuclear Fission Research Program *by Rhiannon Meharchand*

[# 324](#) The University of New Mexico fission fragment spectrometer, with preliminary results from LANSCE *by Adam Hecht*

[# 198](#) Recent studies of fission fragment properties at LANSCE *by K. Meierbachtol*

[# 377](#) Average Total Kinetic Energy Measurements of Neutron Induced Fission for ^{235}U , ^{238}U , and ^{239}Pu *by Dana L Duke*

[# 231](#) Relativistic mass of secondary neutrons in fission and fragments in fusion. *by AJAY SHARMA*

NST06: Bio-Materials and Bio-Medical Applications - Part II

Monday at 4:00 PM in [Bonham D](#)

[# 381](#) Improving AMS Detection of the Biomedical Radiotracer ^{41}Ca with Segmented Radio-Frequency Quadrupoles *by Jean-Francois Alary*

[# 89](#) Lipid Compounds Analysis with Argon Gas Cluster Ion Beam Irradiation *by Makiko FUJII*

[# 182](#) Quantitative analysis of iron (Fe) uptake by corn roots using micro-PIXE *by Stephen Juma Mulware*

RE02: Radiation Effects in Metals Using Ion Accelerators

Monday at 4:00 PM in [Presidio C](#)

[# 131](#) Small-Scale Thermal and Mechanical Characterization of Ion Irradiated Structural Metals *by Khalid Hattar*

- [# 325](#) What have we learned about swelling resistance and dispersoid stability in ODS variants of ferritic-martensitic alloys using self-ion bombardment? *by Frank A. Garner*
- [# 269](#) Accessing Defect Dynamics using Intense, Nanosecond Pulsed Ion Beams *by Arun Persaud*
- [# 252](#) The Effects of Simultaneous Molten Salt Corrosion and Radiation Damage Simulated via Ion Beam Irradiation *by Elizabeth S Sooby*
- [# 233](#) Vacancy defects induced in Tungsten by 20 MeV W ions irradiation: Effect of fluence and temperature irradiation *by Marie-France Barthe*

PS02: Plenary Session - Tuesday

Tuesday at 8:00 AM in [Lone Star Ballroom](#)

- [# 482](#) Charged-Particle Therapy Takes Center Stage *by Eugen B. Hug*
- [# 485](#) Facility for Antiproton and Ion Physics *by Thomas Stohlker*

ATF05: Emerging Accelerator Technologies

Tuesday at 10:00 AM in [Presidio A](#)

- [# 283](#) Laser Plasma Accelerators as Driver of Future Light Sources *by Jeroen van Tilborg*
- [# 220](#) Ultrafast electron bunches from a laser-wakefield accelerator at kHz repetition rate *by Alexander G R Thomas*
- [# 3](#) Status of plasma spectroscopy method for CNS Hyper-ECR ion source at RIKEN *by Hideshi MUTO*
- [# 53](#) Magnetic Control of a Neutralized Ion Beam *by Ryan E. Phillips*
- [# 80](#) Space-Charge Compressed Ion Beam Equilibrium *by Carlos A. Ordonez*
- [# 438](#) Rapid High Dynamic Range Dose Profiling at the University of Maryland Radiation Facility's E-Beam. *by Timothy W Koeth*
- [# 129](#) Broadband source of coherent THz radiation based on compact LINAC. *by Ivan V. Konoplev*

IBA03: IBA of Technologically Important Oxides and Nitrides

Tuesday at 10:00 AM in [Presidio B](#)

- [# 83](#) Comparison of Radiation Damage by Light- and Heavy-Ion Bombardment in Single-Crystal LiNbO₃ *by Hsu-Cheng Huang*
- [# 272](#) In-situ study of damage evolution in SrTiO₃ and MgO using ion beam-induced luminescence *by Miguel L. Crespillo*
- [# 149](#) The New Applications of Rutherford Backscattering Spectrometry/Channeling *by Shude Yao*
- [# 295](#) Effect of transition metal ion implantation on photocatalysis and hydrophilicity of MOD deposited TiO₂, V₂O₅ and mixed oxide films *by Karur R Padmanabhan*
- [# 430](#) The Role of Oxygen Vacancies in Conductivity of SrCrO₃- Films *by Amila Dissanayake*

IBM02: Swift Heavy ion modification of Materials - Nanostructuring

Tuesday at 10:00 AM in [Bonham C](#)

- [# 72](#) Nano-scale Materials *by Leonard C Feldman*
- [# 42](#) Radiation defects in nanoscale: the case of compound materials *by Andrzej Turos*
- [# 14](#) Ion beam induced effects on nanocrystals, alloys and high-k dielectric films *by Srinivasa Rao Nelamarri*
- [# 9](#) An On-line ERDA Study on SHI Induced Desorption of Hydrogen from Porous Silicon Prepared by Anodic Etching of H-implanted Silicon *by V S Vendamani*
- [# 15](#) Swift Heavy Ion induced intermixing effects in HfO₂ based MOS devices *by N. Manikanthababu*
- [# 232](#) Ion irradiation effects on WN_xO_y films *by Noriaki Matsunami*
- [# 64](#) Effect of Swift Heavy Ion Irradiation on Dielectric, Thermal and Structural Properties of Metal/Polymer Composites *by Nand Lal Singh*

MA04: Developments in Target Delineation, Beam Scanning and Dose Delivery

Tuesday at 10:00 AM in [Bonham B](#)

- [# 427](#) Status Update and New Developments in Planning, Verification, and Active Delivery of Particle Beam Therapy *by Reinhard W Schulte*
- [# 466](#) New developments in Monte Carlo based treatment planning for proton therapy *by Bruce A Faddegon*
- [# 469](#) 4D-optimized beam tracking for treatment of moving targets with scanned ion-beam therapy *by John G Eley*
- [# 475](#) Proton therapy using pencil beam spot scanning technology *by Jay Steele*
- [# 109](#) Uncoupled and Achromatic Gantry for Medical Applications *by Nicholaos Tsoupas*
- [# 95](#) Progress in the development of the proton Computed Tomography (pCT) Phase-II scanner at NIU. *by Sergey A Uzunyan*

NP03: Reactions on Unstable Nuclei

Tuesday at 10:00 AM in [Travis C/D](#)

- [# 11](#) Recent Measurements at HELIOS *by Calem R Hoffman*
- [# 134](#) Recent advances with ANASEN at the RESOLUT radioactive beam facility *by Ingo Wiedenhoever*
- [# 13](#) Reaction measurements with SuN *by Artemis Spyrou*
- [# 258](#) Intermediate-energy Coulomb excitation of neutron-rich chromium isotopes *by T. Baugher*
- [# 247](#) Neutron Knockout on Beams of $^{108,106}\text{Sn}$ and ^{106}Cd *by Giordano Cerizza*

NST01: Nanoscale Fabrication and Patterning - Part I

Tuesday at 10:00 AM in [Bonham D](#)

- [# 26](#) Ion Beam Assisted Enhanced Thermoelectric Properties (with Figure of Merit above 2.0) *by Daryush ILA*
- [# 270](#) Ion beam engineered nano metallic substrates for surface enhanced Raman spectroscopy *by Dharshana Nayanajith Wijesundera*
- [# 221](#) Hybrid inorganic-organic composite materials for radiation detection *by Sunil K Sahi*
- [# 7](#) Nano-crystal Formation and Growth from High Fluence Ion Implantation of Au, Ag, or Cu in Silica or MgO *by Daryush ILA*
- [# 285](#) Thermoelectric and Optical Properties of $\text{SiO}_2/\text{SiO}_2+\text{Au}$ Multilayer Thin Films Affected by Thermal Annealing *by S. Budak*
- [# 150](#) Pair Distribution Function Analysis of nanocrystalline ZnS and CdS *by Sunil D Deshpande*

RE04: Radiation Effects in Electronics - Part II

Tuesday at 10:00 AM in [Presidio C](#)

- [# 302](#) Interactions with Neutron Radiation in High-Performance Computing *by Heather Marie Quinn*
- [# 242](#) The Vanderbilt Pelletron - Radiation Effects on Electronics and Materials Characterization *by Michael W. McCurdy*
- [# 133](#) Efficient Reliability Testing of Emerging Memory Technologies Using Multiple Radiation Sources *by William Geoff Bennett*
- [# 225](#) Use of Alpha Particle and Ion Accelerators for Characterization of Soft-Error Reliability in Advanced ICs *by Rachel C Quinn*
- [# 446](#) Degredation of GaAs Photovoltaics Exposed to Reactor Neutrons and Accelerator Ions *by Barney L. Doyle*

AMP01: Atomic and Molecular Physics with keV Ion Beams

Tuesday at 1:30 PM in [Travis A/B](#)

- [# 114](#) XUV photofragmentation of small water cluster ions *by Henrik B. Pedersen*
- [# 316](#) Fast ion beam studies of Intense laser interactions with molecular anions *by Daniel Strasser*
- [# 279](#) Merged beams studies for astrobiology. *by Kenneth Andrew Miller*
- [# 289](#) Development of a high resolution Analyzing Magnet System for heavy molecular ions *by Mohamed O A El Ghazaly*
- [# 47](#) Line ratios of soft X-ray emissions following charge exchange between C^{6+} and Kr *by T. J. J. Lamberton*

[# 178](#) Process Identification and Relative Cross Sections for Low-keV Proton Collisions in N₂ and CO₂ Molecules *by López Patiño Juan*

ATF03: Applications of of SC Linac and SRF Technology

Tuesday at 1:30 PM in [Presidio A](#)

[# 70](#) Superconducting RF Accelerators for Commercial Applications *by Chase H. Boulware*

[# 96](#) SRF DIPOLES FOR DEFLECTING AND CRABBING APPLICATIONS *by Alejandro Castilla*

[# 331](#) Advanced Materials Manufacturing with Superconducting Electron Accelerators *by Justin Joseph Hill*

[# 230](#) Compact Free Electron Lasers Driven By Superconducting Linacs *by W. B Colson*

IBA05: Applications of Nuclear Scattering and Reaction Analysis

Tuesday at 1:30 PM in [Presidio B](#)

[# 330](#) Implantation and analysis of helium by NRA and HI-ERDA at the JANNUS-Saclay laboratory *by Lucile BECK*

[# 275](#) Identifying the Dominant Interstitial Complex in GaAsN Alloys *by Timothy Jen*

[# 271](#) Microbeam contrast imaging analysis of gas-solid interface and NO adsorption studies on Rh(111) surface. *by Karur R Padmanabhan*

[# 407](#) Nuclear reaction analysis of deuterium in ion irradiated and plasma exposed tungsten *by Yongqiang Wang*

MA06: Clinical Progress with Proton Therapy

Tuesday at 1:30 PM in [Bonham B](#)

[# 116](#) The Current Status of Proton Therapy in the Cooperative Group Multi-institutional Clinical Trials Setting *by David S Followill*

[# 465](#) Prospective Clinical Trials of Proton and Photon Radiation for Non-Small Cell Lung Cancer *by Zhongxing Liao*

[# 478](#) Pediatric Proton Therapy - an Update *by Anita Mahajan*

[# 424](#) The ANDANTE Project: A Multidisciplinary Approach to Estimate the Risk of Neutrons in Pediatric Proton Patients *by Reinhard Schulte*

[# 473](#) Summary of Ongoing Clinical Protocols for Proton and Heavier-Ion Therapy *by Richard P Levy*

NP04: Reactor Neutrinos

Tuesday at 1:30 PM in [Travis C/D](#)

[# 448](#) Precision Neutrino Physics with Reactor Antineutrinos *by Karsten M Heeger*

[# 415](#) PROSPECT: A Short Baseline Reactor Antineutrino Oscillation Experiment *by Nathaniel Bowden*

[# 333](#) Reactor neutrino fluxes *by Patrick Huber*

[# 458](#) The miniTImeCUbe, the World's Smallest Neutrino Detector *by John Learned*

[# 278](#) Past and future studies of beta-delayed neutrons with VANDLE *by Karolina Kolos*

NST07: Ripples, Simulation and Experiments - Part I

Tuesday at 1:30 PM in [Bonham D](#)

[# 81](#) Ion irradiation of Si surfaces - what determines the formation of ripple patterns? *by Hans Hofsäss*

[# 78](#) Crater Functions from the Binary Collision Approximation: Energy, Material, and Curvature Dependence *by Scott Norris*

[# 169](#) Functional Nanostructures by Self-Organised Ion Beam Sputtering *by Francesco Buatier de Mongeot*

RE03: Radiation Effects in Electronics - Part I

Tuesday at 1:30 PM in [Presidio C](#)

[# 192](#) The Effect of Space Weather on Electronics *by Heather Marie Quinn*

[# 318](#) A Low Noise Detection Circuit for Probing the Structure of Damage Cascades with IBIC *by Elizabeth C. Auden*

- [# 124](#) Radiation Testing Capability for Electronic Devices and Circuits at Sandia's Ion Beam Laboratory *by Edward S. Bielejec*
- [# 222](#) Localization of Conductive Filaments in TaOx Memristor using Focused Ion Beam Irradiation *by J. L. Pacheco*
- [# 167](#) X-ray Radiation Effect on ZnS:Mn,Eu Fluorescence for Radiation Detection *by Lun Ma*

AMP03: Fundamental Processes in Atomic Physics

Tuesday at 3:30 PM in [Travis A/B](#)

- [# 138](#) Effect of Inactive Electron in Single Ionization of Helium *by Allison L Harris*
- [# 378](#) Collision dynamics studied with a polarized in-ring MOT target *by Daniel Fischer*
- [# 223](#) Variational calculations of positronium-hydrogen scattering for $L=0$ to 5 *by Denton Woods*
- [# 191](#) Atomic Processes in Radiation Dosimetry *by Paul M Bergstrom*
- [# 28](#) Production of Multiply Charged Kr Ions by Synchrotron Radiation *by Antonio C. F. Santos*
- [# 6](#) Origin of L satellites in X-Ray emission spectra of elements with ^{26}Fe to ^{92}U *by Surendra Poonia*

IBA09: General Ion Beam Analysis II

Tuesday at 3:30 PM in [Presidio B](#)

- [# 79](#) Ion Beam Analysis in Extreme Environment: investigation of radioactive samples at the micrometric scale *by caroline raepsaet*
- [# 136](#) Monitoring of ion purity in high-energy implant via RBS. *by Arthur W Haberl*
- [# 214](#) Thickness evaluation of doped BiFeO₃ thin films using different techniques *by Ion Burducea*
- [# 250](#) Ion Beam Analysis of Shale rock for Hydrocarbon and Micro-structural Measurement *by Khalid Hossain*
- [# 287](#) Ionoluminescence: An Important Ion Beam Analytical Method *by Emmanuel Njumbe Epie*

MA07: Clinical Progress with Heavier-Ion Therapy

Tuesday at 3:30 PM in [Bonham B](#)

- [# 488](#) Evolving Role of Charged-Particle Irradiation: Potential and Risks of Clinical Treatment with Particles Heavier than Protons *by Richard P. Levy*
- [# 489](#) Clinical activity with protons and carbon ions at the National Center for Oncological Hadrontherapy (CNAO) in Italy *by Marco Krengli*
- [# 493](#) Overview Summary of Clinical Heavier-Ion Progress in Japan *by Naruhiro Matsufuji*

NP05: High Energy Density Physics

Tuesday at 3:30 PM in [Travis C/D](#)

- [# 310](#) Radiochemical Measurements of Neutron Reaction Products at the National Ignition Facility *by Dawn Shaughnessy*
- [# 195](#) High Energy Density Plasmas (HEDP) for studies of basic nuclear science, Stellar Nucleosynthesis and Big Bang Nucleosynthesis *by Johan A Frenje*
- [# 142](#) Measurement of the T+T Neutron Spectrum Using the National Ignition Facility *by Daniel B. Sayre*
- [# 452](#) Charged-Particle Diagnostics for Inertial Confinement Fusion *by Anna Catherine Hayes*
- [# 12](#) Partial charge changing cross-sections of 300 A MeV Fe²⁶⁺ ion beam in different target media *by Ashavani Kumar*

NST08: Ripples, Simulation and Experiments - Part II

Tuesday at 3:30 PM in [Bonham D](#)

- [# 296](#) Crater Function Modeling of Ion Bombardment and Ripple Formation *by Harley T. Johnson*
- [# 441](#) Formation and Evolution of Ripples on Ion-Irradiated Semiconductor Surfaces *by Rachel S Goldman*
- [# 173](#) Exotic New Patterns and Virtually Defect-Free Ripples Produced by Ion Sputtering *by R. Mark Bradley*

AMP02: Electron-Ion Collisions with Applications in Nuclear Physics and Astrophysics

Wednesday at 8:00 AM in [Presidio C](#)

- [# 58](#) Electron Coolers and Storage Rings as Spectroscopic Tools for Highly Charged Ions *by Stefan Schippers*
- [# 457](#) Radiance line ratios Ly- β / Ly- α , Ly- γ / Ly- α , Ly- δ / Ly- α , and Ly- ϵ / Ly- α for soft X-ray emissions following charge exchange between C⁶⁺ and Kr *by V M Andrianarijaona*
- [# 399](#) SPARC: Experiments at the High-Energy Storage Ring HESR *by Thomas Stöhlker*
- [# 320](#) Photonuclear studies of the isomeric yield ratios in the production of ^{nat}Ag(g,xn)^{106m,g}Ag with 50-, 60-, and 70-MeV bremsstrahlung *by Md. Shakilur Rahman*
- [# 349](#) Electron spectroscopy at the high-energy endpoint of electron-nucleus bremsstrahlung *by Pierre-Michel Hillenbrand*

HSD07: Modeling and Simulation for Accelerator-Based HS&D Technologies Wednesday at 8:00 AM in [Travis A/B](#)

- [# 50](#) Overview of Accelerators with Potential Use in Homeland Security *by Robert W Garnett*
- [# 31](#) An Ultra Low-Exposure Neutron Based Inspection System for Nuclear Material *by Michael J King*
- [# 94](#) Small Cyclotron Applications and Development *by Richard R Johnson*
- [# 336](#) Superconducting Magnets for Ultra Light and Magnetically Shielded, Compact Cyclotrons for Medical, Scientific, and Security Applications *by Joseph V. Minervini*

IBA02: Low and Medium Energy Ion Scattering

Wednesday at 8:00 AM in [Presidio B](#)

- [# 36](#) Recent progress in fast atom diffraction at surfaces *by Helmut Winter*
- [# 422](#) Multiple scattering simulation: effects at low energy *by Francois Schiettekatte*
- [# 189](#) Medium Energy Ion Scattering investigation of the topological insulator Bi₂Se₃ films *by Hang Dong Lee*
- [# 199](#) Medium energy ions scattering and elastic recoils for thin films and monolayers *by Lyudmila V Goncharova*

MA08: Startup of New Particle Beam Facilities and Overview Summary of Med App Section

Wednesday at 8:00 AM in [Bonham B](#)

- [# 491](#) Navigating the Logistical and Bureaucratic Minefield of Starting Up a New Particle Therapy Facility *by Carl J Rossi*
- [# 490](#) Myths and Realities of Developing a Particle Therapy Center *by Chris Chandler*

NP11: Accelerator Mass Spectrometry II

Wednesday at 8:00 AM in [Travis C/D](#)

- [# 351](#) Application of accelerator mass spectrometry to archaeology, geography and environmental research. *by Wolfgang Kretschmer*
- [# 376](#) Experimental Investigation of Ion Sources for the Detection of Ultra-trace Uranium and Thorium *by Yuan Liu*
- [# 449](#) Basic and applied nuclear physics at CIRCE laboratory *by Giuseppe Porzio*
- [# 135](#) New AMS Facility in Mexico: "Laboratorio de Espectrometría de Masas con Aceleradores": High sensitivity measurements of radioactive isotope concentrations in materials. *by Efraín Chávez*

ATF04: Accelerator Technology for Security and Defense Applications

Wednesday at 9:45 AM in [Presidio A](#)

- [# 39](#) High-Energy Electron-Beam Tomography *by Joseph Bendahan*
- [# 44](#) Nuclear detection & characterization with laser-plasma accelerator driven quasi-monoenergetic photon sources *by Cameron G.R. Geddes*
- [# 97](#) A High Flux Neutron Generator for Explosives Detection *by Evan Sengbusch*
- [# 22](#) Portable High Power X-ray Source Based on a 10 MeV Superconducting Linac *by Terry L Grimm*
- [# 69](#) Linatron Mi6, THE X-Ray Source for Cargo Inspection *by Gongyin Chen*

[# 46](#) Computational Study of Integrated Neutron/Photon Imaging for Illicit Material Detection *by Jessica N. Hartman*

[# 371](#) Intense Combined Source of Neutrons and Photons for Interrogation Based on Compact Deuteron RF Accelerator *by Sergey S Kurennoy*

HSD04: Nuclear and Crime Lab Forensics

Wednesday at 9:45 AM in [Travis A/B](#)

[# 357](#) Nuclear Forensic Analysis Overview *by Patrick M. Grant*

[# 472](#) Post-explosion exercises and accelerator-produced radionuclides *by Ken Moody*

[# 435](#) Exploiting the 'Power and Precision of Lasers' for nuclear forensics *by Jean-Claude Diels*

[# 387](#) Silicon Drift Detectors for Specialized Accelerator and Synchrotron Applications *by Shaul Barkan*

[# 27](#) Development of a Rapid Field Response Sensor for Characterizing Nuclear Detonation Debris *by Sudeep S Mitra*

[# 171](#) Incorporating Environmental Lines of Evidence into Nuclear and Criminal Forensics *by Adam H Love*

IBA01: General Ion Beam Analysis I

Wednesday at 9:45 AM in [Presidio B](#)

[# 494](#) Triassico: A Sphere Manipulating Apparatus for IBA *by Barney L Doyle*

[# 174](#) Rutherford Backscattering Spectrometry: early activities, and future prospect *by Wei-Kan Chu*

[# 335](#) Rutherford backscattering analysis of irradiation-enhanced diffusion kinetics and interface formation of uranium bearing diffusion couples *by Michael S. Martin*

[# 111](#) Temporal dependence of electron transmission through funnel shaped micro-sized glass capillaries *by S J Wickramarachchi*

[# 293](#) Sputtering of a liquid Bi:Ga alloy with keV Ar ions *by Naresh T Deoli*

IBM05: Nanostructuring with Ion Beams

Wednesday at 9:45 AM in [Bonham C](#)

[# 157](#) Silicon and Germanium Nanopatterning and Relaxation Processes during Ion Bombardment *by Karl F Ludwig, Jr.*

[# 390](#) Ion-Slicing of Ultrathin Layers from III-Nitride Bulk Wafers *by Oussama Moutanabbir*

[# 29](#) Focused Ion Beam nano-patterning and single ion implantation perspectives *by Jacques Gierak*

[# 37](#) In-situ morphology and surface chemistry studies during nanopatterning of III-V semiconductors via low energy ion beams *by Osman El-Atwani*

[# 355](#) Ion beam and cluster ion beam engineered nano-metallic substrates for SPR based sensors *by Iram Saleem*

[# 286](#) Thermoelectric Properties of Zn_4Sb_3 and ZrNiSn Thin Films Affected by MeV Si ion-beam *by S. Budak*

NBA02: Applications Using Neutron Generators

Wednesday at 9:45 AM in [Bonham B](#)

[# 420](#) Material Classification by Analysis of Prompt Photon Spectra Induced by 14-MeV Neutrons *by Alexander Barzilov*

[# 368](#) Neutron Generators for Nuclear Recoil Calibration of Liquid Noble Gas TPCs *by Sean MacMullin*

[# 183](#) Recent Fast Neutron Imaging Measurements and Simulations with the Fieldable Nuclear Materials Identification System *by Tracey A. Wellington*

[# 179](#) A Method to Measure Elemental Gamma-Ray Production Cross Sections Using a 14.1 MeV Associated Particle Neutron Generator. *by Haoyu Wang*

[# 175](#) Application of D-D based Neutron Generator System to Quantify Manganese in Bone In Vivo *by Linda H Nie*

[# 185](#) Sensitivity of Associated Particle Neutron Elemental Imaging for Cancer Diagnoses *by David Koltick*

NP07: Beam Development for Nuclear Physics and Isotope Production

Wednesday at 9:45 AM in [Travis C/D](#)

- [# 380](#) On the use of Aluminum Nitride to Improve Aluminum-26 Accelerator Mass Spectrometry Measurements for Earth Science Applications *by Meghan S. Janzen*
- [# 144](#) Monochromatic fast (MeV) neutron "beam" characterization and its use to study elastic scattering in heavy nuclei. *by Efraín Chávez*
- [# 298](#) Development of a Positron Generator for Material Science at CEMHTI *by Jean-Michel Rey*
- [# 373](#) Utilization of a RIB facility for R&D related to radioisotope production *by Daniel W Stracener*

NST09: Cluster Ion Beam Surface Modification

Wednesday at 9:45 AM in [Bonham D](#)

- [# 299](#) Current Progress and Future Prospects of Cluster Ion Beam Process Technology *by Jiro matsuo*
- [# 60](#) Advancement of gas cluster ion beam processes for chemically enhanced surface modification and etching *by Noriaki Toyoda*
- [# 265](#) Study of multiple collision effects in cluster impact by molecular dynamics simulations *by Takaaki Aoki*
- [# 277](#) Gas Cluster Ion Beam Induced Nanostructures on Metal and Alloy Surfaces *by Buddhi Prasanga Tilakaratne*

RE06: Radiation Effects in Ceramic Materials

Wednesday at 9:45 AM in [Presidio C](#)

- [# 163](#) Multi-scale simulation of structural heterogeneity of swift-heavy ion tracks in complex oxides *by Jianwei Wang*
- [# 168](#) Mechanical Properties of Metal Nitrides for Radiation Resistant Coating Applications: A DFT Study *by Tahir Cagin*
- [# 57](#) Nanocomposite Interfaces and their Effects on Defect Evolution following Light Ion Irradiation *by Jeffery A Aguiar*
- [# 100](#) Effects of composition on the response of oxides to highly ionizing radiation *by Cameron Lee Tracy*
- [# 218](#) Heavy Ion Irradiation-Induced Microstructural Change in Helium-Implanted Single Crystal and Nano-Engineered SiC *by Chien-Hung Chen*
- [# 437](#) Ne ion irradiation effects on stuffed $\text{Er}_2(\text{Ti}_{2-x}\text{Er}_x)\text{O}_{7-x/2}$ ($x=0-0.667$) structures *by Juan Wen*

PS03: Plenary Session - Thursday

Thursday at 8:00 AM in [Lone Star Ballroom](#)

- [# 483](#) Advances in Science and Technology for Counter Terrorism *by James Johnson*
- [# 327](#) Application of accelerators in nuclear structural materials research: history, present status and challenges *by Frank A. Garner*

ATF06: Radiation Generators and Components for Energy and Environmental Applications

Thursday at 10:00 AM in [Bowie A](#)

- [# 464](#) Pulsed-Neutron Generator Applications in the Oil Industry *by Bradley A Roscoe*
- [# 253](#) Performance and Technology of High Flux Neutron Generator DD110MB *by Jaakko Hannes Vainionpaa*
- [# 379](#) A Compact Neutron Generator *by Luke T. Perkins*
- [# 268](#) Ungated Field Ionization Sources for Compact Neutron Generators *by Arun Persaud*
- [# 102](#) Laser-free RF-Gun as a combined source of THz and ps-sub-ps X-rays *by Alexei Vladimirovich Smirnov*
- [# 400](#) Energy-tunable Parametric X-ray (PXR) production using medical accelerators *by Bryndol A Sones*

HSD06: Detectors for Accelerator-Based HS&D Technologies

Thursday at 10:00 AM in [Travis A/B](#)

- [# 386](#) Scintillators and Electronics for Transmission Z-Spectroscopy (Z-SPEC) *by Willem G.J. Langeveld*
- [# 450](#) Gamma-insensitive fast neutron detection for active interrogation applications *by Rico Chandra*
- [# 99](#) Detectors for the new technique of High Energy X-ray cargo inspection *by Anatoli Arodzero*

- [# 52](#) Study of a Silicon Photomultiplier for Optical Readout of EJ-299-33A Scintillator *by Alexander Barzilov*
- [# 201](#) X-ray Radar Imaging Technique Using a 2 MeV Linear Electron Accelerator *by Wendi Dreesen*
- [# 32](#) A neutron imager and flux monitor based on Micro Channel Plates (MCP) in electrostatic mirror configuration *by Vincenzo Variale*

IBA07: PIXE Basics and Applications

Thursday at 10:00 AM in [Bowie B](#)

- [# 107](#) Study on transfer coefficients of cesium-137 and other elements from soil to plant by g-ray measurement and PIXE analysis for remediation of Fukushima *by Keizo ISHII*
- [# 442](#) High Throughput PIXE for Large Area High Definition Elemental Imaging *by Tilo Reinert*
- [# 18](#) The PIXE technique: recent applications and trends in Brazil *by Carla Eliete Iochims dos Santos*
- [# 259](#) Large area transition-edge sensor array for particle induced X-ray emission spectroscopy *by Mikko Laitinen*
- [# 33](#) Using PIXE study Alzheimer Disease induced by neo natal iron administration model in rats. *by Paulo Fernandes Costa Jobim*
- [# 113](#) Commissioning and first applications of a new Mexican beam extraction device for PIXE analysis in air. *by Efrain Rafael Chávez*

IBM03: IBMM - Advanced Characterization Capabilities

Thursday at 10:00 AM in [Bonham C](#)

- [# 319](#) Application of Atom Probe Tomography For Studying Irradiation Damage, Ion Beam Implantation, and Related Subjects *by Robert M. Ulfing*
- [# 416](#) Chemical analysis on nanoscale using synchrotron based soft X-ray scanning microscopes *by Tolek Tyliczszak*
- [# 87](#) Time-of-Flight Secondary Ion Mass Spectrometry: a Unique Tool for Characterization of Ion Beam Modified Materials *by Zihua Zhu*
- [# 347](#) Phase stability and microstructure evolution of the metal-oxide multilayer Fe/Cr-TiO₂-Fe/Cr nanocomposite under ion irradiation *by Nan Li*
- [# 459](#) Influence of ions species on radiation damage of metal/oxide (Cr/MgO) interface *by sandeep manandhar*

NBA03: Nonproliferation Analysis Techniques

Thursday at 10:00 AM in [Bonham B](#)

- [# 93](#) Introduction and Survey of laser-Compton gamma-ray Source Development for Nuclear Photonics *by Christopher P. J. Barty*
- [# 206](#) Dense Plasma Focus Z-Pinch: A Short-Pulse Neutron Source Concept for Active Interrogation *by Andrea Schmidt*
- [# 444](#) Accelerators for Discovery Science and Security Applications *by Alan Todd*
- [# 76](#) Improved Neutron Capture Gamma-Ray Data and Evaluation *by B. Sleaford*
- [# 358](#) Determining isotopic concentrations using delayed gamma-rays from active inspection techniques for nuclear materials safeguards *by Alan W Hunt*
- [# 51](#) Modeling of Time Correlated Detection of Fast Neutrons Emitted in Induced SNM Fission *by Amber Guckes*
- [# 45](#) Application of Wavelet Unfolding Technique in Neutron Spectroscopic Analysis *by Jessica N. Hartman*

NP08: Physics at RHIC and JLAB

Thursday at 10:00 AM in [Travis C/D](#)

- [# 343](#) Long-term detector upgrade plans for RHIC and eRHIC *by Jin Huang*
- [# 433](#) The Electron-Ion Collider (EIC) project at Jefferson Lab *by Pawel Nadel-Turonski*
- [# 369](#) Detector Development for Jefferson Lab's 12 GeV Upgrade *by Yi Qiang*
- [# 356](#) Future upgrades for the PHENIX Experiment at RHIC: From PHENIX to sPHENIX and beyond *by Achim Franz*
- [# 322](#) A MAPS based micro-vertex detector for the STAR experiment *by Joachim Schambach*

NST04: Nanostructured Metals and Alloys

Thursday at 10:00 AM in [Bonham D](#)

[# 130](#) Real Time Observation of He Implantation, High-Energy Si Irradiation, and Self-ion Irradiation of Nanocrystalline Au *by Khalid Hattar*

[# 311](#) Ultrafine grained T91 steel processed by equal channel angular extrusion and their response to heavy ion irradiation *by Miao Song*

[# 495](#) Response of nanotwinned metals to heavy ion irradiation *by Kaiyuan Yu*

[# 382](#) Molecular dynamics simulations of defect-boundary interactions in Fe *by DI CHEN*

RE08: Radiation Effects in Chemical and Biological Systems

Thursday at 10:00 AM in [Bowie C](#)

[# 479](#) Radiation effects in Heavy Ion Radiolysis *by Jay A LaVerne*

[# 71](#) Photoprotective properties of a eumelanin building block: Ultrafast excited state relaxation dynamics in indole *by Susanne Ullrich*

[# 453](#) Inorganic oxygen regulator alleviates radiation induced damage to living systems

by Soumen Das

[# 352](#) Controlling Bond Cleavage in Gas-Phase Biomolecules *by Sylwia Ptasinska*

[# 408](#) Advances of the multiscale approach to the assessment of radiation damage with ions *by Eugene Surdutovich*

ATF07: Advances in Compact Neutron Generators

Thursday at 1:30 PM in [Bowie A](#)

[# 216](#) Handheld 10^7 DT neutrons/second pulsed neutron generator using a field ionization source *by Jennifer L Ellsworth*

[# 140](#) High Yield, Gas Target Neutron Generator Development at Phoenix Nuclear Labs *by Evan Sengbusch*

[# 341](#) A fluid-based-arc deuteron ion source for neutron generators *by Paul R. Schwoebel*

[# 251](#) Development and Optimization of a Compact Neutron Generator for Research and Education *by Allan Xi Chen*

[# 468](#) Preliminary Experiments with a High-Intensity Neutron Source Based on a Liquid-Lithium Target *by Ido Silverman*

IBM07: Ion Irradiation in Fission and Fusion Energy Research

Thursday at 1:30 PM in [Bonham C](#)

[# 429](#) Exploring the Radiation Damage Resistance of Nanoscale Interfaces *by Vaithiyalingam Shutthanandan*

[# 61](#) Advanced barrier layers for use under extreme corrosion and irradiation conditions *by Francisco García Ferré*

[# 297](#) "Reverse Epitaxy" induced by ion irradiation *by Xin Ou*

[# 359](#) Study of Tungsten-Yttrium Based Coatings for Nuclear Applications *by Gustavo Martinez*

[# 342](#) Micromechanical Investigation of the Effects of Thermal Shock due to Irradiation in Ferritic-Martensitic Steels *by Pavana Prabhakar*

NP06: Accelerator Mass Spectrometry I

Thursday at 1:30 PM in [Travis C/D](#)

[# 412](#) A mini C-14 AMS with great potential in environmental research in Hungary *by Mihály Molnár*

[# 410](#) Accelerator Mass Spectrometry (AMS): From art to Stars *by Philippe A Collon*

[# 227](#) AMS and nuclear astrophysics - supernovae signatures and nucleosynthesis in the lab *by Anton Wallner*

[# 228](#) Compound specific radiocarbon analysis from indoor air samples via accelerator mass spectrometry. *by Wolfgang Kretschmer*

NST02: Nanoscale Fabrication and Patterning - Part II

Thursday at 1:30 PM in [Bonham D](#)

[# 186](#) Nanoscale Lithography for Few-Nanometer Features using Ion Beams *by John Baglin*

[# 245](#) Kelvin Probe Microscopy Characterization of Buried Graphitic Channels Microfabricated by MeV Ion Beam Implantation *by Ettore Bernardi*

[# 290](#) Ion Beam Analysis of Wet NanoBonding™ of Si-to-SiO₂ and SiO₂-to-Silica for single-device sensing electronics using Atomic Force Microscopy & Three Liquids Contact Angle Analysis to Correlate Components of the Surface Free Energy to Topography and Composition *by Eric R.C. Morgan*

RE01: Radiation Effects in Nanostructures and Nanophase Materials

Thursday at 1:30 PM in [Bowie C](#)

[# 34](#) Controlling helium in radiation tolerant multilayer and nanochannel materials *by Feng Ren*

[# 248](#) Atomistic modeling of mixing and disordering at a Ni/Ni₃Al interface *by Tongsik Lee*

[# 261](#) Microstructural changes of oxide-dispersion-strengthened alloys under extreme ion irradiation *by Chao-chen Wei*

[# 439](#) Analyzing Irradiation Effects on Nano- Yttria Stabilized Zirconia *by Sanchita Dey*

[# 411](#) Mechanical stability of nanoporous gold under ion irradiation *by Yongqiang Wang*

TA01: Accelerators in Undergraduate Education I

Thursday at 1:30 PM in [Bonham B](#)

[# 8](#) Ion Beam facility for Research, Service and Education *by Daryush ILA*

[# 217](#) An accelerator in the Faculty of Science of U.N.A.M *by Beatriz Fuentes*

[# 244](#) Ion beam transport simulations for the 1.7 MV tandem accelerator at the Michigan Ion Beam Laboratory *by Fabian U Naab*

[# 434](#) Undergraduate Education with the Rutgers 12-Inch Cyclotron *by Timothy W Koeth*

AMP05: Fundamental Processes in Collisions involving Molecules

Thursday at 3:30 PM in [Travis A/B](#)

[# 312](#) Close coupling CI-approach for (multi-)electronic processes in atomic and molecular keV-collisions *by Alain Dubois*

[# 55](#) Some Dynamical Features of Molecular Fragmentation by Electrons and Swift Ions *by Eduardo C Montenegro*

[# 181](#) Interaction of multicharged ions with biological molecules *by Roberto Daniel Rivarola*

[# 66](#) Transmission of electrons through insulating PET nanocapillaries: Angular dependence *by D Keerthisinghe*

ATF08: Accelerator Facility Updates

Thursday at 3:30 PM in [Bowie A](#)

[# 374](#) Recent achievements in laser-ion acceleration *by Bjorn Manuel Hegelich*

[# 306](#) DOE Office of Science Accelerator Stewardship Program *by Eric R Colby*

[# 211](#) Status on the developments at the tandem accelerator complex in IFIN-HH *by Dan Gabriel Ghita*

[# 152](#) Current Status of the IAP NASU Accelerator-Based Analytical Facility *by Volodymyr Storizhko*

[# 188](#) Construction and Characteristics of the High Energy Ion Microprobe system at Amethyst Research, Inc. *by Lucas C Phinney*

[# 431](#) A new fast and accurate method for accelerator energy calibration *by Guy Terwagne*

IBA04: IBA Theory and Simulations

Thursday at 3:30 PM in [Bowie B](#)

[# 17](#) CORRECT CALCULATION OF ECPSSR IONIZATION CROSS SECTIONS AT LOW IMPACT ENERGIES *by Ziga Smit*

[# 184](#) Geant4 and beyond for the simulation of multi-disciplinary accelerator applications *by Maria Grazia Pia*

[# 90](#) Simulation of MeV ion transmission through capillaries *by M. Doebeli*

NBA04: Positron and Electron Studies: Basic Physics & Applications

Thursday at 3:30 PM in [Bonham B](#)

- # [92](#) Positron Annihilation Spectroscopy Study of Barnett Shale Core *by Carroll A. Quarles*
- # [226](#) Progress in the design of a 21-cell Multicell Trap for Positron Storage [1] *by Christopher J Baker*
- # [224](#) Electron Beam Transmission through a Cylindrically Symmetric Artificially Structured Boundary *by J. L. Pacheco*
- # [132](#) Neutron induced reactions with the 17 MeV facility at the Athens Tandem Accelerator NCSR "Demokritos" *by Rosa Vlastou*

RE07: In-Situ Characterization of Radiation Damage

Thursday at 3:30 PM in [Bowie C](#)

- # [313](#) Direct observation of microstructural evolution in graphitic materials under ion irradiation *by Jonathan A Hinks*
- # [65](#) Ion microscopy based correlative microscopy techniques for high-sensitivity high-resolution elemental mapping *by Patrick Philipp*
- # [137](#) Design, implementation, and characterization of a triple beam in situ ion irradiation TEM facility *by Daniel Bufford*
- # [74](#) Helium-induced bubble formation on ultrafine and nanocrystalline tungsten under different extreme conditions *by Osman El-Atwani*
- # [67](#) In-situ Raman spectroscopy for investigating modifications in materials under ion irradiation *by Lucile Beck*

TA02: Accelerators in Undergraduate Education II

Thursday at 3:30 PM in [Bonham D](#)

- # [101](#) Characterization of Atmospheric Aerosols in the Adirondack Mountains Using PIXE, SEM/EDX, and Micro-Raman Spectroscopies *by Michael F. Vineyard*
- # [196](#) Radiation Curing Program *by Mark S Driscoll*
- # [403](#) Undergraduate Measurements of Neutron Cross Sections *by S. F. Hicks*
- # [432](#) Applications of Ion Beam Analysis to Consumer Product Testing *by Paul A DeYoung*

PS04: Plenary Session - Friday

Friday at 8:00 AM in [Lone Star Ballroom](#)

- # [481](#) Photon Activation Analysis and its Applications *by Doug P. Wells*
- # [159](#) Overview of Nuclear Astrophysics *by Daniel Bardayan*

AMP04: Strong Field Physics at Accelerators and Storage Rings

Friday at 10:00 AM in [Bowie A](#)

- # [409](#) New Opportunities for Atomic Physics with SPARC *by Reinhold H Schuch*
- # [241](#) Electron- and proton-impact excitation of the heaviest Helium-like ions *by Alexandre Gumberidze*
- # [462](#) Experiments with stored highly-charged ion at the border between atomic and nuclear physics *by Yuri A Litvinov*
- # [345](#) Single differential projectile ionization cross sections ds/dE_e for 50 AMeV U^{28+} in the ESR storage ring *by Siegbert J Hagmann*
- # [262](#) Two Photon Decay in High-Z He-like Ions *by Sergiy Trotsenko*

IBM06: Ion Beam Modification ? Interesting Properties

Friday at 10:00 AM in [Bonham C](#)

- # [49](#) An ideal system for analysis and interpretation of ion beam induced luminescence *by Miguel Luis Crespillo Almenara*
- # [361](#) ION/ELECTRON INDUCED LUMINESCENCE FOR RADIATION DAMAGE PROCESS INTERPRETATION AND IN SITU MATERIAL VERIFICATION. *by Marta Malo*

[# 440](#) Au-implanted CeO₂ thin films for the selective detection of gases in a harsh environment *by Manjula Nandasiri*

[# 112](#) Low temperature and decay lifetime photoluminescence of Eu and Tb nanoparticles embedded into SiO₂ *by Paulo L. Franzen*

[# 344](#) Preliminary study on formation of proton microbeam with continuously variable kinetic energy for 3-Dimensional proton lithography *by Takeru Ohkubo*

NBA01: Neutron, Photon, and Charged Particles Activation Analysis

Friday at 10:00 AM in [Bonham B](#)

[# 455](#) The Analysis Of Large Samples Using Accelerator Activation *by Christian Segebade*

[# 128](#) Usage of quasi-monoenergetic and continuous spectrum neutron generators for cross-section measurements and benchmarking *by Mitja Majerle*

[# 5](#) Feasibility study of photon activation analysis (PAA) of gold-bearing ores *by Sultan Jaber Alsufyani*

[# 115](#) A Comparison of Various Procedures in Photon Activation Analysis (PAA) with the Same Irradiation Setup *by Z. Sun*

NP09: Nuclear Astrophysics

Friday at 10:00 AM in [Bowie B](#)

[# 254](#) Experimental techniques to investigate neutron sources for the s-process *by Manoel Couder*

[# 205](#) Beta decay as a probe of explosive nucleosynthesis in classical novae *by C. Wrede*

[# 164](#) The ²⁶Al(p,γ)²⁷Si reaction at stellar temperatures *by S.D. Pain*

[# 414](#) Nuclear astrophysics at the CIRCE laboratory *by Lucio Gialanella*

[# 73](#) The JENSA gas-jet target for radioactive beam experiments at ReA3 and FRIB *by DW Bardayan*

RE09: Radiation Effects and Industrial Applications of Electron Accelerators

Friday at 10:00 AM in [Bowie C](#)

[# 207](#) Electron Beam Treatment of Wood Thermoplastic Composites *by Andrew Palm*

[# 209](#) Electron Beam Assisted Carbon Fiber Composite Recycling *by Mark S Driscoll*

[# 210](#) Electron Beam, Wood and the Production of Value Added Products *by Mark S Driscoll*

[# 480](#) Recent Advancements in the Applications of Electron Beam Processing in Advanced Technologies *by Marshall Cleland*

[# 235](#) Use of PENELOPE Monte Carlo Code to design a 125 keV electron accelerator irradiator and determine its shielding requirements *by Roberto M Uribe*

[# 200](#) Ozone Generation in Air During Electron Beam Processing *by Marshall R Cleland*

Invited Posters

Will be presented on poster boards Monday through Friday

- AMP01 [# 47](#) Line ratios of soft X-ray emissions following charge exchange between C^{6+} and Kr *by T. J. J. Lamberton*
- AMP01 [# 178](#) Process Identification and Relative Cross Sections for Low-keV Proton Collisions in N_2 and CO_2 Molecules *by López Patiño Juan*
- AMP01 [# 289](#) Development of a high resolution Analyzing Magnet System for heavy molecular ions *by Mohamed O A El Ghazaly*
- AMP03 [# 6](#) Origin of L satellites in X-Ray emission spectra of elements with ^{26}Fe to ^{92}U *by Surendra Poonia*
- AMP03 [# 28](#) Production of Multiply Charged Kr Ions by Synchrotron Radiation *by Antonio C. F. Santos*
- ATF04 [# 46](#) Computational Study of Integrated Neutron/Photon Imaging for Illicit Material Detection *by Jessica N. Hartman*
- ATF04 [# 371](#) Intense Combined Source of Neutrons and Photons for Interrogation Based on Compact Deuteron RF Accelerator *by Sergey S Kurennoy*
- ATF05 [# 53](#) Magnetic Control of a Neutralized Ion Beam *by Ryan E. Phillips*
- ATF05 [# 80](#) Space-Charge Compressed Ion Beam Equilibrium *by Carlos A. Ordonez*
- ATF05 [# 129](#) Broadband source of coherent THz radiation based on compact LINAC. *by Ivan V. Konoplev*
- ATF05 [# 438](#) Rapid High Dynamic Range Dose Profiling at the University of Maryland Radiation Facility's E-Beam. *by Timothy W Koeth*
- IBM02 [# 64](#) Effect of Swift Heavy Ion Irradiation on Dielectric, Thermal and Structural Properties of Metal/Polymer Composites *by Nand Lal Singh*
- IBM02 [# 232](#) Ion irradiation effects on WN_xO_y films *by Noriaki Matsunami*
- IBM03 [# 459](#) Influence of ions species on radiation damage of metal/oxide (Cr/MgO) interface *by sandeep manandhar*
- IBM04 [# 162](#) Modeling the Transport of Secondary Ion Fragments Into a Mass Spectrometer Through Ambient Pressure Using COMSOL Multiphysics Simulation Software. *by John-William Warmenhoven*
- IBM04 [# 165](#) Ambient Pressure MeV-SIMS analysis of contaminated PTFE aerosol filters. *by Julien Demarche*
- IBM05 [# 286](#) Thermoelectric Properties of Zn_4Sb_3 and $ZrNiSn$ Thin Films Affected by MeV Si ion-beam *by S. Budak*
- MA03 [# 337](#) The Potential of a Compact Accelerator for Low Energy Production of Copper Isotopes *by Robert Cywinski*
- NBA03 [# 45](#) Application of Wavelet Unfolding Technique in Neutron Spectroscopic Analysis *by Jessica N. Hartman*
- NP02 [# 231](#) Relativistic mass of secondary neutrons in fission and fragments in fusion. *by AJAY SHARMA*
- NP06 [# 228](#) Compound specific radiocarbon analysis from indoor air samples via accelerator mass spectrometry. *by Wolfgang Kretschmer*
- NST01 [# 7](#) Nano-crystal Formation and Growth from High Fluence Ion Implantation of Au, Ag, or Cu in Silica or MgO *by Daryush ILA*
- NST01 [# 150](#) Pair Distribution Function Analysis of nanocrystalline ZnS and CdS *by Sunil D Deshpande*
- NST01 [# 285](#) Thermoelectric and Optical Properties of SiO_2/SiO_2+Au Multilayer Thin Films Affected by Thermal Annealing *by S. Budak*
- RE04 [# 446](#) Degredation of GaAs Photovoltaics Exposed to Reactor Neutrons and Accelerator Ions *by Barney L. Doyle*

Regular Posters

Will be presented on poster boards Monday through Wednesday

- AMP01 [# 1](#) Negative ion formation in Ion-Molecule collisions *by Angelin Ebanazar John*

AMP01 [# 354](#) Investigations of Fast-Moving Ion Kinematic Effects in Velocity-Map Imaging Spectroscopy *by Kiattichart Chartkunchand*

AMP03 [# 19](#) Origin of L β ₂ X-Ray satellites spectra of 4d transition metals for lead as predicted by HFS calculations *by Surendra Poonia*

AMP03 [# 20](#) Theoretical calculation of L β ₁ Satellites in X-Ray Emission Spectra of 3d transition elements *by Surendra Poonia*

AMP03 [# 118](#) Bare- and dressed-ion impact collisions from neon atoms studied within a nonperturbative mean-field approach *by Tom Kirchner*

AMP03 [# 119](#) Time-dependent density functional theory study of correlation in proton-helium collisions *by Tom Kirchner*

AMP03 [# 121](#) Independent-particle and independent-event calculations for 1.5 MeV/amu O⁸⁺-Li collisions *by Tom Kirchner*

AMP03 [# 332](#) Double Ionization in Ion-Atom Collisions: Mechanisms and Scaling *by Steven T. Manson*

AMP03 [# 463](#) Atomic Physics with Accelerators: Projectile Electron Spectroscopy (APAPES) * *by Ioannis Madesis*

AMP05 [# 120](#) Quantum-mechanical study of ionization and capture in proton-methane collisions *by Tom Kirchner*

AMP05 [# 338](#) Outer-shell double photoionization of CH₂Cl₂ *by Katianne Fernandes de Alcantara*

ATF01 [# 238](#) Surface morphology of brass and bronze treatment by high power ion beam nanosecond duration *by Vladimir S. Kovivchak*

ATF01 [# 366](#) Studies of the Thorium-Uranium Fuel Cycle *by Robert Cywinski*

ATF01 [# 445](#) Commissioning of an in-air irradiation facility with a 30 MeV/A Xenon Beam *by Mariet Anna Hofstee*

ATF02 [# 363](#) PIP: a compact recirculating accelerator for the production of medical isotopes *by Robert Cywinski*

ATF02 [# 395](#) High Intensity Cyclotron for the ISODAR experiment *by Adriana Bungau*

ATF02 [# 477](#) The Perspectives of the Boron Neutron Capture Therapy-Clinical Applications Research and Development in Saudi Arabia *by Ibtesam Saeed Badhrees*

ATF03 [# 180](#) Design of THz Free Electron Laser Oscillator Cavity *by Conor M Pogue*

ATF03 [# 292](#) Results of the SRF Wafer Test Cavity for the Characterization of Superconductors *by Justin Comeaux*

ATF05 [# 59](#) Radial Expansion of a Low Energy Positron Beam Passing Through a Cold Electron Plasma Within a Uniform Magnetic Field. *by Franz F. Aguirre*

ATF05 [# 215](#) Multiple Aperture-Based Antihydrogen Parallel Plate Gravity Experiment *by Alex H Treacher*

ATF06 [# 63](#) Particle Diffusion along Magnetic Null Lines as Sputter or Antiproton Source *by Ryan A Lane*

ATF06 [# 68](#) Artificially Structured Boundary as a Charged Particle Beam Deflector Shield *by Ryan M. Hedlof*

ATF07 [# 203](#) A High-Flux Neutron Generator Facility for Geochronology and Nuclear Physics Research *by Cory S. Waltz*

ATF07 [# 208](#) Development of A Time-tagged Neutron Source for SNM Detection *by Qing Ji*

ATF07 [# 294](#) RFI-Based Ion Linac Systems *by Donald A. Swenson*

ATF08 [# 117](#) Advances in the Development of Positron Beams at the 5.5 MV Van de Graaff Accelerator, IFUNAM *by Oscar G de Lucio*

ATF08 [# 125](#) Status of the CS-30 Cyclotron at Sichuan University and the beam optic design of the external target beam line. *by zhihui Li*

ATF08 [# 204](#) Automatic Frequency Control of a Sub-Harmonic Bunching Cavity *by Thomas Hunt*

ATF08 [# 267](#) Development of an electrostatic quadrupole doublet system for focusing fast heavy ion beams *by Szabolcs Z Szilasi*

ATF08 [# 370](#) Induced Activation in Accelerator Components for the European Spallation Source *by Adriana Bungau*

HSD02 [# 172](#) Active Detection of Shielded Special Nuclear Material In the Presence of Variable High Backgrounds Using a Mixed Photon-Neutron Source *by Philip Nathaniel Martin*

IBA01 [# 35](#) Fundamentals of the layer-by-layer chemical analysis of heterogeneous samples by secondary ions energy-mass spectrometry method *by Olga V. Vilkhivskaya*

IBA01 [# 291](#) Temperature dependence on vapor and hydrogen absorption characteristics of lithium-zirconium-oxide ceramics *by Bun Tsuchiya*

IBA01 [# 303](#) Comparison of thicknesses of deposited copper thin films on silicon substrate using thin film monitor, profilometer and Rutherford backscattering spectroscopy. *by Gyanendra Bohara*

IBA01 [# 471](#) Establishment of an ASEAN ion beam analysis center at Chiang Mai University for novel materials analysis *by U. Tippawan*

IBA01 [# 494](#) Triassico: A Sphere Manipulating Apparatus for IBA *by Barney L Doyle*

IBA02 [# 202](#) Accurate 50-200 keV proton stopping cross sections in solids *by Sergey N Dedyulin*

IBA02 [# 249](#) Description of Ge, Sm, Hf, Ta, and Au ultra-thin targets by Rutherford back-scattering technique for atomic inner K shell ionization studies. *by Camilo Miguel Correa*

IBA02 [# 367](#) The UK MEIS facility - a new future at the IIAA, Huddersfield *by Bob Cywinsky*

IBA03 [# 123](#) Dynamic measurements of hydrogen and lithium distributions in lithium-cobalt-oxide films during heating and charging using elastic recoil detection techniques *by Bun Tsuchiya*

IBA04 [# 176](#) Benchmarking the proton elastic scattering cross sections on ^{19}F and ^{10}B using DE/E silicon telescopes *by A. Stamatopoulos*

IBA04 [# 273](#) Rainbow effect in ion channeling through a single layer of graphene *by Karur R Padmanabhan*

IBA06 [# 362](#) Chemical characterisation of explosives residues by Ambient Pressure MeV-SIMS *by Lidija Matjacic*

IBA07 [# 105](#) PIXE Determination of the Stoichiometry of Ni-Pd and Au-Ag Nano-Particles Prepared by Laser Ablation in Liquid Solution *by M. Roumie*

IBA07 [# 151](#) PIXE Analysis of Powder and Liquid Uranium-Bearing Samples *by Oleksandr Buhay*

IBA07 [# 193](#) Analysis of Atmospheric Aerosols Collected in an Urban Area in Upstate NY Using Proton Induced X-ray Emission (PIXE) Spectroscopy *by Jeremy W Smith*

IBA08 [# 104](#) PIXE identification of pottery production from the necropolis of Jiyeh archaeological site *by M. Roumie*

IBA08 [# 177](#) Ion Beam Analyses of Microcrystalline Quartz Artifacts from the Reed Mound site (ca. 1200 A.D.), Delaware County, Oklahoma *by S. B. Younger-Mertz*

IBM01 [# 40](#) The reduction of the critical H implantation dose for ion-cut by incorporating B doped SiGe/Si superlattice into Si substrate *by Zhongying Xue*

IBM01 [# 41](#) Sharp crack formation in low fluence hydrogen implanted epitaxial Si/B-doped $\text{Si}_{0.70}\text{Ge}_{0.30}/\text{Si}$ structures *by Miao Zhang*

IBM01 [# 139](#) Raman and ion channeling damage analysis of high energy He implanted Si temperature dependence *by Jack Elliot Manuel*

IBM01 [# 213](#) Optimization of irradiation parameters of heavy ion implantation for diamond growth on silicon *by Szabolcs Z Szilasi*

IBM01 [# 315](#) Synthesis of low dimensional embedded Ge nanostructures *by Vikas Baranwal*

IBM01 [# 323](#) The technical difficulties to synthesize staggered multi-layer low energy ion deposition for synthesis of metal nanostructure in Si. *by Mangal S Dhoubhadel*

IBM01 [# 419](#) Phase Changes of Zn and Si Due to Ion Implantation and Thermal Annealing. *by Bimal Pandey*

IBM02 [# 16](#) Synthesis, characterization and radiation damage studies of high-k dielectric (HfO_2) films for MOS device applications *by N. MANIKANTHABABU*

IBM02 [# 48](#) Tunable Resonant Reflected Wavelength of Porous Silicon based DBR Structures Prepared by Radiation Treated Silicon *by V S Vendamani*

IBM02 [# 317](#) Ge nanocrystals embedded in HfO_2 synthesized by RF sputtering followed by RTA or SHI irradiation *by N Manikanthababu*

IBM02 [# 391](#) Swift heavy ions induced self-organization of LiF Surface *by Vikas Baranwal*

IBM02 [# 396](#) Origin of cracks on BaF_2 thin film surface under swift heavy ion irradiation *by Vikas Baranwal*

IBM03 [# 21](#) TEM and Raman Study of GeMn Recrystallized by Helium IBIEC *by ChienHsu Chen*

IBM03 [# 54](#) In-Situ SEM Characterization of Irradiated Stainless Steel *by Amanda Lupinacci*

IBM04 [# 154](#) Channeling and stopping power issues in the study of heavy ion irradiation in MgO *by Chien-Hung Chen*

IBM05 [# 284](#) Effects of MeV Si Ions and Thermal Annealing on Thermoelectric and Optical Properties of SiO₂/SiO₂+Ge Multi-Nanolayer Thin Films *by S. Budak*

IBM05 [# 384](#) Surface enhanced Raman substrates fabricated by gold ion implantation in quartz *by Yanzhi He*

MA02 [# 156](#) Novel electrostatic accelerator *by Prof. Oliver Heid*

NBA01 [# 56](#) Analysis of ZDDP content and thermal decomposition in motor oils using NAA and NMR *by S. Williams*

NBA02 [# 274](#) Delayed Gamma-ray Spectroscopy for Non-destructive Assay of Nuclear Materials *by Bernhard A Ludewigt*

NBA02 [# 365](#) A Method to Measure Prompt Gamma-Ray Production Cross Sections Using a 14.1 MeV Associated Particle Neutron Generator. *by Haoyu Wang*

NP01 [# 145](#) MOMentum Neutron DETector (MONDE) *by Efraín Chávez*

NP01 [# 470](#) Low Energy Levels in the neutron-rich ^{120,122,124,126}Cd Isotopes *by Jon C. Batchelder*

NP01 [# 474](#) POSITRON GENERATOR DEVELOPMENTS: A NEW SETUP FOR CEMHTI *by Jean-Michel Rey*

NP03 [# 266](#) Study of neutron induced reactions on ⁷Be using large angle coincidence spectroscopy *by Jiri Vacik*

NP04 [# 110](#) How to Produce a Reactor Neutron Spectrum Using a Proton Accelerator *by David W Wootan*

NP05 [# 10](#) Total charge changing cross-sections of 300 A MeV Fe²⁶⁺ ion beam in different target media *by Renu Gupta*

NP07 [# 84](#) Neutron Time-of-Flight Measurements; Comparison with Monte Carlo Simulations at the Idaho Accelerator Center *by Mayir Mamtimin*

NP07 [# 86](#) Numerical Simulation of a multicusp ion source for high current H⁻ Cyclotron at RISP *by J.H. Kim*

NP11 [# 487](#) Formation of large cluster anions of Cu with a Cs-sputtering source *by Ran Chu*

RE01 [# 75](#) TUNGSTEN RESPONSE TO TRANSIENT HEAT LOADS GENERATED BY LASER PULSES *by Osman El-Atwani*

RE01 [# 393](#) Physical properties and radiation stability of nanoparticles *by Vladimir V. Uglov*

RE02 [# 326](#) Neutron-atypical phenomena operating in ion simulations of neutron-induced void swelling that complicate the ion-neutron correlation and prediction of neutron-induced swelling *by Frank A. Garner*

RE06 [# 127](#) Metastability of tetragonal zirconia nanoparticle by Sol-Gel-Derived method coupling with carbon irradiation *by Y. C. Yu*

RE06 [# 372](#) Coloration of Lithium Hydride with Alpha Particle Radiation (U) *by Joseph Tesmer*

RE06 [# 389](#) Heavy and light ion irradiation damage effects on delta-phase Sc₄Hf₃O₁₂ *by Juan Wen*

RE08 [# 276](#) Changes in Mechanical properties of Rat Bones under simulated effects of Microgravity and Radiation[†] *by Azida H Walker*

TA01 [# 426](#) RBS Study of the Behavior of PMMA as a Negative Resist for Particle Beam Lithography *by Randolph S. Peterson*

TA02 [# 394](#) Step-by-Step Analysis of Powder XRD Data: A PG Level Experiment *by Gopichand M Dharne*

Conference Abstracts

Abstract 350 MON-PS01-1

[Plenary Talk - Monday 8:30 AM - Lone Star Ballroom](#)

Thorium Based Energy Production Using Accelerators

[Robert Cywinski](#), [Roger J Barlow](#), [Cristian Bungau](#)

International Institute for Accelerator Applications, University of Huddersfield, Queensgate, Huddersfield HD1 3DH, United Kingdom

On the one hand it is widely believed that the twin global crises associated with energy supply and climate change can only be mitigated by a wider deployment of nuclear power, whilst on the other there remains widespread public concern about the safety of existing uranium and plutonium fuelled nuclear reactors, the management of nuclear waste and the issue of proliferation. It is therefore not surprising that there is growing global interest in the possibility that the fertile element thorium, coupled with innovative nuclear technology, may provide an alternative nuclear future that has inherently higher safety margins; that is low waste; that does not include plutonium as part of its fuel cycle, that is intrinsically proliferation resistant; that can effectively burn legacy radiotoxic waste; and is both sustainable and cost effective.

In this talk I will review the potential of thorium nuclear power generation, focussing upon the key role that particle accelerators, and in particular spallation technologies, could play in realising this potential through the development of Accelerator Driven Subcritical Reactor (ADSR) systems, fertile to fissile conversion, and legacy waste management.

Abstract 314 MON-PS01-2

[Plenary Talk - Monday 8:30 AM - Lone Star Ballroom](#)

LAST IMPROVEMENTS ON AGLAE FACILITY AND THEIR APPLICATION TO THE ANALYSIS OF CULTURAL HERITAGE ARTEFACTS

[Claire PACHECO](#)^{1,2}

⁽¹⁾C2RMF, Palais du Louvre 14 quai F. Mitterrand, Paris 75001, France

⁽²⁾FR 3506 New AGLAE, CNRS/MCC, Palais du Louvre 14 quai F. Mitterrand, Paris 75001, France

For more than 20 years, the AGLAE (Accelérateur Grand Louvre pour l'Analyse Elementaire) is exclusively dedicated to IBA of Cultural Heritage objects in the Louvre premises, at the crossroad of social science and hard science. Because Cultural Heritage artifacts are unique, sampling cannot often be considered. Moreover, the conservation state may also prohibit to work under vacuum. For these reasons, an extracted beamline has been developed especially for Cultural Heritage objects on this facility [1]. Multidisciplinary, the New AGLAE project will provide an exceptional and multipurpose beam line with a performance in spatial resolution, beam stability and a capability of multi-particle detection much higher than for the previous facility. This talk will describe the milestones and the state of progress of the project, the new set-up, the imaging system and how this innovative New AGLAE project follows on from the development of the AGLAE facility in accordance with the specificities of the Cultural Heritage objects and their questioning. The first images collected on prestigious Cultural Heritage objects will be presented and commented, showing the limits and the perspectives of the technique. [1] J.C. Dran, J. Salomon, Th. Calligaro, Ph. Walter, Ion beam analysis of art works: 14 years of use in the Louvre, NIMB, June 2004, 219-220, 7-15

Abstract 62 MON-ATF01-1

[Invited Talk - Monday 10:30 AM - Presidio A](#)

The MYRRHA ADS project in Belgium enters the Front End Engineering Phase

[Didier J De Bruyn](#), [Hamid Aït Abderrahim](#), [Peter Baeten](#), [Rafaël Fernandez](#), [Gert Van den Eynde](#)

Belgian Nuclear Research Centre (SCK•CEN), Boeretang 200, Mol 2400, Belgium

MYRRHA (Multi-purpose hYbrid Research Reactor for High-tech Applications) is a multipurpose research facility currently being developed at SCK•CEN, based on the ADS (Accelerator Driven System) concept where proton accelerator, spallation target and subcritical reactor are coupled. MYRRHA will demonstrate the ADS full concept by coupling these three components at a reasonable power level to allow operation feedback, scalable to an industrial demonstrator. As a flexible irradiation facility, the MYRRHA research facility will be able to work in both critical as subcritical modes. In this way, MYRRHA will allow fuel developments for innovative reactor systems, material developments for GEN IV and fusion reactors, and radioisotope production for medical and industrial applications. MYRRHA will be cooled by lead-bismuth eutectic and will play an important role in the development of the Pb-alloys technology needed for the LFR (Lead Fast Reactor) GEN IV concept. MYRRHA will also contribute to the study of partitioning and transmutation of high-level waste. Transmutation of minor actinides (MA) can be completed in an efficient way in fast neutron spectrum facilities (critical reactors and sub-critical ADS). A sub-critical ADS operates in a flexible and safe manner even with a core loading containing a high amount of MA leading to a high transmutation rate. The sub-criticality is therefore rather a necessity for an efficient and economical burning of the MA. The MYRRHA design has progressed through various framework programmes of the European Commission in the context of Partitioning and Transmutation and has now entered into the Front End Engineering Phase covering the period 2012-2015. The engineering company which will handle this phase has started the works in the late 2013. In this paper, we present the most recent developments of the MYRRHA design in terms of primary system, reactor building and plant layout as existing end of 2013.

Abstract 304 MON-ATF01-2

[Invited Talk - Monday 10:30 AM - Presidio A](#)

Fixed field ring methods for high power beams

[Francois G Meot](#)

Collider-Accelerator, BNL, Bldg 911, Upton NY 11973, United States

Cyclotrons and Fixed Field Alternating Gradient ring methods have the potential for producing mega-watt class beams in the GeV energy range, based on conservative technologies and at a lower cost compared to other possible techniques. A review is given, including recent development and progress, ultimate schemes, challenges and objectives, on a background of historical context, and of most recent ADS-Reactor application prospects.

Abstract 360 MON-ATF01-3

[Invited Talk - Monday 10:30 AM - Presidio A](#)

Experimental Subcritical Facility Driven by D-D/D-T Neutron Generator at BARC, India

[Amar Sinha](#), [Tushar Roy](#), [Yogesh Kashyap](#), [Nirmal Ray](#), [Mayank Shukla](#), [Tarun Patel](#), [Shefali Bajpai](#), [Parthsarthi sarkar](#), [Saroj Bishnoi](#)

Neutron & X-ray Physics Division, Bhabha Atomic Research Centre, Purnima lab, Trombay, Mumbai 400085, India

A zero-power, sub-critical assembly driven by a D-D/D-T neutron generator has been developed at Bhabha Atomic Research Centre, India. This facility has been conceived for investigating the static and dynamic neutronics properties of accelerator driven sub-critical systems. This system is modular in design and it is first in the series of subcritical assemblies being designed. The subcritical core consists of natural uranium fuel with high density polyethylene as moderator and beryllium oxide as reflector. The fuel pins are made of metallic uranium with aluminum clad. A total of 160 fuel elements are arranged in a 13 X 13 square lattice with a pitch of 48mm. The central 3 X 3 positions form the central cavity for inserting the neutron source. The fuel is embedded in high density polyethylene moderator matrix. Estimated k_{eff} of the system is ~ 0.89 . One of the unique features of subcritical core is the use of Beryllium oxide (BeO) as reflector and HDPE

as moderator making the assembly a compact modular system. The core and reflector assembly is surrounded by an outer layer of borated polyethylene and cadmium. The subcritical core is coupled to Purnima Neutron Generator which works in D-D and D-T mode with both DC and pulsed operation. It has facility for online source strength monitoring using neutron tagging and programmable source modulation. Preliminary experiments have been carried out for spatial flux measurement and reactivity estimation using pulsed neutron source (PNS) techniques. Further experiments are being planned to measure the reactivity and other kinetic parameters using noise methods. This facility would also be used for carrying out studies on effect of source importance and measurement of source multiplication factor k_{∞} and external neutron source efficiency β in great details. Experiments with D-T neutrons are also underway.

Abstract 194 MON-ATF01-4

[Contributed Talk - Monday 10:30 AM - Presidio A](#)

A Strong Focusing Cyclotron capable of producing 10 mA of proton beam up to 800 MeV and its applications.

[Nathaniel Pogue](#), [Peter McIntyre](#), [Josh Kellams](#), [Karie Melconian](#), [Kyle Damborsky](#), [Akhdiyor Sattarov](#)

Physics and Astronomy Department, Texas A&M University, 3380 University Dr. East, College Station Texas 77845, United States

The Strong Focusing Cyclotron, developed at Texas A&M University's Accelerator Research Lab, can produce greater than 10 mA of proton beam to a desired target at 800 MeV. The implications of this device are diverse and far-reaching. These beams can be used to create accelerated driven fission to destroy nuclear waste and power the U.S. for several millennia, create a flood of neutrons to induce neutron damage in materials to test reactor material lifetimes, medical isotope production, and be used as an investigative tool. The same technology developed for the system have implication in beam therapy, the high intensity frontiers and high energy frontiers. The SFC will be presented along with industrial application that could benefit from its further development, construction, and commissioning.

Abstract 23 MON-ATF01-5

[Contributed Talk - Monday 10:30 AM - Presidio A](#)

A Fast Spectrum Neutron Source for Material Irradiation Using a Superconducting Electron Linac

[Valeriia N Starovoitova](#)¹, [Terry L Grimm](#)¹, [Frank Harmon](#)², [Mayir Mamtimin](#)²

⁽¹⁾*Niowave, Inc, 1012 N. Walnut St, Lansing MI 48906, United States*

⁽²⁾*Idaho Accelerator Center, Idaho State University, 1500 Alvin Ricken Dr, Pocatello ID 83201, United States*

Next generation reactor concepts cater to a common goal of providing safer, longer lasting and economically viable nuclear power plants. Developing radiation damage resistant materials for both in-core and out-of core applications is a critical component of these next generation power plants. Testing these novel materials requires an intense neutron environment. A commonly used tool for testing novel materials is a nuclear reactor providing high density neutron flux.

We are developing a convenient and low-cost alternative: an intense source of fast fission-spectrum neutrons produced from a superconducting electron linac. The source is based on the photo production of neutrons, including (γ, n) production and photofission, with a high power 10-40 MeV electron beam. The end-station is intended to irradiate small mm-scale samples with a neutron flux of 10^{14} n/cm².s. Fluxes greater than 10^{13} n/cm².s can be achieved for larger, cm-scale specimens. Beryllium, tungsten, lead and uranium are being investigated as potential neutron target materials. We will present both Monte-Carlo simulations and preliminary experimental results confirming the predicted fluxes.

Abstract 460 MON-ATF01-6

[Contributed Talk - Monday 10:30 AM - Presidio A](#)

Compact CW Racetrack FFAG for High-intensity Applications

[Carol Joanne Johnstone](#), [Richard Ford](#)

Particle Accelerator Corp, 809 Pottawatomie Trail, Batavia IL 60510, United States

Ultra-compact, high-energy proton accelerators imply both CW operation and high acceleration gradients to mitigate losses, especially at extraction in order to achieve milliamp currents. Losses must be under a per cent to avoid massive shielding and sustainable operation. Conventional cyclotron designs utilize Dee-shaped RF components between pole faces to achieve compactness, however, the accelerating gradient of these structures is low and as relativistic energies are approached, the orbit separation decreases making low-loss extraction difficult and in general unachievable. To achieve higher acceleration gradients which increases the orbit separation at extraction, RF modules must be employed, forcing separated sectors in a cyclotron design, with an unavoidable large increase in footprint. However, the weak-focusing nature of traditional cyclotron fields do not promote long (several meter) straight sections. The addition of strong focusing gradients for the purpose of envelope control - with reversed gradients to capture both transverse planes - to conventional cyclotron fields do allow inclusion of long synchrotron-like straight sections and implementation of high-gradient RF modules, even SCRF cryomodules. This approach, based on Fixed Field Alternating Gradient design, supports a new, racetrack form - essentially a recirculating linear accelerator with FFAG arcs. An ultra-compact, 0.2 - 1 GeV RLA FFAG design with a 3 m x 5-6m footprint that undergoes only 40 acceleration turns and exhibits a very large DA by (using SC pillbox RF cryomodules @10 MV/m) is presented here with complete orbit separation at extraction for CW operation.

Abstract 108 MON-HSD01-1

[Invited Talk - Monday 10:30 AM - Travis A/B](#)

Domestic Nuclear Detection Office's Approach to Detect Concealed Threats

[Joel Rynes](#)

Domestic Nuclear Detection Office, Department of Homeland Security, 245 Murray Lane SW, #0550 DNDO, Washington DC 20528, United States

The Transformational and Applied Research (TAR) Directorate within the Domestic Nuclear Detection Office (DNDO) of the Department of Homeland Security (DHS) has the mission to develop break-through technologies that will have a dramatic impact on capabilities to detect nuclear and radiological threats through an aggressive and expedited research and development (R&D) program. In its role to develop and implement the Global Nuclear Detection Architecture (GNDA), DNDO has defined several technical grand challenges. This talk will discuss TAR's multi-year R&D approach to solve one of these challenges - the detection of nuclear threats even when heavily shielded. Special emphasis will be given on the role of traditional and non-traditional particle acceleration techniques to help solve this challenge.

Abstract 486 MON-HSD01-2

[Invited Talk - Monday 10:30 AM - Travis A/B](#)

Photofission based interrogation techniques for nuclear materials

[Tsahi Gozani](#)

DNDO Consultant, 1050 Harriet St., Palo Alto CA 94301, United States

Detecting the naturally emitted gamma rays (or neutrons, in some cases) by nuclear materials, is helpful and is commonly done these days, and referred to as "Passive Interrogation". However when embedded in cargo the detection of these materials precipitously declines because of the "passive" gamma ray's low energy. The Active Interrogation (AI), where neutrons or high energy x-rays are employed to penetrate deep into the cargo to reach the nuclear material and stimulate fission, overcame the inherent limitations of passive interrogation. The fission process is very rich in nuclear signatures endowed with high energies and temporal behavior, making it more readily detectable. High energy x-rays employed for high resolution radiography of trucks and marine containers can also be applied to reveal the presence of high Z value materials and determine whether they are fissionable by photofission stimulation. The relatively low photofission cross sections (tens of mb, below 10MeV) are readily compensated with the ample intensity of x-rays generated by commercially available electron accelerators like linacs. In fact photofission with linacs was used as early as 1968 to detect SNM as a part of nuclear material safeguards missions. Among the various ways to determine the Z of the interrogated materials there is the spectrum of the transmitted x-ray, which intrinsically contains the energy dependence of the elemental attenuation factors. Photofission is induced in all fissionable materials. To discriminate between fissile and non-fissile-fissionable materials several "2nd order" features, such as the decay time of the delayed gamma rays, delayed neutrons and the ratio between the prompt and these delayed radiations are employed. Detectors for these neutrons and gammas are readily available. High Z and photofission measurements techniques will be discussed.

*) Email address: tgmaven@gmail.com

Abstract 82 MON-HSD01-3

[Invited Talk - Monday 10:30 AM - Travis A/B](#)

Non-intrusive Inspection Using CW Photon Beams

[Cody M. Wilson](#), [William Bertozzi](#), [Areg Danagouliau](#), [Wilbur A. Franklin](#), [Stephen E. Korbly](#), [Robert J. Ledoux](#), [Rustam Niyasov](#)

Passport Systems, Inc., 70 Treble Cove Rd, North Billerica Massachusetts 01862-2232, United States

Homeland security applications such as the screening of sea-bound and air cargo shipping containers involve interrogation of large objects with a strong emphasis on throughput. High energy photons are advantageous for interrogating containers of this size and density. The vast majority of commercially available high energy photon sources make use of a pulsed beam with a duty cycle of approximately 0.1%. The throughput emphasis has driven cargo screening technology to operate these sources at relatively high peak currents while making use of integration techniques such as traditional transmission imaging and dual energy, multi-view systems. Photon sources providing equivalent average currents with vastly increased duty-cycles enable the application of spectroscopic techniques that involve photon or particle counting. Interrogation applications, available photon sources, and potential spectroscopic techniques are surveyed in this presentation, including CW enabled cargo interrogation technologies developed by Passport Systems such as Effective-Z in 3d (EZ-3DTM), nuclear resonance fluorescence (NRF), and prompt neutrons from photofission (PNPF).

Abstract 166 MON-HSD01-4

[Contributed Talk - Monday 10:30 AM - Travis A/B](#)

Mixed source interrogation of steel shielded special nuclear material using an intense pulsed source

[Cassie E Hill](#), [Phillip N Martin](#), [Ceri D Clemett](#), [James Threadgold](#), [Robert Maddock](#), [Ben Campbell](#)

National Nuclear Security, AWE, Aldermaston, Reading Berks RG7 4PR, United Kingdom

This paper presents data from an experimental campaign performed to investigate the benefits of using a mixed photon and neutron radiation source for active detection for homeland security. More than fifty irradiations were performed using an 8 MV induction voltage adder (IVA) at the Naval Research Laboratory, Washington DC. The experiments used a high atomic number converter to produce a Bremsstrahlung photon spectrum which was then used to create a neutron source via a

nuclear interaction with deuterated water (or deuterium oxide, D₂O). This mixed particle source was then used to irradiate a DU sample, inducing fission in the sample. A number of thicknesses of steel shielding were tested in order to compare the performance of the mixed photon and neutron source to a photofission only irradiation. An array of detectors were fielded to record both photons and neutrons resultant from the fission reaction. A correlation between steel shielding and a detection figure of merit can be seen in all cases where the Bremsstrahlung only source was used. The same relationship for the missed photon-neutron source is less consistent. This paper looks specifically at a small selection of the detectors fielded and compares the results to MCNP6 calculations with positive results.

Abstract 30 MON-HSD01-5

[Contributed Talk - Monday 10:30 AM - Travis A/B](#)

A light transportable neutron based inspection system for nuclear material and other contraband

[Michael J King](#), [Tsahi Gozani](#), [Mashal Elsalim](#), [Dan A Strellis](#), [Krystal Alfonso](#), [Matthew Araujo](#)

Rapiscan Laboratories, Inc, 520 Almanor Avenue, Sunnyvale CA 94085, United States

Rapiscan Laboratories has developed a portable pulsed neutron-based active interrogation source for the detection of SNM, drugs and explosive materials. The single-sided system, where both the interrogating source and detector are on the same side utilizes a commercial-off-the-shelf dT electronic neutron generator imbedded inside a beryllium moderator, a shadow shielding module to shield the photon detector from direct 14 MeV neutron interactions and NaI and differential-die away detectors. The system focuses on proximity interrogation with threats located just behind walls and without serious shielding materials. The system utilizes a He-3 based differential die-away detector for the detection of SNM while a 6" x 6" right cylindrical NaI to detect the capture gamma-ray signal from drug and explosive threats. Results with heroin and ammonium nitrate simulants as well as with LEU placed at various distances will be shown.

This work has been supported by the US Department of Homeland Security, Domestic Nuclear Detection Office, under competitively awarded contract/IAA HSHQDC-10-C-00048. This support does not constitute an express or implied endorsement on the part of the Government.

Abstract 155 MON-IBA06-1

[Invited Talk - Monday 10:30 AM - Presidio B](#)

Elemental, Chemical & Molecular Speciation Using MeV Ion Beams: What, How and Why?

[Roger P Webb](#)

Surrey Ion Beam Centre, University of Surrey, Surrey Ion Beam Centre, Guildford Surrey GU2 7XH, United Kingdom

MeV-ion beams have had wide use in mapping surfaces. The ability to focus MeV ions to sub-micron dimensions and to scan them over surfaces allows high quality surface maps to be created. The use of techniques such as PIXE enable trace elemental mapping to become standard in many labs across the world. Coupling this with the ability to pass MeV ion beams through thin windows so that analysis can be performed in ambient conditions on real-world samples makes for a very powerful tool set. However, elemental analysis only reveals a part of the story behind a sample. A lot of interest is in how these elements are combined at the surface - how are the elements linked with each other, in other words, the molecular structure. New tools being developed are providing high resolution molecular concentration maps of surfaces - SIMS and associated techniques have been doing this, of course, for many years, but they are limited to vacuum. Exploiting a technique from the 1970s - PDMS - and combining it with an external beam provides a new tool AP-MeV-SIMS, which can map molecular concentrations with high spatial resolution without vacuum. This does not provide details of the chemical arrangement of the molecules - which bonds are present. XPS provides such information at the very surface layer and is very much a technique limited to analysis in vacuum. New high resolution X-ray detectors on the market have resolutions better than a few eV and it is possible to use these detectors in conjunction with the PIXE technique to obtain not just the trace element population but the bonding states of these elements also - providing chemical information.

Recently the term "Total IBA" has been used to describe coincidental use of PIXE and RBS (and other IBA tools), here we explore the future of the term.

Abstract 436 MON-IBA06-2

[Invited Talk - Monday 10:30 AM - Presidio B](#)

Imaging and Analysis of Fixed Charge Density in the Brain using PIXE and Fe(III)-Ions as a Probe

[Tilo Reinert](#)¹, [Markus Morawski](#)², [Anja Reinert](#)², [Wolfram Meyer-Klaucke](#)³, [Friedrich E. Wagner](#)⁴,
[Thomas Arendt](#)²

⁽¹⁾*Physics Department, University of North Texas, 1155 Union Circle #311427, Denton TX 76203, United States*

⁽²⁾*Paul Flechsig Institute for Brain Research, University of Leipzig, Jahnallee 59, Leipzig 04109, Germany*

⁽³⁾*European Molecular Biology Laboratory (EMBL), Hamburg Unit, DESY, Notkestrasse 85, Hamburg 22607, Germany*

⁽⁴⁾*Physik-Department E15, Technische Universität München, James-Frank-Straße, Garching 85748, Germany*

The brain could not maintain its functions without diffusion and related transport processes on the molecular level. The extracellular matrix with its physico-chemical properties regulates the diffusion through the extracellular space. The extracellular matrix governs the diffusion within the extracellular space via its fixed negative charge density. This density originates mainly from sulfate and carboxyl side groups of the macromolecular components, especially chondroitin sulphate proteoglycans.

We used Fe(III)-cations as probe ions added at different concentrations to rat brain sections. The Fe(III)-probe ions bind to the negatively charged macromolecules, mainly glycosaminoglycans, with high affinity. Thus, the distribution and concentration of the Fe(III)-iron probe reflects the fixed negative charge densities. Using scanning particle induced X-ray emission (μ PIXE) we have quantitatively analyzed the iron concentration in the extracellular space, from which we calculated the fixed negative charge density and the affinity. We also applied extended X-ray absorption fine structure (EXAFS) and Mössbauer spectroscopy to verify the trivalent state of the iron probe. Additionally, from EXAFS analysis the binding sites at the glycosaminoglycans could be narrowed down to sites at sulfate groups.

The results of this analysis show that the extracellular matrix is not only influencing the diffusion parameters by providing rapid reversible cation binding, which in effect slows down diffusion rates. It is also capable, especially in the neuronal microenvironment, to partition mobile ions due to very high negative charge density, thus building diffusion barriers.

Abstract 256 MON-IBA06-3

[Invited Talk - Monday 10:30 AM - Presidio B](#)

SIMS Analysis of Biological Material in 1-, 2- and 3 Dimensions

[Alex Henderson](#)

Manchester Institute of Biotechnology, University of Manchester, 131 Princess Street, Manchester M1 7DN, United Kingdom

Biological materials are inherently complex entities containing many distinct organic molecules. In SIMS, without the separation step commonly used in hyphenated techniques such as GC-MS and LC-MS, we must content with a great many overlapping spectra, each of indeterminate complexity. In order to mitigate these problems it is now commonplace to find multivariate statistical analysis approaches being used in the SIMS laboratory.

Even within this seemingly restrictive environment, we obtain so much information from a SIMS experiment that it is still possible to classify spectra with high precision. In 2D imaging, where we obtain a full spectrum at each pixel, we can

visualise chemical localisation even where we cannot necessarily determine the identity of the chemicals responsible. Using ion beams that exhibit low sub-surface damage characteristics, we can remove organic material during analysis to reach buried interfaces and render the outcome in 3D. Within each of these dimensions there are issues to overcome: ionisation efficiency, sample damage, topography, data volume.

In this presentation we will address the issues found in keV-SIMS, speculating about the possibilities for MeV-SIMS, in the context of the classification of bacterial spectra, 2D imaging of tissue and 3D analysis of single human cells.

Abstract 300 MON-IBA06-4

[Invited Talk - Monday 10:30 AM - Presidio B](#)

MeV-SIMS: A new chemical imaging technique for organic materials

[Jiro Matsuo](#)

Quantum Science and Engineering Center, Kyoto University, Gokasho, Uji Kyoto 611-0011, Japan

Secondary particle emission provides unique opportunities for further insight on ion collision with matter. In particular, molecular ion emission from organic molecules is of interest, not only for fundamental studies on excitation of molecules, but also for practical applications. Desorption Mass Spectroscopy (PDMS) has been reported and was widely used for analysis of organic samples [1]. In this energy range, most of the deposited energy by incoming ions is used for electronic excitation, although nuclei excitation is dominant for the conventional SIMS technique using low energy (keV) ions. Therefore, the enhancement of secondary molecular ion yields corresponds to the electronic stopping power [1, 2].

We have been demonstrated molecular imaging technique with swift heavy ion beams [2, 3]. The molecular distribution (up to 1 kDa) was clearly imaged with a lateral resolution of around 5 μm , opening a new opportunity of chemical imaging. In addition, swift heavy ion beams have high transmission capability in matter and allows us to use this beam in low vacuum pressure to analyze volatile sample, such as liquids, waters and wet biological samples. Molecular imaging equipment combining with orthogonal time of flight (ToF) mass spectrometer has been developed to analyze organic samples containing volatile molecules at 2000 Pa [3]. We call this new technique "wet-SIMS".

Recent progress in this MeV-SIMS will be presented and discussed along with its possible applications for organic material analysis.

Acknowledgement

This work was partially supported by JST, CREST.

References

- 1 A. Hedin, P. Hakansson, M. Salchpour and B. U. R. Sundqvist, Phys. Rev. B, 35, 7371, (1987)
- 3 Y. Nakata, Y. Honda, S. Ninomiya, T. Seki, T. Aoki and J. Matsuo, J. Mass Spectro., 44, 128 (2009)
- 3 J. Matsuo, S. Ninomiya, H. Yamada, K. Ichiki, Y. Wakamatsu, M. Hada, T. Seki, T. Aoki, Surf. Inter. Anal., 42, 1612 (2010)

Abstract 348 MON-IBA06-5

[Contributed Talk - Monday 10:30 AM - Presidio B](#)

Pharmaceutical and biomedical application possibilities of ambient pressure MeV-SIMS

[Julien Demarche](#)¹, [Brian N. Jones](#)¹, [Lidija Matjacic](#)¹, [Vladimir Palitsin](#)¹, [Joke Meeus](#)², [Guy van den Mooter](#)², [Roger P. Webb](#)¹

⁽¹⁾*Surrey Ion Beam Centre, University of Surrey, Nodus Building, GUILDFORD GU27XH, United Kingdom*

⁽²⁾*Department of Pharmaceutical and Pharmacological Sciences, University of Leuven, Campus Gasthuisberg O&N2; Herestraat 49 b921, Leuven 3000, Belgium*

A major breakthrough has been made in recent years, enabling the inclusion of molecular characterisation in the wide range of elemental IBA applications: the use MeV primary ions for secondary ion mass spectrometry (MeV-SIMS). The desorption of large surface molecules (up to hundreds of kDa) induced by MeV heavy ions has been observed, offering applications in key areas such as archaeometry, forensics, biology, or biomedical sciences. MeV ion microbeams can also be extracted into air through a thin exit window, to achieve ambient pressure high resolution imaging at the submicron scale. Sample-altering vacuum conditions would thus be avoided, which is of primary interest for biology and pharmacology applications. These include new polymeric or active pharmaceutical ingredient materials for drug delivery, and biomarkers.

In this work, molecular detection of biocompatible drug delivery polymers has been performed by ambient pressure MeV-SIMS, using 8.8 MeV oxygen ions produced by a 2 MV Tandetron accelerator. Secondary ions were collected thanks to a differentially pumped orthogonal ToF spectrometer. Polymer mixtures of PLGA and PVP, which are common polymeric matrix for long-release injected microspherical drugs, have been probed in broad beam conditions, in order to identify their specific macromolecular footprints for imaging purpose. Conservation of the molecular identity even beyond the SIMS static limit has been proven by MeV heavy ion depth-profiling of a DSPC protein solution spin-coated on silicon. Finally, SIMS of molecular components of the coat and core of a drug tablet has been performed to demonstrate the potential applications of the ambient pressure facility.

Abstract 106 MON-IBA06-6

[Invited Talk - Monday 10:30 AM - Presidio B](#)

Molecular imaging of organic samples using MeV SIMS setup at the heavy ion microprobe in Zagreb

[Ivancica Bogdanovic Radovic](#)¹, [Zdravko Siketic](#)¹, [Dubravka Jembrih-Simbürger](#)³, [Tonci Tadic](#)¹,
[Nikola Markovic](#)¹, [Mirko Hadzija](#)², [Milko Jaksic](#)¹, [Marta Anghelone](#)³

⁽¹⁾*Division of experimental physics, Rudjer Boskovic Institute, Bijenicka 54, PO Box 180, Zagreb 10000, Croatia*

⁽²⁾*Division of molecular medicine, Rudjer Boskovic Institute, Bijenicka 54, PO Box 180, Zagreb 10000, Croatia*

⁽³⁾*Institute of Science and Technology in Art, Academy of Fine Arts Vienna, Schillerplatz 3, Vienna 1000, Austria*

In the present work, TOF-SIMS setup for highly sensitive molecular imaging using focused MeV heavy ions is described. This development is based on the fact that yield of intact organic molecules (with masses from 500 to 10000 Da) is several orders of magnitude larger if the excitation by MeV heavy ions is used instead of the keV ions. As molecular fragmentation is significantly reduced as well, identification of molecular species is much easier which is especially important for chemical compounds with complex organic molecular structure.

The Zagreb Heavy Ion Microbeam focuses heavy ion beams (>5 MeV) from C to I with sub-micrometer resolution enabling chemical imaging at a cellular level. A dedicated pulse processing electronics for MeV SIMS application has been developed. It includes microbeam-scanning control, pulsing of ion microbeam and on line molecular mapping. Examples of MeV TOF SIMS molecular spectra as well as 2D molecular maps obtained using different MeV ions, different biological samples and samples of modern paint materials are presented and discussed.

* This work is supported by the UKF project „Study of modern paint materials and their stability using MeV SIMS and other analytical techniques" and bilateral project between Austria and Croatia „ Application of MeV SIMS for identification and characterization of ageing properties of synthetic painting materials used in contemporary art".

Abstract 255 MON-IBM01-1

[Invited Talk - Monday 10:30 AM - Bonham C](#)

In-situ characterization by RBS/C of damage evolution and thermal recovery on irradiated 3C-SiC

[Haizhou Xue](#)¹, [Miguel Almenara Crespillo](#)¹, [Yanwen Zhang](#)^{1,2}, [William J Weber](#)^{1,2}

⁽¹⁾*Department of Materials Science and Engineering, University of Tennessee, Department of Materials Science and Engineering, University of Tennessee, Knoxville TN 37996, United States*

⁽²⁾*Materials Science and Technology Division, Oak Ridge National Laboratory, Materials Science and Technology Division, Oak Ridge National Laboratory, Oak Ridge TN 37831, United States*

Single crystalline 3C-SiC (3.8 μm in thickness on Si substrate) was irradiated using 900 keV Si^+ ions at ~ 170 K, 7° off surface normal direction to produce a buried damaged layer with disorder levels from a detectable level to near fully amorphization. Subsequently, the pre-damaged sample was annealed **in-situ** in high vacuum conditions at several higher temperatures following an isochronal process. The disorder fraction before and after each annealing process was determined **in situ** by employing Rutherford Backscattering Spectrometry in channeling geometry (RBS/C).

The isochronal annealing was carried out from 190 K to 670 K for 20 minutes, three stages of annealing were identified: below room temperature, between 420 K and 570 K, and above 570 K. The results are in agreement with a previous annealing study in 6H-SiC [1]. Furthermore, after the 323 K annealing, the sample was hold in high vacuum condition at room temperature (~ 300 K) for 700 hours before the 423 K annealing. The extended room temperature storage leads to an additional moderate damage recovery for the pre-damaged regions, and the quantified disorder level has decreased proportionally to the damage level determined right after the 323 K 20-minute annealing.

In this work we present a systematical study of the damage evolution and thermal recovery, by isochronal and isothermal annealing in a wide temperature range, with the aim of determining the activation energy for the damage recovery processes. The ion-induced defects migration and recombination processes will be presented and the possible mechanisms will be discussed.

Synthesis of silver nanoparticles in MgO and YSZ using low energy ion implantation[M. M. Al-Amar](#)¹, [E. Garratt](#)¹, [S. Vilayurganapathy](#)¹, [A. Dissanayake](#)¹, [S. AlFaify](#)², [A. Kayani](#)¹⁽¹⁾Physics, Western Michigan University, 1903 W Michigan Ave, Kalamazoo MI 49008, United States⁽²⁾Physics, King Khalid University, Abha, Saudi Arabia

Ag nanoparticle formation within the near-surface region of MgO(100) and YSZ(111) has been carried out using direct ion implantation of 69 keV Ag⁺ ions to **fluences** of approximately 1×10^{17} ions/cm². Annealing steps followed by UV/Vis and Rutherford backscattering spectrometry characterized the migration and formation of Ag nanoparticles. In MgO, nanoparticle formation was observed after the first annealing cycle at 1000 °C. Ag migration was observed to halt after 30 hours of annealing, corresponding to saturation in nanoparticle size, estimated to at 13 nm. While saturation in nanoparticles was obtained with MgO, Ag was not detected within YSZ after the first annealing cycle, indicating a loss of Ag to the environment during annealing.

Possible interface superconductivity with coherent quantum CDW transport and soliton condensation phase transition in heterogeneously doped ion implanted NbSe3 single crystals[kalyan sasmal](#), [Dharshana Wijesundera](#), [Irene Rusakova](#), [Zhong Tang](#), [Arnold Guloy](#), [Wei-Kan Chu](#), [John H Miller](#)*Physis, Texas Center for Superconductivity, university of houston, 4444 cullen blvd, apt # 1103, houston Tx 77004, United States*

Aharonov-Bohm quantum interference shows oscillations of period $h/2e$ in conductance $\{vs\}$. magnetic flux of CDW rings above 77 K, reveals macroscopically observable quantum behavior. CDW transports electrons through a linear chain compound all together as the Peierls gaps displace in momentum space along with the entire Fermi Sea, similar to a superconductor. The dV/dI vs. bias at several temps showing a significant drop in zero-bias resistance below 46 K across an ion-implanted boundary suggests possible interfacial superconductivity or a related phase transition near the boundary between ion-implanted and un-implanted regions of a CDW in NbSe3. The data suggests condensation of solitons near the interface. Charge soliton ($\pm 2e$) dislocations could accumulate and condense near the boundary either due to injected charge from non-isoelectronic impurities or due to a sharp gradient in optimum CDW phase between the weakly and strongly pinned regions. Implanted NbSe3 also been studied with TEM.

Electroluminescence of NV centers in diamond induced by ion-beam micro-fabricated graphitic electrodes[Jacopo Forneris](#)^{1,2,3}, [Daniele Gatto Monticone](#)^{1,2,3}, [Paolo Traina](#)⁴, [Veljko Grilj](#)⁵, [Ivo Degiovanni](#)⁴, [Ekaterina Moreva](#)⁴, [Natko Skukan](#)⁵, [Milko Jaksic](#)⁵, [Marco Genovese](#)⁴, [Paolo Olivero](#)^{1,2,3}⁽¹⁾Physics Department and NIS Excellence Centre, University of Torino, via Giuria, 1, Torino 10125, Italy⁽²⁾Istituto Nazionale di Fisica Nucleare (INFN), sez. Torino, via Giuria, 1, Torino 10125, Italy⁽³⁾Consorzio Nazionale Interuniversitario per le Scienze fisiche della Materia (CNISM), via Giuria, 1, Torino 10125, Italy⁽⁴⁾Optics Division, Istituto Nazionale di Ricerca Metrologica (INRIM), Strada delle Cacce 91, Torino 10135, Italy⁽⁵⁾Laboratory for Ion Beam Interactions, Ruder Boskovic Institute, Bijenicka 54, P.O. Box 180, Zagreb 10002, Croatia

Focused MeV ion micro-beams are suitable tools for the direct writing of conductive graphitic channels buried in an insulating single-crystal diamond bulk; their micrometric resolution allows for the fabrication of multi-electrode geometries, which have recently been exploited for the development of solid-state detectors [1] and cellular biosensors [2]. In this work we investigate the effectiveness of the fabrication method for the electrical excitation of color centers in diamond, which are regarded as promising candidates for the development of quantum technologies based on single-photon sources [3].

The optical emission from color centers induced by electrical excitation requires the injection of a moderately high current of charge carriers in the diamond subgap states.

With this purpose, buried graphitic electrode pairs with a $\sim 10\ \mu\text{m}$ spacing were fabricated using a 6 MeV C microbeam at $3\ \mu\text{m}$ below the surface of a single-crystal optical-grade diamond sample.

The electrical characterization of the structures showed low currents at low applied bias voltage, associated with the residual damage in the irradiated lattice. Furthermore, a significant, non-destructive current increase (hundreds of μA) was observed at an effective breakdown voltage of tens of volts.

The electroluminescence imaging was combined with a photoluminescence mapping of the sample using a confocal microscopy setup, in order to identify the active regions along the conductive paths and the residual vacancy distribution associated with the fabrication technique. Measurements evidenced bright electroluminescent emission from native neutrally-charged nitrogen-vacancy centers (NV^0); the acquired spectra highlighted the absence of electroluminescence from residual vacancy clusters associated with radiation damage, suggesting a potential effectiveness of the fabrication method for the development of isolated, electrically-driven single-photon sources.

[1] J. Forneris et al. Nucl. Instr. Meth. B 306 (2013) 181

[2] F. Picollo et al. Adv. Mater 25 (2012) 4696

[3] N. Mizuochi et al., Nature Photonics 6 (2012) 299

Abstract 219 MON-IBM01-5

[Contributed Talk - Monday 10:30 AM - Bonham C](#)

High Energy (MeV) Ion Beam Implantation in INT-WS₂

[Mihai Straticiuc](#)¹, [Alla Zak](#)², [Doru Gheorghe Pacesila](#)³, [Adrian Ionut Rotaru](#)³, [Victor Alexandru Runceanu](#)³, [Ion Burducea](#)¹, [Petru Mihai Racolta](#)¹

⁽¹⁾*Applied Nuclear Physics Department, Horia Hulubei National Institute of Physics and Nuclear Engineering (IFIN-HH), 30 Reactorului St., Magurele Ilfov 077125, Romania*

⁽²⁾*Department of Science, Holon Institute of Technology, Golomb St. 52, Holon 58102, Israel*

⁽³⁾*Tandem Accelerators Department, Horia Hulubei National Institute of Physics and Nuclear Engineering (IFIN-HH), 30 Reactorului St., Magurele Ilfov 077125, Romania*

Niobium ions implantation was performed on tungsten disulfide inorganic nanotubes powder (INT-WS₂) synthesized in a fluidized bed reactor (FBR). A dose of 10^{15} ions/cm² and different beam energies, between 1 MeV and 15 MeV, were delivered by using a 3 MV HVEE Tandetron accelerator recently installed at IFIN-HH, in Romania. In order to determine the modifications induced by the ion beam irradiation in the INT-WS₂ pellets, various nuclear and atomic techniques were

applied: Rutherford Backscattering Spectrometry (RBS), Particle Induced X-ray Emission (PIXE) and Transmission Electron Microscopy (TEM).

Abstract 454 MON-IBM01-6

[Contributed Talk - Monday 10:30 AM - Bonham C](#)

Low Energy Ar⁺ Ion Irradiation Induced Surface Modification in Cadmium Zinc Telluride (CdZnTe)

[Jitendra Kumar Tripathi](#), [Sivanandan S Harilal](#), [Ahmed Hassanein](#)

Center for Materials Under Extreme Environment, School of Nuclear Engineering, Purdue University, West Lafayette IN 47907, United States

In recent years, paramount effort has been invested in developing a range of compound semiconductors with wide band gap and high atomic number (Z) for x- and gamma-ray detectors. Consequently, cadmium zinc telluride (Cd_{1-x}Zn_xTe) has emerged as the most promising materials for these applications. Its quite higher Z values and density ensures relatively superior stopping power compared with other conventional semiconductors and operating temperature close to room temperature. In addition, nano-semiconductor offers strong change in their energy band diagram which leads to a significant change in its properties, such as electrical (the change of free charge carriers concentration and their mobility), optical (absorption coefficient, reflectivity coefficient, and radiative recombination efficiency), mechanical and thermal properties. It has been noticed that even a very small amount of change in dopant (Zn) concentration can cause giant change in its physical and electronic properties.

We report on modifications in structural, stoichiometry and optical properties of CdZnTe surface due to 1keV Ar⁺ ion irradiation as function of ion fluence, using extremely high ion flux of 1.7×10^{17} ions cm⁻² s⁻¹. Atomic force microscopy studies show sequentially change in surface structure as a function of ion fluence, from homogeneously populated nano-hole to sub-micron sized holes which are well geometrically defined in shapes on whole sample (5mm×5mm). Using **in-situ** x-ray photoelectron spectroscopy characterizations, we observed a reduction in Zn concentration (at %) as compared to pristine samples. Raman and photoluminescence spectroscopy studies show almost complete depletion of Te inclusions and slight red shifts due to ion irradiations, respectively. These results indicate for the possibility of large-area surface nanostructuring by ion beams which may be implemented in the fabrication of future CdZnTe-based devices.

Abstract 392 MON-IBM01-7

[Contributed Talk - Monday 10:30 AM - Bonham C](#)

XPS Characterization of β-FeSi₂ formed in Si (100) by high fluence implantation of 50 keV Fe ion and post-thermal vacuum annealing

[Wickramaarachige Jayampath Lakshantha](#)¹, [Mangal S Dhaubhadel](#)¹, [Tilo Reinert](#)¹, [Floyd D Mcdaniel](#)¹, [Bibhudutta Rout](#)^{1,2}

⁽¹⁾*Department of Physics, University of North Texas, 210 Avenue A, Denton Texas 76203, United States*

⁽²⁾*Center for Advanced Research and Technology, University of North Texas, 1155 Union Circle #311427, Denton Texas 76203, United States*

Fe-Si alloy have attracted widespread interest for technological and fundamental reasons. The Fe-Si system provides several iron silicides that have varied and exceptional material properties with applications in the electronic industry. Fe-Si crystallizes in two Silicon rich phase, the tetragonal metallic α-FeSi₂ and orthorhombic semiconducting β-FeSi₂ and Phase transition occurs at $\approx 937^\circ\text{C}$ from β-phase to α-phase. Optical and electron spectroscopic studies show that β-FeSi₂ is a semiconductor with narrow direct band gap of 0.8 eV. With this band gap β-FeSi₂ is favorable for optical fiber communication systems operating at a 1.5 μm wavelength. Among the transition-metal silicide, β-FeSi₂ is the only reported light emitter. Iron disilicide is also the only transition-metal silicon compound reported to occur in both semiconducting and metallic phases.

Polycrystalline β -FeSi₂ was fabricated by 50 keV Fe ion implantation in Si (100) and subsequent vacuum annealing. The depth profile of the implanted Fe atoms in Si (100) were simulated by the widely used transportation of ion in matter (TRIM) computer code as well as by the dynamic transportation of ion in matter code (T-DYN). The stoichiometry and depth distribution of Fe were determined by Rutherford Backscattering (RBS) and β -FeSi₂ structure was determined by x-ray diffraction (XRD). Chemical condition specimen was analyzed by using X-ray photoelectron spectroscopy (XPS). The valence band spectra show features that can be attributed to bonding and non-bonding states. In transition metal silicides, bonding is expressed in terms of hybridization. Therefore, we have investigated the photoelectron spectra of samples. The chemical shifts of Fe 2p_{3/2} peak from their metallic to silicide were studied with their evolutions with heat treatment as well as depth distribution. The concentration of Fe as a function of the sample depth was also determined by XPS.

Abstract 305 MON-MA03-1

[Invited Talk - Monday 10:30 AM - Bonham B](#)

Medical isotope production using high intensity accelerator neutrons

[Yasuki Nagai](#)

Nuclear Engineering Research Collaboration Center, Japan Atomic Energy Agency, Tokai-mura, Naka-gun Ibaraki-ken 319-1195, Japan

^{99m}Tc, the daughter nuclide of ⁹⁹Mo, is the most common radioisotope used in diagnosis. An unscheduled shut down of the reactors in Canada and Netherlands in 2008, which happened again recently, caused the shortage of ⁹⁹Mo, which has triggered widespread discussions on the supply of ⁹⁹Mo. We proposed a new route to produce ⁹⁹Mo by neutron-induced reactions using fast neutrons from an accelerator. Since then, we have carried out all important steps necessary to obtain ^{99m}Tc with high-quality using ⁹⁹Mo, which was produced using accelerator neutrons. On the basis of the results, we propose a prototype facility for the Generation of Radioisotopes with Accelerator Neutrons by Deuterons (GRAND). This facility has a potential to produce also therapeutic radionuclides. Radiopharmaceuticals containing ⁹⁰Y, a pure beta-ray emitter, are used to kill targeted cancer cells. ⁶⁷Cu (T_{1/2} = 62 h), which emits both beta-rays and low-energy gamma-rays, is believed to be a promising radionuclide to be used simultaneously for diagnostic imaging and internal therapy, when their appropriate production routes are established. Successful PET medicine imaging using ¹⁸F (T_{1/2} = 1.8 h) triggered a search for a longer half-life PET radionuclide. ⁶⁴Cu (T_{1/2} = 13 h) is a promising PET radionuclide. A charge exchange reaction, such as (n,p) and (n,He), of a sample nucleus has a sizable cross section at E_n=10-18 MeV. In fact, we proposed new routes to produce carrier-free therapeutic radioisotopes of ⁹⁰Y, ⁶⁴Cu, and ⁶⁷Cu using fast neutrons from an accelerator. It should be mentioned that the medical radionuclides, ⁹⁹Mo, ⁶⁴Cu, ⁶⁷Cu and ⁹⁰Y can be produced with little radionuclide impurity using neutrons from a single accelerator, which can produce 40 MeV 5 mA deuterons. I will talk the overview of the GRAND project and the experimental study of ⁹⁹Mo, ⁶⁴Cu, ⁶⁷Cu and ⁹⁰Y.

Abstract 153 MON-MA03-2

[Contributed Talk - Monday 10:30 AM - Bonham B](#)

Direct Production of ^{99m}Tc via ¹⁰⁰Mo(p,2n) on Small Medical Cyclotrons

[Peter A Zavodszky](#)¹, [F. B  nard](#)², [A. Bernstein](#)³, [K. Buckley](#)⁴, [J. Corsault](#)⁵, [A. Celler](#)⁶, [C. Economou](#)⁷, [T. Eriksson](#)⁸, [M. A. Frontera](#)¹, [V. Hanemaayer](#)⁴, [B. Hook](#)⁴, [M. Kovacs](#)⁵, [J. Klug](#)², [S. McDiarmid](#)⁴, [T. J. Ruth](#)^{2,4}, [C. Shanks](#)³, [J. F. Valliant](#)⁷, [S. Zeisler](#)⁴, [U. Zetterberg](#)⁸, [P. Schaffer](#)⁴

⁽¹⁾Global Research Center, General Electric, 1 Research Circle, Niskayuna NY 12309, United States

⁽²⁾British Columbia Cancer Agency, 675 West 10th Avenue, Vancouver BC V5Z 4E6, Canada

⁽³⁾Mdx, GE Healthcare, 3350 N Ridge Ave, Arlington Heights IL 60004, United States

⁽⁴⁾TRIUMF, 4004 Wesbrook Mall, Vancouver BC V6T 2A3, Canada

⁽⁵⁾Nordal Cyclotron & PET Radiochemistry Facility, Lawson Health Research Institute, 268 Grosvenor Street, London ON N6A 4V6, Canada

⁽⁶⁾Department of Radiology, Medical Imaging Research Group, University of British Columbia, 366-828 West 10th Avenue, Vancouver BC V5Z 1L8, Canada

⁽⁷⁾Centre for Probe Development and Commercialization, McMaster University, 1280 Main Street West, Hamilton ON L8S 4K1, Canada

Past and impending shortages are driving the development of alternative production methods for technetium-99m (^{99m}Tc). The supply chain is shifting from a sensitive infrastructure of a few subsidized, aging research reactors employing highly enriched uranium targets to a diverse network of both local and centralized production capability built on non-HEU reactor targets, sub-critical nuclear processes and medical cyclotron production methods.

From the efforts of a number of Canadian institutions and private industry collaborations, direct production of ^{99m}Tc using medical cyclotrons has recently been advanced from a 1970's academic exercise to a commercial, economically viable solution for regional production. Using GE PETtrace 880 machines our team has established preliminary saturated yields of 1.8±0.2 GBq/μA, translating to approximately 70 and 115 GBq after a 3 or 6 hour irradiation respectively. The team is in the process of assessing the accuracy and reliability of this production value with a goal of optimizing yields by up to 50%.

In medical cyclotrons the residual gas in the vacuum tank contributes to the collisional destruction of the H⁺ ions, limiting the maximum output of the machine. With a novel high-current (2-9 kW) solid target design being tested an expanded capacity of the GE PETtrace is being explored. Efficiency of H⁺ ion acceptance, vacuum management or use of an external ion source are potential solutions for different output intensity levels based on customer needs.

Work underway also includes an evaluation of production method impurities, scale-up, clinical validation, and application for regulatory approval with a goal of introducing a cost-effective process before the Canadian NRU reactor ceases medical isotope production in 2016.

Abstract 282 MON-MA03-3

[Contributed Talk - Monday 10:30 AM - Bonham B](#)

Progress Related to Domestic Production of Mo-99: Accelerator Induced Fission in LEU Solution.

[Sergey Chemerisov](#), [Amanda Youker](#), [John Krebs](#), [Peter Tkac](#), [Dominique Stepinski](#), [David Rotsch](#),
[Michael Kalensky](#), [Roman Gromov](#), [Charles Jonah](#), [Thad Heltemes](#), [George Vandegrift](#), [Andrew Hebden](#)

Argonne National Laboratory, 9700 South Cass Avenue, Argonne IL 60439, United States

The National Nuclear Security Administration's Global Threat Reduction Initiative Program is assisting in accelerating the development of a domestic supply of commercial non-HEU based Mo-99. Argonne National Laboratory is supporting SHINE Medical Technologies in their efforts to become a domestic Mo-99 producer. SHINE plans to produce Mo-99 through the fissioning of an LEU solution as uranyl sulfate using the neutrons produced from high power D/T accelerator.

A significant amount of work has been done at Argonne using tracers for development of Mo-99 separation, recovery, purification, and solution cleanup, but a more complete understanding of the radiation effects on chemistry and Mo-99 separation process are needed. Argonne has developed mini-SHINE experimental setup utilizing high current electron linac and photo-neutron target to simulate fission based production of Mo-99 in LEU solution. Those experiments have four major objectives: quantitate the production rate and composition of radiolytic gases generated during operation of the system under varying conditions of power density, solution temperature, and start-up conditions. Provide information on changes of solution composition (peroxide concentration, iodine and nitrogen speciation, pH, conductivity, solids formation), vs. time, temperature, and fission power. Provide fission produced Mo-99 to demonstrate Mo-recovery from the irradiated solution within hours after end of irradiation and produce 2 Ci of Mo-99 for shipment to the commercial partners.

All data collected during the mini-SHINE experiments will be directly representative of what is expected in the SHINE system. Design of the experimental setup and latest results of the mini-SHINE experiments will be discussed in this presentation.

Abstract 43 MON-MA03-4

[Contributed Talk - Monday 10:30 AM - Bonham B](#)

Design and Thermal-Hydraulic Performance of a Helium Cooled Target for the Production of Medical Isotope ^{99m}Tc

[Keith Woloshun¹](#), [Greg Dale¹](#), [Sergey Chemerisov²](#), [Eric Olivas¹](#), [Michael Holloway¹](#), [Ken Hurtle¹](#),
[Frank Romero¹](#), [Dale Dalmás¹](#), [Angela Naranjo¹](#), [James Harvey³](#)

⁽¹⁾Accelerator Operations Technology, Los Alamos National Laboratory, MS H856, PO Box 1663, Los Alamos NM 87545, United States

⁽²⁾Argonne National Laboratory, Lemont IL, United States

⁽³⁾Northstar Medical Technologies, Chicago IL, United States

Abstract

^{99m}Tc , the daughter isotope of ^{99}Mo , is the most commonly used radioisotope for nuclear medicine in the United States. Under the direction of the National Nuclear Security Administration (NNSA), Los Alamos National Laboratory (LANL) and Argonne National Laboratory (ANL) are partnering with NorthStar Medical Technologies to demonstrate the viability of large-scale ^{99}Mo production using electron accelerators. In this process, ^{99}Mo is produced in an enriched ^{100}Mo target through the $^{100}\text{Mo}(\gamma, n)^{99}\text{Mo}$ reaction. This paper describes the design and performance (test results) of the helium-cooled Mo target to date. Modifications of the target size (diameter and length) continue toward an optimum configuration for isotope production maximization, but with volumetric heating as high as 33 kW/cc the cylindrical target has been segmented into disks to keep the peak heat flux under 1000 W/cm². Changes in electron beam spot size and shape, also continually evolving toward an optimum for both production and cooling, impact of the design and performance of the target. The current status and performance predictions are discussed.

Abstract 321 MON-MA03-5

[Contributed Talk - Monday 10:30 AM - Bonham B](#)

Converter and Target Optimization for the Photonuclear Production of Radioisotopes Using Electron Linear Accelerators

[Bindu KC](#), [Valeriia Starovoitova](#), [Douglas P. Wells](#)

Dept. of Physics, Idaho State University, Pocatello ID 83209-8106, United States

In order to satisfy the long term global demand of radioisotopes, the development of novel methods of production is an important component. Photonuclear production of radioisotopes using an electron accelerator can be an excellent alternative method of radioisotope production to conventional methods that use nuclear reactors and cyclotrons. With the right choice of electron beam parameters, irradiation time, bremsstrahlung converter and target design, the specific activity of photo-produced radioisotopes may be increased significantly. An optimum converter thickness and target geometry was found for the photo-proton production of Cu-67 using an electron accelerator at the Idaho Accelerator Center. Considering four different geometries for a 40 gram zinc target, the specific activity of Cu-67 for each target shape were determined. In this study, the optimization procedure of bremsstrahlung converter and target for the photonuclear production of radioisotopes using electron linear accelerator was investigated in general, and the optimum bremsstrahlung converter thickness and target geometry for Cu-67 production through $^{68}\text{Zn}(\gamma, p)^{67}\text{Cu}$ reaction was found.

Abstract 308 MON-NP01-1

[Invited Talk - Monday 10:30 AM - Travis C/D](#)

The IAEA new Accelerator Knowledge Portal

[Aliz Simon](#)¹, [Jacopo Forneris](#)^{1,3}, [Raymond Li](#)¹, [Julien Demarche](#)^{1,4}, [Martina Levay](#)², [Vishal Baldania](#)²,
[Ralf Kaiser](#)¹

⁽¹⁾*Division of Physical and Chemical Sciences, Physics Section, International Atomic Energy Agency (IAEA), P.O. Box 100, Vienna International Centre, Vienna A-1400, Austria*

⁽²⁾*Division of Information Technology, Business Solutions Section, International Atomic Energy Agency (IAEA), P.O. Box 100, Vienna International Centre, Vienna A-1400, Austria*

⁽³⁾*Physics Department, University of Torino, via P. Giuria 1, Torino 10125, Italy*

⁽⁴⁾*Ion Beam Centre, University of Surrey, Guildford GU2 7XH, United Kingdom*

The IAEA Physics Section is pursuing efforts on utilizing accelerators to support fundamental and applied research, characterize and qualify materials of nuclear interest and provide training of a highly educated nuclear workforce.

The IAEA Physics Section is launching a new Accelerator Knowledge Portal (AKP) for the benefit of accelerator scientists, accelerator users and service providers worldwide. The knowledge portal offers not only a database of MV particle accelerators in the world, but it has several networking and community features in an attempt to bring together the accelerator community, as well as provide information to accelerator users and policy makers, too.

The proposed system consists of two parts:

1) The **Accelerator Database Web site**: a publicly accessible and searchable repository providing detailed information about the world's low- and medium energy accelerators (~150 facilities). The content of the database is contributed by research facilities in the Member States.

2) The **Accelerator Collaboration platform and networking site**: for the particle accelerator community. By providing up-to-date information on relevant conferences, workshops and schools; relevant papers and books; links to relevant software packages and database tools etc. users shall be motivated to regularly return to the site, to contribute content themselves and to build a community around the accelerator database.

The AKP is a community driven website. The main aim of this talk is to introduce the new website to the Accelerator community and demonstrate the above features which are opened for the public and some of them exclusively for registered users.

For more information, registration and update your accelerator facility please visit the AKP:
<http://nucleus.iaea.org/sites/accelerators/>.

Abstract 239 MON-NP01-2

[Invited Talk - Monday 10:30 AM - Travis C/D](#)

Proposal for New World Laboratory: XFEL for protein spectroscopy, Higgs Factory for a million Higgs decays, 100 TeV Hadron Collider for supersymmetry

[Peter McIntyre](#)¹, [Saeed Assadi](#)¹, [Richard York](#)², [Nathaniel Pogue](#)¹, [James Gerity](#)¹, [Joshua Kellams](#)¹,
[Thomas Mann](#)¹, [Christopher Mathewson](#)¹, [Akhdiyor Sattarov](#)¹

⁽¹⁾*Physics, Texas A&M University, Dept. of Physics, College Station Texas 77843, United States*

⁽²⁾*Physics, Michigan State University, Dept. of Physics, College Station Texas 77843, United States*

Suggestions have been made for a 80-100 km circumference Future Circular Collider (FCC) that could ultimately contain a circular e^+e^- ring collider operating as a Higgs Factory as well as a 100 TeV hadron collider. A particular opportunity for this purpose would take advantage of the favorable geotechnology of the rock strata at the SSC site in Texas. A tunnel of up to 270 km circumference could be located in the Austin Chalk and Taylor Marl formations there, for which world-record tunnel advance rates have been recorded for the SSC project. An electron-positron ring collider suitable as a Higgs Factory could be located in the SSC tunnel, which is 50% complete, and a 100 TeV Hadron Collider could be located in a 270 km circumference tunnel. The Hadron Collider would utilize 5 Tesla superconducting magnets, which are a mature technology and readily adapted to industrial manufacture. The injector for the Hadron Collider would be located in the SSC tunnel. Positron production and acceleration for injection to the Higgs Factory requires a ~ 9 GeV recirculating linac, which could also provide optimum beams for two industrial applications: XFEL for femtosecond protein crystallography and X-ray lithography for 19 nm device technology for the next generation of computer electronics.

Abstract 346 MON-NP01-3

[Invited Talk - Monday 10:30 AM - Travis C/D](#)

Experimental nuclear astrophysics research using stable beams at small scale accelerators

[Gabor gyula Kiss](#)

Section of Ion Beam Physics, Institute for Nuclear Research (ATOMKI) of the Hungarian Academy of Sciences , Bem tér 18/c, Debrecen 4026, Hungary

The aim of nuclear astrophysics is to understand those nuclear reactions which are responsible for the energy production of stars and/or playing an important role synthesizing the chemical elements and their isotopes. Experimentally, these reactions need to be studied preferably in the energy range relevant for the given sub-process (in so-called Gamow window) or at least as close as possible to it. This means energies well below the Coulomb barrier where charged particle induced reactions have extremely low cross sections. The measurement of these low cross sections requires the use of special experimental techniques.

In this talk I will introduce the experimental nuclear astrophysics research program of Atomki - which is a "typical" institute equipped only with small scale accelerators (1MV Van de Graaf, 5 MV Van de Graaf, K = 20 cyclotron and a brand new 2MV Tandem). Different astrophysical scenarios and the corresponding research (including gamma spectroscopy-, elastic alpha scattering experiments and cross section determinations using indirect techniques) will be introduced.

Recently, a new tandem accelerator was installed at Atomki, using the new extremely bright beams (200 μ A proton and 50 μ A alpha particle) provided by this accelerator, we initiate a new research program aiming the direct measurements of cross sections relevant for the Hydrogen Burning process - which is the most important burning phase taking place e.g. in the Sun. In my talk I will focus on our aims and opportunities.

Abstract 402 MON-NP01-4

[Invited Talk - Monday 10:30 AM - Travis C/D](#)

The TIGRESS Integrated Plunger Device and In-Beam Gamma-Ray Spectroscopy at TRIUMF

[Philip J. Voss](#)

Department of Chemistry, Simon Fraser University, 8888 University Drive, Burnaby BC V5A 1S6, Canada

Radionuclides far from the valley of beta stability exhibit a variety of interesting properties. Quantifying the evolution of nuclear structure with increasing proton-neutron asymmetry is a major focus of current experimental efforts. High precision gamma-ray spectroscopy plays an important role in this pursuit and provides fundamental probes of the nucleus and stringent tests for theoretical models important to our understanding of these many-bodied systems. At TRIUMF, accelerated beams from the ISAC-II facility permit access to nuclear structure information for a wide range of exotic species via in-beam gamma-ray spectroscopy with TIGRESS, a high-efficiency and Compton-suppressed segmented germanium clover detector array.

Several sophisticated ancillary systems enhance the sensitivity of gamma-ray spectroscopy and provide additional experimental observables. These devices couple to the TIGRESS experimental infrastructure, resulting in a highly specialized and quickly reconfigurable experimental facility for nuclear structure studies. Among these, the TIGRESS Integrated Plunger (TIP) device has recently been developed for precision electromagnetic transition rate measurements by Doppler-shift lifetime techniques and low-energy Coulomb excitation. TIP provides a suite of detectors for charged-particle tagging and light-ion identification following a variety of nuclear reaction mechanisms. In particular, a silicon PIN diode wall, annular silicon segmented detector, and CsI(Tl) scintillator wall have together enabled particle-gamma correlations for reaction channel selectivity and kinematic reconstruction in recent measurements.

These in-beam tests have highlighted the experimental flexibility of TIP with simultaneous and complementary transition rate measurements of self-conjugate ^{36}Ar using Doppler-shift attenuation and sub-barrier Coulomb excitation techniques. In addition, light-ion discrimination via pulse shape analysis of captured CsI(Tl) waveforms has been demonstrated by the selection of the ^{28}Mg two-proton evaporation channel from an $^{18}\text{O} + ^{12}\text{C}$ reaction. This presentation will provide a brief overview of the TIGRESS gamma-ray spectroscopy program, with an emphasis on recent developments and the

implementation of TIP.

Abstract 141 MON-NP01-5

[Invited Talk - Monday 10:30 AM - Travis C/D](#)

ROSPHERE - a dedicated in-beam fast timing HPGe-LaBr₃(Ce) array

[Nicolae Marginean](#)

"Horia Hulubei" National Institute for Physics and Nuclear Engineering, Reactorului 30, Bucharest-Magurele 077125, Romania

The ROSPHERE 4pi array, consisting of HPGe and LaBr₃(Ce) detectors, was built and installed at the TANDEM Laboratory of the "Horia Hulubei" National Institute for Physics and Nuclear Engineering in Bucharest, Romania. This experimental setup is optimized to measure lifetimes of excited nuclear levels from several tens of picoseconds up to nanoseconds using electronic timing method. A description of the array and several selected physics results obtained using ROSPHERE will be presented.

Abstract 383 MON-NST03-1

[Invited Talk - Monday 10:30 AM - Bonham D](#)

Radiation effects on nano mechanics of low dimensional carbon systems

[Joseph Wallace](#), [Lin Shao](#)

Department of Nuclear Engineering, Texas A&M University, 335 R Zachry, College Station Texas 77845, United States

Understanding radiation responses of low dimensional carbon systems is important for their property tuning or applications under harsh environments. In this talk, we will report a few new findings on nanomechanics changes of irradiated carbon nanomaterials: (1) the sliding behaviors of few-layer-graphene in which the displaced atoms act as a seed atom to pull out atoms from graphene planes; (2) the bending buckling and compression buckling of carbon nanotube bundles in which inter-tube displacements promote kink formation but also immobilize kink re-arrangements, leading to higher buckling resistance; (3) self arrangements of a graphene flake upon vacancy loading in which defects lower or remove the energy barriers for rolling into a scroll with final curvature radius depending on defect densities. Most of these findings are obtained from molecular dynamics simulations but a few examples of experimental studies will be discussed and compared with the modeling results.

Abstract 190 MON-NST03-2

[Contributed Talk - Monday 10:30 AM - Bonham D](#)

An ion-beam-based technique to characterize thermal property changes of irradiated carbon nanotubes

[Di Chen](#), [Jing Wang](#), [Lloyd Price](#), [Joseph Wallace](#), [Jonathan Gigax](#), [Xuemei Wang](#), [Lin Shao](#)

Department of Nuclear Engineering, Texas A&M University, 3133 TAMU, College Station TX 77843, United States

For applications in thermal management by using carbon nanomaterials, characterization of their thermal properties usually requires complicated procedures and instrument. We demonstrated the feasibility of using an ion-beam-based technique for in situ characterization of irradiated samples without breaking vacuum. This technique utilizes an ion beam focused to a small point as a heat source to create a thermal gradient over a carbon nanotube film. Concurrently, the sample surface is viewed using an IR (infrared) camera to measure the resulting thermal pattern. By analyzing the spatial and time evolution of heating patterns, thermal diffusivity as well as conductivity can be calculated. The technique can be extended to other nanomaterials for studying irradiation induced thermal property changes.

Abstract 197 MON-NST03-3

[Contributed Talk - Monday 10:30 AM - Bonham D](#)

Irradiation induced thermal property changes of carbon nanotubes

[Jing Wang](#)², [Di Chen](#)¹, [Joseph Wallace](#)¹, [Jonathan Gigax](#)¹, [Xuemei Wang](#)¹, [Lin Shao](#)^{1,2}

⁽¹⁾*Nuclear Engineering, Texas A&M University, 3133 TAMU, College Station TX 77840, United States*

⁽²⁾*Materials Science and Engineering, Texas A&M University, 3003 TAMU, College Station TX 77840, United States*

We studied mechanism of thermal property changes after irradiation on carbon nanotube (CNT) films through integrated molecular dynamics (MD) simulations and experiments. Upon ion irradiation of carbon nanotube (CNT) films, both inter-tube defects and intra-tube defects are introduced. Our MD simulations show that interface thermal resistance between nanotubes is greatly reduced since inter-tube defects among them promote a covalent path for phonon transport. Upon thermal annealing, we found that inter-tube defects are more stable while intra-tube defects can be annihilated or reconstructed to complex configurations. As a result of annealing, axial phonon transport increases due to reduced phonon scattering centers and off-axial phonon transport is sustained due to the high stability of inter-tube defects, leading to further thermal conductivity enhancement. Experimental observations also agree with modeling predictions that thermal conductivities of CNT films have been enhanced after 2 MeV hydrogen ion irradiations and conductivities were further improved upon post irradiation annealing treatment.

Abstract 264 MON-NST03-4

[Contributed Talk - Monday 10:30 AM - Bonham D](#)

Laser induced periodic surface structures in nickel-fullerene hybrid composites

[Jiri Vacik](#), [Vasyl Lavrentiev](#), [Vladimir Havranek](#), [Vladimir Hnatowicz](#)

Nuclear Physics Institute, Academy of Sciences of the Czech Republic, Hlavni 130, Husinec - Rez 25068, Czech Republic

Thin hybrid films, synthesized at room temperature by co-deposition of Ni atoms and C₆₀ molecules on Si(100), were irradiated by an energetic laser beam. The structural form of the systems was analyzed by microprobe, micro-Raman and microscopy (SEM) techniques. The single shot had a profound effect on the hybrid composites. For a small laser spot, determined by a narrow aperture (10 micrometers), two-stage micrometer-sized Ni protrusions, with a narrow (few micrometers) encompassing a-C (amorphous carbon) ring and a broad C₆₀-depleted halo was observed. Contrarily, using a defocused laser beam (a large beam spot) an extensive phase separation with vast, interspersed Ni- and C₆₀(a-C)-rich zones were formed. Surprisingly, in the C₆₀(a-C)-rich regions a number of periodic surface patterns (LIPSS) were produced. The LIPSS patterns consist of a massive several-micrometer sized central a-C nucleus, which is surrounded with an array of tens of Ni/C₆₀(a-C) domains. Here, an architecture and a mechanism of the LIPSS fabrication is discussed.

Abstract 443 MON-RE05-1

[Invited Talk - Monday 10:30 AM - Presidio C](#)

Atomic Structure and Radiation Effects in Complex Oxides

[Kurt Edward Sickafus](#)

Materials Science and Engineering, University of Tennessee, 414F Ferris Engineering Building 1508 Middle Way Drive, Knoxville Tennessee 37996-2100, United States

Complex oxides, that is, oxides with multiple cation constituents, often form crystal structures based on simple layered atomic stacking arrangements, but with special atomic patterns within these layers. These atom patterns can be ordered or disordered, depending on stoichiometry or alternatively, depending on physical effects such as thermal or radiation-induced entropic disorder.

In this presentation, we will consider a layered structure model to describe atomic arrangements in a variety of oxides, from corundum to spinel to fluorite to pyrochlore. We will examine how atomic order varies as a function of compound stoichiometry and how atomic disorder is accommodated within these structures. We will also relate these layered atom arrangements to the radiation damage response of certain model oxide compounds. In particular, we will consider radiation damage effects in spinel and fluorite derivative compounds.

Abstract 122 MON-RE05-2

[Contributed Talk - Monday 10:30 AM - Presidio C](#)

Ion radiation damage in Sr₂Fe_{1.5}Mo_{0.5}O_{6-δ} Perovskite

[Ming Tang](#)¹, [Siwei Wang](#)², [Kyle S. Brinkman](#)², [Fanglin Chen](#)³

⁽¹⁾*Materials Science and Technology Division, Los Alamos National Laboratory, P.O. Box 1663, MS G755, Los Alamos New Mexico 87545, United States*

⁽²⁾*Department of Materials Science and Engineering, Clemson University, Clemson South Carolina 29634, United States*

⁽³⁾*Department of Mechanical Engineering, University of South Carolina, Columbia South Carolina 29208, United States*

The incorporation of radioactive elements in fission products (FPs) into complex oxides, where the elements are constrained in the structure and enhanced leaching and radioactive stability can be obtained, is an active area of research in the nuclear fuel cycle. Perovskite structured $\text{Sr}_2\text{Fe}_{1.5}\text{Mo}_{0.5}\text{O}_{6.8}$ (SFM) has the capability of incorporating several FPs (such as Sr and Mo) into the crystalline network simultaneously while maintaining a stabilized structure. The radiation damage effects on the structure changes of this polycrystalline SFM sample is conducted under various ion irradiations including 200 keV He ions to a fluence of 5×10^{20} ions/m², 100 keV H ions to a fluence of 3×10^{21} ions/cm², and 600 keV Kr ions to a fluence of 2.5×10^{19} ions/m² at room temperature.. Grazing angle incident X-ray Diffraction (GIXRD), transmission electron microscope (TEM), Raman, X-ray photoelectron spectroscopy (XPS), and Mossbauer Spectroscopy characterizations are conducted to detect the surface structural changes as well as possible secondary phases of SFM. The irradiated SFM sample decomposes into a layered $\text{Sr}_4\text{FeMoO}_{8.8}$ phase and a metallic Fe phase under light ion (He and H) irradiations. Nano-crystallized secondary phase was observed with particle sizes around 7 nm. These results suggest that irradiation-induced reducing atmospheres may affect the stability of crystalline structure in complex oxides. Experiment results also reveal an amorphization in the heavy ion Kr irradiated sample, while no amorphization is observed in He and H irradiated SFM.

Abstract 406 MON-RE05-3

[Contributed Talk - Monday 10:30 AM - Presidio C](#)

Micro-bumps on the surface of borosilicate glasses induced by ion irradiation

[Tieshan wang](#), [Genfa Zhang](#), [Liang Chen](#), [Wei Yuan](#), [Limin Zhang](#), [Haibo Peng](#), [Xin Du](#)

School of Nuclear Science and Technology, Lanzhou University, Tianshuinan Road 222, Lanzhou Gansu 730000, China

In order to study the irradiation effect of borosilicate glasses, 5MeV Xe^{q+} ions were used to irradiate two kinds of borosilicate glasses. The irradiated samples were characterized by optical microscopy, Atomic Force Microscopy (AFM) and Raman spectroscopy etc. methods. Micro-bumps were observed on the irradiated sample surface which was irradiated over 5×10^{13} ion/cm². The size and density of bumps increase versus the irradiation dose. While the dose is over 9×10^{15} ions/cm², the size and density of bumps are saturated. But the height of bumps increases with further irradiation. Micro-bumps distribute almost homogenous and become orderly after a saturation dose. The bumps are condensed and swelling up. The phase separation of glass surface is found by Raman spectrum. The hardness of irradiated glasses surface decreases about 14 percents after a dose of 2.0×10^{16} ions/cm². Micro-bumps were considered to be formed by phase separation and swelling of volume. The orderly distribution should be caused by inner stress in damaged near surface region. This phenomenon is interesting and might have potential application for changing the optical characterization and function of glass surface.

Abstract 451 MON-RE05-4

[Invited Talk - Monday 10:30 AM - Presidio C](#)

Ion beams studies of the radiation chemistry and radiation damage of materials important in nuclear power.

[Andrew D Smith](#), [Simon M Pimblott](#)

Dalton Cumbrian Facility, University of Manchester, Westlakes Science & Technology Park, Moor Row Cumbria CA24 3HA, United Kingdom

The Dalton Cumbrian Facility (DCF) is a new institute formed in partnership between the University of Manchester and the UK's nuclear power industry. Areas of research interest include the study of radiation damage to materials proposed for the construction of next generation fission and fusion reactors; damage to materials used for containment of long term storage; and the radiation impact to geological structures encountered in sites proposed for deep long term deposition.

A central component of the DCF is a 5 MV tandem electrostatic ion accelerator dedicated to the challenges of the UK nuclear legacy and future generation power production. The Pelletron accelerator is equipped with ion sources capable of

generating either high current light ions (proton & alpha) or lower current high Z ions, whilst the provision of 6 beamlines split between two separate target rooms allows for the installation of end stations to support simulated accelerated radiation damage experiments under ambient or extreme temperature and pressure conditions, or to conduct radiochemistry studies with minimal downtime between experiments.

We will present an outline of the DCF research programme and the capabilities of the DCF accelerator and beamlines in addressing these interests. The presentation will include initial results from the first experiments conducted with the ion beam accelerator and conclude with the addition to our facilities of a second ion beam accelerator to create a dual beam system and the inclusion of Rutherford Backscattering and PIXE ion beam analysis.

Abstract 428 MON-RE05-5

[Contributed Talk - Monday 10:30 AM - Presidio C](#)

Defect Analysis of Heavy Ion-Irradiation of Polyethylene and Composites with Martian Regolith

[Naidu V. Seetala](#), [Naeem Tull-Walker](#)

Department of Mathematics and Physics, Grambling State University, Carver Hall 81, 305 Main Street, Grambling LA 71245, United States

We have used SRIM-2013 computer code to estimate the irradiation parameters and the defect concentrations in Ultra High Molecular Weight Polyethylene (UHMWPE) and composites with the addition of Martian Regolith (UHMWPE-MR) subjected to irradiation with 56Fe heavy ions at an energy of 600 MeV/u to three different doses (10, 32, 64 Gy). Our previously reported Positron Annihilation Lifetime Spectroscopy (PALS) studies showed larger variations in positron lifetime parameters with increasing irradiation dose for UHMWPE polymer compared to UHMWPE+MR composite. TRIM analysis is used to include cascade damage effects and defect concentrations and their variations with irradiation dose are correlated to explain the variations observed in vacancy defects, nanoporosity, and fractional free volume obtained from PALS. The variations in defect parameters may indicate change in defect kinetics as irradiation dose increases such as: 1) vacancy defects aggregation and 2) formation of smaller pores at high doses as some vacancies escape from the hot spots created within the collision cascades at higher doses due to local heating and vacancy mobility increase.

The work is partly supported by NASA-CIPAIR grant, Award# NNX09AU97G.

Abstract 143 MON-ATF02-1

[Invited Talk - Monday 2:00 PM - Presidio A](#)

Accelerator-Driven Subcritical Assembly for the Production of Molybdenum-99

[Evan Sengbusch](#)¹, [Ross Radcliff](#)¹, [Logan Campbell](#)¹, [Arne Kobernick](#)¹, [Tye Gribb](#)¹, [Casey Lamers](#)¹,
[Chris Seyfert](#)¹, [Katrina Pitas](#)², [Greg Piefer](#)²

⁽¹⁾Phoenix Nuclear Labs, 2555 Industrial Drive, Monona WI 53713, United States

⁽²⁾SHINE Medical Technologies, 2555 Industrial Drive, Monona WI 53713, United States

Phoenix Nuclear Labs (PNL) has designed and built a high yield neutron generator that will drive a subcritical assembly developed by SHINE Medical Technologies to produce the medical radioisotope molybdenum-99. The PNL neutron generator demonstrated neutron yields greater than 3×10^{11} n/s in the spring of 2013 using the deuterium-deuterium (DD) fusion reaction. It utilizes a proprietary gas target coupled with a custom 300kV accelerator and a microwave ion source (MWS). Experiences operating and optimizing the various subsystems (ion source, accelerator, focus element, differential pumping stages, and gas target) will be described. System performance will be characterized in terms of beam current and voltage, measured neutron yield, and operational reliability. PNL is targeting delivery of 3 neutron generators with yields of 5×10^{13} deuterium-tritium (DT) n/s in early 2016 to SHINE's molybdenum-99 production facility. The accelerator-driven,

low-enriched uranium (LEU) solution geometry will be optimized for high-efficiency isotope production. Neutrons produced by the PNL neutron generator drive fission in the subcritical LEU solution. Hydrogen and oxygen from radiolysis of water in the solution are continuously recombined during operation. The LEU solution is irradiated for approximately a week, then medical isotopes are extracted from the solution, purified using established techniques and packaged for sale. The LEU solution is recycled, achieving extremely efficient use of uranium and significantly less waste generation than current methods. The process produces medical isotopes that fit seamlessly into existing supply chains while eliminating the use of weapons-grade uranium and reliance on aging nuclear reactors. PNL neutron generator prototype I has demonstrated 1,000+ hours of operation. Prototype II is operational and undergoing system reliability testing. Target solution chemistry has been selected; target geometry has been optimized and prototyped. ^{99}Mo separation at >97% efficiency has been demonstrated.

Abstract 476 MON-ATF02-2

[Contributed Talk - Monday 2:00 PM](#) - [Presidio A](#)

Development of a Visualization System for Charged Particles Shapes Superimposed on the Waveform of the Cyclotron Frequency

[Faisal M Alrumayan](#)^{1,2}, [Amro M Hendy](#)², [Ibtesam Badhress](#)³

⁽¹⁾*Research Centre, King Faisal Specialist Hospital, Takhasosy Road, Riyadh Riyadh 11211, Saudi Arabia*

⁽²⁾*Research Centre, King Faisal Specialist Hospital, Takhasosy Road, Riyadh Riyadh 11211, Saudi Arabia*

⁽³⁾*Department of Physics and Mathematics, King Abdulaziz City for Science and Technology (KACST), Prince Turki Road, Riyadh Riyadh 11211, Saudi Arabia*

Beam instrumentation systems play an important role in determining the quality of beam bunches as they being measured. A fast current transformer (FCT) usually is used to pick beam bunches as they pass through it. Due to their high repetition rate, beam bunches expected from a Cyclotron should be detected by a FCT of rise time and sensitivity of 1 ns and 5 V/A, respectively. Additionally, the small signal from the FCT is connected to a low noise amplifier for eliminating high frequency noise. We have developed an imaging system to visualize the bunches being superimposed on the RF waveform (the cyclotron frequency is 26.9 MHz). Data will be presented.

Abstract 24 MON-ATF02-3

[Contributed Talk - Monday 2:00 PM](#) - [Presidio A](#)

Production of Medical and Industrial Isotopes Using a Superconducting Electron Linac

[Valeriia N Starovoitova](#)¹, [Chase H Boulware](#)¹, [Terry L Grimm](#)¹, [Dyle D Henning](#)¹, [Jerry L Hollister](#)¹,
[Erik S Maddock](#)¹, [Frank Harmon](#)², [Jon L Stoner](#)²

⁽¹⁾*Niowave, Inc, 1012 N. Walnut St, Lansing MI 48906, United States*

⁽²⁾*Idaho Accelerator Center, Idaho State University, 1500 Alvin Ricken Dr, Pocatello ID 83201, United States*

The majority of radioisotopes used in the U.S. today come from foreign suppliers or are generated parasitically in large government accelerators and reactors. Both of these restrictions limit the availability of radioisotopes, especially short-lived ones, and it discourages the development and evaluation of new isotopes and radiopharmaceuticals. Linacs are an excellent alternative to nuclear reactors for production of many isotopes such as ^{67}Cu , ^{99}Mo , and ^{225}Ac . Linacs operate at much lower costs than nuclear reactors and produce far smaller waste streams. Initial capital costs are a fraction of nuclear reactors and time to production is far quicker. Despite these advantages, electron linacs have not been widely used for isotope production as of today, mostly due to the absence of affordable high power accelerators and bremsstrahlung converters.

In this talk we will present the design of a production setup based on a superconducting electron accelerator equipped with a liquid metal bremsstrahlung converter. The converter will be capable of dissipating hundreds of kilowatts of electron beam power and providing very high photon flux density, over 10^{17} photons/cm² per second for a 40 MeV, 2.5 mA electron beam. We will show the results of the initial testing of a prototype Pb-Bi eutectic (LBE) converter. We will also present the results of the studies of conversion efficiency, power handling and yields of several isotopes including ⁶⁷Cu, ⁹⁹Mo, and ²²⁵Ac using a superconducting linac and a liquid metal converter.

Abstract 280 MON-ATF02-4

[Contributed Talk - Monday 2:00 PM - Presidio A](#)

Accelerator Based Domestic Production of Mo-99: Photonuclear Approach

[Sergey Chemerisov](#)¹, [George Vandegrift](#)¹, [Gregory Dale](#)², [Peter Tkac](#)¹, [Roman Gromov](#)¹, [Vakho Makarashvili](#)¹, [Bradley Micklich](#)¹, [Charles Jonah](#)¹, [Keith Woloshun](#)², [Michael Holloway](#)², [Frank Romero](#)², [James Harvey](#)³

⁽¹⁾Argonne National Laboratory, 9700 South Cass Avenue, Argonne IL 60439, United States

⁽²⁾Los Alamos National Laboratory, P.O. Box 1663, Los Alamos NM 87545, United States

⁽³⁾NorthStar Medical Technologies, LLC, 52 Femrite Drive, Madison WI 53718, United States

The National Nuclear Security Administration's (NNSA) Global Threat Reduction Initiative (GTRI), in partnership with commercial entities and the US national laboratories, is working to accelerate the establishment of a reliable domestic supply of Mo-99 for nuclear medicine while also minimizing the civilian use of HEU. Argonne National Laboratory (ANL) and Los Alamos National Laboratory (LANL) are supporting NorthStar Medical Technologies in their efforts to become a domestic Mo-99 producer. NorthStar Medical Technologies, LLC is utilizing the photonuclear reaction in an enriched Mo-100 target for the production of Mo-99.

In this approach a high-power electron accelerator is used to produce the required flux of high energy photons through the bremsstrahlung process. Due to the small photon cross section for the reaction and high cost of the enriched 100Mo material, one would want to use the highest photon flux available. That leads to a high thermal load on the target. The ability to remove heat from the target is a limiting factor in the production of Mo-99. A pressurized gaseous-He cooling system was developed by LANL and installed and tested at ANL to allow study of the thermal performance of the target and production of Mo-99. Irradiation of the target will be conducted at different beam energies to study the side reactions and effect of impurities in enriched Mo-100. Other investigations include calculation for development of the requirement of the facility shielding, beam transport components, beam diagnostic and components reliability studies.

So far we have performed five demonstration of the Mo-99 production, with natural and enriched Mo-100, utilizing liquid (water) and gaseous-He cooling. Those experiments have demonstrated production of the Mo-99 at relatively high beam power on the target and effective separation of the Tc-99m from low-specific-activity Mo targets. This presentation will review the current status of the project.

Abstract 329 MON-HSD03-1

[Invited Talk - Monday 2:00 PM - Travis A/B](#)

An Overview of Active Interrogation

[James D Silk](#)

This talk will present an overview of efforts to develop active interrogation techniques to stimulate fission in uranium at standoff distances. Starting from the earliest days of proof-of-concept experiments using a Varitron medical LINAC, work has progressed using various interrogating species (photons, neutrons, protons, muons) generated from a diverse range of sources such as LINACs, cyclotrons, and laser wakefield generators. Additionally, a brief review of the challenges encountered by the techniques will be presented such as dose, experimental facilities, detectors, etc. Some of these challenges overlap with other CAARI sessions, while others are unique to the long standoff detection mission.

Abstract 146 MON-HSD03-2

[Invited Talk - Monday 2:00 PM - Travis A/B](#)

APPLICATION OF INTENSE, SINGLE-PULSE BREMSSTRAHLUNG TO THE PROBLEM OF FINDING FISSILE MATERIAL*

[R. J. Commisso](#)¹, [J. P. Apruzese](#)¹, [G. Cooperstein](#)¹, [D. D. Hinshelwood](#)¹, [S. L. Jackson](#)¹, [D. Mosher](#)¹, [D. P. Murphy](#)¹, [J. W. Schumer](#)¹, [S. B. Swanekamp](#)¹, [F. C. Young](#)¹, [J. C. Zier](#)¹, [P. F. Ottinger](#)¹, [B. V. Weber](#)¹, [B. F. Phlips](#)², [A. L. Hutcheson](#)², [L. J. Mitchell](#)², [R. S. Woolf](#)², [E. A. Wulf](#)², [A. W. Hunt](#)³, [Z. M. Larsen](#)³, [E. S. Cardenas](#)³

⁽¹⁾Plasma Physics Division, Naval Research Laboratory, 4555 Overlook Ave SW, Washington DC 20375, United States

⁽²⁾Space Sciences Division, Naval Research Laboratory, 4555 Overlook Ave SW, Washington DC 20375, United States

⁽³⁾Idaho Accelerator Center, Idaho State University, 1500 Alvin Ricken Drive, Pocatello ID 83201, United States

Developing techniques for finding contraband fissile material is an important activity for national and international security.¹ Because passive radiation from fissile material is relatively weak and can be readily shielded, "active" techniques have been investigated.² In one approach, fission is induced by bremsstrahlung. The products of the fission are then measured. Usually, relatively low-peak-power linacs produce the bremsstrahlung. Discussed here are results from a new approach called intense pulsed active detection (IPAD).³ With IPAD, TW-level (electrical) generators produce intense, short (< 100-ns) bremsstrahlung pulses. The short pulse allows access to a variety of fission signatures over relatively short counting times (~ 10 microseconds to ~ 1 min). The resulting short fission-product measurement time minimizes the natural background.³ Inductive voltage adders (8 MV/200 kA and 300 kA, 12 MV/300 kA, and 16 MV/600 kA, ~ 50 ns) are used to produce the bremsstrahlung. Induced-fission experiments using depleted uranium resulted in measurement of fission signatures unambiguously higher than the induced and passive backgrounds. These signatures include prompt and delayed neutrons and delayed gammas. Conventional nuclear detectors were modified to operate in the harsh environment and a new, high-energy neutron detector was developed. The MCNPX Monte Carlo transport code was benchmarked against measurements and used to guide experiments and detector design.

1. T. B. Cochran and M. G. McKinzie, "Detecting nuclear smuggling," Sci. Am., 298, pp. 98-104, April 2008.

2. Robert C. Runkle, et al., "Rattling nucleons: New developments in active interrogation of special nuclear material, Nuclear Instruments and Methods in Physics Research A, 663, pp. 75 - 95 (2012).

3. S.B. Swanekamp, et al., IEEE Trans. Nucl. Sci., 58, pp. 2047-2054 (2011).

a. Independent consultants to NRL through Engility Corp., Chantilly VA 20151

b. National Research Council Research Associate

* Work supported by DTRA and ONR.

Narrowband and tunable all-laser-driven inverse-Compton x-ray source

[Sudeep Banerjee](#)¹, [S. Chen](#)¹, [G. Golovin](#)¹, [N. Powers](#)¹, [C. Liu](#)¹, [J. Jhang](#)¹, [B. Zhao](#)¹, [I. Ghebregziabher](#)¹, [J. Mills](#)¹, [K. Brown](#)¹, [C. Petersen](#)¹, [D. P. Umstadter](#)¹, [S. Clarke](#)², [C. Miller](#)², [S. Pozzi](#)²

⁽¹⁾*Physics and Astronomy, University of Nebraska, Lincoln NE 68588, United States*

⁽²⁾*Nuclear Engineering and Radiological Sciences, University of Michigan, Ann Arbor MI 48109, United States*

We discuss the development of a compact x-ray source based on inverse-Compton scattering with a laser-driven electron beam.¹ This source produces a beam of high-energy x-rays in a narrow cone angle (5-10 mrad), at a rate of 10^7 photons-s⁻¹. Tunable operation of the source over a large energy range, with energy spread of ~50%, has also been demonstrated.² Photon energies > 10 MeV have been obtained. The narrowband nature of the source is advantageous for radiography with low dose, low noise, and minimal shielding.

1. S. Chen et al., Phys. Rev. Lett. **110**, 155003 (2013).

2. N. Powers et al., Nat. Photonics **8**, 031302 (2014); published online on 1/12/13.

Advanced Low-Beta Cavity Development for Proton and Ion Accelerators

[Zachary A Conway](#), [Michael P Kelly](#), [Peter N Ostroumov](#)

Physics, Argonne National Laboratory, 9700 S. Cass Ave., Argonne IL 60439, United States

Recent developments in designing and processing low-beta superconducting cavities at Argonne National Laboratory are very encouraging for future applications requiring compact proton and ion accelerators. One of the major benefits of these accelerating structures is achieving real-estate accelerating gradients greater than 3 MV/m very efficiently either continuously or for long-duty cycle operation (> 1%). The technology is being implemented in low-beta accelerator cryomodules for both the Argonne ATLAS Heavy-Ion linac and the Fermilab Proton Improvement Project-II driver accelerator where the cryomodules are required to have real-estate gradients of more than 3 MV/m. In offline testing low-beta cavities with even higher gradients have already been achieved. This presentation will review this work and give examples of where performance can be pushed even further.

A Novel Compact Accelerator for Proton Interrogation

[Carol Johnstone](#), [Richard Ford](#), [Fred Mills](#)

Particle Accelerator Corporation, 809 Pottawatomie Tr, Batavia IL 60510, United States

A promising approach for remote detection of special nuclear materials (SNM) and nuclear weapons is proton interrogation in which an energetic proton beam is passed through cargo, and, if nuclear materials are present, induces emission of

characteristic radiation, which can be identified. An effective application would require an ultra-compact, stable, and mobile proton accelerator delivering a 1-4-GeV beam with a current up to 1 mA; a technology currently not available. A comprehensive trade study was initiated to review the state of the art in accelerator technologies and recent innovations to identify the potential to develop such a practical interrogation system. Two potential hybrid accelerators were identified as a result of this trade study. One successful implementation is a two-stage 800MeV Fixed Field Alternating Gradient Accelerator (FFAG) in a novel compact racetrack format. The second is a two stage 600-MeV "folded" linac with a 330-MeV FFAG injector to decrease the overall length - an even more compact version of the cyclinac concept. The technical innovations and dynamic studies of the FFAG are reported here.

Abstract 98 MON-IBM04-1

[Invited Talk - Monday 2:00 PM - Bonham C](#)

Probing Environmental and Energy Liquid Surfaces and Interfaces Using Time-of-Flight Secondary Ion Mass Spectrometry

[Xiao-Ying Yu](#)¹, [Zihua Zhu](#)², [Bingwen Liu](#)¹, [Matthew Marshall](#)³, [Xin Hua](#)¹, [Zhaoying Wang](#)², [Li Yang](#)⁴, [Abigail Tucker](#)³, [William Chrisler](#)³, [Eric Hill](#)³, [Theva Thevuthasan](#)², [James Cowin](#)⁴

⁽¹⁾*Atmospheric Sciences and Global Climate Change Division, Pacific Northwest National Laboratory, Richland WA 99354, United States*

⁽²⁾*W. R & Wiley Environmental Molecular Science Laboratory, Pacific Northwest National Laboratory, Richland WA 99352, United States*

⁽³⁾*Biological Sciences Division, Pacific Northwest National Laboratory, Richland WA 99352, United States*

⁽⁴⁾*Chemical and Materials Sciences Division, Pacific Northwest National Laboratory, Richland WA 99352, United States*

The surfaces of aqueous phases and films can have unique kinetics and thermodynamics, distinct from the bulk. However, major surface analytical techniques are mostly vacuum-based and direct applications for volatile liquid studies are difficult. We developed a vacuum compatible microfluidic interface to enable surface analysis of liquids and liquid-solid interactions. The unique aspect of our approach is that 1) the detection window is an aperture of 2-3 mm in diameter, which allows direct detection of the liquid surface, and 2) it uses surface tension to hold the liquid within the aperture. The microfluidic reactor is composed of a silicon nitride (SiN) membrane and polydimethylsiloxane (PDMS). Its application in ToF-SIMS as an analytical tool was evaluated. Most recently, we demonstrated *in situ* probing of the electrode-electrolyte solution interface using a new electrochemical probe based on our original invention. A classical electrochemical system consisting of gold working electrode, platinum counter electrode, platinum reference electrode, and dilute potassium iodide electrolyte solution was used to demonstrate real-time observation of the gold iodide adlayer on the electrode and chemical species as a result of redox reactions using cyclic voltammetry (CV) and time-of-flight secondary ion mass spectrometry (ToF-SIMS) simultaneously. It provides direct observation of the surface and diffused layer with chemical speciation in liquids using ToF-SIMS for the first time. Moreover, we extended the microfluidic reactor for biofilm growth and real-time chemical mapping. Our results provided the first ToF-SIMS molecular imaging of the hydrated biofilm using this unique capability.

Abstract 88 MON-IBM04-2

[Invited Talk - Monday 2:00 PM - Bonham C](#)

Possibilities and Limitations of MeV-SIMS for Biological Applications

[Makiko FUJII](#)¹, [Masakazu KUSAKARI](#)², [Toshio SEKI](#)², [Takaaki AOKI](#)³, [Jiro MATSUO](#)¹

⁽¹⁾*Quantum Science and Engineering Center, Kyoto University, Gokasho, Uji Kyoto 611-0011, Japan*

⁽²⁾*Department of Nuclear Engineering, Kyoto University, Gokasho, Uji Kyoto 611-0011, Japan*

⁽³⁾*Department of Electronic Science and Engineering, Kyoto University, Nishikyo-ku, Kyoto Kyoto 615-8510, Japan*

In recent years, mass spectrometry of biological materials has been extensively performed in pharmacokinetic and metabolic studies. Secondary Ion Mass Spectrometry utilizing MeV-energy projectiles as primary probe, MeV-SIMS, is one of the most promising biological analysis techniques because of the high secondary ion yields of large organic molecules and the high convergence property. On the other hand, appropriate sample preparation is required for biological

analysis because biological samples include numerous varieties of volatile substances. MeV-energy SIMS can offer a solution on that aspect as well. Projectiles with energy in the MeV range have a distinctively longer flight path than in the keV-energy range, and a sample chamber with low vacuum conditions can be obtained. We have been developing MeV-SIMS apparatus with orthogonal acceleration time-of-flight mass spectrometer (oa ToF-MS), which allows us to utilize continuous beam and achieves high mass resolution and high secondary ion efficiency.

In this study, liquid sample measurements with MeV-SIMS apparatus are mainly presented. Some fatty acids and higher alcohols with different vapor pressures were analyzed with MeV-SIMS under low vacuum conditions. In addition, studies on the imaging mass spectrometry and detection limit using MeV-SIMS are discussed for biological applications.

Acknowledgement

This study was supported in part by Research Fellowship for Young Scientists from the Japan Society for the Promotion of Science (JSPS).

Abstract 158 MON-IBM04-3

[Invited Talk - Monday 2:00 PM - Bonham C](#)

AP-MeV-SIMS at Surrey - a new ambient pressure SIMS system for molecular concentration mapping.

[Roger P Webb](#)¹, [Geoff W Grime](#)¹, [Vladimir Palitsin](#)¹, [Julien Demarche](#)¹, [Luke D Antwis](#)¹, [Brian N Jones](#)²

⁽¹⁾*Surrey Ion Beam Centre, University of Surrey, Surrey Ion Beam Centre, Guildford Surrey GU2 7XH, United Kingdom*

⁽²⁾*Labec, INFN, via Sansone 1, Florence 50019, Italy*

We describe the Ambient Pressure MeV Secondary Ion Mass Spectrometry system under construction at the University of Surrey. It has been shown that the system is capable of collecting molecular concentration maps on a surface in full ambient conditions. We have so far demonstrated a spatial resolution of 4microns - already better than other ambient pressure techniques available currently. We demonstrate how it is essential to use PIXE as well as MeV-SIMS to obtain the images particularly in the case where there are conducting elements present.

We describe the advantages and disadvantages of this new technique and explain the difficulties of extracting secondary ions through ambient and into a mass spectrometer.

Abstract 467 MON-MA01-1

[Invited Talk - Monday 2:00 PM - Bonham B](#)

Current advances in the biological optimization of proton treatment plans

[Alejandro Carabe](#), [Marcus Fager](#), [Daniel Sanchez](#), [Consuelo Guardiola](#), [Maura Kirk](#), [Malorie Stowe](#), [Brendan Burgdorf](#), [Eric Diffenderfer](#), [Tim Solberg](#)

Radiation Oncology, University of Pennsylvania, 3400 Civic Center Boulevard, Philadelphia Pennsylvania 19104, United States

The variation of the relative biological effectiveness (RBE) of protons along their path offers the possibility of optimizing proton treatment plans to enhance their therapeutic ratio. However, the current uncertainties in the dependency of protons

RBE with biological and physical parameters, makes difficult the clinical implementation of a spatially variable RBE. Current trends in proton treatment planning indicate that Linear Energy Transfer (LET) painting of the target may have favorable dosimetric and biological effects in the treatment. For instance, it has been proven that by increasing the LET in the prostate, it is possible to reduce the dose required to maintain the same biological effectiveness of the treatment by up to 13%, which would have important consequences regarding the dose to the normal tissues as well as the total treatment time. However, the application of LET painting to proton treatment planning requires especial consideration to the robustness of such plans.

The advantage of using LET to optimize proton treatments is that the optimization will be based on a well defined parameter that can be calculated by physical means such as monte carlo (MC) methods. However, especial consideration needs to be given to how LET is calculated in MC as well as clinical relevant aspects such the voxel size of the CT images used to create the treatment plans where these calculations are performed.

Therefore, we will discuss the current uncertainties related to proton RBE with respect variables such as dose, LET and a/b ratios, and treatment planning strategies that could help to minimize the biological impact of such uncertainties. Also, the technological requirements needed for a proton accelerator system to deliver such treatment will be revised. Finally, research trends in the fields of experimental radiobiology and micro-/nano-technology will be discussed in relation to methods to reduce uncertainty in the calculation of proton RBE.

Abstract 461 MON-MA01-2

[Invited Talk - Monday 2:00 PM - Bonham B](#)

High-throughput Mapping of Proton Biologic Effect

[Lawrence Bronk](#)¹, [Fada Guan](#)², [Matt Kerr](#)², [Uwe Titt](#)², [Dragan Mirkovic](#)², [Jeffrey Dinh](#)³, [Steven Lin](#)³,
[Radhe Mohan](#)², [David Grosshans](#)³

⁽¹⁾*Department of Experimental Radiation Oncology, The University of Texas MD Anderson Cancer Center, 1515 Holcombe Blvd, Houston TX 77030, United States*

⁽²⁾*Department of Radiation Physics, The University of Texas MD Anderson Cancer Center, 1515 Holcombe Blvd, Houston TX 77030, United States*

⁽³⁾*Department of Radiation Oncology, The University of Texas MD Anderson Cancer Center, 1515 Holcombe Blvd, Houston TX 77030, United States*

The use of beams containing a broad energy spectrum of protons has made it difficult to thoroughly characterize unique parameters of a single proton beam while simultaneously obscuring spatially-dependent biological effects. With spot scanning, the therapy beam approximately consists of a single beam, enabling us to probe the effects of beam parameters on cellular survival. We aim to relate the biological effects of proton therapy to beam LET and dose using a newly designed irradiation apparatus capable of performing high-throughput screening techniques. The device consists of a custom-fabricated plate holder that enables simultaneous irradiation at 12 different locations along the proton beam path with each location corresponding to a column in a standard 96-well plate. Each column receives a specific LET-dose combination. Numerous dose-LET pairings are examined by incrementing the total number of dose repainting to sample survival data over the entire beam path. In our initial study, H460 lung cancer cells were irradiated using a clinical 80MeV-scanning beam. Irradiation with increasing LETs resulted in decreased cell survival. This trend was obscured at lower LET values in the plateau region but was evident for LET values at and beyond the Bragg peak. Data fits revealed the surviving fraction at a dose of 2Gy (SF2) to be 0.48 for the lowest tested LET (1.55keV/um), 0.47 at the end of the plateau region (4.74keV/um) and 0.33 for protons at the Bragg peak (10.35keV/um). Beyond the Bragg peak SF2s of 0.16 for 15.01keV/um, 0.02 for 16.79keV/um, and 0.004 for 18.06keV/um were measured. We have shown our methodology enables high-content automated screening for proton irradiations over a broad range of LETs. The observed decrease in cellular survival in high-LET regions confirms an increased relative biological effectiveness (RBE) of the radiation and suggests optimization of clinical outcomes will require further evaluation of proton RBE values.

Radiobiological Modeling of High-Throughput Proton Irradiation Cell Survival Experiments

[Christopher Peeler](#)^{1,2}, [Reza Taleei](#)², [Fada Guan](#)², [Lawrence Bronk](#)³, [David Grosshans](#)⁴, [Dragan Mirkovic](#)², [Uwe Titt](#)², [Radhe Mohan](#)²

⁽¹⁾*Graduate School of Biomedical Sciences, University of Texas, 6767 Bertner Ave., Houston TX 77030, United States*

⁽²⁾*Department of Radiation Physics, The University of Texas MD Anderson Cancer Center, 1515 Holcombe Blvd., Houston, TX 77030, United States*

⁽³⁾*Department of Experimental Radiation Oncology, The University of Texas MD Anderson Cancer Center, 1515 Holcombe Blvd., Houston, TX 77030, United States*

⁽⁴⁾*Department of Radiation Oncology, The University of Texas MD Anderson Cancer Center, 1515 Holcombe Blvd., Houston, TX 77030, United States*

Modeling of proton beam biologic effect has been performed on the compiled data sets from a number of different labs, introducing many variables into the data such as differences in experimental techniques, definitions of quantities and their subsequent calculation, and the analytic methods employed. The consequence is that similarly defined experiments, with regard to proton energy and LET and the cell type used, can produce differing results. The purpose of this work is to determine the capability of selected radiobiological models to accurately recreate the results collected from single-institution high-throughput cell survival experiments performed with the H460 human lung cancer cell line. In an attempt to model the results obtained from these experiments, two models have been employed: a basic linear-scaling model and the more mechanistic repair-misrepair-fixation (RMF) model. Linear regression analysis was performed to determine the model coefficients necessary for each to reproduce the results. It was found that both alpha and beta coefficients for protons begin to increase in a non-linear fashion for LET values in the range of approximately 5-18 keV/μm. A linearly scaled alpha value could thus not be employed to reproduce the results. The further consequence of this result was that the RMF model biological coefficients θ and κ could not accurately model the data if constant values were maintained for both. A reasonable reproduction of the data was achieved for constant θ and allowing κ to increase for LET above approximately 5 keV/μm.

Predicted Risks of Second Cancers after Carbon-Ion Therapy versus Proton Therapy

[John G Eley](#)¹, [Thomas Friedrich](#)², [Kenneth L Homann](#)¹, [Anita Mahajan](#)¹, [Marco Durante](#)², [Rebecca M Howell](#)¹, [Michael Scholz](#)², [Wayne D Newhauser](#)³

⁽¹⁾*The University of Texas MD Anderson Cancer Center, 1515 Holcombe Boulevard, Houston TX 77030, United States*

⁽²⁾*GSI Helmholtzzentrum für Schwerionenforschung GmbH, Planckstraße 1, Darmstadt 64291, Germany*

⁽³⁾*Louisiana State University and Agricultural and Mechanical College, 202 Nicholson Hall, Tower Drive, Baton Rouge LA 70803, United States*

Carbon-ion therapy can sometimes provide increased dose conformity and increased relative biological effectiveness (RBE) for tumor control, compared to proton therapy, but nearly equivalent RBE in normal tissue upstream of the target. The purpose of this work was to determine whether carbon-ion therapy would significantly reduce the predicted risk of radiation induced second cancers in the breast for female Hodgkin lymphoma (HL) patients while preserving tumor control compared with proton therapy. To achieve our goals, we prepared RBE-weighted treatment plans for 6 HL patients using scanned proton and carbon-ion therapy. For the breast, we implemented a linear-energy-transfer-dependent risk model for tumor induction and modeled the competing process of cell inactivation. We also studied the possible influence of non-targeted radiation effects on our risk predictions. Our findings indicate that a lower risk of second cancer in the breast might be expected for some Hodgkin lymphoma patients using carbon-ion therapy instead of proton therapy. For our reference scenario, we found the ratio of risk to be 0.77 ± 0.35 for radiogenic breast cancer incidence after carbon-ion therapy versus proton therapy. The incorporation of a non-targeted effects model suggested a possible 3% increase in that ratio of risk, increased for carbon. Our findings were dependent on the RBE values for tumor induction and the radiosensitivity of breast tissue, as well as the physical dose distribution.

Tumor-targeting gold nanoparticles as engineered radiosensitizers for proton therapy: In Vivo Study at the SOBP and Beam Entrance

[Tatiana Wolfe](#), [Jonathan D Grant](#), [Adam R Wolfe](#), [Michael Gillin](#), [Sunil Krishnan](#)

Department of Experimental Radiation Oncology, The University of Texas MD Anderson Cancer Center, Houston TX, United States

Purpose: To assess tumor-growth delay and survival rate in animal models of prostate cancer receiving tumor-targeting gold nanoparticles (AuNP) and proton therapy.

Material and Methods: AuNP were coated with poly-ethylene-glycol (PEG) and conjugated to goserelin acetate. The final construct is a prostate tumor targeting AuNP (gAuNP) that interacts with GnRH receptors on the cell membrane, is endocytosed, and localized within vesicles in the cytoplasm whereas untargeted AuNPs (pAuNPs) are not. Fifty-one mice with prostate xenograft tumors measuring 8mm were included in the study. AuNP were injected intravenously at a final gold concentration of 0.2% w/w 24h prior to irradiation. A special jig was designed to facilitate tumor irradiation perpendicular to the proton beam. Proton energy was set to 200MeV, the radiation field was 18x18cm², and tumors were positioned either at the beam entrance (BE) or at the spread-out Bragg peak (SOBP). Physical doses of 5Gy were delivered to tumors. Experiments were performed on a patient beam line at the Proton Therapy Center.

Results: Animals receiving AuNP had delayed tumor-growth. The tumor volume doubling time (T2V) relative to protons alone was delayed by 11 or 32 days in mice receiving gAuNP irradiated at BE or SOBP, respectively. The T2V for pAuNP groups irradiated at BE or SOBP were 9 or 23 days, respectively. Overall survival (OS) was assessed over a period of 6 months, revealing gAuNP improved OS by 36% or 74% when tumors were irradiated at BE or SOBP, respectively. The same analysis was made for pAuNP and OS was found significant ($p < 0.001$) only for the group irradiated at the SOBP, being improved by 38%.

Conclusions: This in vivo study importantly reveals nanoparticles as potent radiosensitizers of proton therapy. Conjugation to tumor-specific antigens that promote enhanced cellular internalization of nanoparticles improves both tumor-growth delay and survival of mice following proton therapy.

Multi-Reflection Time-of-Flight Mass Spectrograph for Precision Mass Measurements of Short-Lived Nuclei and More

[Yuta Ito](#)¹, [Michiharu Wada](#)¹, [Hermann Wollnik](#)², [Fumiya Arai](#)¹, [Tetsu Sonoda](#)¹, [Peter Schury](#)³

⁽¹⁾Nishina Center for Accelerator-Based Science, RIKEN, 2-1 Hirosawa, Wako City Saitama 351-0198, Japan

⁽²⁾Dept. Chem. and BioChem., New Mexico State University, 1175 N. Horseshoe Dr., Las Cruces New Mexico 88003, United States

⁽³⁾Nishina Center for Accelerator-Based Science, RIKEN, 2-1 Hirosawa, Wako City Saitama 351-0198, Japan

Atomic mass measurements play a vital role in nuclear physics, providing a direct measure of the nuclear binding energy. Systematic mass measurements provide vital inputs for nuclear structure and nuclear astrophysics. It is currently popular to use Penning trap mass spectrometers for such measurements. However, the nuclei amenable to such a technique are limited by the observation time required. Using a multi-reflection time-of-flight mass spectrograph (MRTOF-MS), it is possible to achieve a mass resolving power $R_m \sim 200,000$ with observation times of less than 10 ms for even the heaviest nuclei,

allowing its use in studies of even the shortest-lived nuclei. Accurate mass measurements with a relative precision of $\Delta m/m \sim 5 \times 10^{-8}$ have been demonstrated with the device, and it has been shown to tolerate contaminants without introduction of meaningful deviations in accuracy. It can also be used for simultaneous mass measurements of ions within wide bands of mass-to-charge ratios, which could allow for very economical utilization of radioactive ion beams. Additionally, by replacing the detector at the end of the system with a Bradbury-Neilson gate, the MRTOF-MS could be operated as a high-purity isobar separator.

At RIKEN, the MRTOF-MS will be used for mass measurements of r-process nuclei and as an isobar (and possibly isomer) separator as part of the SLOWRI project. It will be similarly employed for use with trans-Uranium ions as part of the SlowSHE project. We will discuss the various features of the MRTOF-MS, with an emphasis on plans for its use at RIKEN.

Abstract 401 MON-NP10-2

[Contributed Talk - Monday 2:00 PM - Travis C/D](#)

Search for ^{283,284,285}Fl decay chains*

[N. T. Brewer](#)^{1,2}, [V.K. Utyonkov](#)³, [K.P. Rykaczewski](#)¹, [R.K. Grzywacz](#)^{1,2}, [K. Miernik](#)^{1,4}, [J.B. Roberto](#)¹,
[Yu. Ts. Oganessian](#)³, [A. N. Polyakov](#)³, [Yu. S. Tsyganov](#)³, [A. A. Voinov](#)³, [F. Sh. Abdullin](#)³, [S. N. Dmitriev](#)³,
[M. G. Itkis](#)³, [A.V. Sabelnikov](#)³, [R. N. Sagaidak](#)³, [I. V. Shirokovsky](#)³, [M. V. Shumeyko](#)³, [V. G. Subbotin](#)³,
[A. M. Sukhov](#)³, [G. K. Vostokin](#)³, [J. H. Hamilton](#)⁵, [R. A. Henderson](#)⁶, [M. A. Stoyer](#)⁶

⁽¹⁾ORNL, Oak Ridge TN 37831, United States

⁽²⁾University of Tennessee, Knoxville TN 37996, United States

⁽³⁾JINR, RU-141980, Dubna, Russia

⁽⁴⁾University Of Warsaw, Pl 00681, Warsaw, Poland

⁽⁵⁾Vanderbilt University, Nashville TN 37235, United States

⁽⁶⁾LLNL, Livermore CA 94551, United States

Experiments with ^{239,240}Pu targets and ⁴⁸Ca beams were initiated at Dubna in November 2013. These studies, to identify decay chains starting from Z=114, ^{283,284,285}Fl isotopes, are using a new detection system with digital acquisition commissioned by the ORNL-UTK team[1], and implemented at the Dubna Gas Filled Recoil Separator.

The experiments with ^{239,240}Pu are expected to expand our knowledge on the properties of superheavy nuclei and identify new nuclei located at the gap between the Hot Fusion Island and the Nuclear Mainland [2-4]. New data may enrich information on the competition between alpha decay and spontaneous fission (SF) in super heavy nuclei. New equipment and analysis provide better validation and correlation of fast decays.

The calibration experiment at the DGFRS performed with the new detection system and using the ⁴⁸Ca+^{nat}Yb reaction allowed direct observation of α decay from thorium isotopes including the 1- μ s activity of ²¹⁹Th.

Irradiation of the ²³⁹Pu target with ⁴⁸Ca beam began on 6th December 2013. As of the 20th February 2014 a total beam of approximately 1.3×10^{19} projectiles on target was achieved. The status of this experimental campaign will be presented including the evidence for sub-millisecond activity of new Z=114 isotope, ²⁸⁴Fl, highlighting the benefit of validating correlations.

- [1] R. Grzywacz et al., Nucl. Instr. Methods in Phys. Res. B 261, 1103 (2007).
- [2] Yu. Ts. Oganessian, J. Phys. G Nucl. Part. Phys., 34, R165, 2007.
- [3] Yu. Ts. Oganessian, Radiochimica Acta, 99, 429, 2011.
- [4] J. H. Hamilton, S. Hofmann, Yu. Ts. Oganessian, Ann. Rev. Nucl. Part. Sci., 63, 383 (2013).

*Supported by the U.S. DOE Office of Science under contracts DE-AC05-00R22725 (ORNL), DE-FG02-96ER40983 (UTK), DE-FG-05-88ER40407 (Vanderbilt) and DE-AC52-07NA27344 (LLNL), and Russian Foundation for Basic Research Grants, grant No. 13-02-12052.

Abstract 339 MON-NP10-3

[Invited Talk - Monday 2:00 PM - Travis C/D](#)

New opportunities in decay spectroscopy with the GRIFFIN and DESCANT arrays

[Vinzenz Bildstein](#), [GRIFFIN collaboration](#), [DESCANT collaboration](#)

Physics Department, University of Guelph, 50 Stone Rd E, Guelph ON N1G 2W1, Canada

The GRIFFIN (Gamma-Ray Infrastructure For Fundamental Investigations of Nuclei) project is a significant upgrade of the decay spectroscopy capabilities at TRIUMF-ISAC. GRIFFIN will replace the HPGe germanium detectors of the 8π spectrometer with an array of up to 16 large-volume HPGe clover detectors and use a state-of-the-art digital data acquisition system. The existing ancillary detector systems that had been developed for 8π , such as the SCEPTAR array for β -tagging, PACES for high-resolution internal conversion electron spectroscopy, and the DANTE array of LaBr₃/BaF₂ scintillators for fast gamma-ray timing, will be used with GRIFFIN.

GRIFFIN can also accommodate the new neutron detector array DESCANT, enabling the study of beta-delayed neutron emitters. DESCANT consists of up to 70 detector filled with about 2 liters of deuterated benzene. Deuterated benzene has the same PSD capabilities to distinguish between neutrons and γ -rays interacting with the detector as un-deuterated scintillators. In addition, the anisotropic nature of **n-d** scattering as compared to the isotropic **n-p** scattering allows the determination of the neutron energy spectrum directly from the pulse-height spectrum, complementing the time-of-flight information.

The installation of GRIFFIN is well on its way and first experiments are planned for the fall of 2014. The array will be completed in 2015 with the full complement of 16 clovers. DESCANT will be tested with the TIGRESS array in 2014 and ready to be used in experiments by 2015. A detailed overview of GRIFFIN and DESCANT will be presented.

Development of Fast, Segmented Trigger Detector for Decay Studies[M. F. Alshudifat](#), [R. Grzywacz](#), [S. Paulauskas](#)*Physics and astronomy, University of Tennessee-Knoxville, 401 Nielsen Physics Building, 1408 Circle Drive, Knoxville TN 37996, United States*

Segmented scintillator based detector was developed for decay studies. The detector is build with use of position-sensitive photo-multiplier (PSPMT) Hamamatsu H8500 coupled with fast pixelated (16×16) plastic scintillator (Eljen EJ-204). The PSPMT anodes form a two dimensional matrix (8×8), which is used for position reconstruction. Position resolution with average FWHM of ~ 1.1 mm was achieved with ^{137}Cs gamma-ray source. Signals derived from a non-segmented dynode are used for timing. Digital pulse shape analysis algorithm was used for this analysis and the 500 ps timing resolution was achieved. This detector is intended to use in fragmentation type experiments which require segmented detectors in order to enable recoil-decay correlations for applications requiring good timing resolution, e.g. the neutron time-of-flight experiments using versatile array of neutron detectors at low energy (VANDLE).

Alpha- and proton-decay studies in the vicinity of ^{100}Sn .

[Karolina Kolos](#)¹, [Robert Grzywacz](#)^{1,2}, [Katsuhisa Nishio](#)⁴, [Andrei Andreyev](#)³, [Krzysztof Rykaczewski](#)², [Carl Gross](#)², [Shintaro Go](#)¹, [Yongchi Xiao](#)¹, [Victoria Trusdale](#)³, [Robert Wadsworth](#)³, [David Jenkins](#)³, [Charles Barton](#)³, [Michael Bentley](#)³, [Riccardo Orlandi](#), [Kentaro Hirose](#)⁴, [Hiroyuki Makii](#)⁴, [Ichiro Nishinaka](#)⁴, [Hiroshi Ikezoe](#)⁴, [Tutomu Otsuki](#)⁵, [Satoshi Chiba](#)⁶

⁽¹⁾*University of Tennessee, Knoxville TN 37996, United States*⁽²⁾*Physics Division, Oak Ridge National Laboratory, Oak Ridge TN 37830, United States*⁽³⁾*University of York, Heslington YO10 5DD, United Kingdom*⁽⁴⁾*Advanced Science Research Center, JAEA, Tokai 319-1112, Japan*⁽⁵⁾*Research Reactor Institute, Kyoto University, Osaka 590-0494, Japan*⁽⁶⁾*Research Laboratory for Nuclear Reactors, Tokyo Institute of Technology, Tokyo 152-8550, Japan*

The region of nuclei around the doubly magic ^{100}Sn is unique in the nuclear landscape. It allows us to study the structure of nuclei near closed shell ($N=Z=50$) and the proton drip line. The program to study this region was initiated at the HRIBF (ORNL) and led to the numerous technical developments [1, 2] and discovery of the new elements as well as proton emission in rare earth region (see e.g. [3]). We have performed commissioning experiment with heavy-ion induced reactions using the Recoil Mass Spectrometer (RMS) [3] at the JAEA tandem accelerator at the Advanced Science Research Center at Tokai, Japan. In order to test the feasibility of alpha-decay studies two reactions were measured: $^{58}\text{Ni} + ^{56}\text{Fe}$ and $^{58}\text{Ni} + ^{58}\text{Ni}$ with the beam of 1pnA and energy of 225MeV. We have used the unique detection and data acquisition techniques developed at UTK/ORNL [4]. We have identified alpha particles and protons from the decay of $^{108,109}\text{Te}$, ^{109}I and ^{112}Cs , and measured their production yields. We will present the extracted cross-section values for the production of these elements to demonstrate the capability of the RMS device at the ASRC, and discuss possible future improvements and goals for the structure studies.

[2] S.N. Liddick, I.G. Darby, R. Grzywacz, NIM A 669, 70 (2012)

[3] H. Ikezoe et al. , NIM A 376, 420 (1996)

[4] M. Karny et al. Phys. Lett. B 664, 52 (2008)

Abstract 91 MON-NST05-1

[Invited Talk - Monday 2:00 PM - Bonham D](#)

Cell Adhesion and Growth on Modified Surfaces by Plasma and Ion Implantation

[Wagner W R Araujo¹](#), [Fernanda S Teixeira¹](#), [Glenda N da Silva³](#), [Daisy M F Salvadori²](#), [Maria Cecilia Salvadori¹](#)

⁽¹⁾*Department of Applied Physics, University of Sao Paulo, Rua do Matão, Travessa R, 187, Cidade Universitária, Sao Paulo SP 05508-090, Brazil*

⁽²⁾*Department of Pathology, São Paulo State University, Faculty of Medicine, UNESP, Rubião Junior, Botucatu SP 18618-000, Brazil*

⁽³⁾*Department of Clinical Analyses , Pharmacy School, Federal University of Ouro Preto, Ouro Preto MG, Brazil*

Surface modifications have been widely used for cell growth for various applications. In this context, chemical treatments, including plasma surface modification and ion implantation, are commonly used, with considerable changes of surface properties, which influence the adhesion and proliferation of mammalian cells in a strong way. In this study we show and discuss the results of the interaction of living CHO (Chinese Hamster Ovary) cells, in terms of adhesion and growth on glass, SU-8 (epoxi photoresist), PDMS (polydimethylsiloxane) and DLC (hydrogen free diamond-like carbon) surfaces. The choice of the materials was based on their properties and applications. SU-8 is an epoxi-based photo and electron beam resist used in a variety of applications, mainly using microfabrication techniques, such as microfluidics, superhydrophobicity and bio-MEMS. Silver nanoparticles are known for their antibacterial properties. As it is known that implantation of metal into polymer using ion implantation forms nanoparticles inside the polymer, we evaluated the cell growth on buried silver nanoparticles into SU-8 formed by ion implantation. PDMS (polydimethylsiloxane) is a widely used polymeric material with several interesting characteristics, which include high flexibility, optical transparency, biocompatibility and ease to fabricate. Diamond-like carbon (DLC) is an amorphous carbon material with high content of sp³ bonds, providing properties similar to diamond films, being also a biocompatible material. Glass, SU-8 and DLC but not PDMS showed to be good surfaces for cell growth. DLC and SU-8 surfaces were modified and also evaluated concerning to the interaction of living CHO cells. DLC surfaces were treated by oxygen plasma (DLC-O) and sulfur hexafluoride plasma (DLC-F). After 24 hours of cell culture, the number of cells on DLC-O was higher than on DLC-F surface. SU-8 with silver implanted, creating nanoparticles 12 nm below the surface, increased significantly the number of cells per unit of area.

Abstract 229 MON-NST05-2

[Invited Talk - Monday 2:00 PM - Bonham D](#)

APPLICATIONS OF ELECTRON-BEAM IRRADIATION FOR THE PREPARATION OF NOVEL BIOMATERIALS - A REVIEW

[Maria J. A. Oliveira](#), [Mara T. S. Alcântara](#), [Gustavo H. C. Varca](#), [Ademar B. Lugão](#), [Esperidiana A. B. Moura](#)

The present article provides a review of the applications of electron-beam radiation for the development of novel biomaterials. Among various methods applied for the production of biomaterials, the radiation technique has many advantages, as a simple, efficient, clean and environment-friendly process. It usually allows to combine the synthesis and sterilization in a single technological step, thus reducing costs and production time, and possibility of simultaneous immobilization of bioactive materials without any loss in their activity. Electron-beam radiation are being used for synthesis of hydrogels, functional polymers, interpenetrating systems, chemical modification of surfaces, immobilization of bioactive materials, synthesis of functional micro and nanospheres and processing of naturally derived biomaterials. Potential medical applications of these biomaterials include implants, topical dressings, treatment devices and drug delivery systems. Herein, the applications of electron-beam radiation for the development of novel biomaterials are discussed in general, and detailed examples are also drawn from scientific literature and practical work currently under development by authors, such as, hydrogel dressing crosslinked and sterilized by irradiation for treatment of neglected diseases, hidrogel with silver nanoparticles, development of protein nanoparticles using irradiation to crosslink, sterilize and in situ production of protein nanoparticles, among other biomaterials.

Abstract 288 MON-NST05-3

[Contributed Talk - Monday 2:00 PM - Bonham D](#)

Ion Beam Analysis of Materials Used in Hermetic Single-Device Human Implants integrating Bio-sensors with Medical Electronics

[Mark W. Mangus, Jr.](#)^{1,3}, [Marko Neric](#)³, [Kevin T. Nguyen](#)^{2,3,4}, [Aaron M. Slyder](#)³, [Anthony J. Woolson](#)³, [Saloni A. Sinha](#)^{4,5}, [Nicole X. Herbots](#)^{1,2,3}, [Robert J. Culbertson](#)^{1,3}, [Barry J. Wilkens](#)¹, [Clarizza F. Watson](#)², [Eric R.C. Morgan](#)^{2,3,4}, [Ajjiya J. Acharya](#)^{2,3,4,5}

⁽¹⁾LeRoy Eyring Center for Solid State Sciences, Arizona State University, 901 So. Palm Walk, Rm. PSA 213, Tempe Arizona 85287, United States

⁽²⁾R&D, SiO₂ NanoTech LLC, ASU Skysong Innovation Center, Scottsdale Arizona 85287, United States

⁽³⁾Department of Physics, Arizona State University, Mail Stop 1504 P.O. Box 85287-1504, Tempe Arizona 85287-1504, United States

⁽⁴⁾Barrett Honors College, Arizona State University, 751 E. Lemon Mall, Tempe Arizona 85281, United States

⁽⁵⁾Department of Chemistry & Bio-Chemistry, Arizona State University, Mail Stop 1604, Tempe Arizona 85287-1604, United States

Percolation of bodily fluids into single-device medical implants limits device lifetimes to less than a week in permanent glucose sensors for diabetics.[1,2] Ion beam analysis (IBA) can detect bodily fluid elements (H, C, O, Na, Mg, K and Fe) if fluids percolate into medical devices. Rutherford backscattering spectrometry (RBS) can measure impurities in a substrate but, the RBS detection limit, D_{\min}^{RBS} , can be inadequate for light elements on/in a heavier substrate. For RBS of ^4He at 2 MeV, the D_{\min} of C in Si is ~ 5 monolayers (ML). D_{\min} needs to be lower to track contaminants that first shift calibration and then destroy permanent medical sensors.

Nuclear resonance analysis (NRA) can reduce D_{\min} , sometimes significantly, for combinations of incident ions and target isotopes if the incident ion is near resonance energy, enhancing the scattering cross section.

Combining NRA with channeling can improve D_{\min} for low Z elements in high Z crystalline substrates by another factor of 20 to 50, depending on the minimum yield (χ_{\min}). This results in a D_{\min} near 1 ML for C in Si(100). Exploiting Channeling geometry, such as $\langle 111 \rangle$ channeling in Si(100), can extend sampled depths so that D_{\min} is further reduced to ~ 0.1 ML. With backscattering of ^4He from Na in NaCl optical crystals and NaHCO₃ at energies near 4.68 MeV, scattering cross sections are found to be 1.6 times the Rutherford cross section, which reduces D_{\min} for Na. NRA combined with

<111> channeling to detect C, Na, K, P and Fe from blood or saline percolated into SiO₂ on Si(100), bulk silica and TiN on Si(100) will be discussed.

[1] B.J. Wilkens, M.W. Mangus, Jr., N. Herbots, et al. ASU Technol. Discl., Pat. Pend. (2014) [2] N. Herbots et al. Pub. No 13/259,278, PCT/US2010/033301 (2012)

Abstract 447 MON-HSD02-1

[Invited Talk - Monday 4:00 PM - Travis A/B](#)

High Duty Factor Compact Linear Accelerator Systems

[Sami G Tantawi](#)¹, [Zhenghai Li](#)², [Aaron Jensen](#)²

⁽¹⁾Particle Physics and Astrophysics, SLAC/Stanford University, 2575 Sand Hill Rd, Menlo Park California 94025, United States

⁽²⁾Accelerator Division, SLAC, 2575 Sand Hill Rd, Menlo Park California 94025, United States

Recently Demand for high repetition rate and high duty factor linear accelerators has grown. Many application such as free electron lasers, medical linacs ,and linacs for cargo scanning, to name a few, would benefit greatly from linacs with repetition rates greater than 1 KHz and duty factors that approach 1%. To this end, every part of the linac system has to be optimized for ever higher efficiencies. In this paper we will present an optimization process for the overall system and for each individual component from the modulator and the rf source to the accelerator structure with the goal of obtaining an efficient compact system. The system aims for electron beam energies of about 10 MeV in about a meter long structure. Also we aim to achieve average beam power above 10 kW with a wall plug power of less than 50 kW.

Abstract 147 MON-HSD02-2

[Contributed Talk - Monday 4:00 PM - Travis A/B](#)

ARCIS: Adaptive Rail Cargo Inspection System

[Anatoli Arodzero](#), [Salime Boucher](#), [Luigi Faillace](#), [Mark Harrison](#), [Scott Storms](#)

RadiaBeam Technologies, 1717 Stewart Street, Santa Monica CA 90404, United States

Existing requirements for high throughput rail cargo radiography inspection include high resolution (better than 5 mm line pair), penetration beyond 400 mm steel equivalent, material discrimination (organic, inorganic, high Z), high scan speeds (>10 kph, up to 60 kph), low dose and small radiation exclusion zone. To meet and exceed these requirements, research into a number of new radiography methods, new detector materials and design has been initiated.

RadiaBeam Technologies is developing an innovative rail cargo X-ray scanning technique that promises dramatically improved penetration and imaging capability. Our Adaptive Rail Cargo Inspection System, ARCIS, will be able to provide radiographic scanning with material discrimination at speeds consistent with normal commercial operation.

Novel concepts relying on Linac-based, adaptive, modulated energy X-ray sources, new types of fast X-ray detectors (Scintillation-Cherenkov detectors), and fast processing of detector signals are being developed. We discuss requirements and operation mode of Linac-based X-ray source for adaptive cargo inspection system and expected performance improvement.

Parts of this work is support by the U.S. Department of Homeland security, Domestic Nuclear Detection Office, under competitively awarded contract HSHQDC-13-C-B0019. This support does not constitute an express or implied endorsement on the part of the Government.

Abstract 148 MON-HSD02-3

[Contributed Talk - Monday 4:00 PM - Travis A/B](#)

Intra-Pulse Multi-Energy Method for Material Discrimination in X-ray Cargo and Container Inspection

[Aleksandr Saverskiy](#), [Dan-Cristian Dinca](#), [J. Martin Rommel](#)

American Science and Engineering, Inc., 829 Middlesex Turnpike, Billerica MA 01821, United States

The Intra-Pulse Multi-Energy (IPME) method of material discrimination is a novel concept for X-ray inspection of containers and cargo. IPME is aimed at improving the traditional Dual (Multi)-Energy (DE) method and overcoming its main disadvantages: reduction in effective scanning speed and ambiguity caused by sampling different regions of cargo.

The IPME method is proposed by AS&E in two versions: a) forming and analyzing discrete energy levels within a single inspection pulse, and b) creating a pulse with ramping energy and adaptively controlled end-point energy.

First experimental results evaluating the Intra-Pulse method are presented and discussed. The technology for the Intra-Pulse method significantly depends on the availability of X-ray sources capable of providing in-pulse energy modulation and new detector materials for fast data acquisition.

The requirements for X-ray sources based on Linear accelerators (Linac) are analyzed for several classes of cargo inspection systems: "slow moving" gantry, high throughput portal, and fast moving train inspection system.

Specifics of a Linac implementation with intra-pulse energy modulation are discussed. Several original solutions are presented.

Abstract 85 MON-HSD02-4

[Contributed Talk - Monday 4:00 PM - Travis A/B](#)

Air Cargo Mobile Scanner Based on Associated Particle Imaging

[Vladimir G Solovyev](#), [John Stevenson](#), [Joseph Bendahan](#), [Dan Strellis](#)

Rapiscan Laboratories, Inc., 520 Almanor Ave, Sunnyvale CA 94085, United States

Rapiscan Laboratories developed a laboratory prototype mobile cargo scanner, based on a deuterium-tritium (DT) neutron generator with Associated Particle Imaging (API) detector. API technology enables depth mapping (~10 cm spatial resolution) of elemental composition of the scanned cargo content. This information can be used to determine presence of drugs, explosives, and other illicit substances.

The developed scanner has a small footprint, suitable for placement on a cargo van or a small truck, as part of the mobile scanning solution, easily re-locatable between deployments. It was designed to provide a quick (less than a minute)

secondary scan of an LD-3 size container. Only a portion of the container, pre-selected by an x-ray based primary scan is irradiated by neutrons. The rest of the container is shielded by the neutron collimator. It was demonstrated that effectiveness of the collimator is crucial in reducing signal-to-noise ratio and overall system performance.

Development of the system was guided by MCNP simulations. The scanner prototype was tested with drug simulants hidden in high and low density organic and metallic LD-3 size cargoes at Purdue University. System design, modeling and experimental results will be discussed.

Abstract 212 MON-HSD02-5

[Contributed Talk - Monday 4:00 PM - Travis A/B](#)

New Accelerator Design for Homeland Security X-Ray Applications

[Willem GJ Langeveld](#)¹, [Vinod K Bharadwaj](#)², [James Clayton](#)³, [Daniel Shedlock](#)³

⁽¹⁾*Rapiscan Laboratories, Inc., 520 Almanor Ave, Sunnyvale CA 94085, United States*

⁽²⁾*SLAC National Accelerator Laboratory, 2575 Sand Hill Road, Menlo Park CA 94025, United States*

⁽³⁾*Varian Medical Systems, Inc., 3120 Hansen Way, Palo Alto CA 94304, United States*

One goal for security scanning of cargo and freight is determining the type of material that is being imaged. One commonly used technique is dual-energy imaging, i.e. imaging with different x-ray energy spectra and calculating the effective atomic number, Z , of the cargo material by variations in the attenuation because of the different energies used. However, the transmitted x-ray spectrum also depends on the effective Z . Obtaining this spectrum is difficult because individual x ray energies need to be measured at very high count rates. Typical accelerators for security applications offer large bursts of x rays, suitable for current mode integrated imaging. In order to perform x-ray spectroscopy a new accelerator design is required that has the following capabilities: 1. Modulate the number of x rays produced in each delivered pulse by adjusting the accelerator electron beam instantaneous current, thereby delivering adequate signal to measure the spectrum without saturating the spectroscopic detector; and 2. Increasing the duty factor of the x-ray source in order to spread out the arrival of x rays at the detector over time. Current sources are capable of 0.1% duty factor, although usually they are operated at duty factors significantly below that ($\sim 0.04\%$), but duty factors in the range 0.4-1.0% are desired. The higher duty factor can be accomplished by, for example, moving from 300 pulses per second (pps) to 1000 pps. This paper will describe R&D in progress to examine cost effective modifications that could be performed on a typical linear accelerator for these purposes. Key issues will be discussed including LINAC and klystron cooling, the low current electron gun, and modulator upgrades.

This work has been supported by US Department of Homeland Security, Domestic Nuclear Detection Office, under competitively awarded contract HSHQDC-14-C-B0002. This support does not constitute an express or implied endorsement on the part of the Government.

Abstract 237 MON-IBA08-1

[Invited Talk - Monday 4:00 PM - Presidio B](#)

Accelerator based techniques at CEDAD for cultural heritage studies

[Lucio Calcagnile](#)

CEDAD - CEnter for DAting and Diagnostics, Department of Engineering for Innovation -University of Salento, via Monteroni, Lecce Italy 73100, Italy

Since 2003 a 3MV HVE Tandetron accelerator is in operation at CEDAD - CEntre for DAting and Diagnostics - at the University of Salento in Lecce, Italy. During years different research projects have allowed to design and install different beam lines for Ion Beam Analysis and Accelerator Mass Spectrometry. The Tandetron accelerator is now equipped with

two AMS spectrometers and RBS, PIXE-PIGE, nuclear microprobe and high energy ion implantation beam lines. CEDAD has become over the years a multidisciplinary research Centre for applied and fundamental studies for cultural heritage and environmental monitoring by means of radiocarbon and other rare isotopes by AMS and IBA techniques.

In this talk an overview of the history and potentialities of CEDAD and the SIDART, BLU-ARCHEOSYS, IT@CHA projects will be given. It will be shown the potentialities of the integrated approach of the IBA and AMS techniques for performing, with the same accelerator, studies for cultural heritage. Recent investigations will be presented where AMS and IBA have been used to solve specific archaeological problems. Studies on objects with a high cultural or religious value have been possible with a high degree of accuracy which allowed to solve historical controversies, often difficult to solve by alternative approaches. Studies on the Riace Bronzes, the Capitoline she-wolf, Caravaggio, and on the provenience of obsidians tools will be presented in this talk.

Abstract 234 MON-IBA08-2

[Invited Talk - Monday 4:00 PM - Presidio B](#)

High-throughput PIXE analysis of aerosol samples

[Massimo Chiari](#), [Giulia Calzolai](#), [Martina Giannoni](#), [Franco Lucarelli](#), [Silvia Nava](#)

INFN-Florence and Department of Physics and Astronomy, University of Florence, via G. Sansone 1, Sesto Fiorentino 50019, Italy

Particle Induced X-ray Emission (PIXE) technique has been largely used from the beginning for the study of atmospheric aerosols, being for a long time the prevalent technique for the aerosol elemental analysis. Nowadays, in order to remain competitive with other consolidated techniques, like ICP-AES, ICP-MS or Synchrotron Radiation XRF, a proper experimental set-up is important to fully exploit PIXE capabilities.

Based on the experience at INFN LABEC laboratory, the feasibility of very rapid, lasting a few tens of second, "flash-like" PIXE measurements in an external beam set-up of aerosol samples, collected with various sampling devices (low volume samplers, cascade impactors, high-time resolution samplers) and on different sampling substrates (Teflon, Nuclepore, Kapton, Kimfol), will be discussed. Using high extracted proton beam currents, thanks to the use of a durable Si_3N_4 extraction window, and collecting X-ray spectra with multiple Silicon Drift Detectors (SDD) to increase the effective solid angle of PIXE detectors, a large number of low mass samples can be routinely analysed in short times, as mandatory for atmospheric aerosol studies (i.e. for source apportionment), thus putting PIXE in an outstanding position for the elemental analysis of aerosol samples.

The development of such SDD arrays for highly efficient PIXE analysis over the widest range of elements (from Na on) is important for other fields of application as well, for example, for cultural heritage where very low beam currents and doses are required to avoid damaging the artefacts.

The critical aspects of this approach, i.e. the possible damages to the SDDs due to the large backscattered proton flux, will be addressed as well and solutions based on the use of Proton Magnetic Deflectors to filter out the backscattered protons without affecting the detector intrinsic efficiency at low X-ray energies will be presented.

Abstract 103 MON-IBA08-3

[Contributed Talk - Monday 4:00 PM - Presidio B](#)

Characterization of pottery production of Tyre historical site using PIXE technique and cluster analysis

[Mohamad Roumie](#)¹, [Severine Elaigne](#)², [Mohamed El-Bast](#)¹, [Mona Bahja](#)³, [Pierre-Louis Gatier](#)²,
[Malek Tabbal](#)³, [Bilal Nsouli](#)¹

⁽¹⁾Accelerator Laboratory, Lebanese Atomic Energy Commission, Lebanese CNRS, Airport Road, P.O.Box 11-8281, Beirut, Lebanon

⁽²⁾Laboratoire Histoire et Sources des Mondes Antiques, MOM-CNRS, Lyon, France

⁽³⁾Department of Physics, American University of Beirut, Beirut, Lebanon

It is proposed to study the excavated ceramics from Tyre, the prestigious city of antiquity (locally named Sour and located at 85 km south of Beirut, Lebanon). The originality of Tyre in this context is its long permanence of prosperity as a great center of pottery production and maritime trade through the centuries without interruptions, which were experienced by neighboring cities and rivals. In this work, several series of excavated pottery are analyzed in order to characterize the Tyre production, based on the elemental composition, and thus to be distinguished from those of other neighboring workshops (Serapta, Sidon or Acre), possible sites of ceramic production at this period. Particle induced X-ray emission technique PIXE is used to determine the elemental composition of about 107 excavated shards. The elemental composition provided by PIXE and based on 12 most abundant elements, ranging from Mg to Zr, was used in a multivariate statistical program, where two well defined groups were identified.

Abstract 334 MON-MA02-1

[Invited Talk - Monday 4:00 PM - Bonham B](#)

An Overview of Proton Accelerators for Cancer Therapy

[George Coutrakon](#)

dept. of Physics, Northern Illinois University, 202 LaTourette Hall, DeKalb IL 60115, United States

The last decade has brought important developments in accelerator technology for charged particle radiation therapy. Since 2001, more than 15 proton and light ion facilities have started clinical operations worldwide. The two classes of accelerators, cyclotrons and synchrotrons, have been adapted to meet the clinical needs of particle therapy. Starting with Loma Linda University's 250 MeV proton synchrotron in Loma Linda, CA, many vendors have worked to reduce size, cost and weight while adding features such as fast (50 μ sec) beam on-off modulation for respiration gating, rapid (1 sec) energy changes for particle range modulation, and uniform (+/- 5%) beam intensity for pencil beam scanning. Respiration gating is a relatively new feature of accelerators that only allows beam delivery during fixed phases of the patient breathing cycle in order to reduce dose to healthy tissue and allow better targeting of dose to the tumor. The ability to control energy and intensity delivered to each point in the tumor is an essential feature for successful operation of all clinical accelerators which in turn requires careful coordination between accelerator control systems and beam delivery systems in the treatment room. The advent of pencil beam scanning and respiration gating has added newer more stringent accelerator requirements for intensity and energy control in order to avoid under dosing or overdosing of the tumor and neighboring healthy organs. This review paper discusses the spectrum of proton therapy accelerators in clinical use as well as newer evolving technologies.

Abstract 405 MON-MA02-2

[Contributed Talk - Monday 4:00 PM - Bonham B](#)

Overview of Carbon-ion Accelerators for a US-based National Center for Particle Beam Radiation Therapy Research

[Carol Johnstone](#)

Particle Accelerator Corporation, 809 Pottawatomie Tr., Batavia IL 60510, United States

In the DOE report "Accelerators for America's Future," it was noted that critical R&D in particle-beam therapy can only be conducted at a dedicated accelerator-based medical research facility capable of supplying the full range of ion beams from protons to carbon, oxygen or even neon. Such a facility requires beam energies and intensities useful for therapy and imaging but also high beam intensities for advanced radiobiology research and a wide range of Linear Energy Transfer

(LET) values. NCI jointly with DOE recently organized a workshop to define the research and technical needs for advancing charged particle therapy, producing a detailed final report. The recommendations of the DOE-NCI workshop, in particular high dose deposition rates and motion control, imply beam intensity requirements that take us into uncharted territory for particle-beam radiation facilities. This talk will present an overview of the current state of carbon-ion accelerators, R&D in carbon-ion accelerators, and the technical and engineering advances required to meet the challenges for particle-beam research and therapy as envisioned in the NCI/DOE report.

Abstract 301 MON-MA02-3

[Contributed Talk - Monday 4:00 PM - Bonham B](#)

Multiple-room, continuous beam delivery hadrontherapy installation

[Francois G Meot](#)

Collider-Accelerator, BNL, Bldg 911, Upton NY 11973, United States

A protontherapy hospital installation, based on multiple-extraction from a high repetition rate fixed-field synchrotron, and on simultaneous beam delivery to several treatment rooms, is presented and commented. Potential interests as hospital operation efficiency as well as the strong impact of the method on session cost (brought down to X-rays' level of cost) are discussed.

Abstract 25 MON-MA02-4

[Contributed Talk - Monday 4:00 PM - Bonham B](#)

A High Intensity 10 MeV X-ray Generator to Eliminate High Activity Sources Used for Sterilization

[Terry L Grimm](#)¹, [Chase H Boulware](#)¹, [Jerry L Hollister](#)¹, [Erik S Maddock](#)¹, [Valeriia N Starovoitova](#)¹,
[Alan W Hunt](#)²

⁽¹⁾*Niowave, Inc, 1012 N. Walnut St, Lansing MI 48906, United States*

⁽²⁾*Idaho Accelerator Center, Idaho State University, 1500 Alvin Ricken Dr, Pocatello ID 8, United States*

One of the most common ways to sterilize goods is with gamma producing radioactive sources, most commonly Co-60 and Cs-137. However, long-term possession of these sources is undesirable due to security concerns, Nuclear Regulatory Commission oversight, and rising replacement, storage, and disposal costs. In addition, gamma sterilization typically requires relatively long exposure times to achieve dosages necessary for effective sterilization. We are developing a radiation sterilization system based on a 10 MeV superconducting linear accelerator (linac) to provide high radiation doses and thus eliminate disadvantages of utilizing Co-60 and Cs-137 sources.

In this talk we will present the results of the simulations of the photon fluxes and doses and will show that a properly collimated beam from a superconducting linac can generate up to 10^{17} photons/cm² per second. We will demonstrate a conceptual design of the sterilization system, and will present the experimental results of the prototype testing.

Abstract 170 MON-NP02-1

[Invited Talk - Monday 4:00 PM - Travis C/D](#)

The LANSCE Nuclear Fission Research Program

[Rhiannon Meharchand](#)

Los Alamos National Laboratory, Los Alamos NM 87545, United States

The Neutron and Nuclear Science Group at Los Alamos National Laboratory (LANSCE-NS) has a diverse experimental program aimed at studying nuclear fission: prompt fission neutron and gamma output; fission fragment mass, charge, and energy distributions; cross sections for direct and surrogate neutron-induced fission reactions. These data are fundamental to nuclear energy and defense applications.

Experiments take place at the Los Alamos Neutron Science Center (LANSCE) Weapons Neutron Research (WNR) and Lujan Neutron Scattering facilities, spallation neutron sources which provide white neutron spectra over 10 orders of magnitude. An overview of the LANSCE-NS experimental program, focused on measurements related to nuclear fission, will be presented.

Abstract 324 MON-NP02-2

[Invited Talk - Monday 4:00 PM - Travis C/D](#)

The University of New Mexico fission fragment spectrometer, with preliminary results from LANSCE

[Adam Hecht](#), [Richard Blakeley](#), [Lena Heffern](#)

Chemical and Nuclear Engineering, University of New Mexico, 1 University of New Mexico, Albuquerque NM 87131, United States

Fission cross section and fragment yields are important for active interrogation, for understanding secondary reactor heating, and for furthering theory on fission preformation. We have developed a spectrometer at the University of New Mexico (UNM) for particle-by-particle measurements of fragments emitted by fission. This is part of a multi-year detector development and measurement campaign as part of the LANL led SPectrometer for Ion Determination in fission Research (SPIDER) collaboration, with UNM prototyping and testing designs to improve resolution and extract more particle information. We have performed beam measurements with the LANL-LANSCE neutron beam on U-235 and calibration tests with Cf-252, and preliminary results will be presented. The spectrometer design is based on the 2E-2v type Cosi Fan Tutte spectrometer with several improvements implemented and planned to improve efficiency and resolution, towards 1 amu heavy fragment resolution. The fission fragment that is emitted in the appropriate direction passes through a time-of-flight (TOF) region and into an ionization chamber (IC), giving both velocity (v) and kinetic energy (E) measurements. With both the velocity and kinetic energy for each individual fragment, the fission fragment mass may be extracted. With the IC configured as a time projection chamber, IC timing information yields fragment Z information. The incident neutron kinetic energy on the target is known by timing with the LANSCE pulsed beam. A, Z, N and E measurements for both fragments simultaneously from a binary fission event we will also have a measure of neutron multiplicity and reaction cross section to produce that fragment pair as a function of incident neutron energy. We are currently testing an active cathode design on the IC for improved timing and Z resolution, and will implement detectors on both sides of the fission target, two spectrometer arms, for the simultaneous binary fragment measurements for a full 2E-2v spectrometer.

Abstract 198 MON-NP02-3

[Contributed Talk - Monday 4:00 PM - Travis C/D](#)

Recent studies of fission fragment properties at LANSCE

[K. Meierbachtol](#)¹, [F. Tovesson](#)¹, [C. Arnold](#)¹, [R. Blakeley](#)², [T. Bredeweg](#)¹, [D. Duke](#)¹, [A. A. Hecht](#)², [M. Jandel](#)¹, [H. J. Jorgenson](#)¹, [V. Kleinrath](#)³, [R. Meharchand](#)¹, [S. Mosby](#)¹, [R. O. Nelson](#)¹, [B. Perdue](#)¹, [D. Richman](#)¹, [D. Shields](#)¹, [M. White](#)¹

⁽¹⁾LANSCE-NS, Los Alamos National Laboratory, P.O. Box 1663, Los Alamos NM 87545, United States

⁽²⁾*Department of Chemical and Nuclear Engineering, University of New Mexico, 1 University of New Mexico, Albuquerque NM 87131, United States*

⁽³⁾*Department of Nuclear Science and Engineering, Idaho State University, 921 S. 8th Avenue, Pocatello ID 83209, United States*

Research on the neutron-induced fission of actinides has been valuable to both basic science and the applications community. Both bodies have benefited from experimental measurements of the outgoing fragments and their properties to better understand the complex reaction process. Fragment properties of interest include mass, charge, and energy. These measurements are currently limited in neutron excitation energy with inadequate resolution. New instrumentation and data acquisition systems have enabled new measurements of the fragments' mass and total kinetic energy distributions from neutron-induced fission on ^{235}U at the Los Alamos Neutron Science Center (LANSCE), taking advantage of the white neutron spectrum ranging from thermal to 200 MeV produced with the LANSCE accelerator. Current results will be presented for both fragment mass distributions at thermal neutron energies and total kinetic energy distributions over a wide incident neutron energy range. This work is in part supported by LANL Laboratory Directed Research and Development Projects 20110037DR and 20120077DR. LA-UR-14-21322.

Abstract 377 MON-NP02-4

[Contributed Talk - Monday 4:00 PM - Travis C/D](#)

Average Total Kinetic Energy Measurements of Neutron Induced Fission for ^{235}U , ^{238}U , and ^{239}Pu

[Dana L Duke](#)

Los Alamos National Laboratory, P.O. Box 1663, Los Alamos NM 87545, United States

Most of the energy released in neutron-induced fission goes into the kinetic energy of the resulting fission fragments. Additional average Total Kinetic Energy (TKE) information at incident neutron energies relevant to defense- and energy-related applications would provide a valuable observable against which simulations can be benchmarked. These data could also be used as inputs in theoretical fission models. Experiments at the Los Alamos Neutron Science Center - Weapons Neutron Research (LANSCE - WNR), measured TKE of fission products following the neutron induced fission of ^{235}U , ^{238}U , and ^{239}Pu over incident neutron energies from thermal to hundreds of MeV. Depending on isotope, little or no TKE data exist for high neutron energies. Measurements were made using a double Frisch-gridded ionization chamber. Preliminary analysis using the double energy (2E) method will be presented, including fission fragment emission angles, masses, and energies for ^{238}U .

Abstract 381 MON-NST06-1

[Invited Talk - Monday 4:00 PM - Bonham D](#)

Improving AMS Detection of the Biomedical Radiotracer ^{41}Ca with Segmented Radio-Frequency Quadrupoles

[Jean-Francois Alary](#)¹, [Gholamreza Javahery](#)², [William E. Kieser](#)³, [Christopher Charles](#)³, [Xiao-Lei Zhao](#)³, [Albert E. Litherland](#)⁴, [Lisa M. Cousins](#)²

⁽¹⁾*Isobarex Corp., 32 Nixon Road Unit#1, Bolton Ontario L7E 1W2, Canada*

⁽²⁾*IONICS Mass Spectrometry, 32 Nixon Road Unit#1, Bolton Ontario L7E 1W2, Canada*

⁽³⁾*Department of Physics, University of Ottawa, 150 Louis Pasteur, Ottawa Ontario K1N 6N5, Canada*

⁽⁴⁾*Department of Physics, University of Toronto, 60 St. George, Toronto Ontario M5S 1A7, Canada*

⁴¹Ca is an important biomedical radiotracer finding many applications in biological, nutritional and medical studies. The detection of ⁴¹Ca by AMS is however limited by an important background signal of ⁴¹K originating from biological samples and from contaminated cesium in the source. An approach consisting of using PbF₂-assisted in-source fluorination in combination with an Isobar Separator for Anions (ISA), a device incorporating a low energy radio frequency quadrupole (RFQ) gas cell, promises to push down the limit of detection of ⁴¹Ca attainable on small (<3 MV) AMS systems by several orders of magnitude. Such on-line reduction of ⁴¹K should also result in a simplification of biological sample preparation and less concern about variable ⁴¹K contamination of the cesium beam. The selective collision-induced fragmentation of KF₃⁻ versus CaF₃⁻, occurring in the gas cell of an ISA equipped with a double segment RFQ, have been reported earlier⁽¹⁾, leading to K being suppressed by a factor of 1e4 over Ca. We present here the pre-commercial configuration of the ISA, redesigned using a multi-segmented RFQ to enhance further this effect and improve transmission through the gas cell. A segmented RFQ is an appropriate tool to finely control ion energy down to the few eV's separating the fragmentation energies of the two fluoride species. Some practicalities of integrating a low energy RFQ-based device in a high energy AMS system will also be discussed. This pre-commercial ISA will be used at the newly established A. E. Lalonde AMS laboratory at University of Ottawa (Canada).

1) Zhao et al., "A Refined Study of KF₃⁻ Attenuation in RFQ Gas-Cell for ⁴¹Ca AMS", Radiocarbon 55 (2013) 268-281.

Abstract 89 MON-NST06-2

[Contributed Talk - Monday 4:00 PM - Bonham D](#)

Lipid Compounds Analysis with Argon Gas Cluster Ion Beam Irradiation

[Makiko FUJII](#)¹, [Shunichirou NAKAGAWA](#)², [Toshio SEKI](#)², [Takaaki AOKI](#)³, [Jiro MATSUO](#)¹

⁽¹⁾*Quantum Science and Engineering Center, Kyoto University, Gokasho, Uji Kyoto 611-0011, Japan*

⁽²⁾*Department of Nuclear Engineering, Kyoto University, Gokasho, Uji Kyoto 611-0011, Japan*

⁽³⁾*Department of Electronic Science and Engineering, Kyoto University, Nishikyo-ku, Kyoto Kyoto 615-8510, Japan*

In recent years, mass spectrometry of biological materials has been extensively performed in pharmacokinetic and metabolic studies. Imaging Mass Spectrometry (IMS) technique especially is crucially essential to visualize spatial distribution of atoms and molecules in biological tissues and cells. Secondary Ion Mass Spectrometry utilizing Argon Gas Cluster Ion Beam (Ar-GCIB) as primary probe, Ar-GCIB SIMS, is one of the most promising IMS techniques because of the high secondary ion yields of large organic molecules and the less damage induction onto organic components. On the other hand, extremely high sensitivity is required for biological analysis because biological samples include numerous varieties of bio-molecules with quite low concentrations. We have been developing Ar-GCIB SIMS apparatus with orthogonal acceleration time-of-flight mass spectrometer (oa ToF-MS), which allows us to utilize continuous beam and achieves high mass resolution and high secondary ion efficiency. In this study, the detection limit of Ar-GCIB SIMS apparatus was investigated using some lipid compound samples. As a result, it was found that Ar-GCIB SIMS had high quantitative accuracy and the detection limit was lower than 0.1 %. In addition, the damage cross section and the relative sensitivity of some kinds of lipids were investigated using Ar-GCIB SIMS.

Acknowledgement

This study was supported in part by Research Fellowship for Young Scientists from Japan Society for the Promotion of Science (JSPS).

Abstract 182 MON-NST06-3

[Contributed Talk - Monday 4:00 PM - Bonham D](#)

Quantitative analysis of iron (Fe) uptake by corn roots using micro-PIXE

[Stephen Juma Mulware¹](#), [Nabanita Dasgupta-Schubert²](#), [Bibhudutta Rout¹](#), [Reinert Tilo¹](#)

⁽¹⁾*Physics, University of North Texas, 1155 Union Circle #311427, Denton Tx 76203, United States*

⁽²⁾*Inst. de Investigaciones Químico-Biológicas, , Universidad Michoacana de San Nicolás de Hidalgo, , 1155 Union Circle #311427, Ciudad Universitaria Morelia Michoacán C.P 58060, Mexico*

Abstract:

Iron is among the most of the 17 essential nutrients for plants and animals including humans. Deficiencies of essential minerals like Iron affect both the quality and quantity of plant foodstuffs, hence adversely affecting millions of the world's population for whom plants serve as the major dietary source of essential minerals. The WHO estimates that two billion people suffer from some form of Fe deficiency anemia, making it a leading human nutritional disorder in the world today. Thus proper uptake and homeostasis of Fe by plants is critical for their growth and development and ensuring Fe-rich plant food products for human consumption. Plants require Iron for life sustaining processes including respiration and photosynthesis. For them to respond to iron deficiency, plants induce either reduction-based or chelation-based mechanisms to enhance iron uptake from the soil. This process can be improved by engineering plants with enhanced iron content in the growing rhizosphere. In this study, we analyze quantitative iron uptake and distribution by corn roots germinated in different media some of which are laced with Fe (II) and Fe (III) of different concentrations, using micro-PIXE as an analytical technique. The effect of adding carbon nano tubes in the germinating media was also investigated.

Abstract 131 MON-RE02-1

[Invited Talk - Monday 4:00 PM - Presidio C](#)

Small-Scale Thermal and Mechanical Characterization of Ion Irradiated Structural Metals

[Khalid Hattar¹](#), [Ramez Cheaito²](#), [Shreyas Rajasekhara¹](#), [Thomas E. Buchheit¹](#), [Blythe G. Clark¹](#), [Brad L. Boyce¹](#), [Amit Misra^{3,4}](#), [Luke N. Brewer^{1,5}](#), [Patrick E. Hopkins²](#)

⁽¹⁾*Sandia National Laboratories, PO Box 5800, Albuquerque NM 87185, United States*

⁽²⁾*University of Virginia, PO Box 400746, Charlottesville VA 22904, United States*

⁽³⁾*Los Alamos National Laboratory, P.O. Box 1663, Los Alamos NM 87545, United States*

⁽⁴⁾*University of Michigan, 2300 Hayward Street, Ann Arbor MI 48109, United States*

⁽⁵⁾*Naval Postgraduate School, 1 University Cir., Monterey CA 93943, United States*

To accelerate the incorporation of advanced materials into Generation IV nuclear reactors or to extend the lifetime of current Generation II reactors, advance models must reliably predict the performance margins of the structural metals exposed to a combination of radiation, mechanical loading, and corrosive environments. The fidelity of these models and initial screening of potential alloys may be greatly enhanced through the combination of ion irradiation and implantation that can be used to simulate various aspects of neutron exposure. These ion beam techniques permit rapid exposure to high embedded gas concentrations, extensive displacement damage, or controlled combinations thereof. Unfortunately, the inherent limited volume associated with ion irradiation and implantation excludes the traditional techniques used for probing the thermal and mechanical properties of the damaged microstructures. This presentation will highlight a few of the

techniques that have been utilized to investigate the small-scale thermal and mechanical properties of radiation damaged metals.

The challenges and opportunities with various small-scale mechanical testing techniques that have been explored at Sandia to evaluate the mechanical stability of ion irradiated and implanted metals will be reviewed. These techniques span a large gamut including: nanoindentation, micropillar compression, and microtensile experiments. In addition, this presentation will debut the use of time domain thermoreflectance (TDTR) to probe the radiation damage in copper-niobium nanolamellar and erbium coated zirconium alloy produced by various ion irradiation conditions.

This research was partially funded by the U.S. Department of Energy, Office of Science, Office of Basic Energy Sciences, Division of Materials Sciences and Engineering. Sandia National Laboratories is a multi-program laboratory managed and operated by Sandia Corporation, a wholly owned subsidiary of Lockheed Martin Corporation, for the U.S. Department of Energy's National Nuclear Security Administration under contract DE-AC04-94AL85000.

Abstract 325 MON-RE02-2

[Contributed Talk - Monday 4:00 PM - Presidio C](#)

What have we learned about swelling resistance and dispersoid stability in ODS variants of ferritic-martensitic alloys using self-ion bombardment?

[Frank A. Garner](#)¹, [Mychailo B. Toloczko](#)², [David T. Hoelzer](#)³, [Lin Shao](#)⁴, [Victor V. Bryk](#)⁵, [Oleg V. Borodin](#)⁵, [Victor N. Voyevodin](#)⁵, [Shigeharu Ukai](#)⁶

⁽¹⁾*Radiation Effects Consulting, 2003 Howell Avenue, Richland WA 99354, United States*

⁽²⁾*Pacific Northwest Laboratory, Richland WA 99354, United States*

⁽³⁾*Oak Ridge National Laboratory, Oak Ridge TN 37831, United States*

⁽⁴⁾*Texas A&M University, College Station TX 77843, United States*

⁽⁵⁾*Kharkov Institute of Physics and Technology, Kharkov 7261072, Ukraine*

⁽⁶⁾*Hokkaido University, Sapporo, Japan*

It is recognized that austenitic alloys cannot resist the onset of high-rate swelling beyond ~120-150 dpa, a limitation that precludes fuel burn-up above 11-12% maximum in fast reactors. Other reactor concepts also require dose levels in excess of 150 dpa, perhaps 300 to 600 dpa. Therefore, the reactor materials community has shifted to ferritic and ferritic-martensitic (FM) alloys which are known to swell much less than austenitics. There is particularly strong interest in oxide-dispersion-strengthened (ODS) variants of these alloys to extend the service range to higher temperatures.

While some ODS FM alloys have been irradiated in fast reactors, the attained doses do not exceed 100 dpa. Therefore, there is a concerted effort to explore the response of these alloys to high dose irradiation using self-ion irradiation, especially concerning stability of dispersoids and resistance to void swelling. Two ion simulation programs are being used in a joint effort, one using 1.8 MeV Cr ions at KIPT, and another at TAMU using 3.5 MeV Fe ions. Depending on the alloy investigated, doses as high as 500 dpa have been employed.

Using irradiation parameters previously established for non-ODS FM alloys (HT9, EP-450, EK-181, ChS-139), irradiation of EP-450-ODS, 14YWT and several heats of MA957 was conducted at KIPT, while irradiation of MA956 and 9Cr-ODS was conducted at TAMU.

It has been observed that the uniformity of initial dispersoid distribution is key; otherwise the local swelling can vary from almost zero to very large levels within adjacent grains. In general, dispersoids appear to retard the onset of void swelling

compared to non-ODS steels, with the exception of MA956 where the dispersoids appear to facilitate void nucleation. There are significant differences among the various alloys in both void swelling and dispersoid stability. These results provide guidance for future studies to develop improved FM-ODS alloys.

Abstract 269 MON-RE02-3

[Contributed Talk - Monday 4:00 PM - Presidio C](#)

Accessing Defect Dynamics using Intense, Nanosecond Pulsed Ion Beams

[Arun Persaud](#)¹, [Hua Guo](#)², [Steve M Lidia](#)¹, [William L Waldron](#)¹, [Peter Hosemann](#)³, [Andrew M Minor](#)^{2,4}, [Thomas Schenkel](#)¹

⁽¹⁾*Accelerator and Fusion Research Division, E. O. Lawrence Berkeley National Laboratory, 1 Cyclotron Road, Berkeley CA 94720, United States*

⁽²⁾*Materials Sciences Division, E. O. Lawrence Berkeley National Laboratory, 1 Cyclotron Road, Berkeley CA 94720, United States*

⁽³⁾*Nuclear Engineering Department, University of California, Berkeley CA 94720, United States*

⁽⁴⁾*Department of Materials Science and Engineering, University of California, Berkeley CA 94720, United States*

Experiments using fast pump and probe beams can access the dynamics of radiation damage from ion implantation at time scales in the picosecond to the microsecond range. At these short timescales, a very high ion-beam current is required to create enough damage to be probed. The Neutralized Drift Compensation Experiment (NDCX-II) at Berkeley National Laboratory is able to provide these high current beams delivering tens of nano-Coulombs of charge in a nanosecond pulse. We will discuss the present status of the facility, which is able to deliver up to 30nC of Li ions with a pulse length of 20-500ns at 100-300keV. Furthermore, we will present the current effort to finalize the machine to meet its design goal of a sub-1ns pulse width of Li ions at an energy of 1.2MeV.

The results of ongoing experiments will be presented, where the NDCX-II beam is used to investigate the defect dynamics of lithium ions in crystalline silicon membranes by observing the transmitted ions. Due to the properties of the ion beam (e.g. angular distribution), some ions in the beam will channel through the sample, whereas others will not. The latter will create more damage in the sample, which will influence the number of subsequent ions that can channel. We are currently working on experiments that utilize this phenomenon to probe the time dynamics of the defects. Furthermore, we will discuss our effort to expand these experiments to other target materials and probes, as well as different ion species.

This work was supported by the Office of Science of the U.S. DOE and by the LDRD Program at Lawrence Berkeley National Laboratory under contract no. DE-AC02-05CH11231. AM was supported by the Center for Defect Physics, an Energy Frontier Research Center funded by the U.S. DOE, Office of Science, Basic Energy Sciences.

Abstract 252 MON-RE02-4

[Contributed Talk - Monday 4:00 PM - Presidio C](#)

The Effects of Simultaneous Molten Salt Corrosion and Radiation Damage Simulated via Ion Beam Irradiation

[Elizabeth S Sooby](#)¹, [Magda S Caro](#)², [Robert Houlton](#)², [Feng Lu](#)¹, [Akhdiyor I Sattarov](#)¹, [Joseph Tesmer](#)², [Yongqiang Wang](#)², [Peter M McIntyre](#)¹

⁽¹⁾*Physics and Astronomy, Texas A&M University, 4242 TAMU, College Station TX 77843, United States*

⁽²⁾*Ion Beam Accelerator Laboratory, Los Alamos National Laboratory, Los Alamos NM, United States*

Molten salt reactors, both salt fueled and salt cooled, have been studied as safe sources for nuclear energy since the 1960's. A novel technology for Accelerator-based Destruction of Actinides in Molten salt (ADAM) is being developed at Texas A&M University as a method to destroy the transuranics in used nuclear fuel. The core structural components will be exposed to radiation damage by fast-spectrum neutrons and corrosion in 600 C chloride-based molten fuel salt. An experiment to expose pure nickel, a primary vessel material candidate, to simultaneous molten salt corrosion and ion-beam damage is staged at the Ion Beam Materials Laboratory at Los Alamos National Laboratory. A 5.5 MeV, 3 micro-A proton beam will pass through the window and deposit approximately 10 DPA at the molten salt interfacing surface. A surrogate fuel salt, $\text{CeCl}_3\text{-NaCl}$, is contained in a dry atmosphere capsule held at 550 C. Irradiation occurs over one week, allowing 100 hours of molten salt exposure. The initial post-irradiation observations and initial microscopy results are presented here.

Abstract 233 MON-RE02-5

[Contributed Talk - Monday 4:00 PM - Presidio C](#)

Vacancy defects induced in Tungsten by 20 MeV W ions irradiation: Effect of fluence and temperature irradiation

[Moussa Sidibe](#)¹, [Pierre Desgardin](#)¹, [Patrick Trocellier](#)², [Yves Serruys](#)², [Marie-France Barthe](#)¹

⁽¹⁾CEMHTI, CNRS, Orleans University, 3A rue de la férollerie, Orléans 45071, France

⁽²⁾DEN/DMN/SRMP, CEA, Centre d'Études Nucléaires de Saclay, Gif sur Yvette 91191, France

The International Thermonuclear Experimental Reactor (ITER) will be a step in the demonstration of the scientific and technological feasibility of producing energy using a fusion reaction. The divertor is a critical component, it will be subjected to intense particle bombardment (neutron, He, H...), high heat fluxes, and operating temperatures between 780K and 1780K. Tungsten was chosen for the plasma facing components in the divertor region of ITER, because of its good properties such as low sputtering erosion, good thermal conductivity as well as high melting point. Particle bombardment creates atomic displacement and damage in material that can lead to a degradation of its macroscopic properties.

In this work we investigate vacancy defects induced in polycrystalline tungsten samples with 20 MeV W ions irradiations by using positron annihilation spectroscopy. Irradiations have been performed at different fluences and induced damage dose of 0.25, 1 and 12 dpa (as calculated by using SRIM), in region probed by positron (0-700nm), and the effect of irradiation temperature has been investigated.

The nature, concentration and evolution of vacancy defects as a function of fluence and temperature has been studied by using the Slow Positron Beam coupled to Doppler Broadening spectrometer of the CEMHTI laboratory (Orleans, France), to probe vacancy defects in the first μm under the surface of the sample.

After irradiation the measurements show that vacancy clusters are created in W and that their size change as a function of damage dose and temperature.

Abstract 482 TUE-PS02-1

[Plenary Talk - Tuesday 8:00 AM - Lone Star Ballroom](#)

Charged-Particle Therapy Takes Center Stage

[Eugen B. Hug](#)

ProCure Proton Therapy Center, 103 Cedar Grove Lane, Somerset NJ 08873, United States

Abstract 485 TUE-PS02-2

[Plenary Talk - Tuesday 8:00 AM - Lone Star Ballroom](#)

Facility for Antiproton and Ion Physics

[Thomas Stohlker](#)

Helmholtz Institut Jena, Friedrich-Schiller University, GSI, Darmstadt, Germany

FAIR, the Facility for Antiproton and Ion Research, is the next generation facility for fundamental and applied research with antiproton and ion beams [1]. It will provide worldwide unique accelerator and experimental facilities, allowing for a large variety of unprecedented fore-front research in physics and applied sciences [2]. Key features of FAIR are intense beams of antiprotons and ions up to the heaviest and even exotic nuclei in virtually all charge states, covering an energy range from rest up to 30 GeV/u. Special emphasis will be devoted to the experimental facilities and the anticipated research programs related to atomic and fundamental physics with highly-charged ions [3] and slow anti-protons [4] and will focus on most recent developments.

[1] W.F. Henning et al., An International Accelerator Facility for Beams of Ions and Antiprotons, GSI, Darmstadt, 2001, http://www.gsi.de/GSI_Future/cdr

[2] T. Aumann, K.H. Langanke, K. Peters, Th. Stöhlker, EPJ Web of Conferences 3, 01006 (2010)

[3] <http://www.gsi.de/sparc>

[4] http://www.gsi.de/fs3/start/fair/fair_experimente_und_kollaborationen/sparc/anlagen/flair.htm

Abstract 283 TUE-ATF05-1

[Invited Talk - Tuesday 10:00 AM - Presidio A](#)

Laser Plasma Accelerators as Driver of Future Light Sources

[Jeroen van Tilborg](#), [Carl B Schroeder](#), [Brian H Shaw](#), [Wim P Leemans](#)

Lawrence Berkeley National Laboratory, 1 Cyclotron Road, Berkeley CA 94720, United States

In laser-plasma accelerators (LPAs), the cm-scale interaction of ultra-intense laser pulses with underdense plasmas leads to the production of well-directed electron beams. LPAs have already enabled the availability of high-quality GeV electron

beams at compact laser facilities. One of the emerging pillars of the community is the application of LPAs as driver of novel light source technology, ranging from long-wavelength THz radiation to high-energy X-rays and gammas. This novel radiation source benefits from the key advantages of LPAs, including

- The hyper-spectral nature of the source (electrons, X-rays, gamma rays, THz radiation, laser)
- Ultra-short pulse durations (~ 10 fs)
- Intrinsically small timing jitter (few fs)
- High peak-current ($> \text{kA}$) electron beams and intense photon fluxes
- Small facility footprint (compact accelerator)
- Flexibility in hardware lay-out

In this talk the focus will concern the production of coherent X-ray pulses. This can be achieved with an LPA-driven free-electron laser (FEL). By seeding the FEL with a coherent photon beam, further improvements in system compactness and stability are feasible. It is predicted that over 10^{11} photons per pulse (~ 10 fs duration, photon energy ~ 30 eV) can be produced, triggering applications in non-linear X-ray optics, X-ray pump/probe experiments, and single-shot X-ray diffraction. I will address the stringent quality requirements on the LPA e-beam, and discuss approaches our group and others have taken to achieve this. Experimental results on incoherent LPA-driven X-ray production are presented, as well as our recent results on laser-driven high-harmonic generation off a spooling tape as FEL seed source. It will be discussed how the various components (LPA e-beam production, transport and phase-space manipulation, coherent seed generation, and undulator-based X-ray production) can be integrated towards an LPA-driven FEL.

This work was supported by the National Science Foundation under contracts 0917687 and 0935197, and the United States Department of Energy under Contract No. DE-AC02-05CH11231.

Abstract 220 TUE-ATF05-2

[Invited Talk - Tuesday 10:00 AM - Presidio A](#)

Ultrafast electron bunches from a laser-wakefield accelerator at kHz repetition rate

[Zhaohan He](#)¹, [Vivian Lebailly](#)², [John A Nees](#)¹, [Bixue Hou](#)¹, [Karl Krushelnick](#)¹, [Benoit Beaurepaire](#)²,
[Jerome Faure](#)², [Victor Malka](#)², [Alexander G R Thomas](#)¹

⁽¹⁾*University of Michigan, Ann Arbor, United States*

⁽²⁾*Laboratoire d'Optique Appliquée, Paris, France*

We report on laser wakefield electron acceleration using a high-repetition-rate, sub-TW power laser. By tightly focusing 30 fs laser pulses with up to 20 mJ pulse energy on a 100 μm scale gas target, high amplitude plasma waves are excited that trap and accelerated electrons. Our experiments are carried out at an unprecedented 0.5 kHz repetition rate, allowing 'real-time' optimization of accelerator parameters using a genetic algorithm. We were able to improve the electron beam charge and angular distribution each by an order of magnitude and even to control the energy distribution. We show that electron bunches with a peak energy of around 100 keV can be produced and that using a solenoid magnetic lens, the electron bunch distribution can be shaped. The resulting transverse and longitudinal coherence is suitable for producing single shot diffraction images from crystalline samples. The high repetition rate, the stability of the electron source, and the fact that its uncorrelated bunch duration is below 100 fs make this approach promising for the development of sub-100 fs ultrafast electron diffraction experiments.

Status of plasma spectroscopy method for CNS Hyper-ECR ion source at RIKEN

[Hideshi MUTO](#)^{1,2,3}, [Yukimitsu Ohshiro](#)², [Shoichi Yamaka](#)², [Shin-ichi Watanabe](#)^{2,3}, [Michihiro Oyaizu](#)⁴, [Shigeru Kubono](#)^{2,3,5}, [Hidetoshi Yamaguchi](#)², [Masayuki Kase](#)³, [Toshiyuki Hattori](#)⁶, [Susumu Shimoura](#)²

⁽¹⁾Center of General Education, Tokyo University of Science, Suwa, 5000-1 Toyohira, Chino Nagano 391-0292, Japan

⁽²⁾Center for Nuclear Study, University of Tokyo, 2-1 Hirosawa, Riken Campus, Wako Saitama 351-0198, Japan

⁽³⁾Nishina Center for Accelerator-Based Science, RIKEN, 2-1 Hirosawa, Wako Saitama 351-0198, Japan

⁽⁴⁾Institute of Particle and Nuclear Studies, High Energy Accelerator Research Organization, 1-1 Oho, Tsukuba Ibaraki 305-0801, Japan

⁽⁵⁾Institute of Modern Physics, Chinese Academy of Sciences, 509 Nanchang Road, Lanzhou 730000, China

⁽⁶⁾Heavy Ion Cancer Therapy Center, National Institute of Radiological Sciences, 49-1 Anagawa, Inage Chiba 263-8555, Japan

The optical line spectra of multi-charged gaseous and metal ion beams from ECR plasma have been observed using a grating monochromator with photomultiplier. Separation of ion species of the same charge to mass ratio with an electromagnetic mass analyzer is almost impossible. However, this new method simplifies the observation of the targeted ion species in the plasma during beam tuning. In this paper we describe present condition of the Hyper-ECR ion source tuning with this plasma spectroscopy method.

Comparison of Radiation Damage by Light- and Heavy-Ion Bombardment in Single-Crystal LiNbO₃

[Hsu-Cheng Huang](#)¹, [Jerry I. Dadap](#)¹, [Richard M. Osgood, Jr.](#)¹, [Sandeep Manandhar](#)², [Rama Sesha R Vemuri](#)², [Vaithiyalingam Shutthanandan](#)², [Girish Malladi](#)³, [Hassaram Bakhru](#)³

⁽¹⁾Center for Integrated Science & Engineering, Columbia University, New York New York 10027, United States

⁽²⁾Environmental Molecular Sciences Laboratory, Pacific Northwest National Laboratory, Richland Washington 99352, United States

⁽³⁾College of Nanoscale Science and Engineering, State University of New York at Albany, Albany New York 12222, United States

Lithium niobate (LiNbO₃) is one of the most widely used complex oxides, exhibiting important materials functionality such as ferroelectricity, piezoelectricity, electro-optic, and nonlinear-optical effects. Radiation damage in such insulating oxides is important for various technological applications and as well as for understanding the response of materials to extreme environments. It has been reported that light-ion (He⁺) irradiation will induce damage including the formation of point defects, compositional change, long- and short-range strain and local volume swelling [1, 2]. In this work, **in-situ** RBS/Channeling (Rutherford Backscattering Spectroscopy), confocal micro-Raman imaging, optical microscopy (OM), scanning electron microscopy (SEM), and atomic force microscopy (AFM) are used to investigate heavy-ion (iron) radiation damage. Different Raman probing geometries, together with the use of RBS/C provide complementary damage information and its distribution. Surface deformation features including partial exfoliation and lattice disorder along ion trajectories were observed. The effects of different iron doses, post-implantation treatments such as annealing, and the comparison of damage with light-ion (He⁺) irradiation are also discussed. Our discussion will emphasize implications for applications in optical modulation.

[1] **Opt. Mater. Express** **4**, 338-345 (2014).

[2] **Opt. Mater. Express** **3**, 126-142 (2013).

In-situ study of damage evolution in SrTiO₃ and MgO using ion beam-induced luminescence

[Miguel L. Crespillo](#)¹, [Yanwen Zhang](#)^{1,2}, [William J. Weber](#)¹

⁽¹⁾*Materials Science & Engineering Dept., University of Tennessee, Knoxville Tennessee 37996, United States*

⁽²⁾*Materials Science & Technology Division, Oak Ridge National Laboratory, Oak Ridge Tennessee 37831, United States*

Ion beam-induced luminescence (IL or IBIL) is a sensitive technique, often applied for characterization of dielectric and semiconductor materials. It provides information on the electronic structure of the solid, particularly on intra-gap levels associated to impurity and defect centers, such as those introduced by irradiation. In particular, the luminescence induced by ion-beam irradiation, commonly named ionoluminescence, is an appropriate technique to investigate the microscopic processes accompanying the generation of damage, its kinetic evolution with the irradiation fluence, and the formation of color centers. Compared to conventional post-irradiation techniques, measuring IL of materials, enables **in-situ** measurements of the evolution of network degradation and the formation of new structures.

A new optical experimental setup has been developed at the UT-ORNL Ion Beam Materials Laboratory to perform the ionoluminescence measurements from some scintillation materials, including some model oxides: SiO₂, quartz, SrTiO₃, and MgO. High-purity single crystals with low defect concentrations have been used in this work. Irradiations were performed in a multipurpose end-station, using low currents. The light emitted from the samples was transmitted through a silica window port placed at 30° with respect to the ion beam, and collected by focusing with a lens into a silica optical fiber located outside of the vacuum chamber. The light was guided to a spectrometer equipped with a back illuminated CCD camera. The evolution of the ion-beam-induced luminescence spectrum was monitored for wavelengths from 250 to 1000 nm with a spectral resolution better than 0.05 nm.

The goal of this work focuses on studying the kinetics of damage evolution by measuring electron/ion-induced luminescence from irradiation-induced defects in SrTiO₃ and MgO crystals at cryogenic temperatures (from ~ 100 K to room temperature). A study of separate and integrated radiation effects between nuclear and electronic damage in nuclear materials will be presented and discussed.

The New Applications of Rutherford Backscattering Spectrometry/Channeling

[Shude Yao](#), [Quan Bai](#), [Engang Fu](#), [Lin Li](#), [Fengfeng Cheng](#), [Ren Bin](#), [Tao Fa](#)

State Key Laboratory of Nuclear Physics and Technology, Peking University, Beijing 86-100871, China

Rutherford Backscattering Spectrometry/Channeling(RBS/C) is a mature and applicable ion beam analysis technology. In recent years, we applied and developed this technique for a series of new materials to measure their multiple special structural characteristics, such as: elastic strain, ordering affect, features of inserted layer in heteroepitaxial film ; detail of radiation damage layer; diffusion or interdiffusion behaviors for various elements of multilayer, and so on.

Research and control the composition and structure of novel hybrid III-V group and II-VI group semiconductors are critical for their optoelectronic and microelectronic interested properties and widely applications. In this study, we reported on the relation regularities between ingredient, component, thickness of the inserted layer in the heteroepitaxial films with the

depth, width of the corresponding RBS spectrum deep pit. The results from RBS/C are very accurate and reliable. We also found a way to measure and assess the extent of radiation damage by RBS/C accurately.

Abstract 295 TUE-IBA03-4

[Contributed Talk - Tuesday 10:00 AM - Presidio B](#)

Effect of transition metal ion implantation on photocatalysis and hydrophilicity of MOD deposited TiO_2 , V_2O_5 and mixed oxide films

[Chandra Thapa](#), [Punya Talagala](#), [Xhorlina Marco](#), [Karur R Padmanabhan](#)

Physics and Astronomy, Wayne State University, 666 West Hancock, Detroit MI 48201, United States

Thin TiO_2 , V_2O_5 and mixed oxide films deposited using Metalorganic Deposition (MOD) technique and implanted with transition metal ions were measured for photocatalysis and hydrophilicity. The implantation conditions were predetermined using SRIM code and the oxides were characterized by XRD, Raman spectroscopy and RBS. Hf^+ and V^+ and Fe^+ implanted TiO_2 films exhibited best photocatalytic efficiency while Co^+ implantations in the oxide demonstrated poorer efficiency than unimplanted films. The water contact angle measurements of the films before and after photoactivation showed good hydrophilicity corresponding to saturation contact angle for V^+ implanted and ion beam mixed TiO_2 - HfO_2 films. It appears high oxygen vacancies and deep electron-hole traps could be attributed as major factors for high photocatalytic efficiency. In addition lower surface acidities of mixed oxide films seem to enhance hydrophilicity compared to implanted single oxide films probably due to higher number of oxygen vacancies on the surface and implantation induced defects.

Abstract 430 TUE-IBA03-5

[Contributed Talk - Tuesday 10:00 AM - Presidio B](#)

The Role of Oxygen Vacancies in Conductivity of SrCrO_3 - Films

[Amila Dissanayake](#)¹, [Hongliang Zhang](#)², [Yingge Du](#)¹, [Robert Colby](#)¹, [Sandeep Manandhar](#)¹,
[Vaithiyalingam Shutthanandan](#)¹, [Scott Chambers](#)²

⁽¹⁾*EMSL, Pacific Northwest National Lab, 902 innovation Blvd, Richland Washington 99352, United States*

⁽²⁾*Pacific Northwest National Lab, 902 innovation Blvd, Richland Washington 99352, United States*

There is a great deal of current interest in finding new materials that can effectively harvest sunlight for both photovoltaic conversion and powering photochemical reactions. Therefore, finding photovoltaic and photochemically active materials that absorb in the visible is of especially high interest. Mixed perovskite oxide semiconductors are an attractive system for light harvesting applications, including alloys with bandgaps across the visible spectrum, made from materials that are inexpensive and abundant. Since LaCrO_3 is a wide bandgap semiconductor and SrCrO_3 is conducting, the $(\text{La,Sr})\text{CrO}_3$ alloy system can potentially be tuned to absorb in the visible region. However, the degree of conductivity in SrCrO_3 films seems to depend upon defects in the material and in particular oxygen vacancies. The structure and resulting properties of SrCrO_3 films grown on LaAlO_3 by molecular beam epitaxy (MBE) are investigated using resonant Rutherford backscattering spectrometry (RRBS), conventional and scanning transmission electron microscopy (TEM/STEM). The precise oxygen deficiency is measured using RRBS and was found that the as grown films are 15% O-deficient. STEM results clearly showed that the as-grown films with poor conductivities have ordered oxygen vacancies aligned along (111) planes. There is a marked improvement in the conductivity after annealing in oxygen. Detail RRBS and TEM analysis of the samples before and after the oxygen annealing will be shown, demonstrating the role of defects and oxygen vacancies on the resulting conductivity.

Nano-scale Materials[Leonard C Feldman](#)

Institute for Advanced Materials, Devices and Nanotechnology, Rutgers University, 607 Taylor Rd, New Brunswick NJ 08901, United States

Modern material research has provided the means of creating structures controlled at the atomic scale. Familiar examples include the formation of hetero-structures grown with atomic precision, monolayer (graphene and graphene-like) films, nanostructures with designed electronic properties, shaped nano-plasmonic materials and new organic structures employing the richness of organic chemistry. The current forefront of such nano-materials research includes the creation and control of new materials for energy, bio/medical and electronics applications. The performance of these diverse materials, and hence their performance, is invariably linked by their fabrication and their interfacial structure. Interfaces are the critical component and least understood aspect of such materials-based structures.

Ion beam analysis, and its role in interfacial definition, will be described in the context of a number of such forefront projects underway at the Rutgers Institute for Advanced Materials, Devices and Nanotechnology (IAMDN). These include: 1) self-assembled monolayers on organic single crystals resulting in enhanced surface mobility; 2) monolayer scale interfacial analysis of complex oxide hetero-structures to elucidate the p the enhanced two-dimensional electron mobility; 3) characterization of the semiconductor-dielectric interface in the SiC/SiO₂ system for energy efficient power transmission.

Nanoscale materials require nanoscale ion beam analysis. We briefly describe IAMDN progress on this front employing the Zeiss-Orion 0.25nm He ion beam and the Rutgers-NION Scanning Transmission Electron Microscope with ~ 12 meV electron energy loss resolution.

Fellow Researchers: R. A. Bartynski, E. Garfunkel, T. Gustafsson, H.D. Lee, D. Mastrogiovanni, V. Podzorov, L. S. Wielunski, G. Liu, J. Williams, S. Dhar, S. Rosenthal, P. Cohen, E. Conrad, Yi Xu, P. Batson

Radiation defects in nanoscale: the case of compound materials[Andrzej Turos](#)

Institute of Electronic Materials Technology, Wolczynska 133, Warsaw 01-919, Poland

Ion beams are currently used for analysis and modification of nanometer scale materials. Therefore, understanding of radiation effects in nanomaterials is urgently required for designing new materials. The mechanism of defect formation and agglomeration upon ion bombardment in single element materials is quite well known. Typically, a continuous growth of damage clusters up to amorphisation has been observed. The situation dramatically changes in the case of compound

materials. Migration, recombination and agglomeration of defects produced in different sublattices lead to microstructure transformations resulting in a complicated, multistep defect accumulation process.

The elementary processes in nanoscale are extremely difficult to follow experimentally, hence, the basic studies are mostly based on the Molecular Dynamics (MD) simulations. The experimental validation of such computer simulations is the key issue in defect studies. Here the approach based on the analysis of defect accumulation curves will be presented. The dissipation of the energy deposited by the incident particle is considered in the thick medium and a variety of analytical methods like: ion channeling, TEM and XRD have been used. The materials studied were compound semiconductors AlGaAs and GaN.

Our study of defect accumulation revealed that collisional damage evolves in dislocation loops and stacking faults. Comparison of defect mobility at 15K and RT indicated that an athermal process is responsible for defect agglomeration. The driving force being the lattice stress produced by displaced atoms. However, as indicated by MD simulations, antisite defects can also play a role. Upon continuous ion bombardment the extended defects grow leading to a strain build up in the implanted region. Once the critical value of the stress has been attained plastic deformation takes place leading to a complicated, almost unrecoverable defect structure. Basing on these observations defect transformation models will be proposed and compared to MD simulations.

Abstract 14 TUE-IBM02-3

[Invited Talk - Tuesday 10:00 AM - Bonham C](#)

Ion beam induced effects on nanocrystals, alloys and high-k dielectric films

[Srinivasa Rao Nelamarri¹](#), [Saikiran V²](#), [Manikanthababu N²](#), [Nageswara Rao S V S²](#), [Anand P Pathak²](#)

⁽¹⁾*Department of Physics, Malaviya National Institute of Technology Jaipur, JLN Marg, Jaipur Rajasthan 302017, India*

⁽²⁾*School of Physics, University of Hyderabad, Central University (P.O), Hyderabad Andhra Pradesh 500046, India*

Ion beams are one of the most important tools for materials processing, modification, and also for materials analysis. In particular, ion irradiation is an effective method for the modification of materials at nano-scale. Properties of various nanomaterials are being tuned using swift heavy ion beam irradiation by changing their size and shape. Here we report the effects of ion beam irradiation on Ge nanocrystals (NCs) which have been synthesized by RF magnetron co-sputtering technique followed by rapid thermal annealing. Variation of NC size with ion beam parameters is explained on the basis of energy deposited by incident ion inside the target material. Titanium-nickel (TiNi) alloys have attracted great attention due to their superior electronic and mechanical properties and extensive effort has been devoted to investigate these alloys. High energy ion beam irradiation induced phase transformation and modifications of TiNi alloys are being investigated and results will be discussed in detail. Finally, ion beam irradiation effects on high-k oxide thin films will also be presented during the conference.

Abstract 9 TUE-IBM02-4

[Contributed Talk - Tuesday 10:00 AM - Bonham C](#)

An On-line ERDA Study on SHI Induced Desorption of Hydrogen from Porous Silicon Prepared by Anodic Etching of H-implanted Silicon

[V S Vendamani^{1,2}](#), [Saif A Khan³](#), [M Dhanunjaya¹](#), [A P Pathak¹](#), [SVS Nageswara Rao¹](#)

⁽¹⁾*School of Physics, University of Hyderabad, Gachibowli., Hyderabad, Andhra Pradesh 500046, India*

⁽²⁾*Dept. of Physics, Pondicherry University, Kalapet., Puducherry Puducherry 605014, India*

⁽³⁾*Material Science Division,, Inter-University Accelerator Center,, Aruna Asaf Ali Marg, Vasantkunj Sector B., New Delhi, New Delhi 110067, India*

Porous silicon is considered to be a potential material in the field of electronics and optoelectronics because of its strong luminescence in visible/ infrared region. Ion implantation is a powerful technique for modifying the near-surface properties of porous silicon (pSi). Here we present a study on Swift Heavy Ion (SHI) induced desorption of hydrogen from porous silicon synthesized by hydrogen implanted c-Si wafers. The p-type (100) Si was implanted with 50 keV hydrogen ions at fluence of 1×10^{16} ions/cm². Some of these implanted samples were subjected to Rapid Thermal Annealing (RTA) at 450⁰ C under N₂ atmosphere while some of them were irradiated by 80 MeV Ni ions with fluence of 5×10^{13} Ni/cm² to study the SHI induced annealing effects. Further, all these samples were used to prepare porous silicon under specific anodic conditions. The hydrogen content and SHI induced desorption have been investigated on these samples by online Elastic Recoil Detection Analysis (ERDA) by using 100 MeV Ag ions. The comparative annealing behaviours on porous silicon formation as well as hydrogen desorption under various irradiation fluence will be discussed in detail.

Abstract 15 TUE-IBM02-5

[Contributed Talk - Tuesday 10:00 AM - Bonham C](#)

Swift Heavy Ion induced intermixing effects in HfO₂ based MOS devices

[N. Manikanthababu](#)¹, [Chan Taw Kuei](#)², [A. P. Pathak](#)¹, [X. W. Tay](#)², [N. ARUN](#)¹, [Yang Ping](#)³, [M. B. H. Breese](#)^{2,3}, [T. Osipowicz](#)², [S. V. S. Nageswara Rao](#)¹

⁽¹⁾*SCHOOL OF PHYSICS, UNIVERSITY OF HYDERABAD, P.O. CENTRAL UNIVERSITY, HYDERABAD ANDHRA PRADESH 500046, India*

⁽²⁾*Department of Physics, National University of Singapore, Singapore Singapore 117542, India*

⁽³⁾*Singapore Synchrotron Light Source, National University of Singapore, Singapore Singapore 117542, India*

In the semiconductor industry, SiO₂ has served as a conventional gate material for the last five decades. As the thickness of the SiO₂ gate dielectric is scaled down to 1 nm, leakage current becomes a major and serious issue. The proposed solution is to replace the conventional SiO₂ gate dielectric by a higher dielectric constant material. HfO₂ has been opted as a competent material among all other high-k dielectric materials owing to its compatibility with Si technology. A combination of SiO₂ and HfO₂ dielectric films deposited on Si forming a simple MOS structure seems to be more effective. A detailed study on Swift Heavy Ion (SHI) induced intermixing effects on ALD grown HfO₂ (3 nm)/SiO₂ (0.7 nm)/Si samples will be presented. These samples were irradiated by 120 MeV Au ions at 1×10^{13} , 5×10^{13} and 1×10^{14} ions/cm² fluences. SHI induced intermixing effects were evident from High Resolution Rutherford Backscattering Spectrometry (HRBS) and X-Ray Reflectometry (XRR) measurements performed on these samples. Further, electrical measurements like I-V (leakage current) and C-V will be performed using semiconductor device analyzer. The effects of SHI induced intermixing on the structural and electrical properties of these samples will be discussed in detail.

*Corresponding author E-mail: svnsp@uohyd.ernet.in & nageshphysics@gmail.com

Tel: +91-40-23134329, Fax: +91-40-23010227 / 23010181

Abstract 427 TUE-MA04-1

[Invited Talk - Tuesday 10:00 AM - Bonham B](#)

Status Update and New Developments in Planning, Verification, and Active Delivery of Particle Beam Therapy

[Reinhard W Schulte](#)

Radiation Medicine, Loma Linda University Medical Center , Loma Linda CA 92354, United States

Proton and ion beam therapy technology lags behind modern photon IMRT techniques. Only equivalent technology and similar planning margins will eventually allow a meaningful comparison between the different forms of radiation therapy. Clinical trials are, however, vital to define the indications for the different modalities and will eventually make clinical decisions based on tumor type, biology, and proximity of organs at risk reality. The technology development should thus be driven by clinical goals rather than the other way around. In this overview talk, the current status and new developments in particle accelerators, biological treatment planning, particle imaging, and adaptive therapy will be presented.

Abstract 466 TUE-MA04-2

[Invited Talk - Tuesday 10:00 AM - Bonham B](#)

New developments in Monte Carlo based treatment planning for proton therapy

[Bruce A Faddegon](#)

Radiation Oncology, University of California San Francisco, 1600 Divisadero Street, San Francisco ca 94941, United States

The Monte Carlo method is proving to be a valuable tool in treatment planning for proton therapy. Calculation of dose distributions have proven critical for accounting of source and geometry details including the treatment head and patient with the accuracy and detail required in radiotherapy. Applications are expanding to account for all types of temporal variations in the beam, treatment head and patient, to provide validation images for range verification with positron emission tomography and the emerging technology of proton computed tomography, and to estimate radiobiological effect to account for the spatial variation of physical aspects of the energy deposition including linear energy transfer. The emergence of this powerful tool for accurate and detailed radiotherapy simulation is strongly facilitated by the provision of systems to make it much easier for practitioners to harness the power of the Monte Carlo method while limiting supplementary requirements of programming or related computer skills. Techniques are being employed to make the simulations faster. Benchmarks are being measured to make the simulations more accurate. Continued developments are rapidly leading to wide acceptance of Monte Carlo simulation in proton therapy.

Abstract 469 TUE-MA04-3

[Invited Talk - Tuesday 10:00 AM - Bonham B](#)

4D-optimized beam tracking for treatment of moving targets with scanned ion-beam therapy

[John G Eley](#)¹, [Wayne D Newhauser](#)², [Robert Lüchtenborg](#)³, [Christian Graeff](#)³, [Christoph Bert](#)³

⁽¹⁾*Radiation Physics, UT MD Anderson Cancer Center, 1840 Old Spanish Trail, Houston TX 77054, United States*

⁽²⁾*Physics and Astronomy, Louisiana State University, 202 Nicholson Hall, Tower Drive, Baton Rouge LA 70803, United States*

⁽³⁾*Biophysik, GSI Helmholtzzentrum für Schwerionenforschung GmbH, Planckstraße 1, Darmstadt Hessen 64291, Germany*

Scanned ion-beam therapy for moving targets requires consideration of organ motion effects for treatment planning and delivery. The purpose of our study was to determine whether 4D-optimized beam tracking with scanned carbon-ion therapy could potentially benefit patients with thoracic cancers subject to respiratory motion. We implemented a 4D-optimization algorithm in a research treatment planning system for heavy-ion therapy. We also implemented changes in the treatment control system (TCS) for the experimental carbon-ion beamline at the GSI Helmholtz Centre for Heavy Ion Research in Darmstadt, Germany (GSI). The new TCS allows synchronization between 4D-optimized treatment plans and phases of respiration, which are monitored in real-time during treatment via motion sensors. We found that 4D-optimized ion beam tracking therapy can reduce the maximum dose to critical structures near a moving target by as much as 53%, compared to 3D-optimized ion beam tracking therapy, and can improve target dose homogeneity for targets in heterogeneous tissue. We validated these findings experimentally using the scanned carbon-ion synchrotron at GSI.

Abstract 475 TUE-MA04-4

[Invited Talk - Tuesday 10:00 AM - Bonham B](#)

Proton therapy using pencil beam spot scanning technology

[Alexander Winnebeck](#), [Martin Wegner](#), [Holger Goebel](#), [Juergen Heese](#), [Jay Steele](#)

PTX, Varian Medical Systems, Palo Alto CA 93204, United States

Proton therapy comprises all radio-oncological treatments using proton beams to cure cancerous tumors. After giving a brief introduction to the related biological and physical basics, an overview of the different beam delivery techniques like double scattering, uniform scanning, and spot scanning will be presented.

This talk focuses on one beam delivery technique, namely Varian's state-of-the-art pencil beam spot scanning technology. The concept of this technique will be illustrated and the workflow of a treatment together with some technical insights will be discussed.

Finally the measured performance and the first clinical results from Scripps Proton Therapy Center using Varian's latest spot scanning technology are presented.

Abstract 109 TUE-MA04-5

[Invited Talk - Tuesday 10:00 AM - Bonham B](#)

Uncoupled and Achromatic Gantry for Medical Applications

[Nicholaos Tsoupas](#)¹, [Vladimir Litvinenko](#)², [Dmitry Kayran](#)³

⁽¹⁾CAD, BNL, Building 911B, Upton NY 11973, United States

⁽²⁾CAD, BNL, Building 911B, Upton NY 11973, United States

⁽³⁾CAD, BNL, Building 911B, Upton NY 11973, United States

The angular orientation of a medical gantry introduces linear beam coupling which causes an angular dependence of the beam spot size at the isocenter of the gantry. This dependence of the beam spot size on the angular orientation of the gantry can be eliminated by imposing the achromatic and uncoupled constraints on the beam optics of the gantry. In this presentation we discuss the beam optics of a gantry which satisfies these two constraints and we show that the beam spot size at the location of the isocenter is independent on the angular orientation of the gantry.

Abstract 95 TUE-MA04-6

[Contributed Talk - Tuesday 10:00 AM - Bonham B](#)

Progress in the development of the proton Computed Tomography (pCT) Phase-II scanner at NIU.

[Sergey A Uzunyan](#)

Physics Department, Northern Illinois University, Department of Physics, 232 La Tourette Hall, DeKalb IL 60115, United States

Proton imaging can provide more accurate dose delivery compared to achievable

via traditional X-ray computed tomography, while also inducing a lower dose for image production.

We describe the development of a second generation proton Computed Tomography (pCT) scanner at Northern Illinois University (NIU) in

collaboration with Fermilab and Delhi University. The scanner is designed to demonstrate pCT can be used in a clinical environment

with the ability of collecting data required for 2D or 3D image reconstruction in about 10 minutes. We report on the progress in

the commissioning of the major scanner components: the Range Stack Calorimeter, the Tracker, and the Data Acquisition system, and present

the preliminary analysis of tests conducted at the ProCure Proton center in Warrenville, IL.

Abstract 11 TUE-NP03-1

[Invited Talk - Tuesday 10:00 AM - Travis C/D](#)

Recent Measurements at HELIOS

[Calem R Hoffman](#)

Physics, Argonne National Laboratory, 9700 S. Cass Ave, Argonne IL 60439, United States

Transfer reaction studies in nuclear structure research have been instrumental in achieving our current description of nuclei. Traditionally, such experiments were carried out using a beam of light particles impinging on a heavy stable target. However, because of large strides in the quality and the availability of radioactive ion-beams, this important technique now must be carried out in inverse kinematics. Transfer reactions in inverse kinematics present numerous challenges, including worsening energy resolutions due to kinematic compression, lower outgoing particle energies, and larger backgrounds. The Helical Orbit Spectrometer (HELIOS) is a detection system that was developed specifically to measure transfer reactions in inverse kinematics. HELIOS provides an improvement in energy resolution of up to five-times that of a traditional detector array while maintaining a high particle detection efficiency. The novel feature of HELIOS is use of a nearly 3 Tesla solenoid inside which the reactions take place. Outgoing particles are then measured at fixed longitudinal distance from the target (on beam axis) after completion of a single cyclotron orbit as opposed to at a fixed laboratory angle. This subtle mapping from laboratory angle to longitudinal position removes the aforementioned kinematic compression effect, thus improving the overall Q-value resolution. HELIOS also provides a natural way to identify particles of interest, independent of energy, through their measured cyclotron period. The design and implementation of HELIOS at the Argonne Tandem Linear Accelerator System (ATLAS) on the site of Argonne National Laboratory will be presented along with physics highlights from recent measurements.

Abstract 134 TUE-NP03-2

[Invited Talk - Tuesday 10:00 AM - Travis C/D](#)

Recent advances with ANASEN at the RESOLUT radioactive beam facility

[Ingo Wiedenhoefer](#)¹, [G. V. Rogachev](#)^{1,3}, [J. Blackmon](#)², [L. T. Baby](#)¹, [J. Belarge](#)¹, [E. D. Johnson](#)¹, [E. Koshchiy](#)^{1,3}, [A. Kuchera](#)¹, [K. Macon](#)², [M. Matos](#)², [D. Santiago-Gonzalez](#)¹

⁽¹⁾*Department of Physics, Florida State University, 315 Keen Building, Tallahassee FL 32306, United States*

⁽²⁾*Department of Physics and Astronomy, Louisiana State University, 221-C Nicholson Hall, Tower Dr., Baton Rouge LA 70803, United States*

⁽³⁾*Cyclotron Institute, Texas A&M University, College Station TX 77843, United States*

The resonant facility at Florida State University's accelerator laboratory produces beams of short-lived nuclei using the in-flight method. Beams such as ^6He , ^7Be , ^8Li , ^8B , ^{19}O and ^{25}Al have been successfully used in experiments. Recently, the program has focused on experiments with the new anasen detector system, which was commissioned in 2011 and 2012 during a series of experiments. Anasen is an active-target detector system developed for resonant scattering and transfer reactions.

In particular, anasen was used in two experiments studying the energetic location of the $d_{3/2}$ -orbital in neutron-rich nuclei, which is of interest as it determines the location of the neutron drip-line in the Oxygen isotopes. Another program pursued with anasen is the measurement of (α, p) reactions to establish the reaction rates of astrophysical events. The anasen project is a collaboration between Florida State University and Louisiana State University. It is funded by an NSF Major Research Instrumentation grant.

Abstract 13 TUE-NP03-3

[Invited Talk - Tuesday 10:00 AM - Travis C/D](#)

Reaction measurements with SuN

[Artemis Spyrou](#)^{1,2,3}, [S. Quinn](#)^{1,2,3}, [A. Simon](#)^{1,3}, [A. Dombos](#)^{1,2,3}, [T. Rauscher](#)⁴, [M. Wiescher](#)⁵

⁽¹⁾*National Superconducting Cyclotron Laboratory, Michigan State University, East Lansing MI 48824, United States*

⁽²⁾*Department of Physics and Astronomy, Michigan State University, East Lansing MI 48824, United States*

⁽³⁾*Joint Institute for Nuclear Astrophysics, Michigan State University, East Lansing MI 48824, United States*

⁽⁴⁾*Centre for Astrophysical Research, School of Physics, Astronomy, and Mathematics, University of Hertfordshire, Hatfield AL10 9AB, United Kingdom*

⁽⁵⁾*Department of Physics, University of Notre Dame, Notre Dame IN 46556, United Kingdom*

Charged particle capture reactions are extremely important for several astrophysical processes responsible for the nucleosynthesis of heavy elements. Nucleosynthesis in core collapse supernovae, supernova type Ia, X-ray bursts and others, include (p, g) and sometimes (α, g) reactions as well as their inverse ones. The majority of these reactions involve radioactive nuclei, which makes it hard to measure using the traditional techniques where a proton or alpha-beam impinges on a heavy stable target. It is therefore of paramount importance to develop tools that allow for such reactions to be explored in inverse kinematics at radioactive beam facilities.

For this purpose we have developed the Summing NaI (SuN) detector at the National Superconducting Cyclotron Laboratory, at Michigan State University. The detector is a 16x16 inch NaI cylinder with a borehole along its axis where the target can be placed. The detector was commissioned at the University of Notre Dame and first (p, g) and (α, g) reaction

cross sections were measured on a variety of stable targets in the mass region between Ni and Nb. For these measurements we applied the gamma-summing technique which is the equivalent of total absorption spectroscopy in reaction studies. Results from the stable beam/target measurements will be presented together with their implications on stellar nucleosynthesis. In addition, results from the first application of the gamma-summing technique in inverse kinematics will also be presented and the path toward radioactive beam experiments will be described.

Abstract 258 TUE-NP03-4

[Contributed Talk - Tuesday 10:00 AM - Travis C/D](#)

Intermediate-energy Coulomb excitation of neutron-rich chromium isotopes

[T. Baugher](#)¹, [A. Gade](#)^{2,4}, [R. V. F. Janssens](#)³, [S. M. Lenzi](#)⁵, [D. Bazin](#)^{2,4}, [B. A. Brown](#)^{2,4}, [M. P. Carpenter](#)³, [A. N. Deacon](#)⁶, [S. J. Freeman](#)⁶, [T. Glasmacher](#)^{2,4}, [G. F. Grinyer](#), [F. G. Kondev](#)³, [S. McDaniel](#)², [A. Poves](#)⁷, [A. Ratkiewicz](#)¹, [E. Ricard-McCutchan](#)³, [D. K. Sharp](#), [I. Stefanescu](#), [K. A. Walsh](#)^{2,4}, [D. Weisshaar](#)^{2,4}, [S. Zhu](#)³

⁽¹⁾*Physics and Astronomy, Rutgers University, Piscataway NJ, United States*

⁽²⁾*National Superconducting Cyclotron Laboratory, East Lansing MI, United States*

⁽³⁾*Physics Division, Argonne National Laboratory, Argonne IL, United States*

⁽⁴⁾*Department of Physics and Astronomy, Michigan State University, East Lansing, United States*

⁽⁵⁾*Dipartimento di Fisica e Astronomia dell'Università and INFN, Sezione di Padova, Padova, Italy*

⁽⁶⁾*School of Physics and Astronomy, Schuster Laboratory, University of Manchester, Manchester, United Kingdom*

⁽⁷⁾*Departamento de Física Teórica e IFT-UAM/CSIC, Universidad Autónoma de Madrid, Madrid, Spain*

In the nuclear shell model, the magic numbers, caused by large gaps in the nuclear energy levels, are well-established for nuclei near stability, but have been observed to change in the exotic regime. Traditional shell gaps can be reduced or disappear altogether while new ones can emerge. This can be explained by shifts in the single-particle energy levels due to the monopole components of the proton-neutron tensor interaction, for example. This shell evolution can lead to new regions of deformation and rapidly changing nuclear structure far from stability. The region below ⁶⁸Ni has been of interest recently since the enhanced 2⁺ energy and small quadrupole transition probability in ⁶⁸Ni suggested the possibility of an N=40 sub-shell gap, while nearby the iron and chromium isotopes were observed to be collectively approaching N=40. Intermediate-energy Coulomb-excitation experiments at the NSCL, combined with detailed simulations, have quantified the quadrupole collectivity in the iron isotopes out to N=42 and in the chromium isotopes out to N=40. The results pose sensitive benchmarks for state-of-the-art large-scale shell-model calculations and a recent effective interaction developed for this region and emphasize the importance of the 0g_{7/2} and 1d_{5/2} neutron orbitals beyond the N=40 sub-shell gap for describing nuclear structure in these isotopes. This work was funded in-part by the NSF under contract PHY-0606007; by the US DOE, Office of Nuclear Physics, under contracts DE-AC02-06CH11357 and DE-FG02-08ER41556 and by the UK Science and Technology Facilities Council (STFC). AP is supported by the MICINN (Spain) (FPA2011-29854) and by the Comunidad de Madrid (Spain) (HEPHACOS S2009-ESP-1473). TB is supported in-part by Rutgers University under NSF grant 1067906.

Abstract 247 TUE-NP03-5

[Contributed Talk - Tuesday 10:00 AM - Travis C/D](#)

Neutron Knockout on Beams of ^{108,106}Sn and ¹⁰⁶Cd

[Giordano Cerizza](#)

Physics and Astronomy, University of Tennessee - Knoxville, 401 Nielsen Physics Building, 1408 Circle Drive, Knoxville TN 37996, United States

Characterizing the nature of single-particle states outside of double shell closures is essential to a fundamental understanding of nuclear structure. This is especially true for those doubly magic nuclei that lie far from stability and where the shell closures influence nucleo-synthetic pathways. The region around ^{100}Sn is one of the most important due to the proximity of the $N=Z=50$ magic numbers, the proton-drip line, and the end of the rp-process. However, owing to the low production rates, there is a lack of spectroscopic information and no firm spin-parity assignment for ground states of odd-A isotopes close to ^{100}Sn . Neutron knockout reaction experiments on beams of $^{108,106}\text{Sn}$ and ^{106}Cd have been performed at the NSCL. By measuring gamma rays and momentum distributions from reaction residues, the spins of the ground and first excited states for $^{107,105}\text{Sn}$ have been established. The results also show a degree of mixing in the ground states of the isotopes $^{108,106}\text{Sn}$ between the $d_{5/2}$ and $g_{7/2}$ single particle-states. The results are compared to reaction calculations. Single-, double-, and triple-neutron knockout reactions on the ^{106}Cd beam have been observed. The spin-parity of ^{105}Cd is already known, therefore, the measurement of the momentum distributions of the ground and first excited states of this residue is an important validation of the technique used for the light tin isotopes.

Abstract 26 TUE-NST01-1

[Invited Talk - Tuesday 10:00 AM - Bonham D](#)

Ion Beam Assisted Enhanced Thermoelectric Properties (with Figure of Merit above 2.0)

[Daryush ILA](#)

Department of Chemistry and Physics, Fayetteville State University, 1200 Murchison Rd., Fayetteville NC 28301, United States

The reasons why thermoelectric generators (TEG) have not been used extensively to generate electricity or charge batteries can be summarized as: their low efficiencies, high temperature operation, and non-conformal nature. TEGs based on recently produced thermoelectric materials can operate starting at room temperature as the heat source or the cold source, as long as a temperature difference (dT) of a few degrees Kelvin is available, which leads to a potential difference, and a current is then generated. This enables us to capture the power generated, per few square centimeters, by the human body, while the ambient temperature is at or below 300K, in order to charge a cell phone battery, to charge the batteries for jogging LED indicators and more. Currently, few off-the-shelf TEGs can provide enough power to achieve the above goals, despite their bulkiness, despite their lack of flexibility and despite their low efficiency. In this presentation, we will report our work on production of thin films of thermoelectric materials which have higher figure of merit, and conformal shape, and which can operate at lower temperature difference (dT) than currently available TEGs (patent awarded & patent pending). Our work stems from the properties of regimented quantum dot quasi-lattices, consisting of nanocrystals of gold and/or silver separated at one to a few Angstroms from each other that display novel electrical and thermal properties as well as interesting optical properties. We will discuss how ion irradiation has been used by our team in order to achieve properties similar to those predicted theoretically for regimented quantum dot quasi-lattices. We will review a series of materials that have resulted from our investigation, some operating at temperatures around 300K and some at about 400K.

Abstract 270 TUE-NST01-2

[Invited Talk - Tuesday 10:00 AM - Bonham D](#)

Ion beam engineered nano metallic substrates for surface enhanced Raman spectroscopy

[Dharshana Nayanajith Wijesundera](#)¹, [Yanzhi He](#)¹, [Iram Saleem](#)¹, [Yang Li](#)², [Buddhi P Tilakaratne](#)¹, [Jiming Bao](#)², [Indrajith Rajapaksa](#)³, [Emmanuel Epie](#)¹, [Xuemei Wang](#)¹, [Irene Rusakova](#)¹, [Wei-Kan Chu](#)¹

⁽¹⁾Physics and Texas Center for Superconductivity, University of Houston, 4800 Calhoun Rd, Houston TX 77004, United States

⁽²⁾Dept. of Electrical & Computer Engineering, University of Houston, 4800 Calhoun Rd, Houston TX 77004, United States

⁽³⁾Department of Electrical Engineering and Computer Science, University of California, Irvine, Irvine CA, United States

A method for engineering substrates for surface enhanced Raman spectroscopy (SERS) by metal (Ag and Au) ion implantation in Si and SiO₂ matrix is demonstrated. The implantation dose and beam current density are chosen such that the metal concentration in the matrix exceeds the solid solubility limit, causes aggregation of Ag and nucleates Ag nano particles. The embedded nano particles are then partially exposed by a wet etch process and functionalized with a SERS

probe. Our measurements show that the so fabricated nano-composite substrates are effective as reproducible SERS substrates.

Abstract 221 TUE-NST01-3

[Invited Talk - Tuesday 10:00 AM - Bonham D](#)

Hybrid inorganic-organic composite materials for radiation detection

[Sunil K Sahi](#), [Wei Chen](#)

DEPARTMENT OF PHYSICS, THE UNIVERSITY OF TEXAS AT ARLINGTON, BOX 19059, ARLINGTON TX 76019, United States

Inorganic single crystals and organic scintillators (plastic or liquid) are the two widely used materials for radiation detection (scintillation) applications. High light output, fast decay time, high stopping power, good transparency and low cost are some basic requirements of a good radiation detector. The present day scintillators do not fulfill these entire criterions. The inorganic single crystals has high stopping power due to higher density and hence the better efficiency. But these single crystals are difficult to synthesize and are very expensive. On the other hand, organic scintillators have poor stopping power because of low Z-value. This limits the applications of these organic scintillators for gamma spectroscopy. Inorganic-organic hybrid materials, which combined the properties of inorganic and organic materials, could be a possible solution to these drawbacks. Here, we have explored the possibility of inorganic-organic hybrid materials for radiation detection. To make the hybrid materials we have synthesized the nanocrystals of inorganic materials and embedded into the polymer matrix. We have characterized the nanocrystals phase using X-ray diffraction (XRD). Transmission Electron Microscope (TEM) was used to determine the size of the nanocrystals. The optical properties of the hybrid materials are measured. The as synthesized hybrid materials showed, enhanced luminescence properties under ultra-violet (UV) and X-ray excitation and could be a promising materials for high energy(X-ray or gamma ray) detection.

Abstract 302 TUE-RE04-1

[Invited Talk - Tuesday 10:00 AM - Presidio C](#)

Interactions with Neutron Radiation in High-Performance Computing

[Heather Marie Quinn](#)

ISR3, Space Data Systems, Los Alamos National Laboratory, MSD440, Los Alamos NM 87544, United States

Interactions with terrestrial radiation is one of a number of ways that high-performance computers can fail. Many of these computers are designed with thousands of microprocessors and petabytes of volatile memory, which makes them vulnerable to single-event effects (SEEs). In these systems, SEEs can cause microprocessors to crash, change values in memory and change computational output. In this talk, we will cover how neutron radiation affects high-performance computers, results of testing high-performance computing sub-systems in neutron radiation, and efforts to suppress the effect of neutron radiation in high-performance computers.

Abstract 242 TUE-RE04-2

[Invited Talk - Tuesday 10:00 AM - Presidio C](#)

The Vanderbilt Pelletron - Radiation Effects on Electronics and Materials Characterization

[Michael W. McCurdy](#)¹, [Marcus H. Mendenhall](#)^{1,2}, [Robert A. Reed](#)^{1,2}, [Bridget R. Rogers](#)³, [Ronald D. Schrimpf](#)^{1,2}

⁽¹⁾*Institute for Space and Defense Electronics, Vanderbilt University, Nashville TN 37212, United States*
⁽²⁾*Department of Electrical Engineering and Computer Science, Vanderbilt University, Nashville TN 37212, United States*
⁽³⁾*Department of Chemical and Biomolecular Engineering, Vanderbilt University, Nashville TN 37212, United States*

The Vanderbilt University School of Engineering installed a National Electrostatics Corporation (NEC) model 6SDH tandem 2 MV Pelletron in May 2011. It has an Alphatross ion source capable of injecting several ion species. Hydrogen, helium, and oxygen are currently used and chlorine is in process of implementation.

Two beamlines are available. A custom vacuum chamber dedicated to electronics radiation effects is at the end of the +15 degree beamline. It has internal dimensions of approximately 20 inches high and 23.5 inches in diameter. A positioning stage with x-y translation and rotation about the vertical is installed. Multiple coaxial and ribbon electrical feedthroughs are available. Scattering foils in the beamline provide a uniform field of irradiation of 1-3/8 inch diameter. Beam flux is variable and typical experiments run from less than 1E+5 to approximately 5E+9 particles/(cm²*s). Without scattering foils the beam flux can be over 1E+10 particles/(cm²*s). The beam spot size is adjustable but with unknown uniformity. Single event upset, single event transient, displacement damage and total ionizing dose experiments on various electronic devices have been conducted to date with this end station.

An NEC RC43 Analytical End Station terminates the -15 degree beamline. This end station is turbo pumped and load locked, capable of obtaining base pressure in the low 10-8 Torr range. The computer controlled 4-axis manipulator is capable of polar scans for channeling analyses with a resolution of $\approx 0.01^\circ$. Thus far we have used this end station for RBS analyses of films and nanoparticles, forward scattering measurements, as well as experiments investigating the sensitivity of ceramic oxide phosphors to proton damage.

This report will discuss more details of the VU Pelletron, past and current research efforts as well as use by industry.

Abstract 133 TUE-RE04-3

[Invited Talk - Tuesday 10:00 AM - Presidio C](#)

Efficient Reliability Testing of Emerging Memory Technologies Using Multiple Radiation Sources

[William Geoff Bennett](#)¹, [Nicholas C Hooten](#)¹, [Ronald D Schrimpf](#)¹, [Robert A Reed](#)¹, [Michael L Alles](#)¹,
[En X Zhang](#)¹, [Mike McCurdy](#)¹, [Dimitri Linten](#)², [Malgorzata Jurzak](#)², [Andrea Fantini](#)²

⁽¹⁾*Electrical Engineering and Computer Science, Vanderbilt University, 2301 Vanderbilt Place PMB 351826, Nashville TN 37235, United States*

⁽²⁾*imec, Kapeldreef 75, 3001 Leuven, Belgium*

The commercial memory industry, now more than ever, is looking at CMOS Flash alternatives to provide continued scaling of data storage elements. Meanwhile, radiation tolerant memory researchers and designers are investigating these new technologies to see if they could provide higher reliability in radiation environments than their CMOS counterparts. For these novel devices, different radiation sources can give insight into specific mechanisms driving their radiation response. Presented are the various uses of different radiation sources as it pertains to a Hf/HfO₂ 1T1R resistive random access memory (RRAM). The total ionizing dose (TID) response was measured using an ARACOR x-ray generator, which will not contribute atomic displacements in the resistive element, but will generate significant amounts of charge in the HfO₂. Protons from Vanderbilt's Pelletron accelerator were used to cause atomic displacements, resulting in a recoverable failure mode not seen with x-rays.

Single-event upsets (SEUs), where incident ions change the state of the stored bit in memory (1 to 0, or 0 to 1) were first discovered in RRAMs using backside two photon absorption at Vanderbilt University. SEUs occur when charge

generated in the access transistor generate a voltage pulse across the RRAM capable of writing to the cell. Attempts to replicate these upsets using the 14 MeV Oxygen atoms proved fruitless due to the relatively low amount of deposited energy. For higher levels of energy deposition, a variety of ions were used from Lawrence Berkeley National Lab's 88" cyclotron. This allowed for the demonstration of not only SEUs, but also multiple-event upsets (MEUs), where cumulative effects from multiple ions add together to produce a single upset. The availability and cost effectiveness of the Pelletron accelerator and TPA facilities allowed preliminary experiments to shape research on more energetic beam-lines like LBNL, reducing testing costs and producing a greater amount of research.

Abstract 225 TUE-RE04-4

[Contributed Talk - Tuesday 10:00 AM - Presidio C](#)

Use of Alpha Particle and Ion Accelerators for Characterization of Soft-Error Reliability in Advanced ICs

[Rachel C Quinn](#)¹, [T D Loveless](#)², [J S Kauppila](#)², [J A Maharrey](#)¹, [S Jagannathan](#)¹, [E X Zhang](#)¹, [M W McCurdy](#)², [M L Alles](#)², [R A Reed](#)², [L W Massengill](#)²

⁽¹⁾*Electrical Engineering and Computer Science, Vanderbilt University, 2301 Vanderbilt Place PMB 351826, Nashville TN 37235-1826, United States*

⁽²⁾*ISDE, VU Station B 351553, Nashville TN 37235-1553, United States*

The response of electronic devices to ionizing radiation is a reliability concern for commercial and space applications. Particle accelerators are used to characterize the response to heavy-ions and predict failure rates for space applications. With technology scaling it has become increasingly important to understand device reliability for commercial applications as a wide spectrum of terrestrial particles can generate a sufficient amount of charge to induce soft errors. Isotropic low-activity button sources are often used to predict commercial device response to alpha particles present in terrestrial environments (such as packaging material emission). Button sources emit a spectrum of particles over various angles and energies. They can also emit a spectrum of ionizing particle species.

Circuit designers often use radiation hardening techniques that depend on the relative location and spacing between transistors. The energy and angle of the incident radiation impact how the circuit responds to an ionizing particle. Isotropic button sources provide useful data for predicting error rate, but cannot be used to understand the mechanisms causing upsets in the devices. Using particle accelerators for irradiation experiments gives further insight into a circuit's response to radiation for a subset of angles and particle energies. This information is valuable in continuing improvement of radiation hardened by design circuits.

In this work, we demonstrate the combined use of an alpha accelerator (Vanderbilt University Pelletron 6MeV alpha beam) and heavy-ion accelerator (Lawrence Berkeley National Laboratory cyclotron 10MeV/AMU heavy ion cocktail) to comprehensively characterize the single-event response of 32 nm SOI flip-flops. Comparison with results produced using Californium-252 and Americium-241 button sources demonstrates how the Pelletron can provide unique insight into the angular sensitivity of the circuit, which is an important consideration when predicting error rates for a given environment or configuration.

Abstract 114 TUE-AMP01-1

[Invited Talk - Tuesday 1:30 PM - Travis A/B](#)

XUV photofragmentation of small water cluster ions

[Henrik B. Pedersen](#)

Department of Physics and Astronomy, Aarhus University, Ny Munkegade 120, Aarhus 8000, Denmark

The smallest water cluster ions, $\text{H}^+(\text{H}_2\text{O})_{n=1-2}$, are fundamental building blocks of both proton solvation in bulk water [1] and isolated protonated water clusters [2]. Moreover, the presence of water cluster ions in the ionosphere of the earth [3] as well as other planetary atmospheres [4] is well established. For example in the earth's ionosphere, water cluster ions are formed through a complex chemistry initiated by molecular ionization by high-energy solar photons or cosmic rays. Interestingly, the photochemistry of the water cluster ions in the extreme ultraviolet (XUV) range, where valence ionization is possible, has been experimentally essentially unexplored.

In a series of experiments [5-7] using a crossed photon-ion beams experiment installed at the PG2 beamline [8] of the FLASH [9] (Free electron LASer in Hamburg), we have studied the XUV-photolysis of the water radical ion (H_2O^+) as well as the fundamental small water clusters ions of the Eigen (H_3O^+) and Zundel ($\text{H}_2\text{O}-\text{H}^+-\text{OH}_2$) forms.

The experiments take explicit advantage of the extreme photon intensities available at FLASH, and use coincident imaging detection of photoelectrons, photoions, and neutral fragments to deduce both fragmentation channel branching ratios as well as detailed initial-to-final state reaction routes.

[1] D. Marx et al., Nature (London) 397, 601 (1999).

[2] G. Niedner-Schattenburg, Angew. Chem., Int. Ed. 47,1008 (2008).

[2] R. P. Wayne, **Chemistry of Atmospheres**, 3rd ed. (Oxford University Press, New York, 2000).

[4] M. Larsson, W. D. Geppert, and G. Nyman, Rep. Prog. Phys.**75**, 066901 (2012).

[5] L. Lammich **et al.**, Phys. Rev. Lett. **105**, 253003 (2010)

[6] H. B. Pedersen **et al.**, Phys. Rev A **87**, 013402 (2013)

[7] C. Domesle **et al.**, Phys. Rev A **88**, 043405 (2013)

[8] M. Martins **et al.**, Rev. Sci. Instrum. **77**, 115108 (2006).

[9] W. Ackermann **et al.**, Nat. Photon. **1**, 336 (2007).

Fast ion beam studies of Intense laser interactions with molecular anions

[Daniel Strasser](#)

Institute of Chemistry, Hebrew university of Jerusalem, Givat Ram Campus, Jerusalem 9602, Israel

I will present experimental studies of the interaction of shaped intense laser pulses with molecular anions using fast ion beam methods. A dedicated photofragment spectrometer that allows us to detect and resolve the charge over mass ratio of neutral and cationic products will be described. In the case of the SF_6^- molecular anion, dissociative ionization channels that lie more than 20eV above the threshold energy for double detachment are reported and saturation intensities are determined for the observed final channels. Product yields are analyzed as a function of the femtosecond laser pulse energy, pulse shape and polarization ellipticity to reveal the nature of the efficient non-sequential multiple detachment mechanism. The observed strong suppression of multiple detachment by pre-pulses, induced with negative third order dispersion of the transform limited fs laser pulse, is interpreted as suppression of a non-sequential process by early single detachment. Furthermore, in contrast to the relatively simple picture of a rescattering mechanism characterized by acute sensitivity to polarization ellipticity that dominates double ionization of neutral species and was reported for the atomic F^- anion, multiple detachment of the molecular anion is found to exhibit only mild ellipticity dependence. In addition, preliminary data of SF_6^- based cluster anions will be presented and discussed.

Abstract 279 TUE-AMP01-3

[Invited Talk - Tuesday 1:30 PM - Travis A/B](#)

Merged beams studies for astrobiology.

[Kenneth Andrew Miller](#)¹, [Nathalie de Ruette](#)¹, [Aodh Patrick O'Connor](#)¹, [Xavier Urbain](#)², [Daniel Wolf Savin](#)¹

⁽¹⁾*Astrophysics Laboratory, Columbia University, 550 W. 120th street, New York New York 10027-6601, United States*

⁽²⁾*Institute of Condensed Matter and nanosciences, Universite de Louvain, Chemin du Cyclotron 2 a 1348, Louvain la Nueve, Belgium*

The chain of chemical reactions leading towards life is thought to begin in molecular clouds when atomic carbon and oxygen are fixed into molecules. Reactions of neutral atomic C with H_3^+ is one of the first steps in gas phase chemistry leading to the formation of complex organic molecules within such clouds. Water, believed to be vital for life, can form via a chain of gas-phase reactions that begin with neutral atomic O reacting with H_3^+ . Uncertainties in the rate coefficient for these reactions hinder our ability to understand the first links in the chemical chain leading towards life. Theory provides little insight as fully quantum mechanical calculations for reactions involving four or more atoms are too complex for current capabilities. On the other hand, measurements of cross sections and rate coefficients for reactions of atoms with molecular ions are extremely challenging. This is due to the difficulty in producing sufficiently intense and well characterized beams of neutral atoms.

We have developed a novel merged beam apparatus to study reactions of neutral atoms with molecular ions at the low collision energies relevant for molecular cloud studies. Photo-detachment of atomic anion beams, with an 808-nm (1.53-eV) laser beam, is used to produce beams of neutral C and O, each in their ground term as occurs in molecular clouds. The neutral beam is then merged with a velocity matched, co-propagating H_3^+ beam, in order to study reactions of C and O on H_3^+ . The merged beams method allows us to use fast beams (keV in the lab frame) to achieve relative collision energies down to ≈ 10 meV. Using the measured merged beams rate coefficient, we are able to extract cross sections which can then be used to better understand molecular cloud chemistry.

Abstract 70 TUE-ATF03-1

[Invited Talk - Tuesday 1:30 PM - Presidio A](#)

Superconducting RF Accelerators for Commercial Applications

[Chase H. Boulware](#), [Terry L. Grimm](#), [Valeriia N. Starovoitova](#), [Jerry L. Hollister](#)

Niowave, Inc., 1012 N. Walnut St., Lansing MI 48906, United States

Superconducting RF linacs can operate continuously with higher average beam intensity (current) than any other type of accelerator (cyclotron, copper linac, etc.). Niowave, Inc. has developed complete turn-key superconducting electron linacs for a broad range of commercial applications. In addition to the niobium accelerating structure, the complete system includes the liquid helium refrigerator, high power microwave source, radiation shielding and licensing. This integrated system enables a company or university research group to quickly and inexpensively use the electron beam for a number of applications, including high-power x-ray sources, production of medical radioisotopes, high-flux neutron sources, and high-power free-electron lasers. Linacs with beam energy of 0.5 to 50 MeV and average beam power of 1 W to 1 MW are under development, and two integrated helium refrigerator models have been developed with leading experts in the cryogenic industry. This contribution will discuss these integrated accelerator systems and their applications.

Abstract 96 TUE-ATF03-2

[Contributed Talk - Tuesday 1:30 PM](#) - [Presidio A](#)

SRF DIPOLES FOR DEFLECTING AND CRABING APPLICATIONS

[Alejandro Castilla](#)^{1,2,3}, [Jean R. Delayen](#)^{1,2}

⁽¹⁾*Center For Accelerator Science, Old Dominion University, Department of Physics Old Dominion University OCNPS Bldg., Room 306
4600 Elkhorn Ave., Norfolk Virginia 23529, United States*

⁽²⁾*Center for Advanced Studies of Accelerators, Thomas Jefferson Lab, Center for Advanced Studies of Accelerators Thomas Jefferson
National Accelerator Facility 12000 Jefferson Avenue, Mail Stop 7B, Newport News Virginia 23606, United States*

⁽³⁾*Departamento de Fisica - DCI, Universidad de Guanajuato Campus Leon, Loma del Bosque No. 103 Col. Lomas del Campestre C.P
37150 A.Postal E-143, Leon Guanajuato 37150, Mexico*

Designs of superconducting rf dipole cavities have been studied for diverse applications, such as an rf separator at the Jefferson Lab 12 GeV upgrade, and as part of the crabbing correction scheme for both the LHC luminosity upgrade and the medium energy electron-ion collider (MEIC) at Jefferson Lab. In each case, specific design and operation requirements have been addressed. Proof of principle prototypes have been built and tested for these particular applications (at 499, 400, and 750 MHz respectively) by Jefferson Lab and Niowave, Inc. In the present talk, a survey of the design parameters and cryogenic test results will be presented.

Abstract 331 TUE-ATF03-3

[Contributed Talk - Tuesday 1:30 PM](#) - [Presidio A](#)

Advanced Materials Manufacturing with Superconducting Electron Accelerators

[Justin Joseph Hill](#)

Materials Science Engineering Technologies, Mainstream Engineering Corporation, 200 Yellow Place, Rockledge FL 32955, United States

Superconducting (SC) linear accelerators (LINAC) for electron beams (Ebeams) open up new opportunities for advanced materials processing since they can continuously deliver extremely high energy and brightness electrons at high power. Unlike normal conducting systems SC systems produce a continuous beam. The increased energy delivery rate of SC systems enables the production of far-from-equilibrium materials and selective processing within a material surface and subsurface. Higher energy Ebeams penetrate deeper within a material and increase the processed depth.

Through a public-private partnership lead by the Office of Naval Research and including NASA, DoE, the Florida Institute of Technology, Space Florida, CareerSource Brevard and the Space Coast EDC, Mainstream Engineering is commissioning a Niowave SC Ebeam LINAC system specifically designed to investigate advanced materials processing, production and additive manufacturing. The goal of Mainstream's Electron Beam Enabled Advanced Manufacturing (EBEAM) center is to develop materials that are uniquely produced with SC systems and alleviate significant technological deficiencies. The center will also be available to other interested research groups to further identify the value of this system.

Given that SC Ebeam LINAC systems have not been available for materials processing R&D, Mainstream Engineering identified candidate materials through simulation of structure-property changes during Ebeam irradiation. The simulation combines a Monte Carlo model of electron trajectories in the solid material, an energy and electric field dispersion model, and a thermal energy distribution model. The average power of the simulated Ebeam system was varied to mimic SC and normal conducting systems. Only materials that could be uniquely produced with the SC system were considered. Based on a techno-economic analysis, several high-value and low-risk materials and technologies were targeted for validation with the SC system. Mainstream will discuss the EBEAM facility, the simulation results, and the target materials for the first phase of Ebeam operation.

Abstract 230 TUE-ATF03-4

[Contributed Talk - Tuesday 1:30 PM - Presidio A](#)

Compact Free Electron Lasers Driven By Superconducting Linacs

[W. B Colson¹](#), [J. Blau¹](#), [K. Cohn¹](#), [C. Pogue²](#), [T. L. Grimm²](#), [C. H. Boulware²](#)

⁽¹⁾Physics Department, Naval Postgraduate School, Monterey CA 93943, United States

⁽²⁾Niowave Inc., Lansing MI 48906, United States

Free Electron Lasers (FELs) are attractive for commercial applications because they are continuously tunable over a wide range, "designable" to even wider ranges, and can be powerful, efficient, and reliable systems with near perfect laser mode quality. In 1994, a National Academy of Sciences Committee representing broad areas of chemistry, biology, and physics, made the strong recommendation that smaller, laboratory sized FELs should be developed.

The FEL Group in the Physics Department of the Naval Postgraduate School and Niowave, Inc. are collaborating to design several compact FEL systems using superconducting spoke RF cavities. Accelerators range in size from 1m to 4m length and reach electron beam energies of 2MeV to 40MeV, respectively, with milliamps of average current. A short ten period undulator, approximately 30cm long, provides a periodic, transverse magnetic field coupling the electron beam to coherent radiation ranging from THz to infrared depending on the electron beam energy. In the 2MeV accelerator, the radiation process can be super-radiant due to the long millimeter wavelength, while the 40MeV accelerator generates infrared wavelengths in a conventional FEL oscillator configuration. An intermediate 8MeV accelerator powers an FEL oscillator with short picosecond pulses providing a kilowatt of THz power in a compact source.

Abstract 330 TUE-IBA05-1

[Invited Talk - Tuesday 1:30 PM - Presidio B](#)

Implantation and analysis of helium by NRA and HI-ERDA at the JANNUS-Saclay laboratory

[Lucile BECK¹](#), [Patrick TROCELLIER¹](#), [Thomas LOUSSOUARN¹](#), [Frédéric LEPRETRE¹](#), [Sylvain VAUBAILLON^{1,2}](#), [Yves SERRUYS¹](#)

⁽¹⁾Laboratoire JANNUS, CEA, DEN, Service de Recherches de Métallurgie Physique, CEA-Saclay, Gif sur Yvette 91120, France

⁽²⁾Laboratoire JANNUS, CEA, INSTN, UEPTN, CEA-Saclay, Gif sur Yvette 91120, France

The JANNUS facility at CEA-Saclay (France) is devoted to the study of damage mechanisms, synergistic effects of multi-beam irradiation and ion beam modification of materials. For that purpose, three electrostatic accelerators (3 MV Pelletron, 2.5 MV Van de Graaff and 2 MV tandem Pelletron) are coupled in order to perform single, dual and triple beam irradiations in a dedicated triple beam chamber. In addition, the facility is equipped with two lines and chambers for ion beam analysis. The complementarity of these devices provides a relevant tool for the characterization of implanted materials.

In nuclear materials, helium is an element of interest due to its production by nuclear reactions in reactor structural materials or in nuclear waste. The interactions of helium with these materials can be studied by implantation of $^3\text{He}^+$ or $^4\text{He}^+$ and consecutive annealing. After implantation, two routes are possible for the determination of helium profiles and concentrations. ^3He profiles are measured by the $^3\text{He}(\text{d}, \text{p})^4\text{He}$ nuclear reaction and ^4He profiles are determined by heavy-ion ERDA.

In this contribution, the facility will be described focussing on instrumental developments for helium analysis (NRA and HI-ERDA). The recent system for HI-ERDA and the first measurements will be presented in details.

Abstract 275 TUE-IBA05-2

[Contributed Talk - Tuesday 1:30 PM - Presidio B](#)

Identifying the Dominant Interstitial Complex in GaAsN Alloys

[Timothy Jen¹](#), [Gulin Vardar¹](#), [Yongqiang Wang²](#), [Rachel Goldman¹](#)

⁽¹⁾Material Science Engineering, University of Michigan, 2300 Hayward Street, Ann Arbor MI 48109, United States

⁽²⁾Materials Science and Technology Division, Los Alamos National Laboratory, P.O. Box 1663, MS G755, Los Alamos NM 87545, United States

Dilute nitride semiconductors, an example of highly mismatched alloys (HMAs), are promising for a wide range of applications including long-wavelength light-emitters, high performance electronic devices, and high efficiency solar cells. The properties of HMAs are often described with a model focusing on the influence of individual solute atoms, assuming that all solute atoms "see" the same atomic environment. In the case of GaAsN alloys, single local environment models predict a N composition-dependent energy band gap which agrees **qualitatively** with experiment. However, such models do not **quantitatively** explain non-monotonic composition-dependent effective masses [1] and persistent photoconductivity [2]. We recently reported significant composition-dependent incorporation of N into non-substitutional sites, as either (N-N)_{As} or (N-As)_{As} interstitials [3][4]. To distinguishing (N-N)_{As} and (N-As)_{As} interstitials in GaAsN alloys, we compare [100], [110], and [111] channeling and non-channeling (random) NRA spectra with Monte Carlo (MC) simulations with full numerical integration of ion trajectories. The MC simulation was validated via a comparison of simulated and measured NRA spectra for palladium with deuterium impurities. For these simulations, we assume that (N-N)_{As} is aligned along the [111] direction and (N-As)_{As} deviates from the [111] direction by 0.6 Å [5]. Since the NRA channeling yields are the highest (lowest) in the [111] ([100]) direction, (N-As)_{As} is likely the dominant N-pair complex. The simulated spectra exhibit similar trends, namely the highest (lowest) yields in the [111] ([100]) directions, suggesting that (N-As)_{As} is the dominant interstitial pair.

Abstract 271 TUE-IBA05-3

[Contributed Talk - Tuesday 1:30 PM - Presidio B](#)

Microbeam contrast imaging analysis of gas-solid interface and NO adsorption studies on Rh(111) surface.

[Karur R Padmanabhan](#)

Physics and Astronomy, Wayne State University, 666 West Hancock, Detroit MI 48201, United States

Microbeam channeling in the CCM and CSTIM mode were employed in the analysis of a gas-solid interface and lattice location of adsorbed atoms on epitaxial film surfaces. Backscattered and channeled transmission MeV ions through a thin single and double Si window-gas cell were detected and analyzed under varying cell pressure. Channeling contrast images generated by distortion induced dechanneling of ions and c_{\min} values indicate an almost linear relationship with partial pressure in the cell. Desorption of NO at different partial pressures and temperatures on an epitaxial Rh film deposited on a Si (111) window were studied using the cell arrangement. The Rh back surface shows higher c_{\min} as expected due to higher dechanneling. NO dissociates completely at temperatures between 275 K and 340 K. The lattice locations of N and O in the channeling mode with NRA indicates that O occupies interstitial sites in Rh (111) and dissociation of NO becomes progressively inhibited due to site blocking from 275 K at to 400 K as preadsorbed oxygen appears to inhibit NO decomposition and N concentration increases beyond 455K.

Abstract 407 TUE-IBA05-4

[Contributed Talk - Tuesday 1:30 PM - Presidio B](#)

Nuclear reaction analysis of deuterium in ion irradiated and plasma exposed tungsten

[Yongqiang Wang¹](#), [Joseph L. Barton²](#), [Joseph Tesmer¹](#), [Russ P. Doerner²](#), [George R. Tynan²](#)

⁽¹⁾*Materials Science and Technology Division, Los Alamos National Laboratory, Los Alamos New Mexico 87545, United States*

⁽²⁾*Department of Mechanical and Aerospace Engineering, University of California - San Diego, La Jolla California 92093, United States*

Effective tritium removal from plasma facing material is critical to the successful operation of International Thermonuclear Experimental Reactor (ITER). In this report, we will use deuterium as a surrogate for tritium to study the effect of radiation damage and hydrogen isotope exchange on the tritium retention and release in polycrystalline tungsten. ITER grade W coupons were first treated with D plasma with a fluence of 10^{26} ions/m² and ion energies of 150 eV in PISCES. Each sample was then exposed to varying doses of H plasma with similar sample temperature and plasma conditions to various fluences, to examine the effectiveness of isotope exchange as a means of tritium removal. To examine the effect of the radiation damage by fusion neutrons on the tritium removal, some of the W samples were intentionally pre-damaged at various levels of displacements per atom (dpa) using MeV Cu ions before the plasma exposures. The $D(^3\text{He}, p)^4\text{He}$ nuclear reaction with various incident energies was used to measure D concentration profiles up to a depth of 7.7 μm . High fidelity deuterium depth profile in each of the W specimens was obtained by fitting the measured proton energy spectra with SIMNRA code. To corroborate NRA results, thermal desorption spectroscopy (TDS) was also used to determine the deuterium retained throughout the bulk of the W sample. This presentation will report and discuss our latest findings in this research area.

Abstract 116 TUE-MA06-1

[Invited Talk - Tuesday 1:30 PM - Bonham B](#)

The Current Status of Proton Therapy in the Cooperative Group Multi-institutional Clinical Trials Setting

[David S Followill](#), [Paige A Summers](#)

Radiation Physics, M. D. Anderson Cancer Center, 1515 Holcombe Blvd, Unit 607, Houston TX 77030, United States

While proton therapy has been used for over 20 years to treat cancer patients, it has only recently (past 7 years) escalated to a level that it plays a more active role in NCI funded clinical trials. The first step in participation is completing NCI's published approval requirements for the use of proton therapy in its clinical trials. The IROC Houston QA center (RPC)

was tasked with coordinating and implementing NCI's approval process and a QA program establishing a minimum consistent baseline of required quality for proton centers enrolling patients. The five IROC Houston-coordinated approval steps for each proton delivery method include completion of the proton facility questionnaire, annual monitoring of beam output, electronic transfer of treatment plans, successful irradiation of two anthropomorphic phantoms (prostate and spine) and successful completion of an onsite dosimetry review visit. Once approved, an institution may have to complete additional trial specific credentialing, such as irradiation of an IROC Houston's protocol-specific proton phantoms. To date, the RPC has approved twelve proton centers (11 USA and 1 Japanese) of the 14 clinically active centers. These approvals cover scattered, uniform scanning, and spot scanning proton therapy delivery techniques. The RPC has performed 17 proton site visits and is developing consensus data to establish acceptance criteria for site visit measurements that will ensure clinical trial consistency. This need for a clinical trial proton quality assurance program is critical as new proton therapy protocols are developed that require collaboration of many proton centers. Currently there are 5 adult and 8 pediatric trials that allow proton therapy with new concepts being developed monthly. An appropriate QA program has been established to ensure quality and consistency as proton therapy is further incorporated into multi-institutional clinical trials.

Work supported by grants CA10953, CA059267, and CA81647 (NCI, DHHS).

Abstract 465 TUE-MA06-2

[Invited Talk - Tuesday 1:30 PM - Bonham B](#)

Prospective Clinical Trials of Proton and Photon Radiation for Non-Small Cell Lung Cancer

[Zhongxing Liao](#)

Radiation Oncology, The university of Texas MDANDERSON Cancer Center, 1515 Holcombe boulevard, Unit 97, Houston TX 77030, United States

Attempts to improve clinical outcomes for patients with lung cancer have led to the

used of charged particle therapy in an effort to exploit the physical properties of such particles to escalate the dose to the tumor while simultaneously limiting the dose to nearby structures, thereby enhancing the therapeutic ratio and potentially improving cancer cure rates. The physical and dosimetric characteristics of proton therapy make it an ideal radiation modality for lung cancer, having the potential to reduce toxicity, improve patient quality of life (QOL), increase tumor dose, and improve OS of patients with lung cancer. This potential has generated very high interest in the use of proton beam therapy for cancer, and the number of proton facilities has increased steadily worldwide. However, the lack of level I evidence of the effectiveness of proton therapy and concerns regarding its cost and benefits have remained problematic. No standards or guidelines have been established specifically for aspects of quality assurance, treatment planning, and delivery of proton radiation therapy.

Given the rapid proliferation of new proton treatment facilities, it is a critical time to objectively and scientifically assess the potential of protons versus photons for the treatment of lung cancer. The speaker will present the rationale, hypothesis and current status of prospective trials comparing protons and photons in the management of lung cancer.

Pediatric Proton Therapy - an Update[Anita Mahajan](#)*Radiation Oncology, MD Anderson Cancer Center, 1515 Holcombe Boulevard, Unit 097, Houston TX 77030, United States*

Over the past 50 years, great advances have been made in increasing the overall survival of pediatric patients with cancer. Many of our patients now enjoy long term survival with modern multi-disciplinary cancer care. We have learned that many of the survivors of pediatric malignancies have an increased risk of health issues, poorer education attainment, decreased ability to become independent and increased risk of secondary malignancies. Even though these later effects are due to many factors including the patient's genetic make up, life style, and treatment factors, it is known that radiation therapy contributes to many of the late toxicities that survivors experience.

Radiotherapy remains a integral treatment for local control. Technical advances have allowed better tumor delineation and treatment delivery. Concurrent therapies have allowed for decreased radiation dose. Proton therapy, when used to with modern imaging, targeting and multi-disciplinary care is a radiation modality that has great promise to reduce radiation related acute and late toxicities in this vulnerable population.

In this talk, the issues of radiation related toxicities in pediatric patients will be reviewed. The potential benefit of proton therapy in this population will be demonstrated. Current efforts and accumulating evidence will be summarized to provide an overview of the use of proton therapy in children.

The ANDANTE Project: A Multidisciplinary Approach to Estimate the Risk of Neutrons in Pediatric Proton Patients[Andrea Ottolenghi](#)¹, [Vere Smyth](#)¹, [Reinhard Schulte](#)², [On behalf of the ANDANTE project](#)¹⁽¹⁾*Università degli Studi di Pavia, Pavia, Italy*⁽²⁾*Radiation Medicine, Loma Linda University Medical Center, Loma Linda CA 92354, United States*

ANDANTE is a European project with 7 European institutions and one U.S. partner. The project integrates the disciplines of radiation physics, molecular biology, systems biology modeling, and epidemiology to investigate the relative risk of induction of cancer from exposure to neutrons in proton therapy compared to photons. The biology studies of project will focus on three specific induced cancers following pediatric photon radiotherapy: salivary gland, thyroid gland, and breast. Stem cells from each of the types of tissue will be exposed to well characterized beams of neutrons, and biological markers of possible tumorigenesis will be used to develop relative biological effectiveness (RBE) models. A track structure model and experimental system will be developed to simulate and measure the nanodosimetric quantities under experimental conditions and to explore the relationships between exposure parameters (neutron energy spectra, doses and nanodosimetric cluster size distributions) and response. The combination of radiation biology and biophysics/systems biology will generate a strongly directed epidemiological investigation to validate the parameters of an RBE model that ties dosimetric data to cancer risk. We will explore the usefulness of retrospective clinical data from pediatric proton therapy patients compared to existing cohorts of pediatric photon radiation therapy patients. The limitations of the epidemiological approach will be addressed on the one hand by using the discipline for model validation rather than model generation, and, on the other hand, a future prospective study, if possible with multi-institutional participation, will be designed in order to accumulate sufficient statistical power. The creation of a multi-center cohort of pediatric patients is a decisive task at the current phase where the number of pediatric proton therapy patients is on the rise world-wide. The overarching objective of the project is

to determine the radiobiological quality of neutron fields outside therapeutic proton beams for specific tissues and neutron energies, which can then be validated using pediatric proton therapy data in the future.

Abstract 473 TUE-MA06-5

[Invited Talk - Tuesday 1:30 PM - Bonham B](#)

Summary of Ongoing Clinical Protocols for Proton and Heavier-Ion Therapy

[Richard P Levy](#), [Bosco Giap](#), [David Shia](#), [Barrett O'Donnell](#), [Phuong Vop](#), [Fantine Giap](#)

Scripps Proton Therapy Center, 9730 Summers Ridge Road, San Diego CA 92121, United States

Since 1954 when the very first patient was treated at Lawrence Berkeley National Lab with heavy-charged particles, more than 100,000 patients in total have now been treated with protons, and another 20,000 patients have been treated with carbon and other heavier ions at over 50 facilities worldwide. During the first several decades of this endeavor, particle therapy was accessible only at a small number of programs. More recently, however, this therapy has become available at a rapidly increasing number of facilities worldwide. This expansion of the discipline has led to the development of many more clinical trials, designed to optimize particle-beam therapy and to compare the results achieved with those resulting from other treatment methods.

Presently, more than 100 clinical protocols worldwide are actively involved in the effort to improve our understanding of these clinical guidelines. The purpose of this presentation is to offer a broad overview of these protocols, highlighting the specific disease categories that are now being studied using proton and/or heavier-ion therapy, and how the parameters of dose-escalation, beam conformity, and RBE modeling are being evaluated for various disease sites and stages.

Abstract 448 TUE-NP04-1

[Invited Talk - Tuesday 1:30 PM - Travis C/D](#)

Precision Neutrino Physics with Reactor Antineutrinos

[Karsten M Heeger](#)

Department of Physics, Yale University, New Haven CT 06511, United States

Experiments with reactor antineutrinos have played an important role throughout the history of neutrino physics. Reactor neutrinos enable precision studies of neutrino oscillation, allow us to search for signs of new physics, and are a tool for reactor monitoring. In this talk we will review the results from recent reactor neutrino experiments and discuss the prospects for studying neutrino properties with reactor antineutrinos.

Abstract 415 TUE-NP04-2

[Invited Talk - Tuesday 1:30 PM - Travis C/D](#)

PROSPECT: A Short Baseline Reactor Antineutrino Oscillation Experiment

[Nathaniel Bowden](#)

Lawrence Livermore National Laboratory, Livermore CA, United States

While much progress has been made in understanding the neutrino sector in recent decades, persistent hints at the existence of additional sterile neutrino flavors remain an unanswered puzzle. These include unexplained event excesses in the LSND and MiniBOONE experiments, suggestions from astrophysical measurements, and the "Reactor Antineutrino Anomaly". There is a strong desire in the neutrino physics community for new experimental inputs that can provide definitive confirmation or exclusion of these suggestive indications via the measurement of oscillation patterns.

Here we describe the efforts of the PROSPECT Collaboration to develop a short baseline reactor experiment using one of several unique U.S. research reactor facilities. Through careful siting and design, such an experiment would be sensitive to sterile neutrino driven oscillations in both baseline length and antineutrino energy. Furthermore, the fuel composition of these facilities provides the opportunity to perform a precision measurement of the U235 antineutrino spectrum. Here we will describe the experimental concept, the challenges that must be addressed, and the overlap with efforts to develop compact antineutrino detectors for reactor monitoring and safeguards.

LLNL-ABS-651772

This work was performed under the auspices of the U.S. Department of Energy by Lawrence Livermore National Laboratory under Contract DE-AC52-07NA27344.

Abstract 333 TUE-NP04-3

[Invited Talk - Tuesday 1:30 PM - Travis C/D](#)

Reactor neutrino fluxes

[Patrick Huber](#)

Physics, Virginia Tech, 850 West Campus Drive, Blacksburg VA 24061, United States

Nuclear reactors have been recognized as an intense source of electron antineutrinos for more than 50 years and given the importance of reactor neutrino experiments for fundamental science, a great deal of effort has been devoted to predict the details of neutrino emissions. Till 2011 there was a standard result in the literature which formed the basis for interpreting all reactor neutrino experiments performed to date. However, new attempts at computing reactor neutrino spectra led to the surprising result that fluxes may be larger than previously thought. In this presentation, I will discuss the general problem of computing reactor neutrino fluxes and explain in detail how state-of-the-art calculations attempt to control the uncertainties. I also will comment on our current limitations in improving these calculations.

Abstract 458 TUE-NP04-4

[Invited Talk - Tuesday 1:30 PM - Travis C/D](#)

The miniTimeCube, the World's Smallest Neutrino Detector

[John Learned](#)

Department of Physics and Astronomy, University of Hawaii, 327 Watanabe Hall, 2505 Correa Road, Honolulu Hawaii 96822, United States

The miniTimeCube is a 2 liter detector for inverse beta decay interactions of electron antineutrinos from reactors. It employs an unprecedented number of pixels (1536) and fast waveform digitization to achieve ~50 picosecond time resolution at the single photoelectron level. Streaming digitized signals from the backs of the twenty four 64 anode multi-

channel plate photodetectors, permits fast signal recognition and background rejection. Simulations indicate reconstruction of the positron track and good (mm) recognition of interaction vertex and neutron capture on the Boron in the doped scintillating plastic target. The mTC also has excellent capability for recognition of neutrons from radioactive sources, calculation of directions and hence source location. Tests are now underway at NIST, Gaithersburg, Md, first at a source facility and then near the 20 MW reactor. We will report progress, show some current data and discuss future plans.

Abstract 278 TUE-NP04-5

[Contributed Talk - Tuesday 1:30 PM - Travis C/D](#)

Past and future studies of beta-delayed neutrons with VANDLE

[Karolina Kolos](#)¹, [Robert Grzywacz](#)^{1,3}, [Miguel Madurga](#)¹, [Nick Stone](#)², [Jirina Stone](#)², [Ivan Borzov](#)⁵, [Krzysztof Rykaczewski](#)³, [William A Peters](#)⁴, [Carl J Gross](#), [David Miller](#)¹, [Dan W Stracener](#)³, [Daniel W Bardayan](#)³, [Nathan T Brewer](#)⁶, [Jolie A Cizewski](#)⁷, [Lucia Cartegni](#)¹, [Joe Hamilton](#)⁶, [Sergey Ilyushkin](#)⁹, [Carola Jost](#)¹, [Marek Karny](#)^{4,8}, [Brett Manning](#)⁷, [Anthony Mendez II](#)³, [Krzysztof Miernik](#)⁸, [Steven W Padgett](#)¹, [Stanley V Paulauskas](#)¹, [Andrew Ratkiewicz](#)⁷, [Jeff Winger](#)⁹, [Marzena Wolinska-Cichocka](#)³, [Ed Zganjar](#)¹⁰

⁽¹⁾University of Tennessee, Knoxville TN 37996, United States

⁽²⁾University of Oxford, Oxford OX1 3PU, United Kingdom

⁽³⁾Physics Division, Oak Ridge National Laboratory, Oak Ridge TN 37830, United States

⁽⁴⁾Oak Ridge Associated Universities, Oak Ridge TN 37831, United States

⁽⁵⁾Joint Institute of Nuclear Research, Dubna 141980, Russia

⁽⁶⁾Vanderbilt University, Nashville TN 37235, United States

⁽⁷⁾Rutgers University, New Brunswick NJ 08903, United States

⁽⁸⁾University of Warsaw, Warsaw 00-681, Poland

⁽⁹⁾Mississippi State University, Starkville MS 39762, United States

⁽¹⁰⁾Louisiana State University, Baton Rouge LA 70803, United States

Beta-delayed neutron emission is an increasingly important decay mechanism as the drip line is approached and its detailed understanding is essential to model the astrophysical r-process but also in more practical applications as the safe operation of nuclear power reactors. In order to study beta delayed neutron emission from very neutron rich nuclei, the "Versatile Array of Neutron Detectors at Low Energy" (VANDLE) was developed. This instrument was recently commissioned and used in on-line experiments using fission fragments at the Holifield Radioactive Ion Beam Facility and also in direct reaction experiments at NSCL and Notre Dame. VANDLE is capable of detecting neutrons over a wide range of energies (100-6000keV) due to the innovative use of digital electronics. A brief overview of past results near doubly magic ⁷⁸Ni will be presented. Among several future projects for VANDLE, we propose a world-first measurement of the angular distribution of the beta-delayed radiation from oriented ^{137,139}I and ^{87,89}Br nuclei, polarized at a low temperature at the NICOLE facility (ISOLDE, CERN). Spin and parity of excited states will be determined through the angular distribution of neutrons and gammas. This measurement will investigate the role of orbital angular momentum in beta-delayed neutron emission.

Abstract 81 TUE-NST07-1

[Invited Talk - Tuesday 1:30 PM - Bonham D](#)

Ion irradiation of Si surfaces - what determines the formation of ripple patterns?

[Hans Hofsäss](#), [Kun Zhang](#), [Omar Bobes](#)

2nd Institute of Physics, University Göttingen, Friedrich-Hund-Platz 1, Göttingen 37077, Germany

Although ripple pattern formation during ion irradiation of Si surfaces has been studied extensively in the past, there are still a number of open questions, some of which will be addressed in this contribution.

(i) The pattern formation mechanism, i.e. curvature dependent erosion or curvature dependent mass redistribution, was extensively discussed in the past. Our calculated curvature coefficients based on Monte Carlo simulations, as well as our measurements of the ripple propagation velocity reveal a significant contribution of curvature dependent erosion.

(ii) An experimental observation is the absence of surface patterns on Si for Ne and Ar ion irradiation in the energy regime between about 1.5 keV and 20 keV, whereas patterns are observed for Xe ion irradiation. We discuss possible reasons for this behavior.

(iii) Pattern formation models rely on the assumption of an incompressible viscous surface layer. We will show, that the initial density of the Si substrate material (c-Si, sputter deposited a-Si, evaporated a-Si, ion irradiated a-Si) also influences the pattern formation.

(iv) Co-deposition of metal atoms during normal incidence ion irradiation is known to generate pronounced dot and ripple patterns, most probably triggered by phase separation processes. Here, we present new results showing similar pattern formation for ion irradiation of amorphous $\text{Me}_x\text{Si}_{1-x}$ compound films.

Abstract 78 TUE-NST07-2

[Invited Talk - Tuesday 1:30 PM - Bonham D](#)

Crater Functions from the Binary Collision Approximation: Energy, Material, and Curvature Dependence

[Scott Norris](#)¹, [Wolfhard Moeller](#)²

⁽¹⁾*Mathematics, Southern Methodist University, 3200 Dyer Street, Dallas TX 75275, United States*

⁽²⁾*Institute of Ion Beam Physics and Materials Research, Helmholtz Zentrum Dresden-Rossendorf, Dresden-Rossendorf, Germany*

The framework of "crater functions" has emerged as an appealing way to simultaneously estimate the relative contributions of erosion and redistribution to the equations governing surface evolution during ion irradiation. Though originally applied only to the output of Molecular Dynamics (MD) simulations, it is equally compatible with simulations performed using the Binary Collision Approximation (BCA). Although potentially less accurate at low energies, the BCA method is significantly faster than MD, allowing the exploration of a much larger parameter space in the same amount of time.

In this talk, we will demonstrate the use of both the SDTrimSP and TRI3DST simulation tools within the crater function framework. We will discuss the relative advantages and disadvantages of such methods relative to MD in the context of Argon-irradiated Silicon. Then, we will describe systematic parametric studies, focusing on a variety of energies and materials for which experimental data are available. Finally, we will report on simulations that include curved surfaces, comparing the predictions of the framework in that case, with its predictions when only flat-target data are available.

Abstract 169 TUE-NST07-3

[Invited Talk - Tuesday 1:30 PM - Bonham D](#)

Functional Nanostructures by Self-Organised Ion Beam Sputtering

[Francesco Buatier de Mongeot](#)

Dipartimento di Fisica, Università di Genova, Via Dodecaneso, 33, Genova GE 16166, Italy

I will review recent results relative to the self-organised formation of laterally ordered arrays of periodic nanostructures induced by ion beam sputtering (IBS) on crystalline metal systems, demonstrating that controlled manipulation of the nanoscale morphology allows to finely tune important physical properties of the nanostructures ranging from catalysis to magnetic anisotropy. In the second part of my talk I will show that the lessons derived from crystalline model systems can be successfully extended to the formation of nanoscale patterns on low-cost polycrystalline metal films supported on dielectric substrates. By increasing ion dose, the rippled metal film decomposes into an array of disconnected nanowires when the troughs of the valleys reach the supporting insulating substrate [1]. The metal nanowire arrays exhibit anisotropic resistivity with low sheet resistances in the 3-5 Ohm/square range and high optical transparency in the 70-80 % range, alternatives to the best TCOs employed in photovoltaic or OLED applications. Additionally, far-field optical characterisation demonstrates that the nanowires exhibit a tunable plasmonic response, a crucial issue in view of plasmon enhanced bio-sensing applications [2].

Finally I will show that nanostructured glass substrates featuring bio-mimetic light trapping can be obtained by defocused ion beam sputtering through a stencil mask formed by the Au nanowire arrays. The high aspect ratio features confer broadband anti-reflection functionality to the textured glass substrate and at the same ensure a high efficiency for diffuse scattering (Haze). The potentiality of the patterned glass substrates in promoting photon harvesting is demonstrated by comparing the performance of thin film amorphous silicon solar cells grown on the nanostructured glass templates with that of reference devices grown on flat glass [3].

[1] D. Chiappe, et al. Small 9, 913-919 (2013)

[2] B. Fazio, et al. ACS Nano , 5 5945 (2011)

[3] C.Martella et al. Nanotechnology 24, 225201 (2013)

Abstract 192 TUE-RE03-1

[Invited Talk - Tuesday 1:30 PM - Presidio C](#)

The Effect of Space Weather on Electronics

[Heather Marie Quinn](#)

ISR3, Space Data Systems, Los Alamos National Laboratory, MSD440, Los Alamos NM 87544, United States

The space radiation environment is both dynamic and potentially damaging to spacecrafts. While dependent on location and solar cycle, most satellite subsystems must be robust to naturally occurring protons, heavy ions, electrons and X rays that occur in many near earth and interplanetary missions. These types of radiation can cause electronics to degrade permanently or suffer from transient reliability problems. New technology insertion in space programs can be very difficult, as the risk from radiation-induced failures is very high. Use of laboratory radiation sources can be helpful in determining whether new technology can be used successfully in space before the system is launched. In this talk, we will present information about the space weather environment, the use of radiation sources to reduce risk to spacecraft projects and how pre-launch radiation testing matches on-orbit behavior.

Abstract 318 TUE-RE03-2

[Invited Talk - Tuesday 1:30 PM - Presidio C](#)

A Low Noise Detection Circuit for Probing the Structure of Damage Cascades with IBIC

[Elizabeth C. Auden](#), [Barney L. Doyle](#), [Edward Bielejec](#), [Gyorgy Vizkelethy](#), [William R. Wampler](#)

Ion Beam Laboratory, Sandia National Laboratories, MS 1056, Albuquerque NM 87185-1056, United States

Energetic particles displace atoms in the semiconductor lattice, but the physical structure of electrically active defects in the resulting damage cascades has never been observed microscopically. Ion Beam Induced Charge (IBIC) can be used to probe the structure of damage cascades caused by a single heavy ion by following such a single ion implant with light ion IBIC.

In this experiment, the Sandia nanoimplanter is used to implant a single 100 keV bismuth ion in the depletion or field free region of a reverse biased laterally oriented silicon diode. Once the bismuth ion's arrival is detected by the current pulse created when electron hole pairs are generated as it traverses the depletion region, a beam of 100 keV lithium ions is scanned across the surface of the diode. The IBIC signal is strong when the beam scans undamaged regions of the diode. When the lithium beam scans damaged regions of the diode, the IBIC signal drops due to Shockley-Read-Hall recombination from midgap defects. Damage cascade structures can therefore be resolved down to the resolution of the lithium beam, or ~10 nm.

Two physical parameters govern the choice of the diode and the charge sensitive pre-amplification circuit used to detect damage through an IBIC signal: diode dead layer thickness and circuit noise. The passivation layers of the diode must be thin enough for the bismuth and lithium ions to penetrate the passivation and interlevel metallization levels into the region where charge made by the lithium ions either diffuse or drift. In addition, the noise generated from leakage currents, capacitances, and thermal fluctuations in the circuit must be sufficiently suppressed to detect the change in the IBIC signal between undamaged and damaged regions of the diode. The optimal choice of detector, FET, and charge sensitive pre-amplifier will be discussed in the talk.

Abstract 124 TUE-RE03-3

[Contributed Talk - Tuesday 1:30 PM - Presidio C](#)

Radiation Testing Capability for Electronic Devices and Circuits at Sandia's Ion Beam Laboratory

[Edward S. Bielejec](#), [G Vizkelethy](#), [B L Doyle](#), [D K Serkland](#), [R M Fleming](#), [J L Pacheco](#), [D Hughart](#),
[M Marinella](#), [D B King](#)

Sandia National Laboratories, 1515 Eubank Blvd, Albuquerque NM 87185-1056, United States

We present an overview of the radiation effects testing capability for electronics devices and circuits at Sandia's Ion Beam Laboratory (IBL). This overview will cover the four main accelerators (6 MV Tandem Accelerator, 3 MV Pelletron Accelerator, 400 kV HVEE Accelerator and the 100 kV NanoImplanter) along with the associated radiation effects testing capability on each. For example, we have multiple beam-lines for the testing of electronic devices and circuits that allow for in-situ capability such as: (1) photoluminescence, (2) deep-level transient spectroscopy, (3) concurrent 100 kV electron irradiation, and (4) electrically testing under a wide range of ion beam irradiation conditions including spot sizes on target as large as 5x5 mm² and over a temperature range from 40 to 400 K. We have on-going studies exploring the radiation effects on Silicon BJTs, III-V HBTs, Si and III-V diodes, Si APDs, TaOx Memristor devices and we have performed in-situ irradiations on AlGaIn/GaN HEMTs, HafOx Capacitors and AlGaIn/GaN Hall Bars to name a few examples. We have developed a flexible electronic device/circuit testing capability that allows for in-situ device/circuit operation with well determined fluence, spot size and targeting techniques. An example of some of our on-going studies include exploring an observed reverse annealing behavior in PnP HBTs as a function of ion species and relating this to changes in the local damage clusters which in turn have dramatic effects on early-time gain of the device. This is directly probing the locally formed defect complexes and their evolution in time. Experiments such as this are the mainstay of our radiation effects testing program and directly elucidate the physics of defects in semiconductors.

Sandia is a multi-program laboratory operated by Sandia Corporation, a Lockheed Martin Company, for the United States Department of Energy's National Nuclear Security Administration under Contract DE-AC04-94AL85000.

Abstract 222 TUE-RE03-4

[Contributed Talk - Tuesday 1:30 PM](#) - [Presidio C](#)

Localization of Conductive Filaments in TaOx Memristor using Focused Ion Beam Irradiation

[J. L. Pacheco](#), [D. Hughart](#), [G. Vizkelethy](#), [B. L. Doyle](#), [E. Bielejec](#), [M. Marinella](#)

Sandia National Laboratories, 1515 Eubank SE, Albuquerque NM 87123, United States

We have used a series of focused ion beam irradiations to determine the spatial location of the conductive filaments in TaOx memristor devices. These devices were irradiated using high energy silicon ions from the microbeam on the Sandia National Laboratories Tandem accelerator. We determined that the conductive filaments that led to the hysteretic IV curves characteristic of memristor operation were located at the edges of the device structure. These initial experiments were limited by the spatial resolution achieved with a focused ion beam of approximately 1 μm in diameter. We are preparing a similar experiment to improve on the spatial resolution by raster scanning a focused ion beam from our newly developed nano-Implanter (nI) to determine the location of the conductive filaments. The nI is a 100 kV focused ion beam system capable of achieving a spot size smaller than 10 nm on target and can provide ion beams from approximately 1/3 of the periodic table using a combination of mass velocity filter and liquid metal alloy ion sources. We will use 200 keV Si⁺⁺ beam focused to a 10-20 nm spot to determine the spatial location of the conductive filaments as a function of device history and ion fluence. The improved spatial resolution will allow us to determine if the hysteretic IV is due to a single conductive filament or from a series of partially conductive filaments. These filaments change conductivity as a function of ion irradiation induced damage (in particular; oxygen vacancy creation) and can be mapped by performing in-situ resistance measurements as a function of beam location. This experiment will provide a physical insight into the origins of memristor operation.

Sandia is a multi-program laboratory operated by Sandia Corporation, a Lockheed Martin Company, for the United States Department of Energy's National Nuclear Security Administration under Contract DE-AC04-94AL85000.

Abstract 167 TUE-RE03-5

[Contributed Talk - Tuesday 1:30 PM](#) - [Presidio C](#)

X-ray Radiation Effect on ZnS:Mn,Eu Fluorescence for Radiation Detection

[Lun Ma](#)¹, [Ke Jiang](#)², [Xiaotang Liu](#)³, [Wei Chen](#)¹

⁽¹⁾*Department of Physics and the SAVANT Center, University of Texas at Arlington, 502 Yates St. , Arlington TX 76019, United States*

⁽²⁾*Center for Biofrontiers Institute, University of Colorado at Colorado Springs, 1420 Austin Bluffs Pkwy, Colorado Springs Co 80918, United States*

⁽³⁾*Department of Applied Chemistry, College of Science South China Agricultural University, Guangzhou Guangdong 510642, China*

We have prepared manganese and europium co-doped zinc sulfide (ZnS:Mn,Eu) phosphors and investigated X-ray radiation effect on their fluorescence emissions. In addition to the red fluorescence at 583 nm due to the d-d transition of Mn ions, an intense violet emission at 420 nm is newly observed in ZnS:Mn,Eu phosphors. It is found that X-ray radiation quenches the 420 nm emission intensity but does not affect the Mn emission at 583 nm. The ratio of fluorescence intensities (FIR) at 420 nm and 583 nm has been monitored and recorded as a function of X-ray doses that exposed upon the ZnS:Mn,Eu phosphors. Empirical formulas of X-ray doses as a function of the FIRs are provided to estimate the quantity of applied X-ray radiation. Finally, possible mechanisms of X-ray radiation induced fluorescence quenching are discussed. Both X-ray induced (Eu²⁺)⁺ ions and defects are suggested as possible reasons of the 420 nm fluorescence intensity quenching. The X-ray radiation effect on the FIR of the two emissions in ZnS:Mn,Eu may provide a new, sensitive and reliable method for radiation detection.

Abstract 138 TUE-AMP03-1

[Invited Talk - Tuesday 3:30 PM - Travis A/B](#)

Effect of Inactive Electron in Single Ionization of Helium

[Allison L Harris](#)

Physics Department, Illinois State University, Campus Box 4560, Normal IL 61790, United States

The frozen core approximation has been successfully used for decades to model 4-Body collisions as 3-Body processes. Recently, computational advancements have allowed for full 4-Body models to be used to calculate fully differential cross sections (FDCS) for single ionization of helium. These 4-Body models show discrepancies with their 3-Body model counterparts. We have identified four possible sources of the discrepancies between the models. These four possible sources are: the initial state helium wave function, the final state He⁺ wave function, the final state potential for the outgoing electrons, and the perturbation. To identify which of these four sources causes in the differences in FDCS, we have performed a comprehensive study of 3-body and 4-body models for a wide range of incident projectile energies, ionized electron energies, and scattering angles.

Abstract 378 TUE-AMP03-2

[Invited Talk - Tuesday 3:30 PM - Travis A/B](#)

Collision dynamics studied with a polarized in-ring MOT target

[Daniel Fischer](#)¹, [Johannes Goullon](#)¹, [Renate Hubele](#)¹, [Michael Schuricke](#)¹, [Natalia Ferreira](#)¹, [Michael Schulz](#)²

⁽¹⁾*Max Planck Institute for Nuclear Physics, Saupfercheckweg 1, Heidelberg 69117, Germany*

⁽²⁾*Physics Department and LAMOR, Missouri University of Science & Technology, Rolla MO 65409, United States*

Studying atomic collisions enhances our understanding of the fundamental few-body problem in quantum dynamics. In the present contribution the dynamics of ionizing ion-lithium collisions is investigated. The experimental data is obtained with a novel experimental technique (MOTReMi) combining a magneto-optically trapped (MOT) Li target with a Reaction Microscope (ReMi) enabling the momentum resolved and coincident detection of the target fragments. This apparatus was implemented in the ion storage ring TSR providing electron-cooled projectile beams with high currents and low momentum spread. Due to the high resolution and by means of optical excitation, for the first time initial state selective fully differential cross sections for ion-impact induced ionization became available. Transitions of 1s, 2s, and 2p target electrons were investigated shedding light on the role of the projectile coherence length, electronic correlation and target polarization effect.

Abstract 223 TUE-AMP03-3

[Contributed Talk - Tuesday 3:30 PM - Travis A/B](#)

Variational calculations of positronium-hydrogen scattering for L=0 to 5

[Denton Woods](#)¹, [S.J. Ward](#)¹, [P. Van Reeth](#)²

⁽¹⁾*Physics, University of North Texas, 210 Avenue A, Denton Texas 76203, United States*

⁽²⁾*Physics, University College London, Gower St., London WC1E 6BT, United Kingdom*

We are investigating low-energy elastic positronium-hydrogen (Ps-H) scattering for partial waves from $L=0$ to $L=5$ using the complex Kohn variational method and variants of this, including the Kohn and the generalized Kohn methods [1]. To describe Ps-H scattering, we use elaborate trial wavefunctions which include a large number of Hylleraas-type terms for the short-range part, including all 6 interparticle distances. We plan to compare the S-, P-, and D-wave phase shifts to the phase shifts from close coupling calculations [2,3] and also to compare the $L=0$ to 5 phase shifts with Born approximation phase shifts. While there is no rigorous bound to the phase shifts for positive energies, we plan to show how systematically adding short-range terms appear to improve the phase shifts.

1. Denton Woods, P. Van Reeth and S.J. Ward, <http://meetings.aps.org/Meeting/MAR14/Event/215763>; submitted to APS for DAMOP 2014; Denton Woods, S.J. Ward and P. Van Reeth, <http://meetings.aps.org/link/BAPS.2013.DAMOP.Q1.122> (and references within).

2. Jennifer E. Blackwood, Mary T. McAlinden and H. R. J. Walters, Phys. Rev. A, **65**, 032517-1 (2002).

3. H. R. J. Walters, A.C.H. Yu, S. Sahoo and Sharon Gilmore, Nucl. Instrum. and Methods Phys. Res. B **221**, 149 (2004).

Abstract 191 TUE-AMP03-4

[Contributed Talk - Tuesday 3:30 PM - Travis A/B](#)

Atomic Processes in Radiation Dosimetry

[Paul M Bergstrom](#)

Radiation Physics Division, National Institute of Standards and Technology, 100 Bureau Dr, Gaithersburg MD 20899, United States

Radiation dosimetry metrology depends on accurate data for photon and electron interactions with atoms in a few materials over a wide range of energies. The photon-atom processes include photoionization, photon scattering and pair production. The electron-atom processes include bremsstrahlung and elastic and inelastic electron-atom scattering. The recent emphasis in the application of these data has been in trying to quantify the uncertainties in widely used tabulations. These uncertainties are approached from a physical point of view here. Assumptions regarding the modeling of the form of the interaction as well as the departures from the atomic description are examined for these processes.

Abstract 79 TUE-IBA09-1

[Invited Talk - Tuesday 3:30 PM - Presidio B](#)

Ion Beam Analysis in Extreme Environment: investigation of radioactive samples at the micrometric scale

[caroline raepsaet](#)^{1,2}, [hicham khodja](#)^{1,2}, [philippe bossis](#)³, [sylvain peugot](#)⁴

⁽¹⁾CEA/DSM/IRAMIS/NIMBE/LEEL, CEA/Saclay, Gif sur Yvette cedex 91191, France

⁽²⁾UMR 3299 SIS2M/LEEL, CEA/Saclay, gif sur yvette cedex 91191, France

⁽³⁾CEA/DEN/DANS/DMN/SEMI, CEA, CEA/Saclay, gif sur yvette cedex 91191, France

⁽⁴⁾CEA/DEN/MAR/DTCD/SECM/LMPA, CEA, CEA/Marcoule, Bagnols-sur-Cèze 30207, France

For many years, Ion Beam Analysis (IBA) techniques have been widely used all over the world in material sciences to study corrosion processes, interface phases formation, light element diffusion... In the specific field of the electronuclear industry, most phenomena are at first stage investigated in the laboratories on non-radioactive samples. However, this first approach has to be completed by the study after real functioning conditions, on highly radioactive materials.

Being strongly involved in nuclear research programs, CEA equipped one of the two beam lines of the nuclear microprobe [1] of Saclay, France, in order to extend IBA to radioactive samples. Located in a controlled area, this facility has been dimensioned to accept radiative but non-contaminant samples, handled in hot cells with slaved arms. The analysis chamber, situated in a concrete shielded cell, contains charged particle detectors allowing ERDA, RBS and NRA.

Operational since 1998, this facility has been used in the framework of two main programs. The first one concerns the corrosion of Zr-based alloy fuel cladding tubes after in-core service in Pressurized Water Reactors (PWR). Hydrogen content and distribution have been measured by ERDA through the cladding thickness, and lithium and boron content by NRA in the outer oxide layer of the clad. The second one is related to the influence of self-irradiation on the thermal diffusion of helium in various matrices, (U,Pu)O₂ fuel and waste disposal glasses: measurements by NRA of the modification of implanted ³He depth profiles are made before and after annealing.

After describing the facility, we will give an overview of the measurements which have been performed.

[1] H. Khodja, E. Berthoumieux, L. Daudin, JP. Gallien, Nucl. Inst. Meth. B181 (2001) 83.

Abstract 136 TUE-IBA09-2

[Contributed Talk - Tuesday 3:30 PM - Presidio B](#)

Monitoring of ion purity in high-energy implant via RBS.

[Arthur W Haberl](#)¹, [Wayne G Skala](#)¹, [Hassaram Bakhru](#)²

⁽¹⁾*Ion Beam Laboratory, University at Albany, 1400 Washington Avenue, Albany NY 12222, United States*

⁽²⁾*College of Nanoscale Science and Engineering, 255 Fuller Road, Albany NY 12203, United States*

The UAlbany Dynamitron is used for high-energy ion implantation as well as for routine materials analysis. Its ion source can be run using any one of fourteen different gases, leading to concerns of contamination during an implantation. The system has the usual well-calibrated mass-separation in a magnetic analyzer. A pre- or post-implant mass spectrum through this analyzer can give a useful understanding of unintended ions within the source beam, but it does not provide direct identification for such ions as CO or diatomic nitrogen-14 when implanting silicon-28. Since these possible components have the same momentum, the beamline mass separator will transmit them all. Because backscattered ions from the mass-separated beam will have only atomic scattering, this allows for element detection following the breakup of any molecular ion components. The verification system consists of a back-angle particle detector along with a movable temporary target consisting of a very thin film of gold on a carbon or silicon substrate. The backscattered spectrum can then be analyzed for the presence of unwanted elements. While this does not provide for removal of the unwanted components, it does provide for the identification and measurement of the problem. We show the physical layout, software and extra details necessary for successful use of the technique.

Abstract 214 TUE-IBA09-3

[Contributed Talk - Tuesday 3:30 PM - Presidio B](#)

Thickness evaluation of doped BiFeO₃ thin films using different techniques

[Ion Burducea](#)¹, [Mihai Straticiu](#)¹, [Petru Mihai Racolta](#)¹, [Mariuca Gartner](#)², [Victor Fruth](#)²

⁽¹⁾*Applied Nuclear Physics Department, Horia Hulubei National Institute of Physics and Nuclear Engineering - IFIN HH, 30 Reactorului St., Magurele 077125, Romania*

⁽²⁾*Institute of Physical Chemistry, 202 Splaiul Independentei St., Bucharest 060021, Romania*

BiFeO₃ (BFO) thin films have become attractive nanostructures because of their potential applications in a new generation of multifunctional devices. Strontium doped and pure BFO thin layers were deposited on silicon and microscope glass slide substrates using liquid precursors and dip coating technique. In order to have a more complete characterization of the obtained materials and their quality along with conventional techniques nuclear methods were also used. Structural and morphological observations were realized by means of XRD and SEM investigation. The thicknesses of the deposited layers were evaluated by spectro-ellipsometry (SE) and Rutherford Backscattering Spectrometry (RBS) techniques. RBS measurements were done at the new 3MV Tandetron accelerator available at Horia Hulubei National Institute of Physics and Nuclear Engineering (IFIN- HH). The results revealed a good correlation between values obtained with different evaluation techniques.

Abstract 250 TUE-IBA09-4

[Contributed Talk - Tuesday 3:30 PM - Presidio B](#)

Ion Beam Analysis of Shale rock for Hydrocarbon and Micro-structural Measurement

[Khalid Hossain¹](#), [Lucas Phinney¹](#), [Clayton Fullwood²](#), [Tim Hossain²](#), [Terry D Golding¹](#)

⁽¹⁾*Amethyst Research Inc, 123 Case Circle, Ardmore OK 73401, United States*

⁽²⁾*Cerium Laboratories, 5204 E. Ben White Blvd., Austin TX 78741, United States*

There has been an explosion in Shale gas extraction recently in US with strong economic benefit. Laboratory analysis of Shale rocks is significantly important in understanding hydrocarbon abundance, geological origin and maturity, pore structures and mineralogical fabric of the sediment. In this context, Amethyst Research and Cerium Labs are exploring comprehensive analytical techniques for organic and inorganic elemental as well as microstructural analysis of Shale rocks. Direct measurement inorganic C accessed by nuclear reaction analysis using 2.5 MV Van de Graaff accelerators. Hydrogen was analyzed by ERDA and C/H ratio was established for comparison. Heavier elements were analyzed by PIXE. Additional sample preparation, structural and compositional analysis was done by FIB/SEM, ICP-OES, and WDXRF. Ion Beam analysis will be presented comparing standard pyrolysis for hydrocarbon measurement. Results exploring porosity and structural variation by ion-microprobe will also be presented.

Abstract 287 TUE-IBA09-5

[Contributed Talk - Tuesday 3:30 PM - Presidio B](#)

Ionoluminescence: An Important Ion Beam Analytical Method

[Emmanuel Njumbe Epie¹](#), [Dharshana N Wijesundera¹](#), [Quark Chen^{1,3}](#), [Jiming Bao²](#), [Yang Li²](#), [Buddhi P Tilakaratne¹](#), [Ananta Adhikari¹](#), [Yanzhi He¹](#), [Iram Saleem¹](#), [Joseph Hernandez¹](#), [Wei Kan Chu¹](#)

⁽¹⁾*Department of Physics and TcSUH Ion Beam Lab, University of Houston, 4800 Calhoun Rd, Houston TX 77004, United States*

⁽²⁾*Department of Electrical and Computer Engineering, University of Houston, 4800 Calhoun Rd, Houston TX 77004, United States*

⁽³⁾*Department of Physics and Center for Nanoscience and Technology, National Sun Yat-Sen University, Koashiung, Taiwan*

Ionoluminescence (IL) also known as Ion Beam Induced Luminescence (IBIL) is the emission of optical (UV-IR) radiations when fast moving ions penetrate matter. IL originates from electronic transitions and recombination processes within the outer shell electrons of the target material, decay of self-trapped excitons, de-excitation of colour centers and impurities. Because of this, IL can provide information about the chemical form of elements (speciation), which complements other ion beam analytical techniques such as RBS, PIXE and PIGE. It also allows for the detection of impurities such as Mn, Cr and Rare Earth Elements as well as point defects in host materials (e.g. minerals) with a minimum detection limit of only a few ppm (mg/g). Although IL is still in its infancy, it is already finding a lot of potential applications in material sciences.

This presentation introduces the IL phenomenon, its band theory interpretation, and some applications.

Evolving Role of Charged-Particle Irradiation: Potential and Risks of Clinical Treatment with Particles Heavier than Protons

[Richard P. Levy](#)

Scripps Proton Therapy Center, 9730 Summers Ridge Road, San Diego CA 92121, United States

Proton irradiation has been developed to achieve the clinical benefit of improved 3D-dose distribution, with biological properties similar to x-rays. Neutron irradiation, though much less 3D-conformal than proton treatment, has been developed to take advantage of increased relative biologic effectiveness (RBE), as manifested by reduced oxygen enhancement ratio (OER), less repair of sublethal or potentially lethal damage, and less variation in sensitivity through the cell cycle. Irradiation with charged particles heavier than protons (e.g., carbon and neon ions) exhibits the unique combination of improved 3D dose distribution and increased RBE. Accelerator technology is rapidly developing to improve the efficiency of delivering these heavier charged particles clinically, but important issues remain regarding optimization of dose and fractionation parameters for the treatment of various tumor types and histologies located in different anatomical sites. Many laboratory animal and in vitro cellular studies, and an increasing number of clinical studies, have been performed to enable better understanding of how to adjust dose-fractionation selection to improve the therapeutic ratio of tumor-cell kill to normal-tissue injury. This paper highlights those findings, and outlines the enhanced therapeutic potential and associated risks of treatment with these heavier charged particles.

Clinical activity with protons and carbon ions at the National Center for Oncological Hadrontherapy (CNAO) in Italy

[Marco Krengli](#)^{1,2}, [Piero Fossati](#)^{1,3}, [Viviana Vitolo](#)¹, [Maria Rosaria Fiore](#)¹, [Alberto Iannalfi](#)¹,
[Barbara Vischioni](#)¹, [Silvia Molinelli](#)¹, [Alfredo Mirandola](#)¹, [Mario Ciocca](#)¹, [Francesca Valvo](#)¹,
[Sandro Rossi](#)¹, [Roberto Orecchia](#)^{1,3}

⁽¹⁾*Centro Nazionale Adroterapia Oncologica (CNAO), Via Campeggi 53, Pavia 27100, Italy*

⁽²⁾*University of "Piemonte Orientale", Via Solaroli 17, Novara 28100, Italy*

⁽³⁾*University of Milan, Via Festa del Perdono 7, Milan 20122, Italy*

The project for the National Center for Oncological Hadrontherapy (Centro Nazionale Adroterapia Oncologica - CNAO) was launched in 2001 thanks to the support of the Italian Ministry of Public Health. It aimed at building a center equipped with a synchrotron able to deliver beams of protons and heavy ions with active scanning. The building includes three treatment rooms, two with fixed horizontal and one with horizontal and vertical beam lines and a diagnostic section with CT-scan, 3-Tesla MRI and PET-scan for target identification and imaging follow-up. After relevant commissioning tests, clinical activity started in September 2011 when the first patient affected by skull base chondrosarcoma was treated with active scanning proton beam. In December 2012, the first treatment with carbon ions was delivered to a patient affected by recurrent adenoid-cystic carcinoma of the head and neck. To date, more than 250 patients included in established clinical protocols have been treated. About 65% of them received carbon ions and 35% protons. In total, 23 clinical protocols have been approved 15 are already ongoing. The most frequently treated tumor types are chordoma and chondrosarcoma of the base of skull and the spine, followed by other head and neck tumors such as adenoid-cystic carcinoma, recurrent pleomorphic adenoma and mucosal melanoma of the upper aero-digestive tract. Preliminary results on the ongoing clinical protocols and new research programs will be presented and discussed.

Overview Summary of Clinical Heavier-Ion Progress in Japan

[Richard P. Levy](#)¹, [Tadashi Kamada](#)², [Naruhiko Matsufuji](#)

⁽¹⁾*Radiation Oncology, Scripps Proton Therapy Center, 9730 Summers Ridge Road, San Diego CA 92121, United States*

⁽²⁾*Research Center Hospital for Charged Particle Therapy, National Institute for Radiological Sciences, 4-9-1 Anagawa, Inage-ku ward, Chiba Chiba-shi 263-8555, Japan*

Combining the properties of increased energy deposition toward range end with increasing biological effectiveness renders heavier ions such as carbon ions attractive for treating deep-seated tumors. Following the pioneering study at the Lawrence Berkeley Laboratory (LBL) in the United States, National Institute of Radiological Sciences (NIRS) of Japan started the carbon ion radiotherapy (C-ion RT) program at the Heavy Ion Medical Accelerator in Chiba (HIMAC) in 1994. Clinical outcome in the past 20 years targeting various tumor sites is proving the expectations toward this modality: significant anti-tumor effects have been achieved with acceptable toxicities in surrounding normal tissues, as well as drastic reduction of overall treatment time in most cases.

Concurrently we have been continuously updating HIMAC: In addition to the original broad-beam irradiation system, a 3D scanning irradiation system has been placed in 2011. A super-conducting rotating gantry coupled with the scanning system will be completed in two years. As of 2014, C-ion RT has been initiated at three more facilities in Japan: Hyogo Ion Beam Medical Center (HIBMC) in Hyogo; Gunma University Heavy Ion Medical Center (GHMC) in Gunma; and SAGA Heavy Ion Medical Accelerator in Tosu (SAGA HIMAT) in Saga. The Ion-beam Radiation Oncology Center in Kanagawa (i-ROCK) is now under construction.

In the treatment planning of C-ion RT, it is indispensable to handle the change in the biological effectiveness appropriately. At HIMAC, a pragmatic biological model, based on Human Salivary Gland cell response coupled with clinical experience from fast neutron radiotherapy, was developed and utilized. The clinical outcome was in good agreement with the model expectation. The model has been upgraded recently to optimize its application to the technique of scanning irradiation. The new model offers versatile estimation of the biological effectiveness of various radiations based on their microdosimetric information, while harmonizing with the original approach.

Abstract 310 TUE-NP05-1

[Invited Talk - Tuesday 3:30 PM - Travis C/D](#)

Radiochemical Measurements of Neutron Reaction Products at the National Ignition Facility

[Dawn Shaughnessy](#)¹, [Narek Gharibyan](#)¹, [Kenton Moody](#)¹, [Patrick Grant](#)¹, [John Despotopoulos](#)^{1,2}

⁽¹⁾*Chemical Sciences Division, Lawrence Livermore National Laboratory, 7000 East Ave., Livermore CA 94551, United States*

⁽²⁾*University of Nevada, 4505 S. Maryland Parkway, Las Vegas NV 89154, United States*

The National Ignition Facility (NIF) is currently the world's most powerful laser, capable of producing very large quantities of neutrons via the fusion of deuterium and tritium fuel. The neutron luminosity of a NIF ignition can produce observable concentrations of activation products from nanogram quantities of radiochemical detector isotopes loaded in the innermost layer of the capsule ablator (closest to the DT fuel) or on the outside of the hohlraum. The production of 14 MeV neutrons

in a single pulse creates an opportunity to measure neutron activation and neutron capture reaction rates in an environment where the contribution from lower-energy, scattered neutrons is insignificant. Using the Solid Radiochemistry (SRC) and Radiochemical Analysis of Gaseous Species (RAGS) diagnostics at NIF, initial results obtained during high neutron yield shots have shown collection of activated hohlraum material, as well as neutron capture products both in the hohlraum and in the collector material itself. As neutron yields continue to increase, there is also the possibility of measuring cross sections from excited nuclear states. These results motivate using NIF as a source for the measurement of nuclear data that is not obtainable at traditional reactor or accelerator facilities. This work performed under the auspices of the U.S. Department of Energy by Lawrence Livermore National Laboratory under Contract DE-AC52-07NA27344.

Abstract 195 TUE-NP05-2

[Invited Talk - Tuesday 3:30 PM - Travis C/D](#)

High Energy Density Plasmas (HEDP) for studies of basic nuclear science, Stellar Nucleosynthesis and Big Bang Nucleosynthesis

[Johan A Frenje](#)

Plasma Science and Fusion Center, Massachusetts Institute of Technology, 175 Albany street, NW17-235, Cambridge MA 02139, United States

Thermonuclear reaction rates and nuclear processes have been explored traditionally by means of conventional accelerator experiments, which are difficult to execute at conditions relevant to stellar nucleosynthesis. Thus, nuclear reactions at stellar energies are often studied through extrapolations from higher-energy data or in low-background underground experiments. Even when measurements are possible using accelerators at relevant energies, thermonuclear reaction rates in stars are inherently different from those in accelerator experiments. The fusing nuclei are surrounded by bound electrons in accelerator experiments, whereas electrons occupy mainly continuum states in a stellar environment. Nuclear astrophysics research will therefore benefit from an enlarged toolkit for studies of nuclear reactions. In this presentation, we report on the first use of High Energy Density Laboratory Plasmas (HEDLP) for studies of nuclear reactions relevant to basic nuclear science, stellar and Big Bang nucleosynthesis. These experiments were carried out at the OMEGA laser facility at University of Rochester and the National Ignition Facility (NIF) at Lawrence Livermore National Laboratory, in which spherical capsules were irradiated with powerful lasers to compress and heat the fuel to high enough temperatures and densities for nuclear reactions to occur. Four experiments will be highlighted in this presentation. In the first experiment, the differential cross section for the elastic neutron-triton (n-T) scattering at 14.1 MeV was measured with significantly higher accuracy than achieved in accelerator experiments. In the second experiment, the $T(t,2n)^4\text{He}$ reaction, a mirror reaction to the $^3\text{He}(^3\text{He},2p)^4\text{He}$ reaction that plays an important role in the proton-proton chain that transforms hydrogen into ordinary ^4He in stars like our Sun, was studied at energies in the range 15-40 keV. In the third experiment, the $^3\text{He}+^3\text{He}$ solar fusion reaction was studied directly, and in the fourth experiment, we probed the $T+^3\text{He}$ reaction, possibly relevant to Big Bang nucleosynthesis.

Abstract 142 TUE-NP05-3

[Invited Talk - Tuesday 3:30 PM - Travis C/D](#)

Measurement of the T+T Neutron Spectrum Using the National Ignition Facility

[Daniel B. Sayre](#)¹, [Carl R. Brune](#)², [Joseph A. Caggiano](#)¹, [Robert Hatarik](#)¹

⁽¹⁾Lawrence Livermore National Laboratory, Livermore CA 94550, United States

⁽²⁾Ohio University, Athens OH 45701, United States

Neutron time-of-flight spectra from inertial confinement fusion experiments with tritium-filled targets have been measured at the National Ignition Facility. These spectra represent a significant improvement in energy resolution and statistics over previous measurements, and afford the first definitive observation of a peak resulting from sequential decay through the ground state of ^5He at low reaction energies $E_{c.m.} < 100$ keV. To describe the spectrum, we have developed an R-matrix model that accounts for interferences from fermion symmetry and decays channels, and show these effects to be non-negligible. We also find the spectrum can be described by sequential decay through $l=1$ states in ^5He , which differs from previous interpretations.

Abstract 452 TUE-NP05-4

[Contributed Talk - Tuesday 3:30 PM - Travis C/D](#)

Charged-Particle Diagnostics for Inertial Confinement Fusion

[Anna Catherine Hayes](#)

T-Division, Los Alamos National Laboratory, B283, Los Alamos NM 87545, United States

Reaction-in-flight neutrons and knock-on charged particle induced reactions provide ideal probes of the stopping power in a burning plasma. In this talk I will present the physics of these reactions and the techniques needed to extract the stopping power from such measurements.

Abstract 12 TUE-NP05-5

[Contributed Talk - Tuesday 3:30 PM - Travis C/D](#)

Partial charge changing cross-sections of 300 A MeV Fe²⁶⁺ ion beam in different target media

[Ashavani Kumar](#), [Renu Gupta](#)

Physics, National Institute of Technology Kurukshetra, Kurukshetra Haryana 136119, India

In the present study, partial charge changing cross-sections of 300 A MeV Fe²⁶⁺ ion beam in Al and combined media of CH₂, CR39 and Al were calculated. The CR39 nuclear track detectors were used to identify the incident charged particles and their fragments. Exposed CR39 detectors were etched in 6N NaOH solution + 1% ethyl alcohol at 70 °C to visualize the tracks produced by primary ion beam and its fragmentations under optical microscope. The temperature was kept constant throughout the etching within ± 0.1 °C. The etched CR39 detectors were analyzed by using an image analysing system; DM6000 M optical microscope attached with a personal computer installed with Leica QWin Plus software. The cone-diameter distributions were fitted by multiple Gaussians using ROOT software analysis toolkit. To determine the partial charge changing cross-sections for $\Delta Z = -23, -22, \dots, -1$, the number of events corresponding to each fragment were determined from multiple Gaussian fitting of diameter distributions within 95.5% confidence levels and the number of incident and survived beam ions were counted within 99.7% confidence levels.

Abstract 296 TUE-NST08-1

[Invited Talk - Tuesday 3:30 PM - Bonham D](#)

Crater Function Modeling of Ion Bombardment and Ripple Formation

[Harley T. Johnson](#)¹, [Jonathan B. Freund](#)^{1,3}, [M. Z. Hossain](#)², [Kallol Das](#)¹

⁽¹⁾*Mechanical Science and Engineering, University of Illinois at Urbana-Champaign, 1206 W. Green St., Urbana IL 61801, United States*

⁽²⁾*Mechanical and Civil Engineering, Caltech, MC 104-44, Pasadena CA 91125, United States*

⁽³⁾*Aerospace Engineering, University of Illinois at Urbana-Champaign, 104 S. Wright St., Urbana IL 61801, United States*

Ion bombardment of solid surfaces is known to cause surface instabilities on a range of materials including metals, semiconductors and insulators. However, the explanations that have been proposed to explain these instabilities do not connect the rich range of experimentally observed patterns to atomistic mechanisms. The Bradley and Harper erosion-smoothing mechanism is the basis for most continuum theoretical analyses of ripple orientation. Here, we focus on atomistic and multiscale mechanisms underpinning the formation and orientation of surface ripples, including their evolution at finite amplitude. We provide the first explanation of the atomistic mechanism that determines ripple orientation, namely the competition between mass accumulation on the surface and the hole creation on the surface within picoseconds of the arrival of each incident ion. The wavelength of ripples is found to be controlled by the smoothing effect

of surface diffusion. Our conclusions are based on both a multiscale numerical model and an analysis of the geometric moments of the molecular dynamics (MD) based crater function, a term we use to describe the average surface height change due to a single ion impact. We describe in detail our MD and multiscale simulation methods, and we show recent extensions to our work, as well as future directions for MD modeling of ion beams.

Abstract 441 TUE-NST08-2

[Invited Talk - Tuesday 3:30 PM - Bonham D](#)

Formation and Evolution of Ripples on Ion-Irradiated Semiconductor Surfaces

[Rachel S Goldman](#)

Materials Science and Engineering, University of Michigan, 2300 Hayward Street, Ann Arbor MI 48105, United States

Ion-beam irradiation of semiconductor surfaces has emerged as a promising approach to generate a variety of self-organized nanostructures, including islands and ripples. For both broad-beam and focused-ion-beam (FIB) irradiation of semiconductors in the fluence range from to 10^{18} cm^{-2} , ripples have been reported to form and grow exponentially with time; further irradiation of rippled surfaces leads to a saturation of the ripple amplitude. Broad-beam irradiation is typically described in terms of the ion angle of incidence with respect to the substrate, θ_b . Meanwhile, the initial FIB beam spot produces trenches which lead to effectively off-normal irradiation of all subsequent spots. Therefore, we consider the effective ion beam angle of incidence, θ_{eff} , which is the angle between the incident ion beam and the local surface normal of the trenches. To date, ripples are typically reported for $\theta_b \neq 0$, and the influence of θ_{eff} on irradiation-induced surface evolution has not been explored. Here, we consider the FIB-irradiation-induced surface evolution of a low binding energy compound, InSb, for which the irradiation-induced variations in θ_{eff} are expected to be maximized [1]. In particular, we will present the influence of θ_{eff} on the formation of ripples for single-pass FIB irradiation and the influence of multiple-pass FIB irradiation on the ripple-nanorod evolution [2]. Our study provides an alternative approach to achieve dense arrays of ripples and nanorods with controllable spacings.

This research was supported by the CSTEC, founded by the DOE under Award No. DE-SC0000957, and also supported in part by the NSF through the MRSEC at the University of Michigan, Grant No. DMR-1120923.

[1] M. Kang, J. H. Wu, W. Ye, Y. Jiang, E. A. Robb, C. Chen, and R. S. Goldman, **Appl. Phys. Lett.** **104**, 052103 (2014).

[2] J.H. Wu and R.S. Goldman, **Appl. Phys. Lett.** **100**, 053103 (2012).

Abstract 173 TUE-NST08-3

[Invited Talk - Tuesday 3:30 PM - Bonham D](#)

Exotic New Patterns and Virtually Defect-Free Ripples Produced by Ion Sputtering

[R. Mark Bradley](#)¹, [Patrick D. Shipman](#)², [Francis C. Motta](#)²

⁽¹⁾*Department of Physics, Colorado State University, Fort Collins CO 80523, United States*

⁽²⁾*Department of Mathematics, Colorado State University, Fort Collins CO 80523, United States*

We have developed a theory that explains the genesis of the strikingly regular hexagonal arrays of nanodots that can form when the surface of a binary compound is subjected to normal-incidence ion bombardment [1]. In our theory, the coupling between the topography of the surface and a thin surface layer of altered composition is the key to the observed pattern formation.

For oblique-incidence bombardment of a binary material, we find that remarkably defect-free ripples can be produced if the ion species, energy and angle of incidence are appropriately chosen [2]. In addition, a "dots-on-ripples" topography can emerge for a different range of parameter values. Nanodots arranged in a hexagonal array sit atop a ripple topography in this novel type of pattern.

A closely related theory yields insight into the results of recent experiments in which silicon was bombarded with a beam of gold ions, yielding patches of ripples with two distinct wave vectors that were oblique to the beam [3]. We have advanced a theory that accounts for the emergence of this fascinating type of order --- in our theory, it is the result of (i) an anisotropic fourth order term in the equations of motion and (ii) the coupling between the surface height and a thin surface layer in which implanted gold is present.

[1] R. M. Bradley and P. D. Shipman, Phys. Rev. Lett. **105**, 145501 (2010).

[2] F. C. Motta, P. D. Shipman and R. M. Bradley, J. Phys. D **45**, 122001 (2012).

[3] S. A. Mollick, D. Ghose, P. D. Shipman and R. M. Bradley, Appl. Phys. Lett. **104**, 043103 (2014).

Abstract 58 WED-AMP02-1

[Invited Talk - Wednesday 8:00 AM - Presidio C](#)

Electron Coolers and Storage Rings as Spectroscopic Tools for Highly Charged Ions

[Stefan Schippers](#)

Institute for Atomic and Molecular Physics, Justus-Liebig-University Giessen, Leihgesterner Weg 217, Giessen 35392, Germany

The electron-ion merged-beams technique has extensively been exploited at heavy-ion storage rings equipped with electron coolers for spectroscopic studies of highly charged ions. Recent experiments comprise the measurement of hyperfine induced transition rates in Be-like ions [1,2], the determination of hyperfine-structure splittings [3,4] and nuclear charge radii [5] in heavy few electron systems, or the spectroscopy of ions with in-flight produced unstable nuclei [6]. This field of research faces a bright future with upcoming new facilities such as the Cryogenic Storage Ring (CSR) [7] at the Max-Planck-Institute for Nuclear Physics in Heidelberg, Germany, the TSR at HIE-ISOLDE [8] at CERN in Geneva, Switzerland and the Facility for Antiproton and Ion Research (FAIR) [9] in Darmstadt, Germany. In my talk I will present selected results and discuss some ideas for future research which will partly be carried out within the Stored Particle Atomic Physics Research Collaboration (SPARC) [10] at GSI/FAIR.

[1] S. Schippers et al., Phys. Rev. Lett. **98** (2007) 033001

[2] S. Schippers et al., Phys. Rev. A **85** (2012) 012513

[3] E. Lindroth et al., Phys. Rev. Lett. **86** (2001) 5027

[4] M. Lestinsky et al., Phys. Rev. Lett. **100** (2008) 033001

[5] C. Brandau et al., Phys. Rev. Lett. **100** (2008) 073201

- [6] C. Brandau et al., Phys. Scr. **T156** (2013) 014050
- [7] C. Krantz et al., J. Phys. Conf. Ser. **300** (2011) 012010
- [8] M. Grieser et al., Eur. Phys. J. Special Topics **207** (2012) 1
- [9] T. Stöhlker et al., arXiv:1401.7595v1
- [10] https://www.gsi.de/work/forschung/appa_pni_gesundheit/atomphysik/forschung/ap_und_fair/sparc.htm

Abstract 457 WED-AMP02-2

[Contributed Talk - Wednesday 8:00 AM - Presidio C](#)

Radiance line ratios $\text{Ly-}\beta / \text{Ly-}\alpha$, $\text{Ly-}\gamma / \text{Ly-}\alpha$, $\text{Ly-}\delta / \text{Ly-}\alpha$, and $\text{Ly-}\epsilon / \text{Ly-}\alpha$ for soft X-ray emissions following charge exchange between C^{6+} and Kr

[V M Andrianarijaona](#)¹, [D. McCammon](#)², [M. Fogle](#)³, [D R Schultz](#)⁴, [D G Seely](#)⁵, [P C Stancil](#)⁶, [C C Havener](#)⁷

⁽¹⁾*Department of Physics, Pacific Union College, Angwin CA 94508, United States*

⁽²⁾*Department of Physics, University of Wisconsin, Madison WI 53706, United States*

⁽³⁾*Department of Physics, Auburn University, Auburn AL 36849, United States*

⁽⁴⁾*Department of Physics, University of North Texas, Denton TX 76203, United States*

⁽⁵⁾*Department of Physics, Albion College, Albion MI 49224, United States*

⁽⁶⁾*Department of Physics and Astronomy, University of Georgia, Athens GA 30602, United States*

⁽⁷⁾*Physics Division, Oak Ridge National Laboratory, Oak Ridge TN 37831, United States*

Using the ion-atom merged beams apparatus at Oak Ridge National Laboratory, the radiance line ratios $\text{Ly-}\beta / \text{Ly-}\alpha$, $\text{Ly-}\gamma / \text{Ly-}\alpha$, $\text{Ly-}\delta / \text{Ly-}\alpha$, and $\text{Ly-}\epsilon / \text{Ly-}\alpha$ for soft X-ray emission following charge exchange between C^{6+} and Kr were measured for collision velocities between 250-3000 km/s. The measurements were done with a microcalorimeter x-ray detector of approximately 10 eV FWHM resolution. There is no Kr theory; Kr has the same ionization potential as H so that the results reported here are compared to calculations done on $\text{C}^{6+} + \text{H}$. The comparison and discussion include the possibility of using Kr as an experimental surrogate for H for the study of single-electron-capture. Also, double-electron-capture is possible for $\text{C}^{6+} + \text{Kr}$ and for any multi-electron target. The true double capture is seen to be only 10% of the single-electron-capture.

Abstract 399 WED-AMP02-3

[Invited Talk - Wednesday 8:00 AM - Presidio C](#)

SPARC: Experiments at the High-Energy Storage Ring HESR

[Thomas Stöhlker](#)², [Yuri Litvinov](#)¹, [Reinhold Schuch](#)³

⁽¹⁾*Atomic Physics, GSI Darmstadt, Planckstrasse 1, Darmstadt 64291, Germany*

⁽²⁾*Helmholtz-Institut Jena, Froebelstieg 3, Jena 07743, Germany*

⁽³⁾*Stockholm University, AlbaNova, Stockholm 10691, Sweden*

An overview about the envisioned program of the research collaboration (Stored Particle Atomic Research Collaboration, <http://www.gsi.de/sparc>) at the future accelerator facility FAIR will be given. In the presentation special emphasis will be given to the planned experiments at high-energy storage-ring HESR where cooled heavy ions up to gamma factor of 5 will be available [2].

- [1] SPARC Technical Proposal (2005) http://www.gsi.de/onTEAM/grafik/1068560945/sparc-technical-proposal_print.pdf

Abstract 320 WED-AMP02-4

[Contributed Talk - Wednesday 8:00 AM - Presidio C](#)

Photonuclear studies of the isomeric yield ratios in the production of $^{nat}\text{Ag}(g,xn)^{106m,g}\text{Ag}$ with 50-, 60-, and 70-MeV bremsstrahlung

[Md. Shakilur Rahman](#)¹, [Guinyun Kim](#)², [Kyung-Sook Kim](#)², [Manwoo Lee](#)², [A.K.M. Moinul Haque Meaze](#)³, [Tae-Ik Ro](#)⁴

⁽¹⁾*Institute of Nuclear Science & Technology, Atomic Energy Research Establishment, Bangladesh Atomic Energy Commission, Ganakbari, Savar, Dhaka Dhaka 1349, Bangladesh*

⁽²⁾*Department of Physics, Kyungpook National University, 1370 Sankyuk-dong, Buk-gu, Daegu 702-701, Korea*

⁽³⁾*Department of Physics, University of Chittagong, Chittagong 4331, Bangladesh*

⁽⁴⁾*Department of Physics, Dong-A University, 840 Hadan-dong, Saha-gu, Busan 604-714, Korea*

Isomeric yield ratio by photonuclear reactions is a powerful tool for studying angular momentum transfer in a nuclear reaction that leads a valuable information on the spin dependence of the nuclear level density parameter, spin cut off parameter as well as information on the probability of excitation, the energy, and spin distributions. The isomeric yield ratios in the production of $^{nat}\text{Ag}(g,xn)^{106m,g}\text{Ag}$ have been measured by photonuclear reactions with bremsstrahlung beams of end point energy 50-, 60-, and 70-MeV. The high purity natural Ag metallic foils were used and irradiated with bremsstrahlung radiation produced from high energy electron beam struck with 0.1 mm thin tungsten target from the electron beam accelerator at Pohang Accelerator Laboratory (PAL). The photoactivation technique has been used and hence the induced activities in the irradiated foils were measured by off-line g-ray spectrometric system consisting of HPGe detector coupled with PC-based 4K MCA. The isomeric yield ratio in the present measurement (high-spin to low spin) are found to be 0.0186 ± 0.0035 , 0.0201 ± 0.0024 , 0.0208 ± 0.0021 for bremsstrahlung end point energy 50-, 60-, and 70-MeV respectively. In order to improve the accuracy of the measurement, necessary correction factors were attempted in the present study. The measured values of isomeric ratios are compared with the theoretical values by statistical model code TALYS. The details of the formation of the isomer by photonuclear and particle induced reactions together with the literature values of the investigated nuclei are compared and discussed.

Abstract 349 WED-AMP02-5

[Contributed Talk - Wednesday 8:00 AM - Presidio C](#)

Electron spectroscopy at the high-energy endpoint of electron-nucleus bremsstrahlung

[Pierre-Michel Hillenbrand](#)^{1,2}, [Siegbert Hagmann](#)^{1,3}, [Dariusz Banas](#)⁴, [Carsten Brandau](#)^{2,5}, [Reinhard Dörner](#)³, [Enrico DeFilippo](#)⁶, [Alexandre Gumberidze](#)⁵, [Dalong Guo](#)⁷, [Doris Jakubassa-Amundsen](#)⁸, [Michael Lestinsky](#)¹, [Yuri Litvinov](#)¹, [Alfred Müller](#)², [Hermann Rothard](#)⁹, [Stefan Schippers](#)², [Uwe Spillmann](#)¹, [Andrey Surzhykov](#)¹¹, [Sergiy Trotsenko](#)^{1,11}, [Alexander Voitikiv](#)¹⁰, [Thomas Stöhlker](#)^{1,11}

⁽¹⁾*GSI Helmholtzzentrum für Schwerionenforschung, Darmstadt, Germany*

⁽²⁾*Justus-Liebig-Universität, Giessen, Germany*

⁽³⁾*Goethe Universität, Frankfurt, Germany*

⁽⁴⁾*Jan Kochanowski University, Kielce, Poland*

⁽⁵⁾*Extreme Matter Institute, Darmstadt, Germany*

⁽⁶⁾*INFN Catania, Catania, Italy*

⁽⁷⁾*Institute of Modern Physics, Lanzhou, China*

⁽⁸⁾*Ludwig-Maximilians-Universität, München, Germany*

⁽⁹⁾*CIMAP-CIRIL-GANIL, Caen, France*
⁽¹⁰⁾*Max-Planck-Institut für Kernphysik, Heidelberg, Germany*
⁽¹¹⁾*Helmholtz-Institut Jena, Jena, Germany*

The high-energy endpoint of electron-nucleus bremsstrahlung is of particular theoretical interest due to its close relation to photoionization PI and radiative electron capture REC and provides most stringent tests for understanding the coupling between a matter field and an electromagnetic field. In this process, the incoming electron scatters inelastically off an atomic nucleus and transfers almost all of its kinetic energy onto the emitted bremsstrahlung photon. Alternatively the electron can be understood as being radiatively captured into the continuum of the projectile (RECC). Experimentally this process is only accessible using inverse kinematics, where quasi-free target electrons scatter off fast highly charged heavy projectiles. For collisions U88+ + N2 @ 90 MeV/u new measurements of the electron energy distribution in coincidence with the emitted photon have been conducted at the Experimental Storage Ring ESR at GSI, using the upgraded magnetic electron spectrometer. Furthermore electron energy distributions for non-radiative electron capture to continuum (ECC) and the electron loss to continuum (ELC) could be determined. Comparison with various theoretical calculations will be presented.

Abstract 50 WED-HSD07-1

[Invited Talk - Wednesday 8:00 AM - Travis A/B](#)

Overview of Accelerators with Potential Use in Homeland Security

[Robert W Garnett](#)

Accelerator Operations and Technology Division, Los Alamos National Laboratory, MS H817, PO Box 1663, Los Alamos NM 87545, United States

Quite a broad range of accelerators have been applied to solving many of the challenging problems related to Homeland Security and Defense. These accelerator systems range from relatively small, simple, and compact, to large and complex, based on the specific application requirements. They have been used or proposed as sources of primary and secondary probe beams for applications such as radiography and to induce specific reactions that are key signatures for detecting conventional explosives or fissile material. A brief overview and description of these accelerator systems, their specifications, and application will be presented. Some recent technology trends will also be discussed.

Abstract 31 WED-HSD07-2

[Contributed Talk - Wednesday 8:00 AM - Travis A/B](#)

An Ultra Low-Exposure Neutron Based Inspection System for Nuclear Material

[Michael J King](#), [Dan A Strellis](#), [Tsahi Gozani](#), [Mashal Elsalim](#), [Krystal Alfonso](#), [Matthew Araujo](#)

Rapiscan Laboratories, Inc, 520 Almanor Avenue, Sunnyvale CA 94085, United States

Rapiscan Laboratories has developed a pulsed-neutron based active interrogation system for the inspection of nuclear materials inside human occupied passenger vehicles. The goal of the system is to detect nuclear material hidden inside a passenger vehicle while minimizing passenger radiation exposure to less than 25 mrem/scan. The inspection technique is based on differential die-away, which relies on thermalized neutrons to induce fission neutrons in the threat. Thermal neutrons are ideal for inspection purposes in that the fission cross-section increases as the neutron energy decreases as a function of $1/v$ and the quality factor Q-value is 2, minimizing the dose. The experimental system consists of three large-area He-3 based differential die-away detector placed in the bottom, side and transmission geometry. The interrogating source consists of an electronic neutron generator imbedded in a beryllium moderator. Results with the detection of nuclear material yielding a passenger radiation dose of <25 mrem/scan will be shown.

This work has been supported by the US Department of Homeland Security, Domestic Nuclear Detection Office, under competitively awarded contract/IAA HSHQDC-11-C-00092. This support does not constitute an express or implied endorsement on the part of the Government.

Abstract 94 WED-HSD07-3

[Contributed Talk - Wednesday 8:00 AM - Travis A/B](#)

Small Cyclotron Applications and Development

[Richard R Johnson](#), [Leandro AC Piazza](#)

Design Office, Best Cyclotron Systems, Inc., 7643 Fullerton Road, Springfield Road Virginia 22153, United States

The widespread use of Positron Emission Tomography (PET) has resulted in a broad worldwide base of cyclotrons throughout the world. The majority of these devices use technology that may limit application. Those small cyclotrons can have other uses. The characteristics and potential of improved small cyclotron design are presented.

Abstract 336 WED-HSD07-4

[Contributed Talk - Wednesday 8:00 AM - Travis A/B](#)

Superconducting Magnets for Ultra Light and Magnetically Shielded, Compact Cyclotrons for Medical, Scientific, and Security Applications

[Joseph V. Minervini](#)¹, [Alexey Radovinsky](#)¹, [Craig E. Miller](#)¹, [Philip C. Michael](#)¹, [Leslie Bromberg](#)¹,
[Mario Maggiore](#)²

⁽¹⁾*Plasma Science and Fusion Center, Massachusetts Institute of Technology, 77 Massachusetts Avenue, Cambridge MA 02139, United States*

⁽²⁾*National Institute of Nuclear Physics (INFN), Laboratori Nazionali di Legnaro, 2, viale dell'Università, Legnaro PD I-35020, Italy*

Compact superconducting cyclotrons are being considered for use in medical applications such as ion beam radiotherapy and PET isotope production, medium energy nuclear particle accelerators for scientific research, and in portable devices for security applications. The use of superconductors can lower the size and weight of the cyclotron because magnetic fields much higher than the saturation field of iron can be achieved at very high current density, and low power consumption when compared with copper, water-cooled, resistive coils. In this work we show that the superconducting magnetic field coils can be used as the primary method for producing the field shaping needed to generate the field profile required in a cyclotron, avoiding or minimizing the ferromagnetic pole pieces typically used in these machines. Coil number, location, and current are adjusted to produce the required field for either synchrocyclotrons or isochronous machines. In addition, magnetic field coils are used to magnetically shield the device, similarly eliminating the need for a ferromagnetic return yoke or ferromagnetic shields. Results are presented that demonstrate the significant weight advantage and high performance that can be achieved when the iron yoke is eliminated or reduced to a small amount of iron poles for local field shaping. Magnetic shielding of the stray field can even offer improvement over the use of iron shields.

Abstract 36 WED-IBA02-1

[Invited Talk - Wednesday 8:00 AM - Presidio B](#)

Recent progress in fast atom diffraction at surfaces

[Helmut Winter](#)

Institute of Physics, Humboldt Universitaet, Newtonstrasse 15, Berlin D-12489, Germany

Recently pronounced diffraction effects for grazing scattering of fast light atoms and molecules with energies up to some keV under axial surface channeling were observed. The rich diffraction patterns provide information on the interatomic spacings between axial surface channels and on the corrugation of the interaction potential. The latter effect can be used to study the structure of surfaces with fast atoms via interferometric techniques. The new method shows similarities to thermal He atom scattering (HAS), but has a number of advantages as simple tuning of the projectile energy (de Broglie wavelength), an orders of magnitude more efficient detection of scattered projectiles as well as a simple and cost-effective setup. The quantum coherence in the scattering process is preserved by specific features of surface channeling which is investigated in detail via the coincident detection of the diffraction patterns with the energy loss of scattered atoms. It turns out that the suppression of electronic excitations owing to the band gap of insulator surfaces plays a key role for coherent scattering and the application of Fast Atom Diffraction (FAD) in surface science. For He atoms the energy transfer to lattice atoms plays an important role. Recent work on FAD has focused on the longitudinal coherence in the scattering event with the surface and on applications to ordered films formed by organic molecules as the amino acid alanine adsorbed on a Cu(110) surface.

Abstract 422 WED-IBA02-2

[Invited Talk - Wednesday 8:00 AM - Presidio B](#)

Multiple scattering simulation: effects at low energy

[Francois Schiettekatte](#)

Departement de Physique, Universite de Montreal, C.P. 6128, succursale centre-ville, Montreal Quebec H3C 3J7, Canada

Simulations of background signal are important in order to get quantitative analysis of IBA data. Multiple wide-angle scattering is one of the few issue where analytical theory allowing a computation of the effect does not exist. Some analytical simulation software does take this effect into account up to 2nd order (double scattering), which is usually sufficient. But the effect requires a simulation at higher order whenever the cross-section or the distance travelled into a sample become important, both resulting in increasingly numerous collisions. This is the case of medium- and low-energy ion scattering because of the energy dependence of the cross-section. Analysis is therefore limited to the close surface in order to not be in a regime where MS becomes significant. We will show that Monte Carlo (MC) simulations could be used to push the barrier somewhat further.

MC simulations carried out by Corteo, however, are based on some fundamental assumptions. In its implementation of the random phase approximation, it considers a fixed mean free path l_0 . This implies that the maximum impact parameter \mathbf{b} is also fixed for each layer. Conversely, MC simulations carried out by SRIM (usually for ion implantation) use the minimum impulse approximation, where \mathbf{b} is set at a value such that collisions transfer at least a minimum amount of energy to the target atom. Because \mathbf{b} increases with decreasing energy, l_0 decreases, leading to more collisions as the energy decreases, and possibly too few at high energy to simulate accurately an IBA spectrum. Here, these two approximations are compared also with a third one that considers a minimum deflection angle. They are shown to give the same results within the statistical uncertainty, except in the low energy tails where the minimum impulse approximation predicts a yield a few percent higher than the two others.

Abstract 189 WED-IBA02-3

[Contributed Talk - Wednesday 8:00 AM - Presidio B](#)

Medium Energy Ion Scattering investigation of the topological insulator Bi₂Se₃ films

[Hang Dong Lee](#), [Can Xu](#), [Samir Shubeita](#), [Matthew Brahle](#), [Nikesh Koirala](#), [Seongshik Oh](#), [Torgny Gustafsson](#)

Physics and Astronomy Department, Rutgers University, 136 Frelinghuysen Rd, Piscataway NJ 08854, United States

Topological insulators (TI) have emerged as a platform for low-power electronics, spintronics, quantum computations and other applications. They are predicted to have an insulating bulk state and spin-momentum-locked metallic surface states. Among the TI discovered so far, Bi_2Se_3 is one of the most promising for device applications. However, for successful device applications growing high quality, single crystalline Bi_2Se_3 films is indispensable. We have used medium energy ion scattering (MEIS) to study the structure and composition of ultrathin films of a topological insulator, Bi_2Se_3 , grown epitaxially on Si (111) and sapphire substrates using molecular beam epitaxy (MBE). MEIS shows that films grown on sapphire have uniform thickness, excellent stoichiometry and a flat surface while films grown on Si (111) do not. Our results are corroborated by STM analysis. The films grown on sapphire have much enhanced transport properties. This result suggests that the topological properties of Bi_2Se_3 films may depend on the crystal structure. Investigations of crystallinity and its influence on the transport properties of Bi_2Se_3 films will be presented as well. Amorphous Bi_2Se_3 films on sapphire were annealed in ultrahigh vacuum at several different temperatures and in-situ MEIS measurements were carried out to examine the crystallinity depending on annealing temperature. The transport properties of our samples after annealing were also measured by four point probe Hall measurements.

Abstract 199 WED-IBA02-4

[Contributed Talk - Wednesday 8:00 AM - Presidio B](#)

Medium energy ions scattering and elastic recoils for thin films and monolayers

[Lyudmila V Goncharova](#), [Sergey N Dedyulin](#), [Mitchell Brocklebank](#)

Physics and Astronomy, The University of Western Ontario, 1151 Richmond St, London ON N6A3K7, Canada

Modern synthetic approaches and nanofabrication are providing us the means of creating material structures controlled at the atomic scale. Familiar examples include the formation of hetero-structures grown with atomic precision, nanoparticles with designed electronic properties, and new carbon-based devices. One of the challenges here is that electron transport properties of these diverse materials are closely linked to the basic interactions at the interface.

Ion scattering has been very successfully applied in our group to study interfaces of devices based on silicon and higher-mobility semiconductors. We use medium energy ion scattering (MEIS), a powerful tool for depth profiling, with depth resolution of 5-10 Å in the near surface region with electrostatic energy analyzer (ESA). It was applied successfully in the past to analyze for elements heavier than carbon, typically on light substrates. It is potentially interesting to extend this technique to perform elastic recoil detection analysis (ERDA) of light elements, such as H, D, or Li. We were also able to detect residual hydrogen presence in Hf silicate thin films grown by atomic layer deposition. The width of the H⁺ ion peak can be correlated well with the film thicknesses in the 3.6-16 nm range, while conventional ERDA does not differentiate them. We observe some dependence of the H⁺ fraction on recoil angle, H⁺ ions are not observed at any emerging angles above 80°, while the data reported by Marion-Young predicts H fraction of 3-5% in this energy range. The H⁺ fraction is expected to increase with decreasing energy of the recoils (incident energy). We also comment of the limitations of medium energy elastic recoil detection analysis.

Abstract 491 WED-MA08-1

[Invited Talk - Wednesday 8:00 AM - Bonham B](#)

Navigating the Logistical and Bureaucratic Minefield of Starting Up a New Particle Therapy Facility

[Carl J Rossi](#)

Scripps Proton Therapy Center, 9730 Summers Ridge Road, San Diego CA 92121, United States

Abstract 490 WED-MA08-2

[Invited Talk - Wednesday 8:00 AM - Bonham B](#)

Myths and Realities of Developing a Particle Therapy Center

[Chris Chandler](#)

Chief Executive Officer, Proton International, 922 Hawkhorn Ct., Atlanta GA, United States

After decades of development and experience derived from various institutions and vendors, ?modern? particle therapy is here to stay, and these centers are increasing rapidly in number. Benefits to sponsoring institutions include: the ability to differentiate oncology offerings amongst competing healthcare systems; increased patient flow and volume of all oncology services performed in the facility; assurance that patients and medical staff have access to the full complement of advanced radiation therapy modalities; and an increased likelihood that patients will be retained who otherwise might travel to other particle therapy centers.

Having developed and opened multiple such facilities, we have seen clear evidence of these benefits. When you are identified as a provider of advanced radiotherapy services, people are immediately drawn into your healthcare sphere of influence. Even when particle therapy may not be the right modality for certain patients, they will often stay and obtain other services. We must be realistic, however, and learn from the experience of those who have gone before us. This is not just an equipment purchase decision. The clinical envelope and treatment protocols are also critical to your success. What factors have been instrumental to the success of some start-up efforts and to the failure of others? Complexity, financial issues, patient ramp-up, technological solutions promised but not realized, and more.

What is reality in this industry and what is myth? Multiple variables, and how they interact in the overall development and operational strategy for a particle facility, must be carefully evaluated. This talk will evaluate the impact the following variables may have on our particle journey: technological complexity; patient ramp-up and throughput; diag-nostic mix; operational management; and reimbursement.

Abstract 351 WED-NP11-1

[Invited Talk - Wednesday 8:00 AM - Travis C/D](#)

Application of accelerator mass spectrometry to archaeology, geography and environmental research.

[Wolfgang Kretschmer](#), [Andreas Scharf](#), [Matthias Schindler](#), [Alexander Stuhl](#)

Physics Department, University of Erlangen, Erwin-Rommel-Str. 1, Erlangen 91058, Germany

Accelerator mass spectrometry (AMS) is an ultrasensitive method for the measurement of isotope ratios of a long lived radioisotope to a stable isotope (e.g. $^{14}\text{C}/^{12}\text{C} \approx 10^{-12} - 10^{-15}$) with numerous applications in interdisciplinary research. The Erlangen AMS facility, based on an EN tandem accelerator with a Pelletron charging system and a hybrid sputter ion source for solid and gaseous samples is well suited for age determination of carbonaceous materials for periods of up to 50.000 years. The application to geography and archaeology is demonstrated by the investigation of numerous wooden drill cores from historic monasteries, temples and secular buildings in Tibet and Nepal. Here the ^{14}C measurements in combination with tree ring structure lead to an enhanced dating precision via wiggle matching. This can be used to extend existing tree ring chronologies and could help to investigate suggested monsoon variations during the Middle Ages. The historic tower buildings of Tibet and Sichuan are a special cultural heritage which has been rarely studied up to now. The knowledge of the exact age of these buildings could help to better understand the cultural and historical context of their development and their function, and could support the effort to declare them a UNESCO World Heritage site. Another spectacular application to archaeology was the investigation of a Persian mummy found in 2000 in the western part of Pakistan.

An important topic in environmental research is the origin of organic compounds in nature. This can be investigated by the determination of the ^{14}C content of the compound since an anthropogenic input can be deduced from industrial production via oil and coal which contain no ^{14}C , compounds from biogenic sources have the ^{14}C concentration of living organisms. This compound specific radiocarbon analysis has been applied to aldehydes from indoor air samples extracted from different locations.

Experimental Investigation of Ion Sources for the Detection of Ultra-trace Uranium and Thorium

[Yuan Liu](#)¹, [John C. Batchelder](#)^{1,2}, [Ran Chu](#)^{1,3}, [Alfredo Galindo-Uribarri](#)^{1,3}, [Elisa Romero-Romero](#)^{1,3},
[Dan W. Stracener](#)¹

⁽¹⁾*Physics Division, Oak Ridge National Laboratory, 1 Bethel Valley Rd, Oak Ridge TN 37831, United States*

⁽²⁾*Oak Ridge Associated Universities, 1 Bethel Valley Rd, Oak Ridge TN 37831, United States*

⁽³⁾*Department of Physics and Astronomy, University of Tennessee, 401 Nielsen Physics Building, Knoxville TN 37996, United States*

Efforts are presently underway at Oak Ridge National Laboratory to develop ultrasensitive analytical techniques based on accelerator mass spectrometry (AMS) for evaluating the U and Th impurity levels in the underground electroformed copper materials used in a search for neutrinoless double-beta-decay. AMS has been used previously to detect rare actinide isotopes with detection limits of 10^{-11} - 10^{-12} isotope abundance ratios [1]. The ion source typically used for AMS is a Cs-sputter negative ion source, which has an ionization efficiency ranging from 0.01% to 0.1% for U [2-5]. To detect the U and Th impurities in the copper material, a more efficient ion source is required. We are investigating two candidate positive-ion sources: an electron beam plasma ion source and a hot-cavity surface ionization source. The latter promises at least one order of magnitude higher ionization efficiency for U and Th than a Cs-sputter source. Preliminary experimental results will be presented.

Research sponsored by the Laboratory Directed Research and Development Program of Oak Ridge National Laboratory, managed by UT-Battelle, LLC, for the U. S. Department of Energy.

[1] P. Steier, **et al.**, **Nucl. Instr. and Meth. B** 268 (2010) 1045-1049.

[2] M. Srncik, **et al.**, **J. Environ. Radioactivity** 102 (2011) 614-619.

[3] P. Steier, **et al.**, **Nucl. Instr. and Meth. B** 266 (2008) 2246-2250.

[4] M.A.C. Hotchkis, **et al.**, **Nucl. Instr. and Meth. B** 172 (2000) 659-665.

[5] X.Wang, **et al.**, **Nucl. Instr. and Meth. B**

Abstract 449 WED-NP11-3

[Contributed Talk - Wednesday 8:00 AM - Travis C/D](#)

Basic and applied nuclear physics at CIRCE laboratory

[Giuseppe Porzio](#)¹, [Raffaele Buompane](#)¹, [Antonio D'Onofrio](#)¹, [Mario De Cesare](#)¹, [Nicola De Cesare](#)¹,
[Antonino Di Leva](#)², [Lucio Gialanella](#)¹, [Fabio Marzaioli](#)¹, [Filippo Terrasi](#)¹

⁽¹⁾*Mathematics and Physics, Second University of Naples, Via Lincon 5, Caserta 81100, Italy*

⁽²⁾*Physics, University of Naples FEDERICO II, via Cinthia, napoli 80126, Italy*

The Center for Isotopic Research on Cultural and Environmental heritage, operated by Department of Mathematics and Physics of the Second University of Naples, is performing since 2005 both basic research and commercial and R&D activity in the field of fundamental and applied nuclear physics. It features a 3 MV tandem accelerator 9SDH-2 type Pelletron, produced by National Electrostatics Corp. (NEC), Middleton (USA), including two Cs sputtering ion sources (one for stable and another for radioactive beams), an injector featuring an electrostatic analyzer and a magnet equipped with a fast bouncing system, a pelletron two-stage accelerator, a high-energy double focusing magnet and a spherical electrostatic analyzer. A switching magnet drives the beam in one of the 5 beam lines, each equipped with different experimental systems. The accelerator is used both for producing intense reaction-inducing ion beams and for ultrasensitive Accelerator Mass Spectrometry of several long lived cosmogenic isotopes, supporting research activity in nuclear astrophysics, archaeometry by high-precision radiocarbon dating, environmental science by ¹⁴C-based global carbon cycle studies, nuclear safeguards and contrast to illegal nuclear fuel use by actinides AMS, forensic applications of AMS, tribology by ⁷Be implantation, measurement of the ¹¹B/¹⁰B ratio of pure boric acid [B(OH)₃] samples..

The poster will present the specifications and performances of the facility with emphasis on the upgradings and modifications of the original lay-out.

Abstract 135 WED-NP11-4

[Contributed Talk - Wednesday 8:00 AM - Travis C/D](#)

New AMS Facility in Mexico: "Laboratorio de Espectrometría de Masas con Aceleradores": High sensitivity measurements of radioactive isotope concentrations in materials.

[Efraín Chávez](#), [Corina Solís](#), [Eduardo Andrade](#), [Libertad Barrón-Palos](#), [María Esther Ortiz](#), [Arcadio Huerta](#), [Victoria Araujo](#), [Laura Marín](#), [Edgar Adán Jiménez](#)

Instituto de Física, Universidad Nacional Autónoma de México, Ciudad Universitaria, S/N, Coyoacán D. F. 04510, Mexico

LEMA is a new AMS facility in Mexico with the goal of measuring low concentrations of specific (radioactive) isotopes found in matter.

In this presentation, the main features of the facility are described along with some of the first applications in fields like Archeology, Geology and Nuclear Astrophysics.

Abstract 39 WED-ATF04-1

[Invited Talk - Wednesday 9:45 AM - Presidio A](#)

High-Energy Electron-Beam Tomography

[Joseph Bendahan](#), [Dan Strellis](#), [Deepa Angal-Kalininb](#), [J. K. Jones](#), [K. B. Marinov](#)

Science and Technology Facilities Council, Daresbury Science and Innovation Campus, Daresbury, Warrington WA4 4AD, United Kingdom

Low-energy Computed Tomography (CT) systems have shown to detect explosives in luggage. The inspection of larger objects, require higher-energy x-rays to penetrate the longer path and higher density of the objects contents. High-energy CT systems for large objects employ non-rotating sources and are configured horizontally with the object rotating around its axis. It is possible to reconfigure the source and detectors to rotate around the object to allow for the inspection of longer objects. However, the high-speed rotation of the large high-energy source and detectors is impractical.

Rapiscan Laboratories in collaboration with the Science and Technology Facilities Council designed a system for obtaining multiple high-energy electron beams directed at multiple target locations along a defined path. The system generates multiple x-ray views around a large object or cargo container that allow reconstructing three-dimensional density and atomic number (Z) maps of the inspected object. The system transports two interlaced electron energies at a frequency of up to approximately 300hz. A single-energy electron beam is transported if Z information is not required.

The electron beam transport system consists of a number of EBT stations, a transport section to direct the beam from the x-ray source to the EBT sections and components to maintain the electron trajectory. The EBT station contains one magnet to deflect the electron beam from the main trajectory, another magnet to direct the beam to the target and two quadrupoles to focus the beam to the desired focal-spot size. The electron source section has two magnets and slits to filter the low-energy tails. The beam is steered at suitable intervals to maintain the beam trajectory employing.

The High-Energy Electron-Beam Tomography system enables the generation of three-dimensional density and Z images for high-throughput inspection of large and dense objects, for improved detection of contraband and other items of interest.

Abstract 44 WED-ATF04-2

[Invited Talk - Wednesday 9:45 AM - Presidio A](#)

Nuclear detection & characterization with laser-plasma accelerator driven quasi-monoenergetic photon sources

[Cameron G.R. Geddes](#), [Nicholas H. Matlis](#), [Sven Steinke](#), [Min Chen](#), [Eric H. Esarey](#), [Kei Nakamura](#), [Sergey Rykovanov](#), [Carl B. Schroeder](#), [Csaba Toth](#), [Brian J. Quiter](#), [Maurice Garcia-Sciveres](#), [Bernhard Ludewigt](#), [Kai Vetter](#), [Wim P. Leemans](#)

Lawrence Berkeley National Laboratory, 1 Cyclotron Road MS 71-259, Berkeley CA 94720, United States

Near-monoenergetic photon sources at MeV energies offer improved sensitivity at greatly reduced dose for active interrogation, and new capabilities in treaty verification, NDA of spent nuclear fuel and emergency response. Compact high-energy electron linacs are a crucial component to enable compact or transportable photon sources. Laser-plasma accelerators (LPAs) produce GeV electron beams in centimeters, using the plasma wave driven by the radiation pressure of an intense laser. Recent LPA experiments have greatly improved beam quality and efficiency, rendering high quality photon sources based on Thomson scattering realistic. These advances will be reviewed, including control over the laser optical mode and plasma profile extended the acceleration distance producing electrons above 200 MeV from 10 TW. The beat between two colliding pulses was used to control injection into the high energy structure. This produced tunable bunches, with energy spreads below 1.5% FWHM and divergences of 1.5 mrad FWHM. Separate experiments recently demonstrated 0.1 mm-mrad emittance from self injected LPAs using betatron radiation and stable electron beams using

plasma gradient control. The combination of low energy spread and emittance with production of 200 MeV energies from 10 TW lasers, which are now transportable, is important to applications including MeV photon and other light sources, and to injectors for high energy LPAs for HEP. Designs for MeV photon sources utilizing the unique properties of LPA beams, and their applications to nuclear material interrogation and characterization, will be presented.

Abstract 97 WED-ATF04-3

[Invited Talk - Wednesday 9:45 AM - Presidio A](#)

A High Flux Neutron Generator for Explosives Detection

[Evan Sengbusch¹](#), [Ross Radel¹](#), [Logan Campbell¹](#), [Arne Kobernick¹](#), [Tye Gribb¹](#), [Casey Lamers¹](#),
[Chris Seyfert¹](#), [Jin Lee¹](#), [Eric Risley¹](#), [Carl Sherven¹](#), [Steven Roanhaus¹](#), [Greg Piefer²](#)

⁽¹⁾Phoenix Nuclear Labs, 2555 Industrial Drive, Monona WI 53713, United States

⁽²⁾SHINE Medical Technologies, 2555 Industrial Drive, Monona WI 53713, United States

Phoenix Nuclear Labs (PNL) has designed and built a high yield deuterium-deuterium (DD) neutron generator with measured yields greater than 3×10^{11} n/s. The neutron generator utilizes a proprietary gas target coupled with a custom 300kV accelerator and a microwave ion source (MWS). Two prototype neutron generators have been delivered - one to the US Army for neutron radiography and one to SHINE Medical Technologies for medical isotope production - and an order was recently signed for PNL's first commercial delivery, which will take place in late 2014. Experiences operating and optimizing the various subsystems (ion source, accelerator, focus element, differential pumping stages, and gas target) will be described. System performance will be characterized in terms of beam current and voltage, measured neutron yield, and operational reliability. A miniaturized, next-generation prototype for explosives detection is currently under construction via a contract with the US Army. Results from preliminary testing will be presented. Explosives detection speed and standoff distance will be characterized as a function of measured neutron yield in a laboratory setting. The analysis of multiple gamma signals will be explored with multiple different explosives and/or explosive simulants. Anticipated neutron yield from this miniaturized device is 1×10^{11} DD n/s. PNL has partnered with Oshkosh Corporation on multiple explosives detection proposals. The Oshkosh TerraMax Unmanned Ground Vehicle (UGV) is the ideal platform to house the PNL explosives detection system (i.e. adequate payload and available onboard power) for route clearance and convoy-leading IED detection operational scenarios. A description of proposed vehicle implementation plans and anticipated operational capabilities will be provided. Future planned upgrades to the PNL neutron generator will also be discussed in the context of explosives detection and other homeland security applications including the detection of special nuclear material (SNM).

Abstract 22 WED-ATF04-4

[Contributed Talk - Wednesday 9:45 AM - Presidio A](#)

Portable High Power X-ray Source Based on a 10 MeV Superconducting Linac

[Terry L Grimm¹](#), [Chase H Boulware¹](#), [Jerry L Hollister¹](#), [Erik S Maddock¹](#), [Valeriia N Starovoitova¹](#),
[Alan W Hunt²](#)

⁽¹⁾Niowave, Inc, 1012 N. Walnut St, Lansing MI 48906, United States

⁽²⁾Idaho Accelerator Center, Idaho State University, 1500 Alvin Ricken Dr, Pocatello ID 83201, United States

Cargo scanning using either radiographic imaging or active interrogation for Special Nuclear Material (SNM) requires high energy and high intensity x-rays. The most common source of such x-rays is an electron accelerator. Existing pulsed copper accelerators have low duty cycle beams and correspondingly low average current, which limit the quality of x-ray images and SNM detection sensitivity. Furthermore, inspection systems based on copper accelerators typically weigh several tons, have a large footprint, and consume hundreds of kilowatts of electric power. As a result, these machines require a large, fixed site to operate.

To overcome these limitations we are developing a compact, portable, high-efficiency 10 MeV superconducting electron linac. Equipped with a thin liquid metal bremsstrahlung converter, it generates a continuous, high-energy, high-intensity x-ray beam ideal for x-ray radiography or for initiating photonuclear reactions required for active interrogation. Using a superconducting linac as an x-ray source results in a compact and portable scanning system. Despite the high beam intensity, superconducting linacs produce very little electron scatter within the accelerating module, requiring only light shielding and resulting in low radiation doses in the area adjacent to the machine. High efficiency, solid-state radio frequency amplifiers and superconducting accelerating modules allow our linacs to be powered by a portable generator of less than 20 kW. By supplying cryogenic coolant (liquid nitrogen and helium) from insulated dewars, a fully functional, self-contained superconducting linac can be mounted on a small truck for rapid deployment.

In this talk we will present the results of the simulations of the photon fluxes and doses, conceptual design of the system, and the experimental results of the prototype testing.

Abstract 69 WED-ATF04-5

[Contributed Talk - Wednesday 9:45 AM - Presidio A](#)

Linatron Mi6, THE X-Ray Source for Cargo Inspection

[Gongyin Chen](#)¹, [John Turner](#)¹, [Kevin Holt](#)², [David Nisius](#)², [Alan Brooks](#)²

⁽¹⁾Varian Medical Systems, Imaging Components Businesses, 6811 Spencer St., Las Vegas NV 89119, United States

⁽²⁾Varian Medical Systems, Imaging Components Businesses, 425 Barclay Blvd, Lincolnshire IL 60069, United States

Abstract:

We last reported the status and trends in x-ray cargo inspection at CAARI 2008. The trends included improving imaging performance, a variety of platforms, material discrimination and expansion into security applications. Since Varian shipped its first Linatron Mi6 interlaced-pulse dual-energy x-ray source at the end of August 2008, the most important development in cargo inspection industry has been widespread adoption of this x-ray source. The adoption has enabled one-pass material discrimination and to some degree, material identification and automatic detection. A few hundred cargo inspection units powered by Linatron Mi6 have been installed worldwide. This number approximately represents the total unit count of advanced cargo inspection systems outside China.

The Linatron Mi6 produces interlaced pulses of 6MV and 3.5MV x-rays, providing single-pass material discrimination capability with traditional linear-array detectors. Mi6 was based on M6 components with innovation in system architecture. Dose output ranges from approximately 10Rad/min to 800rad/min to fit various cargo inspection platforms and application environments. Spectral filtration and use of energy sensitive detectors further improve material discrimination performance. Although our Linatron Mi9 Linatron, which produces interlaced pulses of 9MV and 6MV x-rays, provides even better material discrimination performance, it is not as widely used due to increased cost of safety shielding. Over the years, we have improved Linatron Mi6's short-term (pulse-to-pulse) stability and longer-term (in the time frame of a scan) stability.

Abstract 357 WED-HSD04-1

[Invited Talk - Wednesday 9:45 AM - Travis A/B](#)

Nuclear Forensic Analysis Overview

[Patrick M. Grant](#)

Forensic Science Center, Livermore National Laboratory, LLNL, MS L-091, Livermore CA 94550, United States

A condensed presentation on the modern practice of pre-detonation nuclear forensic analysis will be given. Following a depiction of the historic nature of nuclear smuggling, examples of both source and route evidentiary aspects of any given investigation will be discussed. The talk will be based on actual casework conducted at the Livermore National Lab Forensic Science Center.

Abstract 472 WED-HSD04-2

[Invited Talk - Wednesday 9:45 AM - Travis A/B](#)

Post-explosion exercises and accelerator-produced radionuclides

[Ken Moody](#)

Forensic Science Center, Lawrence Livermore National Laboratory, 7000 East Ave, mail stop L-236, Livermore CA 94551, United States

Forensic signatures are extracted from residual debris following a nuclear detonation through radiochemical analysis. Proficiency can be maintained through periodic exercises involving samples of mixed fission products produced in nuclear reactors. Addition of accelerator-produced radionuclides to these samples can result in a more stringent test of the methods of analysis of post-explosion debris.

Abstract 435 WED-HSD04-3

[Invited Talk - Wednesday 9:45 AM - Travis A/B](#)

Exploiting the 'Power and Precision of Lasers' for nuclear forensics

[Jean-Claude Diels, Ladan Arissian](#)

Center for High Technology Materials, University of New Mexico, 1313 Goddard SE, Albuquerque NM 87106, United States

In the five decades since its invention, the laser has developed as a source of extremely high power, and/or a tool of extreme precision. Both of these aspects promise to be useful for the detection of products or precursors of nuclear events.

Exploiting the nonlinear propagation properties of high power lasers as well as nonlinear interaction can result in remote and high resolution spectroscopy. The promises of remote sensing with IR and UV filaments will be discussed, including absorption/emission spectroscopy and Stimulated Backward Raman scattering.

Exploiting the ultimate precision offered by intracavity laser interferometry provides the possibility to discriminate between gamma-ray or neutron irradiation, through optical measurements. Our approach is to combine standard spectroscopic diagnostic (monitoring radiation-induced color centers) with ultra-sensitive real-time measurements of the index of refraction. Radiation damage from neutrons is dominated by atomic lattice displacements, while damage from gamma rays is dominated by electron displacements. In preliminary measurements, we have been able to demonstrate a neutron

irradiation induced change in index of refraction in a CaF₂ window, using properties of phase and group velocity coupling in a mode-locked laser cavity.

The method employed will be described and compared to the more sensitive Intracavity Phase Interferometry

that we intend to apply to create a compact instrument capable of monitoring and discerning in real time gamma ray and neutron emission.

Abstract 387 WED-HSD04-4

[Contributed Talk - Wednesday 9:45 AM - Travis A/B](#)

Silicon Drift Detectors for Specialized Accelerator and Synchrotron Applications

[Shaul Barkan](#), [Valeri D. Saveliev](#), [Liangyuan Feng](#), [Yen-Nai Wang](#)

Hitachi High-Technologies Science America, Inc., 19865 Nordhoff St., Northridge CA 91324, United States

High performance silicon drift detector (SDD), the Vortex®, has been successfully applied to accelerator and synchrotron applications. The Vortex® SDD offers a large solid angle, excellent energy resolution, and high count rate performance. Several unique 4-element systems have been developed and are currently being used in high count rate synchrotron applications worldwide. Long Standoff detection and PIXE applications can also benefit from the recent x-ray detector development. The energy resolution at low count rate with spectrometer peaking time of 6 μ s is 124eV.

We pursued several approaches to achieve improved performance:

1. A thicker device which enables the detector to be more efficient at higher energy. The current device's thickness is 0.5 mm with an efficiency of 0.37 at 20 keV and 0.12 at 30 keV. The 1 mm thick SDD efficiency matches the theoretical values of 0.6 and 0.4 for 20 keV and 30 keV, respectively.

2. A 4-element detector array is the current product at HHS-US. Several new designs are under consideration; one of them is an array of 7 elements for synchrotron applications or any other applications required large solid angle and high count rate performance.

3. We have improved the high count-rate performance of the Vortex® SDD by integrating it with state-of-the-art front-end electronics. Recent tests indicate excellent results, showing good promise in boosting the throughput at practical dead times (DT). An output count rate of ~1 Mcps was achieved at 2.3 Mcps input count rate (60% DT) with an energy resolution of less than 200 eV by using 0.1 μ s processor peaking time. The results were stable under different operating conditions.

We will present the energy resolution, counting throughput, peak-to-background and x-ray efficiency results from the 0.5 and 1 mm thick SDDs combined with the new ASIC preamplifier.

Abstract 27 WED-HSD04-5

[Contributed Talk - Wednesday 9:45 AM - Travis A/B](#)

Development of a Rapid Field Response Sensor for Characterizing Nuclear Detonation Debris

[Sudeep S Mitra](#)¹, [Oded Doron](#)¹, [Allan X Chen](#)², [Arlyn J Antolak](#)³

⁽¹⁾*Nuclear Forensics R&D, Sandia National Laboratories, P.O. Box 5800 MS 0968, Albuquerque NM 87185-0968, United States*

⁽²⁾*Adelphi Technology, Inc, Redwood City CA 94063, United States*

⁽³⁾*Radiation and Nuclear Detection Materials and Analysis, Sandia National Laboratories, 7011 East Avenue, MS9402, Livermore CA 94550, United States*

The radioactive decay of nuclear detonation (NUDET) debris samples makes rapid analysis methods highly desirable. Nuclear forensics will greatly benefit from field response techniques that will characterize the debris **in situ**. We present proof-of-principal studies to demonstrate the utility of employing low energy neutrons from a portable pulsed D-D neutron generator for non-destructive isotopic analysis of NUDET debris in the field. In particular, time-sequenced data acquisition, operating synchronously with the pulsing state of the neutron generator, partitions the characteristic elemental gamma-rays according to the type of the reaction; inelastic neutron scattering (INS) reactions during the pulse ON state and thermal neutron capture (TNC) reactions during the OFF state. In real world situations, it is challenging to isolate the INS and TNC gamma-rays from the prompt fission and β -delayed gamma-rays that are expected to be produced during the neutron interrogation. To resolve the temporal signatures, a commercial digital multi-channel analyzer is customized to concurrently acquire data into several multiple time resolved gamma-ray spectra from user-defined time intervals within each of the gate periods of the neutron generator. Results on the modeling and benchmarking of the concept are presented.

Sandia National Laboratories is a multi-program laboratory managed and operated by Sandia Corporation, a wholly owned subsidiary of Lockheed Martin Corporation, for the U.S. Department of Energy's National Nuclear Security Administration under contract DE-AC04-94AL85000.

Abstract 171 WED-HSD04-6

[Invited Talk - Wednesday 9:45 AM - Travis A/B](#)

Incorporating Environmental Lines of Evidence into Nuclear and Criminal Forensics

[Adam H Love](#)

Roux Associates Inc, 555 12th Street, Oakland CA 94607, United States

Nuclear and criminal forensics is always seeking the irrefutable "smoking gun", but often times a single, direct line of evidence does not sufficiently narrow attribution. In some cases, environmental features can contribute additional lines of evidence to further narrow attribution. Accelerator Mass Spectrometry has expanded the ability for environmental data to be collected from smaller samples and/or at higher spatial/temporal resolution. This presentation will discuss applications of accelerator mass spectrometry that can provide environmentally-based lines of evidence that can support source and timing attribution.

Abstract 174 WED-IBA01-1

[Invited Talk - Wednesday 9:45 AM - Presidio B](#)

Rutherford Backscattering Spectrometry: early activities, and future prospect

[Wei-Kan Chu](#)

About a century ago (1913), the first alpha particle scattering experiment was performed by Rutherford, and half a century later, the scattering experiment aided with energy loss information was advanced into a spectrometry (RBS) which is well applied in material and thin film characterization. In this talk, I will review some earlier RBS experiments and events leading toward the writing of a monograph coauthored by Chu, Mayer and Nicolet (Backscattering Spectrometry). I will also comment on the prospects of RBS application in the future.

Abstract 335 WED-IBA01-2

[Invited Talk - Wednesday 9:45 AM - Presidio B](#)

Rutherford backscattering analysis of irradiation-enhanced diffusion kinetics and interface formation of uranium bearing diffusion couples

[Michael S. Martin](#)¹, [Di Chen](#)¹, [Chaochen Wei](#)¹, [Bulent Sencer](#)², [J. R. Kennedy](#)², [Lin Shao](#)¹

⁽¹⁾*Nuclear Engineering, Texas A&M University, College Station TX 77843, United States*

⁽²⁾*Materials & Nuclear Fuel Performance, Idaho National Laboratory, Idaho Falls ID 83415, United States*

Understanding interactions of nuclear fuel and fuel cladding under extreme conditions is critical for optimizing reactor operation and design. In this study, the diffusion kinetics, irradiation-enhanced diffusion kinetics, and intermetallic phase formation at the interface of U/Fe, U/Fe-20Cr, and U/Fe-20Cr-20Ni diffusion couples are measured by RBS. Couples are made by magnetron sputtering of alloy films, and thermal annealing in vacuum at 450 and 550°C with and without concurrent Fe ion irradiation causes interdiffusion. Rutherford backscattering spectra are collected and simulated to obtain diffusion profiles. For all systems, we find Fe ion irradiation enhances U diffusion, and, in some cases, promotes intermetallic phase formation. This method can be used to complement existing diffusion couple studies because it is more sensitive to composition changes and the interface is never exposed to impurities. In this talk, we will also discuss traditional methods involving thermal annealing of mechanically bonded diffusion couples and post irradiation characterization, which show the complexity caused by interface roughness and poor surface contact.

Abstract 111 WED-IBA01-3

[Invited Talk - Wednesday 9:45 AM - Presidio B](#)

Temporal dependence of electron transmission through funnel shaped micro-sized glass capillaries

[S J Wickramarachchi](#)¹, [T Ikeda](#)², [D Keerthisinghe](#)¹, [B S Dassanayake](#)³, [J A Tanis](#)¹

⁽¹⁾*Department of Physics, Western Michigan University, 1903, Kalamazoo MI 49008, United States*

⁽²⁾*RIKEN, Nishina Center for Accelerator Based Science, 2-1 Hirosawa Saitama 351-0188, Japan*

⁽³⁾*Department of Physics, Faculty of Science, University of Peradeniya, Peradeniya, Sri Lanka*

Studying the beam transmission through single glass capillaries (straight, conical and funnel-shaped) offers the possibility of producing micro-beams, which is useful in various biological and technical applications [i]. In the present work, the temporal dynamics of electron transmission through a funnel-shaped borosilicate glass capillary have been studied for 500 and 1000 eV incident electrons for several tilt angles with respect to the incident beam direction. These measurements were done at Western Michigan University. The capillary had inlet/outlet diameters of 800 µm/100 µm and a length of 35 mm. For each angle investigated at 1000 eV the deposited charge was in the range 0 - 800 nC for the incident currents of 21 - 35 pA, except for 5° for which the measurements extended to 7000 nC. Measurements were obtained for the **direct** region near zero degree tilt angle where there are no collisions with the capillary walls, and for the **indirect** region for larger tilt angles where electrons are deflected by the deposited charge or they collide with the capillary walls. The transmission showed slow charging with some oscillations in intensity in both regions for 500 eV. For 1000 eV in the direct region the transmission showed erratic fluctuations, while indirect transmission showed some fluctuations with rapid self-discharging

but the transmission slowly increased with deposited charge. Total blocking was observed at the tilt angle of 5° when the incident charge was higher than ~6500 nC for an incident current of 210 pA into the capillary.

[i] T. Ikeda, T. M. Kojima, T. Kobayashi, W. Meissl, V. Mäkel, Y. Kanai and Y. Yamazaki, J. Phys. Conf. Ser. **399**, 012007 (2012)

Abstract 293 WED-IBA01-4

[Contributed Talk - Wednesday 9:45 AM - Presidio B](#)

Sputtering of a liquid Bi:Ga alloy with keV Ar ions

[Naresh T Deoli](#), [Duncan L Weathers](#)

Ion Beam Modification and Analysis Laboratory, Department of Physics, University of North Texas, 1155 Union Circle # 311427, Denton TX 76203, United States

The differential angular sputtering yield and partial sputtering yields due to Ar⁺ ion bombardment of an inhomogeneous liquid Bi:Ga alloy have been investigated, both experimentally and by computer simulation. Normally incident 25 keV and 50 keV beams of Ar⁺ were used to sputter a target of 99.5 at% Ga and 0.5 at% Bi held at 40° C in ultra-high vacuum (UHV), under which conditions the alloy is known to exhibit extreme Gibbsian surface segregation. The sputtered atoms were collected on high purity aluminium foils, which after sputtering were removed to another chamber for analysis using Rutherford backscattering spectrometry. Angular distributions of sputtered neutrals and sputtering yield obtained from the conversion of areal densities of Bi and Ga atoms on collector foils are presented. The Monte-Carlo based SRIM code was employed to simulate the experiment and obtain the angular distribution of sputtered components. Effects of target surface segregation on the sputtering yields are discussed.

Abstract 157 WED-IBM05-1

[Invited Talk - Wednesday 9:45 AM - Bonham C](#)

Silicon and Germanium Nanopatterning and Relaxation Processes during Ion Bombardment

[Karl F Ludwig, Jr.](#)¹, [Eitan Anzenberg](#)², [John Snyder](#)², [Joy Perkinson](#)³, [Michael J. Aziz](#)³, [Scott Norris](#)⁴

⁽¹⁾*Physics and Materials Science & Engineering, Boston University, 590 Commonwealth Ave., Boston MA 02215, United States*

⁽²⁾*Physics, Boston University, 590 Commonwealth Ave., Boston MA 02215, United States*

⁽³⁾*School of Engineering and Applied Sciences, Harvard University, Cambridge MA 02138, United States*

⁽⁴⁾*Mathematics, Southern Methodist University, Dallas TX 75275, United States*

Understanding the fundamental processes determining the surface evolution of materials undergoing ion bombardment is of significant interest both because energetic ion/atom interactions with surfaces are ubiquitous and because ion beam nanopatterning might be useful for inexpensive structuring of surfaces. However, even for the case of elemental semiconductors, the processes driving surface stability/instability during ion bombardment and the exact nature of the ion-enhanced viscous relaxation on the amorphized surfaces remain poorly understood. We examine real-time grazing-incidence small-angle x-ray scattering and wafer-curvature stress measurements within the context of competing recent theories predicting surface evolution driven by the geometry of craters formed by individual ion impacts and by viscous flow due to stress.

Abstract 390 WED-IBM05-2

[Invited Talk - Wednesday 9:45 AM - Bonham C](#)

Ion-Slicing of Ultrathin Layers from III-Nitride Bulk Wafers

The ability to tailor compound semiconductors and to integrate them onto foreign substrates create wealth of opportunities to enable superior or novel functionalities with a potential impact on various areas in electronics, optoelectronics, spintronics, biosensing, and photovoltaics. In this perspective, this presentation provides a brief description of different approaches to achieve this heterogeneous integration, with an emphasis on the ion-cut process. This process combines semiconductor wafer bonding and undercutting using defect engineering by light ion implantation. Bulk-quality heterostructures frequently unattainable by direct epitaxial growth can be produced, provided that a list of technical challenges is solved, thus offering an additional degree of freedom in the design and fabrication of heterogeneous and flexible devices. Ion cutting is a generic process that can be employed to split and transfer fine monocrystalline layers from various crystals. Materials and engineering issues as well as our current understanding of the underlying physics involved in its application to slice ultrathin layers from freestanding GaN wafer will be presented and discussed.

Abstract 29 WED-IBM05-3

[Invited Talk - Wednesday 9:45 AM - Bonham C](#)

Focused Ion Beam nano-patterning and single ion implantation perspectives

[Jacques Gierak](#)¹, [Eric Bourhis](#)¹, [Adrien Hemamouche](#)¹, [Ali Madouri](#)¹, [Gilles Patriarche](#)¹, [Fabien Montel](#)², [Loïc Auvray](#)²

⁽¹⁾*Laboratoire de Photonique et de Nanostructures-CNRS, Route de Nozay, Marcoussis F-91460, France*

⁽²⁾*Matière et Systèmes Complexes, UMR 7057, Paris Diderot University, Paris F-75205, France*

In this presentation we will review some fundamentals of the Focused Ion Beam (FIB) technique based on scanning finely focused beams of gallium ions having energies in the range 30 to 50 keV over a sample to perform direct writing [1]. It is widely accepted that the spatial extension of the phenomena induced by FIB irradiation represents a severe drawback, limiting the use of this method for the realization of highly localized structures. At the light of advanced analysis techniques we will review the limitations of Gallium FIB for the patterning of III-V heterostructures, thin magnetic layers, artificial defects fabricated onto graphite or graphene and atomically thin suspended membranes.

We will summarize our analysis of the main limitations of the FIB technique in terms of damage generation or local contamination and through selected examples we discuss the ultimate potential of this technique with respect to spatial resolution and ion doses already opening single ion implantation perspectives [2].

We will conclude in presenting the instrumental routes we are exploring aiming at turning FIB processing "limitations" into decisive advantages. Such new routes for the fabrication of devices or surface functionalities are urgently required in some emerging nanosciences applications and their developing markets.

[2] C. T. Nguyen, A. Balocchi, D. Lagarde, T. T. Zhang, H. Carrère, S. Mazzucato, P. Barate, E. Galopin, J. Gierak, E. Bourhis, J. C. Harmand, T. Amand, and X. Marie, Appl. Phys. Lett. 103, 052403 (2013), "Fabrication of an InGaAs spin filter by implantation of paramagnetic centers", Appl. Phys. Lett. 103, 052403 (2013)

Abstract 37 WED-IBM05-4

[Invited Talk - Wednesday 9:45 AM - Bonham C](#)

In-situ morphology and surface chemistry studies during nanopatterning of III-V semiconductors via low energy ion beams

[Osman El-Atwani](#)^{1,2,3}, [Scott Norris](#)⁴, [Sean Gonderman](#)², [Alexander DeMasi](#)⁵, [Karl Ludwig](#)⁵, [Jean Paul Allain](#)^{1,2}

⁽¹⁾Materials Engineering, Purdue University, West Lafayette IN 47907, United States

⁽²⁾Nuclear Engineering, Purdue University, West Lafayette IN 47907, United States

⁽³⁾Birck Nanotechnology Center, Purdue University, West Lafayette IN 47907, United States

⁽⁴⁾Department of Mathematics, Southern Methodist University, Dallas TX 75275, United States

⁽⁵⁾Physics Department, Boston University, Boston MA 02215, United States

It is well known that ion beam irradiation of semiconductor surfaces can lead to nanostructure formation of several sizes and shapes [Ziberi, APL 2008]. However, as future device feature size approaches sub 10-nm scales, working at low energies and understanding the mechanism of nanostructure formation for compound materials (e.g. III-V materials) has become very important. In this talk, we will address crucial experimental work performed on various semiconductor surfaces (III-V semiconductors and silicon) for the purpose of controlling the nanopatterning parameters and understanding the nanostructure formation mechanism. In the case of III-V semiconductors, we will focus on the importance of **in-situ** conditions during the characterization of III-V semiconductors to decipher nanopatterning mechanisms, and illustrate the output of crucial **in-situ** surface characterization (XPS, LEISS) experiments and real time GISAXS studies during nanopatterning of different III-V semiconductor surfaces (GaSb, GaAs, GaP) via low energy Ne, Ar, Kr and Xe irradiation. The results will be correlated with energy deposition simulation results and compared with existing approaches such as Bradley-Shipman, Sondergard's and Norris's theories.

Abstract 355 WED-IBM05-5

[Contributed Talk - Wednesday 9:45 AM - Bonham C](#)

Ion beam and cluster ion beam engineered nano-metallic substrates for SPR based sensors

[Iram Saleem](#), [Yanzhi He](#), [Buddhi Tilakaratne](#), [Epie Njumbe](#), [Dharshana Wijesundera](#), [Wei Kan Chu](#)

Department of Physics, Ion beam processing laboratory, Texas Center for Superconductivity at University of Houston, 4800 Calhoun Road, Houston Texas 77004, United States

Surface plasmon resonance (SPR) based bio sensors have a high sensitivity and exploit a label free real time analytical detection mechanism. We have fabricated plasmonic nano-structured substrates by, ion implantation of gold and silver ions on glass and cluster ion beam irradiation of thin gold films and have studied their effectiveness as potential plasmonic sensors. By adsorbing a mono-layer of thiolated organic compounds on the surface of these substrates we identify the shift in the SPR peaks triggered by the change of dielectric function in the neighborhood of the structures. We further observe the change of SPR resonance frequency due to adsorption, re-adsorption and reactions taking place on the nano structures that can potentially be mapped to reaction mechanics.

Abstract 420 WED-NBA02-1

[Contributed Talk - Wednesday 9:45 AM - Bonham B](#)

Material Classification by Analysis of Prompt Photon Spectra Induced by 14-MeV Neutrons

Neutron based methods are widely used in the field of bulk material analysis. These methods employ characteristic prompt gamma rays induced by a neutron probe for classification of the interrogated object using the elemental parameters extracted from the spectral data. Automatic data analysis and the material's classification algorithms are required for applications where access to nuclear spectroscopy expertise is limited and/or the autonomous robotic operation is necessary. Data obtained with neutron based systems differ from elemental composition evaluations based on chemical formulae due to statistical nature of nuclear reactions, presence of shielding and cladding, and other environmental conditions. Experimental data that are produced by the spectral decomposition can be expressed graphically as sets of overlapping classes in multidimensional space of measured elemental intensities. The dimension of this space is determined by the number of isotopes. The chemical compound measured in various conditions is represented not by a single point in the space, but rather by a cloud-looking set of points (classes), where each point corresponds to the single measurement. To discriminate between classes of various materials, classical decision-tree and pattern recognition algorithms were compared. Results of application of these methods to data sets obtained in measurements with a pulse 14-MeV neutron generator based active interrogation system are discussed.

Abstract 368 WED-NBA02-2

[Contributed Talk - Wednesday 9:45 AM - Bonham B](#)

Neutron Generators for Nuclear Recoil Calibration of Liquid Noble Gas TPCs

[Sean MacMullin](#)

Physics, Purdue University, 525 Northwestern Ave., West Lafayette IN 47907, United States

Liquid noble gas TPCs are among the most promising detectors for direct dark matter searches. As these detectors become large compared to the neutron mean free path, neutrons from a DD or DT generator can be used to perform an in situ nuclear recoil energy calibration using double scatters. Given a position reconstruction of the two scatter vertices, the response of the detector at the first scatter can then be compared to the known nuclear recoil energy implied by the scatter geometry. Although many neutron generators can be run at fluxes above 10^5 neutrons/second, some commercial generators can be specifically modified to allow stable operation at less than 10 neutrons/second, allowing for calibration in a mode with similar rate conditions as during dark matter searches. Details on the method of nuclear recoil calibration in liquid noble gas TPCs with a neutron generator will be presented. The characterization of a low-flux neutron generator will also be discussed.

Abstract 183 WED-NBA02-3

[Contributed Talk - Wednesday 9:45 AM - Bonham B](#)

Recent Fast Neutron Imaging Measurements and Simulations with the Fieldable Nuclear Materials Identification System

[Blake A. Palles](#)¹, [Tracey A. Wellington](#)², [James A. Mullens](#)³, [John T. Mihalcz](#)³, [Dan E. Archer](#)³, [Thad Thompson](#)⁴, [Chuck L. Britton](#)³, [Dianne B. Ezell](#)³, [Nance Ericson](#)³, [Ethan Farquhar](#)³, [Randall Lind](#)³

⁽¹⁾*Department of Nuclear Engineering, University of Tennessee, 207 Pasqua Engineering, Knoxville TN 37996, United States*

⁽²⁾*Bredesen Center for Interdisciplinary Research and Education, University of Tennessee, 443 Greve Hall, Knoxville TN 37996, United States*

⁽³⁾*Oak Ridge National Laboratory, P.O Box 2008 MS 6010, Oak Ridge TN 37831, United States*

⁽⁴⁾*Cadre5, LLC, P.O Box 32566, Knoxville TN 37930, United States*

This paper describes some recent measurements and simulations of the fieldable nuclear materials identification system (FNMIS) under development by the National Nuclear Security Administration (NNSA) for possible future use in arms control and nonproliferation applications. The general configuration of FNMIS has been previously described (INMM 2010

Annual Meeting), and a description of the application-specific integrated circuit (ASIC) electronics designed for FNMIS has been reported (IEEE 2012 Nuclear Science Symposium). This paper presents a comparison of imaging measurements performed at ORNL with a Thermo Fisher API 120 DT generator and the fast-neutron imaging module of FNMIS with Monte Carlo simulations. Simulations using two different associated particle imaging DT generators are also compared; one is the API-120 DT generator with a row of 16 alpha detector pixels (YAP scintillation detector, fiber-optic face plate, and position-sensitive Hamamatsu photomultiplier tube), and the other is a modified ING-27 with a row of 15 semiconductor alpha detector pixels.

Abstract 179 WED-NBA02-4

[Contributed Talk - Wednesday 9:45 AM - Bonham B](#)

A Method to Measure Elemental Gamma-Ray Production Cross Sections Using a 14.1 MeV Associated Particle Neutron Generator.

[David Koltick](#), [Haoyu Wang](#)

Department of Physics and Astronomy, Purdue University, 525 Northwestern Ave., West Lafayette Indiana 47907, United States

Knowledge of gamma-ray production rates is important in many elemental analysis applications using active neutron interrogation techniques. However, past measurements are limited to a single fixed angle having small solid angle coverage. The production is then extrapolated to the full solid angle assuming a uniform angular distribution. Even so past measurements are dominated by high backgrounds and overlapping gamma-ray signals having nearby energy. Reported cross sections can vary by a factor of ~4. In order to improve our knowledge of elemental cross sections, we have constructed a spectrometer using an associated particle neutron generator and an array of 12 NaI detectors each 14 cm square by 16.5 cm deep. The array covers ~30% of the solid angle, extending to within ~35 degrees of the entering and exiting electronically collimated neutron beam, on a circular shell ~21 cm in radius from the target. The major improvements in these measurements come from the 3.0 nanosecond coincident timing required between the prompt gamma-ray detection and the associated alpha particle produced simultaneously with the neutron, and the electronically restricted neutron aperture generated by the required alpha particle detection. The timing requirement greatly reduces the detectors exposure to background. To illustrate the improvements using this technique we present first measurements of the 846.8 keV and the 1238.3 keV prompt gamma-ray cross sections from Fe-56.

Abstract 175 WED-NBA02-5

[Contributed Talk - Wednesday 9:45 AM - Bonham B](#)

Application of D-D based Neutron Generator System to Quantify Manganese in Bone In Vivo

[Linda H Nie](#)¹, [Yingzi Liu](#)¹, [David Koltick](#)², [Wei Zheng](#)¹

⁽¹⁾*School of Health Sciences, Purdue University, 550 Stadium Mall Dr., West Lafayette IN 47907, United States*

⁽²⁾*Physics Department, Purdue University, 525 Northwestern Avenue, West Lafayette IN 47907, United States*

A Deuterium-Deuterium (DD) neutron generator with flux up to 3×10^9 neutrons/sec was set up in our lab for the application in human body composition. One of the applications is to quantify Mn in bone **in vivo**. Overexposure to manganese (Mn) leads to various neurological disorders including "manganism". The progressive and irreversible characteristics of chronic Mn neurotoxicity make early diagnosis of body Mn burden an urgent issue. Data in literature have suggested that the amount of Mn in bone (MnBn) accounts for ~40% of total body burden and the half-life of Mn in bone is much longer than that in other organs. We have been developing and validating the D-D based neutron activation analysis (NAA) system to quantify metals, including Mn, in bone **in vivo**. Thermal neutrons have a high cross section to interact with ⁵⁵Mn and result in ⁵⁶Mn which emits characteristic g-ray of 847 keV. By measuring the 847 keV γ -rays from the irradiated bone, MnBn concentration can be calculated. Optimized settings including moderator, reflector, shielding and their thicknesses were selected based on MCNP5 simulations. Hand phantoms with different Mn concentrations were irradiated using the optimized DD neutron generator irradiation system. The Mn characteristic γ -rays were collected by an HPGe detector system with 100% relative efficiency. Calibration line of MnBn concentration versus Mn/calcium (Ca) count ratio was obtained ($R^2 = 0.98$) using hand phantoms doped with different Mn concentrations. The detection limit (DL) was calculated to be about 0.85 ppm with an equivalent dose of 50 mSv to the hand. The DL can be reduced to 0.6 ppm with two 100%

HPGe detectors. The whole body effective dose delivered to the irradiated subject was calculated to be about 31 μ Sv. Given the average normal MnBn concentration of 1 ppm in general population, this system is promising in MnBn quantification in humans.

Abstract 185 WED-NBA02-6

[Contributed Talk - Wednesday 9:45 AM - Bonham B](#)

Sensitivity of Associated Particle Neutron Elemental Imaging for Cancer Diagnoses

[David Koltick](#), [Haoyu Wang](#)

Department of Physics and Astronomy, Purdue University, 525 Northwestern Ave., West Lafayette Indiana 47907, United States

Associated particle neutron elemental imaging (APNEI) for in vivo and in vitro diagnostic analysis is a potential technology to measure elemental disease signatures. APNEI can produce elemental projective images with spatial resolution as small as ~ 3 mm. The use of APNEI technology for disease diagnoses is based on measured concentrations of many signature elements having large differences between normal and cancerous tissues ranging as large as 50% to more than 1000%. The parameters affecting the image spatial resolution are discussed and measured data supporting performance limits are presented. These included: (1) the D-T beam spot size, (2) effects of the associated α -particle transducer floor, (3) geometry of the α -particle transducer, (4) electronics effects of the α -particle transducer and gamma ray detector, (5) gamma ray detector geometry. The relationship between achievable spatial resolution and elemental sensitivity for iron to total expected patient dose is presented. The expected depth resolution is 10 cm. The expected elemental concentration sensitivity to iron will be presented and compared with the difference between cancerous prostate tissue and normal tissue.

Abstract 380 WED-NP07-1

[Invited Talk - Wednesday 9:45 AM - Travis C/D](#)

On the use of Aluminum Nitride to Improve Aluminum-26 Accelerator Mass Spectrometry Measurements for Earth Science Applications

[Meghan S. Janzen](#)^{1,2,3}, [Alfredo Galindo-Uribarri](#)^{1,2,3}, [Yingkui Li](#)⁴, [Yuan Liu](#)², [Ed Perfect](#)¹

⁽¹⁾*Department of Earth and Planetary Sciences, University of Tennessee, 1412 Circle Dr, Knoxville TN 37996, United States*

⁽²⁾*Physics Division, Oak Ridge National Laboratory, 1 Bethel Valley Rd, Oak Ridge TN 37831, United States*

⁽³⁾*Department of Physics and Astronomy, University of Tennessee, 401 Nielsen Physics Building, Knoxville TN 37996, United States*

⁽⁴⁾*Department Of Geography, University of Tennessee, 304 Burchfiel Geography Building, Knoxville TN 37996, United States*

We present results and discuss the use of AlN as an optimal source material for AMS measurements of cosmogenic aluminum (^{26}Al) isotopes. The measurement of ^{26}Al in geological samples by accelerator mass spectrometry is typically conducted on Al_2O_3 targets. However, Al_2O_3 is not an ideal source material because it does not form a prolific beam of Al^+ required for measuring low-levels of ^{26}Al . Multiple samples of aluminum oxide (Al_2O_3), aluminum nitride (AlN), mixed Al_2O_3 -AlN as well as aluminum fluoride (AlF_3) were tested and compared using the test stand and the stable ion beam (SIB) injector platform at the 25MV tandem electrostatic accelerator at Oak Ridge National Laboratory. Negative ion currents of atomic and molecular aluminum were examined for each source material. It was found that pure AlN target produced substantially higher beam currents than the other materials and that there was some dependence on the exposure of AlN to air. The applicability of using AlN as a source material for geological samples was explored by preparing quartz samples as Al_2O_3 and converting them to AlN using a carbo-thermal reduction technique, which involves reducing the Al_2O_3 with graphite powder at 1600 $^\circ\text{C}$ within a nitrogen atmosphere. The quartz material was successfully converted to AlN. Thus far, AlN proves to be a promising source material and could lead towards increasing the sensitivity of low-level ^{26}Al AMS measurements.

Research sponsored by the Office of Nuclear Physics, U.S. Department of Energy.

Monochromatic fast (MeV) neutron "beam" characterization and its use to study elastic scattering in heavy nuclei.

[Efraín Chávez](#)¹, [Eduardo Andrade](#)¹, [Oscar de Lucio](#)¹, [Arcadio Huerta](#)¹, [Rafael Policroniades](#)²,
[Ghiraldo Murillo](#)², [Miguel Rocha](#)³, [Francisco Favela](#)¹, [Edgar Adán Jiménez](#)¹, [Eliud Moreno](#)²,
[Armando Varela](#)⁴

⁽¹⁾*Instituto de Física, Universidad Nacional Autónoma de México, Av. Universidad 3000, Ciudad Universitaria S/N, Coyoacán D. F. 04510, Mexico*

⁽²⁾*Departamento de Aceleradores, Instituto Nacional de Investigaciones Nucleares, Carretera México Toluca S/N, Ocoyoacac México 52750, Mexico*

⁽³⁾*Escuela Superior de Ingeniería Mecánica y Eléctrica, Instituto Politécnico Nacional, Av. Luis Enrique Erro S/N, Zacatenco, Gustavo A. Madero D. F. 07738, Mexico*

⁽⁴⁾*Centro de Ciencias de la Atmósfera, Universidad Nacional Autónoma de México, Av. Universidad 3000, Ciudad Universitaria S/N, Coyoacán D. F. 04510, Mexico*

Monochromatic fast (MeV) neutron beams are produced at the 5.5 MV CN-Van de Graaff accelerator facility of the IFUNAM ("Instituto de Física, Universidad Nacional Autónoma de México) through the d(d,n)3He nuclear reaction. Each neutron is tagged by the associated 3He, so the unambiguously 3He detection and identification is mandatory. The location and size of the 3He detector inside the reaction chamber defines the direction and shape of the tagged neutron flux (beam).

The use of this tagged monochromatic fast neutron flux in fundamental nuclear physics is described, specifically in relation to the importance of neutron elastic scattering on heavy zero spin nuclei at very low angles.

Development of a Positron Generator for Material Science at CEMHTI

[Jean-Michel Rey](#)^{1,3}, [Marie-France Barthe](#)², [Pascal Debu](#)¹, [Pierre Desgardin](#)², [Patrick Echegut](#)², [Laszlo Liskay](#)¹, [Patrice Perez](#)¹, [Yves sacquin](#)¹, [Serge Visière](#)³

⁽¹⁾*IRFU, CEA, CE Saclay, , Gif sur Yvette 91191, France*

⁽²⁾*CEMHTI, CNRS, 1D av de la Recherche scientifique, Orléans 45071, France*

⁽³⁾*POSITHÔT, 1 le Moulin de Fouchault, Valleres 37190, France*

Positron beams are getting increasing interest for materials science and for fundamental research. Recent progress on positron production using a compact electron accelerator made at CEA-IRFU for the Gbar experiment is providing new prospect for material analysis and non-destructive testing technology using positrons. CNRS-CEMHTI is defining a long term strategy to boost its positron laboratory using an upgraded version of the CEA positron generator manufactured by the POSITHÔT company. This new generator is designed to produce between 2 and 3 x 10⁷ slow positrons per second to feed in parallel several experiments. It will be presented here as well as the future beam developments.

Utilization of a RIB facility for R&D related to radioisotope production

[Daniel W Stracener](#), [B Alan Tatum](#)

The Holifield Radioactive Ion Beam Facility (HRIBF) at Oak Ridge National Laboratory was developed to produce high-quality radioactive ion beams for nuclear physics research. The facility used the Isotope Separation On-Line (ISOL) technique to produce high quality beams of short-lived isotopes for post-acceleration up to a few MeV per nucleon. The beam production systems were designed to maximize the beam quality in terms of intensity and purity. This included production targets with fast release properties, ion sources with high ionization efficiency and/or selectivity, molecular ion extraction, high-resolution electromagnetic mass separators, and using the characteristics of the post-accelerator to minimize or eliminate unwanted beam contaminants. Since the most interesting beams at an ISOL facility are often at the extremes where the production rates are low, a suite of specialized detectors were developed, having high detection efficiency and excellent signal-to-noise discrimination.

HRIBF is no longer an operating RIB facility, but its unique and specialized equipment can be used with great advantage for R&D efforts related to the production of radioisotopes for use in medicine, industry, and research. In particular, the energy range of the light-ion beams from the tandem accelerator is well-suited to many radioisotope production reactions and the mass separators can be used to separate radioisotopes from target material in reactor-produced samples. This talk will describe the types of measurements that can be made using HRIBF systems (e.g., cross-section measurements and nuclear decay properties) along with specific examples of current and past R&D projects. Examples include measurement of the production cross-section of Th-229 at low proton energies, determination of the absolute branching ratio of the 776.5 keV gamma-ray in the decay of Rb-82, and the use of the mass separator to prepare samples with high specific activity.

*Research sponsored by the Office of Nuclear Physics, U.S. Department of Energy.

Abstract 299 WED-NST09-1

[Invited Talk - Wednesday 9:45 AM - Bonham D](#)

Current Progress and Future Prospects of Cluster Ion Beam Process Technology

[Jiro matsuo](#)

Quantum Science and Engineering Center, Kyoto University, Gokasho, Uji Kyoto 611-0011, Japan

A method for generating high-intensity cluster with an average size of 1000 atoms/cluster has been developed at Kyoto University. Since then, the cluster beam process has been developed for advanced nanofabrication and characterization technique. When many atoms constituting a cluster bombard a local area, high-density collision, non-linear effects and lateral sputtering are realized [1]. As each atom in a cluster shares the total kinetic energy, an ultra-low energy ion beam with less than several eV/atom can be easily realized.

One of the emerging applications of cluster ion beams is surface analysis techniques for organic materials [2]. Due the low energy effect, no serious damage is accumulated on organic surfaces during irradiation of large cluster ion beams. Both XPS and SIMS instruments equipped with compact cluster ion gun are commercially available. Fine focused cluster ion beam around 1 μm has been developed for imaging mass of cells and tissues.

Very high speed etching (etching rates above 40 $\mu\text{m}/\text{min.}$) and highly anisotropic etching of Si are demonstrated with non-ionized cluster beam generated with reactive gas molecule ClF_3 [3]. Although the kinetic energy of the non-ionized cluster beam is extremely low (<1 eV/atom), the chemical reaction is dramatically enhanced during the collision of cluster. This result opens up new possibly of cluster ion beam process.

Current developments and possible applications of cluster beam technique will be discussed.

This work was partially supported by JST, CREST.

1 I. Yamada, J. Matsuo, N. Toyoda and A. Kirkpatrick, Mat. Sci.&Eng. R34(2001) 231

2 S. Ninomiya, K. Ichiki, H. Yamada, Y. Nakata, T. Seki, T. Aoki and J. Matsuo, Rapid. Commun. Mass Spectrom. 23, 1601 (2009)

3 K. Koike, Y. Yoshino, T. Senoo, T. Seki, S. Ninomiya, T. Aoki and J. Matsuo, Appl. Phys. Express 3, 126501 (2010)

Abstract 60 WED-NST09-2

[Invited Talk - Wednesday 9:45 AM - Bonham D](#)

Advancement of gas cluster ion beam processes for chemically enhanced surface modification and etching

[Noriaki Toyoda](#)

Graduate school of engineering, University of Hyogo, 2167 Shosha, Himeji Hyogo 671-2280, Japan

Gas cluster ion beams show various unique irradiation effects such as surface smoothing, surface analysis, shallow implantation, surface smoothing, and thin film formations. Upon GCIB impact, dense energy is deposited on surface layer while energy/atom of GCIB is low. It is the origin of low-damage sputtering and high yield sputtering or secondary ion emissions.

One of the unique characteristics of GCIB is the enhancement of chemical reactions without heating the substrates. When reactive GCIBs are used, high-rate etching of various materials is expected. Not only reactions between molecules in the cluster and target atoms, but also chemical reactions between target atoms and the adsorbed gas on target are enhanced.

In this paper, advancement of GCIB process by chemically enhanced surface modification and etching will be reviewed. By utilizing unique surface reactions with GCIB, reactive etchings of various materials are reported.

Abstract 265 WED-NST09-3

[Invited Talk - Wednesday 9:45 AM - Bonham D](#)

Study of multiple collision effects in cluster impact by molecular dynamics simulations

[Takaaki Aoki](#)

Dept. of Electronics Science and Engineering, Grad. School of Engineering, Kyoto University, Nishikyo, Kyoto 6158510, Japan

The multiple collision effect is unique property of cluster ion beam process, which does not occur with conventional monomer ion beam. In this presentation, the mechanism of multiple collisions is discussed based on the results from

various MD simulations. The MD simulation and fundamental experiments of cluster impact suggests several parameters to characterize multiple collisions, such as cluster size and incident energy per atom. For the impact of small and swift cluster impact, the penetration depth is almost the same as that for the monomer ion. This is because that the interaction among cluster atoms is negligible and each projectile atom penetrates into the target in a manner similar to the individual monomer ions. However, cluster impacts generate a large number of secondary and tertiary knocked-on atoms in a narrow region simultaneously, which results in dense damaged tracks around the impact point. As the cluster sizes increases and the incident energy per atom decreases, collisions inside the cluster become significant. The cluster penetrates the target surface and stays intact, while the target atoms are compressed and are pushed away to fill vacant space through the multiple collisions, which leads to crater formation on a flat target surface, or smoothing for non-planar surfaces. As for the much slower and larger cluster impact, there arises an interesting threshold in energy-per-atom, where a cluster atom cannot penetrate the target surface even with the help of the multiple collision effect. From the viewpoint of physical interaction, this collisional process causes no damage. However, the incident cluster deposits some high-density particles and kinetic energy on the target, which contributes to the enhancement of chemical interactions, such as decomposition, adsorption, and desorption of reaction products.

Abstract 277 WED-NST09-4

[Contributed Talk - Wednesday 9:45 AM - Bonham D](#)

Gas Cluster Ion Beam Induced Nanostructures on Metal and Alloy Surfaces

[Buddhi Prasanga Tilakaratne](#), [Wei-Kan Chu](#)

Department of Physics and Texas Center for Superconductivity, University of Houston, 4800 Calhoun Rd, Houston TX 77204, United States

The development of hassle free nano fabrication techniques has become an interesting topic in optical and biological research. Current nano fabrication techniques require complicated lithographic procedures. We utilize Gas Cluster Ion Beam (GCIB) to process surface nanostructures on metal, semiconductor surfaces. A GCIB consists clusters of the size of 3000 argon atoms on average bonded by van der Waal's forces. When GCIB bombard a surface of a substrate at an oblique angle surface atoms undergo different dynamical processes, surface erosion, cluster ion induced effective surface diffusion, isotropic thermal diffusion, and localized sputtering. These dynamical processes vary depending on the substrate temperature. We investigated the temperature dependence of nanostructure formation on gold and silver metal and gold silver alloy surfaces. In this talk, an overview of GCIB induced nanostructure formation on these material surfaces will be presented.

Abstract 163 WED-RE06-1

[Invited Talk - Wednesday 9:45 AM - Presidio C](#)

Multi-scale simulation of structural heterogeneity of swift-heavy ion tracks in complex oxides

[Jianwei Wang](#)¹, [Maik K Lang](#)², [Rodney C Ewing](#)³

⁽¹⁾*Department of Geology and Geophysics, Louisiana State University, E235 Howe-Russell, Baton Rouge LA 70803, United States*

⁽²⁾*Nuclear Engineering Department, The University of Tennessee, 315 Pasqua Nuclear Engineering, Knoxville Tennessee 37996, United States*

⁽³⁾*Geological and Environmental Sciences, Stanford University, Encina Hall, E211, Stanford CA 94305, United States*

Tracks formed by a swift-heavy ion irradiation, 2.2 GeV Au, of isometric Gd₂Ti₂O₇ pyrochlore and orthorhombic Gd₂TiO₅ were modeled using thermal-spike model combined with a molecular-dynamics simulation. The thermal-spike model was used to calculate the energy dissipation over time and space. Using the time, space, and energy profile generated from the thermal-spike model, the molecular-dynamics simulations were performed to model the atomic-scale evolution of the tracks. The advantage of combining these two methods, which is using the output from the continuum model as an input for the atomistic model, is that it provides a means of simulating the coupling of the electronic and atomic subsystems and provides simultaneously atomic-scale detail of the track structure and morphology. The simulated internal structure of the track consists of an amorphous core and a shell of disordered, but still periodic, domains. For Gd₂Ti₂O₇, the shell region has a disordered pyrochlore with a defect fluorite structure and is relatively thick and heterogeneous with different degrees of

disordering. For Gd_2TiO_5 , the disordered region is relatively small as compared with $\text{Gd}_2\text{Ti}_2\text{O}_7$. In the simulation, "facets", which are surfaces with a definite crystallographic orientation, are apparent around the amorphous core and more evident in Gd_2TiO_5 along the [010] than [001], suggesting an orientational dependence of the radiation response. These results show that track formation is controlled by the coupling of several complex processes, involving different degrees of amorphization, disordering, and dynamic annealing. Each of the processes depends on the mass and energy of the energetic ion, the properties of the material, and its crystallographic orientation with respect to the incident ion beam.

Abstract 168 WED-RE06-2

[Contributed Talk - Wednesday 9:45 AM - Presidio C](#)

Mechanical Properties of Metal Nitrides for Radiation Resistant Coating Applications: A DFT Study

[Oscar U Ojeda](#), [Roy A Araujo](#), [Haiyan Wang](#), [Tahir Cagin](#)

Chemical Engineering, Texas A&M University, 3322 TAMU, College Station TX 77843, United States

Metal nitrides compounds like aluminum nitride (AlN), titanium nitride (TiN), tantalum nitride (TaN), hafnium nitride (HfN) and zirconium nitride (ZrN) are of great interest because of their chemical and physical properties such as: high melting point, resistivity, thermal conductivity and extremely high hardness. They are the materials of choice for various applications like protective coating for tools, diffusion barriers or metal gate contact in microelectronics, and lately their potential applications as radiation-resistant shields. In order to assess their use for radiation tolerance we have studied the structural, mechanical and electronic properties. We have evaluated the anisotropic elastic constants and their pressure dependence for three different crystalline phases: B1-NaCl, B2-CsCl, and B3-ZnS crystal structures. In addition to these cubic polymorphs, we also have studied potential hexagonal structures of some of the same metal nitrides. All computations are carried out using first principles Density Functional Theory (DFT) approach.

Abstract 57 WED-RE06-3

[Contributed Talk - Wednesday 9:45 AM - Presidio C](#)

Nanocomposite Interfaces and their Effects on Defect Evolution following Light Ion Irradiation

[Jeffery A Aguiar](#)¹, [Pratik P Dholabhai](#)¹, [Zhenxing Bi](#)², [Mujin Zhu](#)¹, [Engang Fu](#)¹, [Yongqiang Q Wang](#)¹,
[Quanxi X Jia](#)², [Amit Misra](#)², [Blas P Uberuaga](#)¹

⁽¹⁾*Material Science and Technology Division, Los Alamos National Laboratory, P.O. Box 1663, Los Alamos New Mexico 87545, United States*

⁽²⁾*Material Physics and Applications Division, Los Alamos National Laboratory, P.O. Box 1663, Los Alamos New Mexico 87545, United States*

Recent developments have lead researchers to hypothesize nanoceramic composite materials may address concerns of nucleation, growth, migration, and immobilization of point defects to tailor material properties. In a nuclear context, controlling the migration kinetics leads itself to begin understanding fission fragments at higher temperatures and radiation environments. Missing in the literature however are studies considering variants of structural and chemical properties at interfaces that can plausibly tailor defect energetics to alter the properties of these same nanoceramics. To develop a perspective into these structural, chemical, and electrostatic effects at interfaces we will present a study focused on the physical origins for the performance, behavior, and onset of amorphization as a function of interface structure.

Studying interfaces offers opportunities to study inherently complex phenomena in connection with material performance. An example of the degree of control at interfaces to bring about complicated behavior is a change in the termination layer at the interface. The rather simple change can play a major factor in the interfacial energetics and are the same energetics responsible for the microstructural evolution. Comparing the interface structure, chemistry, electrostatics, and response before and after irradiation can thereby lead to the exploration of the underlying parameters that underpin material properties, such as radiation tolerance.

In this work, we examine the evolution of electronic and physical structure in connection with the susceptibility to amorphization at nanoceramic interfaces following light ion irradiation. In detail we will present analytical electron microscopy on a series of irradiated CeO₂-STO and STO-MgO interfaces. The results reveal changes in the interfacial termination layer are structural pinning sites for the onset of amorphization and orientation relationship can vastly change this behavior. The presentation concludes with perspective insight into interfacial properties, radiation damage evolution, and how structural materials can be further tailored towards material properties.

Abstract 100 WED-RE06-4

[Invited Talk - Wednesday 9:45 AM - Presidio C](#)

Effects of composition on the response of oxides to highly ionizing radiation

[Cameron Lee Tracy](#)¹, [Maik Lang](#)², [Fuxiang Zhang](#)¹, [Sulgiye Park](#)³, [Jiaming Zhang](#)³, [Christina Trautmann](#)^{4,5}, [Rodney Charles Ewing](#)³

⁽¹⁾*Department of Materials Science and Engineering, University of Michigan, Ann Arbor MI 48109, United States*

⁽²⁾*Department of Nuclear Engineering, University of Tennessee, Knoxville TN 37996, United States*

⁽³⁾*Department of Geological and Environmental Science, Stanford University, Stanford CA 94305, United States*

⁽⁴⁾*GSI Helmholtz Centre for Heavy Ion Research, 64291 Darmstadt, Germany*

⁽⁵⁾*Technische Universität Darmstadt, 64287 Darmstadt, Germany*

Particles having specific energies of approximately 1 MeV/nucleon or higher interact with solids primarily through electronic excitation. Both nuclear fission fragments and alpha particles fall into this category of highly-ionizing radiation. The structural and chemical modifications they induce in insulating materials are critical parameters in the design of nuclear fuels and wastefoms, as well as the study of actinide-bearing minerals. This damage production can be simulated using swift heavy ions generated at large accelerator facilities. We have irradiated a variety of oxide materials with heavy ions having energies from hundreds of MeV to several GeV. The resulting modifications were characterized using synchrotron x-ray scattering and spectroscopy techniques, along with complementary transmission electron microscopy and Raman spectroscopy.

Oxides exhibit diverse responses to highly-ionizing radiation, ranging from point defect accumulation and redox behavior to phase transitions and amorphization. Within a given class of oxides, the induced modifications often depend strongly on chemical composition. Complex pyrochlore-type oxides (Ln₂M₂O₇) feature both amorphization and disordering within nanometric ion tracks, with the relative extent of the two transformations depending on the energetics of antisite defect formation, as determined by the ionic radii of the cations. In contrast, binary lanthanide sesquioxides (Ln₂O₃) undergo crystalline-to-crystalline transitions to various high temperature phases in response to swift heavy ion irradiation. The phases produced in this process and its extent vary with the thermal phase stability of compounds in this system. Finally, the fluorite-structured actinide oxides (AcO₂) retain their long-range periodicity during ion bombardment, but exhibit unique radiation-induced redox behavior, in which the oxidation state of their cations is reduced. This process is accompanied by the expulsion of anions from the ion-solid interaction volume into the surrounding material, where they agglomerate into defect clusters. Compositional variability in the redox potential of these materials therefore influences their radiation response.

Abstract 218 WED-RE06-5

[Contributed Talk - Wednesday 9:45 AM - Presidio C](#)

Heavy Ion Irradiation-Induced Microstructural Change in Helium-Implanted Single Crystal and Nano-Engineered SiC

[Chien-Hung Chen](#)¹, [Yanwen Zhang](#)^{1,2}, [Engang Fu](#)³, [Yongqiang Wang](#)⁴, [Miguel Luis Crespillo](#)¹, [Chaozhuo Liu](#)⁵, [Steven Christopher Shannon](#)⁶, [William John Weber](#)^{1,2}

- ⁽¹⁾Materials Science & Engineering Dept., University of Tennessee, Knoxville TN 37996, United States
⁽²⁾Materials Science & Technology Division, Oak Ridge National Laboratory, Oak Ridge TN 37831, United States
⁽³⁾State Key Laboratory of Nuclear Physics and Technology, School of Physics, Peking University, Beijing 100871, China
⁽⁴⁾Materials Science and Technology Division, Los Alamos National Laboratory, Los Alamos NM 37545, United States
⁽⁵⁾Physics Dept., College of Science, China University of Petroleum, Qingdao 266580, China
⁽⁶⁾Nuclear Engineering Dept., North Carolina State University, Raleigh NC 27695, United States

Silicon carbide (SiC) is a promising candidate material for nuclear applications due to its good radiation resistance and structural stability at high-temperatures. The irradiation response of nano-engineered (NE) SiC films, containing high densities of stacking faults within nano-crystalline grains, and single crystalline SiC films have been investigated after helium ion implantation and after additional heavy-ion irradiation. Both nano-engineered and single crystalline samples have been irradiated with 65 keV helium ions at 7° off the surface normal at 550 K. The helium distribution profile and microstructural changes in the as-implanted SiC samples have been characterized by forward elastic recoil detection analysis (ERDA) and transmission electron microscopy (TEM), respectively. The implantation and damage depth profiles from Stopping and Range of Ions in Matter (SRIM) calculation are consistent with results from the TEM analysis. No bubbles are observed in the as-implanted single crystalline SiC samples. For the NE SiC, bubble formation occurs for specimens irradiated to He fluences greater than $\sim 3 \times 10^{15}$ ions/cm² (2400 appm helium at the peak concentration). Subsequent 9 MeV Au³⁺ ions irradiation of the helium-implanted NE and single crystal SiC samples has been carried at 700°C to doses from 10 to 30 dpa. The high temperature irradiation results in an increase in bubble size and decrease in bubble density for the NE SiC, and a bimodal bubble size distribution begins to form at helium concentrations exceeding 2400 appm. Compared to the single crystal SiC, the NE SiC contains more nucleation sites that promote bubble nucleation, which is thermally activated at 700 °C, and heavy-ion irradiation of the NE SiC at 700 °C drives a bubble coarsening process that leads to a bimodal size distribution for high helium concentrations.

Abstract 437 WED-RE06-6

[Contributed Talk - Wednesday 9:45 AM - Presidio C](#)

Ne ion irradiation effects on stuffed $\text{Er}_2(\text{Ti}_{2-x}\text{Er}_x)\text{O}_{7-x/2}$ ($x=0-0.667$) structures

[Dongyan yang](#)¹, [Yuhong Li](#)¹, [Chunping Xu](#)¹, [Jian Zhang](#)^{2,3}, [Juan Wen](#)^{1,3}, [Yongqiang Wang](#)³

⁽¹⁾School of Nuclear Science and Technology, Lanzhou University, Lanzhou Gansu 730000, China

⁽²⁾School of Energy Research, Xiamen University, Xiamen Fujian 361005, China

⁽³⁾Materials Science and Technology Division, Los Alamos National Laboratory, Los Alamos New Mexico 87545, United States

A series of "stuffed" titanate pyrochlore $\text{Er}_2(\text{Ti}_{2-x}\text{Er}_x)\text{O}_{7-x/2}$ ($x=0, 0.162, 0.286, 0.424$ and 0.667) compounds have been synthesized successfully using conventional solid state synthesis methods. X-ray diffraction measurements and Raman scattering were used to characterize the structure of the compounds. The results indicated that the disordering degree of the structure increased with increasing x . $\text{Er}_2(\text{Ti}_{2-x}\text{Er}_x)\text{O}_{7-x/2}$ ($x=0-0.667$) samples were irradiated with 400keV Ne^{2+} ions to fluences ranging from 1×10^{14} - 5×10^{15} ions/cm² at cryogenic temperature ($\sim 77\text{K}$). Ion irradiation effects in these samples were examined by using grazing incident X-ray diffraction (GIXRD). The results showed all the samples were amorphized at the maximum experimental ion fluence 5×10^{15} ions/cm², and there are lattice swelling effects for all the irradiated samples prior to amorphous. The relationship between the degree of lattice swelling and x were analyzed.

Abstract 483 THU-PS03-1

[Plenary Talk - Thursday 8:00 AM - Lone Star Ballroom](#)

Advances in Science and Technology for Counter Terrorism

[James Johnson](#)

Science and Technology, Office of National Labs, Department of Homeland Security, 1120 Vermont Ave, Washington DC 20005, United States

The Science and Technology (SandT) Directorate serves as the scientific and analytical core for the Department of Homeland Security. SandT works closely with partners across the Homeland Security Enterprise (HSE) to provide scientific analysis and technology solutions that address the most pressing operational challenges faced in homeland

security. From border security to biological defense to cybersecurity to explosives detection, SandT is at the forefront of integrating R and D across public and private sectors and the international community to meet homeland security needs. SandT's experts (including laboratories) continue to develop and transition advanced capabilities and analytics to HSE operators so they may better prevent, protect against, mitigate, respond to and recover from all hazards and a wide range of homeland security threats. The presentation will provide an overview of the ongoing SandT initiatives and value added propositions that contribute to the advances of Science in Technology to keep our homeland safe.

Abstract 327 THU-PS03-2

[Plenary Talk - Thursday 8:00 AM - Lone Star Ballroom](#)

Application of accelerators in nuclear structural materials research: history, present status and challenges

[Frank A. Garner](#)

Radiation Effects Consulting, Richland WA 99354, United States

Irradiation of materials with energetic charged particles is an valuable tool in many technological endeavors. In some cases, charged particle irradiation is used to produce new materials with improved properties, especially in the electronic field. Surface alteration of metals with charged particles is also a way to improve the hardness of alloys. However, for structural alloys in accelerators, nuclear reactors or space vehicles, irradiation with charged particles and/or neutrons usually leads to a progressive degradation of the important engineering properties that were the basis of alloy selection.

For damage introduced by charged particles impinging on structural components, such degradation can be best studied using the same charged particles, often at accelerated rates compared to that of the studied environment. Two examples are charged particle impingement on space vehicle components and gas implantation into the first wall of fusion reactors, the latter leading to blistering and surface erosion.

However, charged particle irradiation can be used to simulate some features of neutron-induced damage in the structural materials of both fission and fusion devices. Sometimes serious lifetime or safety consequences can arise for relatively low damage levels (e.g. pressure vessel embrittlement) but neutron irradiation to very high exposure levels leads to significant changes not only in physical and mechanical properties, but also in significant changes in component dimensions. The latter is often the life-limiting factor for some reactor internal components.

The three major neutron-induced phenomena are phase instability, void swelling and irradiation creep, all of which affect the dimensional stability of alloys. A review of these phenomena is presented, followed by a review of charged particle simulation experiments conducted to study these material problems. Since neutrons have very large penetration depths but charged particles penetrate much shorter distances, this imposes some significant limitations on the conduct of simulation experiments and their interpretation.

Abstract 464 THU-ATF06-1

[Invited Talk - Thursday 10:00 AM - Bowie A](#)

Pulsed-Neutron Generator Applications in the Oil Industry

[Bradley A Roscoe](#)

Schlumberger-Doll Research, 1 Hampshire St., Cambridge MA 02139, United States

Oilfield service companies, like Schlumberger provide a large variety of services to oil companies to help them identify and assess oil reservoirs and to allow them to optimize their production. A large part of Schlumberger's business is to provide petrophysical information on rock formations in particular on those containing hydrocarbons, i.e. oil and gas. Some parameters of interest are the amount of pore space in the rock, the quantity of oil or gas contained in the rock, the composition of the rock matrix, its permeability etc. Many physical measurements to obtain electromagnetic, acoustic, magnetic resonance and nuclear properties of the formation surrounding the wellbore are used for this purpose. This talk will give an introduction to the application of pulsed neutron generator (PNG) technology in oilfield tools. Such tools have typically an available inner diameter ranging from less than 1.5 in. to 3.5 in and need to operate at temperatures up to 175 °C and at external pressures that may reach 30 kpsi.

Abstract 253 THU-ATF06-2

[Invited Talk - Thursday 10:00 AM - Bowie A](#)

Performance and Technology of High Flux Neutron Generator DD110MB

[Jaakko Hannes Vainionpää](#)¹, [Allen X Chen](#)¹, [Melvin A Piestrup](#)¹, [Charles K Gary](#)¹, [Glen Jones](#)², [Richard H Pantell](#)³

⁽¹⁾ *Adelphi Technology, 2003 E Bayshore Rd, Redwood City CA 94063, United States*

⁽²⁾ *G&J Enterprice, 7486 Brighton Ct, Dublin CA 94568, United States*

⁽³⁾ *Department of Electrical Engineering, Stanford University, Stanford CA, United States*

The new model DD110MB neutron generator from Adelphi Technology produces thermal (< 0.5 eV) neutron fluxes that are comparable to those achieved in a nuclear reactor. Thermal neutron fluxes of $0.5\text{-}1 \cdot 10^8$ neutrons/(cm²-sec) are expected. This flux is achieved using four ion beams arranged concentrically around a target chamber containing a compact moderator with a central sample cylinder. Fast neutron yield of $\sim 2 \cdot 10^{10}$ n/s is created at the titanium surface of the target chamber. The thickness and material of the moderator is selected to maximize the thermal neutron flux at the center. The 2.5 MeV neutrons are quickly thermalized to energies below 0.5 eV and concentrated at the sample cylinder. The maximum flux of thermal neutrons at the target is achieved when approximately half of the neutrons at the sample area are thermalized. In this paper we present simulation results used to optimize the geometries and materials in the neutron generator. The neutron flux can be used for neutron activation analysis (NAA) prompt gamma neutron activation analysis (PGNAA) for determining the concentrations of elements in many materials. Another envisioned use of the generator is production of radioactive isotopes. DD110MB is small enough for modest-sized laboratories and universities. Compared to nuclear reactors the DD110MB produces comparable thermal flux but provides reduced administrative and safety requirements and it can be run in pulsed mode, which is beneficial in many neutron activation techniques.

Abstract 379 THU-ATF06-3

[Invited Talk - Thursday 10:00 AM - Bowie A](#)

A Compact Neutron Generator

[Luke T. Perkins](#), [Kevin L. Hiles](#), [James E. Fay](#), [Robert L. Bethke](#), [Ryan P. McCaffrey](#), [Sameer Pandya](#),
[Robert A. Adolph](#)

Princeton Technology Center, Schlumberger, 20 Wallace Road, Princeton Junction NJ 08550, United States

Neutron generators have been used successfully in various oil well logging applications since the 1960s. The initial application was the determination of the macroscopic neutron capture cross section of the formation by measuring the die-away of capture gamma rays following a burst of neutrons. Measurements such as porosity logging and formation evaluation using capture and inelastic gamma ray spectroscopy were added as the technology matured. The pulsed neutron generator (PNG) has always added significant length to the logging tool, constrained the placement of the nuclear detectors in the tool and added length between the measurement and the bottom of the tool, preventing the evaluation of a part of the bottom section of the borehole. A shorter generator not only avoids these complications but makes it possible to put sensors axially above and below the source, enabling multiple measurements at a short distance from the radiation generator. We

review the latest compact PNG from Schlumberger, discuss its geometry and performance, and introduce its use in the Litho Scanner* high-definition spectroscopy service.

*Mark of Schlumberger

Abstract 268 THU-ATF06-4

[Invited Talk - Thursday 10:00 AM - Bowie A](#)

Ungated Field Ionization Sources for Compact Neutron Generators

[Arun Persaud](#)¹, [Rehan Kapadia](#)², [Kuniharu Takei](#)², [Ali Javey](#)^{1,2}, [Thomas Schenkel](#)¹

⁽¹⁾*Accelerator and Fusion Research Division, E. O. Lawrence Berkeley National Laboratory, 1 Cyclotron Road, Berkeley CA 94720, United States*

⁽²⁾*Department of Electrical Engineering and Computer Sciences, University of California, Berkeley CA 94720, United States*

The ability to replace radiological sources with generators depends on matching the size and energy requirements of the application. Furthermore, cost and usability (e.g. lifetime) play an important role. For many applications, such as oil-well logging, these factors lead to stringent requirements that the replacement sources must fulfill. In this talk we will present the results of our investigations using field emitter tips to build a compact neutron generator as an alternative technology to those used currently. Field emitter tips are an interesting choice, since they can provide a low-energy, plasma-free ion source for neutron production. Field emitters are a well established technology for electron production. To generate ions, however, higher fields are necessary and lifetime issues need to be addressed. Our approach uses non-gated field emitters in a diode-like structure. The geometry of the sharp emitter tips leads to an amplification of the applied electric field in the tip region, so that a local field strength of the order of 20 V/nm can be reached. These fields are needed to ionize nearby gas molecules. Using deuterium as a working gas, deuterium ions can be created and accelerated in the applied field. Neutrons can be produced in a fusion reaction when these ions interact with a deuterated target. We will discuss the results of this study, as well as the remaining open questions and the maximum output yields we see attainable using this technology.

This work was supported by the Office of Proliferation Detection(DNN R&D) of the US Department of Energy at the Lawrence Berkeley National Laboratory under contract number DE-AC02-05CHI1231.

Abstract 102 THU-ATF06-5

[Contributed Talk - Thursday 10:00 AM - Bowie A](#)

Laser-free RF-Gun as a combined source of THz and ps-sub-ps X-rays

[Alexei Vladimirovich Smirnov](#)¹, [Ronald Agustsson](#)¹, [Salime Boucher](#)¹, [Thomas Grandsaert](#)¹, [Josiah J Hartzell](#)¹, [Marcos Ruelas](#)¹, [Stephan Storms](#)¹, [Zheng Ning](#)¹, [Alex Murokh](#)¹, [Tara Campese](#)¹, [Luigi Faillace](#)¹, [Avinash Verma](#)¹, [Yujong Kim](#)^{2,3}, [Pikad Buaphad](#)², [Anthony Andrews](#)³, [Brian Berls](#)³, [Chris Eckman](#)³, [Kevin Folkman](#)³, [Ashley Knowles-Swingle](#)³, [Chad O'Neill](#)³, [Mike Smith](#)³

⁽¹⁾*R&D (Research & Development), Radiabeam TECHNOLOGIIES, 1717 STEWART, SANTA MONICA CA 90404, United States*

⁽²⁾*Idaho State University, 921 S. 8th Avenue, Pocatello ID 83209, United States*

A coherent, mm-sub-mm-wave source driven by an inexpensive RF electron gun proposed for wide research applications as well as auxiliary inspection and screening, safe imaging, cancer diagnostics, surface defectoscopy, and enhanced time-domain spectroscopy. It allows generating of high peak and substantial average THz-sub-THz radiation power provided by beam pre-bunching and chirping in the RF gun followed by microbunching in magnetic compressor, and resonant Cherenkov radiation of an essentially flat beam in a robust, ~inch-long, planar, mm-sub-mm gap structure. The proof-of-principle has been successfully demonstrated in Phase I on a 5 MeV beam of L-band thermionic injector of Idaho Accelerator Center. The system can also deliver an intense, ps-sub-ps bursts of low-to-moderate dose of X-ray radiation produced by the same beam required for pulsed radiolysis as well as to enhance screening efficiency, throughput and safety.

Abstract 400 THU-ATF06-6

[Contributed Talk - Thursday 10:00 AM - Bowie A](#)

Energy-tunable Parametric X-ray (PXR) production using medical accelerators

[Bryndol A Sones](#)

Physics and Nuclear Engineering, US Military Academy, Bartlett Hall, West Point NY 10996, United States

X-rays were used to probe for information about crystals' periodic structures nearly 100 years ago. Today because of their well-defined X-ray interaction behavior, crystals are commonly used as "monochromators" at synchrotron radiation facilities to diffract spectrally pure X-rays and as "analyzers" in X-ray interaction experiments to collect information about a target specimen. In both cases, the crystal is a tool used with existing X-rays produced through other means. In the past decade, Parametric X-rays (PXR) experiments have demonstrated that crystals can now be the source of X-rays from an interaction with relativistic electrons. The rotation of a crystal target in an electron beam smoothly varies the PXR energy and produces an energy-tunable, quasi-monochromatic, and directionally intense X-rays that may be used for medical imaging applications. The first demonstration of PXR imaging was reported from the Rensselaer Polytechnic Institute (RPI) 60 MeV LINAC facility in 2005. Concurrently, other PXR production experiments at μ A-levels were done at the LEBRA 100 MeV LINAC facility in Japan, and those researchers advanced the PXR imaging effort by using it as a coherent X-ray source in Diffraction Enhanced Imaging (DEI) experiments where a second crystal was used as analyzer to image a mouse kidney in 2012. This paper continues from early work at RPI and examines the feasibility of using medical electron accelerators found in hospitals to produce PXR. Specifically, the Varian TrueBeam accelerator is evaluated with use with a variety of crystals to include Si, Ge, LiF, Mo, and W. By contrast to earlier PXR experiments, the Varian accelerator has lower electron energy (22 MeV), a higher electron beam current (mA), and a larger and more uniform beam area. The trade-offs of these parameters are presented and the initial experiments are proposed for collaborative work with Memorial Sloan Kettering Cancer Center (MSKCC) in NYC.

Abstract 386 THU-HSD06-1

[Invited Talk - Thursday 10:00 AM - Travis A/B](#)

Scintillators and Electronics for Transmission Z-Spectroscopy (Z-SPEC)

[Willem G.J. Langeveld](#), [Martin Janecek](#)

Rapiscan Laboratories, Inc., 520 Almanor Ave, Sunnyvale CA 94085, United States

The bremsstrahlung x-ray spectrum in high-energy, high-intensity x-ray cargo inspection systems is attenuated and modified by cargo materials in a Z-dependent way. Spectroscopy of detected x rays is thus useful to measure the approximate Z of the cargo. Due to the broad features of the energy spectrum, excellent energy resolution is not required. Such "Z-Spectroscopy" (Z-SPEC) is possible under certain circumstances. A statistical approach, Z-SCAN (Z-determination by Statistical Count-rate ANALysis), can also be used, complementing Z-SPEC at high count rates. Both require fast x-ray detectors and fast digitizers. Preferentially, Z-SPEC, Z-SCAN and cargo imaging are implemented in a single detector array to reduce cost, weight, and complexity. To preserve good spatial resolution of the imaging subsystem, dense scintillators are required. Z-SPEC, in particular, benefits from very fast scintillators, in order to avoid signal pile-up.

We have studied ZnO, BaF₂ and PbWO₄, as well as suitable photo-detectors, read-out and digitization electronics. ZnO is (currently) not suitable because it self-absorbs its scintillation light. BaF₂ emits in the UV, either requiring fast wavelength shifters or UV-sensitive solid state read-out devices, and it also has a long decay time component. PbWO₄ is the most attractive because it does not have these problems, but it is significantly slower and has low light output. There is thus a need for alternative fast high-density scintillators that emit visible light. Alternatively, there is a need for a fast solid-state read-out device that is sensitive to UV light for use with BaF₂, or other UV-emitting scintillators. We plan to present preliminary results of tests made with PbWO₄.

This work has been supported by US Department of Homeland Security, Domestic Nuclear Detection Office, under competitively awarded contract HSHQDC-14-C-B0002. This support does not constitute an express or implied endorsement on the part of the Government.

Abstract 450 THU-HSD06-2

[Invited Talk - Thursday 10:00 AM](#) - [Travis A/B](#)

Gamma-insensitive fast neutron detection for active interrogation applications

[Rico Chandra](#), [Giovanna Davatz](#), [David Murer](#), [Ulisse Gendotti](#)

Arktis Radiation Detectors Ltd, Raffelstrasse 11, Zurich 8045, Switzerland

This paper shall present fast neutron detectors that are more cost effective and less gamma sensitive than liquid scintillators and stilbene. The detectors' sensitive medium is low-cost, compressed natural helium (⁴He). ⁴He has a very low charge density, minimizing gamma ray interactions, and limiting the energy deposit of recoil electronics. Moreover, ⁴He offers a high light yield for neutron interactions, fast timing, and outstanding pulse shape discrimination properties. The presented detectors are read out by a multitude of solid-state silicon photomultipliers (SiPMs) dispersed throughout the scintillating gas, making the detectors rugged and scalable. Signal processing is carried out directly within the detector to yield a simple TTL output per detected neutron, eliminating the necessity for high voltage supply, digitizer, and pulse shape analysis. Gamma rejection up to 200 uSv/hr has been demonstrated to not degrade neutron detection efficiency. The presented detectors allow achieving fast neutron efficiency over square meter areas for unprecedented low costs.

Abstract 99 THU-HSD06-3

[Contributed Talk - Thursday 10:00 AM](#) - [Travis A/B](#)

Detectors for the new technique of High Energy X-ray cargo inspection

[Anatoli Arodzero](#)^{1,2}

⁽¹⁾*RadiaBeam Technologies, 1717 Stewart Street, Santa Monica CA 90404, United States*

⁽²⁾*Nuclear Science and Engineering, Massachusetts Institute of Technology, 77 Massachusetts Avenue, NW13-221, Cambridge MA 02139, United States*

Existing requirements for high throughput rail cargo radiography inspection include high resolution (better than 5 mm line pair), penetration beyond 400 mm steel equivalent, material discrimination (organic, inorganic, high Z), high scan speeds (>10 kph, up to 60 kph), low dose and small radiation exclusion zone. To meet and exceed these requirements research into a number of new radiography methods has been initiated. The factors limiting performance of current High Energy X-ray cargo inspection methods has been identified.

Novel inspection concepts relying on Linac-based, adaptive, modulated energy X-ray sources, new types of fast X-ray detectors (Scintillation-Cherenkov detectors), and fast processing of detector signals are being developed. Crystalline inorganic detector materials, which may be suitable for these applications, will be discussed. These materials should

combine a balance of scintillation and Cherenkov light and allow using Silicon Photomultipliers (SiPM, MPPC) for signal readout. The specification for "ideal" scintillation materials for these applications will be considered.

This work has been partly supported by US Department of Homeland Security, Domestic Nuclear Detection Office, under competitively awarded contract/IAA HSHQDC-13-C-B0019. This support does not constitute an express or implied endorsement on the part of the Government.

Abstract 52 THU-HSD06-4

[Contributed Talk - Thursday 10:00 AM](#) - [Travis A/B](#)

Study of a Silicon Photomultiplier for Optical Readout of EJ-299-33A Scintillator

[Alexander Barzilov](#), [Amber Guckes](#)

Mechanical Engineering, University of Nevada, Las Vegas, 4505 S Maryland Parkway, Las Vegas Nevada 89154, United States

The recent problem of a shortage of Helium-3 isotope poses a significant challenge in supporting existing neutron detection systems and the development of future technologies. Many applications require detection of fast neutrons that are emitted in fissions or generated in (alpha,n) isotopic sources, and accelerator-based sources such as (d,d) and (d,t). Counters that rely on thermal neutron detection require a moderator; they are not rigid and have count rate limitations. The plastic scintillator EJ-299-33A with neutron / photon pulse shape discrimination properties enables measurements of fast neutron flux segregating gamma-ray signals. The feasibility of optical readout of scintillation photons using a silicon photomultiplier (SiPM) was studied for this scintillator. This talk will focus on results of experimental testing of the EJ-299-33A equipped with the 64-pixel, 2"x2" SENSIL SiPM in the mixed flux of neutrons and photons emitted by a plutonium-beryllium source.

Abstract 201 THU-HSD06-5

[Contributed Talk - Thursday 10:00 AM](#) - [Travis A/B](#)

X-ray Radar Imaging Technique Using a 2 MeV Linear Electron Accelerator

[Wendi Dreesen](#)¹, [David Schwellenbach](#)¹, [Rick Wood](#)², [Mark Browder](#)², [Nick Kallas](#)¹, [James Potter](#)³

⁽¹⁾*Physics and Analysis, National Security Technologies, 182 East Gate Drive, Los Alamos NM 87544, United States*

⁽²⁾*Lockheed Martin, PO Box 650003, Dallas TX 75265, United States*

⁽³⁾*JP Accelerator Works, Inc, 2245 47th St, Los Alamos NM 87544, United States*

X-ray radar imaging, patented in 2013 by James R. Wood, combines standard radar techniques with the penetration power of x-rays to image scenes. Our project strives to demonstrate the technique using a 2 MeV linear electron accelerator to generate the S-band-modulated x-ray signals. X-ray detectors such as photodiodes and scintillators are used to detect the signals in backscatter and transmission detection schemes. The S-band microstructure is imposed on the variable width electron pulse and this modulation carries over to the bremsstrahlung x-rays after the electron beam is incident upon a copper-tungsten alloy target. Using phase/distance calculations and a low-jitter system, we expect to detect different object distances by comparing the measured phase differences. The experimental setup, which meets strict jitter requirements, and preliminary experimental results are presented.

Abstract 32 THU-HSD06-6

[Contributed Talk - Thursday 10:00 AM](#) - [Travis A/B](#)

A neutron imager and flux monitor based on Micro Channel Plates (MCP) in electrostatic mirror configuration

[Vincenzo Variale](#)

INFN-sezione di Bari, via Orabona 4, Bari 70126, Italy

In the last years, Micro Channel Plates (MCP) devices have been largely employed both for detection of ionizing radiation and as image intensifier (infrared range). It has also been demonstrated that MCPs can be applied in neutron detection and imaging with many advantages. The use of MCP for neutron detection was proposed for the first time in 1987 at Los Alamos [1] for fast neutrons. More recently, MCP have been proposed as thermal neutron detectors, combined with a suitable converter [2,3].

In this contribution, a new high transparency device based on MCP for the monitoring the flux and spatial profile of a neutron beam will be described. The assembly consists of a Carbon foil with a ^6Li deposit, placed in the beam, and a MCP equipped with a phosphor screen readout viewed by a CCD camera, placed outside the beam. Secondary emitted electrons (SEE) produced in the C foil by the α -particles and tritons from the $^6\text{Li}+n$ reaction, are deflected to the MCP detector by means of an electrostatic mirror, suitably designed to preserve the spatial resolution. The conductive layer on the phosphor can be used for neutron counting, and to obtain time-of-flight information.

A peculiar feature of this device is that the use of an electrostatic mirror minimizes the perturbation of the neutron beam, i.e. absorption and scattering. It can be used at existing time-of-flight facilities, in particular at the n_TOF facility at CERN, for monitoring the flux and special profile of the neutron beam in the thermal and epithermal region.

In this work, the device principle and design will be presented, together with the main features in terms of resolution and neutron detection efficiency.

Abstract 107 THU-IBA07-1

[Invited Talk - Thursday 10:00 AM - Bowie B](#)

Study on transfer coefficients of cesium-137 and other elements from soil to plant by g-ray measurement and PIXE analysis for remediation of Fukushima

[Keizo ISHII](#)¹, [Akiho FUJITA](#)², [Shigeo MATSUYAMA](#)¹, [Atsuki TERAOKA](#)¹, [Hirotugu ARAI](#)¹

⁽¹⁾*Research Center for Remediation Engineering of Environments Contaminated with Radioisotopes, Graduate School of Engineering, Tohoku University, 6-6-01-2 Aza-Aoba, Aramaki, Aoba-ku, Sendai 980-8579, Japan*

⁽²⁾*Department of Quantum Science and Energy Engineering, Graduate School of Engineering, Tohoku University, 6-6-01-2 Aza-Aoba, Aramaki, Aoba-ku, Sendai 980-8579, Japan*

The great East Japan earthquake occurred 11 March 2011 and then the big tsunami hit the east coast of the eastern Japan. It caused the accident of Fukushima first nuclear power plant. The huge amount of radioisotopes of ^{131}I , ^{134}Cs , ^{137}Cs and others were scattered on the prefectures of the eastern Japan. This radiation pollution worried us about the internal exposure by taking contaminated foods. At the present, the cesium radioactivity of foods is almost less than several Bq/kg, however, people are still worried. In order to relieve people's anxiety, the research on seeking for plants not containing radioactive cesium is needed. So, we have investigated the transfer coefficient of radioactive cesium from soil to plants.

We collected ten kinds of contaminated wild plants and soil. We measured γ -rays from ^{137}Cs and ^{40}K in the plants and the soil where the plants were cultivated, and then estimated their transfer coefficients which were 0.02~0.03 in the case of ^{137}Cs .

We investigated also the transfer coefficients of Na, Mg, Al, Si, P, S, K, Ca, Mn, Fe, Co, Zn, Rb and Sr using PIXE analysis. The transfer coefficients of almost all elements were less than 0.5.

We checked the linear relation between the concentration of ⁴⁰K obtained by the g-ray measurement and that of natural K by the PIXE analysis in the plants and the soil, and confirmed it except for some plants.

From the results of g-ray measurement and PIXE analysis, we investigated the relation between the specific activity of Cs and the concentration of other elements in the plants. It was found that the concentrations of K, Rb and Zn were proportional to specific activities of Cs except *Persicaria longiseta*. This result helps search for low Cs radioactivity vegetables and it will contribute to the remediation of agriculture in Fukushima.

Abstract 442 THU-IBA07-2

[Invited Talk - Thursday 10:00 AM - Bowie B](#)

High Throughput PIXE for Large Area High Definition Elemental Imaging

[Tilo Reinert](#)¹, [Nirav Barapatre](#)², [Markus Jäger](#)³, [Markus Morawski](#)⁴

⁽¹⁾*Department of Physics, University of North Texas, 1155 Union Circle #311427, Denton TX 76203, United States*

⁽²⁾*Institute for Experimental Physics II, University of Leipzig, Linnéstraße 5, Leipzig 04103, Germany*

⁽³⁾*Faculty of Mathematics and Computer Science, University of Leipzig, PF 100920, Leipzig 04009, Germany*

⁽⁴⁾*Paul Flechsig Institute for Brain Research, University of Leipzig, Jahnallee 59, Leipzig 04109, Germany*

Usually particle induced X-ray emission analysis (PIXE), especially with a nuclear microprobe, is connected with rather long data acquisition times in the order of hours even for moderate resolutions if trace element sensitivity is required. This unfavorable performance criteria originates from the intrinsic low X-ray yield in standard PIXE experimental setups, that is in the order of a few tens counts per µg/g element content and µC charge of accumulated proton beam. For a higher sample throughput at the same sensitivity, the data acquisition time must be reduced. Increasing the two well known parameters detector efficiency and beam brightness, will lead to the desired higher X-ray count rates.

With the advancement in accelerator, ion source and nuclear microprobe technology, an improvement in count rate of about an order of magnitude is feasible. Today brighter proton beams achieve beam current densities well above 1 nA/µm². Additionally, the availability of the compact silicon drift X-ray detectors (SDD) allow reasonably priced multi-detector arrangements with solid angles as large as 1.2 sr. However, the immense improvements in count rate also require digital data acquisition and signal processing to handle the high data rate.

Today's technology is able to provide large area high definition PIXE elemental imaging. We have taken 12 mega-pixel elemental images of a coronal section of rat brain of about 130 mm² in size.

Abstract 18 THU-IBA07-3

[Invited Talk - Thursday 10:00 AM - Bowie B](#)

The PIXE technique: recent applications and trends in Brazil

[Carla Eliete Iochims dos Santos](#)¹, [Johnny Ferraz Dias](#)², [Marcia Rizzutto](#)¹, [Paulo Fernandes Costa Jobim](#)², [Suene Bernardes dos Santos](#)¹, [Manfredo Harri Tabacniks](#)¹

⁽¹⁾*Group for Applied Physics with Accelerators, Physics Institute, University of Sao Paulo, Rua do Matão Travessa R, 187, Sao Paulo SP 05314-970, Brazil*

⁽²⁾*Ion Implantation Laboratory, Physics Institute, University of Rio Grande do Sul, Av Bento Gonçalves 9500, Porto Alegre RS 91501-970, Brazil*

It is well known by the IBA community that the PIXE technique is a handy tool to characterize different materials regarding their elemental composition and distribution. In Brazil, the first results with PIXE were related to atmosphere pollution in the eighties, at the Physics Institute from Sao Paulo. Since then, many different issues were addressed to PIXE also in Porto Alegre and Rio de Janeiro. The aim of this work is to show and discuss the main aspects of PIXE and its applications in Brazil, focusing research programs, related problems and trends. Since its beginning, the capabilities of PIXE pushed the technique to different applications in the field of biomedical, toxicology of ecosystems and contamination aspects of food and inorganic materials in general. For example, PIXE became a good option to study food and beverage processing, because the composition of a range of elements can be determined during different stages of the processes using basically one analytical technique. By its interdisciplinary feature, the PIXE community has been working closely with biologists and researchers from related areas to investigate, for instance, the role of elements during neurophysiological processes, neurodegenerative diseases, and if some elements could be used as biological markers for cancer diseases like melanoma. However, multidisciplinary research poses several challenges, especially a better channel of communication between PIXE community and researchers from these different fields. Other PIXE applications in Brazil are the analyses and study of artworks and cultural heritage objects; environmental pollution and ecosystem toxicological exposure. The PIXE perspectives and trends including the external beam and microprobe setup, which one could be combined with others ion beam techniques in order to provide a complete set of information regarding the material molecular and elemental composition, structure and morphology.

Abstract 259 THU-IBA07-4

[Contributed Talk - Thursday 10:00 AM - Bowie B](#)

Large area transition-edge sensor array for particle induced X-ray emission spectroscopy

[Mikko Palosaari¹](#), [Kimmo Kinnunen¹](#), [Ilari Maasilta¹](#), [C Reintsema²](#), [D Schmidt²](#), [J Fowler²](#), [R Doriese²](#), [Joel Ullom²](#), [Marko Käyhkö¹](#), [Jaakko Julin¹](#), [Mikko Laitinen¹](#), [Timo Sajavaara¹](#)

⁽¹⁾*Department of Physics, University of Jyväskylä, P.O. Box 35, Jyväskylä 40014, Finland*

⁽²⁾*National Institute of Standards and Technology, Boulder CO 80305, United States*

Transition-edge sensors (TES) have matured to the state that they are used in number of applications, thanks to their superior energy resolution and sensitivity. Here we present a new measurement setup, where TES detector arrays are used to detect X-rays in Particle Induced X-ray Emission (PIXE) using proton and He beams from 1.7 MV Pelletron accelerator in Jyväskylä, Finland. The energy resolution of a TES detector, when used in PIXE, is over an order of magnitude better compared to conventional Si or Ge based detectors. This makes it possible to recognize spectral lines in materials analysis that have previously been impossible to resolve, and even resolve chemical information from the analyzed sample. Our 160 sensors with total area of 15.6 mm² are cooled to the operation temperature of about 100 mK with a cryogen-free Adiabatic Demagnetization Refrigerator (ADR), with a special X-ray snout designed at NIST. The read-out consists of a 256 pixel time-division NIST SQUID multiplexer.

In this paper the Jyväskylä TES detector will be described, and the analysis results from the reference materials (NIST SRM 611 and SRM 1157) and especially from atomic layer deposited thin films will be presented. The potential applications of TES-PIXE having measured energy resolution of about 3 eV will also be discussed.

Abstract 33 THU-IBA07-5

[Contributed Talk - Thursday 10:00 AM - Bowie B](#)

Using PIXE study Alzheimer Disease induced by neo natal iron administration model in rats.

[Paulo Fernandes Costa Jobim¹](#), [Carla Eliete Iochims Dos Santos³](#), [Denise Puglia¹](#), [Tatiele Ferrarri¹](#), [Nadia Schroder²](#), [Noemia Albuquerque²](#), [Betânia Melo Cambrielina²](#), [Johnny Ferraz Dias¹](#)

⁽¹⁾Physics Institute, UFRGS, Bento Gonçalves, 9500, Porto Alegre Rio Grande do Sul 91501-970, Brazil

⁽²⁾Biosciences Institute, PUCRS, Ipiranga, 6681, Porto Alegre Rio Grande do Sul 90619-900, Brazil

⁽³⁾Physics Institute, USP, Rua do Matão, 187, São Paulo São Paulo 05314-970, Brazil

Iron, the most abundant metal in the human body, is essential for many key biological processes related to development of the nervous system. Studies have shown that iron deficiency during neurological development leads to permanent cognitive deficits. However, clinical and experimental evidence suggest a role of iron excess in neurodegenerative diseases. An abnormal iron homeostasis might triggering factor for different neurodegenerative disorders such as Parkinson's and Alzheimer's. Some studies suggested that memory dysfunction associated with iron treatment may be viewed as a model of cognitive decline related to neurodegenerative disorders. Thus, we use PIXE to confirm such suggestion. To do that neonatal iron treatment was made when the animals achieved 12 day old by the oral administration of a daily dose of iron 35 mg/kg and 75mg/kg or vehicle (control group). When the animals became adults, 3 months later, they were submitted to perfusion process with saline to washing out their blood and their brains were quickly removed and carefully dissected. The hippocampal and cortical region were dried in an oven at 100 °C for approximately 3h. The X-rays emitted from the samples were detected by a Si (Li) detector with an energy resolution of about 160 eV at 5.9 keV. The present study made use of the bovine liver standard from the National Institute of Standards and Technology (NIST reference material 1577b) for standardization purposes. The PIXE spectra were fitted as thick samples by the GUPIXWIN software package in order to obtain the elemental concentrations. The results presented here shows that iron accumulation in cortex is significant higher in 75mg/kg group, but not 35mg/kg group, in comparison with control group. Additional preclinical and clinical studies are necessary for further support the applicability of PIXE to quantification of iron and other heavy metals in the brain associated to neurodegenerative disorders.

Abstract 113 THU-IBA07-6

[Contributed Talk - Thursday 10:00 AM - Bowie B](#)

Commissioning and first applications of a new Mexican beam extraction device for PIXE analysis in air.

[Efraín Rafael Chávez](#)¹, [Eduardo Andrade](#)¹, [Oscar Genaro de Lucio](#)¹, [Arcadio Huerta](#)¹, [Francisco Favela](#)¹, [corina Solís](#)¹, [Edgar Adán Jiménez](#)¹, [Hesiquio Vargas](#)¹, [Rafael Policroniades](#)², [Ghivaldo Murillo](#)², [Eliud Moreno](#)², [Armando Varela](#)³, [Javier Miranda](#)^{3,4}

⁽¹⁾Instituto de Física, Universidad Nacional Autónoma de México, Av. Universidad 3000, Ciudad Universitaria S/N, Coyoacán D. F. 04510, Mexico

⁽²⁾Departamento de Aceleradores, Instituto Nacional de Investigaciones Nucleares, Carretera México Toluca S/N, Ocoyoacac México 52750, Mexico

⁽³⁾Centro de Ciencias de la Atmósfera, Universidad Nacional Autónoma de México, Av. Universidad 3000, Ciudad Universitaria S/N, Coyoacán D. F. 04510, Mexico

⁽⁴⁾Permanent Address: Instituto de Física, Universidad Nacional Autónoma de México, Av. Universidad 3000, Ciudad Universitaria S/N, Coyoacán D. F. 04510, Mexico

As part of the modification of the peripheral instrumentation around the 5.5 CN-Van de Graaff Laboratory of the "Instituto de Física" at the "Universidad Nacional Autónoma de México" (IFUNAM), one of the beam lines recently made available thanks to the installation of a switching magnet, has been equipped with a beam extraction device.

This device was designed, constructed, tested and commissioned by our group.

In this work, the device is presented along with the first applications to material characterization by particle induced X-Ray Emission (PIXE).

Abstract 319 THU-IBM03-1

[Invited Talk - Thursday 10:00 AM - Bonham C](#)

Application of Atom Probe Tomography For Studying Irradiation Damage, Ion Beam Implantation, and Related Subjects

[Robert M. Ulfing](#), [David J. Larson](#), [Ty J. Prosa](#), [Thomas F. Kelly](#)

CAMECA Instruments Inc., 5500 Nobel Drive, Madison WI 53711, United States

Atom Probe Tomography (APT) was and still is a key analytical technique for the development of high performance alloys, especially for turbines used in power plants and aerospace applications. Recent performance improvements have widened the application of the technique beyond metallic specimens into a wide variety of applications and its inherent three-dimensional sub-nanometer chemical and isotopic characterization make it uniquely suited to investigate nanoscale changes in materials due to irradiation damage. Here we will review the application of APT and APT data analysis techniques to characterize ion beam and irradiation damage in radiation damage resistant metals, ceramics, and other materials. Analytical methods inherent to APT to characterize cluster composition, density, and growth as well as interface segregation, will be reviewed.

Abstract 416 THU-IBM03-2

[Invited Talk - Thursday 10:00 AM - Bonham C](#)

Chemical analysis on nanoscale using synchrotron based soft X-ray scanning microscopes

[Tolek Tyliczszak](#)

Advanced Light Source, Lawrence Berkeley National Laboratory, 1 Cyclotron Rd. MS 6-2100, Berkeley California 94720, United States

Modern synchrotrons can produce intense and highly coherent X-ray beam. X-ray absorption very much depends on the elemental and chemical speciation of the absorbing sample. Coherent, intense synchrotron radiation can be focus to a relatively small spots allowing using X-ray absorption for chemical analysis on nanoscale. Soft X-rays are especially attractive because of its relatively high sensitivity to chemical bonding for light elements.

At the Advanced Light Source, there are four soft X-ray scanning microscopes, which can do the chemical analysis. A typical spatial resolution is about 20 nm for imaging and about 50 nm for chemical analysis. In last few years, there is a new development of combining scanning microscopy with a recording a diffraction pattern at each point. Because the focused beam is coherent, the diffraction patterns can be reconstructed to significantly enhance the spatial resolution. This new technique, called ptychography, can result in demonstrated images with down to 3 nm resolution and 6 nm for the chemical analysis.

Status of the soft X-ray spectromicroscopy will be presented on examples from environmental science, polymer science, catalyst research, atmospheric research, cometary research and geological research. Special emphasize will be given on in-situ and in-operando measurements of batteries and fuel cells. Important aspect of radiation damage during soft X-ray spectromicroscopy measurements in comparison with energy loss TEM chemical mapping will be also discussed.

Abstract 87 THU-IBM03-3

[Invited Talk - Thursday 10:00 AM - Bonham C](#)

Time-of-Flight Secondary Ion Mass Spectrometry: a Unique Tool for Characterization of Ion Beam Modified Materials

[Zihua Zhu](#)¹, [Weilin Jiang](#)², [Ke Jin](#)³, [Yanwen Zhang](#)^{3,4}

⁽¹⁾*Environmental Molecular Sciences Laboratory, Pacific Northwest National Laboratory, P.O. Box 999, Richland WA 99354, United States*

⁽²⁾*Energy and Environment Directorate, Pacific Northwest National Laboratory, P.O. Box 999, Richland WA 99354, United States*

⁽³⁾*Department of Materials Science & Engineering, University of Tennessee, Knoxville TN 37996, United States*

⁽⁴⁾*Materials Science & Technology Division, Oak Ridge National Laboratory, Oak Ridge TN 37831, United States*

Rutherford backscattering (RBS) and other ion beam-related analysis techniques (e.g., elastic recoil detection analysis (ERDA) and nuclear reaction analysis (NRA)) have been among the most popular techniques to characterize the depth profile of implanted ions. However, RBS has several limitations. For example, (1) it is difficult to distinguish elements with similar masses (e.g., ⁹⁰Zr in SrTiO₃), and (2) it is hard to measure light elements in high mass matrix. Time-of-flight secondary ion mass spectrometry (ToF-SIMS) has been used in characterizing depth distribution of implanted ions for more than twenty years. Compared to RBS, ToF-SIMS has several unique advantages. First, ToF-SIMS can provide high mass resolution ($M/DM > 10000$), so mass interference is normally not a problem. Second, 10 microns depth profiling is feasible for ToF-SIMS, but RBS can only go 1-2 microns deep. In addition, depth resolution of ToF-SIMS can go down to sub-nanometer, and sensitivity of ToF-SIMS is approximately 1-3 orders of magnitude better than RBS (element dependent), which make ToF-SIMS one of the best tools for performing ultra-shallow depth profiling. The major drawback of ToF-SIMS depth profiling is quantification. Matrix effect makes SIMS quantification not straightforward. Therefore, ToF-SIMS and RBS can be regarded as complementary techniques in characterizing depth distribution of implanted ions. Interesting results have been demonstrated when combining these two analytical techniques. In this talk, several representative examples will be presented and discussed.

Abstract 347 THU-IBM03-4

[Invited Talk - Thursday 10:00 AM - Bonham C](#)

Phase stability and microstructure evolution of the metal-oxide multilayer Fe/Cr-TiO₂-Fe/Cr nanocomposite under ion irradiation

[Nan Li](#)¹, [Yun Xu](#)², [Jeffery Aguiar](#)², [Jon Baldwin](#)¹, [Yongqiang Wang](#)², [Anderoglu Osman](#)², [Amit Misra](#)¹, [Blas Ueberuaga](#)²

⁽¹⁾*MPA-CINT, Los Alamos National Laboratory, Los Alamos, Los Alamos NM 87545, United States*

⁽²⁾*MST-8, Los Alamos National Laboratory, Los Alamos, Los Alamos NM 87545, United States*

Metal-oxide multilayer thin film nanocomposite was used as a simple model for oxide-dispersion- strengthened (ODS) steels. To study the phase stability of the composite film, it was irradiated with 10MeV Ni³⁺ ions at temperature 500 °C to dose of 10dpa. Microchemistry and microstructure evolution of metal/oxide multilayer was investigated using High resolution TEM and STEM-EDS. At Fe/Cr-TiO₂ interface, amorphous domain was detected in TiO₂ layer, while Fe/Cr layer stay the same crystalline structure as the pristine sample. Interdiffusion of chromium into TiO₂ layer was detected by STEM-EDS, which could possibly contribute to the amorphization of TiO₂ after irradiation. The knowledge obtained from this work provides guidelines for designing metal-oxide composite with desired radiation tolerance under irradiation.

Abstract 93 THU-NBA03-1

[Invited Talk - Thursday 10:00 AM - Bonham B](#)

Introduction and Survey of laser-Compton gamma-ray Source Development for Nuclear Photonics

[Christopher P. J. Barty](#)

NIF & Photon Science Directorate, Lawrence Livermore National Laboratory, P. O. Box 808, L-580, Livermore CA 94551, United States

Tunable, polarized, mono-energetic, gamma-ray beams may be created via the optimized Compton scattering of pulsed lasers off of ultra-bright electron beams. Above 2 MeV, the peak brilliance of these sources can exceed that of the world's largest synchrotrons by more than 15 orders of magnitude. For the first time the efficient pursuit of nuclear science and applications with photon beams, i.e. Nuclear Photonics is becoming possible. Potential applications are numerous and

include isotope-specific nuclear materials management, element-specific medical radiography and radiology, non-destructive, isotope-specific, material assay and imaging, precision spectroscopy of nuclear resonances and photon-induced fission. This presentation will review the optimization of laser-Compton light sources and applications, introduce the methods by which these sources may be used for nuclear safeguards and nuclear security, and review plans and status of large-scale activities at the Lawrence Livermore National Laboratory in California, KEK in Japan and the Extreme Light Infrastructure - Nuclear Physics facility in Europe.

Abstract 206 THU-NBA03-2

[Invited Talk - Thursday 10:00 AM - Bonham B](#)

Dense Plasma Focus Z-Pinch: A Short-Pulse Neutron Source Concept for Active Interrogation

[Andrea Schmidt](#)¹, [Jennifer Ellsworth](#)¹, [Steve Falabella](#)¹, [Anthony Link](#)¹, [Brian Rusnak](#)¹, [Jason Sears](#)¹,
[Vincent Tang](#)¹, [David Rose](#)², [Dale Welch](#)²

⁽¹⁾*National Security Engineering Division, Lawrence Livermore National Lab, 7000 East Ave L-227, LIVERMORE California 94550, United States*

⁽²⁾*Voss Scientific LLC, 418 Washington St. SE, Albuquerque New Mexico 87108, United States*

The Z-pinch phase of a dense plasma focus (DPF) operated with deuterium or DT gas emits a short (10s of nanoseconds), bright pulse of neutrons. Table-top versions of this device, with ~kJ-scale capacitor banks emit $\sim 10^7$ neutrons in a single deuterium pulse [1], (peak $> 10^{14}$ n/s). Megajoule DPFs emit $\sim 10^{12}$ neutrons in a deuterium pulse (peak $> 10^{19}$ n/s). This makes the DPF an ideal active interrogation source for innovative assay techniques such as differential die-away and active coincidence counting, recently proposed for treaty verification. DPFs use refillable gas targets, enabling DD and DT modes on the same device. Additionally, the DPF neutron source has ~2mm spot size and could provide a new approach for high-resolution neutron transmission imaging. Historically, DPF devices have been empirically optimized because they are governed by complex physical processes that are difficult to model. We recently developed the first fully kinetic model of a DPF device [2], successfully predicting neutron yields, ion beam energies, and ~GHz EM oscillations which past fluid simulations have not reproduced. We can now use this predictive capability to vary electrode shape, drivers, and impurities to optimize and tailor the DPF output for specific applications.

This work performed under the auspices of the U.S. Department of Energy by Lawrence Livermore National Laboratory (LLNL) under Contract DE-AC52-07NA27344 and supported by the Laboratory Directed Research and Development Program (11-ERD-063) at LLNL. This work supported by Office of Defense Nuclear Nonproliferation Research and Development within U.S. Department of Energy's National Nuclear Security Administration, and the Defense Advanced Research Programs Agency. Computing support for this work came from the LLNL Institutional Computing Grand Challenge program. The views expressed are those of the author and do not reflect the official policy or position of the Department of Defense or the U.S. Government. [1]J. Ellsworth, RSI, 2014. [2]A. Schmidt, PRL, 2012.

Abstract 444 THU-NBA03-3

[Contributed Talk - Thursday 10:00 AM - Bonham B](#)

Accelerators for Discovery Science and Security Applications

[Alan Todd](#), [Hans Bluem](#), [Jangho Park](#), [John Rathke](#), [Tom Schultheiss](#)

Advanced Energy Systems, 27 Industrial Boulevard, Unit E, Medford New York 11763, United States

Several ongoing Advanced Energy Systems (AES) accelerator projects that span applications in Discovery Science to Security are described. The design and performance of the IR and THz free electron laser (FEL) at the Fritz-Haber-Institut der Max-Planck-Gesellschaft in Berlin that is now an operating user facility for Physical Chemistry research in molecular and cluster spectroscopy as well as surface science, will be highlighted. The device was designed to meet challenging specifications, including a final energy adjustable in the range of 15 to 50 MeV, low longitudinal emittance (< 50 keV-psec) and transverse emittance ($< 20 \pi$ mm-mrad), at more than 200 pC bunch charge with a micropulse repetition

rate of 1 GHz and a macropulse length of up to 15 μ s. Secondly, we will describe an ongoing effort to develop an ultrafast electron diffraction (UED) source that is scheduled for completion in 2015 with prototype testing taking place at the BNL ATF facility. This tabletop X-band system will find application in time-resolved chemical imaging and as a resource for drug-cell interaction analysis. A third active area at AES is accelerators for security applications where we will cover some top-level aspects of systems that are under development and in testing for stand-off and portal detection.

Abstract 76 THU-NBA03-4

[Contributed Talk - Thursday 10:00 AM - Bonham B](#)

Improved Neutron Capture Gamma-Ray Data and Evaluation

[M. S. Basunia](#)¹, [F. Becvar](#)², [T. Belgia](#)⁶, [L. Bernstein](#)^{1,7}, [H. Choi](#)³, [J. Escher](#)⁷, [R. Firestone](#)¹, [Ch. Genreith](#)⁸, [F. Gunsing](#)⁵, [A. Hurst](#)¹, [M. Krticka](#)², [Zs. Revay](#)⁴, [M. Rossbach](#)⁸, [N. Summers](#)⁷, [L. Szentmiklosi](#)⁶, [B. Sleaford](#)⁷

⁽¹⁾Lawrence Berkeley National Laboratory, 1 Cyclotron Rd., Berkeley CA 94720, United States

⁽²⁾Faculty of Mathematics and Physics, Charles University in Prague, Prague, Czech Republic

⁽³⁾Nuclear Engineering Department, Seoul National University, Seoul, Korea

⁽⁴⁾Forschungszentrum Heinz Maier-Leibnitz (FRM II), Technische Universität, Munich, Germany

⁽⁵⁾CEA, Saclay, France

⁽⁶⁾Centre for Energy Research, Hungarian Academy of Sciences, Budapest, Hungary

⁽⁷⁾Lawrence Livermore National Laboratory, Livermore CA 94550, United States

⁽⁸⁾Safety Research and Reactor Technology, IEK-6, Institute for Energy and Climate Research, Juelich, Germany

The neutron-capture reaction is of fundamental use in identifying and analyzing the gamma-ray spectrum from an unknown object as it gives a fingerprint of which isotopes are present. Many isotopes have capture gamma lines from 5-10 MeV potentially making them easier to see. There are data gaps in the Evaluated Nuclear Data File (ENDF) libraries used by modeling codes (the actinides have no lines for example) and we are filling these with the Evaluated Gamma-ray Activation File (EGAF), a reactor measured database of lines and cross sections for over 260 isotopes. For medium to heavy nuclei, the unresolved part of the gamma cascades are not measured and are modeled using the statistical nuclear structure code Dicebox. ENDF libraries require cross sections for neutron energies up to 20 MeV and we plan to continue this approach through the resolved resonance region. Some benchmarking with gamma spectra from neutron time of flight experiments is possible but data is very limited. In the unresolved resonance and high energy regions, are using Hauser-Feshbach modeling to predict the cross sections of capture gamma spectra in regions where multiple competing output channels are open. This work is performed in part under the auspices of the U.S. Department of Energy by Lawrence Livermore National Laboratory under Contract DE-AC52-07NA27344.

Abstract 358 THU-NBA03-5

[Contributed Talk - Thursday 10:00 AM - Bonham B](#)

Determining isotopic concentrations using delayed gamma-rays from active inspection techniques for nuclear materials safeguards

[Alan W Hunt](#)^{1,2}, [Edward T. E. Reedy](#)², [Vladimir Mozin](#)³, [Bernhard A. Ludewigt](#)⁴, [Heather A. Seipel](#)², [Edna S. Cardenas](#)², [Mike Smith](#)¹, [Andrea Favalli](#)⁵, [Metodi Iliev](#)⁵

⁽¹⁾Idaho Accelerator Center, Idaho State University, Stop 8263, Pocatello ID 83209-8263, United States

⁽²⁾Department of Physics, Idaho State University, Stop 8106, Pocatello ID 83209-8106, United States

⁽³⁾Lawrence Livermore National Laboratory, 7000 East Ave., Livermore CA 94550, United States

⁽⁴⁾Lawrence Berkeley National Laboratory, 1 Cyclotron Rd., Berkeley CA 94720, United States

⁽⁵⁾Los Alamos National Laboratory, Los Alamos NM 87545, United States

There has been a substantial research and development effort into active inspection technologies that can nondestructively detect, identify and quantify special nuclear materials for advanced safeguards and nuclear forensics applications. These active inspection technologies use a probing radiation source to stimulate fission reactions and then monitor for secondary emissions as a direct signature of fissile or fertile materials. In this presentation, results of delayed gamma-ray

spectroscopy measurements will be demonstrated from the active inspection of samples containing ^{235}U , ^{239}Pu or a combination of the two. On average, seven delayed gamma-rays are emitted per fission reaction on timescales that range from hundreds of milliseconds out to years. Since the fission fragment distribution is dependent on the fissioning isotope, the discrete delayed gamma-ray lines provide a fingerprint of the interrogated material, allowing the determination of isotopic content. Fission in the targets was induced by thermalized neutrons created by a pulsed electron linac with maximum energy of 25 MeV and a ^9Be neutron converter. A mechanically cooled HPGe detector collected delayed gamma-ray spectra between irradiation periods. Using advanced accelerator controls, the irradiation/detection periods could be varied from tens of milliseconds to hours, thereby emphasizing the shorter or longer lived fission fragments. In particular, the goal was to find irradiation/detection time structures, which produced spectra with pronounced differences in the discrete gamma-ray lines from the fission of ^{235}U and ^{239}Pu . Spectra from the longer time structures (e.g. 15/15 min irradiation/detection) had a plethora of discrete delayed gamma-ray lines from Rb isotopes, indicating the fission of ^{235}U but lacked strong lines emphasizing the fission of ^{239}Pu . With shorter time structures (e.g. 90/90 s irradiation/detection), the presence of ^{239}Pu was identified by discrete gamma-rays from the decay of ^{106}Tc . Using these unique gamma-rays, the isotopic content of the target containing the two different isotopes can be determined.

Abstract 51 THU-NBA03-6

[Contributed Talk - Thursday 10:00 AM - Bonham B](#)

Modeling of Time Correlated Detection of Fast Neutrons Emitted in Induced SNM Fission

[Amber Guckes](#), [Alexander Barzilov](#), [Norman Richardson](#)

Mechanical Engineering, University of Nevada, Las Vegas, 4505 S Maryland Parkway, Las Vegas NV 89154, United States

Neutron multiplicity methods are widely used in assay of fissile materials. Fission reactions can release multiple neutrons simultaneously. Time correlated detection of neutrons by surrounding sensors provides a coincidence signature unique to fission events and thus enables to distinguish it from other events. Fission neutrons are mainly fast. Thermal neutron sensors require moderation of neutrons prior to a detection event; therefore, the neutron's energy and event's timing information may be distorted resulting in the wide time windows in the correlation analysis. Fast neutron sensing using scintillators allows shortening the time correlation window. Four detectors based on the EJ-299-33A plastic scintillator with neutron / photon pulse shape discrimination properties were modeled in MCNP6 as fast neutron sensors. The fast neutron detection using this sensor array was studied for the induced fission of Pu-239, U-235 and (alpha,n) neutron sources. It was observed that when the detectors are exposed to the fission source, double and triple coincidences occur. This talk will focus on results of computational modeling of time correlated detection of neutrons emitted in induced fission of SNM by plastic scintillator sensors and He-3 detectors equipped with a moderator.

Abstract 343 THU-NP08-1

[Invited Talk - Thursday 10:00 AM - Travis C/D](#)

Long-term detector upgrade plans for RHIC and eRHIC

[Jin Huang](#)

Physics Department, Brookhaven National Laboratory, Bldg 510 C, Upton New York 11973, United States

The Relativistic Heavy Ion Collider (RHIC) at Brookhaven National Laboratory collides a large variety of heavy ion species and provides the only spin-polarized proton collisions in the world. Currently, two experiments, PHENIX and STAR, are operating at RHIC. Both of them have planned for detector upgrades within the next ten years that would provide complementary new detection capabilities in order to study hot and cold nuclear matter. The PHENIX collaboration has proposed a major upgrade, the sPHENIX detector, which consists of large acceptance electromagnetic and hadronic calorimetry built around the superconducting solenoid magnet that was recently acquired from the decommissioned BaBar experiment at SLAC. The STAR collaboration proposes to strengthen its forward detection capability with additional instrumentation consisting of tracking, particle ID and calorimetry. With the addition of a high intensity electron beam, an realization of an electron-ion collider (EIC), eRHIC, is envisioned to begin operation around 2025, that will provide spin-polarized e+p and e+A collisions and allow exploring new frontiers in hadronic structure and dense nuclear matter. Both sPHENIX and STAR have plans to evolve into eRHIC detectors and distinct technology choices for new instrumentation in

the electron-going, barrel and hadron-going directions were proposed to enhance their capabilities in e+P and e+A collisions. In addition, a new major detector is also being proposed to utilize the full physics capability of eRHIC in the future. In this talk, I will describe the detector designs and performance studies for each of these projects.

Abstract 433 THU-NP08-2

[Invited Talk - Thursday 10:00 AM - Travis C/D](#)

The Electron-Ion Collider (EIC) project at Jefferson Lab

[Pawel Nadel-Turonski](#)

Physics, Jefferson Lab, 12000 Jefferson Ave, Newport News VA 23185, United States

The Electron-Ion Collider (EIC) is envisioned as the next-generation US facility for exploring the strong interaction, aimed at mapping the spin- and spatial structure of the quark- and gluon sea in the nucleon, understanding the emergence of hadronic matter from color charge, and probing the gluon fields in nuclei. Both Jefferson Lab and Brookhaven are developing implementations supporting the full generic EIC program, and collaborate on, for instance, detector R&D. The EIC at JLab would use the recently upgraded 12 GeV CEBAF as a full-energy lepton injector. It will use innovative design, such as a figure-8 ring layout for improved spin control (allowing polarized deuterium), but try to minimize the technical risks. The first stage, called the Medium-energy EIC (MEIC) will provide kinematic coverage for the full range between JLab 12 GeV and HERA (or a future LHeC). A key feature of the MEIC is an extended detector and interaction region fully integrated with the accelerator (which is designed around it). The goal for the full-acceptance detector is to measure the complete final state. In particular, it will tag spectators with a resolution \ll than the Fermi momentum, catch all nuclear and partonic target fragments, and to provide a wide coverage in $-t$ for recoil baryons from exclusive (diffractive) reactions at all beam energies. The combination of a high luminosity, polarized lepton and ion beams, and full-acceptance detectors fully will make the EIC a quantum leap in our understanding of the fundamental structure of matter.

Abstract 369 THU-NP08-3

[Contributed Talk - Thursday 10:00 AM - Travis C/D](#)

Detector Development for Jefferson Lab's 12 GeV Upgrade

[Yi Qiang](#)

Physics, Jefferson Lab, 12000 Jefferson Ave, Newport News VA 23606, United States

Jefferson Lab will soon finish its highly anticipated 12 GeV upgrade. With doubled maximum energy, Jefferson Lab's Continuous Electron Beam Accelerator Facility (CEBAF) will enable new experimental program with substantial discovery potential to address important topics in nuclear, hadronic and electroweak physics. In order to take the full advantage of the high energy high luminosity beam, new detectors are being developed, designed and constructed to fit the needs of different physics topics. The talk will give an overview of various new detector technologies to be used for 12 GeV experiments. It will then focus on the development of two solenoid based spectrometers, the GlueX and SoLID spectrometers. The GlueX experiment in Hall-D will study the complex properties of gluons through exotic hybrid meson spectroscopy, and is currently in the final stage of assembling the whole new GlueX spectrometer with hermetic detector package particularly designed for spectroscopy and the associated partial wave analysis. Hall-A, on the other hand, is developing the SoLID spectrometer to capture the 3D image of the nucleon from semi-inclusive processes and also study the intrinsic property of quarks through mirror symmetry breaking. Such a spectrometer will have the capability to handle very high event rate while still maintain a large acceptance in the forward region.

Abstract 356 THU-NP08-4

[Contributed Talk - Thursday 10:00 AM - Travis C/D](#)

Future upgrades for the PHENIX Experiment at RHIC: From PHENIX to sPHENIX and beyond

[Achim Franz](#)

Physics Department, Brookhaven National Laboratory, 510C, Upton NY 11973-5000, United States

A series of major upgrades are being planned for the PHENIX experiment at the Relativistic Heavy Ion Collider (RHIC) to enable a comprehensive measurement of jets in relativistic heavy ion collisions in order to study the phase transition of normal nuclear matter to the Quark Gluon Plasma near its critical temperature. These upgrades will include a number of major new detector systems. The former BaBar solenoid magnet will be incorporated in the first stage, sPHENIX, and will include two new large calorimeters, one electromagnetic and another hadronic, for measuring jets in heavy ion collisions. These calorimeters will cover a region of ± 1.1 in pseudorapidity and 2π in phi, and will result in a factor of 6 increase in acceptance over the present PHENIX detector. The HCAL will be based on scintillator plates interspersed between steel absorber plates that are read out using wavelength shifting fibers. It will have a total depth of $\sim 5 \lambda_{\text{abs}}$ that will be divided into two longitudinal sections, and will have an energy resolution $\sim 50\%/\sqrt{E}$ for single particles and $<100\%/\sqrt{E}$ for jets. The EMCAL will be a tungsten - scintillating fiber design, and will have a depth of $\sim 17 X_0$ and an energy resolution of $\sim 15\%/\sqrt{E}$. Both calorimeters will be read out using silicon photomultipliers and waveform digitizing electronics. This talk will discuss the evolution of the current PHENIX detector to sPHENIX and beyond, the R&D that is being pursued to develop the various detectors that will be needed, and the opportunities and challenges for each of their technologies, with emphasis on the central electromagnetic and hadronic calorimeters for sPHENIX, including results from a recent beam test of prototypes of both of these detectors at Fermilab.

Abstract 322 THU-NP08-5

[Contributed Talk - Thursday 10:00 AM - Travis C/D](#)

A MAPS based micro-vertex detector for the STAR experiment

[Joachim Schambach](#)¹, [Eric Anderssen](#)², [Giacomo Contin](#)², [Leo Greiner](#)², [Joe Silber](#)², [Thorsten Stezelberger](#)², [Xiangming Sun](#)², [Michal Szelezniak](#)³, [Flemming Videbaek](#)⁴, [Chinh Vu](#)², [Howard Wieman](#)², [Sam Woodmansee](#)²

⁽¹⁾*Physics Department, University of Texas at Austin, Austin TX 78712, United States*

⁽²⁾*Nuclear Science Division, Lawrence Berkeley Nation Lab, Berkeley CA 94720, United States*

⁽³⁾*Institut Pluridisciplinaire Hubert Curien, Strasbourg, France*

⁽⁴⁾*Brookhaven National Lab, Upton NY 11973, United States*

For the 2014 heavy ion run of RHIC a new micro-vertex detector called the Heavy Flavor Tracker (HFT) was installed in the STAR experiment. The HFT consists of three detector subsystems with various silicon technologies arranged in 4 approximately concentric cylinders close to the STAR interaction point designed to improve the STAR detector's vertex resolution and extend its measurement capabilities in the heavy flavor domain. The two innermost HFT layers are placed at a radius of 2.7 cm and 8 cm from the beam line. These layers are constructed with 400 high resolution sensors based on CMOS Monolithic Active Pixel Sensor (MAPS) technology arranged in 10-sensor ladders mounted on 10 thin carbon fiber sectors to cover a total silicon area of 0.16 m². Each sensor of this PiXeL ("PXL") sub-detector combines a pixel array of 928 rows and 960 columns with a 20.7 μm pixel pitch together with front-end electronics and zero-suppression circuitry in one silicon wafer providing a sensitive area of $\sim 3.8 \text{ cm}^2$. This sensor technology features 185.6 μs readout time and 170 mW/cm² power dissipation. This low power dissipation allows the PXL detector to be air-cooled, and with the sensors thinned down to 50 μm results in a global material budget of only 0.37% radiation length per layer. A novel mechanical approach to detector insertion allows to effectively install and integrate the PXL sub-detector within a 12 hour period during an on-going STAR run. The detector requirements and the different aspects of its production as well as the performance after installation will be presented in this talk.

Abstract 130 THU-NST04-1

[Invited Talk - Thursday 10:00 AM - Bonham D](#)

Real Time Observation of He Implantation, High-Energy Si Irradiation, and Self-ion Irradiation of Nanocrystalline Au

[Khalid Hattar](#)¹, [Claire Chisholm](#)^{2,3}, [Daniel Bufford](#)¹, [Andrew M. Minor](#)^{2,3}

⁽¹⁾*Radiation Solid Interactions, Sandia National Laboratories, PO Box 5800, Albuquerque NM 87185, United States*

⁽²⁾*Department of Material Science and Engineering, University of California, Berkeley, 210 Hearst Mining Building, Berkeley CA 94720, United States*

⁽³⁾*National Center for Electron Microscopy, Lawrence Berkeley National Laboratory, 1 Cyclotron Rd, Berkeley CA 94720, United States*

Understanding the dynamics of structural evolution that occurs in nanocrystalline metals during exposure to various forms of radiation is important in both predicting the radiation tolerance of the metal and optimizing the parameters for ion beam modification. This presentation will highlight the utility of using **in situ** ion irradiation transmission electron microscopy (I³TEM) to study the resulting structural evolution, as a function of ion beam conditions in a model nanocrystalline system; annealed physical vapor deposited, electron transparent, gold thin films. Three extreme irradiation conditions will be demonstrated in this presentation: 10 keV He implantation, 2.8 to 3.6 MeV Au irradiation, and 48 MeV Si irradiation. The 10 keV He implantation should impart minimal displacement damage, and ions should stop within the TEM foil. Accordingly, it was found that the evolution of He bubbles was highly dependent on dose rate at room temperature, but at nearly all dose levels bubbles could be formed via post implantation annealing. In contrast, the Au ions should impart the most displacement damage, and thus resulted in isolated or overlapping cascade events with multiple defect clusters per cascade. Finally, the 48 MeV Si experiments predominantly resulted in the formation of a single defect structure per observable ion strike approaching that of ion track conditions. This presentation will conclude with a current status of the I³TEM facility at Sandia National Laboratories and vision for its application to other nanostructured systems of relevance.

This research was partially funded by the U.S. Department of Energy, Office of Science, Office of Basic Energy Sciences, Division of Materials Sciences and Engineering. Sandia National Laboratories is a multi-program laboratory managed and operated by Sandia Corporation, a wholly owned subsidiary of Lockheed Martin Corporation, for the U.S. Department of Energy's National Nuclear Security Administration under contract DE-AC04-94AL85000.

Abstract 311 THU-NST04-2

[Contributed Talk - Thursday 10:00 AM - Bonham D](#)

Ultrafine grained T91 steel processed by equal channel angular extrusion and their response to heavy ion irradiation

[Miao Song](#)¹, [Xinghang Zhang](#)^{1,2}, [Karl T Hartwig](#)^{1,2}

⁽¹⁾*Department of materials science and engineering, Texas A&M University, College station TEXAS 77843, United States*

⁽²⁾*Department of mechanical engineering, Texas A&M University, College station TEXAS 77843, United States*

We investigated the microstructure and radiation response of T91 steel subjected to equal channel angular extrusion (ECAE). ECAE was performed at 300 and 625 °C up to 2 passes. The microstructure varied significantly with the processing condition. Heavy ion irradiation up to $9 \times 10^{16}/\text{cm}^2$ at 450°C is also performed. The UFG T91 processed by ECAE show less defect and swelling compared to their coarse grained counterpart. These observations are explained through competition of point defects between GBs and free surfaces, and a GB modified injected interstitial concept.

Abstract 495 THU-NST04-3

[Invited Talk - Thursday 10:00 AM - Bonham D](#)

Response of nanotwinned metals to heavy ion irradiation

[Kaiyuan Yu](#)

Texas A&M University, College Station TX 77842, United States

We report the response of nanotwinned metals to heavy ion irradiation, including the removal of stacking fault tetrahedral by twin boundaries and the variation of coherent and incoherent twin boundaries. Stacking fault tetrahedra are detrimental defects in neutron or proton irradiated structural metals with face-centered-cubic structures, and their removal is very challenging. We present an alternative solution to remove stacking fault tetrahedra discovered during room-temperature, **in situ** Kr ion irradiation of epitaxial nanotwinned Ag with an average twin spacing of ~ 8 nm. A large number of stacking fault tetrahedra are removed during their interactions with abundant coherent twin boundaries. Consequently the density of stacking fault tetrahedra in irradiated nanotwinned Ag is much lower than that in its bulk counterpart. Two fundamental interaction mechanisms are identified, and compared to predictions by molecular dynamics simulations. **In situ** studies also reveal a new phenomenon: radiation induced frequent migration of coherent and incoherent twin boundaries. Such twin boundary migration is closely correlated to the absorption of radiation generated dislocation loops. Potential migration mechanisms are discussed.

Abstract 382 THU-NST04-4

[Contributed Talk - Thursday 10:00 AM - Bonham D](#)

Molecular dynamics simulations of defect-boundary interactions in Fe

[DI CHEN, LIN SHAO](#)

Department of Nuclear Engineering, Texas A&M University, Department of Nuclear Engineering, Texas A&M University, College Station TX 77843, United States

Understanding fundamentals of defect-boundary interactions in Fe is important for the development of radiation tolerant Fe-based alloys for nuclear engineering applications. Although it has become a general consensus that grain boundary acts as defect sinks for both interstitials and vacancies, little is known about how the loaded defects at a grain boundary recombines. If defect removal after defect loading at a boundary has limitations, the defect sink property expects to be saturated or turned off under continuous ion bombardments. Using molecular dynamics simulations, we have shown that defect annihilation at a grain boundary is complicated. The recombination is realized through one dimensional defect movement and both allowable moving directions and associated energy barriers are sensitive to boundary misalignment angles. Based on these findings, optimized boundary configurations having the highest defect removal capability are proposed.

Abstract 479 THU-RE08-1

[Invited Talk - Thursday 10:00 AM - Bowie C](#)

Radiation effects in Heavy Ion Radiolysis

[Jay A LaVerne](#)

Radiation Laboratory and Department of Physics, University of Notre Dame, 314 Radiation Laboratory, Notre Dame IN 46556, United States

Most radiation chemistry research performed with accelerators utilize fast electrons or light ions, but a variety of other types of ions are available and the radiolytic outcome can vary significantly. Radiolytic decomposition is driven by a combination of physical energy deposition events followed by chemical reaction and diffusion and radiolytic yields can vary by orders of magnitude depending on the incident radiation type and energy. Even media that are universally considered to be radiation inert can undergo considerable decomposition under the right conditions. Simple fundamentals of track structure and its effects will be described and their effects illustrated. Comparisons will be shown for the dependence of a variety of materials on the type of incident radiation and reasons for the observed differences given.

Abstract 71 THU-RE08-2

[Invited Talk - Thursday 10:00 AM - Bowie C](#)

Photoprotective properties of a eumelanin building block: Ultrafast excited state relaxation dynamics in indole

[Susanne Ullrich](#), [Timothy J Godfrey](#), [Hui Yu](#)

Department of Physics and Astronomy, University of Georgia, Physics Building, Athens GA 30602, United States

Skin is often cited as the body's biological defense system against ultraviolet radiation, and the color of our skin, predominantly determined by the pigment eumelanin, is presumed to be a major factor in this protection scheme. Through internal conversion processes, ultraviolet energy initially absorbed by the eumelanin chromophores is dissipated quickly-on femtosecond timescales-and converted into harmless heat.

We have investigated the excited state relaxation dynamics of indole, a eumelanin chromophore, using three complementary gas-phase pump-probe spectroscopic techniques: (1) time-resolved photoelectron spectroscopy, (2) time-resolved ion yield, and (3) time-resolved H-atom kinetic energy release. Our studies demonstrate the involvement of the low-lying 1L_a and 1L_b states with $^1\pi\pi^*$ character and the $^1\pi\sigma^*$ state in the deactivation process. This confirms recent ab initio studies that electronic excited states with notable σ^* character, centered at X - H (where X = O or N) bonds, play a particular important role in efficient photoprotection of many biomolecular building blocks.

Abstract 453 THU-RE08-3

[Invited Talk - Thursday 10:00 AM - Bowie C](#)

Inorganic oxygen regulator alleviates radiation induced damage to living systems

[Soumen Das](#)¹, [Ram K Tripathi](#)², [Jefferson Shinpaugh](#)³, [Sudipta Seal](#)¹

⁽¹⁾*Advanced Materials Processing and Analysis Center, Nanoscience and Technology Center, University of Central Florida United States, Orlando FL, United States*

⁽²⁾*NASA Langley Research Center, NASA, Hampton VA, United States*

⁽³⁾*Department of Physics, East Carolina University, Greenville NC, United States*

At the nanoscale, cerium oxide nanoparticles (nanoceria) possess oxygen vacancies on the surface or delocalized electron density on the cerium atom which are believed to be catalytic sites of nanoceria. Nanoceria, due to the presence of oxygen defects, can regulate levels of radicals including reactive oxygen and nitrogen species, as well as the local oxygen environment. Due to the very low reduction potential of Ce^{3+}/Ce^{4+} redox couple, the catalytic surface can be regenerative and therefore make this nanomaterial very unique for different potential applications, ranging from glass polishing, automotive catalytic converters to medical diagnosis and therapy. Radiation exposures to cells induce free radical formation to cells and biological systems. Therefore, a small dose of regenerative nanoceria can regulate the level of free radicals and ameliorate radiation-induced damages. First, in an **in vitro** study nanoceria have shown to protect normal breast epithelial cells survival and minimize DNA damage against 10Gy radiation (x-ray). However, nanoceria did not show any protection towards breast cancer cells and increases radiation lethality for the tumor cells. This phenomenon can be explained in term of nanoceria's microenvironment (pH of the environment) dependent behavior that nanoceria behave as an antioxidant in neutral to near-neutral pH (normal cell) or oxidase in acidic pH (cancer cells). Similar observations were reported in several **in vivo** studies where nanoceria (pre-treatment) behaved as a radio-sensitizer for cancer cells while protecting normal healthy cells against radiation. Nanoceria administration not only supported survival of animals, it also significantly reduced complications associated with radiation exposure. We have also shown that 90% of mice survived after 15Gy thorax irradiation when the mice received nanoceria 2hr post radiation (10% survived in control). Work on nanoceria effect on biological system against particle radiation is under progress. These results strongly suggest nanoceria can be a safe and effective radiation countermeasure.

Abstract 352 THU-RE08-4

[Invited Talk - Thursday 10:00 AM - Bowie C](#)

Controlling Bond Cleavage in Gas-Phase Biomolecules

[Sylvia Ptasinska](#)

Radiation Laboratory and Department of Physics, University of Notre Dame, Notre Dame IN 46556, United States

The high energy quanta of impinging radiation can generate a large number ($\sim 5 \times 10^4$) of secondary electrons per 1 MeV of energy deposited. When ejected in condensed phase water, the kinetic energy distribution of these free or quasi-free electrons is peaked below 10 eV. Low energy electrons also dominate the secondary electron emission distribution from biomolecular targets exposed to different energies of primary radiation. Due to the complexity of the radiation-induced processes in the condensed-phase environment, the mechanisms of secondary electrons induced damage in biomolecules still need to be investigated. However, based on results from theory and different experiments accumulated within the last decade, it is now possible to determine fundamental mechanisms that are involved in many chemical reactions induced in isolated gas-phase biomolecules by low energy electrons. The central finding of the recent research was the discovery of the bond and site selectivity in the dissociative electron attachment process to biomolecules. It has been demonstrated that by tuning the energy of the incoming electron we can gain control over the location of the bond cleavage.

Abstract 408 THU-RE08-5

[Invited Talk - Thursday 10:00 AM - Bowie C](#)

Advances of the multiscale approach to the assessment of radiation damage with ions

[Eugene Surdutovich](#)¹, [Andrey V. Solov'yov](#)²

⁽¹⁾*Physics, Oakland University, 2200 N. Squirrel Rd., Rochester MI 48309, United States*

⁽²⁾*Theoretical Physics, Goethe University, Max-von-Laue-Str. 1, Frankfurt am Main 60438, Germany*

The multiscale approach to the physics of radiation damage with ions has been developed in order to relate physical effects caused by the propagation of ions in tissue to the subsequent biological damage on the phenomenon-based ground. This relation is usually achieved by obtaining of the dependence of probability of cell-survival or other biological effects on the dose deposited in the target. The comparison of these dependencies for ion projectiles with x-rays determines the relative biological effectiveness (RBE) of radiation. In contrast to other methods, which determine the RBE empirically, the multiscale approach analyzes a number of physical, chemical, and biological effects taking place on different temporal, spatial, and energy scales; and the dependencies of damage probabilities on dose are obtained on the basis of these effects. The method is mostly analytical; however some effects are studied using molecular dynamics or Monte Carlo simulations. In the most recent work, the probabilities of plasmid DNA damage were studied and the probability of survival of A549 cells was predicted on this basis. Important in this regard is the effect of shock waves caused by the ion's traverse. These waves participate in the transport of the reactive species such as free radicals to relatively large distances from the ion's paths. The multiscale approach leads to the development of the recipe for the phenomenon-based calculation of RBE. Such a recipe could be used in radiation optimization codes and other applications.

Abstract 216 THU-ATF07-1

[Invited Talk - Thursday 1:30 PM - Bowie A](#)

Handheld 10^7 DT neutrons/second pulsed neutron generator using a field ionization source

[Jennifer L Ellsworth](#)¹, [Steven Falabella](#)¹, [Brian Naranjo](#)², [Seth Putterman](#)², [Brian Rusnak](#)¹, [Vincent Tang](#)¹

⁽¹⁾*Lawrence Livermore National Laboratory, 7000 East Ave., Livermore CA 94550, United States*

⁽²⁾*Dept. of Physics, University of California Los Angeles, Los Angeles CA 90095, United States*

Active interrogation using neutrons is an effective method for detecting shielded nuclear material. A lightweight, lunch-box-sized, battery-operated neutron source would enable new concepts of operation in the field. We are developing at-scale components for a highly portable, completely self-contained, pulsed DT neutron source producing 14 MeV neutrons with average yields of 10^7 n/s. A gated, field ionization ion source using etched electrodes has been developed that produces pulsed ion currents up to 500 nA. A compact Cockcroft-Walton high voltage source will be used to accelerate ions into a metal hydride target for neutron production. We will present the status of component development and integrated testing activities with both deuterated and tritiated targets.

This work was performed under the auspices of the U.S. Department of Energy by Lawrence Livermore National Laboratory under Contract DE-AC52-07NA27344.

Abstract 140 THU-ATF07-2

[Invited Talk - Thursday 1:30 PM - Bowie A](#)

High Yield, Gas Target Neutron Generator Development at Phoenix Nuclear Labs

[Evan Sengbusch](#)¹, [Ross Radel](#)¹, [Logan Campbell](#)¹, [Arne Kobernick](#)¹, [Tye Gribb](#)¹, [Casey Lamers](#)¹,
[Chris Seyfert](#)¹, [Preston Burrows](#)¹, [Greg Piefer](#)²

⁽¹⁾Phoenix Nuclear Labs, 2555 Industrial Drive, Monona WI 53713, United States

⁽²⁾SHINE Medical Technologies, 2555 Industrial Drive, Monona WI 53713, United States

Phoenix Nuclear Labs (PNL) has designed and built a high yield deuterium-deuterium (DD) neutron generator with measured yields greater than 3×10^{11} n/s. The neutron generator utilizes a proprietary gas target coupled with a custom 300kV accelerator and a microwave ion source (MWS). A pressure differential of 1,000,000X is achieved between the high pressure gas target and the accelerator and ion source region in order to stop the ion beam within a reasonable distance in the target (~70cm in the present configuration). Two prototype neutron generators have been delivered; one to the US Army for neutron radiography and one to SHINE Medical Technologies for medical isotope production. PNL furthermore signed its first commercial order in late 2013 and will deliver a generator to the United Kingdom late in 2014. Experiences operating and optimizing the various subsystems (ion source, accelerator, focus element, differential pumping stages, and gas target) will be described. System performance will be characterized in terms of beam current and voltage, measured neutron yield, and operational reliability. Preliminary results utilizing the neutron generator technology for various federally and commercially funded applications, including thermal neutron radiography, medical isotope production, nuclear instrumentation testing and calibration, and explosives detection will be presented. Multiple next-generation systems are presently being designed and built at PNL with an emphasis on further increasing neutron yield and reliability and on decreasing the physical size and price of the system. Modifications currently underway include further increases in voltage and current, the use of a solid target (e.g. for fast neutron radiography), and transitioning to a mixed deuterium-tritium (DT) beam with the gas target system. The latter modification will result in a neutron yield increase of approximately 50X. PNL is targeting delivery of 3 neutron generators with yields of 5×10^{13} DT n/s in early 2016 to SHINE's molybdenum-99 production facility.

Abstract 341 THU-ATF07-3

[Contributed Talk - Thursday 1:30 PM - Bowie A](#)

A fluid-based-arc deuteron ion source for neutron generators

[Paul R. Schwoebel](#)

Physical Sciences Division, SRI International, 333 Ravenswood Avenue, Menlo Park CA 94025, United States

An arc discharge between hydrocarbon fluid-coated electrodes is investigated as a deuteron ion source for compact neutron generators. The use of deuterated fluid-coated electrodes provides the high deuteron yields typical of arc-type ion sources with deuterated metal electrodes, but without permanent electrode erosion due to the self-healing nature of the fluid.

Thomson mass spectrometer studies show the arc produces principally atomic hydrogen ions. Optical emission spectra of the arc are dominated by hydrogen Balmer lines and carbon lines, including the Swan-bands of C_2 . Average arc currents up to 50 A to 100 A have been run for times ranging between 1 and 10 μs . The ion current extracted is $\sim 10\%$ of the arc current, in agreement with ion current fractions extracted from arcs between metal electrodes. The chief gas species produced during the arc is hydrogen. Neutron production and source lifetime experiments as a function of arc current and duration will be presented.

Abstract 251 THU-ATF07-4

[Contributed Talk - Thursday 1:30 PM - Bowie A](#)

Development and Optimization of a Compact Neutron Generator for Research and Education

[Allan Xi Chen](#)¹, [Jaako Hannes Vainionpaa](#)¹, [Melvin M. Piestrup](#)¹, [Charles K. Gary](#)¹, [Glenn Jones](#)²,
[Richard H. Pantell](#)³

⁽¹⁾*Adelphi Technology Inc, Redwood City California 94063, United States*

⁽²⁾*G & J Jones Enterprise, Dublin California 94568, United States*

⁽³⁾*Electrical Engineering, Stanford University, Stanford California 94305, United States*

The new DD-109 model neutron generator by Adelphi Technology Inc. has been enhanced to achieve higher neutron fluxes and improved neutron live-time in a more compact size. The DD-109 uses the $^2H(d,n)^3He$ reaction to produce 2.45 MeV neutrons. Deuterons are first produced in a small Electron-Cyclotron-Resonance (ECR) ion source, which are then accelerated to 125 keV and bombard a titanium bonded copper target. The neutron generator head is housed in a 6 inch diameter x 12 inch long chamber and produces steady neutron yields up to 2×10^9 n/s. Continuous operation periods of up to 10 hours have been demonstrated with neutron live-time > 99.2%. For applications requiring pulsed neutrons, the ECR ion source can be retrofitted with a pulser option to produce >50 micro-second neutron pulses. This neutron generator should be attractive to universities and research institutions requiring a reliable source of fast neutrons in a compact package.

Abstract 468 THU-ATF07-5

[Contributed Talk - Thursday 1:30 PM - Bowie A](#)

Preliminary Experiments with a High-Intensity Neutron Source Based on a Liquid-Lithium Target

[Shlomi Halfon](#)^{1,2}, [Gitai Feinberg](#)^{1,2}, [Alex Arenshtam](#)¹, [Daniel Kijel](#)¹, [Michael Paul](#)², [Leo Weismann](#)¹,
[Dan Berkovits](#)¹, [Ilan Eliyahu](#)¹, [Arik Kreisel](#)¹, [Guy Shimel](#)¹, [Asher Shor](#)¹, [Ido Silverman](#)¹

⁽¹⁾*Nuclear Physics and Engineering, Soreq, Road 4111, Yavne 81000, Israel*

⁽²⁾*Racah Institute of Physics, Hebrew University, Jerusalem 91904, Israel*

A prototype of a compact Liquid Lithium Target (LiLiT), able to constitute an intense accelerator-based neutron source was successfully tested for the first time with an intense 1.9 MeV, 1.3 mA (~ 2.5 kW) continuous-wave proton beam. The high-power liquid-lithium target is designed to produce neutrons through the $^7Li(p,n)^7Be$ reaction and to overcome the major problem of removing the thermal power generated by the proton beam at high intensity (1.91-2.5 MeV, >3 mA). The neutron source is intended to be used for nuclear astrophysical research, boron neutron capture therapy (BNCT) in hospitals and material studies for fusion reactors.

The liquid-lithium loop of LiLiT generate a stable lithium jet at high velocity on a concave supporting wall with free surface for the incident proton beam (up to 10 kW). The liquid-lithium flow at velocity of ~ 4 m/s driven by an electromagnetic (EM) induction pump. The lithium flow is collected into a containment tank where a heat exchanger dissipates the beam power. Radiological risks due to the 7Be produced in the reaction will be handled though cold trap and appropriate shielding.

With a proton beam energy just above the ${}^7\text{Li}(p,n)$ threshold of 1880 keV, the neutron yield was continuously monitored by a fission-chamber detector positioned at 0° with regard to the proton beam while the intensity of the proton beam on the lithium target was monitored by the yield of g rays, dominated by the inelastic ${}^7\text{Li}(p,p'g)$ reaction. Gold activation targets positioned in the forward direction show that the average neutron intensity during the experiment was $\sim 2 \times 10^{10}$ neutrons/s. Preliminary experiments have been done to measure the Maxwellian Averaged Cross Section (MACS) of the ${}^{94}\text{Zr}(n,\gamma){}^{95}\text{Zr}$ and ${}^{96}\text{Zr}(n,\gamma){}^{97}\text{Zr}$ reactions.

Abstract 429 THU-IBM07-1

[Invited Talk - Thursday 1:30 PM - Bonham C](#)

Exploring the Radiation Damage Resistance of Nanoscale Interfaces

[Vaithiyalingam Shutthanandan](#)

EMSL, Pacific Northwest National Lab, 902 innovation Blvd, Richland Washington 99352, United States

The interaction of radiation with materials controls the performance, reliability, and safety of conventional and advanced nuclear power systems. Energetic particles produced by nuclear reactions displace atoms in surrounding materials from their lattice sites, resulting in high local temperatures and formation of vacancies and interstitials that are deleterious to important material properties. Recent research suggests that nanospaced internal interfaces are powerful sinks for vacancies and interstitials. Revolutionary improvements in radiation tolerance may be attainable if methods can be found to manipulate interface structures at the nanoscale to tailor their properties for optimal interface stability and point defect recombination, and to serve as traps for gaseous transmutants such as helium and hydrogen. In this talk, we present our experimental results of application of heavy ion beam radiation to study the stability of a well ordered interface of (1) Cr/MgO (2) Cr-V alloy film/MgO and (3) Fe/Y₂O₃. All these films were grown by molecular beam epitaxial method (MBE). First two systems were exposed to 1 MeV Au⁺ ions over doses ranging from 0.1 to 150 displacement per atom (dpa) and subsequent interface stability was studied using *in situ* RBS/Channeling and *ex situ* High-resolution transmission electron microscopy (HRTEM) and Atom probe tomography. The third system was radiated with 25 keV helium ions using Helium ion microscopy and the subsequent helium bubble formations were studied using HRTEM. In general, the degree of disorder in the Cr-V/MgO interface slightly increases with increasing irradiation damage, but the degree of disorder was far below the random level expected. On the other hand, we found that on the helium implanted Fe/Y₂O₃ sample, the He ions clustered to form bubbles at both the interface and within the interior of both Fe and Y₂O₃ matrices. The bubbles that formed at the interface are significantly larger than bubbles formed in either matrix.

Abstract 61 THU-IBM07-2

[Contributed Talk - Thursday 1:30 PM - Bonham C](#)

Advanced barrier layers for use under extreme corrosion and irradiation conditions

[Francisco García Ferré^{1,2}](#), [Patrick Trocellier³](#), [Marco G Beghi²](#), [Lucile Beck³](#), [Yves Serruys³](#), [Fabio Di Fonzo¹](#)

⁽¹⁾Center for Nano Science and Technology, Istituto Italiano di Tecnologia, Via G. Pascoli 70/3, Milano MI 20133, Italy

⁽²⁾Dipartimento di Energia, Politecnico di Milano, Via Ponzio 34/3, Milano MI 20133, Italy

⁽³⁾CEA/DEN/SRMP Laboratoire JANNUS, CEA, Gif-Sur-Yvette F-91191, France

In future generation nuclear systems cooled by Heavy Liquid Metals (HLMs), fuel cladding will be exposed to an extremely harsh environment, in which radiation dose will approach 150 displacements per atom (dpa) at a temperature of up to 800°C. In addition, corrosion of structural steels by HLMs stands as a major bottleneck. In this framework, Al₂O₃ coatings are being investigated for protecting steels [1].

Here, fully dense and compact, nanocrystalline/amorphous Al_2O_3 coatings are grown by Pulsed Laser Deposition. The mechanical properties of the coating are assessed with high accuracy and precision through a novel opto-mechanical method [2], whereas the adhesive strength is evaluated by nanoscratch tests. The deposition process is tailored so as to obtain an advanced material with metal-like mechanical properties ($E=195\pm9$ GPa and $\nu=0,29\pm0,02$), strong interfacial bonding and outstanding resistance to wear. Corrosion aspects are examined by short- (500 hours) and mid-term (2000 hours) exposure of samples to stagnant HLWs at 600°C. Post-test analysis reveals no signs of corrosion [1].

Concerning high dose radiation damage, the performance of the alloy substrate-ceramic coating system is studied by irradiation with heavy ions up to over 150 dpa at 600°C at the JANNUS platform of the CEA center of Saclay. The irradiated samples are examined by profilometry, SEM, TEM, nanoindentation and nanoscratch measurements. Results are compared to previous work on ion [3] and neutron [4] irradiation of crystalline Al_2O_3 , showing to which the coating is expected to exhibit formation of dislocation loops, along with macroscopic swelling up to $\approx 10\%$ or more.

[1] F. Garc  a Ferr  , M. Ormellese, F. Di Fonzo, M.G. Beghi. *Corr Sci* 77 (2013) 375

[2] F. Garc  a Ferr   et al. *Acta Mater* 61 (2013) 2662

[3] S.J. Zinkle. *J Nucl Mater* 219 (1995) 113

[4] F.W. Clinard Jr. et al. *J Nucl Mater* 122 (1984) 1386

Abstract 297 THU-IBM07-3

[Invited Talk - Thursday 1:30 PM - Bonham C](#)

"Reverse Epitaxy" induced by ion irradiation

[Xin Ou, Stefan Facsko](#)

*Institute of Ion Beam Physics and Materials Research , Helmholtz-Zentrum Dresden-Rossendorf, Bautzner Landstrasse 400, Dresden
sachen, Germany*

Arrays of semiconductor nanostructures have the potential for nanoelectronic and optoelectronic applications. Besides the conventional low efficiency lithographic techniques broad ion beam irradiation is a simple and mass productive technique to fabricate nanostructure patterns on semiconductor surfaces.[1] Based on a "self-organized" erosion process, periodic ripple, hole, or dot arrays can be produced on various semiconductor surfaces.

However, the main drawback of this method is that the irradiated semiconductor surfaces are amorphized. [1, 2] For device fabrication, a crystalline surface of high quality is indispensable. In this work we report the recent discovery of single crystal Ge nanopattern formation based on a "reverse epitaxy" process.[3] The low energy ion irradiation is performed in a defined temperature window. Vacancies created during ion beam irradiation distribute according to the crystallographic anisotropy, which results in an orientation-dependent pattern formation on single crystal Ge surface. This process shows nicely the equivalence of epitaxy with deposited adatoms and "reverse epitaxy" with ion induced surface vacancies on semiconductors. The formation of these patterns is interpreted as the result of a surface instability due to an Ehrlich-Schwoebel barrier for ion induced surface vacancies. The simulation of the pattern formation is performed by a continuum equation accounting for the effective surface currents.

The formation mechanism of these patterns is quite general and can be extended to other semiconductors, e.g. Si and compound semiconductors. Thus our work establishes an entirely new and complementary epitaxial method for the fabrication of high-quality faceted semiconductor nanostructures. A physical model for nanopatterning of crystalline semiconductor surfaces with ion beam irradiation will be demonstrated based on comparison between experimental results and computer simulations.

[1] Stefan Facsko et al., *Science* 285, 1551 (1999).

[2] Xin Ou et al., *AIP Advances*, 1, 042174 (2011).

[3] Xin Ou et al., *Physical Review Letters* 111, 016101 (2013).

Study of Tungsten-Yttrium Based Coatings for Nuclear Applications

[Gustavo Martinez](#)¹, [Jack Chessa](#)¹, [Shuttha Shutthanandan](#)³, [Theva Tevuthasan](#)³, [Michael Lerche](#)²,
[Ramana Chintalapalle](#)¹

⁽¹⁾*Mechanical Engineering, University of Texas at El Paso, 500 West University Avenue, El Paso TX 79968, United States*

⁽²⁾*McClellan Nuclear Research Center, One Shields Avenue, Davis CA 95616, United States*

⁽³⁾*Environmental Molecular Sciences Laboratory, Pacific Northwest National Laboratory, Richland WA 98934, United States*

The challenging environment associated with a fusion reactor will require the utilization of advanced materials in order to enable successful development of fusion energy for the future. Tungsten (W)-based materials have been considered for nuclear reactor applications for its outstanding properties such as high melting point, low vapor pressure, high thermal conductivity, and low thermal expansion coefficient. However, pure W exhibits low fracture toughness at all temperatures and a high ductile to brittle transition, which depends on the chemistry and microstructure. In an attempt to overcome these challenges the present work was focused on the W-Y based alloy coatings grown by RF sputter-deposition using W and W-Y targets in the W(95%)-Y(5%) and W(90%)-Y(10%) composition. The microstructure, surface morphology and mechanical properties of Tungsten and Tungsten-Yttrium (W-Y) nanostructured films with varying sputtering pressure P_{Ar} and varying Yttrium content in the film. It is noted that the film phase can be tailored with the sputtering pressure as the appearance of the metastable β -W phase is related to the lowered deposition flux of W atoms, increased film porosity and correspondingly to the higher probability of oxygen incorporation, all this related to sputtering pressure. The samples were irradiated by 5 MeV Au ions at different fluences ranging from 1×10^{14} to 1×10^{16} ions/cm². GIXRD analysis of the irradiated samples reveals that the structure of W-Y film undergoes microstructure evolution, where gradual crystal degradation leading to amorphization is noted. Also grain growth occurs at the lower Au ion fluence. The damages are also correlated to mechanical Hardness and young modulus measured using nano-indentation technique.

Micromechanical Investigation of the Effects of Thermal Shock due to Irradiation in Ferritic-Martensitic Steels

[Pavana Prabhakar](#)

Mechanical Engineering, University of Texas at El Paso, Engineering Building A-114, 500 W. University Avenue, El Paso TX 79968, United States

Ferritic-martensitic steels appear to be promising candidates for next generation advanced nuclear reactors. They have superior thermal properties compared to austenitic stainless steels, like thermal conductivity, low thermal expansion, larger high-temperature strength, low void swelling rate, under neutron irradiation. These excellent thermal properties make them ideal materials for next generation nuclear reactors with much higher operation temperature and irradiation environments. But, a serious concern is the embrittlement of irradiated alloys due to segregation of alloying elements, and the formation of a number of precipitates under high-dose irradiation. This type of irradiation induced diffusion and phase segregation can influence the life period and safety of the nuclear walls. Therefore, a thorough understanding of such behavior of these materials is essential and extremely important. In this paper, a micromechanical investigation of the effects of thermal shock caused damage in irradiated Ferritic-Martensitic steels will be conducted.

Effects like radiation induced hardening, embrittlement, swelling and creep will be accounted for in the modeling. The microscopic effects that cause the above mentioned macroscopic changes in the alloy will be investigated. That is, at the microscale, the effect of irradiations on the dislocation mobility and grain boundary interactions, and the resulting changes will be predicted. The microscopic evaluations will be carried out using a novel finite element method formulation for grain boundary evolution due to the radiation effects. Changes like, static and dynamic recrystallization, black dot damage formations due to irradiation will be included in the micromodel through damage and failure laws. For the micromechanical modeling, inputs from experiments will be obtained to construct the model. Also, the micromodel will account for phase

transformations caused by excessive thermal shock caused by irradiations. The thermal shock effects caused due to irradiation will be determined from the micromodel, and validated with experiments.

Abstract 412 THU-NP06-1

[Invited Talk - Thursday 1:30 PM - Travis C/D](#)

A mini C-14 AMS with great potential in environmental research in Hungary

[Mihály Molnár¹](#), [László Rinyu¹](#), [Róbert Janovics¹](#), [István Major¹](#), [Mihály Veres¹](#), [Timothy A.J. Jull^{1,2}](#)

⁽¹⁾*Hertelendi Laboratory of Environmental Studies, MTA Atomki - Isotoptech Zrt, Bem ter 18/c, Debrecen 4026, Hungary*

⁽²⁾*NSF Arizona AMS Laboratory, 1118 East Fourth St, Tucson Arizona 85721, United States*

Radiocarbon (C-14) dating is widely applied in environmental protection, archaeology, geology, hydrology, climatology and many other essential scientific branches all over the world. In Hungary C-14 measurements are also applied in archaeology just as well as in nuclear environmental protection since the 1980's. In 2011 a more developed and modern technology took over our old C-14 measuring methods, which is based on isotope separation by accelerator mass spectrometry and not on activity measurements. The advantage of the new method is that it requires much less sample quantity (0.1-100 mg) than the older one (1-100 g) which significantly limited the scale of possible applications and research fields. Besides, accelerator mass spectrometry (AMS) technique could give them ten times higher throughput instead of the recently used method.

In this project a further improved AMS technique dedicated for radiocarbon studies was developed by ETHZ (Zürich, Switzerland) in connection with environmental research, in particular equipped with a gas inlet system to transfer CO₂ gas sample into the AMS ion source.

Installation and successful Final Acceptance of the EnvironMICADAS was completed by the autumn of 2011. Background is about 50 kyrs BP. Ion current is about 40 mA at low energy side (C-12 negative ions) while transmission is 40% through the vacuum isolated 200 kV mini tandem accelerator. Relative uncertainty after a half day measurement of primary C-14 standard (Ox-II, NIST 4990C) was better than +/-0.3%. Results of a secondary standard (Oxa-I, NIST 4990) and IAEA C-14 reference material (IAEA-C1, -C2, -C7, -C8 and -C9) met perfectly with the expected values. In the first two year of operation more than 5000 samples were analyzed in the new AMS lab of Hungary.

Abstract 410 THU-NP06-2

[Invited Talk - Thursday 1:30 PM - Travis C/D](#)

Accelerator Mass Spectrometry (AMS): From art to Stars

[Philippe A Collon](#)

Physics, University of Notre Dame, 225 Nieuwland Science Hall, Notre Dame IN 46556, United States

Evolving from detection methods and techniques developed in nuclear physics, Accelerator Mass Spectrometry (AMS) makes it possible to unambiguously identify the A and Z of a specific ion. This identification enables the separation of rare ions of interest from an isobaric background often many orders of magnitude higher. This technique has lead to many applications ranging from archaeometry and environmental science to research in paleoclimates, nuclear astrophysics and meteor research. The talk will concentrate on the use of the gas-filled magnet technique used in conjunction with

Accelerator Mass Spectrometry (AMS) to measure radionuclide concentrations and reaction cross-sections of importance in stellar nucleosynthesis and galactic radioactivities.

Such a system (**MANTIS; Magnet for Astrophysical Nucleosynthesis studies Through Isobar Separation**) based on an FN Tandem accelerator was set-up and commissioned at the Nuclear Science Laboratory (NSL) at the University of Notre Dame together with graduate and undergraduate students and is used as an AMS system for the measurements of radioisotopes like ^{60}Fe and ^{93}Zr , as well as the study of production nuclear production cross sections such as $^{40}\text{Ca}(a, g)^{44}\text{Ti}$ and $^{33}\text{S}(a, p)^{36}\text{Cl}$. Currently a new radiocarbon dating program is being implemented to serve the local university community such as the departments of Anthropology and biology. A number of future projects as well as some geared towards applied methods will also be presented.

Abstract 227 THU-NP06-3

[Invited Talk - Thursday 1:30 PM - Travis C/D](#)

AMS and nuclear astrophysics - supernovae signatures and nucleosynthesis in the lab

[Anton Wallner](#)

Department of Nuclear Physics, Research School of Physics and Engineering, The Australian National University, Garran Road, Acton ACT 0200, Australia

Accelerator mass spectrometry (AMS) represents a sensitive technique for studying long-lived radionuclides through ultra-low isotope ratio measurements. In this talk I will highlight two applications related to nuclear astrophysics:

(i) the search for live supernova(SN)-produced radionuclides in terrestrial archives: such studies probe directly specific nucleosynthesis sites and will help understanding heavy element nucleosynthesis in massive stars. New data suggest an unexpected low abundance of interstellar ^{244}Pu ($t_{1/2}=81$ Myr) - a perfect nuclide to study r-process nucleosynthesis that serves also as a probe for r-process sites. Another long-lived isotope produced in SNe is ^{60}Fe ($t_{1/2}=2.6$ Myr). Previous measurements at TU Munich of a Pacific Ocean crust-sample showed an enhanced ^{60}Fe signal that is interpreted as of extraterrestrial origin, possibly from a close-by SN about 2-3 Myr ago (K. Knie, Phys. Rev. Lett., 93, 171103 (2004)). I will show the sensitivity of ^{60}Fe -AMS at the ANU using a gas-filled magnet setup with the goal to search for live ^{60}Fe in deep-sea sediments. I will also detail a new approach to determine its disputed half-life value.

(ii) the simulation of stellar nucleosynthesis processes in the laboratory via the study of dedicated nuclear reactions to elucidate current open questions in astrophysics. The combination of sample activation and subsequent AMS measurement was applied to key nuclear reactions in s-process nucleosynthesis where off-line decay counting is difficult or impossible.

Abstract 186 THU-NST02-1

[Invited Talk - Thursday 1:30 PM - Bonham D](#)

Nanoscale Lithography for Few-Nanometer Features using Ion Beams

[John Baglin](#)

K10/D1, IBM Almaden Research Center, 650 Harry Road, San Jose CA 95120, United States

For many advanced applications of nanotechnology - such as fabrication of semiconductor devices or magnetic memories, or bio-sensors - high resolution, high-fidelity performance of resist lithography and patterning are crucially important. For example, the ITRS Semiconductor Roadmap, currently seeks ways to routinely produce features having edge definition of 1 nm or less, with correspondingly precise critical dimensions. In principle, the intrinsically small lateral dimensions of an ion track in photo-resist should offer significant advantages over those of the laterally scattered electrons or photons that have long been the standard for chip lithography. However, the line edge roughness (LER) after ion beam exposure of a typical resist layer is subject to stochastic shot noise. Furthermore, the inherent 3D granularity of this exposure can lead to irregular depth-dependent development of the resist. However, such inherent granularity might be minimized by choosing novel ion beam parameters, resist structure, and process cycle.

We have developed new insights and new exposure strategies by modeling patterned exposure (10 nm stripes at 10 nm pitch) of various layered resist types (e.g. PMMA or HSQ) to beams of various incident ion energies and species. The simulation was made by adapting the SRIM Monte Carlo program to recognize and aggregate the entire exposure pattern in 3 dimensions, using pixels of 1 nm. We will display typical resulting exposure distributions, noting the intrinsic thresholds for either positive tone or negative tone response.

These studies suggest that the problem of stochastic noise can be substantially addressed by using concurrent or sequential multiple exposure to a series of beam species, and by using suitably tailored resists.

Abstract 245 THU-NST02-2

[Contributed Talk - Thursday 1:30 PM - Bonham D](#)

Kelvin Probe Microscopy Characterization of Buried Graphitic Channels Microfabricated by MeV Ion Beam Implantation

[Ettore Bernardi](#), [Federico Picollo](#), [Alfio Battiato](#), [Paolo Olivero](#), [Ettore Vittone](#)

Physics Department and ?NIS? Inter-departmental centre, University of Torino, Via P. Giuria 1, Turin 10125, Italy

The possibility of fabricating sub-superficial graphitic microchannels in diamond offers several promising opportunities in the fields of cellular bio-sensing [1] and particle radiation [2].

In this work, we present an investigation by Kelvin Probe Microscopy (KPM) of a graphitic microchannel fabricated by using a 1.8 MeV He⁺ microbeam scanning over the surface of a single-crystal diamond. A linear pattern (50 nm wide and 1 mm long) was irradiated at a fluence well above the graphitization threshold. Before the implantation process, the diamond's surface were covered with a copper layer in order to reduce the ion penetration depth without modifying the beam energy, choosing in this way the depth of the highly-damaged layer with from the diamond surface. Further metal deposition of variable-thickness masks was then realized in order to implant channels with emerging end-points [3]. High temperature annealing was performed in order to induce the graphitization of the highly-damaged buried region.

The presence of a conductive channel, buried at a depth of 1 mm, was clearly evidenced, in the presence of current flowing in the channels, by KPM maps of the electrical potential of the surface region overlying the channel. Moreover, the KPM profiling shows regions of opposite contrast located at different distances from the channel' endpoints. This effect is attributed to the dissimilarity between the electrical resistance path on the graphitic microchannel and the electrical resistance path on the superficial conductive layer induced by the high thermal annealing.

The results have significant implications for future fabrication of all-carbon graphite/diamond devices, both in the fields of cellular biosensing and radiation detection.

[1] F. Picollo et al., Advanced Materials 25 (2013) 4696

[2] J. Forneris et al., Nuclear Instruments and Methods in Physics Research B 306 (2013) 169

[3] F. Picollo et al., New Journal of Physics 14 (2012) 053011

Abstract 290 THU-NST02-3

[Invited Talk - Thursday 1:30 PM - Bonham D](#)

Ion Beam Analysis of Wet NanoBonding™ of Si-to-SiO₂ and SiO₂-to-Silica for single-device sensing electronics using Atomic Force Microscopy & Three Liquids Contact Angle Analysis to Correlate Components of the Surface Free Energy to Topography and Composition

[Shawn D. Whaley](#)^{1,2}, [Nicole X. Herbots](#)^{1,2,3}, [Ross B. Bennett-Kennett](#)^{1,2}, [Eric R.C. Morgan](#)^{1,2}, [Robert J. Culbertson](#)^{1,3}, [Rob L. Rhoades](#)⁴, [Scott N. Drews](#)⁴, [Clarizza F. Watson](#)², [J. D. Bradley](#), [David A. Sell](#)^{1,2}, [Peter Rez](#)¹, [Barry J. Wilkens](#)³, [Mark W. Mangus](#), [Heather M. Johnson](#)

⁽¹⁾Department of Physics, Arizona State University, Mail Stop 1504, Tempe AZ 85287-1504, United States

⁽²⁾R&D, SiO₂ NanoTech LLC, ASU Skysong Innovation Center, Scottsdale AZ 85287, United States

⁽³⁾LeRoy Eyring Center for Solid State Sciences, Ion Beam Facility for Materials Analysis (IBeAM) User Facility, Arizona State University, Mail Stop 5406, Tempe AZ 85287-5406, United States

⁽⁴⁾R&D, Entrepix Inc, 4717 E Hilton Ave #200, Phoenix AZ 85034, United States

To integrate silica-based sensors into single devices electronics, Wet Nano-Bonding™ uses β -cristobalite-like Si₂O₄H₄ nucleated on Si(100) as precursor phase with r.m.s ~ 0.06 ± 0.02 nm across 1-12" wafers to catalyze cross-bonds between silica and Si surfaces, and SiO₂ -to-silica in contact at the nano-scale, thanks to extended, 20-30 nm-wide atomic terraces. Nano-Bonding uses anneals at T ≤ 180°C in H₂O/O₂ ambient with steam pressurization to eliminate wafer warp, and the Herbots-Atluri (H-A) process [1] to nucleate the precursor phases to form bonding inter-phases over large interface domains via unique molecular and surface geometries [2].

Si₂O₄H₄ can react at low temperatures in H₂O saturated air [1,2]. When put in contact with highly hydrophilic, oxygen-deficient phases of etched silica [2], a cross-bonding inter-phase can form between the two and result in a Nano-Bonding inter-phase² of Si-to-SiO₂, as well SiO₂ to various silicates, including optical silica.

Ion Beam Analysis (IBA) is conducted prior to, and after Nano-Bonding, after (1) precursor phase formation, (2) nano-contacting, (3) Nano-Bonding catalyzed at T = 180 °C, (4) de-bonding. Mechanical strength correlates with structure and composition changes measured by IBA, initial and final topographies measured by Tapping Mode Atomic Force Microscopy, and Three Liquid Contact Angle Analysis with the Van Oss theory. The latter separates contributions from Lifshitz-VanderWaals interactions to total surface free energy from donors and acceptors. IBA also correlates with changes

in hydro-affinity. SiO₂ does not nano-bond reliably because dry O₂ leads to surface free energies as low as 26 ± 1.5 mJ/m². Nano-Bonding occurs more easily in saturated H₂O/O₂ ambient, where surface free energies are 41.5 ± 0.5 mJ/m². An atomistic model was computed via surface energy minimization of Nano-Bonding inter-phases.

[1] US patent 6,617,637 (2003), 7,581,365 (2010).

[2] N. Herbots et al. Pub. No 13/259,278, PCT/US2010/033301 (2012).

Abstract 34 THU-RE01-1

[Invited Talk - Thursday 1:30 PM - Bowie C](#)

Controlling helium in radiation tolerant multilayer and nanochannel materials

[Feng Ren](#)¹, [Yongqiang Wang](#)², [Mengqing Hong](#)¹, [Hongxiu Zhang](#)¹, [changzhong Jiang](#)¹

⁽¹⁾*Department of Physics and Center for Ion Beam Application, Wuhan University, Wuhan Hubei 430072, China*

⁽²⁾*Materials Science and Technology Division, Los Alamos National Laboratory, Los Alamos NM 87545, United States*

Volumetric swelling, surface blistering, exfoliation and embrittlement partially induced by the aggregation of gas bubbles are serious problems for materials in nuclear reactors. In this talk, we demonstrate that the nanochannel films possess greater He management capability and radiation tolerance. For a given fluence, the He bubble size in the nanochannel film decreases with increasing the nanochannel density. For a given nanochannel density, the bubble size increases with increasing fluence initially but levels off to a maximum value. For the 30 keV, 2×10^{17} He⁺ ions/cm² irradiated CrN RT films, the maximum He release ratio of 79% is observed. TEM images show larger bubbles appeared in the Ag film and the V/Ag multilayer under 40 keV, 5×10^{16} He⁺ ions/cm² ion irradiation, while few small He bubbles formed in the nanochannel V films and small bubbles with high densities appeared in the bulk V when the fluence of He⁺ ions reaches 1×10^{17} ions/cm². The abundant surfaces in the nanochannel films are perfect defect sinks and thereby large sized He bubbles and supersaturated defects are less likely to be developed in these high radiation tolerant materials.

Abstract 248 THU-RE01-2

[Contributed Talk - Thursday 1:30 PM - Bowie C](#)

Atomistic modeling of mixing and disordering at a Ni/Ni₃Al interface

[Tongsik Lee](#)¹, [Alfredo Caro](#)², [Michael J. Demkowicz](#)¹

⁽¹⁾*Department of Materials Science and Engineering, Massachusetts Institute of Technology, Cambridge MA 02139, United States*

⁽²⁾*Materials Science and Technology Division, Los Alamos National Laboratory, Los Alamos NM 87545, United States*

L1₂-ordered g' precipitates embedded in a g matrix impart excellent mechanical properties to nickel-base superalloys. The atomistic mechanisms of the stability of these precipitates under irradiation are not fully understood. We perform molecular dynamics simulations of coherent Ni/Ni₃Al interfaces, sequentially inducing multiple 10 keV displacement cascades, to study the irradiation-induced disordering and dissolution of the ordered layer. Changes in local composition and local order parameter are monitored as a function of irradiation dose. Simulation results demonstrate that the Ni₃Al precipitate at room temperature disorders rapidly at a low dose and then dissolves in the disordered state at higher doses, in accordance with experimental observations. Atomic mixing process and broadening of the interface are discussed in terms of the influence of the solute-atom concentration on the effective interdiffusivity. This work was supported by the Laboratory Directed Research and Development (LDRD) program at Los Alamos National Laboratory under Project No. 20130118DR, under DOE Contract DE-AC52-06NA25396.

Microstructural changes of oxide-dispersion-strengthened alloys under extreme ion irradiation

[Chao-chen Wei](#)¹, [Di Chen](#)², [Tianyi Chen](#)², [Lloyd Price](#)², [Jonathan Gigax](#)², [Eda Aydogan](#)³, [Xuemei Wang](#)², [Frank A Garner](#)⁴, [Lin Shao](#)^{2,3}

⁽¹⁾University of Tennessee, 414 Ferris Hall 1508 Middle Drive, Knoxville TN 37996-2100, United States

⁽²⁾Department of Nuclear Engineering, Texas A&M University, 335R Zachry, College Station TX 77843, United States

⁽³⁾Department of Materials Science and Engineering, Texas A&M University, 3003 TAMU, College Station TX 77843, United States

⁽⁴⁾Radiation Effects Consulting, 2003 Howell Avenue, Richland WA 99354, United States

As one candidate material for fuel cladding in advanced reactor designs, oxide-dispersion strengthened (ODS) alloys have been intensively studied during the past decades. In this study, we have shown that swelling behaviors of MA956 ODS alloys are complicated under accelerator-based ion irradiation testing. The void nucleation and growth, induced by 3.5 MeV Fe self ion irradiation, are influenced by the combined effects from (1) preferred vacancy trapping by oxide particles, (2) defect imbalance due to distribution difference of interstitials and vacancies, and (3) injected interstitials due to extra atoms introduced by ion irradiations. Furthermore, instability and partial amorphization of oxide particles under extreme high dpa irradiation will be discussed.

Analyzing Irradiation Effects on Nano- Yttria Stabilized Zirconia

[Sanchita Dey](#), [James Valdez](#)², [Yongqiang Wang](#)², [Terry G Holesinger](#)², [Ricardo H. R. Castro](#)¹

⁽¹⁾Chemical Engineering & Materials Science, UC Davis, 1 Shield Ave, CHMS dept, Davis California 95616, United States

⁽²⁾Los Alamos National Laboratory, Los Alamos New Mexico 87545, United States

One recent topic of interest among the nuclear community is application of nano-materials for improved radiation tolerance. Nano-materials are strong candidates for this application as they offer higher interface area which provide high density of defects sinks; diminishing radiation-induced amorphization by a self-healing mechanism. In this work, we study trends on the radiation damage in Yttria Stabilized Zirconia nano-crystals. The nano-powders were sintered by Spark Plasma Sintering with three different grain sizes (25nm, 38 nm, and ~200nm). Then the sintered samples were irradiated with 400 keV Kr ions to get a controlled irradiated layer and investigated using Transmission Electron Microscopy. The images for the nano samples revealed 3 distinct zones: a region with significant radiation-induced grain growth, with clean boundaries (few dislocations), an interface region with still evidences of grain growth and crack propagation, and non-irradiated zone. On the other hand, the bulk sample shows presence of mainly two different regions: damaged irradiated zone and non-irradiated zone, without cracks but with a significantly larger amount of dislocations.

Mechanical stability of nanoporous gold under ion irradiation

[Yongqiang Wang](#)¹, [Magda Caro](#)¹, [Engang Fu](#)², [L.A. Zepeda-Ruiz](#)³, [E. Martinez](#)¹, [W. Mook](#)¹, [Mike Nastasi](#)⁴, [Alfredo Caro](#)¹

⁽¹⁾Materials Science and Technology Division, Los Alamos National Laboratory, Los Alamos New Mexico 87545, United States

⁽²⁾School of Physics, Peking University, Beijing, China

⁽³⁾Physical and Life Sciences Directorate, Lawrence Livermore National Laboratory, Livermore California 94550, United States

⁽⁴⁾Nebraska Center for Energy Sciences Research, University of Nebraska-Lincoln, Lincoln Nebraska 68508, United States

In previous work, we studied the response of nanoporous gold (np-Au) foams under irradiation at room temperature and different dose-rates [E. Fu, et al. APL 101 (2012) 191607]. Our experimental findings show that 400 keV Ne⁺⁺ ion irradiation for a total dose of 1 dpa leads to the formation of Stacking Fault Tetrahedra (SFTs) at high and intermediate dose-rate, while no SFTs are formed at low dose-rate. An atomic-view of the process was previously reported based on Molecular Dynamics simulations (MD). It was observed that vacancy migration distance and nanofoams ligament size play a key role in explaining the dose-rate dependent defect accumulation.

In this work, we go a step further and make use of nanoindentation techniques to investigate the changes in np-Au foams mechanical properties. We study their deformation behavior under compression before and after ion irradiation at room temperature. We discuss our experimental findings in view of recent MD simulations of ligament deformation behavior under compression [L. Zepeda-Ruiz, et al., APL 103 (2013) 031909]. Simulations predict that nanoscale foams soften under irradiation in very good agreement with our hardness nanoindentation measurements.

Abstract 8 THU-TA01-1

[Contributed Talk - Thursday 1:30 PM - Bonham B](#)

Ion Beam facility for Research, Service and Education

[Daryush ILA](#)

Chemistry and Physics, Fayetteville State University, 1200 Murchison Rd. , 15475, Fayetteville NC 28301-4297, United States

The Center for Irradiation of Materials (CIM) at Huntsville, Alabama was founded by the D. ILA to conduct research and services to meet the needs of the local aerospace community. Soon students and colleagues from various Alabama universities, various states, and other countries added their needs and expatiations to the scope of work at the CIM. Soon after the establishment of CIM the Ion Beam Modification of Materials course, Ion Beam Analysis of materials course and summer training were added to the list of needs and expectations from CIM team, in order to enhance the education and research capabilities at AAMU and provide services needed by the Aerospace, Defense community and Industries at Huntsville, Alabama, as well as several other cities within 1000 miles of Huntsville, AL. As the result of establishment of the CIM the annual grants was increased to additional \$7M per year and annual contract because of the CIM was increased by nearly \$5M/year. The total number of summer students trained at this facility was between 10 to 20 students each summer and nearly two dozen graduate students per year took the IBMM/IBA graduate courses and used this facility regularly. The major focus of this program is ion beam modification materials in order to change chemical, physical and mechanical properties, as well as develop new and innovation method of IBMM and IBA. The optical, electrical, thermal and mechanical properties of ion beam modified materials were, mostly, measured in situ at CIM. Similarly, various devices designed and prototyped at CIM, such as Bio-Chem sensors, detectors, nanopours, ion beam sources, and optical devices. In this talk we will present the historical perspective of this joint effort and plans for similar capability.

Abstract 217 THU-TA01-2

[Contributed Talk - Thursday 1:30 PM - Bonham B](#)

An accelerator in the Faculty of Science of U.N.A.M

[Beatriz Fuentes, Juan Lopez](#)

Departamento de Fisica, Facultad de Ciencias, Universidad Nacional Autonoma de Mexico, Mexico D.F. 04510, Mexico

A low energy accelerator was built in the Faculty of Science of the National Autonomous University of Mexico (UNAM) for atomic and molecular experiments. We present results performed by undergraduate and graduate physics students in different stages of the construction. Experiments include characterization of the velocity filter, identification of Hydrogen ions and TOF spectra.

Abstract 244 THU-TA01-3

[Contributed Talk - Thursday 1:30 PM - Bonham B](#)

Ion beam transport simulations for the 1.7 MV tandem accelerator at the Michigan Ion Beam Laboratory

[Fabian U Naab](#), [Ovidiu F Toader](#), [Gary S Was](#)

Nuclear Engineering and Radiological Sciences, University of Michigan, 2600 Draper Road, Ann Arbor Michigan 48109, United States

The Michigan Ion Beam Laboratory houses a 1.7 MV tandem accelerator. For many years this accelerator was configured to run with three ion sources: a TORoidal Volume Ion Source (TORVIS), a Duoplasmatron source and a Sputter source. In this article we describe an application we have created using the code SIMION[®] to simulate the trajectories of ion beams produced with the ion sources mentioned above through this accelerator.

The goal of this work is to have an analytical tool to understand the effect of each of the electromagnetic components of the accelerator on the ion trajectories. Each ion trajectory simulation starts at the aperture of the ion source and ends at the position of the target. The effect of each of the electromagnetic components in the accelerator is shown in detailed plots.

Using these simulations, new accelerator operators or accelerators users quickly understand how the whole machine works. Furthermore, these simulations allow analyzing modifications in the ion beam optics of the accelerator by adding, removing or replacing components or changing its relative positions.

Abstract 434 THU-TA01-4

[Invited Talk - Thursday 1:30 PM - Bonham B](#)

Undergraduate Education with the Rutgers 12-Inch Cyclotron

[Timothy W Koeth](#)

Institute for Research in Electronics and Applied Physics, University of Maryland, IREAP, Energy Research Facility, Building #223, College Park MD 20742, United States

The Rutgers 12-Inch Cyclotron is a 1.2 MeV research-grade proton accelerator dedicated to undergraduate education. From its inception, it has been intended for instruction and has been designed to demonstrate classic beam physics phenomena. The machine is easily reconfigured, allowing experiments to be designed and performed within one academic semester giving our students a hands-on opportunity to operate an accelerator and directly observe many fundamental beam physics concepts, including axial and radial betatron motion, destructive resonances, weak and azimuthally varying field (AVF) focusing schemes, DEE voltage effects, and more. Built by more than a dozen generations of undergraduates, the Rutgers 12-Inch Cyclotron has also given its students a unique research and development introduction to the field of accelerator physics and associated hardware. These experiences have lead, to-date, six students to pursue academic and industrial careers in accelerator physics. The most recent cyclotron students are preparing a MgF₂ target for precise energy calibration of the proton beam by exploiting the narrow resonances and energetic gamma rays of the ¹⁹F(p,γ)¹⁶O reaction, thus conferring upon our cyclotron the sorcery of nuclear physics.

Abstract 312 THU-AMP05-1

[Invited Talk - Thursday 3:30 PM - Travis A/B](#)

Close coupling CI-approach for (multi-)electronic processes in atomic and molecular keV-collisions

[Alain Dubois](#)¹, [Gabriel Labaigt](#)¹, [Ingjald Pilskog](#)², [Nicolas Sisourat](#)¹

⁽¹⁾*Laboratoire de Chimie Physique-Matiere et Rayonnement, Universite Pierre et Marie Curie - CNRS, 11 rue Pierre et Marie Curie, Paris 75005, France*

⁽²⁾*Department of Earth Science, University of Bergen - The Norwegian Academy of Science and Letters - VISTA, Allégaten 41, Bergen 5007, Norway*

We present a new approach to describe multielectronic processes occurring in ion-atom/molecule collisions at impact energies ranging from 0.1 to 500 keV.u⁻¹. The treatment is based on the semiclassical approximation [1] in which the time-dependent Schrödinger equation is solved non perturbatively, taking into account all the electrons of the collision system. To insure both the correct spin multiplicity and spatial symmetry we use the permutation group theory together with Young diagrams [2] instead of combinations of Slater determinants. This allows to describe exactly multielectronic processes, involving valence and inner shell electrons.

In the conference we shall illustrate this approach with the study of genuine two- and three-electron systems. First A^{q+} - H₂ collisions [3] will be considered in the sudden approximation, i.e. when the molecular geometry (internuclear distance and molecular orientation) is assumed to be frozen during the scattering. We shall concentrate on the study of single and double capture process, with emphasis to the processes where doubly excited states of A^{(q-2)+} are populated. In the final part of the talk results for H⁺-Li(1s²2s¹) collisions will be presented. This system has been studied extensively [4-6] and therefore presents the advantages (i) to allow to test the present treatment and (ii) to provide an interesting benchmark of processes involving inner- and valence-shell electrons in a coupled way.

[1] B.H. Bransden and M.R.C. McDowell, Charge Exchange and the Theory of Ion-Atom Collisions (Oxford University Press, 1992).

[2] F. A. Matsen, J. Phys. Chem. **68**, 3282 (1964).

[3] I. Pilskog, N. Sisourat, J. Caillat and A. Dubois, Phys. Rev. A **85**, 042712 (2012).

[4] S. L. Varghese, W. Waggoner, and C. L. Cocke, Phys. Rev. A **29**, 2453 (1984).

[5] F. Aumayr and H. P. Winter, 1985 Phys. Rev. A **31**, 67 (1985).

[6] R. D. Dubois, Phys. Rev. A **32**, 3319 (1985).

Abstract 55 THU-AMP05-2

[Invited Talk - Thursday 3:30 PM - Travis A/B](#)

Some Dynamical Features of Molecular Fragmentation by Electrons and Swift Ions

[Eduardo C Montenegro](#), [Lucas M Sigaud](#), [Wania Wolff](#), [Hugo Luna](#), [Natalia Ferreira](#)

Physics, Universidade Federal do Rio de Janeiro, Av. Athos da Silveira Ramos, 149, Centro de Tecnologia - bloco A - Cidade Universitária, Rio de Janeiro RJ 21941-972, Brazil

To date, the large majority of studies on molecular fragmentation by swift charged particles have been carried out using simple molecules for which reliable Potential Energy Surfaces are available to interpret the measured fragmentation yields. For complex molecules the scenario is quite different and such guidance is not available, obscuring even a simple organization of the data which are currently obtained for a large variety of molecules of biological or technological interest. In this work we show that a general and relatively simple methodology can be used to obtain a broad picture of the fragmentation pattern of an arbitrary molecule. The electronic ionization or excitation cross section of a given molecular orbital, which is the first part of the fragmentation process, can be well scaled by a simple and general procedure at high projectile velocities [1,2]. The fragmentation fractions arising from each molecular orbital can then be achieved by matching the calculated ionization with the measured fragmentation cross sections. Examples for water, oxygen, chlorodifluoromethane and pyrimidine molecules will be presented. The use of this methodology coupled with the DETOF technique [3,4] allows to identify and obtain absolute cross sections not only for bands associated to small kinetic energy releases, but also for some specific fragmentation mechanisms such as non-local fragmentation or fragmentation through Rydberg molecular states.

[1] E. C. Montenegro, G. M. Sigaud, and R. D. DuBois, Phys. Rev. A .87 (2013) 012706.

[2] W. Wolff, **et al.** J. Chem. Phys. 140 (2014) 064309.

[3] Natalia Ferreira, **et al.** Phys. Rev. A.86 (2012) 012702.

[4] L. Sigaud, **et al.** J. Phys. B: At. Mol. Opt. Phys. 45 (2012) 215203

Abstract 181 THU-AMP05-3

[Invited Talk - Thursday 3:30 PM - Travis A/B](#)

Interaction of multicharged ions with biological molecules

[Roberto Daniel Rivarola](#)

IFIR - FCEIA, CONICET - UNR, Esmeralda y Ocampo, Rosario Santa Fe 2000, Argentina

The understanding of the physical mechanisms producing energy deposition on biological matter, under ion beam irradiation, is a subject of principal interest in radiotherapy and, in particular in hadrontherapy. Different electronic processes like electron emission and charge exchange appear as the main candidates to get an appropriate description. By using distorted wave models and the first-order Born approximation with correct boundary conditions, different molecular targets irradiated with single and multiple charged ions impacting at intermediate and high collisions velocities are investigated. Among them, we must mention the four nucleobases and the sugar phosphate backbone of DNA as well as the RNA uracil. Electron emission multiple differential, single differential and total cross sections are compared with very good success to represent recent experimental data. For electron capture, measurements are much scarcer and only a few values of total cross sections can be contrasted with theoretical predictions. First calculations show that the energy deposited on the target is governed by charge exchange from core orbitals. On the contrary, outer electrons dominate target ionization total cross sections and also electron capture ones. However, using a modification of the Rutherford formula combined with the Born approximation to describe electron ionization, it is proved that energy deposition is dominated by the electron capture reaction, at high enough impact velocities. We focus also our interest in the case of water molecular targets, considering that it is the main compound of the biological tissue. Different physical effects are analyzed, which allow a better interpretation of the existing data, as for example the influence of the dynamic screening produced by the electrons

remaining bound to the residual target on the emitted ones. In order to compare the energy deposition patterns at nanometer scale in liquid water and DNA material, results obtained using a simplified cellular nucleus are presented.

Abstract 66 THU-AMP05-4

[Contributed Talk - Thursday 3:30 PM - Travis A/B](#)

Transmission of electrons through insulating PET nanocapillaries: Angular dependence

[D Keerthisinghe](#)¹, [B S Dassanayake](#)², [S Wickramarachchi](#)¹, [N Stolterfoht](#)³, [J A Tanis](#)¹

⁽¹⁾Physics, Western Michigan University, 1903, W. Michigan Ave, Kalamazoo Michigan 49008, United States

⁽²⁾Physics, University of Peradeniya, Department of Physics, University of Peradeniya, Peradeniya 20400, Sri Lanka

⁽³⁾Materialien und Energie, Helmholtz-Zentrum Berlin, Helmholtz-Zentrum Berlin für Materialien und Energie, Berlin D 14109, Germany

The energy dependence of electrons traveling through insulating capillaries was studied [1] after the first experimental work for highly charged ions on non-conducting foils (HCIs) by Stolterfoht et al. in 2002 [2]. The transmission of HCIs through insulating polyethylene (PET) nanocapillaries without a change in charge state or energy was defined as **guiding**. In the present work electron transmission through insulating PET foils was studied including the angular dependence and the time (charge) evolution for two samples with different dimensions. The samples had diameters of 100 and 200 nm, the same thickness foil 12 μ m and different pore densities of $5 \times 10^8/\text{cm}^2$ and $5 \times 10^7/\text{cm}^2$, respectively. The samples, made at the GSI Laboratory in Darmstadt, Germany, were coated on both the front and back surfaces with gold to carry away excess charges deposited on them. The angular dependence study was carried out for incident electron energies of 300, 500 and 800 eV after the sample reached equilibrium by varying the electron observation angles for different sample tilt angles. Depending on the transmitted electron spectra, three regions were categorized with different characteristics and are referred to as direct, guiding and the transition region between them. Transmission of electrons with negligible energy loss for sample tilt and observation angles close to zero degrees was observed as well as guided electrons for larger tilt angles obeying $\psi \approx 0$. The angular widths were independent of the sample tilt angles within given regions, with values of $\sim 0.7^\circ$ in the direct region and $\sim 1.5^\circ$ in the guiding region, respectively. The angular dependence was observed for both samples and did not depend on the capillary diameter or pore density.

[1] S. Das et al., Phys. Rev. A **76** 042716 (2007).

[2] N. Stolterfoht et al., Phys. Rev. Lett. **88** 133201 (2002).

Abstract 374 THU-ATF08-1

[Invited Talk - Thursday 3:30 PM - Bowie A](#)

Recent achievements in laser-ion acceleration

[Bjorn Manuel Hegelich](#)

Physics, The University of Texas at Austin, 2515 Speedway, Stop C1510, Austin TX 78732, United States

Laser-driven ion acceleration has been recognized for its paradigm changing potential in the late 1990's with the advent of ultrahigh intensity, high energy, short pulse lasers, producing fields of many TV/m, more than a million times stronger than any conventional accelerator. I here review the recent progress in laser-ion acceleration achieved by employing new

acceleration mechanism and targets and leading to the first substantial increase in ion energies from laser-accelerators in a decade.

In experiments on the 150TW Trident laser, we showed for the first time in a decade a substantial increase in proton energies from a laser-ion accelerator accelerating protons to greater than 160 MeV, with a laser of $\sim 1/10^{\text{th}}$ the power and energy of the original PW laser. Carbon ions were accelerated to 1 GeV, a factor 5x higher than the previous record. These results were obtained by using the Break-Out Afterburner (BOA) acceleration mechanism, rather than the standard Target Normal Sheath Acceleration (TNSA). We furthermore demonstrated a laser-to-ion energy conversion efficiency of $\sim 10\%$ into high energy ions. The experimental results are in agreement with 2D and 3D particle-in-cell simulations and are well described by a semi-analytic model. They are backed by direct optical measurements of relativistic transparency, one of the main driving physics mechanisms behind BOA acceleration. This detailed understanding of the process enables us to now apply BOA to other applications, e.g. we used BOA acceleration of Deuterons to demonstrate the brightest laser-driven neutron source, producing $>10^{10}$ neutrons/shot, more than 10^8 neutrons per Joule laser energy.

The original Trident experiments are now being repeated at other facilities. Recent results from the Phelix laser at GSI and the Texas Petawatt laser at UT Austin are in good agreement with the earlier results from Trident as well as with simulations.

Abstract 306 THU-ATF08-2

[Contributed Talk - Thursday 3:30 PM - Bowie A](#)

DOE Office of Science Accelerator Stewardship Program

[Eric R Colby](#), [Michael Zisman](#), [Manouchehr Farkhondeh](#), [Eliane Lessner](#), [Kenneth Olsen](#)

Office of Science, U. S. Department of Energy, 19901 Germantown Road, Germantown MD 20874, United States

Since the Accelerators for America's Future (AfAF) Symposium in 2009, the U. S. Dept. of Energy's Office of High Energy Physics (DOE-HEP) has worked to broaden its accelerator R&D activities beyond supporting only discovery science to include medicine, energy and environment, defense and security, and industry. Accelerators play a key role in many aspects of everyday life, and improving their capabilities will enhance U.S. economic competitiveness and the scientific research that drives it. In 2011, a community task force was initiated by DOE-HEP to develop more fully the information from the original AfAF Symposium. Subsequently, a DOE-HEP concept (coordinated with the other cognizant Office of Science program offices) was developed for long-term accelerator R&D stewardship. Here, we describe the evolution of the stewardship program, the mission of the new program, the broad criteria for participation, and initial steps being taken to implement it. Several initiatives are currently being considered to launch the program, and these will be outlined. Involvement of the accelerator and user communities in developing ideas for future stewardship activities will be crucial to the ultimate success of the program.

Abstract 211 THU-ATF08-3

[Contributed Talk - Thursday 3:30 PM - Bowie A](#)

Status on the developments at the tandem accelerator complex in IFIN-HH

[Dan Gabriel Ghita](#)¹, [Daniel Vasile Mosu](#)¹, [Tiberiu Bogdan Sava](#)¹, [Mihai Straticiuc](#)³, [Ion Burducea](#)³, [Cristian Costache](#)², [Doru Pacesila](#)¹, [Catalin Stan-Sion](#)³, [Mihaela Enachescu](#)³, [Corina Simion](#)⁴, [Oana Gaza](#)¹, [Nicoleta Mihaela Florea](#)², [Alexandru Petre](#)³, [Dan Pantelica](#)²

⁽¹⁾Tandem Accelerators Department, IFIN-HH, 30, Reactorului street, Magurele Ilfov 077125, Romania

⁽²⁾Nuclear Physics Department, IFIN-HH, 30, Reactorului street, Magurele Ilfov 077125, Romania

⁽³⁾Applied Nuclear Physics Department, IFIN-HH, 30, Reactorului street, Magurele Ilfov 077125, Romania

⁽⁴⁾Environmental Physics Department, IFIN-HH, 30, Reactorului street, Magurele Ilfov 077125, Romania

The tandem accelerator complex in IFIN-HH is a main research and development facility in Romania. Apart from the 9 MV Pelletron tandem that has been brought up to today's standards in the last years and is extensively used, as an user facility, for basic and applied physics experiments, two new HVEE Tandetron accelerators were installed in 2012 at IFIN-HH. A state of the art AMS facility built around a 1 MV HVEE Tandetron accelerator was developed. The AMS laboratory started its activity by measuring radiocarbon for archeological studies, but other isotopic ratios measurements are planned for the next period, with practical applications in geology, environmental studies, pharmacology and other research fields. The 3 MV HVEE Tandetron accelerator for ion beam analysis and ion implantation is used for the moment mainly in environmental studies and material physics. Realized and future planned improvements and results are presented.

Abstract 152 THU-ATF08-4

[Contributed Talk - Thursday 3:30 PM - Bowie A](#)

Current Status of the IAP NASU Accelerator-Based Analytical Facility

[Volodymyr Storizhko](#), [Oleksandr Buhay](#), [Andriy Kramchenkov](#), [Oleksandr Drozdenko](#), [Oleksandr Ponomarev](#)

Nuclear Physics, Institute of Applied Physics NAS of Ukraine, 58, Petropavlivs'ka str., Sumy 40000, Ukraine

A microanalysis facility based on the 2 MV electrostatic accelerator has been constructed and put into operation at the Institute of Applied Physics, National Academy of Sciences of Ukraine (IAP NASU). Six end stations are presently operative and two are under construction:

1. Ion microprobe with SE imaging, mPIXE, mRBS and mERDA techniques.

In the high-current mode the beam spot size is 1.2x2 mm, with ion current being 100 nA; in the low-current mode the spot size is 0.6x2 mm and ion current is 1 pA. The microprobe includes an ion-optic system known as the separated "Russian Qudruplet". Integrated doublets of magnetic quadrupole lenses have been designed and constructed at the IAP NASU.

2. High-resolution RBS end station quipped with a precision magnetic spectrometer and an X-ray detector for the PIXE technique.

The end station for HRBS is equipped with a double-focusing magnetic spectrometer which has relative energy resolution of $3.2E-3$. The scattering chamber is furnished with a special flange to accommodate the X-ray detector, permitting a simultaneous use of PIXE and HRBS.

3. High-resolution RBS and ERDA end station provided with a precision electrostatic spectrometer and an automated goniometer for ion channeling.

The electrostatic spectrometer has relative energy resolution better than $3E-4$. The UHV scattering chamber is equipped with a precision automated goniometer for experiments on ion channeling as well as with sample holder for investigations of melted metal surfaces.

4. Ion-induced luminescence end station.

5. PIGE end station with gamma detectors of two types: NaI scintillation detector and HPGe detector.

6. Quasimonochromatic X-ray source based on the electrostatic accelerator

Abstract 188 THU-ATF08-5

[Contributed Talk - Thursday 3:30 PM - Bowie A](#)

Construction and Characteristics of the High Energy Ion Microprobe system at Amethyst Research, Inc.

[Lucas C Phinney](#), [Khalild Hossain](#)

Amethyst Research, Inc., 123 Case Circle, Ardmore OK 73401, United States

Recently a high energy ion microprobe has been installed at the Analytical Laboratory of Amethyst Research, Inc (ARI). The microprobe is installed on one of the beamlines of a 2.5 MV Van-de-Graaff accelerator. The microprobe utilizes the Louisiana Magnetic Doublet (LMD) quadrupole magnets for the focusing system. The microprobe system will be used in focusing mainly light ion beams such as H, He³, and He⁴. The beam spot size has been characterized and analyzed. Experiments at ARI will include measurements using μ -PIXE, μ -RBS, Ion Beam Induced Charge (IBIC) collection and Ion Beam Induced Luminescence (IBIL) techniques. The IBIL instrumentation includes an Ocean Optics USB4000 spectrometer for spectral analysis and a Hamamatsu Photomultiplier tube for monochromatic/panchromatic imaging. The goal of the IBIC and IBIL measurements will be in locating and characterizing defects in group II-VI and III-V hetero-structures on Silicon-based substrates. In this presentation the design, construction and some of the initial results of the microprobe will be discussed.

Abstract 431 THU-ATF08-6

[Contributed Talk - Thursday 3:30 PM - Bowie A](#)

A new fast and accurate method for accelerator energy calibration

[Guy Terwagne](#), [Yvon Morciaux](#)

LARN-PMR, University of Namur, rue de Bruxelles, 61, Namur 5000, Belgium

Accurate determination of the energy of an accelerator is very important especially when nuclear cross-sections are measured. Particles emitted after Rutherford elastic scattering (RBS), non-Rutherford elastic scattering (BS or ERDA) or nuclear reactions (NRA) are often detected in a passivated implanted planar silicon detector (PIPS) or a surface barrier detector (SSD). The calibration of those detectors depends on the energy of the incident beam.

We have developed a simple and original system for measuring the thickness of dead layer in PIPS or SSD detectors. Using a tri- α s source, we can measure spectra at two different incident angles (0° and 60°) and the dead layer is then directly measured. We describe also an original and fast method for the energy calibration of accelerators independently from the energy of the incident particles. We have compared this calibration technique with two other methods using (p,n) threshold reactions and (p,g) resonances or resonant (α,α) scattering.

CORRECT CALCULATION OF ECPSSR IONIZATION CROSS SECTIONS AT LOW IMPACT ENERGIES

[Ziga Smit](#)¹, [Gregory Lapicki](#)²

⁽¹⁾*Faculty of Mathematics and Physics, University of Ljubljana, Jadranska 19, Ljubljana SI-1000, Slovenia*

⁽²⁾*Department of Physics, East Carolina University, Greenville North Carolina NC 27858, United States*

The ECPSSR theory is popularly used for the calculation of light particle induced ionization cross sections of inner atomic shells. In its original form, developed by Brandt and Lapicki until 1981, it corrects the PWBA calculation for the perturbed stationary state (PSS), Coulomb deflection (C), relativistic (R) and projectile energy loss (E) effects. At low projectile velocities, there is marked discrepancy between the original calculation of Brandt and Lapicki and several modern computer codes, such as the ISICS and ERCS08 programs. Though the cross sections at these low energies are hardly measurable, it is important to investigate the effect from the fundamental point of view. We show that the reason for the differences is application of wrong integration limits for momentum transfer, which does not take into account the relativistic effects properly. The correct expressions for integration limits of momentum transfer are presented. Calculations with correct and incorrect integration limits were made and compared with the relativistic PWBA cross sections based on hydrogenic Dirac wave functions and including the necessary corrections. A straightforward modification of the existing computer codes is suggested.

Geant4 and beyond for the simulation of multi-disciplinary accelerator applications

[Maria Grazia Pia](#)¹, [Matej Batic](#)², [Marcia Begalli](#)³, [Min Cheol Han](#)⁴, [Steffen Hauf](#)⁵, [Gabriela Hoff](#)⁶,
[Chan Hyeong Kim](#)⁴, [Han Sung Kim](#)⁴, [Sung Hun Kim](#)⁴, [Markus Kuster](#)⁵, [Paolo Saracco](#)¹, [Georg Weidenspointner](#)⁵

⁽¹⁾*INFN Sezione di Genova, Via Dodecaneso 33, Genova 16146, Italy*

⁽²⁾*Sinergise, Ljubljana, Slovenia*

⁽³⁾*State University Rio de Janeiro, Rio de Janeiro, Brazil*

⁽⁴⁾*Hanyang University, Seoul, Korea*

⁽⁵⁾*XFEL GmbH, Hamburg, Germany*

⁽⁶⁾*PUCRS, Porto Alegre, Brazil*

This talk presents an overview of Geant4 simulation capabilities and new developments relevant to the scientific domain of CAARI.

Geant4 is a toolkit for the simulation of particle interactions with matter. Although its development was originally motivated by large scale, high energy experiments at the CERN LHC (Large Hadron Collider), it is currently widely used in an ample variety of experimental environments. Geant4 reference is the most cited publication in Thomson-Reuter's "Nuclear Science and Technology" and "Instruments and Instrumentation" categories, which encompass scientific literature since 1970.

Despite its widespread application in diverse experimental domains, Geant4 use appears to be marginal in the CAARI environment. This presentation discusses the impact of Geant4 simulation capabilities on scientific and industrial investigations represented at CAARI: it presents an overview of Geant4 functionality relevant to this field, along with a review of experimental applications and a scientometric analysis of its use. Special emphasis is given to recent developments of physics models in the low energy domain, new results of Geant4 experimental validation, and original uncertainty quantification methods of the outcome of the simulation.

Finally, this presentation highlights the challenges to current simulation tools deriving from novel experimental R&D, and introduces new projects that are taking shape to address the simulation requirements of future experiments.

Abstract 90 THU-IBA04-3

[Contributed Talk - Thursday 3:30 PM - Bowie B](#)

Simulation of MeV ion transmission through capillaries

[M. Doebeli](#)¹, [M. J. Simon](#)¹, [C. L. Zhou](#)², [A. Cassimi](#)², [I. Monnet](#)², [A. Méry](#)², [C. Grygiel](#)², [S. Guillous](#)²,
[T. Madi](#)², [A. Benyagoub](#)², [H. Lebius](#)², [A. M. Müller](#)¹, [M. Schulte-Borchers](#)¹, [H. Shiromaru](#)³, [H. A. Synal](#)¹

⁽¹⁾*Ion Beam Physics, ETH Zurich, Otto-Stern-Weg 5, Zurich 8050, Switzerland*

⁽²⁾*CIMAP, CEA/CNRS/ENSICAEN/UCBN, BP 5133, Caen 14070, France*

⁽³⁾*Department of Chemistry, Tokyo Metropolitan University, Hachioji, Tokyo 192-0397, Japan*

Supposed beam guiding and focussing properties of conical glass capillaries for MeV ions have obtained some attention. We have developed a SRIM based 3D Monte Carlo code to simulate ion transmission through micro-capillaries. Experimental results obtained with collimated ion beams of 1 MeV He⁺ and 71 MeV Xe¹⁹⁺ are perfectly reproduced by the simulation. No important guiding effects are observed. These results suggest that transmission properties of capillaries for ion beams in the investigated velocity range are determined by elastic scattering of the ions by the capillary material.

Abstract 92 THU-NBA04-1

[Invited Talk - Thursday 3:30 PM - Bonham B](#)

Positron Annihilation Spectroscopy Study of Barnett Shale Core

[Fnu Ameena](#)¹, [Helge Alsleben](#)², [Carroll A. Quarles](#)¹

⁽¹⁾*Physics and Astronomy, Texas Christian University, TCU Box 298840, Fort Worth TX 76129, United States*

⁽²⁾*Geology, Texas Christian University, TCU Box 298830, Fort Worth TX 76129, United States*

Measurements are reported of positron annihilation lifetime and Doppler broadening parameters on 14 samples of Barnett shale core selected from 196 samples ranging from depths of 6107 to 6402 feet. The Barnett shale core was taken from EOG well Two-O-Five 2H located in Johnson county TX. The selected samples are dark clay-rich mudstone consisting of fine grained clay minerals. The samples are varied in shape, typically a few inches long and about 1/2 inch in width and thickness, and are representative of the predominant facies in the core. X-ray fluorescence (XRF), X-ray diffraction (XRD), petrographic analysis and geochemical analysis of total organic carbon (TOC) were already available for each of the selected samples. The lifetime data are analyzed in terms of three lifetime components with the shortest lifetime fixed at 125 ps. The second lifetime is attributed to positron annihilation in the bulk and positron trapping; and the third lifetime is due to positronium. Correlations of the lifetimes, intensities, the average lifetime and S and W parameters with TOC, XRF and XRD parameters will be discussed. The observed correlations suggest that positron spectroscopy may be a useful tool in characterizing shale.

Abstract 226 THU-NBA04-2

[Invited Talk - Thursday 3:30 PM - Bonham B](#)

Progress in the design of a 21-cell Multicell Trap for Positron Storage [1]

[Christopher J Baker](#), [James R Danielson](#), [Noah C Hurst](#), [Clifford M Surko](#)

Physics Department, University of California, San Diego, 9500 Gilman Drive #0319, La Jolla CA 92093-0319, United States

The potential applications of a high capacity and/or portable antimatter trap are wide and varied. Prior to the construction of a novel multicell Penning-Malmberg trap [2,3], intended to store up to 10^{12} positrons, a test structure has been developed. This test structure consists of a large master cell of radius 38mm, 3 off-axis storage cells of radii 4mm, 6mm and 8mm, and an on-axis storage cell of radius 8mm. All cells contain an azimuthally segmented electrode, are independently controllable and are located within a UHV system and 5T magnetic field. This configuration allows us to investigate and test many of the parameters and techniques needed to successfully store 10^{12} particles in 21 cells. Recent work has been focused on transfer dynamics; moving a plasma off axis via autoresonant diocotron excitation [4] and transferring it between the master and a storage cell. Details of these processes and recent results will be presented.

[1] This work supported by the U. S. DTRA.

[2] Danielson, Weber, Surko, Phys. Plasmas **13**, 123502 (2006).

[3] Danielson, Hurst, Surko, AIP Conf. Proc. **1521**, 101 (2013).

[4] Fajans, Gilson, Friedland, Phys. Rev. Lett. **82**, 4444 (1999).

Abstract 224 THU-NBA04-3

[Invited Talk - Thursday 3:30 PM - Bonham B](#)

Electron Beam Transmission through a Cylindrically Symmetric Artificially Structured Boundary

[J. L. Pacheco](#)^{1,2}, [C. A. Ordonez](#)¹, [D. L. Weathers](#)¹

⁽¹⁾*Department of Physics, University of North Texas, 1155 Union Circle #311427, Denton TX 76203, United States*

⁽²⁾*Sandia National Laboratories, 1515 Eubank SE, Albuquerque NM 87123, United States*

Experimental research on charged particle transmission through an electro- magneto-static field configuration created by a cylindrically symmetric Artificially Structured Boundary (ASB) is presented. The ASB produces a periodic set of magnetic field cusps that are plugged electrostatically. In the system presented, the reflection or modification of charged particle trajectories occurs near the material wall boundary, where the confining fields have a relatively high strength. Away from the boundary, an essentially field free region exists, where confined particles are expected to reside. Such a system is expected to have applications as a charged particle or plasma trap and as a beam guide. An overview of the experimental system is given. Results that pertain to electron beam transmission through the system are also shown. The hardware and software developed to operate this system as a charged particle trap are described briefly.

This material is based upon work supported by the Department of Energy under Grant No. DE-FG02-06ER54883 and by the National Science Foundation under Grant No. PHY-1202428.

Neutron induced reactions with the 17 MeV facility at the Athens Tandem Accelerator NCSR "Demokritos"

[Rosa Vlastou](#)¹, [Maria Anastasiou](#)¹, [Maria Diakaki](#)¹, [Antigoni Kalamara](#)¹, [Michael Kokkoris](#)¹, [Michael Serris](#)², [Michael Axiotis](#)³, [Anastasios Lagoyannis](#)³

⁽¹⁾*Physics, National Technical University of Athens, Zografou Campus, Athens 15780, Greece*

⁽²⁾*Hellenic Army Academy, Vari, Athens 166 73, Greece*

⁽³⁾*Institute of Nuclear Physics, NCSR "Demokritos", Agia Paraskevi, Athens 15310, Greece*

Studies of neutron induced reactions are of considerable interest, not only for their importance to fundamental research in Nuclear Physics and Astrophysics, but also for practical applications in nuclear technology, dosimetry, medicine and industry. These tasks require improved nuclear data and higher precision cross sections for neutron induced reactions

In the 5.5 MV tandem T11/25 Accelerator Laboratory of NCSR "Demokritos" monoenergetic neutron beams have been produced in the energy range ~ 16-19 MeV using a new Ti-tritiated target of 373 GBq activity, consisting of 2.1 mg/cm² Ti-T layer on a 1mm thick Cu backing, by means of the ³H(d,n)⁴He reaction. The corresponding beam energies obtained from the accelerator, were 0.8-3.7 deuterons. The maximum flux has been determined to be of the order of 10⁵-10⁶n/cm² s, implementing reference reactions, while the flux variation of the neutron beam is monitored by using a BF₃ detector. The beam has been used for the measurement of (n,2n) cross sections on several isotopes of Hf, Ir and Au at 16.9 and 17.3MeV with the activation technique. These reactions have already been investigated in the energy region 8-11 MeV using the neutron beam produced by means of the ²H(d,n)³He reaction. Statistical model calculations using the code EMPIRE 3.1 and taking into account pre-equilibrium emission were performed on the data measured in this work as well as on data reported in literature.

A short review will be also presented on the activities related with the neutron facility in the 5.5 MV tandem T11/25 Accelerator Laboratory of NCSR "Demokritos" in Greece.

Direct observation of microstructural evolution in graphitic materials under ion irradiation

[Jonathan A Hinks](#)¹, [Graeme Greaves](#)¹, [Sarah J Haigh](#)², [Cheng-Ta Pan](#)², [Stephen E Donnelly](#)¹

⁽¹⁾*School of Computing and Engineering, University of Huddersfield, Queensgate, Huddersfield HD1 3DH, United Kingdom*

⁽²⁾*School of Materials, University of Manchester, Material Science Centre, Grosvenor Street, Manchester M13 9PL, United Kingdom*

Dimensional change in graphitic materials under displacing radiation is a known phenomenon in which contraction occurs in the a/b-directions (i.e. in the basal planes) and expansion occurs in the c-direction (i.e. normal to the basal planes). The implications of these changes are important for technologies such as current and future nuclear reactor designs incorporating graphite as a core material and for the processing of graphene-based devices.

By selection of appropriate ion species and energy, it has been possible to control damage profiles across the thickness of single thin-crystals of graphite whilst under observation in a transmission electron microscope at the Microscope and Ion Accelerator for Materials Investigations (MIAMI) facility at the University of Huddersfield, United Kingdom. Using this approach, greater damage levels and thus greater dimensional change can be induced in the lower region of a sample

relative to the upper region. This induces strain within the sample resulting in the creation of dislocations which can assemble into ordered arrays and in buckling of the material leading to kink bands. The dynamic nature of the microstructural evolution has been captured and will be presented alongside an explanation of the physical phenomena driving the observed changes.

The fundamental atomic processes which cause dimensional change under displacing irradiation in graphene and graphite are not well understood. Additional low temperature experiments will be presented which demonstrate that similar results are obtained well below the activation temperature for the thermal diffusion of vacancies and interstitials which are a requirement for the point-defect-driven mechanisms proposed in the literature. Alternative mechanisms will also be discussed in the context of the results presented.

Abstract 65 THU-RE07-2

[Invited Talk - Thursday 3:30 PM](#) - [Bowie C](#)

Ion microscopy based correlative microscopy techniques for high-sensitivity high-resolution elemental mapping

[Patrick Philipp](#), [David Dowsett](#), [Santhana Eswara](#), [Yves Fleming](#), [Tom Wirtz](#)

Science and Analysis of Materials (SAM), CRP - Gabriel Lippmann, 41, rue du Brill, Belvaux 4422, Luxembourg

Progress in materials science and life sciences depends on the capabilities of analytical tools. For investigations at the nanoscale, techniques providing chemical or elemental information with high lateral resolution and high sensitivity are of prime importance. For imaging with high lateral resolution, transmission electron microscopy (TEM), helium ion microscopy (HIM) and scanning probe microscopy (SPM) are excellent tools with sub-nm to sub-Å lateral resolution. However, these techniques have the drawback of providing no, or only limited, chemical information. In electron microscopy, some information is obtained by EELS and EDS, but the sensitivity is limited. By contrast, secondary ion mass spectrometry (SIMS) offers detection limits down to the ppb range combined with a high dynamic range and a high mass resolution range which allows for the differentiation between isotopes. The latter is important because of the increasing use of isotopic labelling. Yet, the lateral resolution in SIMS is limited to 50 nm.

Imaging with the highest possible chemical sensitivity and a high lateral resolution has been obtained by developing concepts and three dedicated prototype instruments which combine TEM, HIM and SPM with in-situ SIMS. Preliminary results are encouraging: excellent detection limits are obtained by using reactive gas flooding without affecting the imaging capabilities of TEM, HIM and SPM. Hence, the combination of high-resolution microscopy and high-sensitivity chemical mapping on a single instrument represents a new level of correlative microscopy.

In this talk, we will present the recently developed instruments, give an overview of the obtained performances, present typical examples of applications and make a comparison between ex-situ and in-situ combination of these techniques.

Abstract 137 THU-RE07-3

[Contributed Talk - Thursday 3:30 PM](#) - [Bowie C](#)

Design, implementation, and characterization of a triple beam in situ ion irradiation TEM facility

[Daniel Bufford](#), [Barney Doyle](#), [Daniel Buller](#), [Khalid Hattar](#)

Radiation-Solid Interactions, Sandia National Laboratories, PO Box 5800, Albuquerque NM 87185, United States

Over the past 50 years, **in situ** ion irradiation transmission electron microscopy (TEM) has proven invaluable for characterizing the behavior of defects produced in materials by energetic particles in real time at nanometer length scales. Combinations of beams of different atomic species and energies often lead to synergistic defect behavior not seen with single beams. Such results highlight the importance of conducting multiple beam experiments to better understand material response in complex radiation conditions. Sandia National Laboratories* recently developed a facility capable of studying both displacement damage and ion implantation by exposing TEM samples or coupons to beams from a 0.8-6 MV EN Tandem and 0.5-10 kV Colutron G-1 accelerator either individually or concurrently. Here, we present calculations from the theoretical beam line design, which determined the feasibility of mixing beams of different rigidity and steering them into the sample despite strong magnetic fields from electron optics inside the TEM.

The facility's capability was further extended to allow up to three simultaneous incident species by carefully selecting a mixed source gas with equal mass and ionization state components (**e.g.** He and D₂). We discuss results from elastic recoil detection experiments, which revealed the relative composition of this He/D₂ beam. Finally we show **in situ** ion irradiation TEM results demonstrating the response of a model system (Au) to single, dual, and triple beams. Most interestingly, we show bubble/void formation and annihilation in real time from heavy ion cascades during triple beam Au + He/D₂ irradiation.

This research was funded by the U.S. Department of Energy, Office of Science, Office of Basic Energy Sciences, Division of Materials Sciences and Engineering. Sandia National Laboratories is a multi-program laboratory operated by Sandia Corporation, a wholly owned subsidiary of Lockheed Martin company, for the U.S. Department of Energy's National Nuclear Security Administration under contract DE-AC04-94AL85000.

Abstract 74 THU-RE07-4

[Contributed Talk - Thursday 3:30 PM - Bowie C](#)

Helium-induced bubble formation on ultrafine and nanocrystalline tungsten under different extreme conditions

[Osman El-Atwani](#)^{1,2}, [Khalid Hattar](#)³, [Sivanandan Harilal](#)¹, [Ahmed Hassanein](#)¹

⁽¹⁾Nuclear Engineering, Purdue University, 400 central drive, West Lafayette IN 47907, United States

⁽²⁾Birck Nanotechnology Center, Purdue University, 400 central drive, West Lafayette IN 47907, United States

⁽³⁾Department of Radiation Solid Interactions, Sandia National Laboratories, Albuquerque NM 87185, United States

Ultrafine- and nanocrystalline-grained materials are postulated as irradiation tolerant materials due to their high grain boundary area.[1] Formation of ultrafine- and nanocrystalline-grained tungsten materials of high angle grain boundaries is one of the proposed solutions[2] to mitigate helium-induced irradiation damage. We have experimentally investigated the effect of irradiation conditions (temperature and energy combination) on the performance of grain boundaries as helium sinks in ultrafine- and nanocrystalline-grained tungsten formed by severe plastic deformation. Irradiations were performed at displacement and non-displacement energies and low and high temperatures. Morphology investigation was performed using in-situ and ex-situ irradiation/ transmission electron microscopy (TEM). At non-displacement energies (70 eV), regardless of temperature or vacancy migration conditions, bubbles were uniformly distributed with no preferential bubble formation on grain boundaries. At displacement energies, through in-situ irradiation/TEM experiments, bubbles were shown to preferentially form on the grain boundaries only at high temperatures where vacancy migration occurs. The decoration of grain boundaries with large faceted bubbles occurred on nanocrystalline grains of less than 60 nm size. The results, which were compared to recent theories and simulations, demonstrate the importance of vacancy supply, He-vacancy complex formation and their migration on the performance of grain boundaries as helium sinks and the associated irradiation tolerance of ultrafine-and nanocrystalline-grained tungsten to bubble formation in the grain matrix.

[1] T.D. Shen, S. Feng, M. Tang, J.A. Valdez, Y. Wang, K.E. Sickafus, Appl. Phys. Lett. , 90 (2007) 263115.

[2]G. Federici, C.H. Skinner, J.N. Brooks, J.P. Coad, C. Grisolia, A.A. Haasz, A. Hassanein, V. Philipps, C.S. Pitcher, J. Roth, W.R. Wampler, D. G. Whyte, Nuclear Fusion. 41 (2001) 1967

Abstract 67 THU-RE07-5

[Contributed Talk - Thursday 3:30 PM - Bowie C](#)

In-situ Raman spectroscopy for investigating modifications in materials under ion irradiation

[Sandrine Miro](#), [Eric Bordas](#), [Frédéric Leprêtre](#), [Patrick Trocellier](#), [Yves Serruys](#), [Lucile Beck](#)

JANNUS, CEA, DEN, Service de Recherches de Métallurgie Physique, CEA-Saclay, Gif-sur-Yvette 91191, France

Raman spectroscopy is an efficient technique to study microstructural evolution in materials under irradiation. It is possible to investigate such material modifications as **phase** and **stress** evolution and to monitor **damage build-up**. For that purpose, a Raman microscope has been installed at the multiple-irradiation platform JANNUS-Saclay (France). This spectrometer can analyze points but also has mapping and imaging capabilities. Results on various materials have been recently obtained after single, dual and triple beam ion irradiations: radiation effects in ceramics [Thomé **et al.**, APL 102, 2013; Pellegrino **et al.**, NIM B, in press], detection of hydrogen in ODS steels [Brimbal **et al.**, JNM 447, 2014].

Raman investigation can also be performed **in-situ** in order to observe the dynamic evolution of materials under continuous ion bombardment. A new system has been developed and installed on the triple beam chamber of the JANNUS-Saclay irradiation facility. The Raman probe consists of a compact fiber optic head located in the vacuum chamber at 3 cm of the irradiated sample. Spectra are measured during irradiation and collected by a 40 meter long fiber linked to the Raman spectrometer.

This paper will describe the **in-situ** Raman device and preliminary results will be presented.

Abstract 101 THU-TA02-1

[Invited Talk - Thursday 3:30 PM - Bonham D](#)

Characterization of Atmospheric Aerosols in the Adirondack Mountains Using PIXE, SEM/EDX, and Micro-Raman Spectroscopies

[Michael F. Vineyard](#), [Scott M. LaBrake](#), [Salina F. Ali](#), [Benjamin J. Nadarski](#), [Alexandrea D. Safiq](#),
[Jeremy W. Smith](#), [Joshua T. Yoskowitz](#)

Department of Physics and Astronomy, Union College, 807 Union Street, Schenectady New York 12308, United States

We have an active undergraduate research program at the Union College Ion-Beam Analysis Laboratory (UCIBAL) focused on the study of airborne pollution in Upstate New York. One of the sites that we are monitoring is located at Piseco Lake in the Adirondack Mountains. An environmental problem of particular concern in the Adirondacks for the last forty years is acid rain. While some progress has been made in recent years, the rainfall in the Adirondacks is still quite acidic. We are making detailed measurements of the composition of atmospheric aerosols as a function of particle size using proton-induced X-ray emission (PIXE), scanning electron microscopy with energy-dispersive X-ray spectroscopy (SEM/EDX), and Micro-Raman spectroscopy (MRS). These measurements provide valuable data to help identify the sources and understand the transport, transformation, and effects of airborne pollutants in Upstate New York. The samples are collected with a PIXE International nine-stage, cascade impactor that separates particulate matter by aerodynamic diameter. The PIXE experiments are performed using the 1.1-MV Pelletron accelerator in UCIBAL, while the SEM/EDX

and MRS analyzes are performed with instruments in the Union College Interdisciplinary Instrumentation Suite. Preliminary results indicate significant concentrations of sulfur in small particles that can travel great distances, and that this sulfur may be in the form of oxides that can contribute to acid rain. The sample collection and analyzes will be described, and results will be presented.

Abstract 196 THU-TA02-2

[Contributed Talk - Thursday 3:30 PM - Bonham D](#)

Radiation Curing Program

[Mark S Driscoll](#)¹, [Jennifer L Smith](#)¹, [Charles M Spuches](#)²

⁽¹⁾*UV/EB Technology Center, SUNY ESF, One Forestry Drive, Syracuse NY 13210, United States*

⁽²⁾*Outreach, SUNY ESF, One Forestry Drive, Syracuse NY 13210, United States*

The State University of New York College of Environmental Science and Forestry is offering a three-course suite of graduate-level online courses that focuses on radiation curing of resins. The Radiation Curing Program (RCP) responds to current and emerging demand for ultraviolet radiation and electron beam (UV/EB) training and education. Sustainable materials and manufacturing is a vital sector of the U.S. economy. Radiation curing processes (UV/EB) are an innovative high-growth field in advanced manufacturing. RCP is designed for current employees in radiation curing related industries as well as those preparing to enter the field. RCP introduces fundamentals of polymer chemistry pertinent to functional inks, coatings, resins and adhesives. Courses will address common commercially available radiation curing equipment, their interactions with curable formulations and representative surfaces/substrates, and techniques for monitoring cure reactions. The three courses are Introduction to Polymer Coatings, Radiation Curing of Polymer Technologies and Radiation Curing Equipment, Instrumentation and Safety. This presentation will give an overview of why the program was developed and the courses.

Abstract 403 THU-TA02-3

[Contributed Talk - Thursday 3:30 PM - Bonham D](#)

Undergraduate Measurements of Neutron Cross Sections

[S. F. Hicks](#)¹, [J. R. Vanhoy](#)², [A. J. French](#)¹, [Z. C. Santoni](#)¹, [B. C. Crider](#)³, [S. Liu](#)^{3,4}, [M. T. McEllistrem](#)³, [E. E. Peters](#)⁴, [F. M. Prados-Estévez](#)^{3,4}, [T. J. Ross](#)^{3,4}, [S. W. Yates](#)^{3,4}

⁽¹⁾*Department of Physics, University of Dallas, Irving Texas 75062, United States*

⁽²⁾*Department of Physics, United States Naval Academy, Annapolis Maryland 21402, United States*

⁽³⁾*Department of Physics and Astronomy, University of Kentucky, Lexington Kentucky 40506-0055, United States*

⁽⁴⁾*Department of Chemistry, University of Kentucky, Lexington Kentucky 40506-0055, United States*

Undergraduate physics and chemistry majors at the University of Dallas (UD) have investigated basic properties of nuclei through γ -ray and neutron spectroscopy following inelastic neutron scattering. The former have been used primarily for nuclear structure investigations, while the latter have been used to measure neutron scattering cross sections important for fission reactor applications. Recently ($n,n'\gamma$) measurements have been made on ^{54,56}Fe to deduce neutron cross sections for scattering to excited states in these nuclei by measuring the γ -ray production cross sections to states not easily resolved in neutron spectroscopy. Students learn to build nuclear level schemes and to deduce transitions by examining γ -ray production as a function of incident neutron energy. From these γ -ray excitation functions, students can determine level energies, branching ratios for decays from excited levels, and feeding contributions from higher-lying levels, which are all necessary for determining the neutron cross sections.

All measurements have been completed at the University of Kentucky Accelerator Laboratory (UKAL) using a 7-MV Model CN Van de Graaff accelerator, along with the neutron production and neutron and γ -ray detection systems located there. University of Dallas students who complete nuclear physics research typically spend 2-4 weeks completing measurements at UKAL and 6-8 weeks analysing data at UD during the summer. Students participate in accelerator operation, experimental setup, data acquisition, and in the analyses of all data. An overview of the research program and student contributions to the research important for the design and implementation of next generation fission reactors will be discussed.

This research is supported by the U.S. Department of Energy Nuclear Energy University Programs and by the Cowan Physics Fund at the University of Dallas.

Abstract 432 THU-TA02-4

[Invited Talk - Thursday 3:30 PM - Bonham D](#)

Applications of Ion Beam Analysis to Consumer Product Testing

[Graham F Peaslee²](#), [Paul A DeYoung¹](#)

⁽¹⁾*Physics Dept., Hope College, 12 Graves Pl, Holland MI 49423, United States*

⁽²⁾*Chemistry Dept., Hope College, 35 E. 12th St., Holland MI 49423, United States*

There are a wide variety of ion beam analysis techniques available to the undergraduate institution that has an accelerator facility. Over the past decade Hope College students have used these techniques in research projects that result in publications in fields as diverse as forensic science, biochemistry, materials science and geochemistry. In most cases, a well-developed method is applied to a new situation where elemental analysis (PIXE or PIGE), layer composition (RBS or PESA), or both are desired. In many disciplines there exist alternative analytical measurements that are equivalent in sensitivity or speed of analysis, which lead to interesting comparisons between instrumental techniques, but rarely new knowledge. In the last two years Hope College undergraduates have begun to apply PIXE and PIGE methods to the routine analysis of halogenated environmental contaminants. While other methods exist to measure halogens in the environment or in consumer products, there are none which can match the sensitivity and speed of sample analysis offered by these ion beam analysis techniques. This allows much larger sample sizes to be tested compared to traditional wet chemistry techniques, which can lead to fundamental new insights into fate and transport of these environmental contaminants. Examples of these techniques applied to flame retardant and stain treatment detection in consumer products will be presented, together with what new directions could be explored by involved large numbers of undergraduate researchers.

Abstract 481 FRI-PS04-1

[Plenary Talk - Friday 8:00 AM - Lone Star Ballroom](#)

Photon Activation Analysis and its Applications

[Doug P. Wells](#)

South Dakota School of Mines and Technology, Rapid City South Dakota 57701, United States

Nuclear activation analysis using neutrons, charged particles and photons has a long history, with many applications in environmental, cultural and forensic disciplines. Neutrons, positive ions and photons each have their respective relative advantages. In the case of photons from electron-beam bremsstrahlung, these relative advantages are (i) high penetrability, enabling analysis of larger objects that are nearly uniformly activated, (ii) non-destructive analysis of high-value or irreplaceable objects, (iii) production of mostly proton-rich isotopes, yielding typically shorter activation half-lives that enable more rapid return of objects to their owners and (iv) highly-directional beams that potentially enable in-field applications. These particular relative advantages have only been partially exploited. There remain many important applications that have not been fully exploited. Among these are (i) industrial, criminal and arms-control forensics, (ii) provenance applications in archaeology, paleontology and museum sciences, (iii) contraband attribution and interdiction,

(iv) mining and hazardous/precious waste assay, (v) environmental studies in pollution fate and transport and (vi) nuclear non-proliferation. This talk will focus on potential of these applications, and the state of the art in these areas.

Abstract 159 FRI-PS04-2

[Plenary Talk - Friday 8:00 AM - Lone Star Ballroom](#)

Overview of Nuclear Astrophysics

[K. Ernst Rehm](#)¹, [Daniel Bardayan](#)²

⁽¹⁾*Physics Division, Argonne National Laboratory, 9700 South Cass Av., Argonne IL 60439, United States*

⁽²⁾*Department of Physics, University of Notre Dame, Notre Dame IN 46556, United States*

Stellar explosions are powerful particle accelerators where, through nuclear reactions, a large fraction of the elements in the universe is produced. While in a star the small production cross sections are compensated by its large size and long time scales, studies of these reactions on Earth require high-intensity accelerators and detectors with good efficiencies and low backgrounds. I will provide some examples of these astrophysical studies involving beams of stable and unstable nuclei from accelerators located on the surface of the Earth and in underground laboratories.

This work was supported by the US Department of Energy, Office of Nuclear Physics, under Contract No. DE-AC02-06CH11357.

Abstract 409 FRI-AMP04-1

[Invited Talk - Friday 10:00 AM - Bowie A](#)

New Opportunities for Atomic Physics with SPARC

[Reinhold H Schuch](#)

Physics, Stockholm university, AlbaNova, Stockholm S-10691, Sweden

A status report from the Stored Particle Atomic Research Collaboration (SPARC) and its condition within the new Facility for Antiproton and Ion Research (FAIR) will be given. We also sketch the envisioned program of SPARC. It exploits almost all the key features of FAIR: Ions from rest up to the relativistic energies; ion species up to bare uranium and radioactive nuclei; targets that range from intense photon fluxes to cold electrons and to atoms and solids. These facilities together with new instrumentation offer a range of challenging opportunities for atomic physics and related fields. SPARC@FAIR will soon start up (beginning 2015) with experiments at the low-energy storage ring for heavy highly-charged ions CRYRING that is presently installed at the ESR at GSI. There, high-accuracy experiments in the realm of atomic and nuclear physics will be possible. A brief introduction to these opportunities is given.

Abstract 241 FRI-AMP04-2

[Invited Talk - Friday 10:00 AM - Bowie A](#)

Electron- and proton-impact excitation of the heaviest Helium-like ions

[Alexandre Gumberidze](#)^{1,2}

⁽¹⁾*ExtreMe Matter Institute EMMI, GSI, Planckstrasse 1, Darmstadt 64291, Germany*

Electron-impact excitation (EIE) of bound electrons is one of the most fundamental processes and leads to the specific formation of spectral lines. In particular, it is responsible for the vast majority of x-ray radiation produced in various kinds of plasmas, in high energy density physics experiments and at laboratory fusion devices. Furthermore, relativistic and retardation effects are known to affect the EIE process through the generalized Breit interaction (GBI) [1].

In this contribution, we have extended our previous study [2] of the effect of electron-impact excitation in heavy highly-charged ions (HCI) undergoing collisions with neutral atoms. Namely, in a measurement carried out at the Experimental Storage Ring (ESR) we looked for electron- and proton (nucleus)-impact excitation (PIE) in relativistic collisions between Helium-like uranium ions and hydrogen and argon targets. Here, electron-electron correlation effects can be addressed which are predicted to influence these processes significantly. By performing measurements with different targets as well as with different collision energies, we were able to gain access to and study both; PIE and EIE processes of the ground state of He-like uranium ions in the relativistic collisions.

[1] C. J. Fontes, D. H. Sampson, H. L. Zhang, Physical Review A 51 R12 (1995).

[2] A. Gumberidze et al., Phys. Rev. Lett. 110, 213201 (2013).

Abstract 462 FRI-AMP04-3

[Invited Talk - Friday 10:00 AM - Bowie A](#)

Experiments with stored highly-charged ion at the border between atomic and nuclear physics

[Yuri A Litvinov](#)¹, [Fritz Bosch](#)¹, [Thomas Stöhlker](#)^{1,2,3}, [Shahab Sanjari](#)¹, [Nicolas Winckler](#)¹, [Christophor Kozhuharov](#)¹, [Markus Steck](#)¹, [Fritz Nolden](#)¹, [Xiaolin Tu](#)^{1,4}

⁽¹⁾*Atomic Physics, GSI Helmholtz Center, Planckstrasse 1, Darmstadt 64291, Germany*

⁽²⁾*Helmholtz Institute Jena, Jena 07743, Germany*

⁽³⁾*Friedrich-Schiller-Universität Jena, Jena 07743, Germany*

⁽⁴⁾*Institute of Modern Physics, Chinese Academy of Sciences, Lanzhou 730000, China*

Atomic charge states can significantly influence nuclear decay rates. An obvious example is the electron capture decay probability which depends on the number of bound electrons. A straightforward motivation for studying the beta-decay of highly-charged ions is that stellar nucleosynthesis proceeds at high temperatures where the involved atoms are highly ionized. Furthermore, highly-charged ions offer the possibility to perform basic investigations of beta decay under clean conditions: The decaying nuclei can be prepared as well-defined quantum-mechanical systems, such as e.g. one-electron ions in which all interactions with other electrons are excluded, and thus the complicated corrections due to shake-off effects, electron screening etc. can be removed.

Largest modifications of nuclear half-lives with respect to neutral atoms have been observed in beta decay of fully-ionized nuclei. Presently, the ion-storage ring ESR at GSI is the only facility in the world for addressing radioactive decays of highly-charged ions. Due to the ultra-high vacuum of about 10^{-10} mbar, the high atomic charge states of stored ions can be

preserved for extensive periods of time (minutes, hours). The decay characteristics of electron-cooled stored ions can be accurately measured by employing the non-destructive time-resolved Schottky spectrometry technique.

Recent experiments with stored exotic nuclei, that have been performed at the ESR will be discussed in this contribution. A particular emphasis will be given to two-body beta decays, namely bound-state beta decay and orbital electron capture.

Abstract 345 FRI-AMP04-4

[Contributed Talk - Friday 10:00 AM - Bowie A](#)

Single differential projectile ionization cross sections ds/dE_e for 50 A MeV U^{28+} in the ESR storage ring

[Siegbert J Hagmann](#)^{1,2}, [Pierre-Michel Hillenbrand](#)^{1,3}, [Carsten Brandau](#)⁴, [Michael Lestinsky](#)¹, [Yuri Litvinov](#)^{1,5}, [Alfred Müller](#)³, [Stefan Schippers](#)³, [Uwe Spillmann](#)¹, [Sergiy Trotsenko](#)^{1,6}, [Thomas Stöhlker](#)^{1,6,7}, [Nickolas Winkler](#)¹, [Weidong Chen](#)¹

⁽¹⁾Atomic Physics, Helmholtzzentrum GSI, Darmstadt, Germany

⁽²⁾Inst. f. Kernphysik, University Frankfurt, Frankfurt, Germany

⁽³⁾Strahlenzentrum, University Giessen, Giessen, Germany

⁽⁴⁾EMMI, Helmholtzzentrum GSI, Darmstadt, Germany

⁽⁵⁾Physikalisches Institut, Universität Heidelberg, Heidelberg, Germany

⁽⁶⁾Helmholtz Insitut Jena, Jena, Germany

⁽⁷⁾Physikalisches Insitut, Universität Jena, Jena, Germany

The very high intensity beams of relativistic high Z ions with incident collision energies up to 2.7 A GeV requested for experiments using the SIS100 synchrotron of FAIR requires that $1.3 \cdot 10^{11}$ ions at 2.6 Hz be injected from SIS12/18 into SIS100. The needed luminosity of the beam can only be achieved for such high Z ions when a low charge state q of the ion to be accelerated keeps the particle density via the space charge limit ($\sim A/q^2$) at the highest feasible level. For a thorough understanding of beam loss it is imperative that the mechanisms active in projectile ionization be understood quantitatively to provide benchmarks for advanced **ab initio** theories beyond first order. We have embarked on an experimental investigation of single differential projectile ionization cross sections ds/dE_e (SDCS) for single and multiple ionization of U^{28+} in the ESR storage ring by measuring the electron loss to continuum (ELC) cusp at 0^0 with respect to the beam axis employing our imaging forward electron spectrometer. This was motivated by the high relative fraction of multiple ionization estimated to exceed 40%. We report first results for absolute projectile ionization SDCS for U^{28+} . We find a remarkably high asymmetry for the ELC cusp. This is at strong variance with the line shape expected for validity of first order theories.

Abstract 262 FRI-AMP04-5

[Invited Talk - Friday 10:00 AM - Bowie A](#)

Two Photon Decay in High-Z He-like Ions

[Sergiy Trotsenko](#)

Helmholtz Institute Jena / GSI, Planckstrasse 1, Darmstadt 64291, Germany

The study of two-photon transitions (2E1) in He-like heavy ions is of particular interest due to the sensitivity of its spectral shape to electron-electron correlation and relativistic effects. Therefore, a detailed study of the spectral shape of the two-photon distribution along the helium isoelectronic sequence (the simplest multi-electronic system) is of great importance for understanding the interplay between relativity and electron-electron correlations for medium to high-Z ions. Numerous experimental and theoretical studies have attempted to explore this process, however due to a lack of experimental accuracy sensitivity to relativistic theory has not yet been achieved.

In the present investigation a novel approach for studying the two-photon transition in few-electron high-Z ions is applied. Here, relativistic collisions of Li-like projectiles with low-density gaseous matter have been exploited to selectively populate the desired initial $1s2s$ state, which allows us to measure the undistorted two-photon spectral shape. The $1s2s\ ^1S_0 \rightarrow 1s^2\ ^1S_0$ two-photon decay in He-like high-Z ions was examined and the continuum shape of the two-photon energy distribution was compared with fully relativistic spectral distributions, which in turn are predicted to be Z-dependent. Compared to conventional techniques, the present approach improves statistical and systematic accuracy, which allowed us to achieve for the first time sensitivity to relativistic effects on the two-photon decay spectral shape as well as to discriminate the measured spectrum for tin from theoretical shapes for different elements along the helium isoelectronic sequence.

Abstract 49 FRI-IBM06-1

[Invited Talk - Friday 10:00 AM - Bonham C](#)

An ideal system for analysis and interpretation of ion beam induced luminescence

[Peter David Townsend](#)¹, [Miguel Luis Crespillo Almenara](#)²

⁽¹⁾*Department of Engineering, University of Sussex, Brighton East Sussex BN1 9QH, United Kingdom*

⁽²⁾*Department materials science and engineering, University of Tennessee, 1321 White Avenue, Knoxville Tn 37996-1950, United States*

Luminescence produced during ion beam implantation is apparent from most insulators, but surprisingly the information extracted from it is often far from optimum. Therefore, rather than summarise existing literature the focus here is on the design of an idealised, and feasible, target chamber that could offer far more information than has currently been obtained. Such an improved and multi-faceted approach has a range of options to simultaneously record luminescence spectra generated by the ion beam, explore transient and excited state signals via probes of secondary excitation methods (such as ionisation or photo stimulation). In addition one may monitor optical absorption and lifetime dependent features, plus stress and polarization factors. A particular valuable addition to normal measurements is to have the ability to modulate both the ion beam and the probes. These features allow separation of transient lifetimes, as well as sensing intermediate steps in the defect formation and/or relaxation and growth of new phases and nanoparticle inclusions. It is already known that luminescence methods are the most sensitive probes of defect and imperfection sites in optically active materials. Less familiar is that if the same signal collection is made during controlled cooling or heating of the samples it is effective at revealing phase transitions (both of host and inclusions). Further, simultaneous excitations (e.g. ions and photons) at different temperatures may even lead to different end situations and enable fabrication of unique material structures. References to existing literature will underline that the overall benefits of studying ion beam induced luminescence can be far more fruitful than has normally been considered.

Abstract 361 FRI-IBM06-2

[Invited Talk - Friday 10:00 AM - Bonham C](#)

ION/ELECTRON INDUCED LUMINESCENCE FOR RADIATION DAMAGE PROCESS INTERPRETATION AND IN SITU MATERIAL VERIFICATION.

[Marta Malo](#)

Euratom/CIEMAT fusion association, CIEMAT, Avda Complutense 40, Madrid 28040, Spain

Charge particle accelerators are widely used for radiation damage investigation and testing of materials for nuclear systems and/or aerospace industry, as a means of reproducing radiation effects due to ionization and displacement damage under properly controlled conditions of temperature, pressure, and dose rate.

The Research Centre for Energy, Environment and Technology (CIEMAT), Madrid, Spain features two installations (2 MeV Van de Graaff electron accelerator and a 60 kV ion implanter) specifically developed for in situ material characterization during irradiation, where experimental set ups are mainly focused on the study of volume and surface electrical degradation in insulating materials, key properties of this type of material for fusion applications.

These installations have been equipped with optical systems which permit electron and ion beam induced luminescence to be measured at the same time as recording the electrical conductivity. Both electron and ion induced luminescence give information about defects originally present in the materials, and those produced by irradiation, and hence is considered to be a valuable tool for material modification monitoring during irradiation.

Recent results for combined ion-induced luminescence and surface electrical degradation experiments in aluminas confirmed a correlation between conductivity changes and evolution of emission bands with irradiation dose. Similar experiments under electron irradiation in silicon carbide have also shown the usefulness of luminescence for material characterization and evaluation of radiation effects.

These types of experiments intend to explore the capability of luminescence for real-time materials characterization, which could be implemented for inaccessible components in future fusion devices and present fission reactor experiments, as well as an additional technique for interpretation of the fundamental processes that take place during irradiation.

Abstract 440 FRI-IBM06-3

[Invited Talk - Friday 10:00 AM - Bonham C](#)

Au-implanted CeO₂ thin films for the selective detection of gases in a harsh environment

[Manjula Nandasiri](#)¹, [Nicholas Joy](#)², [Tamas Varga](#)¹, [Arun Devaraj](#)¹, [Robert Colby](#)¹, [Weilin Jiang](#)³,
[Shuttha Shutthanandan](#)¹, [Suntharampillai Thevuthasan](#)¹, [Michael Carpenter](#)²

⁽¹⁾EMSL, Pacific Northwest National Lab, 902 Battelle Boulevard, Richland Washington 99352, United States

⁽²⁾College of Nanoscale Science and Engineering - SUNY, 257, Fuller Road, Albany New York 12203, United States

⁽³⁾FCSD, Pacific Northwest National Lab, 902 Battelle Boulevard, Richland Washington 99352, United States

The plasmonic metal nanoparticles embedded in metal oxide matrices are promising candidates for gas sensing due to the sensitivity of their localized surface plasmon resonance (LSPR) frequency to the changes in the environment. In this study, the plasmonic gas sensing properties of Au nanoparticles embedded in CeO₂ (ceria) were investigated. A CeO₂ thin film with ~300 nm thickness was deposited on Al₂O₃(0001) substrate using oxygen plasma-assisted molecular beam epitaxy and irradiated with 2.0 MeV Au²⁺ ions generated in a tandem accelerator with high fluence of 1×10^{17} ions/cm² at 600°C. Subsequently, Au-implanted CeO₂ (Au/CeO₂) film was annealed at 600°C for 10 hours in air to form well defined Au nanoclusters. Following the Au implantation at 600°C, Glancing incidence x-ray diffraction pattern showed the Au peaks and the reflections associated with ceria-alumina inter-mixing phase (CeAlO₃) in addition to CeO₂ peaks. It suggests the inter-diffusion of metal atoms at the ceria-alumina interface, which is possibly due to the bombardment of high energy Au²⁺

ions at the elevated temperature. Rutherford backscattering spectrometry (RBS) spectra and x-ray photoelectron spectroscopy (XPS) depth profile data further confirmed the inter-diffusion of the metal atoms at the film/substrate interface. Transmission electron microscopy (TEM) image showed a ~60 nm thick CeAlO₃ layer, which is sandwiched between the film and substrate. The x-ray photoelectron spectroscopy (XPS) and RBS depth profiles and TEM image further showed a very low Au concentration in CeAlO₃ layer compared to CeO₂. The 3-D distribution of Au nanoparticles in CeO₂ was also studied using atom probe tomography. Following the ex-situ characterization, the ppm level gas exposure experiments and LSPR analysis showed the promising sensing characteristics of Au/CeO₂ towards the detection of H₂, NO₂ and CO in an air background at 500°C.

Abstract 112 FRI-IBM06-4

[Contributed Talk - Friday 10:00 AM - Bonham C](#)

Low temperature and decay lifetime photoluminescence of Eu and Tb nanoparticles embedded into SiO₂

[Paulo L. Franzen](#), [Felipe L. Bregolin](#)³, [Uilson S. Sias](#)², [Henri I. Boudinov](#), [Moni Behar](#)

⁽¹⁾*Instituto de Física, Universidade Federal do Rio Grande do Sul, Av. Bento Gonçalves, 9500, Porto Alegre Rio Grande do Sul 91501-970, Brazil*

⁽²⁾*Instituto Federal Sul-Rio-Grandense, Praça 20 de Setembro, 455, Pelotas Rio Grande do Sul 96015-360, Brazil*

⁽³⁾*Institute of Ion Beam Physics and Materials Research (FWIM), Helmholtz-Zentrum Dresden-Rossendorf, Bautzner Landstrasse 400, Dresden, Germany*

We have studied the photoluminescence (PL) and decay lifetime of Tb and Eu nanoparticles (NPs) at low temperatures. The NPs were obtained by implanting 3×10^{15} at/cm² 100 keV Eu ions into a thermally grown SiO₂ matrix. During implantation the sample was kept at 300 °C and after the implantation the samples were annealed for 1 hour at 500 °C in O₂ atmosphere. The Tb samples showed a featured emission spectra in the visible, with two prominent peaks at 542 and 550 nm, whose shape is almost unchanged for different temperatures. The PL has a maximum yield at 12 K and decreases with increasing temperature reaching a minimum at 300 K. The lifetime is wavelength independent in the entire range and doesn't change for different temperatures, remaining constant at a value of 1.5 ms. Regarding Eu NPs emission, two spectral regions were identified, one with a narrow emission bands (from 570 to 750 nm) and the other with a broad emission band (from 400 to 550 nm). Both PL regions show a minimum yield at 12 K, and next it rises with increasing temperatures, reaching the maximum around 100 K. Then, the PL yields start to decrease, reaching at 300 K a value similar to the one obtained at 12 K. For the Eu NPs PL lifetime, two different results were obtained. The long wavelength spectral region shows a lifetime of the order of 1.0 ms independent of the temperature. Conversely, the short wavelength region has a decay time of 50 μs for any given temperature. At low temperatures however, the sample presents a second and much longer decay time in the order of several milliseconds. Our results can be explained with a model like that proposed by Calcott et al.

Abstract 344 FRI-IBM06-5

[Contributed Talk - Friday 10:00 AM - Bonham C](#)

Preliminary study on formation of proton microbeam with continuously variable kinetic energy for 3-Dimensional proton lithography

[Takeru Ohkubo](#), [Yasuyuki Ishii](#), [Tomihiko Kamiya](#)

Takasaki Advanced Radiation Research Institute, Japan Atomic Energy Agency, 1233 Watanuki-machi, Takasaki Gunma 370-1292, Japan

Focused proton beam of several hundreds of keV with micrometer scale range become a powerful tool for 3-Dimensional (3D) proton lithography. Ion beam, especially proton beam, has a longer penetration depth into a certain material than electron beam with the same kinetic energy has. When the proton beam's kinetic energy increases, the penetration depth becomes longer. Using different kinetic energies of proton beams for one sample in proton lithography, a 3D structure can be made by the beam writing directly. Since those beams are, so far, generated from large accelerators with a long beam transport line, a compact system with higher energy, whose size is same level as FIB, is necessary for industrial applications.

A new compact focused gaseous ion beam (gas-FIB) system with an acceleration voltage of a few hundreds of kV was developed to form microbeams using a plasma-type ion source. Ion beam is accelerated and focused simultaneously by a pair of electrodes and therefore a total length of the gas-FIB system becomes much shorter than that of a conventional microbeam system. Furthermore, the beam can be focused to the same point with a constant working distance by adjusting voltages of every electrode proportionally even if kinetic energy of the beam is changed. This is the key point of gas-FIB to be expected as a powerful tool for 3D fabrication. A penetration depth can be changed continuously while proton beam is irradiated to a sample.

The preliminary experiments were carried out to show the availability of the gas-FIB system as a writing tool for 3D proton lithography. The beam diameters with various kinetic energies were several micrometers measured at the almost same point, which is smaller than about 20 micrometers obtained by previous experiments presented in CAARI2012. More detailed results will be discussed at the presentation.

Abstract 455 FRI-NBA01-1

[Invited Talk - Friday 10:00 AM - Bonham B](#)

The Analysis Of Large Samples Using Accelerator Activation

[Christian Segebade](#)

Idaho Accelerator Center, Idaho State University, 1500 Alvin Ricken Dr, Pocatello Idaho 83201, United States

The detection power of modern instrumental analytical method has increased dramatically; analysing microgram samples detection limits in the picogram/g range are not unusual nowadays. However, sometimes large amounts of material have to be analysed. A typical case is the analysis of inhomogeneous matter, e.g. electric and electronic waste. This is of urgent interest regarding the enormous world-wide increase rate of this material. There are few methods only by which sample masses in the gram to kilogram range can be analysed without too much effort. One of these is photon activation analysis (PAA) using bremsstrahlung from an electron linear accelerator (LINAC) for activation. This machine, equipped with an electron beam scanner, can produce a large volume bremsstrahlung field with appreciable homogeneity. Sample volumes up to about 10 litres can be exposed. After exposure the activation products are measured with classical high resolution gamma spectrometers. Electronic waste samples of about 1.5 kg were analysed. The results were compared with those obtained by conventional methods. The agreement of the results ranged from "good" to "satisfactory". However, due to the extremely inhomogeneous distribution of some elements the agreement between the respective results was unsatisfactory since the data obtained by conventional methods were obtained by multiple analyses of sample masses of 100 - 300 milligrams.

Abstract 128 FRI-NBA01-2

[Invited Talk - Friday 10:00 AM - Bonham B](#)

Usage of quasi-monoenergetic and continuous spectrum neutron generators for cross-section measurements and benchmarking

[Mitja Majerle](#), [Pavel Bem](#), [Jan Novak](#), [Eva Simeckova](#), [Milan Stefanik](#)

Department of Nuclear Reactions, Nuclear Physics Institute of the ASCR, v.v.i., Rez 130, Rez 25068, Czech Republic

Nuclear facilities based on fusion or accelerator driven technologies are nowadays still on the design desks, but being seriously considered for future power plants. These new concepts will operate in different neutron spectrum than today well understood classical reactors, and there is an increasing need for studies of materials, neutron monitoring, ... at neutron energies above 20 MeV.

It is a known fact that experimentally obtained neutron cross-section data above 20 MeV are rare and uncertain. There are few facilities which are suitable for the material studies at neutron energies above this limit. The neutron generators based on reactions of accelerated protons with Li, Be or D₂O targets providing quasi-monoenergetic and continuous neutron spectra proved to be a good option for such purpose.

The U120M cyclotron located at the Nuclear Physics Institute of the ASCR provides the protons for the neutron generators based on thin Li and thick Be and D₂O targets. The generators and their usage in the frames of the cross-section measurement programs are presented here. The special stress is put on the quasi-monoenergetic neutron beams with the monoenergetic peaks in the energy interval 20-35 MeV and relevant measurements. Quality assurance of such measurements (absolute number of neutrons, unfolding procedures, ..) and the achievable accuracy are addressed. The characteristics of the cyclotron and their potential usage are discussed in conclusion.

Abstract 5 FRI-NBA01-5

[Contributed Talk - Friday 10:00 AM - Bonham B](#)

Feasibility study of photon activation analysis (PAA) of gold-bearing ores

[Sultan Jaber Alsufyani](#), [Lauren Liegey](#), [Valeriia Starovoitova](#), [Erdinch Tatar](#)

Department of physics, Idaho State University, 921 S 8th Ave, Pocatello Idaho 83209, United States

Elemental analysis techniques find use in a variety of applications and industries. In particular, mining and metallurgy industries require reliable high quality geochemical and mineralogical analyses of rocks, minerals, and ores in a timely manner. Precious metals and gold in particular, can be analyzed by many techniques. As of today lead collection fire assay is considered the most definitive technique for finding gold concentration in ores.

In this paper we are going to show the results of the feasibility study of another analytical technique, photon activation analysis, to assay gold bearing ores. We will show that by activating gold containing samples with 25-40 MeV bremsstrahlung photons, we can accurately determine concentration of gold. During photon activation analysis the high-energy photon interacts with the gold nuclide, ¹⁹⁷Au and a neutron is ejected resulting in an unstable ¹⁹⁶Au isotope which emits characteristic gamma rays while decaying down to the ground state. If a reference material is used, gamma-spectroscopy of the irradiated samples yields the concentration of gold straightforwardly.

PAA is a fast and sensitive technique, which does not require sample preparation and under certain irradiation conditions its detection limit can reach ppb level. In order to find these optimum irradiation conditions we have investigated the effect of electron's energy and cooling time on the detection level of gold. Several samples with gold content from 0.1 to 10 ppm were irradiated using 25-40 MeV electron beam. Gamma-spectroscopy on irradiated samples was performed. It was found that the detection limit of gold using ¹⁹⁶Au(γ,n)¹⁹⁵Au reaction varied from 80 to 150 ppb and the optimum electron energy was found to be around 30 MeV. The optimum cooling time was found to be 120 hours. The influence of impurities in the ore (matrix effect) on gold detection limit was investigated as well and found to be significant.

A Comparison of Various Procedures in Photon Activation Analysis (PAA) with the Same Irradiation Setup

[Z. Sun](#)¹, [D. Wells](#)², [C. Segebade](#)³, [S. Chemerisov](#)¹

⁽¹⁾*Chemical Sciences and Engineering, Argonne National Laboratory, 9700 S. Cass Ave., Argonne IL 60439, United States*

⁽²⁾*Physics Department Rapid City, , South Dakota School of Mines & Technology, 501 E. Saint Joseph St., Rapid City SD 57701, United States*

⁽³⁾*Idaho Accelerator Center, Idaho State University, 921 S. 8th Ave. , Pocatello ID 83209, United States*

A sample of known elemental concentration was activated in the bremsstrahlung photon beam which was created by a pulsed electron LINAC. Several procedures of photon activation analysis, including those applied with/without reference material and with/without photon flux monitor, were conducted to make a comparison of their precision and accuracy in practice. Experimental results have shown that: (1) the relative procedures generated better values despite the fact that the absolute measurement can produce very close outcome in some selected elements; (2) Among relative procedures, the method with internal flux monitor yields higher quality of the analytical results. In this article, the pros and cons of each procedure are discussed as well.

Experimental techniques to investigate neutron sources for the s-process

[Manoel Couder](#)

Physics, University of Notre Dame, 124 Nieuwland Science Hall, Notre Dame IN 46556, United States

The $^{13}\text{C}(\alpha, n)^{16}\text{O}$ and $^{22}\text{Ne}(\alpha, n)^{25}\text{Mg}$ reactions produce neutrons during the Helium burning phase of massive stars evolution or the Asymptotic Giant Branch part of the life of a star. Slow capture of those neutrons by heavier nuclei produces the so-called s-process elements. Currently, the studies of those two reactions are limited by environmental and beam induced background. In this talk, two complementary techniques will be discussed. The status of the St. George recoil separator commissioning at the University of Notre Dame and the design and development of CASPAR a low energy underground accelerator laboratory will be presented.

Beta decay as a probe of explosive nucleosynthesis in classical novae

[C. Wrede](#)^{1,2,3}, [M. B. Bennett](#)^{1,2}, [S. N. Liddick](#)^{1,2,4}, [D. W. Bardayan](#)⁵, [A. Bowe](#)^{1,2}, [A. A. Chen](#)⁶, [K. A. Chipps](#)^{7,8,9}, [N. Cooper](#)¹⁰, [C. Fry](#)^{1,2}, [B. Glassman](#)^{1,2}, [D. Irvine](#)⁶, [J. Jose](#)¹¹, [C. Langer](#)^{2,12}, [N. Larson](#)^{2,4}, [E. I. McNeice](#)⁶, [Z. Meisel](#)^{1,2}, [F. Montes](#)^{2,12}, [F. Naqvi](#)¹⁰, [S. D. Pain](#)⁸, [P. O'Malley](#)⁵, [R. Orteiz](#)^{1,2}, [W. J. Ong](#)⁴, [J. Pereira](#)^{2,12}, [D. Perez-Loureiro](#)^{1,2}, [C. Prokop](#)^{2,4}, [J. Quaglia](#)^{2,12,13}, [S. Quinn](#)^{1,2}, [M. Santia](#)^{1,2}, [H. Schatz](#)^{1,2,12}, [S. B. Schwartz](#)^{1,2,14}, [A. Simon](#)^{2,12}, [S. Shanab](#)^{1,2}, [A. Spyrou](#)^{1,2,12}, [S. Suchyta](#)^{2,4}, [E. Thiagalingam](#)⁶, [P. Thompson](#)^{8,9}, [M. Walters](#)⁶

⁽¹⁾*Department of Physics and Astronomy, Michigan State University, East Lansing MI 48824, United States*

⁽²⁾*National Superconducting Cyclotron Laboratory, Michigan State University, East Lansing MI 48824, United States*

⁽³⁾*Department of Physics, University of Washington, Seattle WA 98195, United States*

⁽⁴⁾*Department of Chemistry, Michigan State University, East Lansing MI 48824, United States*

⁽⁵⁾*Department of Physics, University of Notre Dame, Notre Dame IN 46556, United States*

⁽⁶⁾*Department of Physics and Astronomy, McMaster University, Hamilton ON L8S 4M1, Canada*

⁽⁷⁾Department of Physics and Astronomy, Colorado School of Mines, Golden CO 80401, United States

⁽⁸⁾Oak Ridge National Laboratory, Oak Ridge TN 37831, United States

⁽⁹⁾Department of Physics and Astronomy, University of Tennessee, Knoxville TN 37996, United States

⁽¹⁰⁾Department of Physics and Wright Nuclear Structure Laboratory, Yale University, New Haven CT 06520, United States

⁽¹¹⁾Departament Física i Enginyeria Nuclear (UPC) and Institut d'Estudis Espacials de Catalunya (IEEC), Barcelona E-08034, Spain

⁽¹²⁾Joint Institute for Nuclear Astrophysics, Michigan State University, East Lansing MI 48824, United States

⁽¹³⁾Department of Electrical Engineering, Michigan State University, East Lansing MI 48824, United States

⁽¹⁴⁾Department of Geology and Physics, University of Southern Indiana, Evansville IN 47712, United States

Classical novae are common thermonuclear explosions in the Milky Way galaxy, occurring on the surfaces of white-dwarf stars that are accreting hydrogen-rich material from companion stars. Nucleosynthesis in classical novae depends on radiative proton-capture reaction rates on radioactive nuclides. Many of these reactions cannot be measured directly at current accelerator facilities due to the lack of intense, high quality, radioactive-ion beams at the relevant energies. Since most of these reactions proceed via resonant capture, their rates can be determined indirectly by measuring the properties of the resonances. At the National Superconducting Cyclotron Laboratory, we have used the beta-delayed gamma decays of ^{26}P and ^{31}Cl to populate resonances in ^{26}Si and ^{31}S and study the radiative proton captures on ^{25}Al and ^{30}P , respectively. These were two of the three most important nuclear-physics uncertainties associated with the observable products of nova nucleosynthesis. The ^{26}P experiment has enabled a more accurate estimate of the nova contribution to the long-lived Galactic ^{26}Al detected with gamma-ray telescopes. The ^{31}Cl experiment, currently under analysis, will calibrate potential nova thermometers and mixing meters based on elemental abundance ratios, and facilitate the identification of pre-solar nova grain candidates found in primitive meteorites based on isotopic ratios.

Abstract 164 FRI-NP09-3

[Invited Talk - Friday 10:00 AM - Bowie B](#)

The $^{26}\text{Al}(p,\gamma)^{27}\text{Si}$ reaction at stellar temperatures

[S.D. Pain¹](#), [D.W. Bardayan¹](#), [J.C. Blackmon²](#), [K.Y. Chae³](#), [K.A. Chipps⁴](#), [J.A. Cizewski⁵](#), [K.L. Jones³](#), [R.L. Kozub⁶](#), [C. Matei⁷](#), [M. Matos²](#), [B.H. Moazen³](#), [C.D. Nesaraja¹](#), [P.D. O'Malley⁵](#), [J. Okolowicz⁸](#), [W.A. Peters⁵](#), [S.T. Pittman³](#), [M. Ploszajczak⁹](#), [K.T. Schmitt³](#), [J.F. Shriner Jr.⁶](#), [M.S. Smith¹](#), [D.W. Stracener¹](#)

⁽¹⁾Oak Ridge National Laboratory, Oak Ridge, United States

⁽²⁾Louisiana State University, Baton Rouge, United States

⁽³⁾University of Tennessee, Knoxville, United States

⁽⁴⁾Colorado School of Mines, Golden, United States

⁽⁵⁾Rutgers University, Piscataway, United States

⁽⁶⁾Tennessee Technological University, Cookeville, United States

⁽⁷⁾Oak Ridge Associated Universities, Oak Ridge, United States

⁽⁸⁾Polish Academy of Sciences, Radzikowskiego, Poland

⁽⁹⁾Grand Accélérateur National d'Ions Lourds, Caen, France

The long-lived radioactive nuclide ^{26}Al was the first radioisotope detected by direct astronomical observation of a γ ray associated with the beta decay of its ground state. The nuclide has since become a predominant target for γ -ray astronomy, with highly detailed directional studies indicating its galactic distribution, including the first all-sky survey of an individual γ line. Massive stars have been highlighted as dominant source of ongoing synthesis of ^{26}Al and its distribution in the interstellar medium. At these stellar temperatures, the $^{26}\text{Al}(p,\gamma)^{27}\text{Si}$ reaction is expected to be the main destruction mechanism for ^{26}Al , thus impacting the net ^{26}Al production. However, the strengths of low-lying resonances in ^{27}Si which govern this rate are not sufficiently constrained experimentally due to their low energies.

The $^{26}\text{Al}(d,p)^{27}\text{Al}$ reaction has been measured to determine spectroscopic information on the mirror states to astrophysically-important resonances in ^{27}Si , and thereby constrain the reaction rate via these resonances. The measurement was conducted at the Holifield Radioactive Ion Beam Facility at Oak Ridge National Laboratory, using a beam of ~ 5 million ^{26}Al per second. Proton ejectiles were detected in the SIDAR and ORRUBA silicon detector arrays. Details of the astrophysical motivation, experiment, and results will be discussed.

Work supported in part by the US Department of Energy and the National Science Foundation

Abstract 414 FRI-NP09-4

[Contributed Talk - Friday 10:00 AM - Bowie B](#)

Nuclear astrophysics at the CIRCE laboratory

[Lucio Gialanella](#)^{1,2}

⁽¹⁾*Dipartimento di Matematica e Fisica, Seconda Università di Napoli, Viale Lincoln 5, Caserta 81100, Italy*

⁽²⁾*INFN Sezione di Napoli, INFN, Via Cinzia anc, Napoli 80100, Italy*

Nuclear astrophysics at the CIRCE laboratory

The laboratory at CIRCE (Center for Isotopic Research on Cultural and Environmental heritage), Caserta, Italy is equipped with a 3 MV Pelletron tandem accelerator.

The focus of CIRCE is on applied research on cultural and environmental heritage. However, since a few years a program in Nuclear Astrophysics has been undertaken. Experiments are performed using the recently installed recoil mass separator ERNA (European Recoil separator for Nuclear Astrophysics) for radiative capture reactions and a scattering chamber with charged particle detection array for charged particle spectroscopy.

The experimental program includes $7\text{Be}(p,\gamma)$, $14,15\text{N}(\alpha,\gamma)$, $12\text{C}+12\text{C}$, and $12\text{C}(\alpha,\gamma)$.

A short overview of the laboratory will be given, and the experimental program in Nuclear Astrophysics will be discussed in details.

Abstract 73 FRI-NP09-5

[Contributed Talk - Friday 10:00 AM - Bowie B](#)

The JENSA gas-jet target for radioactive beam experiments at ReA3 and FRIB

[DW Bardayan](#), [S. Ahn](#), [JC Blackmon](#), [J. Browne](#), [KA Chipps](#), [U Greife](#), [A Kontos](#), [LE Linhardt](#), [M Matos](#), [SD Pain](#), [ST Pittman](#), [A Sachs](#), [H Schatz](#), [KT Schmitt](#), [MS Smith](#), [P Thompson](#), [JENSA Collaboration](#), [PD O'Malley](#)

Physics, University of Notre Dame, 225 NSH, Notre Dame IN 46556, United States

A high-density supersonic gas-jet target named JENSA (Jet Experiments in Nuclear Structure and Astrophysics) has been constructed and commissioned at Oak Ridge National Laboratory. The target creates a localized (~ 4 mm wide) high-density ($\sim 10^{19}$ atoms/cm²) concentration of gaseous atoms (H, He, N, etc...) that are suitable for use in high-resolution

experiments with radioactive beams. The interaction point of the beam with the gas-jet target is surrounded by silicon strip detectors from the SuperORRUBA (Oak Ridge Rutgers University Barrel Array) to detect reaction products with good energy (~30 keV) and angular resolution (~1 degree). Already completed experiments as well as plans to study scattering and transfer reactions on exotic beams at ReA3 will be presented. The coupling of the JENSA with the future recoil separator SECAR at the Facility for Rare Isotope Beams FRIB will also be discussed.

Abstract 207 FRI-RE09-1

[Invited Talk - Friday 10:00 AM - Bowie C](#)

Electron Beam Treatment of Wood Thermoplastic Composites

[Andrew Palm](#)¹, [Mark S Driscoll](#)¹, [Jennifer L Smith](#)¹, [L Scott Larsen](#)²

⁽¹⁾*UV/EB Technology Center, SUNY ESF, One Forestry Drive, Syracuse NY 13210, United States*

⁽²⁾*New York State Energy Research and Development Authority, 17 Columbia Circle, Albany NY 12203, United States*

Wood thermoplastic composites are a building material that is a nontoxic alternative to pressure treated lumber, and a stronger, sustainable alternative to plastic lumber. Durability and weight have been expressed as primary performance issues. Past research has focused on coupling agents and nanoparticles as additives to increase strength properties of the composites. The focus of this study was to examine the potential benefits of radiation crosslinked thermoplastic composites. Wood fiber reinforcement in a polyethylene matrix was irradiated at five different dose levels, post extrusion, with an electron beam. The composite materials were evaluated using flexural and hardness tests and scanning electron microscopy. The mechanical properties were enhanced and scanning electron microscopy showed very little evidence of wood fiber degradation.

Abstract 209 FRI-RE09-2

[Invited Talk - Friday 10:00 AM - Bowie C](#)

Electron Beam Assisted Carbon Fiber Composite Recycling

[Mark S Driscoll](#)¹, [Jennifer L Smith](#)¹, [Andrew Palm](#)¹, [L Scott Larsen](#)²

⁽¹⁾*UV/EB Technology Center, SUNY ESF, One Forestry Drive, Syracuse NY 13210, United States*

⁽²⁾*New York State Energy Research and Development Authority, 17 Columbia Circle, Albany NY 12203, United States*

Carbon fiber composites (CFC) are seeing more and more use due to their high strength and low weight. Initially they were used for very high priced items used in military and specialty civilian applications. Today commercial aerospace industry relies heavily on CFC with new jets from Airbus and Boeing being over 50% CFC. The auto industry is using CFC at a growing rate with some experts suggesting that production CFC cars are in the near future. Sporting equipment has also seen a large increase in the use of CFC over the past few years. When these items reach the end of their useful life how will they be treated. There are three main options; landfill, burn or recycle them. This presentation will discuss how electron beam irradiation could assist in the recycling of CFC and the possibility of low cost chopped carbon fibers.

Abstract 210 FRI-RE09-3

[Invited Talk - Friday 10:00 AM - Bowie C](#)

Electron Beam, Wood and the Production of Value Added Products

[Mark S Driscoll](#)¹, [Jennifer L Smith](#)¹, [L Scott Larsen](#)²

⁽¹⁾*UV/EB Technology Center, SUNY ESF, One Forestry Drive, Syracuse NY 13210, United States*

⁽²⁾*New York State Energy Research and Development Authority, 17 Columbia Circle, Albany NY 12203, United States*

Wood is a natural composite composed of cellulose, hemicellulose and lignin. The strong interaction of these three components makes wood incredibly strong and durable. This leads to high cost to process wood for uses other than a structural material. Electron beam irradiation of wood can reduce the molecular weight and crystallinity of the cellulose and thus reduce the strength and energy required to process wood for other uses. For example energy required to mill wood to 40 mesh is reduced about an order of magnitude when the wood is irradiated to 1000 kGy. This presentation will focus on how electron beam irradiation of wood can assist in the production of value added products from wood and how electron beams can be intergrated into a wood based bio-refinery.

Abstract 480 FRI-RE09-4

[Invited Talk - Friday 10:00 AM - Bowie C](#)

Recent Advancements in the Applications of Electron Beam Processing in Advanced Technologies

[Mohamad Al-Sheikhly](#)¹, [Marshall Cleland](#)

⁽¹⁾*University of Maryland, College Park MD 20742, United States*

⁽²⁾*IBA Industrial, Edgewood NY 11717, United States*

In recent years, the field of radiation engineering has played an increasingly significant role in the development and enhancement of innovative emerging technologies. With proven success in a wide variety of applications ranging from radiation therapy for cancer treatment to corrosion inhibition in nuclear power plants, the potential uses for ionizing radiation in advanced technologies are virtually limitless.

Applications for nanotechnology:

At present, there are numerous emerging nanotechnologies in which radiation applications play a significant role. Based on present pioneering research programs, examples of future trends in radiation applications in nanotechnology include the following:

Light charged particles and photons: low linear energy transfer (LET) irradiation, such as gamma radiolysis, electron beam irradiation (0.3-10 MeV), and positron irradiation play major roles in the synthesis, manufacturing, and material characterization of nanotechnology. This includes applications such as the manufacturing of nanocomposites, the synthesis of nanogels for drug delivery systems, the radiation-induced grafting of nanotubes, and positron irradiation for characterization of nanostructures

Applications for processing and manufacturing:

Ionizing radiation, particularly electron beam radiation, provides a key tool for the development and implementation of advanced technologies in radiation processing and manufacturing, with applications ranging from radiation curing of coatings to environmental remediation of harmful wastes. Examples of such applications include:

The sterilization and crosslinking of medical materials such as knee and hip replacements using ionizing radiation

The radiation-induced synthesis of magnetic nanoparticle-organic polymer hybrid materials which have potential uses in a variety of applications including magnetic data storage, medical diagnostic imaging, and drug delivery

The fabrication of advanced polymer electrolyte membranes, essential components of fuel cells for renewable energy, through radiation-induced grafting

Radiation-induced inter and intra-molecular crosslinking by an electron beam for the synthesis of nano-hydrogels is a new field with applications in drug and vaccine delivery

Abstract 235 FRI-RE09-5

[Contributed Talk - Friday 10:00 AM - Bowie C](#)

Use of PENELOPE Monte Carlo Code to design a 125 keV electron accelerator irradiator and determine its shielding requirements

[Nuttapong Phantkankum](#), [Roberto M Uribe](#)

College of Applied Engineering Sustainability and Technology, Kent State University, 375 Terrace Drive, Kent OH 44242, United States

The Monte Carlo code PENELOPE has been used in order to calculate the shielding requirements and the dose delivered to a dosimeter, for a low energy electron accelerator that is being assembled at KSU using parts from a donated Advanced Electron Beam 125 keV electron accelerator. The presentation will focus on the determination of appropriate materials to produce the shielding of the accelerator, as well as their required dimensions and finally of the dose calculations in a layer of 100 mm of water used as a detector. Assembly diagrams of the whole system will be presented as well.

Abstract 200 FRI-RE09-6

[Contributed Talk - Friday 10:00 AM - Bowie C](#)

Ozone Generation in Air During Electron Beam Processing

[Marshall R Cleland](#), [Richard A Galloway](#)

Administration, IBA Industrial, Inc., 151 Heartland Blvd., Edgewood NY 11717, United States

Ozone, the triatomic form of oxygen, can be generated by exposing normal diatomic oxygen gas to energetic electrons, X-rays, nuclear gamma rays, short-wavelength ultraviolet radiation (UV) and electrical discharges. Ozone is toxic to all forms of life, and governmental regulations have been established to protect people from excessive exposures to this gas. The human threshold limit values (TLV) vary from 60 to 100 parts per billion (ppb) in air, depending on the agency or country involved. Much higher concentrations can be produced inside industrial electron beam (EB) facilities, so methods for ozone removal must be provided. Equations for calculating the ozone yield vs absorbed energy, the production rate vs absorbed power, and the concentration in the air of an EB facility are presented in this paper. Since the production rate and concentration are proportional to the EB power dissipated in air, they are dependent on the design and application of the irradiation facility. Examples of these calculations are given for a typical EB process to cross-link insulated electrical wire or plastic tubing. The electron energy and beam power are assumed to be 1.5 MeV and 75 kW.

Surface morphology of brass and bronze treatment by high power ion beam nanosecond duration[Vladimir S. Kovivchak](#), [Tatayna V. Panova](#), [Kirill A. Mikhailov](#)*Department of Physics, Omsk State University, pr. Mira, 55a, Omsk 644077, Russia*

Studying the effect of volatile components on the formation of the surface morphology of alloys and the change in the composition under the action of a high power ion beam (HPIB) is of scientific and applied interest. Copper based alloys were chosen as the objects of the study, these included: brass LS 59-1 (37.35-42.2% Zn, 0.8-1.9% Pb), bronze BrOS 10-10 (9-11% Sn, 8-11% Pb), bronze BrAJ 9-4 (8-10% Al, 2-4% Fe) with easily fusible and highly volatile components in their composition, e.g., zinc, lead, tin, and aluminum. Irradiation was performed on a Temp accelerator by a proton-carbon (30% H^+ and 70% C^+) beam with an average energy of 300 keV, a duration of 60 ns, in the current density range of 20 - 150 A/cm² with a variation in the number of irradiation pulses from 1 to 5. The change in the morphology and surface composition of copper alloys (brass LS 59-1, bronzes BrOS 10-10 and BrAJ 9-4) upon irradiation with HPIB is studied. It is shown that craters are mainly formed at the location of lead or sulfur inclusions. The formation of the morphology, first of all craters, on the surface of copper alloys containing elements with different volatilities under HPIB action depends not only on the vapor pressure during evaporation of the most volatile component and their concentrations, but also on the homogeneity of the distribution of these elements over volume. The volatile elements localized in the surface layer with a thickness less than the projected path of beam ions most strongly affect the surface roughness under such exposure. Zinc enrichment of the surface observed for brass is probably due to condensation and the formation of zinc nanoparticles as a result of its cooling during expansion in vacuum. The micron-sized particles of the alloy forming under repeated HPIB irradiation, as a rule, are depleted of the most highly volatile component of the alloy.

Studies of the Thorium-Uranium Fuel Cycle[Cristian Bungau](#), [Robert Cywinski](#), [Roger Barlow](#), [Adriana Bungau](#)*School of Applied Sciences, University of Huddersfield, Queensgate, Huddersfield HD1 3DH, United Kingdom*

Accelerator Driven Subcritical Reactors have been proposed as a more comprehensive alternative to conventional nuclear reactors for both energy production and for burning radioactive waste. The addition of several new classes to the GEANT4 Monte Carlo code enabled the code to calculate for the first time the changes in the number of neutrons inside the reactor as a function of time, which are needed for reactor criticality calculations. This extended version of GEANT4 can also be used to simulate the Thorium-Uranium fuel cycles in ADSR systems.

Commissioning of an in-air irradiation facility with a 30 MeV/A Xenon Beam[Mariet Anna Hofstee](#), [Sytye Brandenburg](#), [Marc-Jan van Goethem](#), [Reint Ostendorf](#), [Harry Kiewiet](#),
[Jan de Jong](#)*AGOR Cyclotron, KVI-CART, University of Groningen, Zernikelaan 25, Groningen NL 9747 AA, Netherlands*

We have expanded our in-air irradiation facility used for radiation effect and radiobiology experiments with a modified setup to be able to irradiate samples with heavy ion beams up to 30 MeV/A Xenon. The XY-translation stage has been enhanced with z-translation and theta rotation capabilities. The beam diagnostics have been adjusted and the degrader

system modified to work with heavy ion beams. A new cocktail of 30 MeV/A beams ranging from molecular deuterium to Xenon has been developed for use with this facility. Further developments, such as improving the real-time diagnostics and increasing the beam energy, are anticipated.

Abstract 362

[Regular Poster - Poster Sessions](#)

Chemical characterisation of explosives residues by Ambient Pressure MeV-SIMS

[Lidija Matjacic](#)¹, [Nadia Abdul-Karim](#)², [Brian Jones](#)¹, [Vladimir Palitsin](#)¹, [Julien Demarche](#)¹, [Roger Webb](#)¹

⁽¹⁾*Ion Beam Centre, University of Surrey, Guildford, Surrey, GU2 7XH, Guildford GU2 7XH, United Kingdom*

⁽²⁾*University College London, Gower Street, London WC1E 6BT, United Kingdom*

While secondary ion mass spectroscopy (SIMS) is a well-established analytical technique for high-resolution molecular imaging, recent years have seen the emergence of a new technique resorting to MeV heavy ions beams to produce secondary ions from an insulating sample surface: "MeV-SIMS".

These MeV beams present the twofold advantage to be focusable down to the micron while being scanned, and to be extractable through a thin Si₃N₄ window and travel a few millimetres in air. Hence, imaging with a submicron resolution is possible under ambient conditions, avoiding vacuum effects on sample, simplifying sample preparation, and significantly decreasing the total analysis' time. Large intact molecules (up to hundreds of kDa) can be gently vaporised from the surface, while low currents ensure a non-destructive probing technique. Elemental characterisation can also be performed simultaneously by PIXE. Therefore, applications are found in many different areas like biomedicine for living cells studies, environmental analysis for establishment of air pollution, forensics for chemical analysis of fingerprint or cultural heritage for conservation and restoration purposes.

In this work, we present the application of Ambient Pressure MeV SIMS for the detection of explosive residues. Secondary molecular ions were detected under 8.8 MeV ¹⁶O⁴⁺ ion probing of PETN (*M*=316.14gmol⁻¹), HTMD (*M*=208.17 gmol⁻¹) and RDX (*M*=222.12 gmol⁻¹) explosive residues before and after explosion, in positive and negative ion mode. Elemental imaging was simultaneously performed by PIXE analysis to spot residues. Molecular signature of explosive residues and their fragments have been investigated in the spectra, with comparison to standard keV SIMS mapping performed on the same samples. The potential for further analysis to establish greater identification data base for explosives residue will be discussed.

Abstract 40

[Regular Poster - Poster Sessions](#)

The reduction of the critical H implantation dose for ion-cut by incorporating B doped SiGe/Si superlattice into Si substrate

[Zhongying Xue](#), [Da Chen](#), [Zengfeng Di](#), [Xing Wei](#), [Miao Zhang](#), [Xi Wang](#)

State Key Laboratory of Functional Materials for Informatics, Shanghai Institute of Microsystem and Information Technology, Chinese Academy of Sciences, 865 Changning Road, Shanghai, 200050, China, Shanghai Shanghai 200050, China

As well known, the typical H implantation dose for Si splitting is 6×10¹⁶/cm². Here, we present a method to achieve ion cut with 3×10¹⁶/cm² H fluence by incorporating B doped SiGe/Si superlattice (SL) into substrate, where the B concentration is 1×10¹⁸/cm³.

The sample with the structure of 135 nm $\text{Si}_{0.75}\text{Ge}_{0.25}$ /100nm Si/15 nm B-doped $\text{Si}_{0.83}\text{Ge}_{0.17}$ -Si SLs/Si substrate (sample B) was fabricated by reduced pressure chemical vapor deposition system. The 15 nm B-doped $\text{Si}_{0.83}\text{Ge}_{0.17}$ -Si SLs consists of three periods of 3 nm $\text{Si}_{0.83}\text{Ge}_{0.17}$ /2 nm Si with B concentration of $1 \times 10^{18}/\text{cm}^3$. A 135 nm $\text{Si}_{0.75}\text{Ge}_{0.25}$ /100nm Si/15 nm B-doped $\text{Si}_{0.83}\text{Ge}_{0.17}$ /Si substrate sample (sample A) was also fabricated for comparison. Both of the samples were implanted by 26 keV H^+ ions with the dose of $3 \times 10^{16}/\text{cm}^2$ and annealed at 600 C for 0.5 hour in a N_2 atmosphere.

The scanning electron microscope (SEM) micrographs, atomic force microscope (AFM) images and cross sectional transmission electron microscopy (XTEM) micrographs reveal that the film splitting takes place along the interfaces on both sides of the SL layer randomly instead of along the H ion range, which evidences the present approach not only decreases the critical H ion dose remarkably, but also controls the location of crack formation precisely. SIMS hydrogen profiles manifest that compared to sample A, the hydrogen trapping effect of sample B is enhanced significantly due to the existence of SL layer, and the H concentration is as high as $1.65 \times 10^{21}/\text{cm}^3$.

In summary, we have presented an approach to achieve film exfoliation by using half of the typical H fluence required for conventional ion cut process. It is found that the B doped SiGe/Si superlattice is a high efficiency H trapping center due to its multiple interfaces, so film splitting could occur at the SL/Si interface using $3 \times 10^{16}/\text{cm}^2$ H fluence.

Abstract 41

[Regular Poster - Poster Sessions](#)

Sharp crack formation in low fluence hydrogen implanted epitaxial Si/B-doped $\text{Si}_{0.70}\text{Ge}_{0.30}$ /Si structures

[Da Chen](#), [Zengfeng Di](#), [Zhongying Xue](#), [Xing Wei](#), [Miao Zhang](#)

State Key Laboratory of Functional Materials for Informatics, Shanghai Institute of Microsystem and Information Technology, Chinese Academy of Sciences, 865 Changning Road, Shanghai, 200050, China, Shanghai Shanghai 200050, China

An approach to transfer a high-quality Si layer for the fabrication of silicon-on-insulator wafers has been proposed based on the investigation of crack formation in H-implanted Si/B-doped $\text{Si}_{0.70}\text{Ge}_{0.30}$ /Si structures.

The epitaxial growth of a Si/B-doped $\text{Si}_{0.70}\text{Ge}_{0.30}$ heterostructure was carried out on 8-inch Si (001) wafers in a commercial reduced pressure chemical vapor deposition (RPCVD) system. The concentration of B was $3 \times 10^{19}/\text{cm}^3$. In order to study the effect of the thickness on H trapping by the SiGe layer, the thickness of the buried $\text{Si}_{0.70}\text{Ge}_{0.30}$ layer was varied from 3 nm to 70 nm. Subsequently, the grown heterostructures were implanted by 24 keV, 26 keV and 33 keV H^+ ions with the fluence of $3 \times 10^{16}/\text{cm}^2$ and annealed at 600 C for 0.5 h in a N_2 atmosphere, respectively.

The SEM micrographs, cross-sectional TEM micrographs and SIMS hydrogen profiles reveal the crack formation position is closely correlated to the thickness of the buried $\text{Si}_{0.70}\text{Ge}_{0.30}$ layer. For H-implanted Si containing a 3 nm thick B-doped $\text{Si}_{0.70}\text{Ge}_{0.30}$ layer, localized continuous cracking occurs at the interfaces on both sides of $\text{Si}_{0.70}\text{Ge}_{0.30}$ interlayer. Upon increasing the thickness of the buried $\text{Si}_{0.70}\text{Ge}_{0.30}$ layer to 15 nm and 70 nm, cracking was observed along the interface between the Si substrate and the B-doped $\text{Si}_{0.70}\text{Ge}_{0.30}$ layer, thus resulting in the formation of continuous sharp crack. We explain the strain-facilitated layer transfer in low fluence hydrogen implantation as being due to the existence of shear stress at both sides of the buried $\text{Si}_{0.70}\text{Ge}_{0.30}$ interlayer and subsequent trapping of hydrogen, which lead to crack in a well controlled manner.

From the TEM micrographs and SIMS hydrogen profiles, it is evident that the present approach is capable of controlling the depth of crack formation by growing a B-doped interlayer at a desired depth.

Abstract 139

[Regular Poster - Poster Sessions](#)

Raman and ion channeling damage analysis of high energy He implanted Si temperature dependence

[jack Elliot Manuel](#), [Bibhudutta Rout](#), [Szabolcs Z Szilasi](#), [Gyanendra Bohara](#), [Gary A Glass](#)

Physics, University of North Texas, 1155 Union Circle, #311427, Denton Tx 76203, United States

Raman scattering and ion channeling techniques were used to study the damage to Si implanted with high energy (3 MeV) He ions. Damage analysis was performed on samples subjected to different fluences and beam densities (current) at various ambient temperatures. Damage characteristics of the substrate were studied by comparing the Raman signal which is specific to amorphization of Si to ion channeling results which are sensitive to small volume crystalline defects. The results show that the damage morphology is dependent on both ion fluence and beam density. Varying the temperature of the substrate during implantation alters the damage morphology of the crystal.

Abstract 213

[Regular Poster - Poster Sessions](#)

Optimization of irradiation parameters of heavy ion implantation for diamond growth on silicon

[Szabolcs Z Szilasi](#), [Jack Manuel](#), [Gyanendra Bohara](#), [Gary Glass](#), [Bibhudutta Rout](#)

Ion Beam Modification and Analysis Laboratory (IBMAL), University of North Texas, 210 Avenue A, Denton Texas 76203-1427, United States

Nucleation and growth rate of diamond films on Si are strongly affected by numerous factors. One of these is the surface treatment of silicon by scratching, seeding, ion implantation, electrical biasing, laser irradiation, etc. The aim of this study is to understand the effects on film growth and adhesion produced by heavy ion implantation of silicon. The optimal irradiation parameters will be determined to attain high selectivity for film growth and enhancement of nucleation and adhesion on silicon substrates.

Abstract 315

[Regular Poster - Poster Sessions](#)

Synthesis of low dimensional embedded Ge nanostructures

[Vikas Baranwal](#)¹, [J W Gerlach](#)², [B Rauschenbach](#)², [H Karl](#)³, [D Kanjilal](#)⁴, [Avinash C Pandey](#)¹

⁽¹⁾Nanotechnology Application Centre, University of Allahabad, Nanotechnology Application Centre, Science Faculty, Allahabad Uttar Pradesh 211002, India

⁽²⁾Material Science, Leibniz-Institut für Oberflächenmodifizierung, Leibniz-Institut für Oberflächenmodifizierung, Permoserstraße 15, Leipzig 04318, Germany

⁽³⁾Institut für Physik, Universität Augsburg, Institut für Physik, Universität Augsburg, Augsburg, Augsburg 86135, Germany

⁽⁴⁾Inter University Accelerator Centre, Inter University Accelerator Centre, Aruna Asaf Ali Marg, New Delhi 110067, India

Ge quantum dots (QDs) have attracted a lot of research interest in the last few years because of their excellent optical and electronic properties which can be utilized for applications in the field of optoelectronic devices [1]. QDs can be incorporated in semiconductor devices such as light emitting diodes [2], lasers [3] and field effect transistors [4]. Ge QDs seem to be very promising due to their larger Bohr exciton radius (~25.3 nm) as compared to that of Si (~4 nm) [5]. Ion implantation is widely used to make quantum dot composites due to having several merits over other techniques like i) electric and optical selective area doping, electrical isolation ii) the ability to produce arbitrary combinations of nanodots and hosts, which enables tailoring the material function for specific applications [6,7].

Ge ions of 150 keV energy were implanted with three different fluences starting from 2.5×10^{16} ions/cm² to 7.5×10^{16} ions/cm² into SiO₂ matrix. The implanted samples were annealed at 950°C for 30 minutes. Structural properties of Ge embedded SiO₂ matrix was studied using high resolution XRD. Depth profile of Ge was obtained by using TOF-SIMS.

References:

1. K. D. Hirschman et al., Nature 384 (1996) 338
2. J. Sabarinathan et al., Appl. Phys. Lett. 81 (2002) 3876
3. D. L. Huffaker et al., Appl. Phys. Lett. 73 (1998) 2564
4. H. Drexler et al., Phys. Rev. Lett. 73 (1994) 2252
5. Y. Maeda et al., Appl. Phys. Lett. 59 (1991) 3168
6. V. Baranwal et al., J. App. Phys. 103 (2008) 124904.
7. V. Baranwal et al., App. Surf. Sci. 253 (2007) 5317

Abstract 323

[Regular Poster - Poster Sessions](#)

The technical difficulties to synthesize staggered multi-layer low energy ion deposition for synthesis of metal nanostructure in Si.

[Mangal S Dhoubhadel](#), [Wikramaarachchige J Lakshanth](#), [Bibhudutta Rout](#), [Floyd D McDaniel](#)

Department of Physics, University of North Texas, 1155 Union Circle, #311427, Denton Texas 76203, United States

The indirect band gap of Si is primarily responsible for its poor optical properties. By modifying Si with ion irradiation, one can circumvent the indirect band gap for photonic devices. Defects as well as presence of metallic nanosystems in the Si are proven to be a source of enhancement of optical properties, such as absorptions or emissions in the Si system. These properties have direct application in photovoltaic cells, optical emitters, and optical sensors. According to photo absorption depth profile in Si, blue light penetrates about 10 nm (10^{-9} m), whereas red light can go as deep as 1 μ m (10^{-6} m). To accommodate a broad visible EM spectrum (white light), the optically sensitive nanoclusters (optical center) can be engineered and distributed strategically at the optically most efficient location (depth). However, multi-energy ion deposition for staggered layers of metal ion deposition is found to be challenging. The experimental results significantly differ from the widely used Transport of Ions in Matter (TRIM) simulation code, due to the surface degradation from the ion irradiation. The Dynamic Transport of Ions in Matter (TDYN) simulations were carried out to investigate the depth profiling on Ag and Au in silicon for various fluencies. We will present the experimental results using Rutherford Backscattering Spectrometry (RBS) and x-ray photoelectron spectrometry (XPS) depth profiling to compare the TDYN and TRIM simulations.

Phase Changes of Zn and Si Due to Ion Implantation and Thermal Annealing.[Bimal Pandey](#), [Duncan L Weathers](#)*Ion Beam Modification and Analysis Laboratory, Department of Physics, University of North Texas, 1115 Union Circle # 311427, Denton TX 76203, United States*

Phase changes of zinc (Zn) and silicon (Si) were studied by using molecular ion implantation followed by thermal annealing. 35 keV ZnO molecular ions were implanted to a fluence of 1×10^{17} atoms/cm² into Si at room temperature. The implanted sample was annealed in a mixture of 96% Ar and 4% H₂ for 1 h at different temperatures. The ion fluence into the implanted sample was confirmed by using Rutherford backscattering spectrometry (RBS). In the as-implanted sample, Si was observed to have formed SiO₂ but only an elemental phase of Zn was observed. When the sample was annealed at 700 °C Zn and ZnO phases were observed, but when the sample was annealed at 900 °C ZnO bonding was absent and Zn₂SiO₄ and Zn phases were observed. Particle sizes, phase formation and depth profiles were studied using different characterizations techniques including high resolution transmission electron microscopy (HRTEM), energy dispersive x-ray spectroscopy (EDS), x-ray diffraction spectroscopy (XRD) and x-ray photoelectron spectroscopy (XPS).

The Potential of a Compact Accelerator for Low Energy Production of Copper Isotopes[Naomi Ratcliffe](#), [Robert Cywinski](#), [Paul Beasley](#)*IIAA, University of Huddersfield, School of Applied Sciences, Queensgate, Huddersfield HD1 3DH, United Kingdom*

The recent, 2010, technetium crisis has sparked a drive in finding replacement sources or alternative isotopes for vital medical diagnostic procedures. The prolonged temporary shut down of the world's two main supply centres of technetium, the most commonly used medical radioisotopes for SPECT (Single Photon Emission Tomography), meant that over 90% of the world's nuclear imaging procedures had to be cancelled or postponed. These facilities, along with several smaller ones, are facing permanent shut down, before 2020, and there is currently no replacement source set to take over. One possible solution is to increase the use of some of the current PET (Positron Emission Tomography) isotopes as a replacement for Tc-99m. One of the main problems with current PET isotopes is availability. PET is still quite an expensive procedure and is not widely available, one of the reasons for this is that many of the positron emitting isotopes used have very short half-lives and must be used in close proximity to the production site. The main method of producing these isotopes is by medical cyclotron, with the ability to produce a proton beam of ~20MeV these are large expensive machines that are only available at larger sites. The aim of this work has been to explore the potential of a cheap compact low energy (<10MeV) accelerator, which could fit in the basement of the average sized hospital, to provide a wider spread application of these isotopes. The most advantageous method is to use low threshold (p,n) reactions with enriched targets to produce proven PET radioisotopes such as Cu-60, Cu-61, and Cu-62. In this way it is possible to produce suitable activity for multiple doses of medical grade isotopes via a method that can be implemented quickly in order to ensure supply and availability of vital medical procedures.

POSITRON GENERATOR DEVELOPMENTS: A NEW SETUP FOR CEMHTI[Jean-Michel Rey](#)^{1,3}, [Marie-France Barthe](#)², [Pascal Debu](#)¹, [Pierre Desgardin](#)², [Patrick Echegut](#)², [Laszlo Liskay](#)¹, [Patrice Perez](#)¹, [Yves Sacquin](#)¹, [Serge Visière](#)³⁽¹⁾IRFU, CEA, CE Saclay, Gif sur Yvette 91191, France⁽²⁾CEMHTI, CNRS, 1D av de la Recherche Scientifique, Orleans 45071, France

Positron beams are getting increasing interest for materials science and for fundamental research. Recent progress on positron production using a compact electron accelerator made at CEA-IRFU for the Gbar experiment is providing new prospect for material analysis and non-destructive testing technology using positrons. CNRS-CEMHTI is defining a long term strategy to boost its positron laboratory using an upgraded version of the CEA positron generator manufactured by the POSITHÔT company. This new generator is designed to produce between 2 and 3×10^7 slow positrons per second to feed in parallel several experiments. It will be presented here as well as the future beam developments.

Abstract 145

[Regular Poster - Poster Sessions](#)

MOmentum Neutron DETector (MONDE)

[Efraín Chávez¹](#), [Pedro Santa Rita¹](#), [Francisco Favela¹](#), [Juan Gerardo Flores¹](#), [Antonio Tonatiuh Ramos¹](#), [Arcadio Huerta¹](#), [Libertad Barrón-Palos¹](#), [Quiela Curiel¹](#), [Eduardo Andrade¹](#), [Oscar de Lucio¹](#), [María Esther Ortiz¹](#), [Eliud Moreno²](#), [Rafael Policroniades²](#), [Ghiraldo Murillo²](#), [Armando Varela³](#)

⁽¹⁾Instituto de Física, Universidad Nacional Autónoma de México, Ciudad Universitaria S/N, Coyoacán D. F. 04510, Mexico

⁽²⁾Departamento de Aceleradores, Instituto Nacional de Investigaciones Nucleares, Carretera México Toluca S/N, Ocoyoacac México 52750, Mexico

⁽³⁾Centro de Ciencias de la Atmósfera, Universidad Nacional Autónoma de México, Av. Universidad 3000, Ciudad Universitaria S/N, Coyoacán D. F. 05410, Mexico

MONDE is a large area ($150 \times 60 \text{ cm}^2$) plastic scintillating slab (5 cm thick), viewed by 16 photomultiplier tubes from the sides. Fast neutrons (MeV) entering the detector will produce a recoiling proton (nearly 50% efficiency for 2 MeV neutrons) that will induce a light spark at the spot of the collision. The signals from the 16 detectors are processed to deduce the position of the spark. Time signals from both the ^3He detector and MONDE can be combined to deduce a time of flight (TOF). Finally, the position information together with the TOF yields the full momentum vector of each detected neutron.

In this work we present two different algorithms to deduce the position of the spark from the 16 signals of the photomultipliers and compare the calculated (expected) resolution to actual data. MONDE is presently in its final testing stage. It is scheduled to come on line by June 2014.

Abstract 470

[Regular Poster - Poster Sessions](#)

Low Energy Levels in the neutron-rich $^{120,122,124,126}\text{Cd}$ Isotopes

[Jon C. Batchelder¹](#), [N. T. Brewer^{3,5}](#), [C. J. Gross²](#), [R. Grzywacz^{2,3}](#), [J. H. Hamilton⁵](#), [M. Karny²](#), [A. Fijalkowska^{3,4}](#), [S. H. Liu²](#), [K. Miernik²](#), [S. W. Padgett³](#), [S. V. Paulauskas³](#), [K. P. Rykaczewski²](#), [A. V. Ramayya⁵](#), [D. W. Stracener²](#), [M. Wolinska-Cichocka^{2,4}](#)

⁽¹⁾UNIRIB/ORISE, ORAU, JIHIR/ORN, Bld 6008, Oak Ridge TN 37831-6374, United States

⁽²⁾Physics Division, ORNL, Oak Ridge TN, United States

⁽³⁾University of Tennessee, Knoxville TN, United States

⁽⁴⁾Faculty of Physics, University of Warsaw, Warsaw, Poland

⁽⁵⁾Vanderbilt University, Nashville TN, United States

The lowest lying levels in the neutron-rich even-even Cd isotopes have structures that resemble an anharmonic vibrator coupled to 2-proton intruder states. Deviations from this simple picture have been shown to occur in $^{112-116,120}\text{Cd}$ isotopes [1,2]. In particular, none of the observed 0^+ and 2^+ states previously assigned as three phonon states decay in a manner

consistent with a multiphonon state. If the explanation for the discrepancy between observed and expected decays of these states at least partially arises from mixing with intruder states, the picture should become more clear further from the neutron mid-shell as there will be less mixing of the N-phonon and intruder levels due to the increase in energy of intruder states. In order to determine the systematics of these states in Cd across the neutron shell we have measured the beta decays of the heavier even-mass $^{122,124,126}\text{Ag}$ isotopes.

Silver-122,124,126 ions were produced via the proton-induced fission of ^{238}U at the HRIBF at ORNL. Fifty MeV protons were bombarded on a UCx target, and the fission products were then separated by the High Resolution Isobar Separator and deposited on a moving tape collector directly in the center of the LeRIBSS (Low-Energy RIB Spectroscopy Station) array. Many new levels in $^{122,124,126}\text{Cd}$ have been observed. These results will be presented and discussed.

[1] K. L. Green, **et al.**, Phys. Rev. C **80**, 032502(R) (2009).

[2] J. C. Batchelder, **et al.**, Phys. Rev. C. **86**, 064311 (2012).

Abstract 363

[Regular Poster - Poster Sessions](#)

PIP: a compact recirculating accelerator for the production of medical isotopes

[Carol Johnstone](#)², [Robert Cywinski](#)¹, [Robert Edgecock](#)¹, [Adina Toader](#)¹, [Roger Barlow](#)¹

⁽¹⁾International Institute for Accelerator Applications, Huddersfield University, Huddersfield HD1 3DH, United Kingdom

⁽²⁾Fermi National Accelerator Laboratory, Batavia IL, United States

PIP is a proposed proton non-scaling fixed-field alternating-gradient (nsFFAG) accelerator which uses an internal target for the production of medical isotopes. Conceptually the FFAG provides strong focusing, avoiding the losses experienced by cyclotrons. For many medical isotopes the productions cross-section peaks strongly as a function of beam energy, and the recirculating beam of PIP gives high efficiency of production as protons which lose energy in the target foil will have this energy replaced for the next pass. The energy can be selected (in the range of MeV to tens of MeV) by altering the radial position of the target foil, and beam extraction is also possible. The machine design and its performance (acceptance and acceleration) are described. We show that PIP's compact, cost-efficient and simple design means that the machine can be installed to service a single hospital, producing doses on demand, as and when needed by patients.

Abstract 395

[Regular Poster - Poster Sessions](#)

High Intensity Cyclotron for the ISODAR experiment

[Adriana Bungau](#)², [Andreas Adelman](#)¹, [Jose Alonso](#)⁴, [William Barletta](#)⁴, [Roger Barlow](#)², [Larry Bartoszek](#)⁴, [Luciano Calabretta](#)³, [Daniela Campo](#)³, [Janet Conrad](#)⁴, [Michael Shaevitz](#)⁵, [Joshua Spitz](#)⁴, [Alessandra Calana](#)³, [Matt Touns](#)⁴, [Joe Minervini](#)⁴, [Daniel Winklehner](#)¹, [Luigi Celona](#)³, [Michel Abs](#)⁶, [Willem Kleeven](#)⁴, [Anna Kolano](#)²

⁽¹⁾Paul Scherrer Institute, Villigen CH-5232, Switzerland

⁽²⁾University of Huddersfield, Huddersfield HD1 3DH, United Kingdom

⁽³⁾Istituto Nazionale di Fisica Nucleare, Laboratori Nazionali del Sud I-95123, Italy

⁽⁴⁾Massachusetts Institute of Technology, Cambridge MA02139, United States

⁽⁵⁾Columbia University, New York NY 10027, United States

⁽⁶⁾IBA, Louvain-le-Neuve, Belgium

The scientific international community in recent years has an increasing interest on the neutrino properties. The aim of the IsoDAR (Isotope Decay At Rest) experiment is to look for the existence of sterile neutrinos. To perform this experiment, a cyclotron able to deliver proton beam current up to 10 mA is proposed. Due to the required higher average beam current and the experimental underground site, it poses a new ambitious goal in terms of technical solutions.

Abstract 477

[Regular Poster - Poster Sessions](#)

The Perspectives of the Boron Neutron Capture Therapy-Clinical Applications Research and Development in Saudi Arabia

[Ibtesam Saeed Badhrees](#)¹, [Faisal M Alrumayan](#)²

⁽¹⁾*National Center For Mathematics and Physics, King Abdulaziz City for Science and Technology(KACST), Prince Turki Road, Riyadh Riyadh 11442, Saudi Arabia*

⁽²⁾*King Faisal Specialist Hospital-Research Center(KFH-RC), King Faisal Hospital, Takhasosy Road, Riyadh Riyadh 11211, Saudi Arabia*

Boron Neutron Capture Therapy (BNCT) is a binary form of experimental radiotherapy based on the administration of a drug able to concentrate the isotopes in a tumor cells and on a subsequent irradiation of the target with low energy neutrons. Even though the first evidence of the success of this treatment dated back years ago, BNCT showed successful treatment results especially in malignant melanoma, and glioblastoma. In order for the BNCT to be successful, a sufficient amount of Boron (¹⁰B) must be selectively delivered to the tumor, and enough thermal neutrons must be absorbed by them.

The CS-30 Cyclotron at King Faisal Specialist Hospital & Research Centre (KFSH-RC) is a positive ion machine capable of accelerating Protons of 20 uA of beam current at 26.5 MeV. Although the beam intensity from the CS-30 is low, and the key to success in using it for BNCT therapy is by using high beam current at low energy, yet cell irradiation may need just few Micro-Amps at 1 MeV of energy to activate the Boron (¹⁰Be) atoms inside the irradiate cells.

In this paper we are presenting preliminary experiments in generating thermal neutron flux using Beryllium target and a Moderator to control the energy of the neutrons.

Abstract 165

[Invited Poster - Poster Sessions](#)

Ambient Pressure MeV-SIMS analysis of contaminated PTFE aerosol filters.

[Brian N Jones](#)¹, [Julien Demarche](#)², [Lidija Matjacic](#)², [Vladimir Palitsin](#)², [Giulia Calzolari](#)¹, [Massimo Chiari](#)¹, [Roger P Webb](#)²

⁽¹⁾*Labec, INFN, via Sansone 1, Florence 50019, Italy*

⁽²⁾*Surrey Ion Beam Centre, University of Surrey, Surrey Ion Beam Centre, Guildford Surrey GU2 7XH, United Kingdom*

MeV-SIMS is a relatively new technique with the capability of performing Secondary Ion Mass Spectrometry analysis in full ambient conditions. We have used this technique to explore a set of PTFE filters deployed at various strategic places around Florence in Italy. Normally these filters are analysed using external beam PIXE and other MS.techniques. We have taken a small subset of these to explore what might be achieved using MeV-SIMS.

MeV-SIMS is in principle a good technique for this sort of analysis in that it can provide complimentary molecular information at the same time as generating more conventional PIXE data for trace element analysis. The technique is quick - requiring only a few minutes of analysis to generate a spectrum.

A set of samples have been looked at ranging from a pristine PTFE filter to a heavily contaminated filter which was situated near a busy junction in Florence. Different mass peaks in the positive spectrum which increase with the amount of contamination expected in the filters are observed. The peaks identified will be discussed and the value of this technique coupled with PIXE will be elaborated.

Abstract 162

[Invited Poster - Poster Sessions](#)

Modeling the Transport of Secondary Ion Fragments Into a Mass Spectrometer Through Ambient Pressure Using COMSOL Multiphysics Simulation Software.

[John-William Warmenhoven](#), [Vladimir Palitsin](#), [Roger P Webb](#)

Surrey Ion Beam Centre, University of Surrey, Surrey Ion Beam Centre, Guildford Surrey GU2 7XH, United Kingdom

Total Ion Beam Analysis¹ (IBA) has become a very powerful technique for surface analysis of unknown materials and with the development of MeV-Secondary Ion Mass Spectrometry (MeV-SIMS) from its Plasma Desorption Ionisation Mass Spectrometry (PDMS) roots², there is now a means of also characterising organic molecules with a sensitivity three orders of magnitude higher than conventional keV-SIMS³. This has substantially increased the applications of IBA to include areas such as forensics⁴ and molecular mapping at the subcellular level⁵. The next step is to remove the limitation of size and vacuum compatibility from the samples being analysed by bringing the process into ambient.

Preliminary work at the Surrey Ion Beam Centre shows a system working with a lateral resolution ~4 microns. However, the gap in sensitivity compared to in vacuum experiments is unsatisfactory. To address this issue work is being carried out to characterise the transport of sputter fragments by the helium gas flow surrounding the beamline end station. We use the COMSOL Multiphysics simulation software, employing the Computational Fluid Dynamics (CFD) module coupled with the Particle Tracing module. Efforts are under way to optimise the system with respect to geometry and rate of gas flow with initial results suggesting that the current setup produces a thin laminar flow from the helium inlet to the mass spectrometer capillary.

1.C.Jeynes, et al, **NIMB**, **271**, 107-118, (2012)

2.D.F.Torgerson, et al, **Biochem. Biophys. Res. Comms**, 60(2), 616-621, (1974).

3.Y.Nakata, et al, **JMS**, 44(1), 128-136, (2009)

4.M.J.Bailey, et al, **NIMB**, 268 (11-12), 1929-1932, (2010).

5.Y.Nakata, et al **NIMB**, 267 (12-13), 2144-2148 (2009)

Abstract 154

[Regular Poster - Poster Sessions](#)

Channeling and stopping power issues in the study of heavy ion irradiation in MgO

[Ke Jin](#)¹, [Zihua Zhu](#)², [Vaithiyalingam Shutthanandan](#)², [William J Weber](#)^{1,3}, [Chien-Hung Chen](#)¹,
[Yanwen Zhang](#)^{1,3}

⁽¹⁾*Materials Science and Engineering, University of Tennessee, Knoxville TN, United States*

⁽²⁾*EMSL, Pacific Northwest National Laboratory, Richland WA, United States*

⁽³⁾*Materials Science & Technology Division, Oak Ridge National Laboratory, Oak Ridge TN, United States*

Irradiation effect of slow heavy ions in single-crystal MgO has attracted lots of interest in the past decades and is still an active topic. It is found that many depth profiles of implanted ions shown in previous studies were much deeper than the predictions. Also, they have shown a significantly enhanced skewness, which is not commonly observed in other materials. In the present work, time-of-flight secondary ion mass spectrometer (ToF-SIMS) and Rutherford backscattering spectrometry (RBS) are utilized to study the ion and damage profiles of (100) and (110) oriented MgO irradiated with 1 and 4 MeV Au ions in varies directions. The results show that the inclined ion profiles are predominantly attributed to the channeling effect (especially due to the planar channels) during irradiation. The commonly used "7 degree off normal" method does not work well for MgO samples due to its rock salt structure and the aligned edge cut. An improved way of effectively avoiding the channeling effect is presented in this work. It is also shown that failure of avoiding the planar channel will considerably affect the damage profile, and could be misinterpreted as irradiation-induced or enhanced defect migration. Furthermore, both previous and current studies (after avoiding the channeling implantation) show that the peak position of implanted ions is significantly deeper than the prediction by the stopping and range of ions in matter (SRIM) code. These results are in consistent with our recent finding that the electronic stopping power used in SRIM code is significantly overestimated for slow heavy ions in targets containing light elements.

Abstract 172

[Regular Poster - Poster Sessions](#)

Active Detection of Shielded Special Nuclear Material In the Presence of Variable High Backgrounds Using a Mixed Photon-Neutron Source

[Philip Nathaniel Martin](#), [Ceri Clemett](#), [Cassie Hill](#), [John O'Malley](#), [Ben Campbell](#)

Atomic Weapons Establishment, Aldermaston, Reading Berkshire RG74PR, United Kingdom

This paper describes and compares two approaches to the analysis of active detection data containing high photon backgrounds associated with mixed photon-neutron source flash active detection. Results from liquid scintillation detectors (EJ301/EJ309) fielded at the Naval Research Laboratory (NRL), in collaboration with Atomic Weapons Establishment (AWE), using the NRL Mercury Inductive Voltage Adder (IVA) operating in both a photon and mixed photon-neutron mode at a DU target are presented. The standard approach applying a Figure of Merit (FOM) consisting of background sigma above background is compared with an approach looking to fit only the time decaying photon signal with standard delayed photon emission from ~10MeV end-point energy Bremsstrahlung photofission of DU. Examples where each approach does well and not-so-well are presented together with a discussion of the relative limitations of both approaches to the type of mixed photon-neutron flash active detection being considered.

PIXE identification of pottery production from the necropolis of Jiyeh archaeological site[M. Roumie](#)¹, [U. Wicenciak](#)², [M. El-Bast](#)¹, [B. Nsouli](#)¹⁽¹⁾*Accelerator Laboratory, Lebanese Atomic Energy Commission, Lebanese CNRS, Airport Road, P.O.Box 11-8281, Beirut, Lebanon*⁽²⁾*Antiquity of southern Europe research centre, University of Warsaw, Warsaw, Poland*

The excavations of the ancient Porphyreon of the Jiyeh archeological site, about 28km due south of Beirut, revealed the remains of some pottery production features beneath a level of graves. The discovered material enabled the identification by the archeologists of two different phases of pottery production, dated to the Late Hellenistic and Early Roman periods. Particle induced X-ray emission technique PIXE is used to determine the elemental composition of about 134 the studied excavated shards. The analysis protocol provided almost 20 elements in one spectrum, including majors, minors and traces. The elemental composition provided by PIXE and based on 12 most abundant elements, ranging from Mg to Zr, was used in a multivariate statistical program, then two main groups are defined..

Ion Beam Analyses of Microcrystalline Quartz Artifacts from the Reed Mound site (ca. 1200 A.D.), Delaware County, Oklahoma[S. B. Younger-Mertz](#)¹, [J. E. Manuel](#)², [S. Z. Szilasi](#)², [T. Reinert](#)², [G. A. Glass](#)², [S. W. Hammerstedt](#)³⁽¹⁾*Department of Anthropology, University of Oklahoma, 455 West Lindsey Dale Hall Tower 521, Norman Oklahoma 73019, United States*⁽²⁾*Department of Physics, University of North Texas, 210 Avenue A Physics Building Rm 110, Denton Texas 76203, United States*⁽³⁾*Oklahoma Archaeological Survey, University of Oklahoma, 111 E Chesapeake, Norman Oklahoma 73019, United States*

Ion Beam Analysis is an extremely useful tool for archaeological research. Several classes of artifacts (e.g. metals, lithics, ceramics, glass, bone, pigments, paper) can be analyzed by various ion beam techniques (e.g. PIXE, PIGE, NRA, RBS, ERDA), and the data obtained can be extremely valuable for numerous types of studies (e.g. provenance, age, function, manufacturing techniques, authenticity). In this study, certain microcrystalline quartz artifacts from the Reed Mound site (ca. 1200 A.D.) in Delaware County, Oklahoma were analyzed using particle induced x-ray emission spectrometry (PIXE) and Rutherford backscattering spectrometry (RBS). The goal of this study is to obtain minor and trace element data in order to determine the number of chert sources represented within this sample set using multivariate statistical analyses. The results of this research will facilitate further provenance studies. The sample set analyzed consists of 30 projectile points that were recovered from Reed Mound I in 1937 during excavations conducted by the Works Progress Administration (WPA).

Novel electrostatic accelerator[Prof. Paul Beasley](#), [Prof. Oliver Heid](#)*Siemens AG, Günther Scharowsky Straße 1, Erlangen 91058, Germany*

Over the past five years, concerns have grown over the ongoing reliable supply of Tc-99m, due to reactor shutdowns forcing hospitals to reschedule or cancel urgent medical exams. As a consequence, there have been numerous studies into alternative methods of manufacture using specialised accelerators to high energy cyclotrons. However, the development of

a novel Direct Current (DC) electrostatic accelerator presents a low cost, compact and efficient alternative, utilising modern materials and a different design philosophy. This new low energy concept integrates the DC voltage generator with the insulator and accelerator structure enabling localized and reliable production of Tc-99m and other medical isotopes in hospitals and medical centers.

Abstract 231

[Invited Poster - Poster Sessions](#)

Relativistic mass of secondary neutrons in fission and fragments in fusion.

[AJAY SHARMA](#)

Nuclear Physics, Fundamental Physics Society, Fundamental Physics Society Post Box 107 GPO Shimla, shimla HP 17100, India

The fission is initiated by thermal neutron (0.025eV or 2,185m/s). In the fission reactions neutrons produced are known as fast (secondary) or relativistic neutrons having energy 2MeV (1.954×10^7 m/s or $\sim 7\%$ speed of light). With help of moderator the velocity is reduced to thermal neutrons or in classical limits. The relativistic variation of mass of fast neutron has to be taken in account. The masses of thermal and fast neutrons are 1.0086649156u and 1.01080879u respectively from relativistic variation of mass. But in calculations of Q-value (energy of reactants - energy of products) the masses of fast (secondary) and slow neutrons are taken as same i.e. 1.0086649156u. Nonetheless, it is not justified to take the relativistic velocity (1.954×10^7 m/s) or relativistic mass is taken same as classical velocity (2,185m/s) or classical mass. Thus in the existing literature, then Q value is calculated as 166.728MeV, the masses of products in this case is 235.8736037u. If masses of fast neutrons are considered, then mass of the products must be 235.880035u. The mass of the reactants in both the cases in the i.e. 236.05255948u. The masses of fission fragments Ba¹⁴⁴ and Kr⁸⁹ are taken as classical masses due to non-availability of exact velocities. If the relativistic masses of secondary neutrons are taken in account correctly, then Q value of the reaction is 160.7373MeV. Thus the accepted Q-value is 5.99MeV (or 0.00643u) less, which is comparable with energy of gamma ray emitted in fission. But this decrease in energy is always neglected which is unfair. There may be numerous such reactions involving fission and fusion. If velocity is found in relativistic region, then relativistic mass has to be taken in account in energy considerations.

Abstract 326

[Regular Poster - Poster Sessions](#)

Neutron-atypical phenomena operating in ion simulations of neutron-induced void swelling that complicate the ion-neutron correlation and prediction of neutron-induced swelling

[Frank A. Garner¹](#), [Mychailo B. Toloczko²](#), [Alicia G. Certain³](#), [Lin Shao⁴](#), [Mike P. Short⁵](#), [Valery A. Pechenkin⁶](#), [Sergiy V. Dyuldya⁷](#), [Victor N. Voyevodin⁷](#)

⁽¹⁾Radiation Effects Consulting, Richland WA 99354, United States

⁽²⁾Pacific Northwest National Laboratory, Richland WA 99354, United States

⁽³⁾Pacific Northwest National Laboratory, Richland WA 99354, United States

⁽⁴⁾Texas A&M University, College Station TX 77843, United States

⁽⁵⁾Massachusetts Institute of Technology, Cambridge MA 02139, United States

⁽⁶⁾Institute of Physics and Power Engineering, Obninsk 249033, Russia

⁽⁷⁾Kharkov Institute of Physics and Technology, Obninsk 249033, Russia

Due to limited availability of high-flux test reactors, effort is underway to study advanced alloys for service in next-generation nuclear reactors using surrogate irradiation techniques. Based on successes in the 1980s-1990s using self-ion irradiation to study void swelling and microstructural evolution of austenitic alloys, effort is now directed toward self-ions to study swelling in ferritic-martensitic alloys, as well as in oxide-dispersion-strengthened variants of these alloys.

However, it is important to recognize that swelling obtained in these ion simulation experiments cannot be extrapolated to make precise predictions of swelling in neutron-irradiated steels. This limitation arises due to operation of neutron-atypical phenomena occurring during ion irradiation. Once understood and quantified, however, these atypical phenomena can be incorporated into the ion-neutron correlation and thereby extend the utility of this simulation technique.

This paper reviews the results of a large number of studies focusing on the impact of neutron-atypical phenomena on evolution of swelling vs. depth. After addressing the atypical compressive stress-state of ion irradiation and its resultant redirection of two-thirds of the mass flow toward the specimen surface, the effects of the specimen surface on swelling and definition of the upper-bound of the temperature regime of swelling is discussed. The combined effect of specimen surface and internal gradients of displacement rate on solute redistribution are then considered. The effects of dpa rate, both local and in aggregate, are addressed, all operating to distort the depth distribution of swelling. Most importantly, the effect of the injected interstitial, both as a physical and chemical entity are discussed, with new results presented to show that this effect is much more powerful in the Fe-bcc system compared to the Fe-fcc system, and defines the lower-bound of the swelling temperature range. Finally, results are shown that quantify the strong suppressive effect of beam-rastering on void nucleation.

Abstract 53

[Invited Poster - Poster Sessions](#)

Magnetic Control of a Neutralized Ion Beam

[Ryan E. Phillips](#), [Carlos A. Ordonez](#)

Department of Physics, University of North Texas, 1155 Union Circle #311427, Denton Texas 76203-5017, United States

Charge-neutralized ion beam control is more complex than control of charged beams. Focusing techniques for charged beams are widely studied. However, many of the tools available for controlling charged beams are not suitable for charge-neutralized beams. Presented here is a scheme for controlling charge-neutralized beams using a distortion of a magnetic guide field via the presence of two current carrying wires. The extent to which the beam can be controlled is evaluated using a classical trajectory Monte Carlo simulation. This material is based upon work supported by the Department of Energy under Grant No. DE-FG02-06ER54883, and the National Science Foundation under Grant No. PHY-1202428.

Abstract 80

[Invited Poster - Poster Sessions](#)

Space-Charge Compressed Ion Beam Equilibrium

[Carlos A. Ordonez](#)

Department of Physics, University of North Texas, 1155 Union Circle #311427, Denton Texas 76203-5017, United States

A radially compressed ion beam equilibrium is made possible by the presence of an edge-confined electron plasma. The beam equilibrium consists of a space-charge neutralized ion beam surrounded by a non-neutral annular region. The ion beam isn't directly affected by an externally applied field. The non-neutral annular region consists of a portion of the electron plasma, which extends radially outward beyond the beam edge. The non-neutral annular region produces a radially inward electrostatic field at the beam edge that serves both to keep the beam radially compressed and to guide the beam. The electron plasma is confined along its outer edge by using an artificially structured boundary. The artificially structured boundary produces a short-range, static electromagnetic field that consists of a spatially periodic sequence of magnetic

cusps, which are electrostatically plugged. The spatial period and range of the field are much smaller than the dimensions of the electron plasma. The electron plasma isn't directly affected by an externally applied field, except near the outer edge of the non-neutral annular region, where the confining electromagnetic field resides. The extent to which the ion beam can be compressed is not directly limited by ion space charge, because the space charge of the ion beam is fully neutralized. Slow ions, or even a stationary ion plasma, can be radially confined by the electrostatic field. Effects that are likely to limit the electron density at the plasma edge of the present concept can be mitigated by reducing the radial width of the non-neutral plasma region. The possibility of producing an intense antihydrogen beam is discussed. This material is based upon work supported by the Department of Energy under Grant No. DE-FG02-06ER54883 and by the National Science Foundation under Grant No. PHY-1202428.

Abstract 438

[Invited Poster - Poster Sessions](#)

Rapid High Dynamic Range Dose Profiling at the University of Maryland Radiation Facility's E-Beam.

[Timothy W Koeth](#), [Eric K Montgomery](#)

Institute for Research in Electronics and Applied Physics, University of Maryland, IREAP, Energy Research Facility, Building #223, College Park MD 20742, United States

The University of Maryland Radiation Facilities hosts two electron accelerators for materials irradiation: a modified Varian Clinac-6 (V7715) variable from 2 to 10 MeV, while nominally providing 1 kW on-target and an L3 (TB-20/15) fixed 10 MeV LINAC providing 17 kW of on-target beam power. For convenience, irradiations are performed in air requiring the electron beam of both machines to exit the evacuated beam pipe through a thin titanium window. After departing the beam pipe, the transverse beam profile rapidly diverges. Dose maps have been generated by hundreds of 1cm X 1cm Radiachromic films that take several days to process. We present an experimental technique that utilizes Optical Transition Radiation (OTR) and Digital Micro-mirror Devices (DMD) which offers real-time dose mapping with better than 1mm resolution and a dose dynamic range of 10^5 .

Abstract 129

[Invited Poster - Poster Sessions](#)

Broadband source of coherent THz radiation based on compact LINAC.

[Ivan V. Konoplev](#)¹, [Andrei Seryi](#)¹, [A. Aryshev](#)², [J. Urakawa](#)², [K. Lekomtsev](#)², [M. Shevelev](#)²

⁽¹⁾JAL, Department of Physics, University of Oxford, DWB, Keble Road, Department of Physics, Oxford Oxfordshire OX1 3RH, United Kingdom

⁽²⁾KEK, High Energy Accelerator Research Organization, 1-1 Oho, Tsukuba Ibaraki 305-0801, United Kingdom

The goal of the research presented is to design a compact source of coherent THz radiation driven by femtosecond electron bunches of up to 10MeV single electron energy. We aim to design the oscillator (including accelerator and the power supply) with total volume below 10 m^3 allowing to transport the device and use it in a medium size laboratory. We suggest to use 2D grating of cylindrical topology and photo-injector to reach the objectives. The radiation will be observed via Smith-Purcell radiation mechanism enabling us building a broadband, high field intensity THz source.

Coherent Smith-Purcell radiation (cSPr) is emitted over a wide range of angles, when a relativistic electron beam passes in the vicinity of the periodic grating. The coherence of the radiation is achieved by selecting the size of the grating period d being larger as compared with the longitudinal size of the beam. In this case electron beam emits coherent Smith-Purcell radiation over a broad spectral range. In this paper we propose to use cSPr to build an oscillator driven by relativistic electron bunches and capable of producing broadband THz pulses. Conventionally, such schemes yield very weak signal which may be acceptable for electron bunch diagnostics but insufficient for other applications. To overcome this 2D periodic grating of cylindrical topology is suggested. One of the advantages of this schema is that such a structure is a cavity and it can be pumped with the electron bunch train. To generate the THz broadband radiation we suggest using a

sub-picosecond, 0.8 nC, 8 MeV e-bunches which can be generated using compact accelerators. Preliminary studies illustrate the possibility to observe coherent broadband radiation with the electric field strength of up to 10MV/m, which is very attractive for a number of applications.

Abstract 59

[Regular Poster - Poster Sessions](#)

Radial Expansion of a Low Energy Positron Beam Passing Through a Cold Electron Plasma Within a Uniform Magnetic Field.

[Franz F. Aguirre](#), [Carlos A. Ordonez](#)

Department of Physics, University of North Texas, 1155 Union Circle #311427, Denton TX 76203-1427, United States

The radial expansion of a low energy positron beam passing through a cold electron plasma within a uniform magnetic field is studied using a classical trajectory Monte Carlo simulation. A monoenergetic positron beam at a kinetic energy of 6κ (where κ has the numerical value of Boltzmann's constant and the units of energy) is simulated passing through a cold electron plasma within a uniform magnetic field of 1T. It was found that under certain conditions there is a range of impact parameters where electrons and positrons may become weakly bound (magnetobound states of positronium) and drift perpendicular to the magnetic field before dissociating. The purpose of the simulation is to evaluate the diffusion coefficient D due to the formation and dissociation of those states. In addition, the effects on D and the drift distances by varying the kinetic energy and the magnetic field will be evaluated. A possible implication of the simulation results is related to radial expansion via magnetobound states when preparing an antihydrogen mixing experiment (for example, when antiproton clouds are driven into the positron plasma in a Penning trap). Since a cascade of long drifts may expel any remaining electrons from antiproton plasmas when overlap with a positron cloud commences, if the number of electrons is sufficiently small compared to the number of positrons, the electrons could be quickly ejected. This material is based upon work supported by the Department of Energy under Grant No. DE-FG02-06ER54883 and by the National Science Foundation under Grant No. PHY-1202428.

Abstract 215

[Regular Poster - Poster Sessions](#)

Multiple Aperture-Based Antihydrogen Parallel Plate Gravity Experiment

[Alex H Treacher](#), [Ryan M Hedlof](#), [Carlos H Ordonez](#)

Physics, University of North Texas, 1155 Union Circle #311427, Denton Texas 76203-5017, United States

An experiment is described that could be carried out at the CERN Antiproton Decelerator facility to determine the direction of acceleration of antihydrogen in the earth's gravitational field. The experiment would use two plates separated by a small distance and orientated parallel with the earth's surface. Multiple cylindrical barriers would be used with gaps that allow the antihydrogen to pass through. Shadow regions are created where, with linear motion, the antihydrogen cannot annihilate. However, with parabolic paths, such as those of objects under the influence of gravity, antihydrogen can annihilate within a shadow region. The probability of an atom annihilating in one of the shadow regions is determined. For simplicity the model considers the antihydrogen source as a point and at a temperature of 4 K. This material is based upon work supported by the Department of Energy under Grant No. DE-FG02-06ER54883 and by the National Science Foundation under Grant No. PHY-1202428.

Abstract 123

[Regular Poster - Poster Sessions](#)

Dynamic measurements of hydrogen and lithium distributions in lithium-cobalt-oxide films during heating and charging using elastic recoil detection techniques

[Bun Tsuchiya](#)¹, [Kenji Morita](#)², [Yasutoshi Iriyama](#)³, [Takuya Mjima](#)⁴, [Hidetsugu Tsuchida](#)⁴

⁽¹⁾*Department of General Education, Faculty of Science and Technology, Meijo University, 1-501, Shiogamaguchi, Tempaku-ku, Nagoya 468-8502, Japan*

⁽²⁾*Department of Research, Nagoya Industrial Research Institute, Noa Yotsuya Bld. 2F, 1-13, Yotsuya-tori, Chikusa-ku, Nagoya 464-8019, Japan*

⁽³⁾*Department of Materials, Physics and Energy Engineering, Graduate School of Engineering, Nagoya University, Furo-cho, Chikusa-ku, Nagoya 464-8603, Japan*

⁽⁴⁾*Department of Nuclear Engineering, Kyoto University, Kyoto 606-8501, Japan*

A solid-state lithium ion (Li^+) battery is one of the most remarkable devices for energy production and storage. To realize the product, it is essential that we have information on the transport behavior of Li in the solid-state Li^+ ion batteries. So far, we have successfully been investigated the distribution of Li in Pt-covered LiCoO_2 multi-layer thin films acting as the positive electrode in a solid-state Li^+ ion battery by means of elastic recoil detection (ERD) techniques. The measurement of the ERD revealed the effects of Pt deposition on the hydrogen absorption characteristics of the LiCoO_2 thin films, with segregation of Co to the surface as a catalyst. It is predicted that the presence of H in the LiCoO_2 thin films has a marked influence on Li^+ ion conduction in Li^+ ion battery systems.

Our aim here was to demonstrate the possibility of dynamically measuring the depth profiles of H and Li at the surface and interface, and in the bulk of the LiCoO_2 thin films with approximately 20 nm thick, deposited on $\text{Li}_{1.4}\text{Ti}_2\text{Si}_{0.4}\text{P}_{2.6}\text{O}_{12}\text{-AlPO}_4$ (LATP) substrates by using pulsed laser deposition, under heating and charging conditions by combining ERD with Rutherford backscattering spectrometry (RBS) using 9.0 MeV O^{4+} ion probe beams.

The ERD spectra clearly revealed that the gradual reduction of the concentrations for H, absorbed in the LiCoO_2 thin films, and the constituent Li atoms, was in-situ observed with an increase in temperature up to 423 K. In addition, it was found in the ERD spectra that the degradation of the distribution of Li occurred with the migration of Li atoms from the surface to the interface between LiCoO_2 thin films and LATP with an increase in the number of charge supplied up to approximately 1.44 e/cm^2 .

Abstract 232

[Invited Poster - Poster Sessions](#)

Ion irradiation effects on WN_xO_y films

[Noriaki Matsunami](#)¹, [T. Teramoto](#)², [M. Kato](#)², [S. Okayasu](#)³, [M. Sataka](#)³, [H. Kakiuchida](#)⁴

⁽¹⁾*Materials Science & Engineering, Meijo University, Shiogamaguchi 1-501, Nagoya 468-8502, Japan*

⁽²⁾*Nagoya University, Nagoya 464-8603, Japan*

⁽³⁾*Japan Atomic Energy Agency, Tokai 319-1195, Japan*

⁽⁴⁾*National Institute of Advanced Industrial Science and Technology, Nagoya 463-8560, Japan*

We have investigated ion irradiation effects on modifications of electronic- and atomic- structures of WN_xO_y films on C-plane-cut-sapphire ($\text{C-Al}_2\text{O}_3$). Rutherford backscattering spectroscopy (RBS) of 1.8 MeV He^+ ions leads to the composition, $x=1.1$ and $y=0.4$ within RBS accuracy of 20 %. According to X-ray diffraction, a strong peak appears at the diffraction angle (2θ) $\approx 37^\circ$ and a weak peak at $\approx 78^\circ$. These peaks are assigned as WN rather than W_2N referring to JCPDS card data, though it is known that WN is metastable phase and W_2N is stable phase. No peaks were observed other than WN and $\text{C-Al}_2\text{O}_3$ ($2\theta=41.7^\circ$). It is found that the electrical resistivity of unirradiated film ($0.03 \Omega\text{cm}$) is reduced to $7 \times 10^{-4} \Omega\text{cm}$ and $3 \times 10^{-3} \Omega\text{cm}$ by 100 MeV Xe ion irradiation at $3.5 \times 10^{12} \text{ cm}^{-2}$ and 100 keV N ion irradiation at 10^{16} cm^{-2} , respectively, and that the XRD intensity decreases to $\sim 1/20$ and $1/10$ by these ion irradiation. These results imply that implantation of N in the film suppress the modification, knowing that the film thickness of 40 nm is smaller than the projected range of 100 keV N (77 nm) and hence considerable fraction of N is remained in the film. It also appears that resistivity of unirradiated film increases with decreasing temperature from RT to 30 K like semiconductor and irradiated film shows very weak temperature dependence. Optical absorption monotonically decreases with increasing the wavelength

from 200 to 2500 nm, implying that bandgap does not exist in the region of 0.4- 6 eV and no appreciable change in the optical absorption by the ion irradiation.

Abstract 64

[Invited Poster - Poster Sessions](#)

Effect of Swift Heavy Ion Irradiation on Dielectric, Thermal and Structural Properties of Metal/Polymer Composites

[Nand Lal Singh](#), [Dolly Singh](#)¹, [Anjum Qureshi](#)²

⁽¹⁾*Department of Physics, Faculty of Science, M.S.University of Baroda, Vadodara Gujarat 390 002, India*

⁽²⁾*Nanotechnology Center , Faculty of Engineering and Natural Science, Sabanci University, Orhanali,Tuzla Istanbul 34956, Turkey*

Copper powder dispersed polyvinyl chloride (PVC) composites (PVC-Cu) were prepared by the solution cast method. These composites were irradiated with 140 MeV Ag⁺¹¹ ions at different fluences. The electrical conductivity, dielectric properties and microstructure properties were studied as a function of filler concentration and also ion fluence. The conductivity of the composite systems exhibited strong frequency dependence. The dielectric constant tends to decrease moderately with increasing frequency while the conductivity displayed a reverse trend. It was also observed that the dielectric properties and electrical conductivity gradually increased with filler concentration and also with ion fluence and was explained in terms of hopping conduction mechanism. Thermal properties of PVC/Cu composites are analyzed by differential scanning calorimetry (DSC). An increase in glass transitions (T_g) was observed with increasing filler of copper particles and it also increases at lower irradiation fluence. T_g shifted to lower temperature on further increase of fluence. The microstructure was examined by means of SEM. The scanning electron microscope (SEM) micrographs indicate that the agglomeration of copper particles dispersed within the PVC at the higher copper concentration and yielding a conductive path through the composites, which is also corroborated with electrical conductivity result. The average surface roughness of the composites also changed as revealed from AFM studied.

Abstract 317

[Regular Poster - Poster Sessions](#)

Ge nanocrystals embedded in HfO₂ synthesized by RF sputtering followed by RTA or SHI irradiation

[V Saikiran](#), [N Manikanthababu](#), [S V S Nageswara Rao](#), [A P Pathak](#)

School of Physics, University of Hyderabad, Gachibowli, Hyderabad Andhra Pradesh 500046, India

Trilayered HfO₂/Ge/HfO₂ thin films were fabricated on Si substrate by RF magnetron sputtering of HfO₂ and Ge target. These samples were then annealed through a rapid thermal annealing (RTA) process at 700 and 800°C in order to form the Ge nanocrystals (NCs) in HfO₂ dielectric matrix. X-ray diffraction (XRD) and micro-Raman spectroscopy measurements were carried out to confirm the formation of Ge NCs in the annealed samples. XRD results reveal the formation of crystalline structure due to RTA while the as-deposited samples were amorphous in nature. The average size of the Ge NCs is found to increase with increase in the annealing temperature. According to micro-Raman spectra, the annealed samples exhibit a shift in the peak corresponding to Ge-Ge optical phonon vibrations, which clearly indicates the formation of Ge NCs in HfO₂ matrix. On the other hand, the as-deposited samples were also irradiated with swift heavy ions of 150 MeV Au and 80 MeV Ni at a fluence of 3, e10¹³ ions/cm² as an alternative approach to induce the formation of Ge NCs through ion beam irradiation. XRD and micro-Raman Spectroscopy suggest the presence of Ge NCs in the ion irradiated samples

and the structural characteristics of NCs in the ion-irradiated samples have been compared with those obtained by RTA process.

Abstract 391

[Regular Poster - Poster Sessions](#)

Swift heavy ions induced self-organization of LiF Surface

[Manvendra Kumar](#)¹, [Parasmani Rajput](#)², [Vikas Baranwal](#)¹, [Saif A Khan](#)³, [Fouran Singh](#)³, [D K Avasthi](#)³, [Avinash C Pandey](#)¹

⁽¹⁾Nanotechnology Application Centre, University of Allahabad, Allahabad 211002, India

⁽²⁾Atomic & Molecular Physics Division, Bhabha Atomic Research Center, Mumbai 400085, India

⁽³⁾Inter University Accelerator Centre, Aruna Asaf Ali Marg, PB 10502, New Delhi 110067, India

The electronic energy loss of swift heavy ions in solid creates a highly excited cylindrical zone of few nm in diameter resulting from a transient increase in the temperature along and in the vicinity of the ion path. After cooling down, a defect-rich or even amorphous latent track is formed in general, especially in insulating materials. The resulting alternations in properties (density, micro-structure, morphology, phase composition, etc.) in such insulating materials have been investigated in bulk, while rather limited experiments have been carried out on thin-film.

In the present work, we report self-organization phenomenon in nano-granular LiF thin films due to 120 MeV Ag ions irradiation at an angle of 10° at liquid nitrogen temperature during irradiation. A cracking perpendicular to the beam direction at low fluences of $\sim 1 \times 10^{13}$ ions/cm² is observed, while at higher fluences of 5×10^{13} ions/cm², the materials started to shrink. After application of further high fluences up to 7×10^{13} ions/cm², the LiF layer was reorganised in 1.25 μ m thick and 450 nm high LiF lamellae of the separation distance 2-3 μ m and orientation as found for the cracks and normal to the beam direction.

Abstract 16

[Regular Poster - Poster Sessions](#)

Synthesis, characterization and radiation damage studies of high-k dielectric (HfO₂) films for MOS device applications

[N. MANIKANTHABABU](#), [N. ARUN](#), [A. P. PATHAK](#), [S. V. S. NAGESWARA RAO](#)

SCHOOL OF PHYSICS, UNIVERSITY OF HYDERABAD, P.O. CENTRAL UNIVERSITY, HYDERABAD ANDHRA PRADESH 500046, India

The current trend in miniaturization of MOS devices needs high-k dielectric materials as gate dielectrics. Among all the high-k dielectric materials, HfO₂ enticed most attention and is considered as a potential candidate to achieve the requirements of gate dielectric in semiconductor industry. High dielectric constant (HfO₂) films (10 nm) on Si substrates were synthesized using e-beam evaporation technique for MOS device applications. These samples were characterized by various structural and electrical characterization techniques. Rutherford Backscattering Spectrometry (RBS), X-Ray reflectivity (XRR) and SEM-EDX measurements were performed to determine the thickness and stoichiometry of these films. The results obtained from various measurements are found to be consistent with each other. These samples were further characterized by I-V (leakage current) and C-V measurements after depositing suitable metal contacts. A significant decrease in leakage current and the corresponding increase in device capacitance are observed. Further we have studied the influence of gamma irradiation on the electrical properties of these films as a function of irradiation dose. The observed increase in leakage current accompanied by changes in various other parameters like accumulation capacitance, inversion capacitance, flat-band voltage, mid-gap voltage etc., indicate the presence of various types of defects in irradiated samples. A systematic study of Swift Heavy Ion (SHI) (120 MeV Ag and Au ions) irradiation effects on the same set of samples will also be discussed in detail.

Tunable Resonant Reflected Wavelength of Porous Silicon based DBR Structures Prepared by Radiation Treated Silicon

[V S Vendamani](#)^{1,2}, [P Ramana](#)¹, [Z Y Dang](#)³, [A P Pathak](#)¹, [M B H Breese](#)³, [S V S Nageswara Rao](#)¹

⁽¹⁾*School of Physics, University of Hyderabad, Gachibowli, Hyderabad, Andhra Pradesh 500046, India*

⁽²⁾*Dept. of Physics, Pondicherry University, Kalapet, Puducherry Puducherry 605014, India*

⁽³⁾*Dept. of Physics, Centre for Ion Beam Applications (CIBA), National University of Singapore, Singapore, Singapore Singapore 117542, Singapore*

Porous silicon multilayers have versatile applications including the design of distributed Bragg reflectors. A DBR structure is formed periodic multilayers comprising alternative high and low refractive index layers. Swift Heavy Ion /Gamma irradiation and subsequent anodization of silicon has been very efficient method to fabricate distributed Bragg reflectors. p-type, mirror-polished (boron doped) Si wafers with resistivity $<0.005 \Omega\text{-cm}$, were irradiated by 100 MeV Ag ions at various fluences ranging from 1×10^{11} to 1×10^{14} ions/cm², while the other set of Si samples were subjected to Gamma irradiation with dose ranging from 1 kGy to 6 kGy. The radiation treated silicon samples were anodically etched with two alternative current densities viz, 5 and 45 mA/cm² to fabricate tunable wave reflectors. The DBR structures were synthesized with 50 bilayers to attain high reflection as well as broad stop band. The radiation induced shift in the reflection wavelength has been compared with the unirradiated DBR structures. This study provides useful information for fabricating tunable wave reflectors for optical communication.

Origin of cracks on BaF₂ thin film surface under swift heavy ion irradiation

[Ratnesh Kumar Pandey](#)¹, [Manvendra Kumar](#)¹, [Saif Ahmad Khan](#)², [Vikas Baranwal](#)¹, [Devesh Kumar Avasthi](#)², [Avinash Chandra Pandey](#)¹

⁽¹⁾*Nanotechnology Application Centre, University of Allahabad, Muir Road, Allahabad Uttar Pradesh 211002, India*

⁽²⁾*Inter University Accelerator Centre, JNU, Aruna Asaf Ali Marg, New Delhi New Delhi 110067, India*

Swift heavy ion (SHI) induced morphological changes of 150 nm thick BaF₂ films grown on Si substrate has been studied for 100 MeV Au⁺⁹ ions at different ion fluences in the range of 5×10^{11} - 2×10^{13} ions/cm². Up to the fluence of 1×10^{12} ions/cm², the surface morphology is almost unchanged from pristine, but thereafter, the formation of cracks is seen using Atomic Force Microscopy. The dimensions and density of the cracks is found to increase with ion fluence. Dynamic scaling of surfaces, extracted from two dimensional power spectral density (2D-PSD), demonstrates that the surface roughness exponent (α) values are in the range of 0.2-0.5. While, Growth exponent values are found to be $\beta = 0.1 \pm 0.03$ and 1.08 ± 0.1 for continuous and cracked surfaces respectively. Roughness exponent value, $\alpha = 0.2-0.5$ and higher value of growth exponent, $\beta = 1.08 \pm 0.1$, suggest the dominant role of electronically mediated sputtering over surface diffusion in the observed crack formation on BaF₂ surface at higher fluence values. Shift of X-ray diffraction peaks after irradiation indicates contribution of tensile stress in the crack evolution with ion fluence. Rutherford backscattering measurements reveal the removal of film and exposure of substrate due to crack formation at higher fluences.

Study of neutron induced reactions on ^7Be using large angle coincidence spectroscopy[Jiri Vacik](#)¹, [Vladimir Hnatowicz](#)¹, [Ivo Tomandl](#)¹, [Ulli Köster](#)²⁽¹⁾*Nuclear Physics Institute, Academy of Sciences of the Czech Republic, Hlavni 130, Husinec - Rez 25068, Czech Republic*⁽²⁾*Institute of Laue-Langevin, Rue Jules Horowitz, Grenoble 38042, France*

Neutron induced reactions on the radioactive nuclei ^7Be play an interesting role in nuclear physics and astrophysics. The interactions of thermal neutrons with ^7Be is dominated by the $^7\text{Be}(n_{\text{th}}, p_1)^7\text{Li}$ and $^7\text{Be}(n_{\text{th}}, p_0)^7\text{Li}$ reactions. While ^8Be in the ground state disintegrates into two alpha particles, the decay from the 2^- capture state is prohibited because of the parity violation. The observation of the $^7\text{Be}(n_{\text{th}}, \alpha)^4\text{He}$ reaction (with two 9495 keV alphas) would be thus a unique tool for the study of the parity violation in the strong interactions. The test was carried out on the collimated thermal neutron beam using the large angle coincidence spectroscopy [1]. Both reaction products were detected by two identical semiconductor detectors. The ^7Be nuclei were prepared at the ISOLDE facility by implantation of 60 keV ^7Be ions into Al foil. The results showed that the ratio of the cross sections was determined to be $\sigma(p_1)/\sigma(p_0) = (1.58 \pm 0.06) \times 10^{-2}$, and in the coincidence measurement simultaneous emission of two alpha particles with the energy 8775 keV was observed. This reaction channel, however, corresponds to a two-stage process comprising transition from the neutron capture state (18991 keV) to an intermediate state by emission of the gamma photon followed by the decay into two alphas. The possible candidate of the intermediate state in the highly excited ^8Be nuclei might be the level at 17640 keV (1^+) [2], which is in contrast to the previous reported data [2,3], where the 16626 keV level was considered as the intermediate one. In the experiment no alpha particles with the energy 9495 keV were observed.

Reference:[1] J. Vacik et al., **Proc. MRS 354** (1994) 419.[2] D.R. Tilley, H.R. Keller, G.M. Hale, **Nucl. Phys. A541** (1992) 1.[3] A. Csoto, G.M. Hale, **Phys. Rev. C55** (1997) 2366.**Nano-crystal Formation and Growth from High Fluence Ion Implantation of Au, Ag, or Cu in Silica or MgO**[Daryush ILA](#)¹, [John E. Baglin](#)³, [Robert Lee Zimmerman](#)²⁽¹⁾*Chemistry and Physics, Fayetteville State University, 1200 Murchison Rd. , 15475, Fayetteville NC 28301-4297, United States*⁽²⁾*Chemistry and Physics, Fayetteville State University, 1200 Murchison Rd. , 15475, Fayetteville NC 28301-4297, United States*⁽³⁾*IBM, Almaden Research Center, San Jose CA 95120, United States*

High fluence implantation of metal ions (e.g. Au, Ag, Cu) into a non-reactive glassy host material (e.g. Silica), at a controlled temperature, followed by thermal anneal, can lead initially to a sparse distribution of individual metal atoms, located in interstitial or vacancy sites of collisional displacement of the host atoms. As fluence is increased, nucleation of metal nanocrystallites occurs, possibly followed by aggregation of such crystallites to form larger entities, via an Ostwald

ripening type of process. The energy to enable the diffusion required for such migrations must come from local energy loss by the arriving ions, plus thermal energy in the sample, plus free energy liberated due to the configurational changes, plus any chemical energy that may arise from interactions at broken bonds of the host material.

The complex sequence of physical processes involved can be controlled by many free parameters of the irradiation and thermal conditions. Development of a comprehensive quantitative model for the evolution of the resulting composite material should provide a basis for future engineering of materials having custom-tailored properties (e.g. particle size- and spatial- distribution), supporting a variety of technological applications based on new optical, electrical, or mechanical performance.

This presentation reports a series of related experimental investigations of the systems involving Au or Ag or Cu implantation into Silica or MgO, at MeV energies, coupled with thermal annealing at temperatures from 600C to 1200C. Preliminary results will be discussed, showing consistency with the assignment of characteristic activation energies for the successive process steps.

Abstract 285

[Invited Poster - Poster Sessions](#)

Thermoelectric and Optical Properties of SiO₂/SiO₂+Au Multilayer Thin Films Affected by Thermal Annealing

[S. Budak¹](#), [B. Allen¹](#), [J. Cole¹](#), [M. E. Gulduren²](#), [S. Yang¹](#), [R. B. Johnson³](#)

⁽¹⁾*Electrical Engineering & Computer Science, Alabama A&M University, Normal AL 35762, United States*

⁽²⁾*Department of Physics, University of Alabama in Huntsville, Huntsville AL, United States*

⁽³⁾*Department of Physics, Alabama A&M University, Normal AL 35762, United States*

Thermoelectric devices have been prepared from 100 alternating layers of SiO₂/SiO₂+Au superlattice films using Magnetron DC/RF Sputtering. SEM and EDS have been used to analyze the surface and composition of the thin films. The prepared thin film samples have been annealed at the different temperatures to form quantum clusters in the multi-layer superlattice thin films to decrease the cross plane thermal conductivity, increase the cross plane Seebeck coefficient and increase the cross plane electrical conductivity to increase the figure of merit. We characterized the thin film devices on their thermoelectric and optical properties.

Research sponsored by the Center for Irradiation of Materials (CIM), National Science Foundation under NSF-EPSCOR R-II-3 Grant No. EPS-1158862, DOD under Nanotechnology Infrastructure Development for Education and Research through the Army Research Office # W911 NF-08-1-0425, and DOD Army Research Office # W911 NF-12-1-0063 and National Nuclear Security Admin (DOE/NNSA/MB-40) with grant# DE-NA0001896, NSF-REU with Award#1156137.

Abstract 150

[Invited Poster - Poster Sessions](#)

Pair Distribution Function Analysis of nanocrystalline ZnS and CdS

[Sunil D Deshpande¹](#), [K K Pandey²](#), [G M Dharne¹](#), [S S Deshpande³](#)

⁽¹⁾*Department of Physics, Dr Babasaheb Ambedkar Marathwada University, University Campus, Aurangabad Maharashtra 431004, India*

⁽²⁾*High Pressure and Synchrotron Radiation Physics Division, Bhabha Atomic Research Centre, Trombay, Mumbai Maharashtra 400085, India*

⁽³⁾*Department of Physics, Sant Gadge Baba Amravati University, University Campus, Amravati Maharashtra 444602, India*

Atomic PDF analysis is well suited to investigate the atomic arrangement in nanosized materials¹⁻². II-VI semiconductor nanocrystals have attracted much attention due to their size dependent properties³⁻⁴.

Herein we report the angle dispersive x ray diffraction (ADXRD) measurements on ~3 nm crystallite ZnS and CdS powders recorded on BL-11 Beamline of INDUS Synchrotron Source. The data acquisition was in transmission mode. The wavelength was 0.04666 nm. Detector was MAR 3450 image plate and the sample to detector distance was 185.9178 mm.

The crystallite size was found to be 2.81 nm for ZnS and 3.03 for CdS. The crystallite sizes matched well with the Brus model⁵. The Bravais lattices both the cases (ZnS and CdS) had cubic (diamond) symmetry (SG: F-43m) and lattice parameter to be 0.53707 nm (for ZnS) and 0.580 nm (for CdS). The II-VI (cation-anion) and II-II or VI-VI (cation-cation as well as anion-anion) distances were found to be 0.2336 nm (Zn-S); 0.251 nm (Cd-S) and 0.3798 nm (Zn-Zn); 0.41 nm (Cd-Cd). To verify These distances were verified using **RAD-Gtk 1.0** developed by Petkov⁶.

1. B. Gilbert et al, Science, 305, 651-654, (2004).
2. V. Petkov, Mater.Today, 11, 28-38, (2008)
3. A. J. Hoffman et al. J. Phys. Chem. 96, (13) 5546-5552 (1992)
4. A. Ishibashi, J. Crystal Growth, 159, 555-565 (1996)
5. L. E. Brus, J. Chem. Phys. 80 (9), 4403-4409 (1984)
6. V. Petkov, J. Appl. Crystallography, 22, 387-389 (1989).

Acknowledgements: One of the authors (SDD) acknowledges the financial assistance from the University Grant Commission, New Delhi (F-37/147/2009(SR)). The authors are also grateful to Dr. S. K. Deb, Head, INDUS Synchrotron Users' Division, Raja Ramanna Center for Advanced Technology Indore and Dr. S.M. Sharma, Head, High Pressure and Synchrotron Radiation Physics Division, Bhabha Atomic Research Centre, Trombay, Mumbai 400085 for the ADXRD measurements.

Degradation of GaAs Photovoltaics Exposed to Reactor Neutrons and Accelerator Ions[David Bossert](#), [Darwin K. Serkland](#), [Elizabeth Auden](#), [Barney L. Doyle](#)*Radiation-Solid Interactions, Sandia National Laboratories, 5800 Eubank SE, Albuquerque NM 87185, United States*

The radiation hardness of optoelectronic components, including photodiodes for optical signal detection and power conversion, is important for operation in high radiation environments like fusion and fission reactors and large particle accelerators. A radiation resistant AlGaAs/GaAs photovoltaic (PV) design has been exposed to pulsed and continuous neutron and gamma rays at the Sandia ACRR facility, demonstrating high optical to electrical efficiency to a neutron fluence of over 1×10^{15} neutrons/cm². Device degradation is attributed primarily to decreased carrier lifetime due to displacement damage from fast neutron-induced collision cascades. While an insitu reactor exposure may be the definitive validation for a component, there are a number of shortcomings associated with the test, including a limited range of neutron fluence and flux, and an inability to separate fast neutron effects from high energy gamma rays. Furthermore, the experiment is labor and time intensive and includes the expense of disposing of the activated test apparatus. The use of accelerated ions to simulate neutron collisions avoids these impediments, providing a flexible method of understanding radiation effects more completely. We report on a comparative study of GaAs-based PVs irradiated by neutrons and accelerated heavy ions where the ion energy and species, flux and fluence was varied as a function of diode bias voltage. Initial results have established a nearly identical photocurrent reduction for all the ion conditions when the fluence is converted to units of 1-MeV-equivalent-neutrons/cm².

* Sandia National Laboratories is a multi-program laboratory managed and operated by Sandia Corporation, a wholly owned subsidiary of Lockheed Martin Corporation, for the U.S. Department of Energy's National Nuclear Security Administration under contract DE-AC04-94AL85000.

Development of a high resolution Analyzing Magnet System for heavy molecular ions[Mohamed O A El Ghazaly](#)¹, [Abdullah S Jabr](#)¹, [Morgan Dehnel](#)², [Salma Z Hmeida](#)³, [Pierre Defrance](#)⁴

⁽¹⁾National Center for Mathematics and Physics (NCMP), King Abdulaziz City for Science and Technology (KACST), King Abdullah Road P.O. Box 6086, Riyadh 11442, Saudi Arabia

⁽²⁾D-PACE, Dehnel - Particle Accelerator Components and Engineering, Inc. (D-PACE), D-PACE, P.O. Box 201, Nelson, S.C BC V7L 5P9, Canada

⁽³⁾Polytech Paris-Sud, Université Paris-Sud, Maison de l'ingénieur, bâtiment 620, Orsay cedex F - 91405, France

⁽⁴⁾Institute of Condensed Matter and Nanosciences, Catholic University of Louvain, Chemin du cyclotron 2, Louvain-la-Neuve B-1348, Belgium

Electrostatic storage rings [1] have been introduced as mass-independent storage devices that thereby open up new applications towards biological and macro-particles sciences. They have indeed, allowed ground-breaking advances to be made in the interdisciplinary fields of e.g. biophysics, biochemistry, and radiobiological, as well. An up-to-date complete electrostatic storage ring facility for atomic and molecular physics is being constructed at the King Abdulaziz City for Science and Technology (KACST), in Riyadh, Saudi Arabia [2]. In this context, a high-performance analyzing spectrometer magnet is being developed and constructed to fulfill the specific requirements for the macromolecular ion beam that is to be injected and stored in the ring. This dipole magnet has thereby been designed to provide a double-focused beam of ions of a kinetic energy up to 50keV and masses up to 1500 **amu**, with a high mass resolution recorded to $\Delta m/m = 1:1500$. The analyzer magnet system includes specific entrance and exit slits, designed to sustain further the required mass resolution. Here, we report on the ion-optical simulations and the design of this magnet.

References:

[1] S P Møller 1997, **Nucl. Instr. Meth. A** 394 **281-286**

[2] M. O. A. El Ghazaly, **Eur. Phys. J. Web of Conferences**, (to appear: 2014)

Abstract 47

[Invited Poster - Poster Sessions](#)

Line ratios of soft X-ray emissions following charge exchange between C^{6+} and Kr

[T. J. J. Lamberton](#)¹, [R. T. Hovey](#)¹, [B. N. Singh](#)¹, [V. M. Andrianarijaona](#)¹, [D. McCammon](#)², [M. Fogle](#)³,
[D. G. Seely](#)⁴, [C. C. Havener](#)⁵

⁽¹⁾*Department of Physics, Pacific Union College, Angwin Ca 94508, United States*

⁽²⁾*Department of Physics, University of Wisconsin, Madison WI 53706, United States*

⁽³⁾*Department of Physics, Auburn University, Auburn AL 36849, United States*

⁽⁴⁾*Department of Physics, Albion College, Albion MI 49224, United States*

⁽⁵⁾*Physics Division, Oak Ridge National Laboratory, Oak Ridge TN 37831-6372, United States*

The radiance line ratios $Ly-\beta / Ly-\alpha$, $Ly-\gamma / Ly-\alpha$, $Ly-\delta / Ly-\alpha$, and $Ly-\epsilon / Ly-\alpha$ for soft X-ray emission following charge exchange between C^{6+} and Kr are reported for collision velocities between approximately 250 km/s - 3000 km/s, which are characteristic of the solar wind. The X-ray spectra were obtained using the ion-atom merged beams apparatus at Oak Ridge National Laboratory equipped with a microcalorimeter x-ray detector with a resolution on the order of 10 eV FWHM. A crossing between the measured $Ly-\beta / Ly-\alpha$ and $Ly-\gamma / Ly-\alpha$ is well resolved around 950 ± 50 km/s and could be used as a velocity indicative tool. There is no Kr theory, however Kr has the same ionization potential as H so that the results reported here are compared to a cascade model based on calculations done on $C^{6+} + H$. On the other side, double-electron-capture (DEC) is possible for this system and for any multi-electron target. True double capture is seen to be only 10% of the single-electron-capture (SEC).

Abstract 178

[Invited Poster - Poster Sessions](#)

Process Identification and Relative Cross Sections for Low-keV Proton Collisions in N_2 and CO_2 Molecules

[López Patiño Juan](#)¹, [Fuentes Madariaga Beatriz Elizabeth](#)¹, [Bashir Yousif Farook](#)², [Martínez Horacio](#)³

⁽¹⁾*Facultad de Ciencias, Universidad Nacional Autónoma de México, 3000 universidad avenue, México D. F. 04510, Mexico*

⁽²⁾*Facultad de Ciencias, Universidad Autónoma del Estado de Morelos, Cuernavaca Morelos, Mexico*

⁽³⁾*Instituto de Ciencias Físicas, Universidad Nacional Autónoma de México, Cuernavaca Morelos, Mexico*

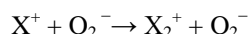
Fragmentation of N_2 and CO_2 molecules has been investigated in the range of energies between 1 and 10 keV. Identification of fragments and relative cross sections were done using Time of Flight (TOF) technique. Single electron capture and ionization processes were found to be the most important reactions present in all the energy range. Dissociative processes are also reported.

Negative ion formation in Ion-Molecule collisions[Angelin Ebanazar John](#), [Rainer Hippler](#)*Institute of Physics, University of Greifswald, Felix-Hausdorff Strasse 6, Greifswald Mecklenburg-Vorpommern 17489, Germany*

Positively charged H^+ , H_2^+ , He^+ , and Ar^+ ions, with impact energies of 50 - 350 keV, have been bombarded with O_2 and SF_6 molecules. The collision cross sections of positive and negative ionic fragments were determined and their dependence on impact energy will be presented.

Besides positively charged ion fragments, the negatively charged secondary ions are an important contribution for various applications especially in atmospheric chemistry and plasma physics.

One of the exciting observation is superoxide O_2^- anion which is a potential reactive oxygen species(ROS). We have proposed the formation of superoxide anion via a charge-transfer reaction with a positively charged projectile as follows,



where the electron transferred to the oxygen molecule originates from the incident ion($X = H_2^+$ or He^+ or Ar^+) having atleast one electron for the reaction. Collision cross sections for O_2^- formation($\sim 10^{-18}$ cm²/molecule) are about 2 orders of magnitude smaller compared to O_2^+ formation($\sim 10^{-16}$ cm²/molecule), which is attributed to the larger energy transfer required. Similarly negatively charged F^- , S^- and SF_6^- secondary ions are formed from SF_6 gas on energetic ion bombardment. Their mass distribution and impact energy dependence have been discussed in detail in-addition to the positively charged secondary ion fragments S^+ , F^+ and SF_n^+ ($n=1-5$).

Investigations of Fast-Moving Ion Kinematic Effects in Velocity-Map Imaging Spectroscopy[Kiattichart Chartkunchand](#), [Kyle R. Carpenter](#), [Jeremy Cheatam](#), [Vernon T. Davis](#), [Paul A. Neill](#),
[Jeffrey S. Thompson](#), [Aaron M. Covington](#)*Department of Physics and Nevada Terawatt Facility, University of Nevada, Reno, 1664 North Virginia Street, Reno NV 89557, United States*

Velocity-Map Imaging (VMI) spectroscopy is a powerful technique that allows for the simultaneous collection of energy- and angle-resolved charged particles. Despite the fact that VMI systems have been in use for over a decade, a systematic analysis quantifying how fast-moving ion beam kinematics might alter captured images has not been published. Kinematic effects may become important for VMI experiments mounted on ion accelerators with beam energies exceeding ~1keV. A preliminary non-relativistic analysis quantifying energy-, ejection angle- and solid angle-effects will be presented utilizing photoelectron images collected following the laser-induced photodetachment of negative ion beams with kinetic energies ranging from ~2-15keV.

Design of THz Free Electron Laser Oscillator Cavity

[Conor M Pogue](#)², [W B Colson](#)¹, [Chase Boulware](#)², [Terry Grimm](#)²

⁽¹⁾*Physics, Naval Postgraduate School, 833 Dyer Road, Monterey CA 93943, United States*

⁽²⁾*Niowave, 1012 North Walnut, Lansing MI 48906, United States*

With the use of superconducting spoke cavities free electron lasers (FELs) with relatively small footprints are becoming a more feasible reality. FELs use a relativistic electron beam in conjunction with a periodic magnetic field to create coherent radiation with a single transverse mode at a designed wavelength. These relatively low energy FELs have many uses as THz sources for medical imaging, security, spectroscopy, and material processing. Here an 8 MeV electron beam drives a THz FEL CW with an output power of ~ 2kW.

The FEL physics allows for a wide wavelength range from 66 mm to 180 mm while allowing moderate gain per pass of ~ 13% using a 10 period undulator. Losses in the 3.4m long cavity arise from clipping on cavity mirrors, clipping at the ends of the undulator, absorption in the mirrors, and outcoupling of the usable radiation. For a point design at ~96um (3THz) wavelength, design criteria for alignment of the 4" diameters mirrors have been simulated showing the mirror tilt tolerance to be <100mrad off of the undulator / cavity axis. The transverse shift tolerances for the cavity mirrors were simulated, and found to be ~0.5mm.

Multiple outcoupling techniques will be studied including typical "hole-outcoupling" where the output coupler has a single small hole to allow ~2% of the power in the cavity. Another possible option involves a "pic-outcoupling" where a mirror is actuated into the optical mode and reflects a small percentage out an output window. Other novel outcoupling techniques including the use of Fresnel mirrors and more elaborate hole-outcoupling techniques may be simulated and considered.

Abstract 292

[Regular Poster - Poster Sessions](#)

Results of the SRF Wafer Test Cavity for the Characterization of Superconductors

[Justin Comeaux](#)¹, [Nate Pogue](#)¹, [Ari Palczewski](#)², [Peter McIntyre](#)¹, [Charles Reece](#)²

⁽¹⁾*Physics and Astronomy, Texas A&M University, 4242 TAMU, College Station Texas 77845, United States*

⁽²⁾*SRF Institute, Thomas Jefferson National Accelerator Facility, 12000 Jefferson Avenue, Newport News Virginia 23606, United States*

The SRF community would greatly benefit from the ability to perform fast, reproducible tests for novel superconductors and preparation techniques. The Wafer Test Cavity was designed to be a platform for measuring the performance and limitations of superconducting samples. Several cavities have been constructed to fulfill this task, however none have the capability to reach a critical field greater than 100 mT presently. The Wafer Test Cavity uses a dielectric lens to focus the field onto the sample pushing the field to 5 times that on the cavity walls. The first results of assembly and testing will be presented.

Abstract 110

[Regular Poster - Poster Sessions](#)

How to Produce a Reactor Neutron Spectrum Using a Proton Accelerator

[Kim A Burns](#), [Robert O Gates](#), [Bruce E Schmitt](#), [David W Wootan](#)

Pacific Northwest National Laboratory, P.O. Box 999, Richland Washington 99352, United States

In this paper a method for reproducing the neutron energy spectrum present in the core of an operating nuclear reactor using an engineered target in an accelerator proton beam is proposed. The protons interact with a target to create neutrons through various (p,n) type reactions. Spectral tailoring of the emitted neutrons can be used to modify the energy of the generated neutron spectrum to represent various reactor spectra. Through the use of moderators and reflectors, the neutron spectrum can be modified to reproduce many different spectra of interest including spectra in small thermal test reactors, large pressurized water reactors, and fast reactors. The particular application of this methodology is the design of an experimental approach for using an accelerator to reduce uncertainties in the interpretation of reactor antineutrino measurements. This approach involves using a proton accelerator to produce a neutron field representative of a power reactor and using this neutron field to irradiate fission foils of the primary isotopes contributing to fission in the reactor, creating unstable, neutron rich fission products that subsequently beta decay and emit electron antineutrinos. Measurement of the energy spectrum of these beta particles provides a distinctive set of systematic considerations for comparison to the original seminal beta spectra measurements. A major advantage of an accelerator neutron source over a neutron beam from a thermal reactor is that the fast neutrons can be slowed down or tailored to approximate various reactor spectra. An accelerator based neutron source that can be tailored to match various reactor neutron spectra provides an advantage for control in studying how changes in the neutron spectra affect parameters such as the resulting fission product beta spectrum.

Abstract 28

[Invited Poster - Poster Sessions](#)

Production of Multiply Charged Kr Ions by Synchrotron Radiation

[Antonio C. F. Santos¹](#), [Sergio Pilling²](#), [Danilo P Almeida³](#)

⁽¹⁾*Nuclear Physics, Universidade Federal do Rio de Janeiro, Av. Athos da Silveira Ramos, 149 Centro de Tecnologia - bloco A - Cidade Universitária - Rio de Janeiro - RJ -, Rio de Janeiro RJ 21941-972, Brazil*

⁽²⁾*Physics, Universidade do Vale do Paraíba, São José dos Campos SP 12244-000, Brazil*

⁽³⁾*Physics, Universidade Federal de Santa Catarina, Florianópolis SC 88040-979, Brazil*

Charge state spectra of krypton ions generated by after photoionization of the L shell of Kr atoms have been measured by the PEPICO technique. Relative abundances of Kr^{q+} ions in charge state up to $8+$ were obtained using monochromatized synchrotron radiation. A comparison with other experimental and theoretical data is presented. The combination of the present data with various theoretical and experimental data suggested that double ionization of Kr atoms by fast electron impact occurs mainly via outer-shell ionization.

Abstract 6

[Invited Poster - Poster Sessions](#)

Origin of L satellites in X-Ray emission spectra of elements with ${}_{26}\text{Fe}$ to ${}_{92}\text{U}$

[Surendra Poonia](#)

X-Ray Spectroscopy Laboratory, Department of Physics, Jai Narain Vyas University, Jodhpur - 342 005, Rajasthan, India, X-Ray Spectroscopy Laboratory, Department of Physics, Jai Narain Vyas University, Jodhpur - 342 005, Rajasthan, India, 10-C, Mahaveer Colony, Opposite Shivam Hospital, Ratanada, Jodhpur, Jodhpur Rajasthan 342001, India

The X-ray satellites La' , La'' , La''' , La'''' , La_3 , La_4 , La_5 , La^{ix} , La^{x} , La_s , Lb_1^{I} , Lb_1^{II} , Lb_1^{III} , Lb_1^{IV} , Lb_2^{I} , $\text{Lb}_2^{(\text{b})}$, Lb_2^{II} , $\text{Lb}_2^{(\text{c})}$, Lg_1 , Lg_2 , Lg_2' , Lg_2'' and $\text{Lg}_2^{2,3}$ observed in the L-emission spectra in elements with $Z = 26$ to 92 , have been calculated. The energies of various transitions have been calculated by available Hartree-Fock-Slater using the semi-empirical Auger transition energies in the doubly ionized atoms and their relative intensities have been estimated by considering cross-sections of singly ionized $2x^{-1}$ ($x = s, p$) states and then of subsequent Coster-Kronig (CK) and shake off processes. In both these processes initial single hole creation is the prime phenomenon and electron bombardment has been the primary source of energy. The calculated spectra have been compared with the measured satellite energies in L emission spectra. Their intense peaks have been identified as the observed satellite lines. The one to one correspondence between the peaks in calculated spectra and the satellites in measured spectra has been established on the basis of the agreement between the separations in the peak energies and those in the measured satellite energies. Group of transitions under the transition

schemes $L_3M_x-M_xM_{4,5}$, $L_2M_x-M_xM_{4,5}$, $L_3M_x-M_xN_{4,5}$ and $L_2M_x-M_xN_{4,5}$ ($x = 1-5$), which give rise to these satellites have been identified. It is observed that the satellite $Lb_2^{(b)}$ in all these spectra can be assigned to superposition of $^3F_4-^3G_5$ and $^3F_4-^3D_3$ transitions and that this must be the most intense of all these satellites, contributing in order of decreasing intensity. Each of the remaining satellites is found to have different origin in different elements. The possible contributions of suitable transitions to all these lines have also been discussed.

Abstract 118

[Regular Poster - Poster Sessions](#)

Bare- and dressed-ion impact collisions from neon atoms studied within a nonperturbative mean-field approach

[Gerald Schenk](#), [Tom Kirchner](#)

Department of Physics and Astronomy, York University, 4700 Keele Street, Toronto Ontario M3J 1P3, Canada

We study electron removal processes in collisions of bare and dressed doubly- and triply-charged ions with neon atoms in the 25 keV/u to 1 MeV/u impact energy regime. The many-electron problem is represented by a single mean field, which in the case of dressed-ion impact includes the projectile electrons. Moreover, the same basis is used to propagate all active orbitals thereby ensuring orthogonality at all times and allowing for a final-state analysis in terms of standard Slater determinantal wave functions. The same approach was used in a recent work for B^{2+} -Ne collisions [1], in which we examined the role of the projectile electrons for target-recoil-charge-state production. The present study expands on that work by (i) considering additional collision channels; (ii) accounting for time-dependent response; (iii) comparing results of equicharged dressed and bare ions in order to shed more light on the role of the projectile electrons.

[1] G. Schenk et al, Phys. Rev. A 88 012712 (2013).

This work is supported by NSERC, Canada.

Abstract 119

[Regular Poster - Poster Sessions](#)

Time-dependent density functional theory study of correlation in proton-helium collisions

[Matthew Baxter](#), [Tom Kirchner](#)

Department of Physics and Astronomy, York University, 4700 Keele Street, Toronto Ontario M3J 1P3, Canada

A recent model to describe electron correlations in time-dependent density functional theory (TDDFT) studies of antiproton-helium collisions [1] is extended to deal with positively charged projectiles. The main complication is that a positively-charged projectile can capture electrons in addition to ionizing them to the continuum. As a consequence, within the TDDFT framework one needs to consider three, instead of just one, correlation integrals when formally expressing the probabilities for the occurring one- and two-electron capture and ionization processes in terms of the density. We discuss an extension of a previously used adiabatic model for the correlation integral to deal with this situation and present results for few keV to few MeV proton-helium collisions obtained from basis-generator-method calculations with microscopic response effects included [2].

[1] M. Baxter and T. Kirchner, Phys. Rev. A 87, 062507 (2013)

[2] M. Keim et al, Nucl. Instr. and Meth. B 233, 240 (2005)

This work is supported by NSERC, Canada.

Abstract 121

[Regular Poster - Poster Sessions](#)

Independent-particle and independent-event calculations for 1.5 MeV/amu O^{8+} -Li collisions

[Tom Kirchner](#)¹, [Nariman Khazai](#)¹, [Laszlo Gulyas](#)²

⁽¹⁾*Department of Physics and Astronomy, York University, 4700 Keele Street, Toronto Ontario M3J 1P3, Canada*

⁽²⁾*Institute of Nuclear Research, Hungarian Academy of Sciences (ATOMKI), PO Box 51, Debrecen H-4001, Hungary*

In a recent experiment, single ionization of lithium atoms by 1.5 MeV/amu O^{8+} impact was considered [1]. The data exhibit two distinct peaks when plotted as a function of the Q-value, i.e., the difference in the energies of the electrons before and after the collision. The peaks were identified as being due to the removal of the 2s- and one of the 1s-electrons, respectively. Since a one-electron continuum distorted-wave with eikonal initial-state (CDW-EIS) calculation for Li(1s) ionization did not agree with the measured electron-energy differential cross section associated with the second peak, it was concluded that it may be due to a two-electron excitation-ionization process [1].

In order to test this interpretation we study the O^{8+} -Li system using independent-particle and independent-event models and single-electron basis generator method and CDW-EIS calculations. We find that pure single ionization of a lithium K-shell electron, which leaves the recoiling target ion in an excited state, is too weak a process to explain the measured cross sections. Rather, our analysis confirms that two-electron excitation-ionization processes occur, but they suggest that the situation is somewhat more involved than speculated in Ref. [1].

[1] D. Fischer et al., Phys. Rev. Lett. 109, 113202 (2012).

This work is supported by NSERC, Canada and OTKA, Hungary.

Abstract 332

[Regular Poster - Poster Sessions](#)

Double Ionization in Ion-Atom Collisions: Mechanisms and Scaling

[Anthony C. F. Santos](#)¹, [Robert D. DuBois](#)², [Steven T. Manson](#)³

⁽¹⁾*Instituto de Física, Universidade Federal do Rio de Janeiro, PO 68528, Rio de Janeiro RJ 21941-972, Brazil*

⁽²⁾*Department of Physics, Missouri University of Science and Technology, Rolla Missouri 64509, United States*

⁽³⁾*Department of Physics & Astronomy, Georgia State University, Atlanta Georgia 30303, United States*

The detailed mechanism(s) as to how double ionization occurs in ion-atom collisions is of great interest; specifically, the importance of processes that are first vs. second order in the ion-atom interaction, and interference between the two orders. Earlier, it was proposed by McGuire that all three terms contribute to the matrix element [1], but recently it was suggested that only first order terms were important [2]. These mechanisms can be separated, to some extent, since they have differing dependences on the velocity and charge of the incident ion. A detailed analysis of available experimental ionization cross sections and cross section ratios for a wide range of systems and impact energies has been assembled and analyzed to try to untangle the competing mechanisms. This analysis supports the McGuire model for double ionization and implies that the first order model of Shao et al. [2] may have only limited applicability. By fitting single ionization cross sections and using experimental data to extract second order contributions to double ionization, as well for the phase difference between the matrix elements for first- and second-order ionization mechanisms (derived by combining the proton and antiproton double ionization cross sections), analytical formulae for the various channels leading to single and double ionization were developed. Multicharged ion data were used to extract projectile Z scaling dependences while proton, antiproton and multicharged ion data for He, Ne, and Ar targets were used to extract target scaling dependences. The data imply that a combination of these scalings and formulae provide reasonable to very good agreement for double outer shell ionization of any atom by any fully stripped projectile for most impact velocities. [1] J.H. McGuire, Phys. Rev. Lett. 49, 1153 (1982). [2] J.X. Shao, X.R. Zou, X.M. Chen, C.L. Zhou, and X.Y. Qiu, Phys. Rev. A 83, 022710 (2011).

Abstract 463

[Regular Poster - Poster Sessions](#)

Atomic Physics with Accelerators: Projectile Electron Spectroscopy (APAPES) *

[Ioannis Madesis](#)^{1,2}, [Anastasios Dimitriou](#)^{1,2}, [Anastasios Lagoyannis](#)², [Michael Axiotis](#)², [Theodore Mertzimekis](#)^{2,3}, [Miltiades Andrianis](#)², [Emmanuel P. Benis](#)⁴, [Sotiris Harissopulos](#)², [Béla Sulik](#)⁵, [Ivan Valastyán](#)⁵, [Theodore J.M. Zouros](#)^{1,2}

⁽¹⁾*Department of Physics, University of Crete, P.O Box 2208, Herakleion GR-71003 , Greece*

⁽²⁾*Tandem Lab, INPP, NCSR Demokritos, P.O Box 60228, Aghia Paraskevi GR-15310 , Greece*

⁽³⁾*Department of Physics, University of Athens, Zografou Campus, Athens GR-15701 , Greece*

⁽⁴⁾*Department of Physics, University of Ioannina, P.O Box 1186, Ioannina GR-45110, Greece*

⁽⁵⁾*Institute for Nuclear Research , MTA ATOMKI, Bem tér 18/c, Debrecen H-4026 , Hungary*

The new research initiative APAPES (<http://apapes.physics.uoc.gr/>) funded by THALES* is presently setting up a new experimental station at the 5.5MV TANDEM of the National Research Center "Demokritos" in Athens with a dedicated beam line for atomic collisions physics research. A complete zero-degree Auger projectile spectroscopy apparatus is being put together to perform high resolution studies of electrons emitted in ion-atom collisions.

A single stage hemispherical spectrometer with a 2-dimensional position sensitive detector combined with a doubly-differentially pumped gas target will be used to perform a systematic isoelectronic investigation of K-Augur spectra emitted from collisions of pre-excited and ground state He-like ions with gas targets using novel techniques. The goal is to provide a deeper understanding of cascade feeding of the $1s2s2p\ ^4P$ metastable states in collisions of He-like ions with gas targets and further elucidate their role in the non-statistical production of excited three-electron $1s2s2p$ states by electron capture, recently a field of conflicting interpretations awaiting further resolution¹.

First beam tests of the apparatus will soon be completed and the spectrometer is expected to become fully operational by the end of this summer. Here, we report on the status of the APAPES project, the description of the beam line, the spectrometer and data acquisition system as well as our plans for the future.

*Co-financed by the European Union (European Social Fund-ESF) and Greek national funds through the Operational Program "Education and Lifelong Learning" of the National Strategic Reference Framework (NSRF)-Research Funding Program: THALES. Investing in knowledge society through the European Social Fund (Grant No. MIS 377289)

¹T. J. M. Zouros, B. Sulik, L. Gulyás and K. Tökési, Selective enhancement of $1s2s2p\ ^4P_1$ metastable states populated by cascades in single-electron transfer collisions of $F^{7+}(1s^2/1s2s\ ^3S)$ ions with He and H_2 targets, Phys. Rev. A 77 (2008) 050701R.

Abstract 19

[Regular Poster - Poster Sessions](#)

Origin of L_{beta}2 X-Ray satellites spectra of 4d transition metals for lead as predicted by HFS calculations

[Surendra Poonia](#)^{1,2}

⁽¹⁾X-Ray Spectroscopy Laboratory, Department of Physics, Jai Narain Vyas University, Jodhpur ? 342 005, Rajasthan, India , X-Ray Spectroscopy Laboratory, Department of Physics, Jai Narain Vyas University, Jodhpur - 342 005, Rajasthan, India , 10-C, Mahaveer Colony, Opposite Shivam Hospital, Ratanada, Jodhpur, Jodhpur Rajasthan 342001, India

⁽²⁾X-Ray Spectroscopy Laboratory, Department of Physics, Jai Narain Vyas University, Jodhpur ? 342 005, Rajasthan, India , X-Ray Spectroscopy Laboratory, Department of Physics, Jai Narain Vyas University, Jodhpur - 342 005, Rajasthan, India , 10-C, Mahaveer Colony, Opposite Shivam Hospital, Ratanada, Jodhpur, Jodhpur Rajasthan 342001, India

The X-ray satellite spectra arising due to $2p_{3/2}^{-1}3x^{-1}3x^{-1}4d^{-1}$ ($x = s, p, d$) transition array, in elements $_{45}Rh$, $_{47}Ag$, $_{49}In$ and $_{51}Sb$, have been calculated. While the energies of various transitions of the array have been determined by using available Hartree-Fock-Slater data on $1s^{-1}2p^{-1}3x^{-1}$ and $2p^{-1}3x^{-1}4d^{-1}$ Auger transition energies and their relative intensities have been estimated by considering cross - sections of singly ionized $2x^{-1}$ ($x = s, p$) states and then of subsequent Coster-Kronig and shake off processes. The calculated spectra have been compared with the measured satellite energies in L_{β_2} spectra. Their intense peaks have been identified as the observed satellite lines. It has been established that all four satellites observed in the L_{β_2} region of the X-ray spectra of various elements and named b_2^I , $b_2^{(b)}$, b_2^{II} and $b_2^{(c)}$ in order of increasing energy are mainly emitted by $2p^{-1}3p^{-1}3p^{-1}4d^{-1}$ transitions. It is observed that out of these four satellites, $b_2^{(b)}$ has the highest intensity in all these spectra and can be assigned to superposition of $^3F_4\text{-}^3G_5$ and $^3F_4\text{-}^3D_3$ transitions and that this must be the most intense of all these satellites. It has been well established that the transitions $^1F_3\text{-}^1G_4$ and $^3D_3\text{-}^3D_3$ is the main source of the emission of the satellite b_2^{II} in the elements $_{45}Rh$ to $_{51}Sb$. Coming to the other two satellites in this region of the spectra, the line $b_2^{(c)}$, observed in the spectra $_{45}Rh$ to $_{49}In$, is mainly assigned to the transition $^3P_1\text{-}^3D_2$. The line b_2^I , is the weakest, observed in the spectra of element $_{45}Rh$, is assigned to the transition $2p^{-1}3p^{-1}3D_3\text{-}3p^{-1}4d^{-1}3F_4$. In the elements $_{47}Ag$ and $_{49}In$, the line b_2^I has been associated with transition $^3F_4\text{-}^3F_4$. Finally, the line b_2^I is assigned to the transitions $^3F_4\text{-}^3G_5$ and $^3F_4\text{-}^3D_3$ transitions in the element $_{51}Sb$.

Abstract 20

[Regular Poster - Poster Sessions](#)

Theoretical calculation of L_{β1} Satellites in X-Ray Emission Spectra of 3d transition elements

[Surendra Poonia](#)

X-Ray Spectroscopy Laboratory, Department of Physics, Jai Narain Vyas University, Jodhpur ? 342 005, Rajasthan, India , X-Ray Spectroscopy Laboratory, Department of Physics, Jai Narain Vyas University, Jodhpur - 342 005, Rajasthan, India , 10-C, Mahaveer Colony, Opposite Shivam Hospital, Ratanada, Jodhpur, Jodhpur Rajasthan 342001, India

The X-ray satellite spectra arising due to $2p_{1/2}^{-1}3x^{-1}-3x^{-1}3d^{-1}$ ($x = s, p, d$) transition array, in elements with $Z = 26$ to 30 , have been calculated. The energies of various transitions of the array have been determined by using available Hartree-Fock-Slater data on $1s^{-1}-2p^{-1}3x^{-1}$ and $2p_{1/2}^{-1}-3x^{-1}3x^{-1}$ Auger transition energies and their relative intensities have been estimated by considering cross sections of singly ionized $2x^{-1}$ ($x = s, p$) states and then of subsequent Coster-Kronig and shake off processes. The calculated spectra have been compared with the measured satellite energies in Lb_1 spectra. Their intense peaks have been identified as the observed satellite lines. The one to one correspondence between the peaks in calculated spectra and the satellites in measured spectra has been established on the basis of the agreement between the separations in the peak energies and those in the measured satellite energies. It has been established that two satellites observed in the Lb_1 region of the x-ray spectra of the elements with $Z = 26$ to 30 and named b_1^I and b_1^{II} in order of increasing energy are mainly emitted by $2p_{1/2}^{-1}3d^{-1}-3d^{-2}$ transitions. The satellite b_1^I has been assigned to the superposition of the transitions $^3F_2-^3F_2$, $^3P_2-^3P_2$ and $^3P_2-^3P_1$, contributing in order of decreasing intensity, and the line b_1^{II} has been assigned to mainly the $^3F_3-^3F_3$ transition.

Abstract 10

[Regular Poster - Poster Sessions](#)

Total charge changing cross-sections of 300 A MeV Fe^{26+} ion beam in different target media

[Renu Gupta](#), [Ashavani Kumar](#)

Physics, National Institute of Technology Kurukshetra, Kurukshetra Haryana 136119, India

In the present study, total charge changing cross-sections of 300 A MeV Fe^{26+} ion beam in Al and combined media of CH_2 , CR39 and Al were calculated by CR39 track etch detectors using an image analysing system; DM6000 M optical microscope attached with a personal computer installed with Leica QWin Plus software. The CR39 nuclear track detectors were used to identify the incident charged particles and their fragments. Exposed CR39 detectors were etched in 6N NaOH solution + 1% ethyl alcohol at $70^\circ C$ to visualize the tracks produced by primary ion beam and its fragmentations under optical microscope. The temperature was kept constant throughout the etching within $\pm 0.1^\circ C$. The present work shows better response of the CR39 track etch detector up to an improved threshold $Z/\beta \sim 4.6$. The cone-diameter distributions were fitted by multiple Gaussians using ROOT software analysis toolkit. The numbers of incident and survived ions were determined within 99.7% confidence levels. The calculated values of total charge changing cross-section were (1663 ± 236) mb in Al target, (1219 ± 29) mb in $CH_2+CR39+Al$ and (1020 ± 121) mb in CH_2+CR39 .

Abstract 202

[Regular Poster - Poster Sessions](#)

Accurate 50-200 keV proton stopping cross sections in solids

[Sergey N Dedyulin](#), [Lyudmila V Goncharova](#)

Department of Physics and Astronomy, The University of Western Ontario, 1151 Richmond St, London ON N6A3K7, Canada

Medium energy ion scattering (MEIS) is used to determine the elemental depth profiling in the first few hundred angstroms of a sample. The interpretation of MEIS spectra requires an accurate knowledge of the rate at which the ions lose their energy - the stopping cross section, ϵ . The rate of energy loss has been fairly well investigated, both experimentally and theoretically, in elemental and compound targets at high energies ($E > 400$ keV/amu). However, in the medium ion energy range where stopping cross section typically has a maximum, experimental data are scarce while most of the existing theories fail to give accurate predictions.

In this work, we report accurate measurements of stopping cross sections for ~ 55 -170 keV protons in Si, Ti and $SrTiO_3$ thin films using MEIS. We developed a new methodology of stopping cross sections calculations from the MEIS spectra. Measured ϵ_{Si} and ϵ_{Ti} agree with the values reported in the NIST database within experimental uncertainties. On the other hand, $SrTiO_3$ data are systematically lower over the whole energy range probed. Among the several factors that could

contribute to the observed discrepancy we eliminated the following: i) the proposed method for calculating stopping cross sections from MEIS spectra is not accurate and ii) literature values for ϵ_{Ti} are overestimated.

Abstract 249

[Regular Poster - Poster Sessions](#)

Description of Ge, Sm, Hf, Ta, and Au ultra-thin targets by Rutherford back-scattering technique for atomic inner K shell ionization studies.

[Camilo Miguel Correa¹](#), [Maria Victoria Manso²](#), [Juan Alejandro Garcia¹](#), [Nora Lia Maidana¹](#), [Manfredo Tabacniks¹](#), [Vito Vanin¹](#), [Suelem Barros¹](#)

⁽¹⁾*Experimental Physics, Insitute of Physics, University of Sao Paulo, Rua do Matao, Travessa R, 187., Sao Paulo SP 05314970, Brazil*

⁽²⁾*Departamento de Ciencias Exactas, Universidade Estadual do Santa Cruz (UESC), Rodovia Ilheus-Itabuna Km 16, Ilheus BA 45662900, Brazil*

The Sao Paulo Microtron research plan comprises the measurement of electron impact inner shell atomic ionization cross-sections, which require the manufacture of thin targets, in the mass-density range of a few to hundreds of micrograms per centimeter square. However, reports that explain in details the procedures for the preparation and characterization of thin targets for atomic data mining are hard to find. One of the most popular methods consists in evaporating a thin deposit of the element on a thin Carbon substrate, which minimizes the bremsstrahlung production both in the target element and in the C backings. Since the target thickness is the main source of uncertainty in the measurement of ionization cross section, these samples require a precise characterization.

This work will show and discuss the characterization of thin targets of Ge, Sm, Hf, Ta and Au evaporated on carbon backings with mass densities lower than 20 $\mu\text{g}/\text{cm}^2$. The technique employs the 2.2 MeV He^{2+} beam of the Tandem Accelerator at LAMFI - IFUSP, where all the targets were irradiated. We used the Rutherford Backscattering of alpha particle technique for measurement of mass density, stoichiometry, and elemental distribution profile along the films. Data analysis was performed off-line using the code SIMNRA [1]. In this study, it was possible to obtain the thickness of each target, corrected by the effects of roughness, oxidation and diffusion between the target element and the carbon substrate. We achieved uncertainties for the thickness below 5% in all measurements.

Abstract 367

[Regular Poster - Poster Sessions](#)

The UK MEIS facility - a new future at the IIAA, Huddersfield

[Jaap Van den Berg¹](#), [Paul Bailey¹](#), [Tim Noakes²](#), [Roger Barlow¹](#), [Bob Cywinsky¹](#), [Sue Kilcoyne¹](#)

⁽¹⁾*International Institute for Accelerator Applications, School of Applied Sciences, University of Huddersfield, Queensgate, Huddersfield W Yorks HD1 3DH, United Kingdom*

⁽²⁾*ASTEC, STFC Daresbury Laboratory, Kecwick Lane, Warrington Cheshire WA4 4AD, United Kingdom*

Medium energy ion scattering (MEIS) is an accelerator based, high depth resolution analytical technique for the characterization of ultra shallow surface layers, both in composition and structure. The UK national MEIS facility, previously located at the STFC Daresbury Laboratory, has served over 20 UK national and international research groups for over 15 years and produced a substantial research output. The facility which has a comprehensive experimental endstation incorporating LEED, Auger target heating, cleaning and evaporation, has now been reestablished at the IIAA in Huddersfield University where it has been equipped with a new accelerator and beamline that produces highly stable beams of 50-200 keV H^+ or He^+ ions.

The MEIS technique is based on the collection and analysis of highly resolved energy and angular spectra of H^+ or He^+ ions scattered off the surface and for crystalline substrates exploits the channeling and blocking phenomena. The unique information MEIS is able to provide on crystalline, metal, alloy, oxide and semi-conductor surfaces as well as amorphous nanolayers will be presented using selected examples from research conducted on the facility in the area of i) surface crystallography (adsorbed atom position, metal layer growth, surface layer expansion /contraction) and ii) high depth resolution profiling (shallow implants, disorder/reordering, high-k dielectric layer interdiffusion, atomic layer deposition film growth and shell enrichment of nano particles for catalysis). Its depth resolution near the surface is sub nm.

The new MEIS facility is now operational and open for collaborative research in existing and novel areas.

Abstract 487

[Regular Poster - Poster Sessions](#)

Formation of large cluster anions of Cu with a Cs-sputtering source

[Ran Chu](#)^{1,2}, [Shiyu Fan](#)^{1,2}, [Alfredo Galindo-Uribarri](#)^{1,2}, [Yuan Liu](#)², [Gerald Mills](#)², [Elisa Romero-Romero](#)^{1,2}

⁽¹⁾*Physics and Astronomy, University of Tennessee, Knoxville TN 37996, United States*

⁽²⁾*Physics Division, Oak Ridge National Laboratory, Oak Ridge TN 37831, United States*

Intense beams of Cu cluster negative ions have been observed with a cesium sputter negative ion source. The formation of large cluster anions in the Cs-sputter source is being investigated. Using different bombarding energies up to 8 keV, sputtered Cu cluster anions containing up to about 50 atoms have been obtained. The sputter targets were made of natural copper metal or powder. Mass analyses reveal that the Cu clusters comprise ^{63,65}Cu isotopes and the composition distributions of the two isotopes follow a binomial distribution of their corresponding natural abundances. We observed breaks in the Cu cluster anion intensity distributions at certain "magic numbers" and odd-even alternation with the odd clusters more abundant than the adjacent even clusters. The preliminary experimental results will be presented.

* Research sponsored by the Laboratory Directed Research and Development Program of Oak Ridge National Laboratory, managed by UT-Battelle, LLC, for the U. S. Department of Energy.

Abstract 46

[Invited Poster - Poster Sessions](#)

Computational Study of Integrated Neutron/Photon Imaging for Illicit Material Detection

[Jessica N. Hartman](#), [Alexander Barzilov](#)

Mechanical Engineering, University of Nevada, Las Vegas, 4505 S Maryland Parkway, Las Vegas Nevada 89154, United States

The feasibility of integration of photon and neutron radiography for nondestructive detection of illicit materials was examined. The MCNP5 code was used to model the radiography system consisting of accelerator-based neutron and photon sources and the imaging detector array, with the object under scrutiny placed between them. Transmission radiography computations were carried out using 2.5-MeV deuterium-deuterium and 14-MeV deuterium-tritium neutron sources, and a 0.3-MeV bremsstrahlung photon source. The radiography tallies for both neutron and photon sources were modeled for the same geometry of the system. For this examination, the objects consisted of a matrix of low-Z and high-Z materials of

various shapes and density. The photon to neutron transmission ratios were determined for each pixel of the detector array and utilized to identify the presence of specific materials in the recorded radiographic images. By focusing on the inherent difference between neutron and photon interactions, it was possible to determine the shape and material composition of complex objects present within a compartment such as a pallet or a shipping container. The use of a single imaging array of scintillation detectors for simultaneous measurements of fast neutrons and photons is discussed. Its function in the dual neutron/photon radiography applications is also addressed.

Abstract 371

[Invited Poster - Poster Sessions](#)

Intense Combined Source of Neutrons and Photons for Interrogation Based on Compact Deuteron RF Accelerator

[Sergey S Kurennoy](#), [Robert W Garnett](#), [Lawrence J Rybarcyk](#)

AOT Division, Los Alamos National Laboratory, PO Box 1663, MS H817, Los Alamos NM 87545, United States

Interrogation of special nuclear materials can benefit from mobile sources providing significant fluxes of neutrons (10^8 at 2.5 MeV, 10^{10} at 14.1 MeV) and of photons ($>10^{12}$ at 1-3 MeV). We propose a source that satisfies these requirements simultaneously plus also provides, via the reaction $^{11}\text{B}(\text{d},\text{n})^{12}\text{C}(\gamma_{15.1})$, a significant flux of 15-MeV photons, which are well penetrating and optimal for inducing photo-fission in actinides. The source is based on a compact (< 5 m) deuteron RF accelerator that delivers an average current of a few mA of deuterons at 3-4 MeV to a boron target and can be operated either in pulsed or continuous mode. The accelerator consists of a short RFQ followed by efficient IH structures with PMQ beam focusing [1], which fit perfectly for deuteron acceleration at low energies. Our estimates, based on recent measurements [2], indicate that the required fluxes of both neutrons and photons can be achieved at ~ 1 mA of 4-MeV deuterons. The goal is to confirm feasibility of the approach and develop requirements for future full-system implementation.

[1] S.S. Kurennoy et al. "H-mode accelerating structures with PMQ beam focusing." **Phys. Rev. ST Accel. Beams**, **15**, 090101 (2012).

[2] T.N. Taddeucci et al. "Neutron and gamma-ray production with low-energy beams." LA-UR-07-2724.

Abstract 494

[Regular Poster - Poster Sessions](#)

Triassico: A Sphere Manipulating Apparatus for IBA

[Barney L Doyle](#)¹, [Cristiano L Fontana](#)^{2,3}

⁽¹⁾*Sandia National Laboratories, Albuquerque, NM,, United States*

⁽²⁾*University of Padua, Padova, Italy*

⁽³⁾*INFN of Padua, Padova, Italy*

We propose here a novel technique to microscopically study the whole surface of millimeter sized spheres. The sphere dimensions can be from 1 mm; the upper limit is defined only by the power and by the mechanical characteristics of the motors used. Three motorized driving rods are arranged so an equilateral triangle is formed by the rod's axes, on such triangle the sphere sits. Movement is achieved by rotating the axes with precise relative speeds and by exploiting the friction between the sphere and the axes surfaces. The sphere can be held in place either by gravity or by an opposing trio of axes. By rotating the rods with specific relative angular velocities, a net torque can be exercised on the sphere that will rotate. No repositioning of the sphere or of the motors is needed to cover the full surface with the investigating tools. There are no fixed positions on the sphere so a continuous movement with no blind spots can be achieved. An algorithm, that takes into

account the kinematics constraints, was developed. The algorithm minimizes the number of rotations needed by the rods, in order to efficiently select a particular position on the sphere surface. The Triassico was initially developed for the National Ignition Facility, of the Lawrence Livermore National Laboratory (Livermore, California, USA), as a sphere manipulation apparatus for R&D of the DT inertial confinement fusion fuel spheres. Other applications span from samples orientation, ball bearing manufacturing, or jewelry.

Abstract 35

[Regular Poster - Poster Sessions](#)

Fundamentals of the layer-by-layer chemical analysis of heterogeneous samples by secondary ions energy-mass spectrometry method

[Nikolay N. Nikitenkov](#), [Olga V. Vilkhivskaya](#), [Alexsey N. Nikitenkov](#), [Vladimir S. Sypchenko](#)

Physical and Technical Institute, Tomsk Politechnical University, PhTI TPU, Lenin ave. 30, Tomsk 634050, Russia

Method SIMS has been developing now in the direction of research of the elements distributions on solid surfaces, improving of depth resolution in composition profiles of chemical elements, etc. This creates a more expensive experimental technique. However, we do not yet know the significant achievements in the direction of chemical analysis of near-surface layers by SIMS method. At the same time, in 1990th we fulfilled a cycle of research works for the usage of the secondary ions energy distributions (SIED) for a chemical analysis. You do not need expensive (pulsed) sources of primary ions and very expensive equipment registration of secondary ions. Results can be obtained with stationary (traditional) primary ion beam and secondary ion detectors. What makes installation much cheaper. Yet, the results of those research works have not gained a wide popularity in the Western hemisphere.

Generally, the following statements were determined concerning chemical analysis:

- The SIED X^+ from heterogeneous targets under certain experimental requirements are the linear superposition of SIED X^+ from separate homogeneities (components) as independent targets (X - chemical element containing all components of a heterogeneous target);
- Target components are manifested in SIED in the form of separate singularities (peaks, plateau) at certain energies and kinds of primary ions, angles of incidence of a primary beam and angles of take off of the secondary ions;
- Energies at which these singularities are placed in SIED are proportional to Gibb's energies of corresponding components.

Depth distributions of chemical compositions have been explored on the following multiphase targets: cobalt at phase transition temperature; oxides on indium and zinc, complex systems such as $\text{In}_x\text{As}_y\text{O}_z/\text{InAs}$, InP/GaAs , $\text{Au}/\text{V}/\text{GaAs}$.

Abstract 291

[Regular Poster - Poster Sessions](#)

Temperature dependence on vapor and hydrogen absorption characteristics of lithium-zirconium-oxide ceramics

[Bun Tsuchiya](#)¹, [Shunji Bandow](#)², [Shinji Nagata](#)³, [Kazutoshi Tokunaga](#)⁴, [Kenji Morita](#)⁵

⁽¹⁾Department of General Education, Faculty of Science and Technology, Meijo University, 1-501, Shiogamaguchi, Tempaku-ku, , Nagoya 468-8502, Japan

⁽²⁾Department of Applied Chemistry, Meijo University, 1-501, Shiogamaguchi, Tempaku-ku, , Nagoya 468-8502, Japan

⁽³⁾Institute for Materials Research, Tohoku University, 2-1-1, Katahira, Aoba-ku, Sendai 980-8577, Japan

⁽⁴⁾Research Institute for Applied Mechanics, Kyushu University, 6-1, Kasugai-park, Kasugai 816-8580, Japan

⁽⁵⁾Department of Research, Nagoya Industrial Research Institute, Noa Yotsuya Bld. 2F, 1-13, Yotsuya-tori, Chikusa-ku, Nagoya 464-8019, Japan

Various technologies for production and storage of H₂ gas have been developed in different ways. For hydrogen storage materials provided with a hydrogen fuel cell used in automobiles, absorption of H₂ gas at room temperature and re-emission of it as H₂ gas at temperatures lower than 423 K, as well as storage capacity higher than 5 wt.% are required.

So far, we have found that composite materials of platinum (Pt) and lithium-zirconium-oxide (Li₂ZrO₃) possess excellent properties on playing both roles as hydrogen-storage and production. However, the each mechanism on absorbing H⁺ ions due to splitting of H₂O adsorbed at the surface, trapping H atoms into some sites, and creating H₂ molecule from the bulk has not been clarified yet.

Our aim in this study is to investigate the dependence of hydrogen absorption and emission characteristics of Li₂ZrO₃ without the catalysis of Pt for the water splitting on temperature, exposed to normal air at room temperature and Ar gas atmospheres including water at various temperatures up to 523 K, using elastic recoil detection (ERD), Rutherford backscattering spectroscopy (RBS), weight gain measurement (WGM) by means of electric balance and thermo gravimetry (TG), and thermal desorption spectroscopy (TDS).

As the results, the WGM showed that the weight gain increased linearly with an increase in the exposure time up to approximately 50 hrs. The weight gain of approximately 2.0 wt.% at 140 hrs kept up to annealing temperature of 413 K, while decreased gradually with an increase in the temperature between 413-523 K. In addition, it was found by combining ERD with RBS techniques that the Li₂ZrO₃ absorbed H at the surface from H₂O vapor, store it in them, and emit 80 % of it as H₂O and H₂ gases resulting in the TDS analysis, when heated at 373 K for 10 min.

Abstract 303

[Regular Poster - Poster Sessions](#)

Comparison of thicknesses of deposited copper thin films on silicon substrate using thin film monitor, profilometer and Rutherford backscattering spectroscopy.

[Gyanendra Bohara](#), [Jack Manuel](#), [Szabolcs Szilasi](#), [Gary Glass](#)

Physics, IBML, University of North Texas, Physics Building Rm 110, 210 Avenue A Denton, TX 76203-1427, Denton TX 76203, United States

Since many years, several efforts have been applied to develop reliable measurement techniques. Among them, three different techniques implemented to measure the thin film thicknesses are briefly discussed in this work. The thicknesses of the copper layers (250 Å to 500 Å) on n-Si (111) wafers have been measured using thin film monitor, optical profilometer and Rutherford backscattering spectroscopy. Cu thin films were prepared on n-Si(111) wafers using thermal evaporation method under the vacuum of 10⁻⁶ Torr and their thicknesses estimated by this method were compared with the thicknesses measured with profilometer and Rutherford backscattering spectroscopy. In this work we see to what extent these measurements agree to each other.

Abstract 471

[Regular Poster - Poster Sessions](#)

Establishment of an ASEAN ion beam analysis center at Chiang Mai University for novel materials analysis

[U. Tippawan](#)¹, [T. Kamwann](#)², [L. D. Yu](#)^{1,3}, [S. Intarasiri](#)⁴, [N. Puttaraksa](#)⁵, [S. Unai](#)⁶, [C. Thongleurm](#)⁴, [K. Won-in](#)⁷, [P. Dararutana](#)⁸, [S. Singkarat](#)^{1,3}

⁽¹⁾Physics and Materials Science, Chiang Mai University, Chiang Mai University, Chiang Mai 50200, Thailand

⁽²⁾Physics, Khon Kaen University, Khon Kaen University, Khon Kaen 40002, Thailand

⁽³⁾Thailand Center of Excellence in Physics, Commission on Higher Education, 328 Si Ayutthaya Road, Bangkok 10400, Thailand

⁽⁴⁾Science and Technology Research Institute, Chiang Mai University, Chiang Mai University, Chiang Mai 50200, Thailand

⁽⁵⁾Atomic Physics Laboratory, RIKEN, 2-1 Hirosawa, Wako, Saitama 351-0198, Japan

⁽⁶⁾Physics, University of Phayao, University of Phayao, Phayao 56000, Thailand

⁽⁷⁾Earth Science, Kasetsart University, Kasetsart University, Bangkok 10900, Thailand

⁽⁸⁾Chemistry, Royal Thai Army, The Royal Thai Army Chemical Department, Bangkok 10900, Thailand

A comprehensive ion beam analysis center uniquely in the ASEAN (Association of Southeast Asian Nations) region has been established at Chiang Mai University, Thailand. The center is equipped with a 1.7-MV Tandetron tandem accelerator with an ion beam analysis beam line. The Tandetron accelerator employs two ion sources, a duoplasmatron ion source and a sputter ion source, capable of producing analyzing ion beams of light species such as hydrogen and helium and heavy species. The beam line is currently able to perform ion beam analysis techniques such as Rutherford Backscattering Spectrometry (RBS), RBS/channeling, Elastic BackScattering (EBS), Particle Induced X-ray Emission (PIXE) and Ionoluminescence (IL) with assistance of commercial and in-house-developed softwares. Micro ion beam for MeV-ion mapping using inexpensive programmable aperture or capillary focusing techniques is being developed. Ion beam analysis experiments and applications have been vigorously developed, especially for novel materials analysis focused on archeological, gemological and biological materials besides other conventional materials. The paper reports all relevant technical details and application examples, demonstrating complex technology establishment in a developing country.

Abstract 286

[Invited Poster - Poster Sessions](#)

Thermoelectric Properties of Zn₄Sb₃ and ZrNiSn Thin Films Affected by MeV Si ion-beam

[S. Budak](#)¹, [S. Guner](#)², [C. I. Muntele](#)³, [D. ILA](#)⁴

⁽¹⁾Electrical Engineering & Computer Science, Alabama A&M University, Normal AL, United States

⁽²⁾Department of Physics, Fatih University, B. Cekmece Istanbul, Turkey

⁽³⁾Cygnus Scientific Services, Huntsville AL, United States

⁽⁴⁾Department of Physics, Fayetteville St. University, Fayetteville NC, United States

High-purity solid zinc and antimony were evaporated by electron beam to grow the β -Zn₄Sb₃ thin film while high-purity zirconium powder and nickel tin powders were evaporated by electron beam to grow the ZrNiSn-based half-Heusler compound thin film. Rutherford backscattering spectrometry (RBS) was used to analyze the composition of the thin films. The deposited thin films were introduced to 5 MeV Si ions bombardments for forming nanostructures in the thin films. The nanostructures produced by MeV ion beam can cause significant change in both the electrical and the thermal conductivity of thin films, thereby improving the efficiency. We used the 3 ω -method (3rd harmonic) measurement system to measure the cross-plane thermal conductivity, the Van der Pauw measurement system to measure the electrical conductivity, and the Seebeck-coefficient measurement system to measure the cross-plane Seebeck coefficient.

Research sponsored by the Center for Irradiation of Materials (CIM), National Science Foundation under NSF-EPSCOR R-II-3 Grant No. EPS-1158862, DOD under Nanotechnology Infrastructure Development for Education and Research through the Army Research Office # W911 NF-08-1-0425, and DOD Army Research Office # W911 NF-12-1-0063 and National Nuclear Security Admin (DOE/NNSA/MB-40) with grant# DE-NA0001896, NSF-REU with Award#1156137.

Effects of MeV Si Ions and Thermal Annealing on Thermoelectric and Optical Properties of SiO₂/SiO₂+Ge Multi-Nanolayer Thin Films

[S. Budak](#)¹, [J. Cole](#)¹, [B. Allen](#)¹, [M. A. Alim](#)¹, [S. Bhattacharjee](#)², [S. Yang](#)¹, [R. B. Johnson](#)³, [C. Muntele](#)⁴

⁽¹⁾Department of Electrical Engineering & Computer Science, Alabama A&M University, Normal AL 35762, United States

⁽²⁾Department of Mechanical and Civil Engineering, Alabama A&M University, Normal AL 35762, United States

⁽³⁾Department of Physics, Alabama A&M University, Normal AL 35762, United States

⁽⁴⁾Cygnus Scientific Services, Cygnus Scientific Services, Huntsville AL 35815, United States

Thermoelectric generator devices have been prepared from 200 alternating layers of SiO₂/SiO₂+Ge superlattice films using Magnetron DC/RF Sputtering. Rutherford Backscattering Spectrometry (RBS) and RUMP simulation software package were used to determine the stoichiometry of Si and Ge in the grown multilayer films and the thickness of the grown multilayer films. SEM and EDS have been used to analyze the surface and composition of the thin films. The 5 MeV Si ion bombardments have been performed using the AAMU Pelletron ion beam accelerator to make quantum clusters in the multi-layer superlattice thin films to decrease the cross plane thermal conductivity, increase the cross plane Seebeck coefficient and increase the cross plane electrical conductivity to increase the figure of merit. The fabricated devices have been annealed at the different temperatures to tailor the thermoelectric and optical properties of the superlattice thin film systems. Impedance spectroscopy has been used to characterize the multi-junction thermoelectric devices. We will be presenting our findings for the thermoelectric and the optical properties of the multilayered SiO₂/SiO₂+Ge thin film systems.

Research sponsored by the Center for Irradiation of Materials (CIM), National Science Foundation under NSF-EPSCOR R-II-3 Grant No. EPS-1158862, DOD under Nanotechnology Infrastructure Development for Education and Research through the Army Research Office # W911 NF-08-1-0425, and DOD Army Research Office # W911 NF-12-1-0063 and National Nuclear Security Admin (DOE/NNSA/MB-40) with grant# DE-NA0001896, NSF-REU with Award#1156137.

Surface enhanced Raman substrates fabricated by gold ion implantation in quartz

[Yanzhi He](#)¹, [Iram Saleem](#)¹, [Yang Li](#)², [Jiming Bao](#)², [Epie Emmanuel Njumbe](#)¹, [Buddhi Tilakaratne](#)¹, [Dharshana Nayanajith Wijesundera](#)¹, [Wei-Kan Chu](#)¹

⁽¹⁾Physics and Texas Center for Superconductivity, University of Houston, 4800 Calhoun Rd, Houston TX 77004, United States

⁽²⁾Dept. of Electrical & Computer Engineering, University of Houston, 4800 Calhoun Rd, Houston TX 77004, United States

We have successfully fabricated substrates for surface enhanced Raman spectroscopy (SERS) by means of gold ion implantation in quartz. The implantation dose and dose rate are chosen such that the implanted concentration of gold in quartz exceeds the solid solubility promoting the formation of gold nano particles embedded, and immobilized in quartz. In this work, we show that these gold-nanoparticle embedded quartz substrates are effective in surface Raman enhancement.

Delayed Gamma-ray Spectroscopy for Non-destructive Assay of Nuclear Materials

[Bernhard A Ludewigt¹](#), [Vladimir Mozin²](#), [Alan W Hunt³](#), [Edward T.E. Reedy³](#), [Luke Campbell⁴](#),
[Andrea Favalli⁵](#)

⁽¹⁾Lawrence Berkeley National Laboratory, Berkeley CA 94720, United States

⁽²⁾Lawrence Livermore National Laboratory, Livermore CA 94550, United States

⁽³⁾Idaho State University, Pocatello ID 83209, United States

⁽⁴⁾Pacific Northwest National Laboratory, Richland WA 99354, United States

⁽⁵⁾Los Alamos National Laboratory, Los Alamos NM 87545, United States

High-energy, beta-delayed gamma-ray spectroscopy is being studied as a technique for the non-destructive assay of nuclear materials at key stages of the fuel cycle, including spent fuel assemblies, and for addressing challenges in homeland security applications. Following neutron irradiation and the collection of delayed gamma-ray spectra, the contributions from different fissionable isotopes, such as U-235, Pu-239, Pu-241, and U-238 in spent nuclear fuel, can be determined by spectral component analysis if the delayed gamma-ray responses of the individual isotopes are accurately known. A series of experimental measurements were performed at the Idaho Accelerator Center (IAC) using a photo-neutron source driven by a pulsed S-band radiofrequency linac to irradiate U-235, Pu-239, U-238 and combined U-235/Pu-239 targets. Gamma-ray spectra were collected for different irradiation/detection time patterns that emphasized delayed gamma-ray lines from fission fragments with different half-lives. Comparisons of measured data with calculations based on nuclear data libraries showed significant discrepancies. Algorithms and methods for quantifying isotopic ratios have been tested on the measured combined U-235/Pu-239 target data. An initial analysis suggests that cycles with irradiation and detection times of around 100 seconds may be optimal for delayed gamma-ray assays.

*This work was supported by the U.S. Department of Energy, NNSA, Office of Nonproliferation and Verification Research & Development.

Abstract 365

[Regular Poster - Poster Sessions](#)

A Method to Measure Prompt Gamma-Ray Production Cross Sections Using a 14.1 MeV Associated Particle Neutron Generator.

[Haoyu Wang](#), [David Koltick](#)

Department of Physics and Astronomy, Purdue University, 525 Northwestern Ave, WEST LAFAYETTE IN 47907, United States

Knowledge of gamma-ray production rates is important in many elemental analysis applications using active neutron interrogation techniques. However, past measurements are limited to a single fixed angle having small solid angle coverage. The production is then extrapolated to the full solid angle assuming a uniform angular distribution. Even so past measurements are dominated by high backgrounds and overlapping gamma-ray signals having nearby energy. Reported cross sections can vary by a factor of ~4. In order to improve our knowledge of elemental cross sections, we have constructed a spectrometer using an associated particle neutron generator and an array of 12 NaI detectors each 14 cm square by 16.5 cm deep. The array covers ~30% of the solid angle, extending to within ~35 degrees of the entering and exiting electronically collimated neutron beam, on a circular shell ~21 cm in radius from the target. The major improvements in these measurements come from the 3.0 nanosecond coincident timing required between the prompt gamma-ray detection and the associated alpha particle produced simultaneously with the neutron, and the electronically restricted neutron aperture generated by the required alpha particle detection. The timing requirement greatly reduces the detectors exposure to background. To illustrate the improvements using this technique we present first measurements of the 846.8 keV and the 1238.3 keV prompt gamma-ray cross sections from Fe-56.

Abstract 84

[Regular Poster - Poster Sessions](#)

Neutron Time-of-Flight Measurements; Comparison with Monte Carlo Simulations at the Idaho Accelerator Center

[Frank Harmon](#), [Heather Seipel](#), [Mayir Mamtimin](#)

Idaho Accelerator Center, Idaho State University, 1500 Alvin Ricken Drive, Pocatello ID 83201, United States

In recent years, research and development at the Idaho Accelerator Center has been conducted on intense photon/neutron production facilities and their application in photon activation analysis, isotope production, national security needs and various nuclear fuel cycle investigations. As an example technical feasibility studies of mixed-field photon/neutron transmutation of certain fission products have been carried out.

In this work it is important to estimate the energy spectrum of radiation fields. Foil activation methods have been used to estimate the flux and energy distributions of photon and neutron field. It is well known that activation foils give only crude estimates of neutron energy distributions. Much better information can be gleaned from properly conducted neutron time-of-flight (nTOF) measurements. In the work reported here a TOF system which was originally developed is used along with the IAC Fast Pulse Linac to measure the neutron energy spectrum emitted from a 40 MeV electron beam driven neutron converter. An evaporation spectrum, similar to a fast fission spectrum, is obtained.

In this paper, experimental setup including electron beam parameters, shielding and detector layout will be discussed. Detailed computer simulations of the same setup are compared to experimental results. Experimental limitations on detectable neutron energies and detector efficiency will be addressed.

Abstract 86

[Regular Poster - Poster Sessions](#)

Numerical Simulation of a multicusp ion source for high current H⁻ Cyclotron at RISP

[J.H. Kim](#)¹, [S.G. Hong](#)^{1,2}, [J.W. Kim](#)¹

⁽¹⁾Rare Isotope Science Project, Institute for Basic Science, 70 Yuseong-daero 1689-gil, Yuseong-gu, Daejeon 305-811, Korea

⁽²⁾Physics, HanNam University, Daejeon 306-791, Korea

The rare isotope science project (RISP) has been launched at 2011 to support a wide range of science programs in nuclear, material, and bio-medical sciences as well as interdisciplinary programs. The production of rare isotope beams at RISP is currently configuring the scheme of employing both In-flight Fragmentation (IF) and the Isotope Separator On-Line (ISOL) method, which is incorporated with a 70 MeV H⁻ cyclotron. The cyclotron will deliver 70 kW beam power to the ISOL targets, where rare isotope beams are generated and re-accelerated by post linear accelerators.

A multicusp ion source used widely in negative hydrogen cyclotrons is designed to have cusp geometries of magnetic field inside plasma chamber, where ions are confining and their mean lifetimes increase. The magnetic confinement produced a number of permanent magnetic poles helps to increase beam currents and reduce the emittance. In this work a numerical simulation is carried to understand the effect of magnetic fields and a number of poles on the plasma structure using the SIMION code. The electron confinement effect becomes stronger and the density increases with increasing the number of poles.

Abstract 127

[Regular Poster - Poster Sessions](#)

Metastability of tetragonal zirconia nanoparticle by Sol-Gel-Derived method coupling with carbon irradiation

[R. T. Huang](#)¹, [C. L. Lee](#)¹, [H. Niu](#)², [Y. C. Yu](#)³

⁽¹⁾*Institute of Materials Engineering, National Taiwan Ocean University, Keelung 20224, Taiwan*

⁽²⁾*Nuclear Science and Technology Development Center, National Tsing Hua University, Hsinchu 30013, Taiwan*

⁽³⁾*Institute of Physics, Academia Sinica, Taipei 11529, Taiwan*

Zirconia has become one of the most important ceramic material for several decades because of its superior physical and electrical properties, high ionic conductivity, excellent chemical durability, and low thermal conductivity in a wide range of industrial application. Moreover, zirconia polymorphs also demonstrate excellent radiation tolerance that could be effectively utilized for nuclear applications, such that they have been suggested as a promising parent material to be used as fuel matrix in nuclear reactors. However, zirconia exhibits three crystallographic polymorphs as a function of temperature at normal atmospheric pressure, which greatly affect the physical and mechanical properties of zirconia utilized as fuel or parent material for nuclear applications. In this study, the research aims to investigate the metastability of tetragonal zirconia ($t\text{-ZrO}_2$) synthesized by the sol-gel method coupling with carbon irradiation, wherein zirconium (IV) n-propoxide and hydroxypropyl cellulose polymer were used to be a precursor and a steric stabilizer, respectively, and these two were compounded in an alcohol solution, followed by drying and calcining. Next, carbon irradiation was also used to try doping the dried zirconia powders which was subsequently calcined in high vacuum. The calcined specimens were examined by x-ray diffractometer and electron microscope to study the evolution of particle sizes, variance of morphologies, and behavior of phase transformation for the synthesized ZrO_2 powders with and without the dopant of carbon calcined separately in high vacuum. Consequentially, a great deal of non-aggregation and submicron size $t\text{-ZrO}_2$ particles (400~600 nm) with sphere and uniform size can be attained when the ratio of molar concentration of water and precursor is equal to 5. Furthermore, the resultant particle, with fluences above 1×10^{16} ions/cm² by using 150 keV carbon ions implantation, appeared a strong aggregation phenomenon, and the size approached to micron scale with t -phase after calcination at the temperature up to 1100°C.

Abstract 372

[Regular Poster - Poster Sessions](#)

Coloration of Lithium Hydride with Alpha Particle Radiation (U)

[Rachel Strickland](#)², [Carol Haertling](#)¹, [Joseph Tesmer](#)¹, [Yongqiang Wang](#)¹

⁽¹⁾*Material Science & Technology, Los Alamos National Laboratory, M/S G770, Los Alamos NM 87545, United States*

⁽²⁾*Conventional Material Science, Aldermaston Weapons Establishment, M/S G770, Aldermaston Reading RG7 4PR, United Kingdom*

Lithium hydride is a solid that has been noted for its color variability, along with its susceptibility to changing colors when irradiated with various radiation sources and energies. We have performed experiments to determine some effects of a radiolysis on LiH. We have used an accelerator in the Ion Beam Materials Laboratory to produce alpha particle doses in LiH at desired energies that are equivalent to decades of exposure from an actinide source near the surface. Color changes that occurred during alpha irradiation were quantified with a spectrophotometer and related to evolved gases, particularly H₂, measured by mass spectrometry. Our data allows prediction of concentrations that could be released over long periods of time in sealed environments.

Abstract 389

[Regular Poster - Poster Sessions](#)

Heavy and light ion irradiation damage effects on delta-phase Sc₄Hf₃O₁₂

[Juan Wen](#)^{1,2}, [Yuhong Li](#)¹, [Ming Tang](#)², [James Valdez](#)², [Yongqiang Wang](#)², [Maulik Patel](#)³, [Kurt Sickafus](#)³

⁽¹⁾*School of Nuclear Science and Technology, Lanzhou University, Lanzhou Gansu 730000, China*

⁽²⁾Materials Science and Technology Division, Los Alamos National Laboratory, Los Alamos New Mexico 87545, United States

⁽³⁾Department of Materials Science and Engineering, University of Tennessee, Knoxville Tennessee 37996, United States

Polycrystalline delta-phase $\text{Sc}_4\text{Hf}_3\text{O}_{12}$ was irradiated with light and heavy ions at room temperature, in order to examine the radiation stability of this compound. The light ion irradiation was performed with 400 keV Ne^{2+} ions to fluences ranging from 1×10^{14} to 1×10^{15} ions/cm², while the heavy ion irradiation was performed with 600 keV Kr^{2+} ions to fluences ranging from 5×10^{14} to 5×10^{15} ions/cm². Irradiated samples were characterized using grazing incidence X-ray diffraction (GIXRD) technique. A complete phase transformation from ordered rhombohedral to disordered fluorite was observed by a fluence of 1×10^{15} ions/cm² with 400 keV Ne^{2+} ions, equivalent to a peak ballistic damage dose of ~ 0.33 displacements per atom (dpa). Meanwhile, the same transformation was also observed by 600 keV Kr^{2+} ions at the same nominal fluence of 1×10^{15} ions/cm², which however corresponds to a peak ballistic damage of ~ 2.2 dpa. There is no radiation induced amorphization observed in this compound up to the highest fluence (equal to a damage dose of 10 dpa) in this study. Experimental results show that light ions are more efficient than heavy ions in producing the retained defects that are presumably responsible for the observed O-D transformation in structure. To better quantify the mechanism of the transformation, the effect of cation antisite-pair defect and anion oxygen Frenkel defect on the O-D phase transformation was considered. Our calculated results appear to support the speculation that the O-D phase transformation in delta-phase $\text{Sc}_4\text{Hf}_3\text{O}_{12}$ is likely caused by anion oxygen Frenkel defects.

Abstract 63

[Regular Poster - Poster Sessions](#)

Particle Diffusion along Magnetic Null Lines as Sputter or Antiproton Source

[Ryan A Lane](#), [Carlos A Ordonez](#)

Physics Department, University of North Texas, 1155 Union Circle #311427, Denton Texas 76203-5017, United States

Particle transport along null magnetic lines is investigated using classical trajectory Monte Carlo simulations and described as a traveling wave and through diffusion equations. A magnetic null line is defined as a one-dimensional region where the magnetic field magnitude is zero. This region may take any shape in three-dimensional space. The field used in the simulations is generated by two infinite wires of negligible thickness carrying identical current and separated by a small distance. Thus, an infinite magnetic null line exists directly between the wires. The particle trajectories are simulated by solving the equations of motion for each simulated particle of a mono-energetic set. Each is considered individually, with all trajectories starting from the same position along the null line. Each trajectory is simulated until it reaches a specified distance from the initial point or a maximum time elapses. The simulation is repeated using a full set for multiple endpoints and maximum times for ten different amounts of current in the wires. Each current value is selected so that no particles can travel more than seven times the distance between the wires from the null line. The fraction of particles that reach the endpoint in a given time is calculated and used to describe particle transport parallel to the null line. The results are given in normalized, dimensionless units and their applications as an antihydrogen source and use in ultra-high purity sputter are discussed. The results are used to find the conditions necessary to obtain a steady and uniform particle flux suitable for ultra-high purity sputter; assuming that plasma is generated near the null line. This material is based upon work supported by the Department of Energy under Grant No. DE-FG02-06ER54883 and by the National Science Foundation under Grant No. PHY-1202428.

Abstract 68

[Regular Poster - Poster Sessions](#)

Artificially Structured Boundary as a Charged Particle Beam Deflector Shield

[Ryan M. Hedlof](#), [Carlos A. Ordonez](#)

Department of Physics, The University of North Texas, 1155 Union Circle #311427, Denton Texas 76203-5017, United States

A classical trajectory Monte Carlo simulation is used to study the possibility of using a planar artificially structured boundary as a charged particle beam deflector shield. The artificially structured boundary (ASB) creates a spatially periodic

magnetostatic field by utilizing a planar array of permanent disk magnets with like poles facing out. A mono-energetic beam of charged particles is incident on the ASB, and the conditions under which charged particles penetrate through the array are determined. This material is based upon work supported by the Department of Energy under Grant No. DE-FG02-06ER54883 and by the National Science Foundation under Grant No. PHY-1202428.

Abstract 105

[Regular Poster - Poster Sessions](#)

PIXE Determination of the Stoichiometry of Ni-Pd and Au-Ag Nano-Particles Prepared by Laser Ablation in Liquid Solution

[M. Roumie¹](#), [R. Mahfouz²](#), [B. Nsouli¹](#), [F.G. Cadete Santos Aires²](#), [J.C. Bertolini²](#)

⁽¹⁾Accelerator Laboratory, Lebanese Atomic Energy Commission, Lebanese CNRS, Airport Road, P.O. Box 118281, Beirut, Lebanon

⁽²⁾IRCELYON, Institut de Recherches sur la Catalyse et l'Environnement de Lyon., CNRS/Universite Lyon 1, 2 Av. A. Einstein, 69626 Villeurbanne cedex, Lyon, France

Synthesized colloidal nanoparticles were prepared by laser ablation in liquids using YAG laser focused on bimetallic targets ($\text{Au}_{75}\text{Ag}_{25}$, $\text{Ni}_{75}\text{Pd}_{25}$ and $\text{Ni}_{95}\text{Pd}_5$). The size and size distribution of the obtained particles in the solution was checked by TEM. The stoichiometric ratio of the particles was determined using ICP, EDX and PIXE, where the obtained results were comparable except for ICP. The PIXE determination of the stoichiometry of Au-Ag nanoparticles showed a composition similar to the target. However, for Ni-Pd, the composition approaches the nominal composition of the target at higher ablation times. PIXE succeed to demonstrate a linear trend of the Ni/Pd stoichiometric ratio vs. time of ablation. The quantification of PIXE composition was done using GUPIX code, using thin film and multilayer approaches.

Abstract 151

[Regular Poster - Poster Sessions](#)

PIXE Analysis of Powder and Liquid Uranium-Bearing Samples

[Oleksandr Buhay](#), [Aram Khachatrian](#), [Volodymyr Storizhko](#)

Department of Nuclear Researches, Institute of Applied Physics, 58, Petropavlivska Str., Sumy 40000, Ukraine

Prevention of illegal traffic of nuclear and radioactive materials (NRM) is one of the key objectives in counterterrorism. Nuclear forensics is an efficient instrument for an advanced monitoring of nuclear and radioactive materials. The main purpose of nuclear forensics is tracing the origin of nuclear and radioactive materials found out beyond the regular monitoring. One of the techniques used for NRM characterization is the PIXE technique allowing proper non-destructive characterization of elemental composition of solid and liquid samples.

We have developed the PIXE analytical technique for powder and liquid uranium-bearing materials. Samples of powdered materials were prepared by moulding the material in aluminium capsules. Graphite powder (5 wt % of a sample mass) was previously added into the sample to improve sample conductivity.

Liquid sample preparation was carried through transformation liquids into solids by mixing some drops of liquid with graphite powder. Yttrium nitrate was also added into a ready-made mixture as an internal standard. The sample was dried. Then the sample was glued onto a copper substrate or moulded to an aluminium capsule, as required by quantity of a substance sampled.

All samples were PIXE analyzed in two stages. At the first stage a 50 μm polyethylene film was used as an X-ray absorber. The task of this stage was to identify the matrix composition. At the second stage an aluminium foil was used as a 40 μm X-ray absorber. The task of the second stage was to determine concentration of heavy elements.

Both spectra were simultaneously processed in the GUPIX software so that agreed results could be obtained. Both the fundamental parameter method and the internal standard method were applied to define the results of quantitative analysis more precisely.

The work is done under the STCU Project P465 »Study of Attribution Signatures of Various Uranium Bearing Materials

Abstract 193

[Regular Poster - Poster Sessions](#)

Analysis of Atmospheric Aerosols Collected in an Urban Area in Upstate NY Using Proton Induced X-ray Emission (PIXE) Spectroscopy

[Jeremy W Smith](#), [Scott M LaBrake](#), [Michael F Vineyard](#), [Salina F Ali](#), [Benjamin J Nadareski](#),
[Alexandrea D Safiq](#), [Joshua T Yoskowitz](#)

Physics and Astronomy, Union College, 807 Union Street, Schenectady NY 12308, United States

We have performed a PIXE analysis of atmospheric aerosol samples collected in Schenectady, NY, to study airborne pollution in an urban environment. The samples were collected using a PIXE International, 9-stage, cascade impactor that separates the airborne particles according to aerodynamic diameter and deposits them on thin Kapton foils. The impacted foils were bombarded with 2.2-MeV proton beams from the Union College 1.1-MV Pelletron accelerator and the emitted X-rays were detected with an Amptek silicon drift detector. The X-ray energy spectra were analyzed using GUPIX software to determine the elemental concentrations in the samples. A broad range of elements from Al to Pb were identified and measurable concentrations of Br and Pb were detected at small particle sizes. The measured Br/Pb ratio of 0.37 ± 0.09 is consistent with results from previous studies and suggests the presence of leaded aviation fuel that may be due to the proximity of the collection site to a small regional airport with a significant amount of general aviation traffic. Data taken during the summer of 2013 through the winter of 2014 to study seasonal variations will be presented.

Abstract 459

[Invited Poster - Poster Sessions](#)

Influence of ions species on radiation damage of metal/oxide (Cr/MgO) interface

[sandeep manandhar](#)^{1,2}, [Kumar Subramaniyam](#)², [Tiffany Kaspar](#)³, [Vaithiyalingam Shutthanandan](#)²

⁽¹⁾Department of Materials Science and Engineering, University of Washington, 302 Roberts Hall, Seattle WA 98195, United States

⁽²⁾EMSL, Pacific Northwest National Laboratory, 3335 Innovation Blvd, Richland WA 99354, United States

⁽³⁾FCSD, Pacific Northwest National Laboratory, 3335 Innovation Blvd, Richland WA 99354, United States

Within recent findings and future research of nuclear energy it has been a relevant requirement for next generation nuclear plants to have new structural materials that can withstand environmental heat up to 1000 °C and doses of hundreds of displacements per atom (dpa) in radiation. In previous work, we have shown that the gold radiation up to 150 dpa did not alter the interface of Cr-MgO single crystal. In this work, the objective is to study the influence of incident ion species on radiation damage of Cr-MgO single crystal interface. Ion radiation experiments have been performed on these films using 0.5 MeV Oxygen ions and 1 MeV Silicon ions. The level of irradiation damage was analyzed *in situ* by Rutherford Backscattering Spectrometry. The results indicated the damage levels are very low at the interfaces and are also independent of choice of ions. Also, the surface damage shows a strong dependence on the mass of the incident ions.

TEM and Raman Study of GeMn Recrystallized by Helium IBIEC[ChienHsu Chen](#)^{1,2}, [Huan Niu](#)¹, [C.P. Lee](#)²⁽¹⁾*Nuclear Science and Technology Development Center, National Tsing Hua University, No. 101, Section 2, Kuang-Fu Road, HsinChu 30013, Taiwan*⁽²⁾*Center for Nano Science and Technology, National Chiao Tung University, No. 1001, University Road, HsinChu 30010, Taiwan*

Mn ions were implanted into Ge substrates at room temperature. Post-annealing was performed using 2MeV He⁺ ion irradiation at a temperature below 500K. The structures of the samples were characterized by Raman scattering and high-resolution transmission electron microscopy before and after ion beam annealing. In this study, we found the Mn⁺ implanted Ge layer had been epitaxially re-grown without formation of 2nd phase. In addition, we found Raman scattering spectrum is useful tool to observe the recrystallization mechanism of GeMn thin film caused by Helium IBIEC.

In-Situ SEM Characterization of Irradiated Stainless Steel[Amanda Lupinacci](#)², [Ashley Reichardt](#)¹, [Zhijie Jiao](#)³, [Peter Chou](#)⁴, [Andrew Minor](#)², [Peter Hosemann](#)¹⁽¹⁾*Nuclear Engineering, UC Berkeley, 4155 Etchevary Hall MC 1730, Berkeley CA 94720, United States*⁽²⁾*Materials Science & Engineering, UC Berkeley, 210 Hearst Mining Building, Berkeley CA 94720, United States*⁽³⁾*Nuclear Engineering, University of Michigan, 2355 Bonisteel Blvd, Ann Arbor MI 48109, United States*⁽⁴⁾*Electric Power Research Institute, 3420 Hillview Ave, Palo Alto CA 94304, United States*

It is the objective of this study to evaluate irradiation induced hardening in 304 SS and radiation induced segregation phenomena on a localized scale. Ion beam irradiation was conducted in an attempt to mimic neutron radiation without activating the steel specimen and making them accessible to fast turn around examination.

Due to the limited penetration depth of ion beams, small scale testing methods such as nanoindentation and microcompression testing are the only practical methods to evaluate the mechanical behavior of the ion-beam irradiated materials. Small scale testing is critical in delivering a comprehensive image of the effect of the microstructural evolution on the mechanical properties of ion beam irradiated Light Water Reactor (LWR) austenitic stainless steels. This testing method enables us to test separately the contribution of both the ion beam irradiation and the subsequent annealing to the mechanical properties. In addition, characterization techniques such as Transmission Electron Microscopy (TEM) and Electron Backscattered Diffraction (EBSD) were utilized to adequately characterize the microstructure that resulted from mechanical testing.

Application of Wavelet Unfolding Technique in Neutron Spectroscopic Analysis[Jessica N. Hartman](#), [Alexander Barzilov](#)*Mechanical Engineering, University of Nevada, Las Vegas, 4505 S Maryland Parkway, Las Vegas Nevada 89154, United States*

Nonproliferation of nuclear materials is important in nuclear power industry and fuel cycle facilities. It requires technologies capable of quickly and efficiently measuring and assessing the radiation signatures of fission events. Neutrons produced in spontaneous or induced fission reactions are mainly fast. The neutron energy information allows characterization of nuclear materials and neutron sources. It can also be applied in remote sensing and source search tasks. The plastic scintillator EJ-299-33A was studied as a fast neutron detector. Since the detector output is the superposition of single-energy response functions of all neutrons entering the scintillator volume, the response to a polyenergetic flux can be unfolded to produce the neutron spectrum. A quick unfolding technique requires a reduction of the number of computer operations performed. This suggests the use of a few variables comparing to hundreds or thousands of data points of the response function. Through the application of wavelets, the number of variables can be limited to only two. The multiple linear regression method yields the intensities of neutron flux of particular energy, hence, enabling the spectroscopic analysis. The wavelet technique was evaluated for the unfolding of neutron spectrum using the scintillator's response functions between 1 MeV and 14 MeV computed with the MCNPX code. Computational results have indicated the wavelet-based spectrum unfolding method is feasible for use in a scintillator detector with neutron / photon pulse shape discrimination properties. This talk will focus on the results of experimental testing of the wavelet unfolding algorithm in the mixed neutron / gamma-ray fluxes of a plutonium-beryllium source equipped with various moderators and collimators.

Abstract 276

[Regular Poster - Poster Sessions](#)

Changes in Mechanical properties of Rat Bones under simulated effects of Microgravity and Radiation [†]

[Azida H Walker¹](#), [Rahul Mehta¹](#), [Nawab Ali²](#), [Max Dobretsov³](#), [Parimal Chowdhury³](#)

⁽¹⁾Physics and Astronomy, University of Central Arkansas, 201 Donaghey Avenue, LSC 171, Conway AR 72035, United States

⁽²⁾Applied Science, University of Arkansas at Little Rock, 2801 S. University Avenue, Little Rock AR 72204, United States

⁽³⁾Biophysics and Physiology, University of Arkansas for Medical Sciences, 4301 W. Markham Street, Little Rock AR 72205, United States

The aim of this study was to determine the changes in elasticity and lattice structure in leg bone of rats which were: 1) under Hind-Limb Suspension (HLS) by tail for 2 weeks and 2) were exposed to radiation of 10 Grays in 10 days. The animals were sacrificed at the end of 2 weeks and the leg bones were surgically removed, cleaned and fixed with a buffered solution. The mechanical strength of the bone (elastic modulus) was determined from measurement of bending of a bone when under an applied force. Two methodologies were used: i) a 3-point bending technique and ii) classical bending where bending is accomplished keeping one end fixed. Three point bending method used a captive actuator controlled by a programmable IDEA drive. This allowed incremental steps of 0.047mm for which the force is measured. The data is used to calculate the stress and the strain. In the second method a mirror attached to the free end of the bone allowed a reflected laser beam spot to be tracked. This provided the displacement measurement as stress levels changed. Analysis of stress vs. strain graph together with solution of Euler-Bernoulli equation for a cantilever beam allowed determination of the elastic modulus of the leg bone for (i) control samples, (ii) HLS samples and (iii) HLS samples with radiation effects. To ascertain changes in the bone lattice structure, the bones were cross-sectioned and imaged with a 20 keV beam of electrons in a Scanning Electron Microscope (SEM). A backscattered detector and a secondary electron detector in the SEM provided the images from well-defined parts of the leg bones. Elemental compositions in combination with mechanical properties (elastic modulus and lattice structure) changes indicated weakening of the bones under space-like conditions of microgravity and radiation.

[†]Supported by Arkansas Space Grant Consortium

Abstract 203

[Regular Poster - Poster Sessions](#)

A High-Flux Neutron Generator Facility for Geochronology and Nuclear Physics Research

[Cory S. Waltz](#)¹, [A. M. Rogers](#)², [T. A. Becker](#)³, [L. A. Bernstein](#)⁴, [K. Van Bibber](#)¹, [D. L. Bleuel](#)⁴, [A. X. Chen](#)⁵, [B. H. Daub](#)⁴, [B. L. Goldblum](#)⁴, [R. B. Firestone](#)², [L. E. Kirsch](#)¹, [K. -N. Leung](#)⁴, [A. Lo](#)¹, [P. R. Renne](#)^{3,6}

⁽¹⁾*Nuclear Engineering, University of California Berkeley, Berkeley California 94720, United States*

⁽²⁾*Lawrence Berkeley National Laboratory, Berkeley California 94720, United States*

⁽³⁾*Berkeley Geochronology Center, 2455 Ridge Road, Berkeley California 94709, United States*

⁽⁴⁾*Lawrence Livermore National Laboratory, Livermore California 94550, United States*

⁽⁵⁾*Dept. of Mechanical Engineering, University of California Berkeley, Berkeley California 94720, United States*

⁽⁶⁾*Dept. of Earth and Planetary Science, University of California Berkeley, Berkeley California 94720, United States*

A facility based on a next-generation, high-flux D-D neutron generator (HFNG) is being commissioned at UC Berkeley. The generator is designed to produce monoenergetic 2.45 MeV neutrons at outputs exceeding 10^{11} n/s. The HFNG is designed around two RF-driven multi-cusp ion sources that straddle a titanium-coated copper target. D+ ions, accelerated up to 150 keV from the ion sources, self-load the target through ion implantation and drive neutron generation through the $d(d,n)^3\text{He}$ fusion reaction. The unique design of the HFNG target permits experimental samples to be placed inside the target volume, allowing the samples to receive the highest neutron flux ($1 \times 10^{11} \text{ cm}^{-2}\text{s}^{-1}$) possible from the generator. A well-integrated cooling system is capable of handling beam power reaching 120 kW impinging on the target.

The proposed science program is focused on pioneering advances in the $^{40}\text{Ar}/^{39}\text{Ar}$ dating technique for geochronology, new nuclear data measurements, basic nuclear science, and education. An overview of the facility and its unique capabilities as well as first measurements from the HFNG 2014 commissioning will be presented.

Work supported by NSF Grant No. EAR-0960138, U.S. DOE LBNL Contract No. DE-AC02-05CH11231, U.S. DOE LLNL Contract No. DE-AC52-07NA27344, and the UC Office of the President.

Abstract 208

[Regular Poster - Poster Sessions](#)

Development of A Time-tagged Neutron Source for SNM Detection

[Qing Ji](#), [Bernhard A. Ludewigt](#), [Joseph Wallig](#), [William Waldron](#)

Lawrence Berkeley National Laboratory, 1 Cyclotron Road, Berkeley CA 94720, United States

It has been shown that associated particle imaging (API) is a powerful technique for special nuclear material (SNM) detection and for the characterization of fissile material configurations. We have been developing a sealed-tube neutron generator that reduces the beam spot size on the neutron production target to 1 mm in diameter for a several-fold increase in directional resolution and simultaneously increases the maximum attainable neutron flux. A permanent magnet 2.45 GHz microwave-driven ion source has been adopted in this time-tagged neutron source. This type of ion source provides a high plasma density that allows the use of a sub-millimeter aperture for the extraction of a sufficient ion beam current and lets us achieve a much reduced beam spot size on target without employing active focusing. The design of this API generator uses a customized radial high voltage insulator to minimize source to neutron production target distance and to provide for a simple ion source cooling arrangement. First experimental results will be presented at the conference.

*This work was supported by NNSA office of Nonproliferation and Verification Research & Development and performed under the auspices of the U. S. Department of Energy by Lawrence Berkeley National Laboratory under contract No. DE-AC02-05CH11231.

RFI-Based Ion Linac Systems[Donald A. Swenson](#)*Ion Linac Systems, Inc., 638 Camino Vista Rio, Bernalillo NM 87004, United States*

A new company, [Ion Linac Systems, Inc.](#), has been formed to promote the development, manufacture, and marketing of intense, RFI-based, Ion Linac Systems. The Rf Focused Interdigital (RFI) linac structure was invented by the author while at Linac Systems, LLC. The first step, for the new company, will be to correct a flaw in an existing RFI-based linac system and to demonstrate "good transmission" through the system. The existing system, aimed at the BNCT medical application, is designed to produce a beam of 2.5 MeV protons with an average beam current of 20 mA. In conjunction with a lithium target, it will produce an intense beam of epithermal neutrons. This system is very efficient, requiring only 180 kW of rf power to produce a 50 kW proton beam. In addition to the BNCT medical application, the RFI-based systems should represent a powerful neutron generator for homeland security, defense applications, cargo container inspection, and contraband detection. The timescale to the demonstration of "good transmission" is early summer of this year. Our website is www.ionlinacs.com.

Compound specific radiocarbon analysis from indoor air samples via accelerator mass spectrometry.[Wolfgang Kretschmer](#), [Matthias Schindler](#), [Andreas Scharf](#)*Physics Department, University of Erlangen, Erwin-Rommel-Str. 1, Erlangen 91058, Germany*

Many volatile organic environmental compounds are potentially dangerous due to their allergic or carcinogen impact on humans. For the establishment of effective countermeasures for lowering their concentration in houses, sources have to be known. Our investigation is focused on aldehyde compounds since their indoor concentration is often above the official guidelines and since they originate from biogenic or anthropogenic sources. Both types of sources can be distinguished by their different ^{14}C content which can be measured via accelerator mass spectrometry (AMS).

For the collection and separation of these gaseous substances they have to be converted into liquid or solid phase by derivatization. This leads to the incorporation of up to six additional carbon atoms into the derivatized sample and hence to a reduced ^{14}C content. To reduce the number of additional carbon atoms and to optimize efficiency and duration of the procedure, different derivatization compounds and methods have been tested with acet- and formaldehyde of known ^{14}C content.

The Erlangen AMS facility, based on an EN tandem accelerator and a hybrid sputter ion source for solid and gaseous samples, is well suited for the measurement of isotope ratios $^{14}\text{C}/^{12}\text{C} \approx 10^{-12} - 10^{-15}$. The ^{14}C concentration of the calibration samples and from indoor air samples in apartments, beer taverns and schools have been determined by AMS, the corresponding results are discussed with regard to potential sources of aldehydes.

TUNGSTEN RESPONSE TO TRANSIENT HEAT LOADS GENERATED BY LASER PULSES

Tungsten (W) has been selected as a plasma-facing component (PFC) in the activated phase of ITER. However, ductile-to-brittle transition is also a major drawback of W, which could produce large macroscopic particles as well as small dust particles. Due to higher energy loads to the diverter surfaces during ITER operation, the surface of PFC will be exposed to extremely high heat flux. Some of the potential damages caused by high heat flux exposure of W include cracking, melting, erosion and splashing. Typically, ion or electron beam facilities are routinely used for simulating ITER-like conditions in the laboratory to study the damage and erosion of PFC materials.¹ However, lasers can also be used for simulating similar features in the laboratory.²

In this study, we exposed W surface with high power laser pulses for investigating the use of laser as an energy source to simulate the behavior of PFC materials under highly transient heat loads. We exposed W with differing laser pulse duration (ms-ns), power density, energy load (number of pulses) and investigated the surface morphology changes. Significant particle emission features are noticed for short pulse (ns) exposure to W target with an energy load of $\sim 0.46 \text{ MJ.m}^{-2}$ due to ductile-to-brittle transition. However, particle emission is found to be significantly less for longer pulse exposure. Regardless of the laser pulse duration (ns-ms), the W surface morphology showed cracks, melting and re-solidification, and splashing. The results obtained with varying W grain sizes (fine and ultrafine) will also be presented. Our results highlight that high power lasers can be used for simulating transient heat flux load experiments similar to the ion beam and plasma interactions with W target.

1. J. Linke et al., **Journal of Nuclear Materials**, **283-287**, 1152-1156 (2000).
2. N. Faid, S. S. Harilal, H. Ding and A. Hassanein, **Nuclear Fusion**, **54**, 012002 (2014)

Abstract 393

[Regular Poster - Poster Sessions](#)

Physical properties and radiation stability of nanoparticles

[Vladimir V. Uglov](#), [Gennadiy E. Remnev](#), [Nikolai T. Kvasov](#), [Vitaliy I. Shymanski](#)

Solid State Physics, Belarusian State University, Nezavisimosty ave. 4, Minsk 220030, Belarus

The dependence of physical properties of materials on their geometrical size is the main criterion determining the boundary L_K between nano-phase and macro-phase. The accepted value $L_K=100 \text{ nm}$ has not physical explanation. In the present work the dependence of Young module, thermal expansion coefficient and crystal lattice parameter on the dimension of a-Fe nanoparticles obtained from computer simulation are discussed. It is shown that the value of L_K does not exceed than 50 nm.

The physical mechanisms of radiation stability increase for nanoparticles are still not clear. In the present work the correlation between theoretical results, experimental results and simulated ones obtained for Young module (E), melting point (T_m), binding energy (E_b), sublimation energy (E_s) and threshold displacement energy (E_d) is discussed. It was suggested the expression for E_d with the physical explanation its components.

A set of dynamical effects occur in the nanoparticles irradiated by the ions with energy more than 20 keV. The elastic and thermoelastic reactions of the crystal lattice on the radiation impact form the force factors influencing on the defects evolution. The simulated results of the spatial redistribution of the defects showed the moving of the defects towards the surface. The described self-organization of nanoparticles during the irradiation is the basis for nanostructured materials with high radiation stability producing.

Abstract 426

[Regular Poster - Poster Sessions](#)

RBS Study of the Behavior of PMMA as a Negative Resist for Particle Beam Lithography

[Randolph S. Peterson](#), [Paul T. Campbell](#), [John L. Davenport](#), [T. Clarke DeMars](#), [Wilson C. Fricke](#), [Zachery W. Goodwin](#), [Bertrand N. Irakoze](#), [Caroline A. Roberts](#), [Joel A. Stewart](#), [Jean Shirimpaka](#), [Frank K. Odom](#), [Michael R. O'Neil](#), [A. Brita Brudvig](#)

Physics Department, University of the South, 735 University Avenue, Sewanee TN 37383, United States

PMMA is widely known as a positive resist for low dose lithography and as a negative resist for high dose lithography. The model often mentioned for the behavior of PMMA as a negative resist is one of cross-linking of broken polymer chains at high lithographic doses from electron or proton beams. However, there are a few experiments that do not observe such cross-linking. A Rutherford backscattering experiment was performed with 2 MeV proton and helium beams on a PMMA resist to observe the oxygen and carbon in the polymer chains as the dose was increased from the positive resist to the negative resist behavior of the PMMA. For a sub-micron layer of PMMA on silicon only carbon was observed and the thickness of the PMMA appeared to decrease with beam dose until a final thickness of carbon was reached.

Abstract 120

[Regular Poster - Poster Sessions](#)

Quantum-mechanical study of ionization and capture in proton-methane collisions

[Arash Salehzadeh](#), [Tom Kirchner](#)

Department of Physics and Astronomy, York University, 4700 Keele Street, Toronto Ontario M3J 1P3, Canada

A recently developed method for first-principles calculations of electron removal from multicenter molecules subjected to ion impact [1] is applied to the proton-methane collision system in the 20 keV to few MeV energy regime. As in our previous work involving water molecules we use a spectral representation of the molecular Hamiltonian and a single-center expansion of the initially populated molecular orbitals to make the problem amenable to the two-center basis generator method for the solution of the time-dependent single-particle equations.

Results for (net) capture and ionization are compared with available experimental data and with results obtained from the simple Bragg additivity rule according to which the molecular cross sections are obtained from adding atomic ones. We observe good overall agreement at high energies. At low and intermediate energies the situation is less clear: while our molecular method clearly outperforms the Bragg rule for capture, the latter seems to fare better in the case of ionization.

[1] M. Murakami et al., Phys. Rev. A 85, 052704 (2012)

This work is supported by NSERC, Canada.

Abstract 338

[Regular Poster - Poster Sessions](#)

Outer-shell double photoionization of CH₂Cl₂

[Katianne Fernandes de Alcantara](#), [Anderson Herbert](#), [Wania Wolff](#), [Lucas Siggaud](#), [Antonio Carlos Fontes dos Santos](#)

Instituto de física , UFRJ, Av Athos da Silveira 149 bloco A , Rio de janeiro RJ 21941-972, Brazil

In this work the roles of the shake-off and knockout processes in the double photoionization of the CH₂Cl₂ molecule have been studied. The probabilities for both mechanisms accompanying valence-shell photoionization have been estimated as a function of incident photon energy using Samson's (1990) and Thomas's (1994) models, respectively. The experimental results are in qualitative accord with the models.

Abstract 117

[Regular Poster - Poster Sessions](#)

Advances in the Development of Positron Beams at the 5.5 MV Van de Graaff Accelerator, IFUNAM

[Oscar G de Lucio](#)¹, [Miguel Pérez](#)¹, [Ulises Mendoza](#)¹, [Juan G Morales](#)¹, [Robert D DuBois](#)²

⁽¹⁾*Instituto de Física, Departamento de Física Experimental, Universidad Nacional Autónoma de México, Cto de la Investigación Científica s/n, Coyoacán DF 04510, Mexico*

⁽²⁾*Department of Physics, Missouri University of Science and Technology, Rolla MO 65409, United States*

In this work we show the advances of a system for developing positron-based methods for materials analysis, which will be used to complement the Ion Beam Analysis (IBA) techniques currently existing at the IFUNAM 5.5 MV Van de Graff Accelerator. Results are presented in two ways: First, we present methods for producing tungsten-based positron moderators, as well as results from characterizing such moderators, including IBA and microscopy techniques, as well as a positron conversion efficiency measurement for the different moderators in the presence of a ²²Na radioactive source. Secondly we present a study of different geometries, for developing a positron transport system, which will allow us to optimize the transmission rate of such system.

Abstract 125

[Regular Poster - Poster Sessions](#)

Status of the CS-30 Cyclotron at Sichuan University and the beam optic design of the external target beam line.

[zhihui Li](#)¹, [jinquan Zhang](#)²

⁽¹⁾*Institute of Nuclear Science and Technology, Sichuan University, No.24 South Section 1, Yihuan Road, Chengdu Sichuan 610065, China*

⁽²⁾*Institute of Modern Physics, CAS, 509, Nachang road, lanzhou Gansu 730000, China*

The CS-30 cyclotron, which was presented by Beijing Research Institute of Automation for Machinery Industry, has been in operation at campus of Institute of Nuclear Science and Technology, Sichuan University since 2004, the status of the machine will be introduced briefly and the beam optic design of the external target beam line will be presented too.

Abstract 204

[Regular Poster - Poster Sessions](#)

Automatic Frequency Control of a Sub-Harmonic Bunching Cavity

[Thomas Hunt](#)¹, [Ashlynn Shatos](#)¹, [Ryan Schwingle](#)¹, [David Schwellenbach](#)², [Wendi Dreesen](#)², [David Bonal](#)³, [Wes Willis](#)³, [Anders Jorgensen](#)¹

⁽¹⁾*Electrical Engineering, New Mexico Institute of Mining and Technology, 801 Leroy Ave, Socorro nm 87801, United States*

⁽²⁾*National Security Technologies, Los Alamos Operations, 182 East Gate Drive, Los Alamos nm 87544, United States*

⁽³⁾*National Instruments, 8100 M-4 Wyoming Blvd NE, PMB #417, Albuquerque nm 87113, United States*

Presented is an automatic approach to determine and track the resonance point of a sub-harmonic bunching cavity and maintain the driving frequency at the cavity resonance frequency. This approach finds the resonance point in 12 seconds and within 1 Hz. Then the driving frequency of the cavity is changed to match the resonance point utilizing Automatic Frequency Control (AFC). The AFC allows the cavity to maintain optimal performance independent of input power, phase, or temperature. Additionally, the waveform control setup program allows for an operator to change the driving waveform between a Continuous Wave (CW), a Pulsed Waveform with a Pulse Repetition Frequency (PRF) between 1 Hz and 300 Hz, and a Single Shot operation with a specified pulse length

This approach was implemented on the National Instruments USRP-2920 using the LabVIEW software environment for development of carrier generation and cavity analysis. It utilizes a comparison of the driving amplitude to the cavity output amplitude to roughly determine the frequency of maximum amplitude. This is followed by fine tune control looking for zero phase difference between a sample of the driving signal and the signal received on the monitor loop. This indicates that the driving frequency is at the resonance point of the cavity. The cavity is characterized by completing linear searches through successively smaller windows arriving at a 1 MHz wide window with a 6.25 KHz step. The fine tune control slowly adjusts the driving frequency to match small shifts in resonance. If a large change in resonance is detected, the previous window is opened and the process re-iterates from there. The new resonance point is determined and the driving frequency is adjusted accordingly, all while maintaining operation.

Abstract 267

[Regular Poster - Poster Sessions](#)

Development of an electrostatic quadrupole doublet system for focusing fast heavy ion beams

[Szabolcs Z Szilasi](#), [Jack Manuel](#), [Gyanendra Bohara](#), [Gary Glass](#)

Ion Beam Modification and Analysis Laboratory, University of North Texas, 210 Avenue A, Denton Texas 76203, United States

In this poster, we report on the progress in the development of the prototype of an electrostatic quadrupole doublet system for focusing fast heavy ion beams. The doublet was built using four chromium and gold coated quartz rods. The coatings were separated allowing two electrodes to be present on each rod. The fine positioning of the electrodes is ensured by a high precision machined stainless steel frame.

Electrostatic quadrupole lenses have some advantages over their magnetic counterparts, the most important of which is the ability to equally focus light and heavy ion beams without changing the excitation of the lens.

Abstract 370

[Regular Poster - Poster Sessions](#)

Induced Activation in Accelerator Components for the European Spallation Source

[Cristian Bungau](#), [Adriana Bungau](#), [Robert Cywinski](#), [Roger Barlow](#)

School of Applied Sciences, University of Huddersfield, Queensgate, Huddersfield HD1 3DH, United Kingdom

The residual activity induced in particle accelerators by high-energy neutrons is a serious issue from the point of view of radiation safety because the long lived radionuclides produced by fast or moderated neutrons, protons and pions causes high levels of activation. Exposure to radiation from induced activation can occur in connection with handling, transport, machining, welding, chemical treatment and storage of irradiated items. These procedures can be extremely difficult because the personnel accumulate dose and if they exceed the permitted limits, remote handling becomes necessary. Activation studies of magnets and collimators are presented here for the High Energy Beam Transport line of the European Spallation Source.

Abstract 176

[Regular Poster - Poster Sessions](#)

Benchmarking the proton elastic scattering cross sections on ^{19}F and $^{\text{nat}}\text{B}$ using DE/E silicon telescopes

[M. Axiotis](#)¹, [M. Kokkoris](#)², [A. Lagoyannis](#)¹, [V. Paneta](#)^{1,2}, [A. Stamatopoulos](#)², [R. Vlastou](#)²

⁽¹⁾*Tandem Accelerator Laboratory, Institute of Nuclear and Particle Physics, National Center for Scientific Research "Demokritos", Aghia Paraskevi 15310, Greece*

⁽²⁾*Department of Physics, National Technical University of Athens, Zografou Campus, Athens 15780, Greece*

The implementation of the existing Ion Beam Analysis (IBA) depth profiling techniques, critically depends on the accuracy of the available differential cross sections for the reactions involved. Unfortunately the existing experimentally determined differential cross-section datasets, as well as the evaluated ones, are still not adequately validated. A carefully designed benchmarking experimental procedure (i.e. the validation of differential cross-section data via the acquisition of thick target spectra from uniform targets of known composition, followed by their detailed simulation) is thus mandatory. Benchmarking can also provide feedback for the adjustment of the parameters of the nuclear model used in the evaluation process and can help in assigning realistic uncertainties to the cross sections. This high precision procedure is seriously impeded in the case of the elastic scattering of protons by certain ultra-low Z nuclei by the existence of background contributions originating from (p, α) reactions.

The present work deals with the benchmarking of $^{19}\text{F}(\text{p,p})^{19}\text{F}$ and $^{\text{nat}}\text{B}(\text{p,p})^{\text{nat}}\text{B}$ since the quantitative determination of fluorine in various samples is of great importance for material science as well as for medical and environmental studies while boron is widely used in the semiconductor industry as a dopant for Si and Ge substrates let alone its use as an essential ingredient of hard coatings on the walls of thermonuclear plants. The experiment was performed using highly pressurized ZnF_2 and boron pellets, in the energy range of 1-4 MeV, for three backward angles, namely at 170°, 150° and 120°. A thin layer of gold was evaporated on each target for normalization purposes.

A DE/E silicon telescope was mounted at each angle exploiting the difference in the stopping power between elastically scattered protons and α -particles. This technique, using event-by-event acquisition based on standard CAMAC electronics, will be further implemented in the case of d-induced reactions in the near future.

Rainbow effect in ion channeling through a single layer of graphene

[Lai Zhang](#)¹, [Zhu Lin Zhang](#)¹, [Karur R Padmanabhan](#)²

⁽¹⁾Anhui University of Science and Technology, 70 Xueyuan South Rd, Tianjia'an, Huainan Anhui 232001, China

⁽²⁾Physics and Astronomy, Wayne State University, 666 West Hancock, Detroit MI 48201, United States

The angular distributions of charged particles transmission through very thin (layer number $N < 10$) layered nanostructures have been studied theoretically based on Lindhard Approximation Method in classical scattering by Screened Coulomb Fields. Interaction potential of the incident projectile and target atoms in a layered structure was obtained starting from the Moliere's approximation of the Thomas-Fermi interaction potential. Interaction of charged particles with few eV to MeV energies incident normally on layered structures such as graphene, MoS₂ and WS₂ have been studied systematically with atomic thermal vibrations taken into account. Our analysis is concentrated on the rainbow effect, which is clearly seen in the angular distributions of charged particles. Using Lindhard approximation, it is seen that the rainbow contour lines are only dependent on the value of E/N for each projectile-target atom pair. Our calculations showed that the atomic thermal vibration effect only plays a minor role in determining these rainbow lines.

Step-by-Step Analysis of Powder XRD Data: A PG Level Experiment

[Shubhangi S Deshpande](#)¹, [Gopichand M Dharne](#)², [Sunil D Deshpande](#)²

⁽¹⁾Physics Department, Sant Gadge Baba Amravati University, University Campus, Amravati Maharashtra 444602, India

⁽²⁾Physics Department, Dr Babasaheb Ambedkar Marathwada University, University Campus, Aurangabad Maharashtra 431004, India

Analysis of powder XRD data is normally carried out using various computer programmes. However, the students do not get an idea of what is happening in such a "blackbox"! Herein we report the student level experiment regarding the step-by-step approach to the XRD data analysis and demonstrate the extraction of the underlying Bravais lattice as well as the lattice parameters for the XRD data for face centered cubic, diamond and hexagonally closed packed specimens. Finally we also demonstrate how to refine the lattice parameter(s) using the Cohen method. For the sake of completeness the determination of crystallite size of nanostructured ZnS using the Scherrer equation is also presented.

Acknowledgements: We are grateful to Professor P R Sarode, Department of Physics, University of Goa, India and Professor C Mande, F. Natl. Acad Sci, F. I Acad Sci for their interest in the topic.

Analysis of ZDDP content and thermal decomposition in motor oils using NAA and NMR

[S. Ferguson¹](#), [J. Johnson¹](#), [D. Gonzales¹](#), [C. Hobbs²](#), [C. Allen¹](#), [S. Williams¹](#)

⁽¹⁾*Department of Physics and Geosciences, Angelo State University, ASU Station #10904, San Angelo Texas 76909, United States*

⁽²⁾*Department of Chemistry and Biochemistry, Angelo State University, ASU Station #10892, San Angelo Texas 76909, United States*

Zinc dialkyldithiophosphates (ZDDPs) are one of the most common antiwear additives present in commercially-available motor oils. The ZDDP concentrations of motor oils are most commonly determined using inductively coupled plasma atomic emission spectroscopy (ICP-AES). We have determined the Zn concentrations of eight commercially-available motor oils and one oil additive using neutron activation analysis (NAA), which has potential for greater accuracy and less sensitivity to matrix effects as compared to ICP-AES. The ³¹P nuclear magnetic resonance (³¹P-NMR) spectra were also obtained for several oil additive samples which have been heated to various temperatures in order to study the thermal decomposition of ZDDPs.

Author Index

Abderrahim, Hamid Aït . . . [# 62](#) in [ATF01](#)
Abdul-Karim, Nadia . . . [# 362](#) in [Posters](#)
Abdullin, F. Sh. . . . [# 401](#) in [NP10](#)
Abs, Michel . . . [# 395](#) in [Posters](#)
Acharya, Ajjya J. . . . [# 288](#) in [NST05](#)
Adelman, Andreas . . . [# 395](#) in [Posters](#)
Adhikari, Ananta . . . [# 287](#) in [IBA09](#)
Adolph, Robert A. . . . [# 379](#) in [ATF06](#)
Aguilar, Jeffery . . . [# 347](#) in [IBM03](#)
Aguilar, Jeffery A . . . [# 57](#) in [RE06](#)
Aguirre, Franz F. . . . [# 59](#) in [Posters](#)
Agustsson, Ronald . . . [# 102](#) in [ATF06](#)
Ahn, S. . . . [# 73](#) in [NP09](#)
Al-Amar, M. M. . . . [# 388](#) in [IBM01](#)
Alary, Jean-Francois . . . [# 381](#) in [NST06](#)
Albuquerque, Noemia . . . [# 33](#) in [IBA07](#)
Alcantara, Katianne Fernandes de . . . [# 338](#) in [Posters](#)
Alcântara, Mara T. S. . . . [# 229](#) in [NST05](#)
AlFaify, S. . . . [# 388](#) in [IBM01](#)
Alfonso, Krystal . . . [# 30](#) in [HSD01](#)
Alfonso, Krystal . . . [# 31](#) in [HSD07](#)
Ali, Nawab . . . [# 276](#) in [Posters](#)
Ali, Salina F . . . [# 193](#) in [Posters](#)
Ali, Salina F. . . . [# 101](#) in [TA02](#)
Alim, M. A. . . . [# 284](#) in [Posters](#)
Allain, Jean Paul . . . [# 37](#) in [IBM05](#)
Allen, B. . . . [# 284](#) in [Posters](#)
Allen, B. . . . [# 285](#) in [NST01](#) and [Posters](#)
Allen, C. . . . [# 56](#) in [Posters](#)
Alles, M L . . . [# 225](#) in [RE04](#)
Alles, Michael L . . . [# 133](#) in [RE04](#)
Almeida, Danilo P . . . [# 28](#) in [AMP03](#) and [Posters](#)
Alonso, Jose . . . [# 395](#) in [Posters](#)
Alrumayan, Faisal M . . . [# 476](#) in [ATF02](#)
Alrumayan, Faisal M . . . [# 477](#) in [Posters](#)
Al-Sheikhly, Mohamad . . . [# 480](#) in [RE09](#)
Alshudifat, M. F. . . . [# 187](#) in [NP10](#)
Alsleben, Helge . . . [# 92](#) in [NBA04](#)
Alsufyani, Sultan Jaber . . . [# 5](#) in [NBA01](#)
Ameena, Fnu . . . [# 92](#) in [NBA04](#)
Anastasiou, Maria . . . [# 132](#) in [NBA04](#)
ANDANTE project, On behalf of the . . . [# 424](#) in [MA06](#)
Anderssen, Eric . . . [# 322](#) in [NP08](#)
Andrade, Eduardo . . . [# 113](#) in [IBA07](#)
Andrade, Eduardo . . . [# 135](#) in [NP11](#)
Andrade, Eduardo . . . [# 144](#) in [NP07](#)
Andrade, Eduardo . . . [# 145](#) in [Posters](#)

Andrews, Anthony . . . [# 102](#) in [ATF06](#)
Andreyev, Andrei . . . [# 385](#) in [NP10](#)
Andrianarijaona, V M . . . [# 457](#) in [AMP02](#)
Andrianarijaona, V. M. . . . [# 47](#) in [AMP01](#) and [Posters](#)
Andrianis, Miltiades . . . [# 463](#) in [Posters](#)
Angal-Kalininb, Deepa . . . [# 39](#) in [ATF04](#)
Anghelone, Marta . . . [# 106](#) in [IBA06](#)
Antolak, Arlyn J . . . [# 27](#) in [HSD04](#)
Antwis, Luke D . . . [# 158](#) in [IBM04](#)
Anzenberg, Eitan . . . [# 157](#) in [IBM05](#)
AOKI, Takaaki . . . [# 88](#) in [IBM04](#)
AOKI, Takaaki . . . [# 89](#) in [NST06](#)
Aoki, Takaaki . . . [# 265](#) in [NST09](#)
Apruzese, J. P. . . . [# 146](#) in [HSD03](#)
Arai, Fumiya . . . [# 353](#) in [NP10](#)
ARAI, Hirotugu . . . [# 107](#) in [IBA07](#)
Araujo, Matthew . . . [# 30](#) in [HSD01](#)
Araujo, Matthew . . . [# 31](#) in [HSD07](#)
Araujo, Victoria . . . [# 135](#) in [NP11](#)
Araujo, Roy A . . . [# 168](#) in [RE06](#)
Araujo, Wagner W R . . . [# 91](#) in [NST05](#)
Archer, Dan E. . . . [# 183](#) in [NBA02](#)
Arendt, Thomas . . . [# 436](#) in [IBA06](#)
Arenshtam, Alex . . . [# 468](#) in [ATF07](#)
Arissian, Ladan . . . [# 435](#) in [HSD04](#)
Arnold, C. . . . [# 198](#) in [NP02](#)
Arodzero, Anatoli . . . [# 99](#) in [HSD06](#)
Arodzero, Anatoli . . . [# 147](#) in [HSD02](#)
ARUN, N. . . . [# 15](#) in [IBM02](#)
ARUN, N. . . . [# 16](#) in [Posters](#)
Aryshev, A. . . . [# 129](#) in [ATF05](#) and [Posters](#)
Assadi, Saeed . . . [# 239](#) in [NP01](#)
Auden, Elizabeth . . . [# 446](#) in [RE04](#) and [Posters](#)
Auden, Elizabeth C. . . . [# 318](#) in [RE03](#)
Auvray, Loïc . . . [# 29](#) in [IBM05](#)
Avasthi, D K . . . [# 391](#) in [Posters](#)
Avasthi, Devesh Kumar . . . [# 396](#) in [Posters](#)
Axiotis, M. . . . [# 176](#) in [Posters](#)
Axiotis, Michael . . . [# 132](#) in [NBA04](#)
Axiotis, Michael . . . [# 463](#) in [Posters](#)
Aydogan, Eda . . . [# 261](#) in [RE01](#)
Aziz, Michael J. . . . [# 157](#) in [IBM05](#)
Baby, L. T. . . . [# 134](#) in [NP03](#)
Badhrees, Ibtesam Saeed . . . [# 477](#) in [Posters](#)
Badhress, Ibtesam . . . [# 476](#) in [ATF02](#)
Baeten, Peter . . . [# 62](#) in [ATF01](#)
Baglin, John . . . [# 186](#) in [NST02](#)
Baglin, John E. . . . [# 7](#) in [NST01](#) and [Posters](#)
Bahja, Mona . . . [# 103](#) in [IBA08](#)
Bai, Quan . . . [# 149](#) in [IBA03](#)

Bailey, Paul . . . [# 367](#) in [Posters](#)
Bajpai, Shefali . . . [# 360](#) in [ATF01](#)
Baker, Christopher J . . . [# 226](#) in [NBA04](#)
Bakhru, Hassaram . . . [# 83](#) in [IBA03](#)
Bakhru, Hassaram . . . [# 136](#) in [IBA09](#)
Baldania, Vishal . . . [# 308](#) in [NP01](#)
Baldwin, Jon . . . [# 347](#) in [IBM03](#)
Banas, Dariusz . . . [# 349](#) in [AMP02](#)
Bandow, Shunji . . . [# 291](#) in [Posters](#)
Banerjee, Sudeep . . . [# 243](#) in [HSD03](#)
Bao, Jiming . . . [# 270](#) in [NST01](#)
Bao, Jiming . . . [# 287](#) in [IBA09](#)
Bao, Jiming . . . [# 384](#) in [Posters](#)
Baranwal, Vikas . . . [# 315](#) in [Posters](#)
Baranwal, Vikas . . . [# 391](#) in [Posters](#)
Baranwal, Vikas . . . [# 396](#) in [Posters](#)
Barapatre, Nirav . . . [# 442](#) in [IBA07](#)
Bardayan, D.W. . . . [# 164](#) in [NP09](#)
Bardayan, Daniel . . . [# 159](#) in [PS04](#)
Bardayan, DW . . . [# 73](#) in [NP09](#)
Bardayan, Daniel W . . . [# 278](#) in [NP04](#)
Bardayan, D. W. . . . [# 205](#) in [NP09](#)
Barkan, Shaul . . . [# 387](#) in [HSD04](#)
Barletta, William . . . [# 395](#) in [Posters](#)
Barlow, Roger . . . [# 363](#) in [Posters](#)
Barlow, Roger . . . [# 366](#) in [Posters](#)
Barlow, Roger . . . [# 367](#) in [Posters](#)
Barlow, Roger . . . [# 370](#) in [Posters](#)
Barlow, Roger . . . [# 395](#) in [Posters](#)
Barlow, Roger J . . . [# 350](#) in [PS01](#)
Barrón-Palos, Libertad . . . [# 135](#) in [NP11](#)
Barrón-Palos, Libertad . . . [# 145](#) in [Posters](#)
Barros, Suelem . . . [# 249](#) in [Posters](#)
Barthe, Marie-France . . . [# 233](#) in [RE02](#)
Barthe, Marie-France . . . [# 298](#) in [NP07](#)
Barthe, Marie-France . . . [# 474](#) in [Posters](#)
Barton, Charles . . . [# 385](#) in [NP10](#)
Barton, Joseph L. . . . [# 407](#) in [IBA05](#)
Bartoszek, Larry . . . [# 395](#) in [Posters](#)
Barty, Christopher P. J. . . . [# 93](#) in [NBA03](#)
Barzilov, Alexander . . . [# 45](#) in [NBA03](#) and [Posters](#)
Barzilov, Alexander . . . [# 46](#) in [ATF04](#) and [Posters](#)
Barzilov, Alexander . . . [# 51](#) in [NBA03](#)
Barzilov, Alexander . . . [# 52](#) in [HSD06](#)
Barzilov, Alexander . . . [# 420](#) in [NBA02](#)
Basunia, M. S. . . . [# 76](#) in [NBA03](#)
Batchelder, John C. . . . [# 376](#) in [NP11](#)
Batchelder, Jon C. . . . [# 470](#) in [Posters](#)
Batic, Matej . . . [# 184](#) in [IBA04](#)
Battiato, Alfio . . . [# 245](#) in [NST02](#)

Baugher, T. . . . [# 258](#) in [NP03](#)
Baxter, Matthew . . . [# 119](#) in [Posters](#)
Bazin, D. . . . [# 258](#) in [NP03](#)
Beasley, Paul . . . [# 337](#) in [MA03](#) and [Posters](#)
Beasley, Prof. Paul . . . [# 156](#) in [Posters](#)
Beatriz Elizabeth, Fuentes Madariaga . . . [# 178](#) in [AMP01](#) and [Posters](#)
Beaurepaire, Benoit . . . [# 220](#) in [ATF05](#)
Beck, Lucile . . . [# 61](#) in [IBM07](#)
Beck, Lucile . . . [# 67](#) in [RE07](#)
BECK, Lucile . . . [# 330](#) in [IBA05](#)
Becker, T. A. . . . [# 203](#) in [Posters](#)
Becvar, F. . . . [# 76](#) in [NBA03](#)
Begalli, Marcia . . . [# 184](#) in [IBA04](#)
Beghi, Marco G . . . [# 61](#) in [IBM07](#)
Behar, Moni . . . [# 112](#) in [IBM06](#)
Belarge, J. . . . [# 134](#) in [NP03](#)
Belgya, T. . . . [# 76](#) in [NBA03](#)
Bem, Pavel . . . [# 128](#) in [NBA01](#)
Bénard, F. . . . [# 153](#) in [MA03](#)
Bendahan, Joseph . . . [# 39](#) in [ATF04](#)
Bendahan, Joseph . . . [# 85](#) in [HSD02](#)
Benis, Emmanuel P. . . . [# 463](#) in [Posters](#)
Bennett, M. B. . . . [# 205](#) in [NP09](#)
Bennett, William Geoff . . . [# 133](#) in [RE04](#)
Bennett-Kennett, Ross B. . . . [# 290](#) in [NST02](#)
Bentley, Michael . . . [# 385](#) in [NP10](#)
Benyagoub, A. . . . [# 90](#) in [IBA04](#)
Bergstrom, Paul M . . . [# 191](#) in [AMP03](#)
Berkovits, Dan . . . [# 468](#) in [ATF07](#)
Berls, Brian . . . [# 102](#) in [ATF06](#)
Bernardi, Ettore . . . [# 245](#) in [NST02](#)
Bernstein, A. . . . [# 153](#) in [MA03](#)
Bernstein, L. . . . [# 76](#) in [NBA03](#)
Bernstein, L. A. . . . [# 203](#) in [Posters](#)
Bert, Christoph . . . [# 469](#) in [MA04](#)
Bertolini, J.C. . . . [# 105](#) in [Posters](#)
Bertozzi, William . . . [# 82](#) in [HSD01](#)
Bethke, Robert L. . . . [# 379](#) in [ATF06](#)
Bharadwaj, Vinod K . . . [# 212](#) in [HSD02](#)
Bhattacharjee, S. . . . [# 284](#) in [Posters](#)
Bi, Zhenxing . . . [# 57](#) in [RE06](#)
Bielejec, E. . . . [# 222](#) in [RE03](#)
Bielejec, Edward . . . [# 318](#) in [RE03](#)
Bielejec, Edward S. . . . [# 124](#) in [RE03](#)
Bildstein, Vinzenz . . . [# 339](#) in [NP10](#)
Bin, Ren . . . [# 149](#) in [IBA03](#)
Bishnoi, Saroj . . . [# 360](#) in [ATF01](#)
Blackmon, J. . . . [# 134](#) in [NP03](#)
Blackmon, J.C. . . . [# 164](#) in [NP09](#)
Blackmon, JC . . . [# 73](#) in [NP09](#)

Blakeley, R. . . . [# 198](#) in [NP02](#)
Blakeley, Richard . . . [# 324](#) in [NP02](#)
Blau, J. . . . [# 230](#) in [ATF03](#)
Bleuel, D. L. . . . [# 203](#) in [Posters](#)
Bluem, Hans . . . [# 444](#) in [NBA03](#)
Bobes, Omar . . . [# 81](#) in [NST07](#)
Bogdanovic Radovic, Ivancica . . . [# 106](#) in [IBA06](#)
Bohara, Gyanendra . . . [# 139](#) in [Posters](#)
Bohara, Gyanendra . . . [# 213](#) in [Posters](#)
Bohara, Gyanendra . . . [# 267](#) in [Posters](#)
Bohara, Gyanendra . . . [# 303](#) in [Posters](#)
Bonal, David . . . [# 204](#) in [Posters](#)
Bordas, Eric . . . [# 67](#) in [RE07](#)
Borodin, Oleg V. . . . [# 325](#) in [RE02](#)
Borzov, Ivan . . . [# 278](#) in [NP04](#)
Bosch, Fritz . . . [# 462](#) in [AMP04](#)
Bossert, David . . . [# 446](#) in [RE04](#) and [Posters](#)
bossis, philippe . . . [# 79](#) in [IBA09](#)
Boucher, Salime . . . [# 102](#) in [ATF06](#)
Boucher, Salime . . . [# 147](#) in [HSD02](#)
Boudinov, Henri I. . . . [# 112](#) in [IBM06](#)
Boulware, Chase . . . [# 180](#) in [Posters](#)
Boulware, Chase H . . . [# 22](#) in [ATF04](#)
Boulware, Chase H . . . [# 24](#) in [ATF02](#)
Boulware, Chase H . . . [# 25](#) in [MA02](#)
Boulware, C. H. . . . [# 230](#) in [ATF03](#)
Boulware, Chase H. . . . [# 70](#) in [ATF03](#)
Bourhis, Eric . . . [# 29](#) in [IBM05](#)
Bowden, Nathaniel . . . [# 415](#) in [NP04](#)
Bowe, A. . . . [# 205](#) in [NP09](#)
Boyce, Brad L. . . . [# 131](#) in [RE02](#)
Bradley, J. D. . . . [# 290](#) in [NST02](#)
Bradley, R. Mark . . . [# 173](#) in [NST08](#)
Brahlek, Matthew . . . [# 189](#) in [IBA02](#)
Brandau, Carsten . . . [# 345](#) in [AMP04](#)
Brandau, Carsten . . . [# 349](#) in [AMP02](#)
Brandenburg, Sytze . . . [# 445](#) in [Posters](#)
Bredeweg, T. . . . [# 198](#) in [NP02](#)
Breese, M B H . . . [# 48](#) in [Posters](#)
Breese, M. B. H. . . . [# 15](#) in [IBM02](#)
Bregolin, Felipe L. . . . [# 112](#) in [IBM06](#)
Brewer, Luke N. . . . [# 131](#) in [RE02](#)
Brewer, Nathan T . . . [# 278](#) in [NP04](#)
Brewer, N. T. . . . [# 401](#) in [NP10](#)
Brewer, N. T. . . . [# 470](#) in [Posters](#)
Brinkman, Kyle S. . . . [# 122](#) in [RE05](#)
Britton, Chuck L. . . . [# 183](#) in [NBA02](#)
Brocklebank, Mitchell . . . [# 199](#) in [IBA02](#)
Bromberg, Leslie . . . [# 336](#) in [HSD07](#)
Bronk, Lawrence . . . [# 461](#) in [MA01](#)

Bronk, Lawrence . . . [# 492](#) in [MA01](#)
Brooks, Alan . . . [# 69](#) in [ATF04](#)
Browder, Mark . . . [# 201](#) in [HSD06](#)
Brown, B. A. . . . [# 258](#) in [NP03](#)
Brown, K. . . . [# 243](#) in [HSD03](#)
Browne, J. . . . [# 73](#) in [NP09](#)
Brudvig, A. Brita . . . [# 426](#) in [Posters](#)
Brune, Carl R. . . . [# 142](#) in [NP05](#)
Bryk, Victor V. . . . [# 325](#) in [RE02](#)
Buaphad, Pikad . . . [# 102](#) in [ATF06](#)
Buatier de Mongeot, Francesco . . . [# 169](#) in [NST07](#)
Buchheit, Thomas E. . . . [# 131](#) in [RE02](#)
Buckley, K. . . . [# 153](#) in [MA03](#)
Budak, S. . . . [# 284](#) in [Posters](#)
Budak, S. . . . [# 285](#) in [NST01](#) and [Posters](#)
Budak, S. . . . [# 286](#) in [IBM05](#) and [Posters](#)
Bufford, Daniel . . . [# 130](#) in [NST04](#)
Bufford, Daniel . . . [# 137](#) in [RE07](#)
Buhay, Oleksandr . . . [# 151](#) in [Posters](#)
Buhay, Oleksandr . . . [# 152](#) in [ATF08](#)
Buller, Daniel . . . [# 137](#) in [RE07](#)
Bungau, Adriana . . . [# 366](#) in [Posters](#)
Bungau, Adriana . . . [# 370](#) in [Posters](#)
Bungau, Adriana . . . [# 395](#) in [Posters](#)
Bungau, Cristian . . . [# 350](#) in [PS01](#)
Bungau, Cristian . . . [# 366](#) in [Posters](#)
Bungau, Cristian . . . [# 370](#) in [Posters](#)
Buompane, Raffaele . . . [# 449](#) in [NP11](#)
Burducea, Ion . . . [# 211](#) in [ATF08](#)
Burducea, Ion . . . [# 214](#) in [IBA09](#)
Burducea, Ion . . . [# 219](#) in [IBM01](#)
Burgdorf, Brendan . . . [# 467](#) in [MA01](#)
Burns, Kim A . . . [# 110](#) in [Posters](#)
Burrows, Preston . . . [# 140](#) in [ATF07](#)
Cadete Santos Aires, F.G. . . . [# 105](#) in [Posters](#)
Caggiano, Joseph A. . . . [# 142](#) in [NP05](#)
Cagin, Tahir . . . [# 160](#) in [AMP03](#)
Cagin, Tahir . . . [# 168](#) in [RE06](#)
Calabretta, Luciano . . . [# 395](#) in [Posters](#)
Calana, Alessandra . . . [# 395](#) in [Posters](#)
Calcagnile, Lucio . . . [# 237](#) in [IBA08](#)
Calzolari, Giulia . . . [# 165](#) in [IBM04](#) and [Posters](#)
Calzolari, Giulia . . . [# 234](#) in [IBA08](#)
Cambrielina, Betânia Melo . . . [# 33](#) in [IBA07](#)
Campbell, Ben . . . [# 166](#) in [HSD01](#)
Campbell, Ben . . . [# 172](#) in [Posters](#)
Campbell, Logan . . . [# 97](#) in [ATF04](#)
Campbell, Logan . . . [# 140](#) in [ATF07](#)
Campbell, Logan . . . [# 143](#) in [ATF02](#)
Campbell, Luke . . . [# 274](#) in [Posters](#)

Campbell, Paul T. . . . [# 426](#) in [Posters](#)
Campese, Tara . . . [# 102](#) in [ATF06](#)
Campo, Daniela . . . [# 395](#) in [Posters](#)
Carabe, Alejandro . . . [# 467](#) in [MA01](#)
Cardenas, E. S. . . . [# 146](#) in [HSD03](#)
Cardenas, Edna S. . . . [# 358](#) in [NBA03](#)
Caro, Alfredo . . . [# 248](#) in [RE01](#)
Caro, Alfredo . . . [# 411](#) in [RE01](#)
Caro, Magda . . . [# 411](#) in [RE01](#)
Caro, Magda S. . . . [# 252](#) in [RE02](#)
Carpenter, M. P. . . . [# 258](#) in [NP03](#)
Carpenter, Michael . . . [# 440](#) in [IBM06](#)
Carpenter, Kyle R. . . . [# 354](#) in [Posters](#)
Cartegni, Lucia . . . [# 278](#) in [NP04](#)
Cassimi, A. . . . [# 90](#) in [IBA04](#)
Castilla, Alejandro . . . [# 96](#) in [ATF03](#)
Castro, Ricardo H. R. . . . [# 439](#) in [RE01](#)
Celler, A. . . . [# 153](#) in [MA03](#)
Celona, Luigi . . . [# 395](#) in [Posters](#)
Cerizza, Giordano . . . [# 247](#) in [NP03](#)
Certain, Alicia G. . . . [# 326](#) in [Posters](#)
Chae, K.Y. . . . [# 164](#) in [NP09](#)
Chakrabarty, Arnab . . . [# 160](#) in [AMP03](#)
Chambers, Scott . . . [# 430](#) in [IBA03](#)
Chandler, Chris . . . [# 490](#) in [MA08](#)
Chandra, Rico . . . [# 450](#) in [HSD06](#)
Charles, Christopher . . . [# 381](#) in [NST06](#)
Chartkunchand, Kiattichart . . . [# 354](#) in [Posters](#)
Chávez, Efraín . . . [# 135](#) in [NP11](#)
Chávez, Efraín . . . [# 144](#) in [NP07](#)
Chávez, Efraín . . . [# 145](#) in [Posters](#)
Chávez, Efrain Rafael . . . [# 113](#) in [IBA07](#)
Cheaito, Ramez . . . [# 131](#) in [RE02](#)
Cheatam, Jeremy . . . [# 354](#) in [Posters](#)
Chemerisov, S. . . . [# 115](#) in [NBA01](#)
Chemerisov, Sergey . . . [# 280](#) in [ATF02](#)
Chemerisov, Sergey . . . [# 282](#) in [MA03](#)
Chemerisovb, Sergey . . . [# 43](#) in [MA03](#)
Chen, ChienHsu . . . [# 21](#) in [Posters](#)
Chen, Chien-Hung . . . [# 154](#) in [Posters](#)
Chen, Chien-Hung . . . [# 218](#) in [RE06](#)
Chen, Da . . . [# 40](#) in [Posters](#)
Chen, Da . . . [# 41](#) in [Posters](#)
Chen, Di . . . [# 190](#) in [NST03](#)
Chen, Di . . . [# 197](#) in [NST03](#)
Chen, Di . . . [# 261](#) in [RE01](#)
Chen, Di . . . [# 335](#) in [IBA01](#)
CHEN, DI . . . [# 382](#) in [NST04](#)
Chen, Fanglin . . . [# 122](#) in [RE05](#)
Chen, Gongyin . . . [# 69](#) in [ATF04](#)

Chen, Liang . . . [# 406](#) in [RE05](#)
Chen, Min . . . [# 44](#) in [ATF04](#)
Chen, Quark . . . [# 287](#) in [IBA09](#)
Chen, S. . . . [# 243](#) in [HSD03](#)
Chen, Tianyi . . . [# 261](#) in [RE01](#)
Chen, Wei . . . [# 167](#) in [RE03](#)
Chen, Wei . . . [# 221](#) in [NST01](#)
Chen, Weidong . . . [# 345](#) in [AMP04](#)
Chen, A. A. . . . [# 205](#) in [NP09](#)
Chen, Allan X . . . [# 27](#) in [HSD04](#)
Chen, Allen X . . . [# 253](#) in [ATF06](#)
Chen, A. X. . . . [# 203](#) in [Posters](#)
Chen, Allan Xi . . . [# 251](#) in [ATF07](#)
Cheng, Fengfeng . . . [# 149](#) in [IBA03](#)
Chessa, Jack . . . [# 359](#) in [IBM07](#)
Chiari, Massimo . . . [# 165](#) in [IBM04](#) and [Posters](#)
Chiari, Massimo . . . [# 234](#) in [IBA08](#)
Chiba, Satoshi . . . [# 385](#) in [NP10](#)
Chintalapalle, Ramana . . . [# 359](#) in [IBM07](#)
Chipps, K.A. . . . [# 164](#) in [NP09](#)
Chipps, KA . . . [# 73](#) in [NP09](#)
Chipps, K. A. . . . [# 205](#) in [NP09](#)
Chisholm, Claire . . . [# 130](#) in [NST04](#)
Choi, H. . . . [# 76](#) in [NBA03](#)
Chou, Peter . . . [# 54](#) in [Posters](#)
Chowdhury, Parimal . . . [# 276](#) in [Posters](#)
Chrisler, William . . . [# 98](#) in [IBM04](#)
Chu, Ran . . . [# 376](#) in [NP11](#)
Chu, Ran . . . [# 487](#) in [Posters](#)
Chu, Wei-Kan . . . [# 174](#) in [IBA01](#)
Chu, Wei-Kan . . . [# 270](#) in [NST01](#)
Chu, Wei-Kan . . . [# 277](#) in [NST09](#)
Chu, Wei-Kan . . . [# 384](#) in [Posters](#)
Chu, Wei-Kan . . . [# 425](#) in [IBM01](#)
Chu, Wei Kan . . . [# 287](#) in [IBA09](#)
Chu, Wei Kan . . . [# 355](#) in [IBM05](#)
Chunduru, Amareswara Prasad . . . [# 307](#) in [Posters](#)
Ciocca, Mario . . . [# 489](#) in [MA07](#)
Cizewski, J.A. . . . [# 164](#) in [NP09](#)
Cizewski, Jolie A . . . [# 278](#) in [NP04](#)
Clark, Blythe G. . . . [# 131](#) in [RE02](#)
Clarke, S. . . . [# 243](#) in [HSD03](#)
Clayton, James . . . [# 212](#) in [HSD02](#)
Cleland, Marshall . . . [# 480](#) in [RE09](#)
Cleland, Marshall R . . . [# 200](#) in [RE09](#)
Clemett, Ceri . . . [# 172](#) in [Posters](#)
Clemett, Ceri D . . . [# 166](#) in [HSD01](#)
Cohn, K. . . . [# 230](#) in [ATF03](#)
Colby, Robert . . . [# 430](#) in [IBA03](#)
Colby, Robert . . . [# 440](#) in [IBM06](#)

Colby, Eric R . . . [# 306](#) in [ATF08](#)
Cole, J. . . . [# 284](#) in [Posters](#)
Cole, J. . . . [# 285](#) in [NST01](#) and [Posters](#)
collaboration, DESCANT . . . [# 339](#) in [NP10](#)
collaboration, GRIFFIN . . . [# 339](#) in [NP10](#)
Collaboration, JENSA . . . [# 73](#) in [NP09](#)
Collon, Philippe A . . . [# 410](#) in [NP06](#)
Colson, W B . . . [# 180](#) in [Posters](#)
Colson, W. B . . . [# 230](#) in [ATF03](#)
Comeaux, Justin . . . [# 292](#) in [Posters](#)
Commisso, R. J. . . . [# 146](#) in [HSD03](#)
Conrad, Janet . . . [# 395](#) in [Posters](#)
Contin, Giacomo . . . [# 322](#) in [NP08](#)
Conway, Zachary A . . . [# 364](#) in [HSD03](#)
Cooper, N. . . . [# 205](#) in [NP09](#)
Cooperstein, G. . . . [# 146](#) in [HSD03](#)
Correa, Camilo Miguel . . . [# 249](#) in [Posters](#)
Corsault, J. . . . [# 153](#) in [MA03](#)
Costache, Cristian . . . [# 211](#) in [ATF08](#)
Couder, Manoel . . . [# 254](#) in [NP09](#)
Cousins, Lisa M. . . . [# 381](#) in [NST06](#)
Coutrakon, George . . . [# 334](#) in [MA02](#)
Covington, Aaron M. . . . [# 354](#) in [Posters](#)
Cowin, James . . . [# 98](#) in [IBM04](#)
Crespillo, Miguel Almenara . . . [# 255](#) in [IBM01](#)
Crespillo, Miguel L. . . . [# 272](#) in [IBA03](#)
Crespillo, Miguel Luis . . . [# 218](#) in [RE06](#)
Crespillo Almenara, Miguel Luis . . . [# 49](#) in [IBM06](#)
Crider, B. C. . . . [# 403](#) in [TA02](#)
Culbertson, Robert J. . . . [# 288](#) in [NST05](#)
Culbertson, Robert J. . . . [# 290](#) in [NST02](#)
Curiel, Quiela . . . [# 145](#) in [Posters](#)
Cywinski, Robert . . . [# 337](#) in [MA03](#) and [Posters](#)
Cywinski, Robert . . . [# 350](#) in [PS01](#)
Cywinski, Robert . . . [# 363](#) in [Posters](#)
Cywinski, Robert . . . [# 366](#) in [Posters](#)
Cywinski, Robert . . . [# 370](#) in [Posters](#)
Cywinsky, Bob . . . [# 367](#) in [Posters](#)
Dadap, Jerry I. . . . [# 83](#) in [IBA03](#)
Dale, Greg . . . [# 43](#) in [MA03](#)
Dale, Gregory . . . [# 280](#) in [ATF02](#)
Dalmas, Dale . . . [# 43](#) in [MA03](#)
Damborsky, Kyle . . . [# 194](#) in [ATF01](#)
Danagouliau, Areg . . . [# 82](#) in [HSD01](#)
Dang, Z Y . . . [# 48](#) in [Posters](#)
Danielson, James R . . . [# 226](#) in [NBA04](#)
Dararutana, P. . . . [# 471](#) in [Posters](#)
Das, Kallol . . . [# 296](#) in [NST08](#)
Das, Soumen . . . [# 453](#) in [RE08](#)
Dasgupta-Schubert, Nabanita . . . [# 182](#) in [NST06](#)

Dassanayake, B S . . . [# 66](#) in [AMP05](#)
Dassanayake, B S . . . [# 111](#) in [IBA01](#)
Daub, B. H. . . . [# 203](#) in [Posters](#)
Davatz, Giovanna . . . [# 450](#) in [HSD06](#)
Davenport, John L. . . . [# 426](#) in [Posters](#)
Davis, Vernon T. . . . [# 354](#) in [Posters](#)
De Bruyn, Didier J . . . [# 62](#) in [ATF01](#)
De Cesare, Mario . . . [# 449](#) in [NP11](#)
De Cesare, Nicola . . . [# 449](#) in [NP11](#)
de Jong, Jan . . . [# 445](#) in [Posters](#)
de Lucio, Oscar . . . [# 144](#) in [NP07](#)
de Lucio, Oscar . . . [# 145](#) in [Posters](#)
de Lucio, Oscar G . . . [# 117](#) in [Posters](#)
de Lucio, Oscar Genaro . . . [# 113](#) in [IBA07](#)
de Ruelle, Nathalie . . . [# 279](#) in [AMP01](#)
Deacon, A. N. . . . [# 258](#) in [NP03](#)
Debu, Pascal . . . [# 298](#) in [NP07](#)
Debu, Pascal . . . [# 474](#) in [Posters](#)
Dedyulin, Sergey N . . . [# 199](#) in [IBA02](#)
Dedyulin, Sergey N . . . [# 202](#) in [Posters](#)
DeFilippo, Enrico . . . [# 349](#) in [AMP02](#)
Defrance, Pierre . . . [# 289](#) in [AMP01](#) and [Posters](#)
Degiovanni, Ivo . . . [# 246](#) in [IBM01](#)
Dehnel, Morgan . . . [# 289](#) in [AMP01](#) and [Posters](#)
Delayen, Jean R. . . . [# 96](#) in [ATF03](#)
Demarche, Julien . . . [# 158](#) in [IBM04](#)
Demarche, Julien . . . [# 165](#) in [IBM04](#) and [Posters](#)
Demarche, Julien . . . [# 308](#) in [NP01](#)
Demarche, Julien . . . [# 348](#) in [IBA06](#)
Demarche, Julien . . . [# 362](#) in [Posters](#)
DeMars, T. Clarke . . . [# 426](#) in [Posters](#)
DeMasi, Alexander . . . [# 37](#) in [IBM05](#)
Demkowicz, Michael J. . . . [# 248](#) in [RE01](#)
Deoli, Naresh T . . . [# 293](#) in [IBA01](#)
Desgardin, Pierre . . . [# 233](#) in [RE02](#)
Desgardin, Pierre . . . [# 298](#) in [NP07](#)
Desgardin, Pierre . . . [# 474](#) in [Posters](#)
Deshpande, Sunil D . . . [# 150](#) in [NST01](#) and [Posters](#)
Deshpande, Sunil D . . . [# 394](#) in [Posters](#)
Deshpande, S S . . . [# 150](#) in [NST01](#) and [Posters](#)
Deshpande, Shubhangi S . . . [# 394](#) in [Posters](#)
Despotopoulos, John . . . [# 310](#) in [NP05](#)
Devaraj, Arun . . . [# 440](#) in [IBM06](#)
Dey, Sanchita . . . [# 439](#) in [RE01](#)
DeYoung, Paul A . . . [# 432](#) in [TA02](#)
Dhanunjaya, M . . . [# 9](#) in [IBM02](#)
Dharne, G M . . . [# 150](#) in [NST01](#) and [Posters](#)
Dharne, Gopichand M . . . [# 394](#) in [Posters](#)
Dhaubhadel, Mangal S . . . [# 392](#) in [IBM01](#)
Dholabhai, Pratik P . . . [# 57](#) in [RE06](#)

Dhoubhadel, Mangal S . . . [# 323](#) in [Posters](#)
Di, Zengfeng . . . [# 40](#) in [Posters](#)
Di, Zengfeng . . . [# 41](#) in [Posters](#)
Di Fonzo, Fabio . . . [# 61](#) in [IBM07](#)
Di Leva, Antonino . . . [# 449](#) in [NP11](#)
Diakaki, Maria . . . [# 132](#) in [NBA04](#)
Dias, Johnny Ferraz . . . [# 18](#) in [IBA07](#)
Dias, Johnny Ferraz . . . [# 33](#) in [IBA07](#)
Diels, Jean-Claude . . . [# 435](#) in [HSD04](#)
Diffenderfer, Eric . . . [# 467](#) in [MA01](#)
Dimitriou, Anastasios . . . [# 463](#) in [Posters](#)
Dinca, Dan-Cristian . . . [# 148](#) in [HSD02](#)
Ding, Jian . . . [# 4](#) in [Posters](#)
Dinh, Jeffrey . . . [# 461](#) in [MA01](#)
Dissanayake, A. . . . [# 388](#) in [IBM01](#)
Dissanayake, Amila . . . [# 430](#) in [IBA03](#)
Dmitriev, S. N. . . . [# 401](#) in [NP10](#)
Dobretsov, Max . . . [# 276](#) in [Posters](#)
Doebeli, M. . . . [# 90](#) in [IBA04](#)
Doerner, Russ P. . . . [# 407](#) in [IBA05](#)
Dombos, A. . . . [# 13](#) in [NP03](#)
Donnelly, Stephen E . . . [# 313](#) in [RE07](#)
D'Onofrio, Antonio . . . [# 449](#) in [NP11](#)
Doriese, R . . . [# 259](#) in [IBA07](#)
Dörner, Reinhard . . . [# 349](#) in [AMP02](#)
Doron, Oded . . . [# 27](#) in [HSD04](#)
dos Santos, Suene Bernardes . . . [# 18](#) in [IBA07](#)
Dos Santos, Carla Eliete Iochims . . . [# 33](#) in [IBA07](#)
Dowsett, David . . . [# 65](#) in [RE07](#)
Doyle, Barney . . . [# 137](#) in [RE07](#)
Doyle, B L . . . [# 124](#) in [RE03](#)
Doyle, Barney L . . . [# 494](#) in [Posters](#)
Doyle, B. L. . . . [# 222](#) in [RE03](#)
Doyle, Barney L. . . . [# 318](#) in [RE03](#)
Doyle, Barney L. . . . [# 446](#) in [RE04](#) and [Posters](#)
Dreesen, Wendi . . . [# 201](#) in [HSD06](#)
Dreesen, Wendi . . . [# 204](#) in [Posters](#)
Drews, Scott N. . . . [# 290](#) in [NST02](#)
Driscoll, Mark S . . . [# 196](#) in [TA02](#)
Driscoll, Mark S . . . [# 207](#) in [RE09](#)
Driscoll, Mark S . . . [# 209](#) in [RE09](#)
Driscoll, Mark S . . . [# 210](#) in [RE09](#)
Drozdenko, Oleksandr . . . [# 152](#) in [ATF08](#)
Du, Xin . . . [# 406](#) in [RE05](#)
Du, Yingge . . . [# 430](#) in [IBA03](#)
Dubois, Alain . . . [# 312](#) in [AMP05](#)
DuBois, Robert D . . . [# 117](#) in [Posters](#)
DuBois, Robert D. . . . [# 332](#) in [Posters](#)
Duke, D. . . . [# 198](#) in [NP02](#)
Duke, Dana L . . . [# 377](#) in [NP02](#)

Durante, Marco . . . [# 456](#) in [MA01](#)
Dyuldya, Sergiy V. . . . [# 326](#) in [Posters](#)
Echegut, Patrick . . . [# 298](#) in [NP07](#)
Echegut, Patrick . . . [# 474](#) in [Posters](#)
Eckman, Chris . . . [# 102](#) in [ATF06](#)
Economou, C. . . . [# 153](#) in [MA03](#)
Edgecock, Robert . . . [# 363](#) in [Posters](#)
El Ghazaly, Mohamed O A . . . [# 289](#) in [AMP01](#) and [Posters](#)
Elaigne, Severine . . . [# 103](#) in [IBA08](#)
El-Atwani, Osman . . . [# 37](#) in [IBM05](#)
El-Atwani, Osman . . . [# 74](#) in [RE07](#)
El-Atwani, Osman . . . [# 75](#) in [Posters](#)
El-Bast, M. . . . [# 104](#) in [Posters](#)
El-Bast, Mohamed . . . [# 103](#) in [IBA08](#)
Eley, John G . . . [# 456](#) in [MA01](#)
Eley, John G . . . [# 469](#) in [MA04](#)
Eliyahu, Ilan . . . [# 468](#) in [ATF07](#)
Ellsworth, Jennifer . . . [# 206](#) in [NBA03](#)
Ellsworth, Jennifer L . . . [# 216](#) in [ATF07](#)
Elsalim, Mashal . . . [# 30](#) in [HSD01](#)
Elsalim, Mashal . . . [# 31](#) in [HSD07](#)
Enachescu, Mihaela . . . [# 211](#) in [ATF08](#)
Epie, Emmanuel . . . [# 270](#) in [NST01](#)
Epie, Emmanuel Njumbe . . . [# 287](#) in [IBA09](#)
Ericson, Nance . . . [# 183](#) in [NBA02](#)
Eriksson, T. . . . [# 153](#) in [MA03](#)
Esarey, Eric H. . . . [# 44](#) in [ATF04](#)
Escher, J. . . . [# 76](#) in [NBA03](#)
Eswara, Santhana . . . [# 65](#) in [RE07](#)
Ewing, Rodney C . . . [# 163](#) in [RE06](#)
Ewing, Rodney Charles . . . [# 100](#) in [RE06](#)
Ezell, Dianne B. . . . [# 183](#) in [NBA02](#)
Fa, Tao . . . [# 149](#) in [IBA03](#)
Facsko, Stefan . . . [# 297](#) in [IBM07](#)
Faddeggon, Bruce A . . . [# 466](#) in [MA04](#)
Fager, Marcus . . . [# 467](#) in [MA01](#)
Faillace, Luigi . . . [# 102](#) in [ATF06](#)
Faillace, Luigi . . . [# 147](#) in [HSD02](#)
Falabella, Steve . . . [# 206](#) in [NBA03](#)
Falabella, Steven . . . [# 216](#) in [ATF07](#)
Fan, Shiyu . . . [# 487](#) in [Posters](#)
Fantini, Andrea . . . [# 133](#) in [RE04](#)
Farid, Nazar . . . [# 75](#) in [Posters](#)
Farkhondeh, Manouchehr . . . [# 306](#) in [ATF08](#)
Farook, Bashir Yousif . . . [# 178](#) in [AMP01](#) and [Posters](#)
Farquhar, Ethan . . . [# 183](#) in [NBA02](#)
Faure, Jerome . . . [# 220](#) in [ATF05](#)
Favalli, Andrea . . . [# 274](#) in [Posters](#)
Favalli, Andrea . . . [# 358](#) in [NBA03](#)
Favela, Francisco . . . [# 113](#) in [IBA07](#)

Favela, Francisco . . . [# 144](#) in [NP07](#)
Favela, Francisco . . . [# 145](#) in [Posters](#)
Fay, James E. . . . [# 379](#) in [ATF06](#)
Feinberg, Gitai . . . [# 468](#) in [ATF07](#)
Feldman, Leonard C . . . [# 72](#) in [IBM02](#)
Feng, Liangyuan . . . [# 387](#) in [HSD04](#)
Ferguson, S. . . . [# 56](#) in [Posters](#)
Fernandez, Rafaël . . . [# 62](#) in [ATF01](#)
Ferreira, Natalia . . . [# 55](#) in [AMP05](#)
Ferreira, Natalia . . . [# 378](#) in [AMP03](#)
Ferrari, Tatiele . . . [# 33](#) in [IBA07](#)
Fijalkowska, A. . . . [# 470](#) in [Posters](#)
Fiore, Maria Rosaria . . . [# 489](#) in [MA07](#)
Firestone, R. . . . [# 76](#) in [NBA03](#)
Firestone, R. B. . . . [# 203](#) in [Posters](#)
Fischer, Daniel . . . [# 378](#) in [AMP03](#)
Fleming, Yves . . . [# 65](#) in [RE07](#)
Fleming, R M . . . [# 124](#) in [RE03](#)
Florea, Nicoleta Mihaela . . . [# 211](#) in [ATF08](#)
Flores, Juan Gerardo . . . [# 145](#) in [Posters](#)
Fogle, M . . . [# 457](#) in [AMP02](#)
Fogle, M. . . . [# 47](#) in [AMP01](#) and [Posters](#)
Folkman, Kevin . . . [# 102](#) in [ATF06](#)
Followill, David S . . . [# 116](#) in [MA06](#)
Fontana, Cristiano L . . . [# 494](#) in [Posters](#)
Ford, Richard . . . [# 404](#) in [HSD03](#)
Ford, Richard . . . [# 460](#) in [ATF01](#)
Forneris, Jacopo . . . [# 246](#) in [IBM01](#)
Forneris, Jacopo . . . [# 308](#) in [NP01](#)
Fossati, Piero . . . [# 489](#) in [MA07](#)
Fowler, J . . . [# 259](#) in [IBA07](#)
Franklin, Wilbur A. . . . [# 82](#) in [HSD01](#)
Franz, Achim . . . [# 356](#) in [NP08](#)
Franzen, Paulo L. . . . [# 112](#) in [IBM06](#)
Freeman, S. J. . . . [# 258](#) in [NP03](#)
French, A. J. . . . [# 403](#) in [TA02](#)
Frenje, Johan A . . . [# 195](#) in [NP05](#)
Freund, Jonathan B. . . . [# 296](#) in [NST08](#)
Fricke, Wilson C. . . . [# 426](#) in [Posters](#)
Friedrich, Thomas . . . [# 456](#) in [MA01](#)
Frontera, M. A. . . . [# 153](#) in [MA03](#)
Fruth, Victor . . . [# 214](#) in [IBA09](#)
Fry, C. . . . [# 205](#) in [NP09](#)
Fu, Engang . . . [# 57](#) in [RE06](#)
Fu, Engang . . . [# 149](#) in [IBA03](#)
Fu, Engang . . . [# 218](#) in [RE06](#)
Fu, Engang . . . [# 411](#) in [RE01](#)
Fuentes, Beatriz . . . [# 217](#) in [TA01](#)
FUJII, Makiko . . . [# 88](#) in [IBM04](#)
FUJII, Makiko . . . [# 89](#) in [NST06](#)

FUJITA, Akiho . . . [# 107](#) in [IBA07](#)
Fullwood, Clayton . . . [# 250](#) in [IBA09](#)
Gade, A. . . . [# 258](#) in [NP03](#)
Galindo-Uribarri, Alfredo . . . [# 376](#) in [NP11](#)
Galindo-Uribarri, Alfredo . . . [# 380](#) in [NP07](#)
Galindo-Uribarri, Alfredo . . . [# 487](#) in [Posters](#)
Galloway, Richard A . . . [# 200](#) in [RE09](#)
Garcia, Juan Alejandro . . . [# 249](#) in [Posters](#)
García Ferré, Francisco . . . [# 61](#) in [IBM07](#)
Garcia-Sciveres, Maurice . . . [# 44](#) in [ATF04](#)
Garner, Frank A . . . [# 261](#) in [RE01](#)
Garner, Frank A. . . . [# 325](#) in [RE02](#)
Garner, Frank A. . . . [# 326](#) in [Posters](#)
Garner, Frank A. . . . [# 327](#) in [PS03](#)
Garnett, Robert W . . . [# 50](#) in [HSD07](#)
Garnett, Robert W . . . [# 371](#) in [ATF04](#) and [Posters](#)
Garratt, E. . . . [# 388](#) in [IBM01](#)
Gartner, Mariuca . . . [# 214](#) in [IBA09](#)
Gary, Charles K . . . [# 253](#) in [ATF06](#)
Gary, Charles K. . . . [# 251](#) in [ATF07](#)
Gates, Robert O . . . [# 110](#) in [Posters](#)
Gatier, Pierre-Louis . . . [# 103](#) in [IBA08](#)
Gatto Monticone, Daniele . . . [# 246](#) in [IBM01](#)
Gaza, Oana . . . [# 211](#) in [ATF08](#)
Geddes, Cameron G.R. . . . [# 44](#) in [ATF04](#)
Gendotti, Ulisse . . . [# 450](#) in [HSD06](#)
Genovese, Marco . . . [# 246](#) in [IBM01](#)
Genreith, Ch. . . . [# 76](#) in [NBA03](#)
Gerity, James . . . [# 239](#) in [NP01](#)
Gerlach, J W . . . [# 315](#) in [Posters](#)
Gharibyan, Narek . . . [# 310](#) in [NP05](#)
Ghebregziabher, I. . . . [# 243](#) in [HSD03](#)
Ghita, Dan Gabriel . . . [# 211](#) in [ATF08](#)
Gialanella, Lucio . . . [# 414](#) in [NP09](#)
Gialanella, Lucio . . . [# 449](#) in [NP11](#)
Giannoni, Martina . . . [# 234](#) in [IBA08](#)
Giap, Bosco . . . [# 473](#) in [MA06](#)
Giap, Fantine . . . [# 473](#) in [MA06](#)
Gierak, Jacques . . . [# 29](#) in [IBM05](#)
Gigax, Jonathan . . . [# 190](#) in [NST03](#)
Gigax, Jonathan . . . [# 197](#) in [NST03](#)
Gigax, Jonathan . . . [# 261](#) in [RE01](#)
Gillin, Michael . . . [# 484](#) in [MA01](#)
Glasmacher, T. . . . [# 258](#) in [NP03](#)
Glass, Gary . . . [# 213](#) in [Posters](#)
Glass, Gary . . . [# 267](#) in [Posters](#)
Glass, Gary . . . [# 303](#) in [Posters](#)
Glass, Gary A . . . [# 139](#) in [Posters](#)
Glass, G. A. . . . [# 177](#) in [Posters](#)
Glassman, B. . . . [# 205](#) in [NP09](#)

Go, Shintaro . . . [# 385](#) in [NP10](#)
Godfrey, Timothy J . . . [# 71](#) in [RE08](#)
Goebel, Holger . . . [# 475](#) in [MA04](#)
Goldblum, B. L. . . . [# 203](#) in [Posters](#)
Golding, Terry D . . . [# 250](#) in [IBA09](#)
Goldman, Rachel . . . [# 275](#) in [IBA05](#)
Goldman, Rachel S . . . [# 441](#) in [NST08](#)
Golovin, G. . . . [# 243](#) in [HSD03](#)
Goncharova, Lyudmila V . . . [# 199](#) in [IBA02](#)
Goncharova, Lyudmila V . . . [# 202](#) in [Posters](#)
Gonderman, Sean . . . [# 37](#) in [IBM05](#)
Gonzales, D. . . . [# 56](#) in [Posters](#)
Goodwin, Zachery W. . . . [# 426](#) in [Posters](#)
Goullon, Johannes . . . [# 378](#) in [AMP03](#)
Gozani, Tsahi . . . [# 30](#) in [HSD01](#)
Gozani, Tsahi . . . [# 31](#) in [HSD07](#)
Gozani, Tsahi . . . [# 486](#) in [HSD01](#)
Graeff, Christian . . . [# 469](#) in [MA04](#)
Grandsaert, Thomas . . . [# 102](#) in [ATF06](#)
Grant, Patrick . . . [# 310](#) in [NP05](#)
Grant, Jonathan D . . . [# 484](#) in [MA01](#)
Grant, Patrick M. . . . [# 357](#) in [HSD04](#)
Greaves, Graeme . . . [# 313](#) in [RE07](#)
Greife, U . . . [# 73](#) in [NP09](#)
Greiner, Leo . . . [# 322](#) in [NP08](#)
Gribb, Tye . . . [# 97](#) in [ATF04](#)
Gribb, Tye . . . [# 140](#) in [ATF07](#)
Gribb, Tye . . . [# 143](#) in [ATF02](#)
Grilj, Veljko . . . [# 246](#) in [IBM01](#)
Grime, Geoff W . . . [# 158](#) in [IBM04](#)
Grimm, Terry . . . [# 180](#) in [Posters](#)
Grimm, Terry L . . . [# 22](#) in [ATF04](#)
Grimm, Terry L . . . [# 23](#) in [ATF01](#)
Grimm, Terry L . . . [# 24](#) in [ATF02](#)
Grimm, Terry L . . . [# 25](#) in [MA02](#)
Grimm, T. L. . . . [# 230](#) in [ATF03](#)
Grimm, Terry L . . . [# 70](#) in [ATF03](#)
Grinyer, G. F. . . . [# 258](#) in [NP03](#)
Gromov, Roman . . . [# 280](#) in [ATF02](#)
Gromov, Roman . . . [# 282](#) in [MA03](#)
Gross, Carl . . . [# 385](#) in [NP10](#)
Gross, Carl J . . . [# 278](#) in [NP04](#)
Gross, C. J. . . . [# 470](#) in [Posters](#)
Grosshans, David . . . [# 461](#) in [MA01](#)
Grosshans, David . . . [# 492](#) in [MA01](#)
Grygiel, C. . . . [# 90](#) in [IBA04](#)
Grzywacz, R. . . . [# 470](#) in [Posters](#)
Grzywacz, R.K. . . . [# 401](#) in [NP10](#)
Grzywacz, Robert . . . [# 278](#) in [NP04](#)
Grzywacz, Robert . . . [# 385](#) in [NP10](#)

Grzywacz, R. . . . [# 187](#) in [NP10](#)
Guan, Fada . . . [# 461](#) in [MA01](#)
Guan, Fada . . . [# 492](#) in [MA01](#)
Guardiola, Consuelo . . . [# 467](#) in [MA01](#)
Guckes, Amber . . . [# 51](#) in [NBA03](#)
Guckes, Amber . . . [# 52](#) in [HSD06](#)
Guillous, S. . . . [# 90](#) in [IBA04](#)
Gulduren, M. E. . . . [# 285](#) in [NST01](#) and [Posters](#)
Guloy, Arnold . . . [# 425](#) in [IBM01](#)
Gulyas, Laszlo . . . [# 121](#) in [Posters](#)
Gumberidze, Alexandre . . . [# 241](#) in [AMP04](#)
Gumberidze, Alexandre . . . [# 349](#) in [AMP02](#)
Guner, S. . . . [# 286](#) in [IBM05](#) and [Posters](#)
Gunsing, F. . . . [# 76](#) in [NBA03](#)
Guo, Dalong . . . [# 349](#) in [AMP02](#)
Guo, Hua . . . [# 269](#) in [RE02](#)
Gupta, Renu . . . [# 10](#) in [Posters](#)
Gupta, Renu . . . [# 12](#) in [NP05](#)
Gustafsson, Torgny . . . [# 189](#) in [IBA02](#)
Haberl, Arthur W . . . [# 136](#) in [IBA09](#)
Hadzija, Mirko . . . [# 106](#) in [IBA06](#)
Haertling, Carol . . . [# 372](#) in [Posters](#)
Hagmann, Siegbert . . . [# 349](#) in [AMP02](#)
Hagmann, Siegbert J . . . [# 345](#) in [AMP04](#)
Haigh, Sarah J . . . [# 313](#) in [RE07](#)
Halfon, Shlomi . . . [# 468](#) in [ATF07](#)
Hamilton, Joe . . . [# 278](#) in [NP04](#)
Hamilton, J. H. . . . [# 401](#) in [NP10](#)
Hamilton, J. H. . . . [# 470](#) in [Posters](#)
Hammerstedt, S. W. . . . [# 177](#) in [Posters](#)
Han, Min Cheol . . . [# 184](#) in [IBA04](#)
Hanemaayer, V. . . . [# 153](#) in [MA03](#)
Harilal, Sivanandan . . . [# 74](#) in [RE07](#)
Harilal, Sivanandan . . . [# 75](#) in [Posters](#)
Harilal, Sivanandan S . . . [# 454](#) in [IBM01](#)
Harissopulos, Sotiris . . . [# 463](#) in [Posters](#)
Harmon, Frank . . . [# 23](#) in [ATF01](#)
Harmon, Frank . . . [# 24](#) in [ATF02](#)
Harmon, Frank . . . [# 84](#) in [Posters](#)
Harris, Allison L . . . [# 138](#) in [AMP03](#)
Harrison, Mark . . . [# 147](#) in [HSD02](#)
Hartman, Jessica N. . . . [# 45](#) in [NBA03](#) and [Posters](#)
Hartman, Jessica N. . . . [# 46](#) in [ATF04](#) and [Posters](#)
Hartwig, Karl T . . . [# 311](#) in [NST04](#)
Hartzell, Josiah J . . . [# 102](#) in [ATF06](#)
Harvey, James . . . [# 43](#) in [MA03](#)
Harvey, James . . . [# 280](#) in [ATF02](#)
Hassanein, Ahmed . . . [# 74](#) in [RE07](#)
Hassanein, Ahmed . . . [# 75](#) in [Posters](#)
Hassanein, Ahmed . . . [# 454](#) in [IBM01](#)

Hatarik, Robert . . . [# 142](#) in [NP05](#)
Hattar, Khalid . . . [# 74](#) in [RE07](#)
Hattar, Khalid . . . [# 130](#) in [NST04](#)
Hattar, Khalid . . . [# 131](#) in [RE02](#)
Hattar, Khalid . . . [# 137](#) in [RE07](#)
Hattori, Toshiyuki . . . [# 3](#) in [ATF05](#)
Hauf, Steffen . . . [# 184](#) in [IBA04](#)
Havener, C C . . . [# 457](#) in [AMP02](#)
Havener, C. C. . . . [# 47](#) in [AMP01](#) and [Posters](#)
Havranek, Vladimir . . . [# 264](#) in [NST03](#)
Hayes, Anna Catherine . . . [# 452](#) in [NP05](#)
He, Yanzhi . . . [# 270](#) in [NST01](#)
He, Yanzhi . . . [# 287](#) in [IBA09](#)
He, Yanzhi . . . [# 355](#) in [IBM05](#)
He, Yanzhi . . . [# 384](#) in [Posters](#)
He, Zhaohan . . . [# 220](#) in [ATF05](#)
Hebden, Andrew . . . [# 282](#) in [MA03](#)
Hecht, Adam . . . [# 324](#) in [NP02](#)
Hecht, A. A. . . . [# 198](#) in [NP02](#)
Hedlof, Ryan M . . . [# 215](#) in [Posters](#)
Hedlof, Ryan M. . . . [# 68](#) in [Posters](#)
Heeger, Karsten M . . . [# 448](#) in [NP04](#)
Heese, Juergen . . . [# 475](#) in [MA04](#)
Heffern, Lena . . . [# 324](#) in [NP02](#)
Hegelich, Bjorn Manuel . . . [# 374](#) in [ATF08](#)
Heid, Prof. Oliver . . . [# 156](#) in [Posters](#)
Heltemes, Thad . . . [# 282](#) in [MA03](#)
Hemamouche, Adrien . . . [# 29](#) in [IBM05](#)
Henderson, Alex . . . [# 256](#) in [IBA06](#)
Henderson, R. A. . . . [# 401](#) in [NP10](#)
Hendy, Amro M . . . [# 476](#) in [ATF02](#)
Henning, Dyle D . . . [# 24](#) in [ATF02](#)
Herbert, Anderson . . . [# 338](#) in [Posters](#)
Herbots, Nicole X. . . . [# 288](#) in [NST05](#)
Herbots, Nicole X. . . . [# 290](#) in [NST02](#)
Hernandez, Joseph . . . [# 287](#) in [IBA09](#)
Hicks, S. F. . . . [# 403](#) in [TA02](#)
Hiles, Kevin L. . . . [# 379](#) in [ATF06](#)
Hill, Cassie . . . [# 172](#) in [Posters](#)
Hill, Eric . . . [# 98](#) in [IBM04](#)
Hill, Cassie E . . . [# 166](#) in [HSD01](#)
Hill, Justin Joseph . . . [# 331](#) in [ATF03](#)
Hillenbrand, Pierre-Michel . . . [# 345](#) in [AMP04](#)
Hillenbrand, Pierre-Michel . . . [# 349](#) in [AMP02](#)
Hinks, Jonathan A . . . [# 313](#) in [RE07](#)
Hinshelwood, D. D. . . . [# 146](#) in [HSD03](#)
Hippler, Rainer . . . [# 1](#) in [Posters](#)
Hirose, Kentaro . . . [# 385](#) in [NP10](#)
Hmeida, Salma Z . . . [# 289](#) in [AMP01](#) and [Posters](#)
Hnatowicz, Vladimir . . . [# 264](#) in [NST03](#)

Hnatowicz, Vladimir . . . [# 266](#) in [Posters](#)
Hobbs, C. . . . [# 56](#) in [Posters](#)
Hoelzer, David T. . . . [# 325](#) in [RE02](#)
Hoff, Gabriela . . . [# 184](#) in [IBA04](#)
Hoffman, Calem R . . . [# 11](#) in [NP03](#)
Hofsäss, Hans . . . [# 81](#) in [NST07](#)
Hofstee, Mariet Anna . . . [# 445](#) in [Posters](#)
Holesinger, Terry G . . . [# 439](#) in [RE01](#)
Hollister, Jerry L . . . [# 22](#) in [ATF04](#)
Hollister, Jerry L . . . [# 24](#) in [ATF02](#)
Hollister, Jerry L . . . [# 25](#) in [MA02](#)
Hollister, Jerry L . . . [# 70](#) in [ATF03](#)
Holloway, Michael . . . [# 43](#) in [MA03](#)
Holloway, Michael . . . [# 280](#) in [ATF02](#)
Holt, Kevin . . . [# 69](#) in [ATF04](#)
Homann, Kenneth L . . . [# 456](#) in [MA01](#)
Hong, Mengqing . . . [# 34](#) in [RE01](#)
Hong, S.G. . . . [# 86](#) in [Posters](#)
Hook, B. . . . [# 153](#) in [MA03](#)
Hooten, Nicholas C . . . [# 133](#) in [RE04](#)
Hopkins, Patrick E. . . . [# 131](#) in [RE02](#)
Horacio, Martínez . . . [# 178](#) in [AMP01](#) and [Posters](#)
Hosemann, Peter . . . [# 54](#) in [Posters](#)
Hosemann, Peter . . . [# 269](#) in [RE02](#)
Hossain, Khalid . . . [# 250](#) in [IBA09](#)
Hossain, Khalild . . . [# 188](#) in [ATF08](#)
Hossain, Tim . . . [# 250](#) in [IBA09](#)
Hossain, M. Z. . . . [# 296](#) in [NST08](#)
Hou, Bixue . . . [# 220](#) in [ATF05](#)
Houlton, Robert . . . [# 252](#) in [RE02](#)
Hovey, R. T. . . . [# 47](#) in [AMP01](#) and [Posters](#)
Howell, Rebecca M . . . [# 456](#) in [MA01](#)
Hu, Xiuqin . . . [# 4](#) in [Posters](#)
Hua, Xin . . . [# 98](#) in [IBM04](#)
Huang, Hsu-Cheng . . . [# 83](#) in [IBA03](#)
Huang, Jin . . . [# 343](#) in [NP08](#)
Huang, R. T. . . . [# 127](#) in [Posters](#)
Hubele, Renate . . . [# 378](#) in [AMP03](#)
Huber, Patrick . . . [# 333](#) in [NP04](#)
Huerta, Arcadio . . . [# 113](#) in [IBA07](#)
Huerta, Arcadio . . . [# 135](#) in [NP11](#)
Huerta, Arcadio . . . [# 144](#) in [NP07](#)
Huerta, Arcadio . . . [# 145](#) in [Posters](#)
Hug, Eugen B. . . . [# 482](#) in [PS02](#)
Hughart, D . . . [# 124](#) in [RE03](#)
Hughart, D. . . . [# 222](#) in [RE03](#)
Hunt, Thomas . . . [# 204](#) in [Posters](#)
Hunt, Alan W . . . [# 22](#) in [ATF04](#)
Hunt, Alan W . . . [# 25](#) in [MA02](#)
Hunt, Alan W . . . [# 274](#) in [Posters](#)

Hunt, Alan W . . . [# 358](#) in [NBA03](#)
Hunt, A. W. . . . [# 146](#) in [HSD03](#)
Hurst, A. . . . [# 76](#) in [NBA03](#)
Hurst, Noah C . . . [# 226](#) in [NBA04](#)
Hurtle, Ken . . . [# 43](#) in [MA03](#)
Hutcheson, A. L. . . . [# 146](#) in [HSD03](#)
Iannalfi, Alberto . . . [# 489](#) in [MA07](#)
Ikeda, T . . . [# 111](#) in [IBA01](#)
Ikezoe, Hiroshi . . . [# 385](#) in [NP10](#)
ILA, D. . . . [# 286](#) in [IBM05](#) and [Posters](#)
ILA, Daryush . . . [# 7](#) in [NST01](#) and [Posters](#)
ILA, Daryush . . . [# 8](#) in [TA01](#)
ILA, Daryush . . . [# 26](#) in [NST01](#)
Iliev, Metodi . . . [# 358](#) in [NBA03](#)
Ilyushkin, Sergey . . . [# 278](#) in [NP04](#)
Intarasiri, S. . . . [# 471](#) in [Posters](#)
Iochims dos Santos, Carla Eliete . . . [# 18](#) in [IBA07](#)
Irakoze, Bertrand N. . . . [# 426](#) in [Posters](#)
Iriyama, Yasutoshi . . . [# 123](#) in [Posters](#)
Irvine, D. . . . [# 205](#) in [NP09](#)
ISHII, Keizo . . . [# 107](#) in [IBA07](#)
Ishii, Yasuyuki . . . [# 344](#) in [IBM06](#)
Itkis, M. G. . . . [# 401](#) in [NP10](#)
Ito, Yuta . . . [# 353](#) in [NP10](#)
Jabr, Abdullah S . . . [# 289](#) in [AMP01](#) and [Posters](#)
Jackson, S. L. . . . [# 146](#) in [HSD03](#)
Jagannathan, S . . . [# 225](#) in [RE04](#)
Jäger, Markus . . . [# 442](#) in [IBA07](#)
Jaksic, Milko . . . [# 106](#) in [IBA06](#)
Jaksic, Milko . . . [# 246](#) in [IBM01](#)
Jakubassa-Amundsen, Doris . . . [# 349](#) in [AMP02](#)
Jandel, M. . . . [# 198](#) in [NP02](#)
Janecek, Martin . . . [# 386](#) in [HSD06](#)
Janovics, Róbert . . . [# 412](#) in [NP06](#)
Janssens, R. V. F. . . . [# 258](#) in [NP03](#)
Janzen, Meghan S. . . . [# 380](#) in [NP07](#)
Javahery, Gholamreza . . . [# 381](#) in [NST06](#)
Javey, Ali . . . [# 268](#) in [ATF06](#)
Jembrih-Simbürger, Dubravka . . . [# 106](#) in [IBA06](#)
Jen, Timothy . . . [# 275](#) in [IBA05](#)
Jenkins, David . . . [# 385](#) in [NP10](#)
Jensen, Aaron . . . [# 447](#) in [HSD02](#)
Jhang, J. . . . [# 243](#) in [HSD03](#)
Ji, Qing . . . [# 208](#) in [Posters](#)
Jia, Quanxi X . . . [# 57](#) in [RE06](#)
Jiang, changzhong . . . [# 34](#) in [RE01](#)
Jiang, Ke . . . [# 167](#) in [RE03](#)
Jiang, Weilin . . . [# 87](#) in [IBM03](#)
Jiang, Weilin . . . [# 440](#) in [IBM06](#)
Jiao, Zhijie . . . [# 54](#) in [Posters](#)

Jiménez, Edgar Adán . . . [# 113](#) in [IBA07](#)
Jiménez, Edgar Adán . . . [# 135](#) in [NP11](#)
Jiménez, Edgar Adán . . . [# 144](#) in [NP07](#)
Jin, Ke . . . [# 87](#) in [IBM03](#)
Jin, Ke . . . [# 154](#) in [Posters](#)
Jobim, Paulo Fernandes Costa . . . [# 18](#) in [IBA07](#)
Jobim, Paulo Fernandes Costa . . . [# 33](#) in [IBA07](#)
John, Angelin Ebanezar . . . [# 1](#) in [Posters](#)
Johnson, J. . . . [# 56](#) in [Posters](#)
Johnson, James . . . [# 483](#) in [PS03](#)
Johnson, R. B. . . . [# 284](#) in [Posters](#)
Johnson, R. B. . . . [# 285](#) in [NST01](#) and [Posters](#)
Johnson, E. D. . . . [# 134](#) in [NP03](#)
Johnson, Heather M. . . . [# 290](#) in [NST02](#)
Johnson, Richard R . . . [# 94](#) in [HSD07](#)
Johnson, Harley T. . . . [# 296](#) in [NST08](#)
Johnstone, Carol . . . [# 363](#) in [Posters](#)
Johnstone, Carol . . . [# 404](#) in [HSD03](#)
Johnstone, Carol . . . [# 405](#) in [MA02](#)
Johnstone, Carol Joanne . . . [# 460](#) in [ATF01](#)
Jonah, Charles . . . [# 280](#) in [ATF02](#)
Jonah, Charles . . . [# 282](#) in [MA03](#)
Jones, Brian . . . [# 362](#) in [Posters](#)
Jones, Glen . . . [# 253](#) in [ATF06](#)
Jones, Glenn . . . [# 251](#) in [ATF07](#)
Jones, K.L. . . . [# 164](#) in [NP09](#)
Jones, J. K. . . . [# 39](#) in [ATF04](#)
Jones, Brian N . . . [# 158](#) in [IBM04](#)
Jones, Brian N . . . [# 165](#) in [IBM04](#) and [Posters](#)
Jones, Brian N. . . . [# 348](#) in [IBA06](#)
Jorgensen, Anders . . . [# 204](#) in [Posters](#)
Jorgenson, H. J. . . . [# 198](#) in [NP02](#)
Jose, J. . . . [# 205](#) in [NP09](#)
Jost, Carola . . . [# 278](#) in [NP04](#)
Joy, Nicholas . . . [# 440](#) in [IBM06](#)
Juan, López Patiño . . . [# 178](#) in [AMP01](#) and [Posters](#)
Julin, Jaakko . . . [# 259](#) in [IBA07](#)
Jull, Timothy A.J. . . . [# 412](#) in [NP06](#)
Jurzak, Malgorzata . . . [# 133](#) in [RE04](#)
Kaiser, Ralf . . . [# 308](#) in [NP01](#)
Kakiuchida, H. . . . [# 232](#) in [IBM02](#) and [Posters](#)
Kalamara, Antigoni . . . [# 132](#) in [NBA04](#)
Kalensky, Michael . . . [# 282](#) in [MA03](#)
Kallas, Nick . . . [# 201](#) in [HSD06](#)
Kamada, Tadashi . . . [# 493](#) in [MA07](#)
Kamiya, Tomihiro . . . [# 344](#) in [IBM06](#)
Kamwann, T. . . . [# 471](#) in [Posters](#)
Kanjilal, D . . . [# 315](#) in [Posters](#)
Kapadia, Rehan . . . [# 268](#) in [ATF06](#)
Karl, H . . . [# 315](#) in [Posters](#)

Karny, M. . . . [# 470](#) in [Posters](#)
Karny, Marek . . . [# 278](#) in [NP04](#)
Kase, Masayuki . . . [# 3](#) in [ATF05](#)
Kashyap, Yogesh . . . [# 360](#) in [ATF01](#)
Kaspar, Tiffany . . . [# 459](#) in [IBM03](#) and [Posters](#)
Kato, M. . . . [# 232](#) in [IBM02](#) and [Posters](#)
Kauppila, J S . . . [# 225](#) in [RE04](#)
Kayani, A. . . . [# 388](#) in [IBM01](#)
Käyhkö, Marko . . . [# 259](#) in [IBA07](#)
Kayran, Dmitry . . . [# 109](#) in [MA04](#)
KC, Bindu . . . [# 321](#) in [MA03](#)
Keerthisinghe, D . . . [# 66](#) in [AMP05](#)
Keerthisinghe, D . . . [# 111](#) in [IBA01](#)
Kellams, Josh . . . [# 194](#) in [ATF01](#)
Kellams, Joshua . . . [# 239](#) in [NP01](#)
Kelly, Thomas F. . . . [# 319](#) in [IBM03](#)
Kelly, Michael P . . . [# 364](#) in [HSD03](#)
Kennedy, J. R. . . . [# 335](#) in [IBA01](#)
Kerr, Matt . . . [# 461](#) in [MA01](#)
Khachatrian, Aram . . . [# 151](#) in [Posters](#)
Khan, Saif A . . . [# 9](#) in [IBM02](#)
Khan, Saif A . . . [# 391](#) in [Posters](#)
Khan, Saif Ahmad . . . [# 396](#) in [Posters](#)
Khazai, Nariman . . . [# 121](#) in [Posters](#)
khodja, hicham . . . [# 79](#) in [IBA09](#)
Kieser, William E. . . . [# 381](#) in [NST06](#)
Kiewiet, Harry . . . [# 445](#) in [Posters](#)
Kijel, Daniel . . . [# 468](#) in [ATF07](#)
Kilcoyne, Sue . . . [# 367](#) in [Posters](#)
Kim, Chan Hyeong . . . [# 184](#) in [IBA04](#)
Kim, Guinyun . . . [# 320](#) in [AMP02](#)
Kim, Han Sung . . . [# 184](#) in [IBA04](#)
Kim, J.H. . . . [# 86](#) in [Posters](#)
Kim, J.W. . . . [# 86](#) in [Posters](#)
Kim, Kyung-Sook . . . [# 320](#) in [AMP02](#)
Kim, Sung Hun . . . [# 184](#) in [IBA04](#)
Kim, Yujong . . . [# 102](#) in [ATF06](#)
King, D B . . . [# 124](#) in [RE03](#)
King, Michael J . . . [# 30](#) in [HSD01](#)
King, Michael J . . . [# 31](#) in [HSD07](#)
Kinnunen, Kimmo . . . [# 259](#) in [IBA07](#)
Kirchner, Tom . . . [# 118](#) in [Posters](#)
Kirchner, Tom . . . [# 119](#) in [Posters](#)
Kirchner, Tom . . . [# 120](#) in [Posters](#)
Kirchner, Tom . . . [# 121](#) in [Posters](#)
Kirk, Maura . . . [# 467](#) in [MA01](#)
Kirsch, L. E. . . . [# 203](#) in [Posters](#)
Kiss, Gabor gyula . . . [# 346](#) in [NP01](#)
Kleeven, Willem . . . [# 395](#) in [Posters](#)
Kleinrath, V. . . . [# 198](#) in [NP02](#)

Klug, J. . . . [# 153](#) in [MA03](#)
Knowles-Swingle, Ashley . . . [# 102](#) in [ATF06](#)
Kobernick, Arne . . . [# 97](#) in [ATF04](#)
Kobernick, Arne . . . [# 140](#) in [ATF07](#)
Kobernick, Arne . . . [# 143](#) in [ATF02](#)
Koeth, Timothy W . . . [# 434](#) in [TA01](#)
Koeth, Timothy W . . . [# 438](#) in [ATF05](#) and [Posters](#)
Koirala, Nikesh . . . [# 189](#) in [IBA02](#)
Kokkoris, M. . . . [# 176](#) in [Posters](#)
Kokkoris, Michael . . . [# 132](#) in [NBA04](#)
Kolano, Anna . . . [# 395](#) in [Posters](#)
Kolos, Karolina . . . [# 278](#) in [NP04](#)
Kolos, Karolina . . . [# 385](#) in [NP10](#)
Koltick, David . . . [# 175](#) in [NBA02](#)
Koltick, David . . . [# 179](#) in [NBA02](#)
Koltick, David . . . [# 185](#) in [NBA02](#)
Koltick, David . . . [# 365](#) in [Posters](#)
Kondev, F. G. . . . [# 258](#) in [NP03](#)
Konoplev, Ivan V. . . . [# 129](#) in [ATF05](#) and [Posters](#)
Kontos, A . . . [# 73](#) in [NP09](#)
Korbly, Stephen E. . . . [# 82](#) in [HSD01](#)
Koshchiy, E. . . . [# 134](#) in [NP03](#)
Köster, Ulli . . . [# 266](#) in [Posters](#)
Kovacs, M. . . . [# 153](#) in [MA03](#)
Kovivchak, Vladimir S. . . . [# 238](#) in [Posters](#)
Kozhuharov, Christophor . . . [# 462](#) in [AMP04](#)
Kozub, R.L. . . . [# 164](#) in [NP09](#)
Kramchenkov, Andriy . . . [# 152](#) in [ATF08](#)
Krebs, John . . . [# 282](#) in [MA03](#)
Kreisel, Arik . . . [# 468](#) in [ATF07](#)
Krengli, Marco . . . [# 489](#) in [MA07](#)
Kretschmer, Wolfgang . . . [# 228](#) in [NP06](#) and [Posters](#)
Kretschmer, Wolfgang . . . [# 351](#) in [NP11](#)
Krishnan, Sunil . . . [# 484](#) in [MA01](#)
Krticka, M. . . . [# 76](#) in [NBA03](#)
Krushelnick, Karl . . . [# 220](#) in [ATF05](#)
Kubono, Shigeru . . . [# 3](#) in [ATF05](#)
Kuchera, A. . . . [# 134](#) in [NP03](#)
Kuei, Chan Taw . . . [# 15](#) in [IBM02](#)
Kumar, Ashavani . . . [# 10](#) in [Posters](#)
Kumar, Ashavani . . . [# 12](#) in [NP05](#)
Kumar, Manvendra . . . [# 391](#) in [Posters](#)
Kumar, Manvendra . . . [# 396](#) in [Posters](#)
Kurennoy, Sergey S . . . [# 371](#) in [ATF04](#) and [Posters](#)
KUSAKARI, Masakazu . . . [# 88](#) in [IBM04](#)
Kuster, Markus . . . [# 184](#) in [IBA04](#)
Kvasov, Nikolai T. . . . [# 393](#) in [Posters](#)
Labagit, Gabriel . . . [# 312](#) in [AMP05](#)
LaBrake, Scott M . . . [# 193](#) in [Posters](#)
LaBrake, Scott M. . . . [# 101](#) in [TA02](#)

Lagoyannis, A. . . . [# 176](#) in [Posters](#)
Lagoyannis, Anastasios . . . [# 132](#) in [NBA04](#)
Lagoyannis, Anastasios . . . [# 463](#) in [Posters](#)
Laitinen, Mikko . . . [# 259](#) in [IBA07](#)
Lakshanth, Wikramarachchige J . . . [# 323](#) in [Posters](#)
Lakshantha, Wickramarachchige Jayampath . . . [# 392](#) in [IBM01](#)
Lamberton, T. J. J. . . . [# 47](#) in [AMP01](#) and [Posters](#)
Lamers, Casey . . . [# 97](#) in [ATF04](#)
Lamers, Casey . . . [# 140](#) in [ATF07](#)
Lamers, Casey . . . [# 143](#) in [ATF02](#)
Lane, Ryan A . . . [# 63](#) in [Posters](#)
Lang, Maik . . . [# 100](#) in [RE06](#)
Lang, Maik K . . . [# 163](#) in [RE06](#)
Langer, C. . . . [# 205](#) in [NP09](#)
Langeveld, Willem G.J. . . . [# 386](#) in [HSD06](#)
Langeveld, Willem GJ . . . [# 212](#) in [HSD02](#)
Lapicki, Gregory . . . [# 17](#) in [IBA04](#)
Larsen, Z. M. . . . [# 146](#) in [HSD03](#)
Larsen, L Scott . . . [# 207](#) in [RE09](#)
Larsen, L Scott . . . [# 209](#) in [RE09](#)
Larsen, L Scott . . . [# 210](#) in [RE09](#)
Larson, N. . . . [# 205](#) in [NP09](#)
Larson, David J. . . . [# 319](#) in [IBM03](#)
LaVerne, Jay A . . . [# 479](#) in [RE08](#)
Lavrentiev, Vasyl . . . [# 264](#) in [NST03](#)
Learned, John . . . [# 458](#) in [NP04](#)
Lebailly, Vivian . . . [# 220](#) in [ATF05](#)
Lebius, H. . . . [# 90](#) in [IBA04](#)
Ledoux, Robert J. . . . [# 82](#) in [HSD01](#)
Lee, C. L. . . . [# 127](#) in [Posters](#)
Lee, C.P. . . . [# 21](#) in [Posters](#)
Lee, Hang Dong . . . [# 189](#) in [IBA02](#)
Lee, Jin . . . [# 97](#) in [ATF04](#)
Lee, Manwoo . . . [# 320](#) in [AMP02](#)
Lee, Tongsik . . . [# 248](#) in [RE01](#)
Leemans, Wim P . . . [# 283](#) in [ATF05](#)
Leemans, Wim P. . . . [# 44](#) in [ATF04](#)
Lekomtsev, K. . . . [# 129](#) in [ATF05](#) and [Posters](#)
Lenzi, S. M. . . . [# 258](#) in [NP03](#)
LEPRETRE, Frédéric . . . [# 330](#) in [IBA05](#)
Leprêtre, Frédéric . . . [# 67](#) in [RE07](#)
Lerche, Michael . . . [# 359](#) in [IBM07](#)
Lessner, Eliane . . . [# 306](#) in [ATF08](#)
Lestinsky, Michael . . . [# 345](#) in [AMP04](#)
Lestinsky, Michael . . . [# 349](#) in [AMP02](#)
Leung, K. -N. . . . [# 203](#) in [Posters](#)
Levy, Martina . . . [# 308](#) in [NP01](#)
Levy, Richard P . . . [# 473](#) in [MA06](#)
Levy, Richard P. . . . [# 488](#) in [MA07](#)
Levy, Richard P. . . . [# 493](#) in [MA07](#)

Li, Lin ... [# 149](#) in [IBA03](#)
Li, Nan ... [# 347](#) in [IBM03](#)
Li, Raymond ... [# 308](#) in [NP01](#)
Li, Yang ... [# 270](#) in [NST01](#)
Li, Yang ... [# 287](#) in [IBA09](#)
Li, Yang ... [# 384](#) in [Posters](#)
Li, Yingkui ... [# 380](#) in [NP07](#)
Li, Yuhong ... [# 389](#) in [Posters](#)
Li, Yuhong ... [# 437](#) in [RE06](#)
Li, Zhenghai ... [# 447](#) in [HSD02](#)
Li, zihui ... [# 125](#) in [Posters](#)
Liao, Zhongxing ... [# 465](#) in [MA06](#)
Liddick, S. N. ... [# 205](#) in [NP09](#)
Lidia, Steve M ... [# 269](#) in [RE02](#)
Liegey, Lauren ... [# 5](#) in [NBA01](#)
Lin, Steven ... [# 461](#) in [MA01](#)
Lind, Randall ... [# 183](#) in [NBA02](#)
Linhardt, LE ... [# 73](#) in [NP09](#)
Link, Anthony ... [# 206](#) in [NBA03](#)
Linten, Dimitri ... [# 133](#) in [RE04](#)
Liszkay, Laszio ... [# 474](#) in [Posters](#)
Liszkay, Laszlo ... [# 298](#) in [NP07](#)
Litherland, Albert E. ... [# 381](#) in [NST06](#)
Litvinenko, Vladimir ... [# 109](#) in [MA04](#)
Litvinov, Yuri ... [# 345](#) in [AMP04](#)
Litvinov, Yuri ... [# 349](#) in [AMP02](#)
Litvinov, Yuri ... [# 399](#) in [AMP02](#)
Litvinov, Yuri A ... [# 462](#) in [AMP04](#)
Liu, Bingwen ... [# 98](#) in [IBM04](#)
Liu, C. ... [# 243](#) in [HSD03](#)
Liu, Chaozhuo ... [# 218](#) in [RE06](#)
Liu, S. ... [# 403](#) in [TA02](#)
Liu, Xiaotang ... [# 167](#) in [RE03](#)
Liu, Yingzi ... [# 175](#) in [NBA02](#)
Liu, Yuan ... [# 376](#) in [NP11](#)
Liu, Yuan ... [# 380](#) in [NP07](#)
Liu, Yuan ... [# 487](#) in [Posters](#)
Liu, S. H. ... [# 470](#) in [Posters](#)
Lo, A. ... [# 203](#) in [Posters](#)
Lopez, Juan ... [# 217](#) in [TA01](#)
LOUSSOUARN, Thomas ... [# 330](#) in [IBA05](#)
Love, Adam H ... [# 171](#) in [HSD04](#)
Loveless, T D ... [# 225](#) in [RE04](#)
Lu, Feng ... [# 252](#) in [RE02](#)
Lucarelli, Franco ... [# 234](#) in [IBA08](#)
Lüchtenborg, Robert ... [# 469](#) in [MA04](#)
Ludewigt, Bernhard ... [# 44](#) in [ATF04](#)
Ludewigt, Bernhard A ... [# 274](#) in [Posters](#)
Ludewigt, Bernhard A. ... [# 208](#) in [Posters](#)
Ludewigt, Bernhard A. ... [# 358](#) in [NBA03](#)

Ludwig, Karl ... [# 37](#) in [IBM05](#)
Ludwig, Jr., Karl F. ... [# 157](#) in [IBM05](#)
Lugão, Ademair B. ... [# 229](#) in [NST05](#)
Luna, Hugo ... [# 55](#) in [AMP05](#)
Lupinacci, Amanda ... [# 54](#) in [Posters](#)
Ma, Lun ... [# 167](#) in [RE03](#)
Maasilta, Ilari ... [# 259](#) in [IBA07](#)
MacMullin, Sean ... [# 368](#) in [NBA02](#)
Macon, K. ... [# 134](#) in [NP03](#)
Maddock, Robert ... [# 166](#) in [HSD01](#)
Maddock, Erik S ... [# 22](#) in [ATF04](#)
Maddock, Erik S ... [# 24](#) in [ATF02](#)
Maddock, Erik S ... [# 25](#) in [MA02](#)
Madesis, Ioannis ... [# 463](#) in [Posters](#)
Madi, T. ... [# 90](#) in [IBA04](#)
Madouri, Ali ... [# 29](#) in [IBM05](#)
Madurga, Miguel ... [# 278](#) in [NP04](#)
Maggiore, Mario ... [# 336](#) in [HSD07](#)
Mahajan, Anita ... [# 456](#) in [MA01](#)
Mahajan, Anita ... [# 478](#) in [MA06](#)
Maharrey, J A ... [# 225](#) in [RE04](#)
Mahfouz, R. ... [# 105](#) in [Posters](#)
Maidana, Nora Lia ... [# 249](#) in [Posters](#)
Majerle, Mitja ... [# 128](#) in [NBA01](#)
Major, István ... [# 412](#) in [NP06](#)
Makarashvili, Vakho ... [# 280](#) in [ATF02](#)
Makii, Hiroyuki ... [# 385](#) in [NP10](#)
Malka, Victor ... [# 220](#) in [ATF05](#)
Malladi, Girish ... [# 83](#) in [IBA03](#)
Malo, Marta ... [# 361](#) in [IBM06](#)
Mamtimin, Mayir ... [# 23](#) in [ATF01](#)
Mamtimin, Mayir ... [# 84](#) in [Posters](#)
Manandhar, Sandeep ... [# 83](#) in [IBA03](#)
Manandhar, Sandeep ... [# 430](#) in [IBA03](#)
manandhar, sandeep ... [# 459](#) in [IBM03](#) and [Posters](#)
Mangus, Mark W. ... [# 290](#) in [NST02](#)
Mangus, Jr., Mark W. ... [# 288](#) in [NST05](#)
Manikanthababu, N ... [# 317](#) in [Posters](#)
Manikanthababu, N. ... [# 15](#) in [IBM02](#)
MANIKANTHABABU, N. ... [# 16](#) in [Posters](#)
Mann, Thomas ... [# 239](#) in [NP01](#)
Manning, Brett ... [# 278](#) in [NP04](#)
Manso, Maria Victoria ... [# 249](#) in [Posters](#)
Manson, Steven T. ... [# 332](#) in [Posters](#)
Manuel, Jack ... [# 213](#) in [Posters](#)
Manuel, Jack ... [# 267](#) in [Posters](#)
Manuel, Jack ... [# 303](#) in [Posters](#)
Manuel, J. E. ... [# 177](#) in [Posters](#)
Manuel, jack Elliot ... [# 139](#) in [Posters](#)
Marco, Xhorlina ... [# 295](#) in [IBA03](#)

Marginean, Nicolae . . . [# 141](#) in [NP01](#)
Marín, Laura . . . [# 135](#) in [NP11](#)
Marinella, M . . . [# 124](#) in [RE03](#)
Marinella, M. . . . [# 222](#) in [RE03](#)
Marinov, K. B. . . . [# 39](#) in [ATF04](#)
Markovic, Nikola . . . [# 106](#) in [IBA06](#)
Marshall, Matthew . . . [# 98](#) in [IBM04](#)
Martin, Phillip N . . . [# 166](#) in [HSD01](#)
Martin, Philip Nathaniel . . . [# 172](#) in [Posters](#)
Martin, Michael S. . . . [# 335](#) in [IBA01](#)
Martinez, E. . . . [# 411](#) in [RE01](#)
Martinez, Gustavo . . . [# 359](#) in [IBM07](#)
Marzaioli, Fabio . . . [# 449](#) in [NP11](#)
Massengill, L W . . . [# 225](#) in [RE04](#)
Matei, C. . . . [# 164](#) in [NP09](#)
Mathewson, Christopher . . . [# 239](#) in [NP01](#)
Matjacic, Lidija . . . [# 165](#) in [IBM04](#) and [Posters](#)
Matjacic, Lidija . . . [# 348](#) in [IBA06](#)
Matjacic, Lidija . . . [# 362](#) in [Posters](#)
Matlis, Nicholas H. . . . [# 44](#) in [ATF04](#)
Matos, M . . . [# 73](#) in [NP09](#)
Matos, M. . . . [# 134](#) in [NP03](#)
Matos, M. . . . [# 164](#) in [NP09](#)
Matsufuji, Naruhiro . . . [# 493](#) in [MA07](#)
Matsunami, Noriaki . . . [# 232](#) in [IBM02](#) and [Posters](#)
MATSUO, Jiro . . . [# 88](#) in [IBM04](#)
MATSUO, Jiro . . . [# 89](#) in [NST06](#)
matsuo, Jiro . . . [# 299](#) in [NST09](#)
Matsuo, Jiro . . . [# 300](#) in [IBA06](#)
MATSUYAMA, Shigeo . . . [# 107](#) in [IBA07](#)
McCaffrey, Ryan P. . . . [# 379](#) in [ATF06](#)
McCammon, D . . . [# 457](#) in [AMP02](#)
McCammon, D. . . . [# 47](#) in [AMP01](#) and [Posters](#)
McCurdy, Mike . . . [# 133](#) in [RE04](#)
McCurdy, M W . . . [# 225](#) in [RE04](#)
McCurdy, Michael W. . . . [# 242](#) in [RE04](#)
McDaniel, S. . . . [# 258](#) in [NP03](#)
McDaniel, Floyd D . . . [# 323](#) in [Posters](#)
Mcdaniel, Floyd D . . . [# 392](#) in [IBM01](#)
McDiarmid, S. . . . [# 153](#) in [MA03](#)
McEllistrem, M. T. . . . [# 403](#) in [TA02](#)
McIntyre, Peter . . . [# 194](#) in [ATF01](#)
McIntyre, Peter . . . [# 239](#) in [NP01](#)
McIntyre, Peter . . . [# 292](#) in [Posters](#)
McIntyre, Peter M . . . [# 252](#) in [RE02](#)
McNeice, E. I. . . . [# 205](#) in [NP09](#)
Meaze, A.K.M. Moinul Haque . . . [# 320](#) in [AMP02](#)
Meeus, Joke . . . [# 348](#) in [IBA06](#)
Meharchand, R. . . . [# 198](#) in [NP02](#)
Meharchand, Rhiannon . . . [# 170](#) in [NP02](#)

Mehta, Rahul . . . [# 276](#) in [Posters](#)
Meierbachtol, K. . . . [# 198](#) in [NP02](#)
Meisel, Z. . . . [# 205](#) in [NP09](#)
Melconian, Karie . . . [# 194](#) in [ATF01](#)
Mendenhall, Marcus H. . . . [# 242](#) in [RE04](#)
Mendez II, Anthony . . . [# 278](#) in [NP04](#)
Mendoza, Ulises . . . [# 117](#) in [Posters](#)
Meot, Francois G . . . [# 301](#) in [MA02](#)
Meot, Francois G . . . [# 304](#) in [ATF01](#)
Mertzimekis, Theodore . . . [# 463](#) in [Posters](#)
Méry, A. . . . [# 90](#) in [IBA04](#)
Meyer-Klaucke, Wolfram . . . [# 436](#) in [IBA06](#)
Michael, Philip C. . . . [# 336](#) in [HSD07](#)
Micklich, Bradley . . . [# 280](#) in [ATF02](#)
Miernik, K. . . . [# 401](#) in [NP10](#)
Miernik, K. . . . [# 470](#) in [Posters](#)
Miernik, Krzysztof . . . [# 278](#) in [NP04](#)
Mihalczo, John T. . . . [# 183](#) in [NBA02](#)
Mikhailov, Kirill A. . . . [# 238](#) in [Posters](#)
Miller, C. . . . [# 243](#) in [HSD03](#)
Miller, David . . . [# 278](#) in [NP04](#)
Miller, Kenneth Andrew . . . [# 279](#) in [AMP01](#)
Miller, Craig E. . . . [# 336](#) in [HSD07](#)
Miller, John H . . . [# 425](#) in [IBM01](#)
Mills, Fred . . . [# 404](#) in [HSD03](#)
Mills, Gerald . . . [# 487](#) in [Posters](#)
Mills, J. . . . [# 243](#) in [HSD03](#)
Minervini, Joe . . . [# 395](#) in [Posters](#)
Minervini, Joseph V. . . . [# 336](#) in [HSD07](#)
Minor, Andrew . . . [# 54](#) in [Posters](#)
Minor, Andrew M . . . [# 269](#) in [RE02](#)
Minor, Andrew M. . . . [# 130](#) in [NST04](#)
Miranda, Javier . . . [# 113](#) in [IBA07](#)
Mirandola, Alfredo . . . [# 489](#) in [MA07](#)
Mirkovic, Dragan . . . [# 461](#) in [MA01](#)
Mirkovic, Dragan . . . [# 492](#) in [MA01](#)
Miro, Sandrine . . . [# 67](#) in [RE07](#)
Misra, Amit . . . [# 57](#) in [RE06](#)
Misra, Amit . . . [# 131](#) in [RE02](#)
Misra, Amit . . . [# 347](#) in [IBM03](#)
Mitchell, L. J. . . . [# 146](#) in [HSD03](#)
Mitra, Sudeep S . . . [# 27](#) in [HSD04](#)
Mjima, Takuya . . . [# 123](#) in [Posters](#)
Moazen, B.H. . . . [# 164](#) in [NP09](#)
Moeller, Wolfhard . . . [# 78](#) in [NST07](#)
Mohan, Radhe . . . [# 461](#) in [MA01](#)
Mohan, Radhe . . . [# 492](#) in [MA01](#)
Molinelli, Silvia . . . [# 489](#) in [MA07](#)
Molnár, Mihály . . . [# 412](#) in [NP06](#)
Monnet, I. . . . [# 90](#) in [IBA04](#)

Montel, Fabien . . . [# 29](#) in [IBM05](#)
Montenegro, Eduardo C . . . [# 55](#) in [AMP05](#)
Montes, F. . . . [# 205](#) in [NP09](#)
Montgomery, Eric K . . . [# 438](#) in [ATF05](#) and [Posters](#)
Moody, Ken . . . [# 472](#) in [HSD04](#)
Moody, Kenton . . . [# 310](#) in [NP05](#)
Mook, W. . . . [# 411](#) in [RE01](#)
Morales, Juan G . . . [# 117](#) in [Posters](#)
Morawski, Markus . . . [# 436](#) in [IBA06](#)
Morawski, Markus . . . [# 442](#) in [IBA07](#)
Morciaux, Yvon . . . [# 431](#) in [ATF08](#)
Moreno, Eliud . . . [# 113](#) in [IBA07](#)
Moreno, Eliud . . . [# 144](#) in [NP07](#)
Moreno, Eliud . . . [# 145](#) in [Posters](#)
Moreva, Ekaterina . . . [# 246](#) in [IBM01](#)
Morgan, Eric R.C. . . . [# 288](#) in [NST05](#)
Morgan, Eric R.C. . . . [# 290](#) in [NST02](#)
Morita, Kenji . . . [# 123](#) in [Posters](#)
Morita, Kenji . . . [# 291](#) in [Posters](#)
Mosby, S. . . . [# 198](#) in [NP02](#)
Mosher, D. . . . [# 146](#) in [HSD03](#)
Mosu, Daniel Vasile . . . [# 211](#) in [ATF08](#)
Motta, Francis C. . . . [# 173](#) in [NST08](#)
Moura, Esperidiana A. B. . . . [# 229](#) in [NST05](#)
Moutanabbir, Oussama . . . [# 390](#) in [IBM05](#)
Mozin, Vladimir . . . [# 274](#) in [Posters](#)
Mozin, Vladimir . . . [# 358](#) in [NBA03](#)
Mullens, James A. . . . [# 183](#) in [NBA02](#)
Müller, Alfred . . . [# 345](#) in [AMP04](#)
Müller, Alfred . . . [# 349](#) in [AMP02](#)
Müller, A. M. . . . [# 90](#) in [IBA04](#)
Mulware, Stephen Juma . . . [# 182](#) in [NST06](#)
Muntele, C. . . . [# 284](#) in [Posters](#)
Muntele, C. I. . . . [# 286](#) in [IBM05](#) and [Posters](#)
Murer, David . . . [# 450](#) in [HSD06](#)
Murillo, Ghiraldo . . . [# 113](#) in [IBA07](#)
Murillo, Ghiraldo . . . [# 144](#) in [NP07](#)
Murillo, Ghiraldo . . . [# 145](#) in [Posters](#)
Murokh, Alex . . . [# 102](#) in [ATF06](#)
Murphy, D. P. . . . [# 146](#) in [HSD03](#)
MUTO, Hideshi . . . [# 3](#) in [ATF05](#)
N, Manikanthababu . . . [# 14](#) in [IBM02](#)
Naab, Fabian U . . . [# 244](#) in [TA01](#)
Nadareski, Benjamin J . . . [# 193](#) in [Posters](#)
Nadarski, Benjamin J . . . [# 101](#) in [TA02](#)
Nadel-Turonski, Pawel . . . [# 433](#) in [NP08](#)
Nagai, Yasuki . . . [# 305](#) in [MA03](#)
Nagata, Shinji . . . [# 291](#) in [Posters](#)
Nageswara Rao, S V S . . . [# 317](#) in [Posters](#)
Nageswara Rao, S. V. S. . . . [# 15](#) in [IBM02](#)

NAGESWARA RAO, S. V. S. . . . [# 16](#) in [Posters](#)
NAKAGAWA, Shunichirou . . . [# 89](#) in [NST06](#)
Nakamura, Kei . . . [# 44](#) in [ATF04](#)
Nandasiri, Manjula . . . [# 440](#) in [IBM06](#)
Naqvi, F. . . . [# 205](#) in [NP09](#)
Naranjo, Angela . . . [# 43](#) in [MA03](#)
Naranjo, Brian . . . [# 216](#) in [ATF07](#)
Nastasi, Mike . . . [# 411](#) in [RE01](#)
Nava, Silvia . . . [# 234](#) in [IBA08](#)
Nees, John A . . . [# 220](#) in [ATF05](#)
Neill, Paul A. . . . [# 354](#) in [Posters](#)
Nelamarri, Srinivasa Rao . . . [# 14](#) in [IBM02](#)
Nelson, R. O. . . . [# 198](#) in [NP02](#)
Neric, Marko . . . [# 288](#) in [NST05](#)
Nesaraja, C.D. . . . [# 164](#) in [NP09](#)
Newhauser, Wayne D . . . [# 456](#) in [MA01](#)
Newhauser, Wayne D . . . [# 469](#) in [MA04](#)
Nguyen, Kevin T. . . . [# 288](#) in [NST05](#)
Nie, Linda H . . . [# 175](#) in [NBA02](#)
Nikitenkov, Alexsey N. . . . [# 35](#) in [Posters](#)
Nikitenkov, Nikolay N. . . . [# 35](#) in [Posters](#)
Ning, Zheng . . . [# 102](#) in [ATF06](#)
Nishinaka, Ichiro . . . [# 385](#) in [NP10](#)
Nishio, Katsuhisa . . . [# 385](#) in [NP10](#)
Nisius, David . . . [# 69](#) in [ATF04](#)
Niu, H. . . . [# 127](#) in [Posters](#)
Niu, Huan . . . [# 21](#) in [Posters](#)
Niyasov, Rustam . . . [# 82](#) in [HSD01](#)
Njoroge, Jean . . . [# 160](#) in [AMP03](#)
Njumbe, Epie . . . [# 355](#) in [IBM05](#)
Njumbe, Epie Emmanuel . . . [# 384](#) in [Posters](#)
Noakes, Tim . . . [# 367](#) in [Posters](#)
Nolden, Fritz . . . [# 462](#) in [AMP04](#)
Norris, Scott . . . [# 37](#) in [IBM05](#)
Norris, Scott . . . [# 78](#) in [NST07](#)
Norris, Scott . . . [# 157](#) in [IBM05](#)
Novak, Jan . . . [# 128](#) in [NBA01](#)
Novikov, Ivan . . . [# 420](#) in [NBA02](#)
Nsouli, B. . . . [# 104](#) in [Posters](#)
Nsouli, B. . . . [# 105](#) in [Posters](#)
Nsouli, Bilal . . . [# 103](#) in [IBA08](#)
O'Connor, Aodh Patrick . . . [# 279](#) in [AMP01](#)
Odom, Frank K. . . . [# 426](#) in [Posters](#)
O'Donnell, Barrett . . . [# 473](#) in [MA06](#)
Oganessian, Yu. Ts. . . . [# 401](#) in [NP10](#)
Oh, Seongshik . . . [# 189](#) in [IBA02](#)
Ohkubo, Takeru . . . [# 344](#) in [IBM06](#)
Ohshiro, Yukimitsu . . . [# 3](#) in [ATF05](#)
Ojeda, Oscar U . . . [# 168](#) in [RE06](#)
Okayasu, S. . . . [# 232](#) in [IBM02](#) and [Posters](#)

Okolowicz, J. . . . [# 164](#) in [NP09](#)
 Olivas, Eric . . . [# 43](#) in [MA03](#)
 Oliveira, Maria J. A. . . . [# 229](#) in [NST05](#)
 Olivero, Paolo . . . [# 245](#) in [NST02](#)
 Olivero, Paolo . . . [# 246](#) in [IBM01](#)
 Olsen, Kenneth . . . [# 306](#) in [ATF08](#)
 O'Malley, John . . . [# 172](#) in [Posters](#)
 O'Malley, P. . . . [# 205](#) in [NP09](#)
 O'Malley, P.D. . . . [# 164](#) in [NP09](#)
 O'Malley, PD . . . [# 73](#) in [NP09](#)
 O'Neil, Michael R. . . . [# 426](#) in [Posters](#)
 O'Neill, Chad . . . [# 102](#) in [ATF06](#)
 Ong, W. J. . . . [# 205](#) in [NP09](#)
 Ordonez, Carlos A . . . [# 63](#) in [Posters](#)
 Ordonez, C. A. . . . [# 224](#) in [NBA04](#)
 Ordonez, Carlos A. . . . [# 53](#) in [ATF05](#) and [Posters](#)
 Ordonez, Carlos A. . . . [# 59](#) in [Posters](#)
 Ordonez, Carlos A. . . . [# 68](#) in [Posters](#)
 Ordonez, Carlos A. . . . [# 80](#) in [ATF05](#) and [Posters](#)
 Ordonez, Carlos H . . . [# 215](#) in [Posters](#)
 Orecchia, Roberto . . . [# 489](#) in [MA07](#)
 Orlandi, Riccardo . . . [# 385](#) in [NP10](#)
 Orteiz, R. . . . [# 205](#) in [NP09](#)
 Ortiz, María Esther . . . [# 135](#) in [NP11](#)
 Ortiz, María Esther . . . [# 145](#) in [Posters](#)
 Osgood, Jr., Richard M. . . . [# 83](#) in [IBA03](#)
 Osipowicz, T. . . . [# 15](#) in [IBM02](#)
 Osman, Anderoglu . . . [# 347](#) in [IBM03](#)
 Ostendorf, Reint . . . [# 445](#) in [Posters](#)
 Ostroumov, Peter N . . . [# 364](#) in [HSD03](#)
 Otsuki, Tsutomu . . . [# 385](#) in [NP10](#)
 Ottinger, P. F. . . . [# 146](#) in [HSD03](#)
 Ottolenghi, Andrea . . . [# 424](#) in [MA06](#)
 Ou, Xin . . . [# 297](#) in [IBM07](#)
 Oyaizu, Michihiro . . . [# 3](#) in [ATF05](#)
 Pacesila, Doru . . . [# 211](#) in [ATF08](#)
 Pacesila, Doru Gheorghe . . . [# 219](#) in [IBM01](#)
 PACHECO, Claire . . . [# 314](#) in [PS01](#)
 Pacheco, J L . . . [# 124](#) in [RE03](#)
 Pacheco, J. L. . . . [# 222](#) in [RE03](#)
 Pacheco, J. L. . . . [# 224](#) in [NBA04](#)
 Padgett, Steven W . . . [# 278](#) in [NP04](#)
 Padgett, S. W. . . . [# 470](#) in [Posters](#)
 Padmanabhan, Karur R . . . [# 271](#) in [IBA05](#)
 Padmanabhan, Karur R . . . [# 273](#) in [Posters](#)
 Padmanabhan, Karur R . . . [# 295](#) in [IBA03](#)
 Pain, S.D. . . . [# 164](#) in [NP09](#)
 Pain, SD . . . [# 73](#) in [NP09](#)
 Pain, S. D. . . . [# 205](#) in [NP09](#)
 Palczewski, Ari . . . [# 292](#) in [Posters](#)

Palitsin, Vladimir . . . [# 158](#) in [IBM04](#)
Palitsin, Vladimir . . . [# 162](#) in [IBM04](#) and [Posters](#)
Palitsin, Vladimir . . . [# 165](#) in [IBM04](#) and [Posters](#)
Palitsin, Vladimir . . . [# 348](#) in [IBA06](#)
Palitsin, Vladimir . . . [# 362](#) in [Posters](#)
Palles, Blake A. . . . [# 183](#) in [NBA02](#)
Palm, Andrew . . . [# 207](#) in [RE09](#)
Palm, Andrew . . . [# 209](#) in [RE09](#)
Palosaari, Mikko . . . [# 259](#) in [IBA07](#)
Pan, Cheng-Ta . . . [# 313](#) in [RE07](#)
Pandey, Bimal . . . [# 419](#) in [Posters](#)
Pandey, Avinash C . . . [# 315](#) in [Posters](#)
Pandey, Avinash C . . . [# 391](#) in [Posters](#)
Pandey, Avinash Chandra . . . [# 396](#) in [Posters](#)
Pandey, K K . . . [# 150](#) in [NST01](#) and [Posters](#)
Pandey, Ratnesh Kumar . . . [# 396](#) in [Posters](#)
Pandya, Sameer . . . [# 379](#) in [ATF06](#)
Paneta, V. . . . [# 176](#) in [Posters](#)
Panova, Tatayna V. . . . [# 238](#) in [Posters](#)
Pantelica, Dan . . . [# 211](#) in [ATF08](#)
Pantell, Richard H . . . [# 253](#) in [ATF06](#)
Pantell, Richard H. . . . [# 251](#) in [ATF07](#)
Park, Jangho . . . [# 444](#) in [NBA03](#)
Park, Sulgiye . . . [# 100](#) in [RE06](#)
Patel, Maulik . . . [# 389](#) in [Posters](#)
Patel, Tarun . . . [# 360](#) in [ATF01](#)
Pathak, A P . . . [# 317](#) in [Posters](#)
Pathak, Anand P . . . [# 14](#) in [IBM02](#)
Pathak, A P . . . [# 9](#) in [IBM02](#)
Pathak, A P . . . [# 48](#) in [Posters](#)
Pathak, A. P. . . . [# 15](#) in [IBM02](#)
PATHAK, A. P. . . . [# 16](#) in [Posters](#)
Patriarche, Gilles . . . [# 29](#) in [IBM05](#)
Paul, Michael . . . [# 468](#) in [ATF07](#)
Paulauskas, S. . . . [# 187](#) in [NP10](#)
Paulauskas, Stanley V . . . [# 278](#) in [NP04](#)
Paulauskas, S. V. . . . [# 470](#) in [Posters](#)
Peaslee, Graham F . . . [# 432](#) in [TA02](#)
Pechenkin, Valery A. . . . [# 326](#) in [Posters](#)
Pedersen, Henrik B. . . . [# 114](#) in [AMP01](#)
Peeler, Christopher . . . [# 492](#) in [MA01](#)
Peng, Haibo . . . [# 406](#) in [RE05](#)
Perdue, B. . . . [# 198](#) in [NP02](#)
Pereira, J. . . . [# 205](#) in [NP09](#)
Perez, Patrice . . . [# 298](#) in [NP07](#)
Perez, Patrice . . . [# 474](#) in [Posters](#)
Pérez, Miguel . . . [# 117](#) in [Posters](#)
Perez-Loureiro, D. . . . [# 205](#) in [NP09](#)
Perfect, Ed . . . [# 380](#) in [NP07](#)
Perkins, Luke T. . . . [# 379](#) in [ATF06](#)

Perkinson, Joy . . . [# 157](#) in [IBM05](#)
Persaud, Arun . . . [# 268](#) in [ATF06](#)
Persaud, Arun . . . [# 269](#) in [RE02](#)
Peters, W.A. . . . [# 164](#) in [NP09](#)
Peters, William A . . . [# 278](#) in [NP04](#)
Peters, E. E. . . . [# 403](#) in [TA02](#)
Petersen, C. . . . [# 243](#) in [HSD03](#)
Peterson, Randolph S. . . . [# 426](#) in [Posters](#)
Petre, Alexandru . . . [# 211](#) in [ATF08](#)
peuget, sylvain . . . [# 79](#) in [IBA09](#)
Phantkankum, Nuttapon . . . [# 235](#) in [RE09](#)
Philipp, Patrick . . . [# 65](#) in [RE07](#)
Phillips, Ryan E. . . . [# 53](#) in [ATF05](#) and [Posters](#)
Phinney, Lucas . . . [# 250](#) in [IBA09](#)
Phinney, Lucas C . . . [# 188](#) in [ATF08](#)
Phlips, B. F. . . . [# 146](#) in [HSD03](#)
Pia, Maria Grazia . . . [# 184](#) in [IBA04](#)
Piazza, Leandro AC . . . [# 94](#) in [HSD07](#)
Picollo, Federico . . . [# 245](#) in [NST02](#)
Piefer, Greg . . . [# 97](#) in [ATF04](#)
Piefer, Greg . . . [# 140](#) in [ATF07](#)
Piefer, Greg . . . [# 143](#) in [ATF02](#)
Piestrup, Melvin A . . . [# 253](#) in [ATF06](#)
Piestrup, Melvin M. . . . [# 251](#) in [ATF07](#)
Pilling, Sergio . . . [# 28](#) in [AMP03](#) and [Posters](#)
Pilskog, Ingjald . . . [# 312](#) in [AMP05](#)
Pimblott, Simon M . . . [# 451](#) in [RE05](#)
Ping, Yang . . . [# 15](#) in [IBM02](#)
Pitas, Katrina . . . [# 143](#) in [ATF02](#)
Pittman, S.T. . . . [# 164](#) in [NP09](#)
Pittman, ST . . . [# 73](#) in [NP09](#)
Ploszajczak, M. . . . [# 164](#) in [NP09](#)
Pogue, C. . . . [# 230](#) in [ATF03](#)
Pogue, Nate . . . [# 292](#) in [Posters](#)
Pogue, Nathaniel . . . [# 194](#) in [ATF01](#)
Pogue, Nathaniel . . . [# 239](#) in [NP01](#)
Pogue, Conor M . . . [# 180](#) in [Posters](#)
Policroniades, Rafael . . . [# 113](#) in [IBA07](#)
Policroniades, Rafael . . . [# 144](#) in [NP07](#)
Policroniades, Rafael . . . [# 145](#) in [Posters](#)
Polyakov, A. N. . . . [# 401](#) in [NP10](#)
Ponomarev, Oleksandr . . . [# 152](#) in [ATF08](#)
Poonia, Surendra . . . [# 6](#) in [AMP03](#) and [Posters](#)
Poonia, Surendra . . . [# 19](#) in [Posters](#)
Poonia, Surendra . . . [# 20](#) in [Posters](#)
Porzio, Giuseppe . . . [# 449](#) in [NP11](#)
Potter, James . . . [# 201](#) in [HSD06](#)
Poves, A. . . . [# 258](#) in [NP03](#)
Powers, N. . . . [# 243](#) in [HSD03](#)
Pozzi, S. . . . [# 243](#) in [HSD03](#)

Prabhakar, Pavana . . . [# 342](#) in [IBM07](#)
Prados-Estévez, F. M. . . . [# 403](#) in [TA02](#)
Price, Lloyd . . . [# 190](#) in [NST03](#)
Price, Lloyd . . . [# 261](#) in [RE01](#)
Prokop, C. . . . [# 205](#) in [NP09](#)
Prosa, Ty J. . . . [# 319](#) in [IBM03](#)
Ptasinska, Sylwia . . . [# 352](#) in [RE08](#)
Puglia, Denise . . . [# 33](#) in [IBA07](#)
Puttaraksa, N. . . . [# 471](#) in [Posters](#)
Putterman, Seth . . . [# 216](#) in [ATF07](#)
Qiang, Yi . . . [# 369](#) in [NP08](#)
Quaglia, J. . . . [# 205](#) in [NP09](#)
Quarles, Carroll A. . . . [# 92](#) in [NBA04](#)
Quinn, S. . . . [# 13](#) in [NP03](#)
Quinn, S. . . . [# 205](#) in [NP09](#)
Quinn, Rachel C. . . . [# 225](#) in [RE04](#)
Quinn, Heather Marie . . . [# 192](#) in [RE03](#)
Quinn, Heather Marie . . . [# 302](#) in [RE04](#)
Quiter, Brian J. . . . [# 44](#) in [ATF04](#)
Qureshi, Anjum . . . [# 64](#) in [IBM02](#) and [Posters](#)
Racolta, Petru Mihai . . . [# 214](#) in [IBA09](#)
Racolta, Petru Mihai . . . [# 219](#) in [IBM01](#)
Radel, Ross . . . [# 97](#) in [ATF04](#)
Radel, Ross . . . [# 140](#) in [ATF07](#)
Radel, Ross . . . [# 143](#) in [ATF02](#)
Radovinsky, Alexey . . . [# 336](#) in [HSD07](#)
raepsaet, caroline . . . [# 79](#) in [IBA09](#)
Rahman, Md. Shakilur . . . [# 320](#) in [AMP02](#)
Rajapaksa, Indrajith . . . [# 270](#) in [NST01](#)
Rajasekhara, Shreyas . . . [# 131](#) in [RE02](#)
Rajput, Parasmani . . . [# 391](#) in [Posters](#)
Ramana, P . . . [# 48](#) in [Posters](#)
Ramayya, A. V. . . . [# 470](#) in [Posters](#)
Ramos, Antonio Tonatiuh . . . [# 145](#) in [Posters](#)
Rao, S V S Nageswara . . . [# 48](#) in [Posters](#)
Rao, SVS Nageswara . . . [# 9](#) in [IBM02](#)
Ratcliffe, Naomi . . . [# 337](#) in [MA03](#) and [Posters](#)
Rathke, John . . . [# 444](#) in [NBA03](#)
Ratkiewicz, A. . . . [# 258](#) in [NP03](#)
Ratkiewicz, Andrew . . . [# 278](#) in [NP04](#)
Rauschenbach, B . . . [# 315](#) in [Posters](#)
Rauscher, T. . . . [# 13](#) in [NP03](#)
Ray, Nirmal . . . [# 360](#) in [ATF01](#)
Reece, Charles . . . [# 292](#) in [Posters](#)
Reed, R A . . . [# 225](#) in [RE04](#)
Reed, Robert A . . . [# 133](#) in [RE04](#)
Reed, Robert A. . . . [# 242](#) in [RE04](#)
Reedy, Edward T. E. . . . [# 358](#) in [NBA03](#)
Reedy, Edward T.E. . . . [# 274](#) in [Posters](#)
Rehm, K. Ernst . . . [# 159](#) in [PS04](#)

Reichardt, Ashley . . . [# 54](#) in [Posters](#)
Reinert, Anja . . . [# 436](#) in [IBA06](#)
Reinert, T. . . . [# 177](#) in [Posters](#)
Reinert, Tilo . . . [# 392](#) in [IBM01](#)
Reinert, Tilo . . . [# 436](#) in [IBA06](#)
Reinert, Tilo . . . [# 442](#) in [IBA07](#)
Reintsema, C . . . [# 259](#) in [IBA07](#)
Remnev, Gennadiy E. . . . [# 393](#) in [Posters](#)
Ren, Feng . . . [# 34](#) in [RE01](#)
Renne, P. R. . . . [# 203](#) in [Posters](#)
Revay, Zs. . . . [# 76](#) in [NBA03](#)
Rey, Jean-Michel . . . [# 298](#) in [NP07](#)
Rey, Jean-Michel . . . [# 474](#) in [Posters](#)
Rez, Peter . . . [# 290](#) in [NST02](#)
Rhoades, Rob L. . . . [# 290](#) in [NST02](#)
Ricard-McCutchan, E. . . . [# 258](#) in [NP03](#)
Richardson, Norman . . . [# 51](#) in [NBA03](#)
Richman, D. . . . [# 198](#) in [NP02](#)
Rinyu, László . . . [# 412](#) in [NP06](#)
Risley, Eric . . . [# 97](#) in [ATF04](#)
Rivarola, Roberto Daniel . . . [# 181](#) in [AMP05](#)
Rizzutto, Marcia . . . [# 18](#) in [IBA07](#)
Ro, Tae-Ik . . . [# 320](#) in [AMP02](#)
Roanhaus, Steven . . . [# 97](#) in [ATF04](#)
Roberto, J.B. . . . [# 401](#) in [NP10](#)
Roberts, Caroline A. . . . [# 426](#) in [Posters](#)
Rocha, Miguel . . . [# 144](#) in [NP07](#)
Rogachev, G. V. . . . [# 134](#) in [NP03](#)
Rogers, A. M. . . . [# 203](#) in [Posters](#)
Rogers, Bridget R. . . . [# 242](#) in [RE04](#)
Romero, Frank . . . [# 43](#) in [MA03](#)
Romero, Frank . . . [# 280](#) in [ATF02](#)
Romero-Romero, Elisa . . . [# 376](#) in [NP11](#)
Romero-Romero, Elisa . . . [# 487](#) in [Posters](#)
Rommel, J. Martin . . . [# 148](#) in [HSD02](#)
Roscoe, Bradley A . . . [# 464](#) in [ATF06](#)
Rose, David . . . [# 206](#) in [NBA03](#)
Ross, T. J. . . . [# 403](#) in [TA02](#)
Rossbach, M. . . . [# 76](#) in [NBA03](#)
Rossi, Sandro . . . [# 489](#) in [MA07](#)
Rossi, Carl J . . . [# 491](#) in [MA08](#)
Rotaru, Adrian Ionut . . . [# 219](#) in [IBM01](#)
Rothard, Hermann . . . [# 349](#) in [AMP02](#)
Rotsch, David . . . [# 282](#) in [MA03](#)
Roumie, M. . . . [# 104](#) in [Posters](#)
Roumie, M. . . . [# 105](#) in [Posters](#)
Roumie, Mohamad . . . [# 103](#) in [IBA08](#)
Rout, Bibhudutta . . . [# 139](#) in [Posters](#)
Rout, Bibhudutta . . . [# 182](#) in [NST06](#)
Rout, Bibhudutta . . . [# 213](#) in [Posters](#)

Rout, Bibhudutta . . . [# 323](#) in [Posters](#)
 Rout, Bibhudutta . . . [# 392](#) in [IBM01](#)
 Roy, Tushar . . . [# 360](#) in [ATF01](#)
 Ruelas, Marcos . . . [# 102](#) in [ATF06](#)
 Runceanu, Victor Alexandru . . . [# 219](#) in [IBM01](#)
 Rusakova, Irene . . . [# 270](#) in [NST01](#)
 Rusakova, Irene . . . [# 425](#) in [IBM01](#)
 Rusnak, Brian . . . [# 206](#) in [NBA03](#)
 Rusnak, Brian . . . [# 216](#) in [ATF07](#)
 Ruth, T. J. . . . [# 153](#) in [MA03](#)
 Rybarczyk, Lawrence J . . . [# 371](#) in [ATF04](#) and [Posters](#)
 Rykaczewski, K.P. . . . [# 401](#) in [NP10](#)
 Rykaczewski, Krzysztof . . . [# 278](#) in [NP04](#)
 Rykaczewski, Krzysztof . . . [# 385](#) in [NP10](#)
 Rykaczewski, K. P. . . . [# 470](#) in [Posters](#)
 Rykovanov, Sergey . . . [# 44](#) in [ATF04](#)
 Rynes, Joel . . . [# 108](#) in [HSD01](#)
 S V S, Nageswara Rao . . . [# 14](#) in [IBM02](#)
 Sabelnikov, A.V. . . . [# 401](#) in [NP10](#)
 Sachs, A . . . [# 73](#) in [NP09](#)
 sacquin, Yves . . . [# 298](#) in [NP07](#)
 Sacquin, Yves . . . [# 474](#) in [Posters](#)
 Safiq, Alexandra D . . . [# 193](#) in [Posters](#)
 Safiq, Alexandra D. . . . [# 101](#) in [TA02](#)
 Sagaidak, R. N. . . . [# 401](#) in [NP10](#)
 Sahi, Sunil K . . . [# 221](#) in [NST01](#)
 Saikiran, V . . . [# 317](#) in [Posters](#)
 Sajavaara, Timo . . . [# 259](#) in [IBA07](#)
 Saleem, Iram . . . [# 270](#) in [NST01](#)
 Saleem, Iram . . . [# 287](#) in [IBA09](#)
 Saleem, Iram . . . [# 355](#) in [IBM05](#)
 Saleem, Iram . . . [# 384](#) in [Posters](#)
 Salehzadeh, Arash . . . [# 120](#) in [Posters](#)
 Salvadori, Maria Cecilia . . . [# 91](#) in [NST05](#)
 Salvadori, Daisy M F . . . [# 91](#) in [NST05](#)
 Sanchez, Daniel . . . [# 467](#) in [MA01](#)
 Sanjari, Shahab . . . [# 462](#) in [AMP04](#)
 Santa Rita, Pedro . . . [# 145](#) in [Posters](#)
 Santia, M. . . . [# 205](#) in [NP09](#)
 Santiago-Gonzalez, D. . . . [# 134](#) in [NP03](#)
 Santonil, Z. C. . . . [# 403](#) in [TA02](#)
 Santos, Anthony C. F. . . . [# 332](#) in [Posters](#)
 Santos, Antonio C. F. . . . [# 28](#) in [AMP03](#) and [Posters](#)
 Santos, Antonio Carlos Fontes dos . . . [# 338](#) in [Posters](#)
 Saracco, Paolo . . . [# 184](#) in [IBA04](#)
 sarkar, Parthsarathi . . . [# 360](#) in [ATF01](#)
 sasmal, kalyan . . . [# 425](#) in [IBM01](#)
 Sataka, M. . . . [# 232](#) in [IBM02](#) and [Posters](#)
 Sattarov, Akhdiyor . . . [# 194](#) in [ATF01](#)
 Sattarov, Akhdiyor . . . [# 239](#) in [NP01](#)

Sattarov, Akhdiyor I . . . [# 252](#) in [RE02](#)
Sava, Tiberiu Bogdan . . . [# 211](#) in [ATF08](#)
Saveliev, Valeri D. . . . [# 387](#) in [HSD04](#)
Saverskiy, Aleksandr . . . [# 148](#) in [HSD02](#)
Savin, Daniel Wolf . . . [# 279](#) in [AMP01](#)
Sayre, Daniel B. . . . [# 142](#) in [NP05](#)
Schaffer, P. . . . [# 153](#) in [MA03](#)
Schambach, Joachim . . . [# 322](#) in [NP08](#)
Scharf, Andreas . . . [# 228](#) in [NP06](#) and [Posters](#)
Scharf, Andreas . . . [# 351](#) in [NP11](#)
Schatz, H . . . [# 73](#) in [NP09](#)
Schatz, H. . . . [# 205](#) in [NP09](#)
Schenk, Gerald . . . [# 118](#) in [Posters](#)
Schenkel, Thomas . . . [# 268](#) in [ATF06](#)
Schenkel, Thomas . . . [# 269](#) in [RE02](#)
Schiettekatte, Francois . . . [# 422](#) in [IBA02](#)
Schindler, Matthias . . . [# 228](#) in [NP06](#) and [Posters](#)
Schindler, Matthias . . . [# 351](#) in [NP11](#)
Schippers, Stefan . . . [# 58](#) in [AMP02](#)
Schippers, Stefan . . . [# 345](#) in [AMP04](#)
Schippers, Stefan . . . [# 349](#) in [AMP02](#)
Schmidt, Andrea . . . [# 206](#) in [NBA03](#)
Schmidt, D . . . [# 259](#) in [IBA07](#)
Schmitt, K.T. . . . [# 164](#) in [NP09](#)
Schmitt, KT . . . [# 73](#) in [NP09](#)
Schmitt, Bruce E . . . [# 110](#) in [Posters](#)
Scholz, Michael . . . [# 456](#) in [MA01](#)
Schrimpf, Ronald D . . . [# 133](#) in [RE04](#)
Schrimpf, Ronald D. . . . [# 242](#) in [RE04](#)
Schroder, Nadia . . . [# 33](#) in [IBA07](#)
Schroeder, Carl B . . . [# 283](#) in [ATF05](#)
Schroeder, Carl B. . . . [# 44](#) in [ATF04](#)
Schuch, Reinhold . . . [# 399](#) in [AMP02](#)
Schuch, Reinhold H . . . [# 409](#) in [AMP04](#)
Schulte, Reinhard . . . [# 424](#) in [MA06](#)
Schulte, Reinhard W . . . [# 427](#) in [MA04](#)
Schulte-Borchers, M. . . . [# 90](#) in [IBA04](#)
Schultheiss, Tom . . . [# 444](#) in [NBA03](#)
Schultz, D R . . . [# 457](#) in [AMP02](#)
Schulz, Michael . . . [# 378](#) in [AMP03](#)
Schumer, J. W. . . . [# 146](#) in [HSD03](#)
Schuricke, Michael . . . [# 378](#) in [AMP03](#)
Schury, Peter . . . [# 353](#) in [NP10](#)
Schwartz, S. B. . . . [# 205](#) in [NP09](#)
Schwellenbach, David . . . [# 201](#) in [HSD06](#)
Schwellenbach, David . . . [# 204](#) in [Posters](#)
Schwingle, Ryan . . . [# 204](#) in [Posters](#)
Schwoebel, Paul R. . . . [# 341](#) in [ATF07](#)
Seal, Sudipta . . . [# 453](#) in [RE08](#)
Sears, Jason . . . [# 206](#) in [NBA03](#)

Seely, D G . . . [# 457](#) in [AMP02](#)
Seely, D. G. . . . [# 47](#) in [AMP01](#) and [Posters](#)
Seetala, Naidu V. . . . [# 428](#) in [RE05](#)
Segebade, C. . . . [# 115](#) in [NBA01](#)
Segebade, Christian . . . [# 455](#) in [NBA01](#)
Seipel, Heather . . . [# 84](#) in [Posters](#)
Seipel, Heather A. . . . [# 358](#) in [NBA03](#)
SEKI, Toshio . . . [# 88](#) in [IBM04](#)
SEKI, Toshio . . . [# 89](#) in [NST06](#)
Sell, David A. . . . [# 290](#) in [NST02](#)
Sencer, Bulent . . . [# 335](#) in [IBA01](#)
Sengbusch, Evan . . . [# 97](#) in [ATF04](#)
Sengbusch, Evan . . . [# 140](#) in [ATF07](#)
Sengbusch, Evan . . . [# 143](#) in [ATF02](#)
Serkland, D K . . . [# 124](#) in [RE03](#)
Serkland, Darwin K. . . . [# 446](#) in [RE04](#) and [Posters](#)
Serris, Michael . . . [# 132](#) in [NBA04](#)
Serruys, Yves . . . [# 61](#) in [IBM07](#)
Serruys, Yves . . . [# 67](#) in [RE07](#)
Serruys, Yves . . . [# 233](#) in [RE02](#)
SERRUYS, Yves . . . [# 330](#) in [IBA05](#)
Seryi, Andrei . . . [# 129](#) in [ATF05](#) and [Posters](#)
Seyfert, Chris . . . [# 97](#) in [ATF04](#)
Seyfert, Chris . . . [# 140](#) in [ATF07](#)
Seyfert, Chris . . . [# 143](#) in [ATF02](#)
Shaevitz, Michael . . . [# 395](#) in [Posters](#)
Shanab, S. . . . [# 205](#) in [NP09](#)
Shanks, C. . . . [# 153](#) in [MA03](#)
Shannon, Steven Christopher . . . [# 218](#) in [RE06](#)
Shao, Lin . . . [# 190](#) in [NST03](#)
Shao, Lin . . . [# 197](#) in [NST03](#)
Shao, Lin . . . [# 261](#) in [RE01](#)
Shao, Lin . . . [# 325](#) in [RE02](#)
Shao, Lin . . . [# 326](#) in [Posters](#)
Shao, Lin . . . [# 335](#) in [IBA01](#)
SHAO, LIN . . . [# 382](#) in [NST04](#)
Shao, Lin . . . [# 383](#) in [NST03](#)
SHARMA, AJAY . . . [# 231](#) in [NP02](#) and [Posters](#)
Sharp, D. K. . . . [# 258](#) in [NP03](#)
Shatos, Ashlynn . . . [# 204](#) in [Posters](#)
Shaughnessy, Dawn . . . [# 310](#) in [NP05](#)
Shaw, Brian H. . . . [# 283](#) in [ATF05](#)
Shedlock, Daniel . . . [# 212](#) in [HSD02](#)
Sherven, Carl . . . [# 97](#) in [ATF04](#)
Shevelev, M. . . . [# 129](#) in [ATF05](#) and [Posters](#)
Shia, David . . . [# 473](#) in [MA06](#)
Shields, D. . . . [# 198](#) in [NP02](#)
Shimel, Guy . . . [# 468](#) in [ATF07](#)
Shimoura, Susumu . . . [# 3](#) in [ATF05](#)
Shinpaugh, Jefferson . . . [# 453](#) in [RE08](#)

Shipman, Patrick D. . . . [# 173](#) in [NST08](#)
Shirimpaka, Jean . . . [# 426](#) in [Posters](#)
Shirokovsky, I. V. . . . [# 401](#) in [NP10](#)
Shiromaru, H. . . . [# 90](#) in [IBA04](#)
Shor, Asher . . . [# 468](#) in [ATF07](#)
Short, Mike P. . . . [# 326](#) in [Posters](#)
Shriner Jr, J.F. . . . [# 164](#) in [NP09](#)
Shubeita, Samir . . . [# 189](#) in [IBA02](#)
Shukla, Mayank . . . [# 360](#) in [ATF01](#)
Shumeyko, M. V. . . . [# 401](#) in [NP10](#)
Shutthanandan, Shuttha . . . [# 359](#) in [IBM07](#)
Shutthanandan, Shuttha . . . [# 440](#) in [IBM06](#)
Shutthanandan, Vaithiyalingam . . . [# 83](#) in [IBA03](#)
Shutthanandan, Vaithiyalingam . . . [# 154](#) in [Posters](#)
Shutthanandan, Vaithiyalingam . . . [# 429](#) in [IBM07](#)
Shutthanandan, Vaithiyalingam . . . [# 430](#) in [IBA03](#)
Shutthanandan, Vaithiyalingam . . . [# 459](#) in [IBM03](#) and [Posters](#)
Shymanski, Vitaliy I. . . . [# 393](#) in [Posters](#)
Sias, Uilson S. . . . [# 112](#) in [IBM06](#)
Sickafus, Kurt . . . [# 389](#) in [Posters](#)
Sickafus, Kurt Edward . . . [# 443](#) in [RE05](#)
Sidibe, Moussa . . . [# 233](#) in [RE02](#)
Sigaud, Lucas M . . . [# 55](#) in [AMP05](#)
Siggaud, Lucas . . . [# 338](#) in [Posters](#)
Siketic, Zdravko . . . [# 106](#) in [IBA06](#)
Silber, Joe . . . [# 322](#) in [NP08](#)
Silk, James D . . . [# 329](#) in [HSD03](#)
Silva, Glenda N da . . . [# 91](#) in [NST05](#)
Silverman, Ido . . . [# 468](#) in [ATF07](#)
Simeckova, Eva . . . [# 128](#) in [NBA01](#)
Simion, Corina . . . [# 211](#) in [ATF08](#)
Simon, A. . . . [# 13](#) in [NP03](#)
Simon, A. . . . [# 205](#) in [NP09](#)
Simon, Aliz . . . [# 308](#) in [NP01](#)
Simon, M. J. . . . [# 90](#) in [IBA04](#)
Singh, Dolly . . . [# 64](#) in [IBM02](#) and [Posters](#)
Singh, Fouran . . . [# 391](#) in [Posters](#)
Singh, Nand Lal . . . [# 64](#) in [IBM02](#) and [Posters](#)
Singh, B. N. . . . [# 47](#) in [AMP01](#) and [Posters](#)
Singkarat, S. . . . [# 471](#) in [Posters](#)
Sinha, Amar . . . [# 360](#) in [ATF01](#)
Sinha, Saloni A. . . . [# 288](#) in [NST05](#)
Sisourat, Nicolas . . . [# 312](#) in [AMP05](#)
Skala, Wayne G . . . [# 136](#) in [IBA09](#)
Skukan, Natko . . . [# 246](#) in [IBM01](#)
Sleaford, B. . . . [# 76](#) in [NBA03](#)
Slyder, Aaron M. . . . [# 288](#) in [NST05](#)
Smirnov, Alexei Vladimirovich . . . [# 102](#) in [ATF06](#)
Smit, Ziga . . . [# 17](#) in [IBA04](#)
Smith, M.S. . . . [# 164](#) in [NP09](#)

Smith, Mike . . . [# 102](#) in [ATF06](#)
Smith, Mike . . . [# 358](#) in [NBA03](#)
Smith, MS . . . [# 73](#) in [NP09](#)
Smith, Andrew D . . . [# 451](#) in [RE05](#)
Smith, Jennifer L . . . [# 196](#) in [TA02](#)
Smith, Jennifer L . . . [# 207](#) in [RE09](#)
Smith, Jennifer L . . . [# 209](#) in [RE09](#)
Smith, Jennifer L . . . [# 210](#) in [RE09](#)
Smith, Jeremy W . . . [# 193](#) in [Posters](#)
Smith, Jeremy W . . . [# 101](#) in [TA02](#)
Smyth, Vere . . . [# 424](#) in [MA06](#)
Snyder, John . . . [# 157](#) in [IBM05](#)
Solberg, Tim . . . [# 467](#) in [MA01](#)
Solís, corina . . . [# 113](#) in [IBA07](#)
Solís, Corina . . . [# 135](#) in [NP11](#)
Solovyev, Vladimir G . . . [# 85](#) in [HSD02](#)
Solov'yov, Andrey V . . . [# 408](#) in [RE08](#)
Sones, Bryndol A . . . [# 400](#) in [ATF06](#)
Song, Miao . . . [# 311](#) in [NST04](#)
Sonoda, Tetsu . . . [# 353](#) in [NP10](#)
Sooby, Elizabeth S . . . [# 252](#) in [RE02](#)
Spillmann, Uwe . . . [# 345](#) in [AMP04](#)
Spillmann, Uwe . . . [# 349](#) in [AMP02](#)
Spitz, Joshua . . . [# 395](#) in [Posters](#)
Spuches, Charles M . . . [# 196](#) in [TA02](#)
Spyrou, A. . . . [# 205](#) in [NP09](#)
Spyrou, Artemis . . . [# 13](#) in [NP03](#)
Stamatopoulos, A. . . . [# 176](#) in [Posters](#)
Stancil, P C . . . [# 457](#) in [AMP02](#)
Stan-Sion, Catalin . . . [# 211](#) in [ATF08](#)
Starovoitova, Valeriia . . . [# 5](#) in [NBA01](#)
Starovoitova, Valeriia . . . [# 321](#) in [MA03](#)
Starovoitova, Valeriia N . . . [# 22](#) in [ATF04](#)
Starovoitova, Valeriia N . . . [# 23](#) in [ATF01](#)
Starovoitova, Valeriia N . . . [# 24](#) in [ATF02](#)
Starovoitova, Valeriia N . . . [# 25](#) in [MA02](#)
Starovoitova, Valeriia N . . . [# 70](#) in [ATF03](#)
Steck, Markus . . . [# 462](#) in [AMP04](#)
Steele, Jay . . . [# 475](#) in [MA04](#)
Stefanescu, I. . . . [# 258](#) in [NP03](#)
Stefanik, Milan . . . [# 128](#) in [NBA01](#)
Steinke, Sven . . . [# 44](#) in [ATF04](#)
Stepinski, Dominique . . . [# 282](#) in [MA03](#)
Stevenson, John . . . [# 85](#) in [HSD02](#)
Stewart, Joel A . . . [# 426](#) in [Posters](#)
Stezelberger, Thorsten . . . [# 322](#) in [NP08](#)
Stohlker, Thomas . . . [# 485](#) in [PS02](#)
Stöhlker, Thomas . . . [# 345](#) in [AMP04](#)
Stöhlker, Thomas . . . [# 349](#) in [AMP02](#)
Stöhlker, Thomas . . . [# 399](#) in [AMP02](#)

Stöhlker, Thomas . . . [# 462](#) in [AMP04](#)
Stolterfoht, N . . . [# 66](#) in [AMP05](#)
Stone, Jirina . . . [# 278](#) in [NP04](#)
Stone, Nick . . . [# 278](#) in [NP04](#)
Stoner, Jon L . . . [# 24](#) in [ATF02](#)
Storizhko, Volodymyr . . . [# 151](#) in [Posters](#)
Storizhko, Volodymyr . . . [# 152](#) in [ATF08](#)
Storms, Scott . . . [# 147](#) in [HSD02](#)
Storms, Stephan . . . [# 102](#) in [ATF06](#)
Stowe, Malorie . . . [# 467](#) in [MA01](#)
Stoyer, M. A. . . . [# 401](#) in [NP10](#)
Stracener, D.W. . . . [# 164](#) in [NP09](#)
Stracener, Dan W . . . [# 278](#) in [NP04](#)
Stracener, Daniel W . . . [# 373](#) in [NP07](#)
Stracener, D. W. . . . [# 470](#) in [Posters](#)
Stracener, Dan W. . . . [# 376](#) in [NP11](#)
Strasser, Daniel . . . [# 316](#) in [AMP01](#)
Straticiuc, Mihai . . . [# 211](#) in [ATF08](#)
Straticiuc, Mihai . . . [# 214](#) in [IBA09](#)
Straticiuc, Mihai . . . [# 219](#) in [IBM01](#)
Strellis, Dan . . . [# 39](#) in [ATF04](#)
Strellis, Dan . . . [# 85](#) in [HSD02](#)
Strellis, Dan A . . . [# 30](#) in [HSD01](#)
Strellis, Dan A . . . [# 31](#) in [HSD07](#)
Strickland, Rachel . . . [# 372](#) in [Posters](#)
Stuhl, Alexander . . . [# 351](#) in [NP11](#)
Subbotin, V. G. . . . [# 401](#) in [NP10](#)
Subramaniam, Kumar . . . [# 459](#) in [IBM03](#) and [Posters](#)
Suchyta, S. . . . [# 205](#) in [NP09](#)
Sukhov, A. M. . . . [# 401](#) in [NP10](#)
Sulik, Béla . . . [# 463](#) in [Posters](#)
Summers, N. . . . [# 76](#) in [NBA03](#)
Summers, Paige A . . . [# 116](#) in [MA06](#)
Sun, Xiangming . . . [# 322](#) in [NP08](#)
Sun, Z. . . . [# 115](#) in [NBA01](#)
Surdutovich, Eugene . . . [# 408](#) in [RE08](#)
Surko, Clifford M . . . [# 226](#) in [NBA04](#)
Surzhykov, Andrey . . . [# 349](#) in [AMP02](#)
Suslova, Anastassiya . . . [# 75](#) in [Posters](#)
Swanekamp, S. B. . . . [# 146](#) in [HSD03](#)
Swenson, Donald A. . . . [# 294](#) in [Posters](#)
Synal, H. A. . . . [# 90](#) in [IBA04](#)
Sypchenko, Vladimir S. . . . [# 35](#) in [Posters](#)
Szelezniak, Michal . . . [# 322](#) in [NP08](#)
Szentmiklosi, L. . . . [# 76](#) in [NBA03](#)
Szilasi, Szabolcs . . . [# 303](#) in [Posters](#)
Szilasi, Szabolcs Z . . . [# 139](#) in [Posters](#)
Szilasi, Szabolcs Z . . . [# 213](#) in [Posters](#)
Szilasi, Szabolcs Z . . . [# 267](#) in [Posters](#)
Szilasi, S. Z. . . . [# 177](#) in [Posters](#)

Tabacniks, Manfredo . . . [# 249](#) in [Posters](#)
Tabacniks, Manfredo Harri . . . [# 18](#) in [IBA07](#)
Tabbal, Malek . . . [# 103](#) in [IBA08](#)
Tadic, Tonci . . . [# 106](#) in [IBA06](#)
Takei, Kuniharu . . . [# 268](#) in [ATF06](#)
Talagala, Punya . . . [# 295](#) in [IBA03](#)
Taleei, Reza . . . [# 492](#) in [MA01](#)
Tang, Ming . . . [# 122](#) in [RE05](#)
Tang, Ming . . . [# 389](#) in [Posters](#)
Tang, Vincent . . . [# 206](#) in [NBA03](#)
Tang, Vincent . . . [# 216](#) in [ATF07](#)
Tang, Zhong . . . [# 425](#) in [IBM01](#)
Tanis, J A . . . [# 66](#) in [AMP05](#)
Tanis, J A . . . [# 111](#) in [IBA01](#)
Tantawi, Sami G . . . [# 447](#) in [HSD02](#)
Tatar, Erdinch . . . [# 5](#) in [NBA01](#)
Tatum, B Alan . . . [# 373](#) in [NP07](#)
Tay, X. W. . . . [# 15](#) in [IBM02](#)
Teixeira, Fernanda S . . . [# 91](#) in [NST05](#)
TERAKAWA, Atsuki . . . [# 107](#) in [IBA07](#)
Teramoto, T. . . . [# 232](#) in [IBM02](#) and [Posters](#)
Terrasi, Filippo . . . [# 449](#) in [NP11](#)
Terwagne, Guy . . . [# 431](#) in [ATF08](#)
Tesmer, Joseph . . . [# 252](#) in [RE02](#)
Tesmer, Joseph . . . [# 372](#) in [Posters](#)
Tesmer, Joseph . . . [# 407](#) in [IBA05](#)
Tevuthasan, Theva . . . [# 359](#) in [IBM07](#)
Thapa, Chandra . . . [# 295](#) in [IBA03](#)
Thevuthasan, Suntharampillai . . . [# 440](#) in [IBM06](#)
Thevuthasan, Theva . . . [# 98](#) in [IBM04](#)
Thiagalingam, E. . . . [# 205](#) in [NP09](#)
Thomas, Alexander G R . . . [# 220](#) in [ATF05](#)
Thompson, P . . . [# 73](#) in [NP09](#)
Thompson, P. . . . [# 205](#) in [NP09](#)
Thompson, Thad . . . [# 183](#) in [NBA02](#)
Thompson, Jeffrey S. . . . [# 354](#) in [Posters](#)
Thongleurm, C. . . . [# 471](#) in [Posters](#)
Threadgold, James . . . [# 166](#) in [HSD01](#)
Tilakaratne, Buddhi . . . [# 355](#) in [IBM05](#)
Tilakaratne, Buddhi . . . [# 384](#) in [Posters](#)
Tilakaratne, Buddhi P . . . [# 270](#) in [NST01](#)
Tilakaratne, Buddhi P . . . [# 287](#) in [IBA09](#)
Tilakaratne, Buddhi Prasanga . . . [# 277](#) in [NST09](#)
Tilo, Reinert . . . [# 182](#) in [NST06](#)
Tippawan, U. . . . [# 471](#) in [Posters](#)
Titt, Uwe . . . [# 461](#) in [MA01](#)
Titt, Uwe . . . [# 492](#) in [MA01](#)
Tkac, Peter . . . [# 280](#) in [ATF02](#)
Tkac, Peter . . . [# 282](#) in [MA03](#)
Toader, Adina . . . [# 363](#) in [Posters](#)

Toader, Ovidiu F . . . [# 244](#) in [TA01](#)
Todd, Alan . . . [# 444](#) in [NBA03](#)
Tokunaga, Kazutoshi . . . [# 291](#) in [Posters](#)
Toloczko, Mychailo B. . . . [# 325](#) in [RE02](#)
Toloczko, Mychailo B. . . . [# 326](#) in [Posters](#)
Tomandl, Ivo . . . [# 266](#) in [Posters](#)
Toth, Csaba . . . [# 44](#) in [ATF04](#)
Toups, Matt . . . [# 395](#) in [Posters](#)
Tovesson, F. . . . [# 198](#) in [NP02](#)
Townsend, Peter David . . . [# 49](#) in [IBM06](#)
Toyoda, Noriaki . . . [# 60](#) in [NST09](#)
Tracy, Cameron Lee . . . [# 100](#) in [RE06](#)
Traina, Paolo . . . [# 246](#) in [IBM01](#)
Trautmann, Christina . . . [# 100](#) in [RE06](#)
Treachner, Alex H . . . [# 215](#) in [Posters](#)
Tripathi, Ram K . . . [# 453](#) in [RE08](#)
Tripathi, Jitendra Kumar . . . [# 454](#) in [IBM01](#)
Trocellier, Patrick . . . [# 61](#) in [IBM07](#)
Trocellier, Patrick . . . [# 67](#) in [RE07](#)
Trocellier, Patrick . . . [# 233](#) in [RE02](#)
TROCELLIER, Patrick . . . [# 330](#) in [IBA05](#)
Trotsenko, Sergij . . . [# 345](#) in [AMP04](#)
Trotsenko, Sergiy . . . [# 262](#) in [AMP04](#)
Trotsenko, Sergiy . . . [# 349](#) in [AMP02](#)
Trusdale, Victoria . . . [# 385](#) in [NP10](#)
Tsoupas, Nicholaos . . . [# 109](#) in [MA04](#)
Tsuchida, Hidetsugu . . . [# 123](#) in [Posters](#)
Tsuchiya, Bun . . . [# 123](#) in [Posters](#)
Tsuchiya, Bun . . . [# 291](#) in [Posters](#)
Tsyganov, Yu. S. . . . [# 401](#) in [NP10](#)
Tu, Xiaolin . . . [# 462](#) in [AMP04](#)
Tucker, Abigail . . . [# 98](#) in [IBM04](#)
Tull-Walker, Naeem . . . [# 428](#) in [RE05](#)
Turner, John . . . [# 69](#) in [ATF04](#)
Turos, Andrzej . . . [# 42](#) in [IBM02](#)
Tyliszczak, Tolek . . . [# 416](#) in [IBM03](#)
Tynan, George R. . . . [# 407](#) in [IBA05](#)
Uberuaga, Blas . . . [# 347](#) in [IBM03](#)
Uberuaga, Blas P . . . [# 57](#) in [RE06](#)
Uglov, Vladimir V. . . . [# 393](#) in [Posters](#)
Ukai, Shigeharu . . . [# 325](#) in [RE02](#)
Ulfig, Robert M. . . . [# 319](#) in [IBM03](#)
Ullom, Joel . . . [# 259](#) in [IBA07](#)
Ullrich, Susanne . . . [# 71](#) in [RE08](#)
Umstadter, D. P. . . . [# 243](#) in [HSD03](#)
Unai, S. . . . [# 471](#) in [Posters](#)
Urakawa, J. . . . [# 129](#) in [ATF05](#) and [Posters](#)
Urbain, Xavier . . . [# 279](#) in [AMP01](#)
Uribe, Roberto M . . . [# 235](#) in [RE09](#)
Utyonkov, V.K. . . . [# 401](#) in [NP10](#)

Uzunyan, Sergey A . . . [# 95](#) in [MA04](#)
V, Saikiran . . . [# 14](#) in [IBM02](#)
Vacik, Jiri . . . [# 264](#) in [NST03](#)
Vacik, Jiri . . . [# 266](#) in [Posters](#)
Vainionpaa, Jaakko Hannes . . . [# 253](#) in [ATF06](#)
Vainionpaa, Jaako Hannes . . . [# 251](#) in [ATF07](#)
Valastyán, Ivan . . . [# 463](#) in [Posters](#)
Valdez, James . . . [# 389](#) in [Posters](#)
Valdez, James . . . [# 439](#) in [RE01](#)
Valliant, J. F. . . . [# 153](#) in [MA03](#)
Valvo, Francesca . . . [# 489](#) in [MA07](#)
Van Bibber, K. . . . [# 203](#) in [Posters](#)
Van den Berg, Jaap . . . [# 367](#) in [Posters](#)
Van den Eynde, Gert . . . [# 62](#) in [ATF01](#)
van den Mooter, Guy . . . [# 348](#) in [IBA06](#)
van Goethem, Marc-Jan . . . [# 445](#) in [Posters](#)
Van Reeth, P. . . . [# 223](#) in [AMP03](#)
van Tilborg, Jeroen . . . [# 283](#) in [ATF05](#)
Vandegrift, George . . . [# 280](#) in [ATF02](#)
Vandegrift, George . . . [# 282](#) in [MA03](#)
Vanhoy, J. R. . . . [# 403](#) in [TA02](#)
Vanin, Vito . . . [# 249](#) in [Posters](#)
Varca, Gustavo H. C. . . . [# 229](#) in [NST05](#)
Vardar, Gulin . . . [# 275](#) in [IBA05](#)
Varela, Armando . . . [# 113](#) in [IBA07](#)
Varela, Armando . . . [# 144](#) in [NP07](#)
Varela, Armando . . . [# 145](#) in [Posters](#)
Varga, Tamas . . . [# 440](#) in [IBM06](#)
Vargas, Hesiquio . . . [# 113](#) in [IBA07](#)
Variale, Vincenzo . . . [# 32](#) in [HSD06](#)
VAUBAILLON, Sylvain . . . [# 330](#) in [IBA05](#)
Vemuri, Rama Sessa R . . . [# 83](#) in [IBA03](#)
Vendamani, V S . . . [# 9](#) in [IBM02](#)
Vendamani, V S . . . [# 48](#) in [Posters](#)
Veres, Mihály . . . [# 412](#) in [NP06](#)
Verma, Avinash . . . [# 102](#) in [ATF06](#)
Vetter, Kai . . . [# 44](#) in [ATF04](#)
Videbaek, Flemming . . . [# 322](#) in [NP08](#)
Vilayurganapathy, S. . . . [# 388](#) in [IBM01](#)
Vilkhivskaya, Olga V. . . . [# 35](#) in [Posters](#)
Vineyard, Michael F . . . [# 193](#) in [Posters](#)
Vineyard, Michael F. . . . [# 101](#) in [TA02](#)
Vischioni, Barbara . . . [# 489](#) in [MA07](#)
Visière, Serge . . . [# 298](#) in [NP07](#)
Visière, Serge . . . [# 474](#) in [Posters](#)
Vitolo, Viviana . . . [# 489](#) in [MA07](#)
Vittone, Ettore . . . [# 245](#) in [NST02](#)
Vizkelethy, G . . . [# 124](#) in [RE03](#)
Vizkelethy, G. . . . [# 222](#) in [RE03](#)
Vizkelethy, Gyorgy . . . [# 318](#) in [RE03](#)

Vlastou, R. . . . [# 176](#) in [Posters](#)
 Vlastou, Rosa . . . [# 132](#) in [NBA04](#)
 Voinov, A. A. . . . [# 401](#) in [NP10](#)
 Voitkiv, Alexander . . . [# 349](#) in [AMP02](#)
 Vop, Phuong . . . [# 473](#) in [MA06](#)
 Voss, Philip J. . . . [# 402](#) in [NP01](#)
 Vostokin, G. K. . . . [# 401](#) in [NP10](#)
 Voyevodin, Victor N. . . . [# 325](#) in [RE02](#)
 Voyevodin, Victor N. . . . [# 326](#) in [Posters](#)
 Vu, Chinh . . . [# 322](#) in [NP08](#)
 Wada, Michiharu . . . [# 353](#) in [NP10](#)
 Wadsworth, Robert . . . [# 385](#) in [NP10](#)
 Wagner, Friedrich E. . . . [# 436](#) in [IBA06](#)
 Waldron, William . . . [# 208](#) in [Posters](#)
 Waldron, William L. . . . [# 269](#) in [RE02](#)
 Walker, Azida H. . . . [# 276](#) in [Posters](#)
 Wallace, Joseph . . . [# 190](#) in [NST03](#)
 Wallace, Joseph . . . [# 197](#) in [NST03](#)
 Wallace, Joseph . . . [# 383](#) in [NST03](#)
 Wallig, Joseph . . . [# 208](#) in [Posters](#)
 Wallner, Anton . . . [# 227](#) in [NP06](#)
 Walsh, K. A. . . . [# 258](#) in [NP03](#)
 Walters, M. . . . [# 205](#) in [NP09](#)
 Waltz, Cory S. . . . [# 203](#) in [Posters](#)
 Wampler, William R. . . . [# 318](#) in [RE03](#)
 Wang, Haiyan . . . [# 168](#) in [RE06](#)
 Wang, Haoyu . . . [# 179](#) in [NBA02](#)
 Wang, Haoyu . . . [# 185](#) in [NBA02](#)
 Wang, Haoyu . . . [# 365](#) in [Posters](#)
 Wang, Jianwei . . . [# 163](#) in [RE06](#)
 Wang, Jing . . . [# 190](#) in [NST03](#)
 Wang, Jing . . . [# 197](#) in [NST03](#)
 Wang, Siwei . . . [# 122](#) in [RE05](#)
 wang, Tieshan . . . [# 406](#) in [RE05](#)
 Wang, Xi . . . [# 40](#) in [Posters](#)
 Wang, Xuemei . . . [# 190](#) in [NST03](#)
 Wang, Xuemei . . . [# 197](#) in [NST03](#)
 Wang, Xuemei . . . [# 261](#) in [RE01](#)
 Wang, Xuemei . . . [# 270](#) in [NST01](#)
 Wang, Yen-Nai . . . [# 387](#) in [HSD04](#)
 Wang, Yongqiang . . . [# 34](#) in [RE01](#)
 Wang, Yongqiang . . . [# 218](#) in [RE06](#)
 Wang, Yongqiang . . . [# 252](#) in [RE02](#)
 Wang, Yongqiang . . . [# 275](#) in [IBA05](#)
 Wang, Yongqiang . . . [# 347](#) in [IBM03](#)
 Wang, Yongqiang . . . [# 372](#) in [Posters](#)
 Wang, Yongqiang . . . [# 389](#) in [Posters](#)
 Wang, Yongqiang . . . [# 407](#) in [IBA05](#)
 Wang, Yongqiang . . . [# 411](#) in [RE01](#)
 Wang, Yongqiang . . . [# 437](#) in [RE06](#)

Wang, Yongqiang . . . [# 439](#) in [RE01](#)
Wang, Zhaoying . . . [# 98](#) in [IBM04](#)
Wang, Yongqiang Q . . . [# 57](#) in [RE06](#)
Ward, S.J. . . . [# 223](#) in [AMP03](#)
Warmenhoven, John-William . . . [# 162](#) in [IBM04](#) and [Posters](#)
Was, Gary S . . . [# 244](#) in [TA01](#)
Watanabe, Shin-ichi . . . [# 3](#) in [ATF05](#)
Watson, Clarizza F. . . . [# 288](#) in [NST05](#)
Watson, Clarizza F. . . . [# 290](#) in [NST02](#)
Weathers, Duncan L . . . [# 293](#) in [IBA01](#)
Weathers, Duncan L . . . [# 419](#) in [Posters](#)
Weathers, D. L. . . . [# 224](#) in [NBA04](#)
Webb, Roger . . . [# 362](#) in [Posters](#)
Webb, Roger P . . . [# 155](#) in [IBA06](#)
Webb, Roger P . . . [# 158](#) in [IBM04](#)
Webb, Roger P . . . [# 162](#) in [IBM04](#) and [Posters](#)
Webb, Roger P . . . [# 165](#) in [IBM04](#) and [Posters](#)
Webb, Roger P. . . . [# 348](#) in [IBA06](#)
Weber, William J . . . [# 154](#) in [Posters](#)
Weber, William J . . . [# 255](#) in [IBM01](#)
Weber, William J. . . . [# 272](#) in [IBA03](#)
Weber, William John . . . [# 218](#) in [RE06](#)
Weber, B. V. . . . [# 146](#) in [HSD03](#)
Wegner, Martin . . . [# 475](#) in [MA04](#)
Wei, Chaochen . . . [# 335](#) in [IBA01](#)
Wei, Chao-chen . . . [# 261](#) in [RE01](#)
Wei, Xing . . . [# 40](#) in [Posters](#)
Wei, Xing . . . [# 41](#) in [Posters](#)
Weidenspointner, Georg . . . [# 184](#) in [IBA04](#)
Weismann, Leo . . . [# 468](#) in [ATF07](#)
Weisshaar, D. . . . [# 258](#) in [NP03](#)
Welch, Dale . . . [# 206](#) in [NBA03](#)
Wellington, Tracey A. . . . [# 183](#) in [NBA02](#)
Wells, D. . . . [# 115](#) in [NBA01](#)
Wells, Doug P. . . . [# 481](#) in [PS04](#)
Wells, Douglas P. . . . [# 321](#) in [MA03](#)
Wen, Juan . . . [# 389](#) in [Posters](#)
Wen, Juan . . . [# 437](#) in [RE06](#)
Whaley, Shawn D. . . . [# 290](#) in [NST02](#)
White, M. . . . [# 198](#) in [NP02](#)
Wicenciak, U. . . . [# 104](#) in [Posters](#)
Wickramarachchi, S . . . [# 66](#) in [AMP05](#)
Wickramarachchi, S J . . . [# 111](#) in [IBA01](#)
Wiedenhoefer, Ingo . . . [# 134](#) in [NP03](#)
Wieman, Howard . . . [# 322](#) in [NP08](#)
Wiescher, M. . . . [# 13](#) in [NP03](#)
Wijesundera, Dharshana . . . [# 355](#) in [IBM05](#)
Wijesundera, Dharshana . . . [# 425](#) in [IBM01](#)
Wijesundera, Dharshana N . . . [# 287](#) in [IBA09](#)
Wijesundera, Dharshana Nayanajith . . . [# 270](#) in [NST01](#)

Wijesundera, Dharshana Nayanajith . . . [# 384](#) in [Posters](#)
Wilkens, Barry J. . . . [# 288](#) in [NST05](#)
Wilkens, Barry J. . . . [# 290](#) in [NST02](#)
Williams, S. . . . [# 56](#) in [Posters](#)
Willis, Wes . . . [# 204](#) in [Posters](#)
Wilson, Cody M. . . . [# 82](#) in [HSD01](#)
Winckler, Nicolas . . . [# 462](#) in [AMP04](#)
Winger, Jeff . . . [# 278](#) in [NP04](#)
Winklehner, Daniel . . . [# 395](#) in [Posters](#)
Winkler, Nickolas . . . [# 345](#) in [AMP04](#)
Winnebeck, Alexander . . . [# 475](#) in [MA04](#)
Winter, Helmut . . . [# 36](#) in [IBA02](#)
Wirtz, Tom . . . [# 65](#) in [RE07](#)
Wolfe, Tatiana . . . [# 484](#) in [MA01](#)
Wolfe, Adam R . . . [# 484](#) in [MA01](#)
Wolff, Wania . . . [# 55](#) in [AMP05](#)
Wolff, Wania . . . [# 338](#) in [Posters](#)
Wolinska-Cichocka, M. . . . [# 470](#) in [Posters](#)
Wolinska-Cichocka, Marzena . . . [# 278](#) in [NP04](#)
Wollnik, Hermann . . . [# 353](#) in [NP10](#)
Woloshun, Keith . . . [# 43](#) in [MA03](#)
Woloshun, Keith . . . [# 280](#) in [ATF02](#)
Won-in, K. . . . [# 471](#) in [Posters](#)
Wood, Rick . . . [# 201](#) in [HSD06](#)
Woodmansee, Sam . . . [# 322](#) in [NP08](#)
Woods, Denton . . . [# 223](#) in [AMP03](#)
Woof, R. S. . . . [# 146](#) in [HSD03](#)
Woolson, Anthony J. . . . [# 288](#) in [NST05](#)
Wootan, David W . . . [# 110](#) in [Posters](#)
Wrede, C. . . . [# 205](#) in [NP09](#)
Wulf, E. A. . . . [# 146](#) in [HSD03](#)
Xiao, Yongchi . . . [# 385](#) in [NP10](#)
Xu, Can . . . [# 189](#) in [IBA02](#)
Xu, Chunping . . . [# 437](#) in [RE06](#)
Xu, Yun . . . [# 347](#) in [IBM03](#)
Xue, Haizhou . . . [# 255](#) in [IBM01](#)
Xue, Zhongying . . . [# 40](#) in [Posters](#)
Xue, Zhongying . . . [# 41](#) in [Posters](#)
Yamaguchi, Hidetoshi . . . [# 3](#) in [ATF05](#)
Yamaka, Shoichi . . . [# 3](#) in [ATF05](#)
yang, Dongyan . . . [# 437](#) in [RE06](#)
Yang, Li . . . [# 98](#) in [IBM04](#)
Yang, S. . . . [# 284](#) in [Posters](#)
Yang, S. . . . [# 285](#) in [NST01](#) and [Posters](#)
Yao, Shude . . . [# 149](#) in [IBA03](#)
Yates, S. W. . . . [# 403](#) in [TA02](#)
York, Richard . . . [# 239](#) in [NP01](#)
Yoskowitz, Joshua T . . . [# 193](#) in [Posters](#)
Yoskowitz, Joshua T. . . . [# 101](#) in [TA02](#)
Youker, Amanda . . . [# 282](#) in [MA03](#)

Young, F. C. . . . [# 146](#) in [HSD03](#)
Younger-Mertz, S. B. . . . [# 177](#) in [Posters](#)
Yu, Hui . . . [# 71](#) in [RE08](#)
Yu, Kaiyuan . . . [# 495](#) in [NST04](#)
Yu, Xiao-Ying . . . [# 98](#) in [IBM04](#)
Yu, Y. C. . . . [# 127](#) in [Posters](#)
Yu, L. D. . . . [# 471](#) in [Posters](#)
Yuan, Wei . . . [# 406](#) in [RE05](#)
Zak, Alla . . . [# 219](#) in [IBM01](#)
Zavodszky, Peter A. . . . [# 153](#) in [MA03](#)
Zeisler, S. . . . [# 153](#) in [MA03](#)
Zepeda-Ruiz, L.A. . . . [# 411](#) in [RE01](#)
Zetterberg, U. . . . [# 153](#) in [MA03](#)
Zganjar, Ed . . . [# 278](#) in [NP04](#)
Zhang, Fuxiang . . . [# 100](#) in [RE06](#)
Zhang, Genfa . . . [# 406](#) in [RE05](#)
Zhang, Hongliang . . . [# 430](#) in [IBA03](#)
Zhang, Hongxiu . . . [# 34](#) in [RE01](#)
Zhang, Jiaming . . . [# 100](#) in [RE06](#)
Zhang, Jian . . . [# 437](#) in [RE06](#)
Zhang, jinquan . . . [# 125](#) in [Posters](#)
Zhang, Kun . . . [# 81](#) in [NST07](#)
Zhang, Lai . . . [# 273](#) in [Posters](#)
Zhang, Limin . . . [# 406](#) in [RE05](#)
Zhang, Miao . . . [# 40](#) in [Posters](#)
Zhang, Miao . . . [# 41](#) in [Posters](#)
Zhang, Xinghang . . . [# 311](#) in [NST04](#)
Zhang, Yanwen . . . [# 87](#) in [IBM03](#)
Zhang, Yanwen . . . [# 154](#) in [Posters](#)
Zhang, Yanwen . . . [# 218](#) in [RE06](#)
Zhang, Yanwen . . . [# 255](#) in [IBM01](#)
Zhang, Yanwen . . . [# 272](#) in [IBA03](#)
Zhang, Zhu Lin . . . [# 273](#) in [Posters](#)
Zhang, E X . . . [# 225](#) in [RE04](#)
Zhang, En X . . . [# 133](#) in [RE04](#)
Zhao, B. . . . [# 243](#) in [HSD03](#)
Zhao, Xiao-Lei . . . [# 381](#) in [NST06](#)
Zheng, Wei . . . [# 175](#) in [NBA02](#)
Zhou, C. L. . . . [# 90](#) in [IBA04](#)
Zhu, Mujin . . . [# 57](#) in [RE06](#)
Zhu, S. . . . [# 258](#) in [NP03](#)
Zhu, Zihua . . . [# 87](#) in [IBM03](#)
Zhu, Zihua . . . [# 98](#) in [IBM04](#)
Zhu, Zihua . . . [# 154](#) in [Posters](#)
Zier, J. C. . . . [# 146](#) in [HSD03](#)
Zimmerman, Robert Lee . . . [# 7](#) in [NST01](#) and [Posters](#)
Zisman, Michael . . . [# 306](#) in [ATF08](#)
Zouros, Theodore J.M. . . . [# 463](#) in [Posters](#)

